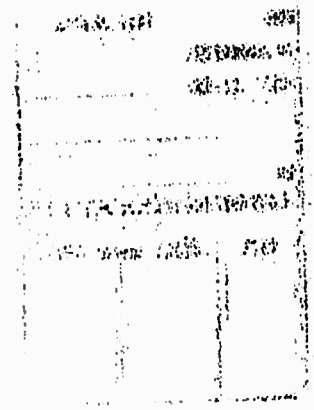


AD-735-722

PLUME CONTAMINATION EFFECTS PREDICTION

The
CONTAM
Computer Program



R.J. Hoffman, W.D. English,
R.G. Oeding, and W.T. Webber
McDonnell Douglas Astronautics Company

FINAL REPORT AND PROGRAM USER'S MANUAL

December 1971

Approved for public release; distribution unlimited.

Air Force Rocket Propulsion Laboratory
United States Air Force
Edwards, California

Reproduced by
NATIONAL TECHNICAL
INFORMATION SERVICE
Springfield, Va. 22151

DDC
RECEIVED
JAN 12 1972
REGITLED
B

UNCLASSIFIED

Security Classification

DOCUMENT CONTROL DATA - R & D		
<i>(Security classification of title, body of abstract and indexing annotation must be entered when the overall report is classified)</i>		
1. ORIGINATING ACTIVITY (Corporate author) McDonnell Douglas Astronautics Company 5301 Bolsa Ave. Huntington Beach, California 92647		2a. REPORT SECURITY CLASSIFICATION Unclassified/Distribution Unlimited 2b. GROUP
3. REPORT TITLE PLUME CONTAMINATION EFFECTS PREDICTION		
4. DESCRIPTIVE NOTES (Type of report and inclusive dates) Final Report		
5. AUTHOR(S) (First name, middle initial, last name) R. J. Hoffman, W. D. English, R. G. Oeding, W. T. Webber		
6. REPORT DATE December 1971	7a. TOTAL NO. OF PAGES 521	7b. NO. OF REFS 82
8a. CONTRACT OR GRANT NO F04611-70-C-0076 b. PROJECT NO c. d.	9a. ORIGINATOR'S REPORT NUMBER(S) AFRPL-TR-71-109 9b. OTHER REPORT NO(S) (Any other numbers that may be assigned this report) MDC G2529	
10. DISTRIBUTION STATEMENT Distribution of this document is unlimited		
11. SUPPLEMENTARY NOTES		12. SPONSORING MILITARY ACTIVITY Air Force Rocket Propulsion Laboratory Air Force Systems Command Edwards, California 92523
13. ABST AC The effect of rocket exhaust plume impingement on sensitive vehicle surfaces is an area of continuing concern in the design of spacecraft, missiles, and reentry vehicle systems. Specifically, the contamination and subsequent degradation of functional surfaces, such as solar cells, thermal control coatings, optical lenses, optical view ports, and highly reflective surfaces, have resulted in compromises of mission effectiveness. The objective of this study was to develop a single computer code capable of predicting the production, transport, and deposition of engine and plume contaminants, and the change in absorptivity, emissivity, reflectivity, and transmissivity of a functional spacecraft surface, such as thermal control coatings and optical view ports and lenses, resulting from plume contaminant deposition or mechanical abrasion (sand blasting). Surface chemical reaction with a deposited plume contaminant layer was not treated. Analytical models and computer subprograms have been developed and integrated to form the <u>CONTAM</u> computer program. Complete User's manuals for each of the computer subprograms as well as the <u>CONTAM</u> program are included in this report, along with details of the analysis and numerical methods. A sample case illustrating the <u>CONTAM</u> program's capability to predict contaminant production and transport is presented. The Marquardt R-6C 5-lb thrust MMH/NTO engine, currently used at NASA/LeRC for their contamination experiment, was chosen. The deposition and surface effects subprogram, <u>SURFACE</u> , was not run because it was felt that meaningful results could not be obtained for this engine with the current version of the <u>SURFACE</u> program. Results for this thruster, pulsed for 50 ms, indicate that a considerable amount of contaminant is formed and transported into the plume when the motor is pulsed periodically.		

DD FORM 1473
1 NOV 65

525

UNCLASSIFIED
Security Classification

FOREWORD

This report was prepared for the Air Force Rocket Propulsion Laboratory (AFRPL), United States Air Force, Edwards, California, under Contract FO4611-70-C-0076, by the McDonnell Douglas Astronautics Company (MDAC), Huntington Beach, California. The Air Force program monitors for this study were Dr. L. P. Quinn (RTSP) and James R. Nunn, Capt., USAF (RTSP). The study was performed during the period August 1970 to August 1971, and the final report submitted to AFRPL for approval on October 4, 1971.

The MDAC study manager for this project was Mr. R. J. Hoffman, Aero/thermodynamics and Nuclear Effects Department, Research and Development. Mr. W. T. Webber, Propulsion Department, was principal investigator for the contaminant production task. Mr. R. G. Oeding, Aero/thermodynamics and Nuclear Effects Department, was principal investigator for the contaminant transport and kinetics tasks. Dr. D. W. English, Propulsion Department, was principal investigator for the surface effects task.

In addition to the authors, many persons contributed significantly to the study effort for which we are grateful. Dr. L. P. Quinn (RTSP), in addition to his duties as contract monitor, helped to guide the technical effort by his continued keen interest in the study and his constructive criticism. Mr. A. D. Warren, principal investigator for the laboratory experiment task, provided the necessary experimental background to interface with the NASA/LeRC contamination experiment. Mr. T. J. Nelson and Mr. G. A. Gaitatzes assisted greatly in the integration and checkout of the computer subprograms. Dr. W. A. Gaubatz provided considerable technical guidance during the development of the contaminant production model and in the parametric study. Mr. T. Ward performed the actual contaminant production parametric study.

We also wish to express our thanks to Dr. H. Mark and his group at NASA/LeRC for allowing MDAC to use his experimental engine data in our computer model development and for providing us with encouragement and needed information concerning his experiment.

This technical report has been reviewed and is approved.

A. D. Brown, Jr., Lt Colonel, USAF
Chief, Technology Division

14. KEY WORDS	LINK A		LINK B		LINK C	
	ROLE	WT	ROLE	WT	ROLE	WT
Contamination						
Plume						
Rocket Exhaust						
Rocket Plume						
Plume Contamination						
Contamination						
Contamination Effects						
Contaminant Production						
Deposition						
Surface Effects						
Surface Properties						
Surface Contamination						

ABSTRACT

The effect of rocket exhaust plume impingement on sensitive vehicle surfaces is an area of continuing concern in the design of spacecraft, missiles, and reentry vehicle systems. Specifically, the contamination and subsequent degradation of functional surfaces, such as solar cells, thermal control coatings, optical lenses, optical view ports, and highly reflective surfaces, have resulted in compromises of mission effectiveness. The objective of this study was to develop a single computer code capable of predicting the production, transport, and deposition of engine and plume contaminants, and the change in absorptivity, emissivity, reflectivity, and transmissivity of a functional spacecraft surface, such as thermal control coatings and optical view ports and lenses, resulting from plume contaminant deposition or mechanical abrasion (sand blasting). Surface chemical reaction with a deposited plume contaminant layer was not treated. Analytical models and computer subprograms have been developed and integrated to form the CONTAM computer program. Complete User's manuals for each of the computer subprograms as well as the CONTAM program are included in this report, along with details of the analysis and numerical methods. A sample case illustrating the CONTAM program's capability to predict contaminant production and transport is presented. The Marquardt R-6C 5-lb thrust MMH/NTO engine, currently used at NASA/LeRC for their contamination experiment, was chosen. The deposition and surface effects subprogram, SURFACE, was not run because it was felt that meaningful results could not be obtained for this engine with the current version of the SURFACE program. Results for this thruster, pulsed for 50 ms, indicate that a considerable amount of contaminant is formed and transported into the plume when the motor is pulsed periodically.

CONTENTS

<u>Section</u>		<u>Page</u>
I	INTRODUCTION	1
II	OBJECTIVES AND SCOPE	9
	1. Objectives	9
	2. Scope	9
III	MODEL DESCRIPTION	11
	1. Combustion Chamber Contaminant Production	11
	a. Feed Systems	13
	b. Atomization	13
	c. Chamber Calculations	14
	d. Wall Calculations	14
	e. Comparison with Experimental Results	14
	2. Contaminant Transport	16
	3. Chemical Kinetics and Condensation in the Nozzle and Plume Flow Field	17
	a. Chemical Kinetics Model	18
	b. Condensation Model	18
	4. Deposition, Abrasion, and Surface Effects	19
	a. Solar Absorptivity	19
	b. Hemispherical Emissivity	19
	c. Surface Abrasion	21
	d. Material Deposition	21
IV	THE <u>CONTAM</u> COMPUTER PROGRAM	23
	1. General Description	23
	a. Combustion Chamber Contaminant Production	25
	b. Contaminant Transport	25
	c. Chemical Kinetics and Condensation	25
	d. Deposition and Surface Property Effects	27
	2. Program Description	27
	3. Program Overlay Structure	27
	4. Program Data Interfaces	29
	a. <u>TCC</u> Data	29
	b. <u>TD2</u> Data	29
	c. <u>TD2P</u> Data	29
	d. <u>SLINES</u> Data	29
	e. <u>KINCON</u>	29

<u>Section</u>		<u>Page</u>
IV	5. Program User's Manual	30
	a. Input to CONTAM	30
	b. Program NAMELISTS	31
	c. CONTAM NAMELISTS	31
	d. Nonstandard Format Inputs	32
	e. Input Card Stack	32
V	SAMPLE CASE RESULTS	35
	1. Definition of Sample Case	35
	2. Contaminant Production - The TCC Program	35
	a. TCC Input - Sample Case (R-6C Engine)	36
	b. TCC Output - Sample Case (R-6C Engine)	51
	3. Contaminant Transport - The MULTRAN. Program	78
	a. Interpretation of TCC Results	78
	b. MULTRAN Input - Sample Case (R-6C Engine	79
	c. MULTRAN Output - Sample Case (R-6C Engine	79
VI	4. Kinetics and Condensation - The KINCON Program	102
	a. Description of Input	103
	b. Description of Output	103
	c. Discussion of Results	107
VI	CONCLUSIONS AND RECOMMENDATIONS	127
	1. Conclusions	127
	2. Recommendations	127
VII	REFERENCES	129
Appendix		
A	TCC—Transient Combustion Chamber Dynamics Computer Program	131
B	MULTRAN—Multiphase Nozzle and Plume Transport Computer Program	285
C	KINCON—Nonequilibrium Chemical Kinetics and Condensation Computer Program	357
D	SURFACE—Deposition and Surface Effects Computer Program	459

ILLUSTRATIONS

<u>Figure</u>		<u>Page</u>
1.	Liquid Bipropellant Plume Impingement Effects (22-lb Thrustor MMH-NTO, O/F = 1.65)	2
2.	Deposition Effects of Rocket Exhaust Impingement After Continuous Long-Duration Firing	4
3.	Effects of Thrustor Exhaust Continuous Long-Duration Firing	5
4.	Effect of Thrustor Exhaust Continuous Long-Duration Firing - Aluminum and Glass Samples	6
5.	Schematic Diagram of Analytical Model Elements and Related Computer Programs	12
6.	Comparison of Experimental and Calculated Wall-Film Contaminant Production as a Function of Propellant/Hardware Temperature	15
7.	Comparison of Calculated and Experimental High Altitude Start	16
8.	Static Pressure and Temperature Profiles for Condensing Nozzle Flow	20
9.	Contaminant Effects Physical Model-Heat Rejection Radiators	20
10.	Schematic of the Plume Contamination Effects Prediction Computer Program, CONTAM	24
11.	Schematic of Contamination Processes and Related Subprogram	26
12.	CONTAM Computer Program Overlay Structure	28

<u>Figure</u>		<u>Page</u>
13.	CONTAM Input Card Stack	33
14.	TCC Graphic Output - Chamber Pressure Versus Time	74
15.	TCC Graphic Output - Oxidizer Valve Trace Versus Time	74
16.	TCC Graphic Output - Oxidizer Voided Versus Time	74
17.	TCC Graphic Output - Oxidizer Injection Rate Versus Time	74
18.	TCC Graphic Output - Stream Beta Angle Versus Time	75
19.	TCC Graphic Output - Oxidizer Droplet Mass Versus Time	75
20.	TCC Graphic Output - Oxidizer on Wall Versus Time	75
21.	TCC Graphic Output - Chamber Oxidizer D32 Versus Time	75
22.	TCC Graphic Output - Gas Outflow Rate Versus Time	76
23.	TCC Graphic Output - Oxidizer Droplet Outflow Versus Time	77
24.	TCC Graphic Output - Oxidizer Film Outflow Versus Time	77
25.	TCC Graphic Output - Film Thickness on Wall Versus Percent Chamber Length at Time = 9 Milliseconds	77
26.	TCC Graphic Output - Film Thickenss on Wall Versus Percent Chamber l Length at Time = 18 Milliseconds	77
27.	Marquardt R-6C Engine - Sample Case - Contaminant Transport (MULTRAN Program)	100
28.	Static Temperature Distribution for 99% Streamline	123

<u>Figure</u>		<u>Page</u>
29.	Gas Velocity Distribution for 99% Streamline	124
30.	H ₂ O, H and O Composition for 99% Streamline	125

BLANK PAGE

TABLES

<u>Table</u>		<u>Page</u>
I	Namelist and Subprogram	31
II	Input Data for Marquardt R-6C Engine TCC	38
III	TCC Output	53
IV	Sample MULTRAN Output-Input Data	80
V	Sample MULTRAN Output - Representative Printout	84
VI	KINCON Sample Case - Data Listing	104
VII	KINCON Sample Case - 0% Streamline	105
VIII	KINCON Sample Case - 90% Streamline	106
IX	KINCON Sample Case - Identification (0% Streamline)	108
X	KINCON Sample Case - Pressure Table (0% Streamline)	109
XI	KINCON Sample Case - Initial Conditions (0% Streamline)	111
XII	KINCON Sample Case - Representative Printout (Axial Position = 0.9767, 0% Streamline)	112
XIII	KINCON Sample Case - Representative Printout (Axial Position = 10.0839, 0% Streamline)	113
XIV	KINCON Sample Case - Representative Printout (Axial Position = 19.8159, 0% Streamline)	114
XV	KINCON Sample Case - Maximum and Minimum for Reaction Production Rates (0% Streamline)	115

<u>Tables</u>		<u>Page</u>
XVI	<u>KINCON</u> Sample Output – Identification (90% Streamline)	116
XVII	<u>KINCON</u> Sample Case – Pressure Table (90% Streamline)	117
XVIII	<u>KINCON</u> Sample Case – Initial Conditions (90% Streamline)	119
XIX	<u>KINCON</u> Sample Case – Representative Printout (Axial Position = 0. 974875, 90% Streamline)	120
XX	<u>KINCON</u> Sample Case – Representative Printout (Axial Position = 24. 4058, 90% Streamline)	121
XXI	<u>KINCON</u> Sample Case – Maximum and Minimum For Reaction Production Rates (90% Streamline)	122

SECTION I

INTRODUCTION

The effect of rocket exhaust plume impingement on sensitive vehicle surfaces is an area of continuing concern in the engineering design of spacecraft, missiles, boosters, and RV systems. Specifically, the contamination and subsequent degradation of functional surfaces, such as solar cells, thermal control coatings, optical lenses, optical view ports, highly reflective (mirrored) surfaces, and sealants, have resulted in compromises of mission effectiveness.

To illustrate the deposition of contaminants problem, several photographic examples of contamination occurring as the result of actual bipropellant engine firings will be presented. These examples were taken from a series of contamination experiments conducted by MDAC under the MOL program.

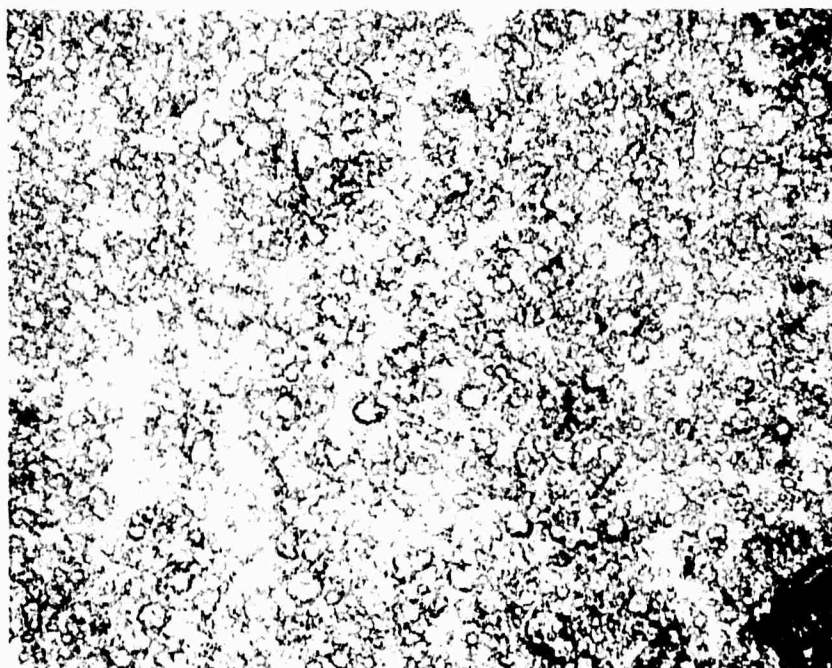
Figure 1 compares a control surface (no impingement) with a surface which has been exposed to normal impingement by the exhaust plume of a liquid bipropellant engine (MMH-NTO). Evidence of surface damage is apparent, and was postulated to be caused by condensed droplets in the core of the plume flow.

During a vacuum chamber subscale thruster test by MDAC at AEDC, a 1-lb thrust Marquardt MMH-NTO rocket engine was fired horizontally so that the exhaust products would impinge upon a vertically oriented test panel containing several surface specimens. Surface specimens included thermal control coatings, polished metal, and specialized glass lenses.

During pulse-mode operation of the motor, copious quantities of brownish, viscous liquid were observed about the nozzle lip and upon the lower external surface of the motor. This liquid exhibited considerable activity, bubbling while suspended from the motor lower external surface apparently due to some boiling and/or decomposition phenomenon. An impingement pattern of sorts was visible upon the test panel that appeared symmetrical but did not agree well (qualitatively) with theoretical predictions of the gas-phase impingement region. The region within the symmetric impingement pattern was coated with viscous liquid and/or solid material that increased in quantity with the number of pulses to which the panel was exposed; the coloration of this material was difficult to identify, but was definitely darker than the panel. Above and below the symmetric impingement region liquids were splattered in very large quantities, particularly near and below the rocket motor where semisolid formations of brownish color were noted; deposition of this variety seemed randomly distributed and was observed fore and aft of the nozzle exit plane. The amount of liquid generated by the rocket motor varied inversely with pulse duration, with



a. CONTROL SAMPLE SHIELDED FROM DIRECT IMPINGEMENT



b. SAMPLE EXPOSED TO NORMAL EXHAUST IMPINGEMENT

Figure 1. Liquid Bipropellant Plume Impingement Effects (22-lb Thrustor MMH-NTO, O/F = 1.65)

maximum amount generated during the 16-msec "minimum impulse" pulses. Thermal control coatings exposed to these exhaust products were visibly coated and suffered losses in reflectance. Similarly, transparent samples suffered transmittance losses. After certain periods of liquid buildup upon the panel, brownish liquids ran down the panel surface. During long-duration firings in excess of several hundred seconds, a well defined symmetric impingement pattern was noted upon the panel. It was difficult to discriminate between liquid and solid formations at this point. The symmetric impingement region gained further definition by virtue of a continuous ridge of solid and/or viscous liquid deposits at the symmetric impingement region boundaries. Posttest microphotography revealed that glass surfaces were coated with micron-sized droplets, even though the incidence angle of exhaust products was (theoretically) very small or nonexistent. Deposits upon the panel and surface samples displayed phase instability at STP conditions, changing from solid to liquid to solid when disturbed physically or environmentally. When the chamber was repressurized to facility ambient conditions, much of the material deposited upon the panel became less viscous and ran off the panel.

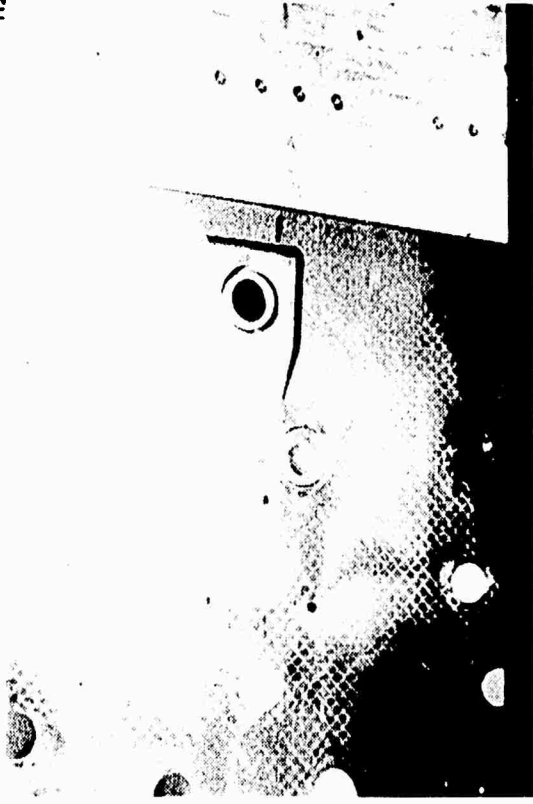
Figures 2 through 4 show some of the deposits observed after various duty cycles.

This report will present the results of a 12-month study for the Air Force Rocket Propulsion Laboratory to develop an analytical model and computer program for the prediction of spacecraft functional surface contamination effects caused by interactions with liquid bipropellant rocket exhaust plumes. Emphasis has been placed on development of computer codes to describe the complex two-phase combustion gas-dynamic processes occurring in a bipropellant combustor and the thermodynamic and kinetic nonequilibrium processes occurring during a two-phase nozzle and plume expansion. Less attention has been given to the detailed modeling of the deposition processes and the subsequent changes in surface properties. Verification of the integrated Plume Contamination Effects Prediction Computer Program will be attempted by comparison with high-altitude bipropellant contaminant tests. It is anticipated that an independent on-going NASA Lewis Research Center experiment, conducted by Dr. Herman Mark and Mr. Jack Cassidy, will provide the necessary engine operating details and contamination effects data to achieve a meaningful correlation.

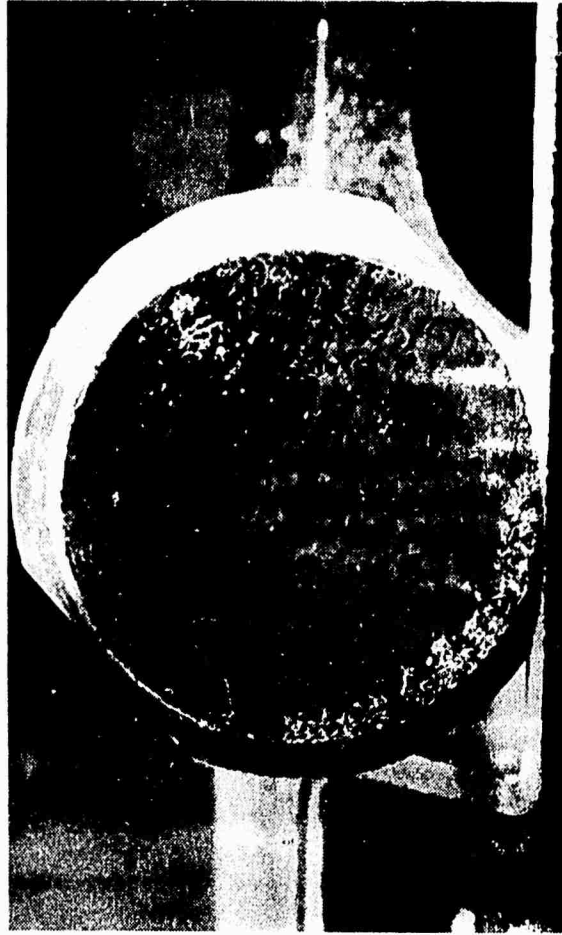
This report is divided into five discrete parts: the main body of the report and four appendixes. In the main body, emphasis is placed on describing the operating characteristics of the integrated Plume Contamination Effects Prediction Computer Program, CONTAM. A description of the program, User's Manual, and sample case run illustrating the ability of CONTAM to predict contaminant production, transport, and condensation are presented. Deposition and surface effects prediction has not been included in the sample case run for CONTAM (main text) but has been discussed in Appendix D. CONTAM consists of four discrete subprogram links, each capable of operating as a separate computer program or as a link to



(a) NEAR-FIELD DEPOSITS ON PANEL



(b) FAR-FIELD DEPOSITS ON PANEL



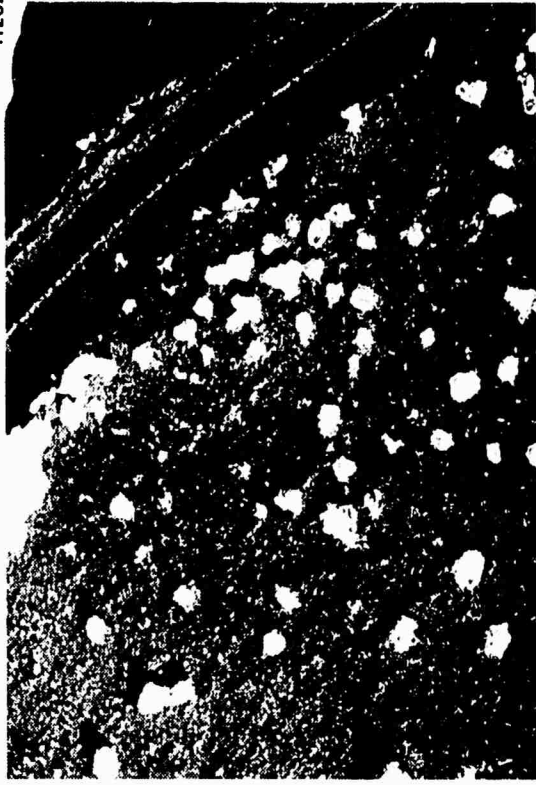
(c) SCHDAHL TAPE SAMPLE SHOWING DEPOSITS



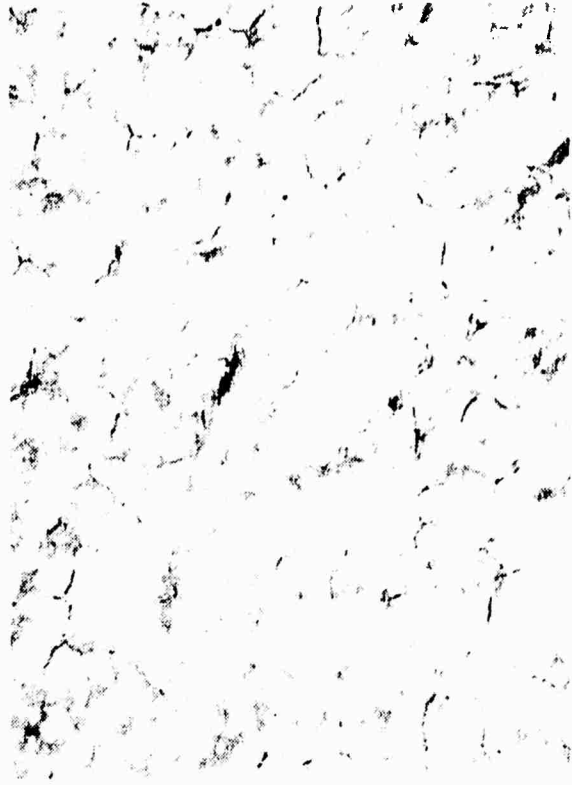
(d) 15X MAGNIFICATION OF (c)

Figure 2. Deposition Effects of Rocket Exhaust Impingement After Continuous Long-Duration Firing

R20Z



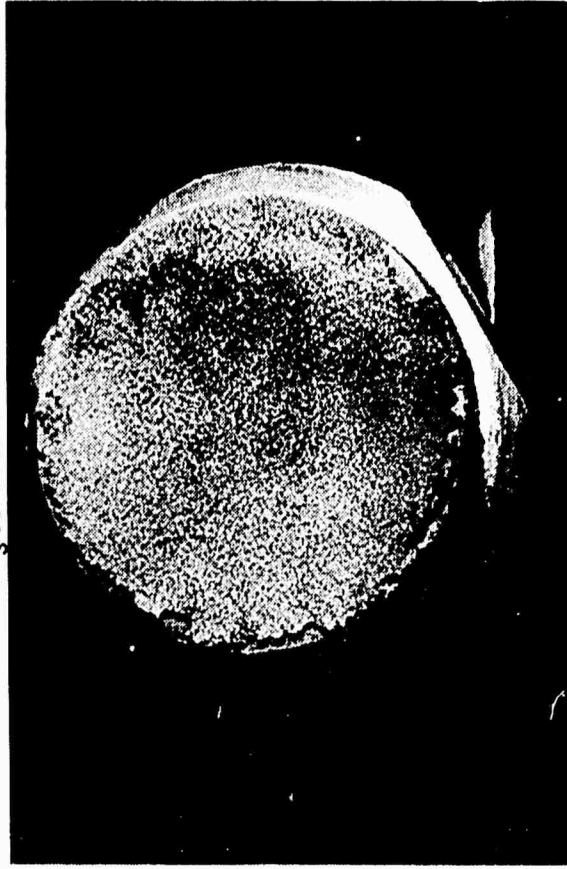
(b) 15X MAGNIFICATION OF (a)



(d) 30X MAGNIFICATION OF (c)



(a) ZnO-KSI O₃ COATING SHOWING FRAGMENTATION



(c) BLACK SPINEL COATING SHOWING DEPOSITS

Figure 3. Effect of Thruster Exhaust Continuous Long-Duration Firing--ZnO-KSiO₃ and Spinel Coatings



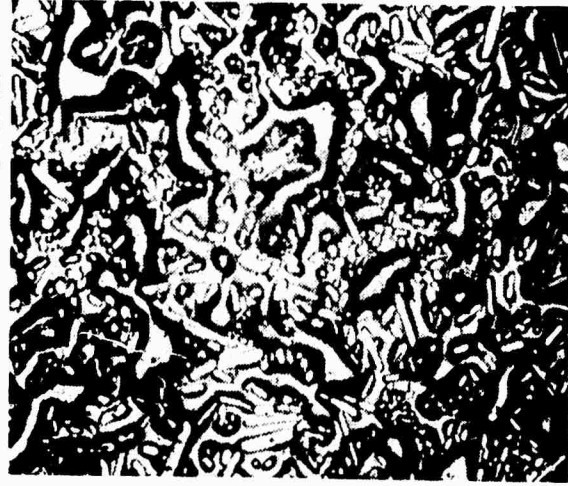
(a) ALUMINUM SAMPLE SHOWING DEPOSITS (10X)



(b) 30X MAGNIFICATION OF (a)



(c) HORIZON SENSOR LENS SHOWING DEPOSITS



(d) 80X MAGNIFICATION OF DEPOSITS ON HORIZON SENSOR LENS

Figure 4. Effect of Thruster Exhaust Continuous Long-Duration Firing - Aluminum and Glass Samples

CONTAM. Each of the subprograms is described in detail in a separate appendix as follows:

- | | |
|---------------------------|--|
| Appendix A <u>TCC</u> | Transient Combustion Chamber Dynamics Computer Program (a bipropellant contaminant production model) |
| Appendix B <u>MULTRAN</u> | Multiphase Nozzle and Plume Transport Computer Program (a multiphase nozzle and plume flow field characterization model) |
| Appendix C <u>KINCON</u> | Nonequilibrium Chemical Kinetics and Condensation Computer Program (a multiphase reacting gas streamtube model) |
| Appendix D <u>SURFACE</u> | Deposition and Surface Effects Computer Program (a plume impingement, deposition, abrasion, and surface contamination effects model) |

In addition to the sample case in the main body of the report, each appendix contains a sample case illustrating additional capabilities of the particular subprogram. Detailed operating information for each subprogram is contained in the User Manual section of each appendix.

This report has been loose-leaf bound to facilitate updating of the various User's Manuals, either by MDAC or other Government and industry users. The author's would greatly appreciate comments, corrections, additions, and suggestions for inclusion in future updates to be distributed to all users. Please send comments to:

R. J. Hoffman
A3-BBBO-20
McDonnell Douglas Astronautics Company
5301 Bolsa Avenue
Huntington Beach, California 92647

SECTION II

OBJECTIVES AND SCOPE

1. OBJECTIVES

The objective of the study is to develop a single computer code capable of predicting the production, transport, and deposition of engine and plume contaminants and the change in absorptivity, emissivity, reflectivity, and transmissivity of a functional spacecraft surface, such as thermal control coatings and optical view ports and lenses, resulting from plume contaminant deposition or mechanical abrasion (sand blasting). Surface chemical reaction with a deposited plume contaminant layer is not treated.

The study has been divided into five main areas:

- (1) Improvement of predictive technology for the characterization of reactive, multiphase rocket nozzle and exhaust plume flows containing propellant contaminants and nonequilibrium combustion products, including condensables.
- (2) Continued development of an analytical model to predict the production of contaminants in bipropellant rocket-engine combustion chambers.
- (3) Development of a semiempirical model to predict changes in surface properties of functional spacecraft surfaces (resulting from deposition or abrasion).
- (4) Integration and coupling of existing computer programs and newly developed computer programs to achieve a systems engineering design tool for the prediction of contaminant effects on spacecraft surfaces.
- (5) Verification of the contamination prediction model by comparison with experimental data.

2. SCOPE

This initial study has been restricted to the development of predictive methods for the production, transport, and deposition of contaminants from hydrazine-family fuels in combination with nitrogen tetroxide and to changes in thermal and optical surface properties of common thermal-control paints and optical lenses. The model development has considered RCS engines in the 5- to 100-lb thrust range; the validity of the model for much larger engines has not been assessed.

Preceding page blank

SECTION III

MODEL DESCRIPTION

Section 4 describes the CONTAM plume contamination effects prediction computer program developed during this study. The analytical models associated with each link of the CONTAM program are discussed in detail in the appropriate appendix. In this section, a summary description of the analytical models employed in the CONTAM program is given.

The general objectives of the study were to construct a single analytical model capable of predicting the effects of bipropellant plume impingement contamination on optical and thermal spacecraft surfaces based only on a knowledge of available engine operating conditions, engine/spacecraft configuration geometries, and spacecraft orbital parameters. To this end, it was necessary to construct a model for the production of contaminants in a bipropellant combustion chamber (unburned propellants ejected through nozzle throat); transport of these contaminants by the expanding gases in the nozzle and exhaust plume; chemical nonequilibrium composition of plume species; condensation of plume species in the expanding plume; abrasion damage and deposition resulting from plume impingement; and, finally, the changes in thermal and optical surface properties, absorptivity, emissivity, transmissivity, and reflectivity resulting from contaminant deposition and/or abrasion damage. In addition, the model considers the effect of engine duty cycle and spacecraft radiant energy transfer on the rate of contaminant deposition over an entire mission profile.

The feasibility of constructing a valid model, considering all of the above aspects, relied heavily upon the existence of several models and computer codes which could be used as a basis for construction of the overall contamination effects prediction model. Several new portions of the model and computer subprograms were developed. Figure 5 schematically illustrates the computation flow logic and the related computer codes. Details of each computer code can be found in the appropriate appendix.

1. COMBUSTION CHAMBER CONTAMINANT PRODUCTION (See Appendix A for further details)

Unburned propellant and intermediate products of combustion (liquid phase) ejected from the combustion chamber are considered first as a source of contaminants. Referring to Figure 5, the Transient Combustion Chamber (TCC) Dynamics Program, developed by Webber and Gaubatz (1) and extensively modified for prediction of contaminant production (2), was used to generate parametric contaminant production data over a range of typical RCS operating conditions. Based on this parametric study, modifications were made to the program to allow its inclusion as part of the overall contamination effects prediction model.

A

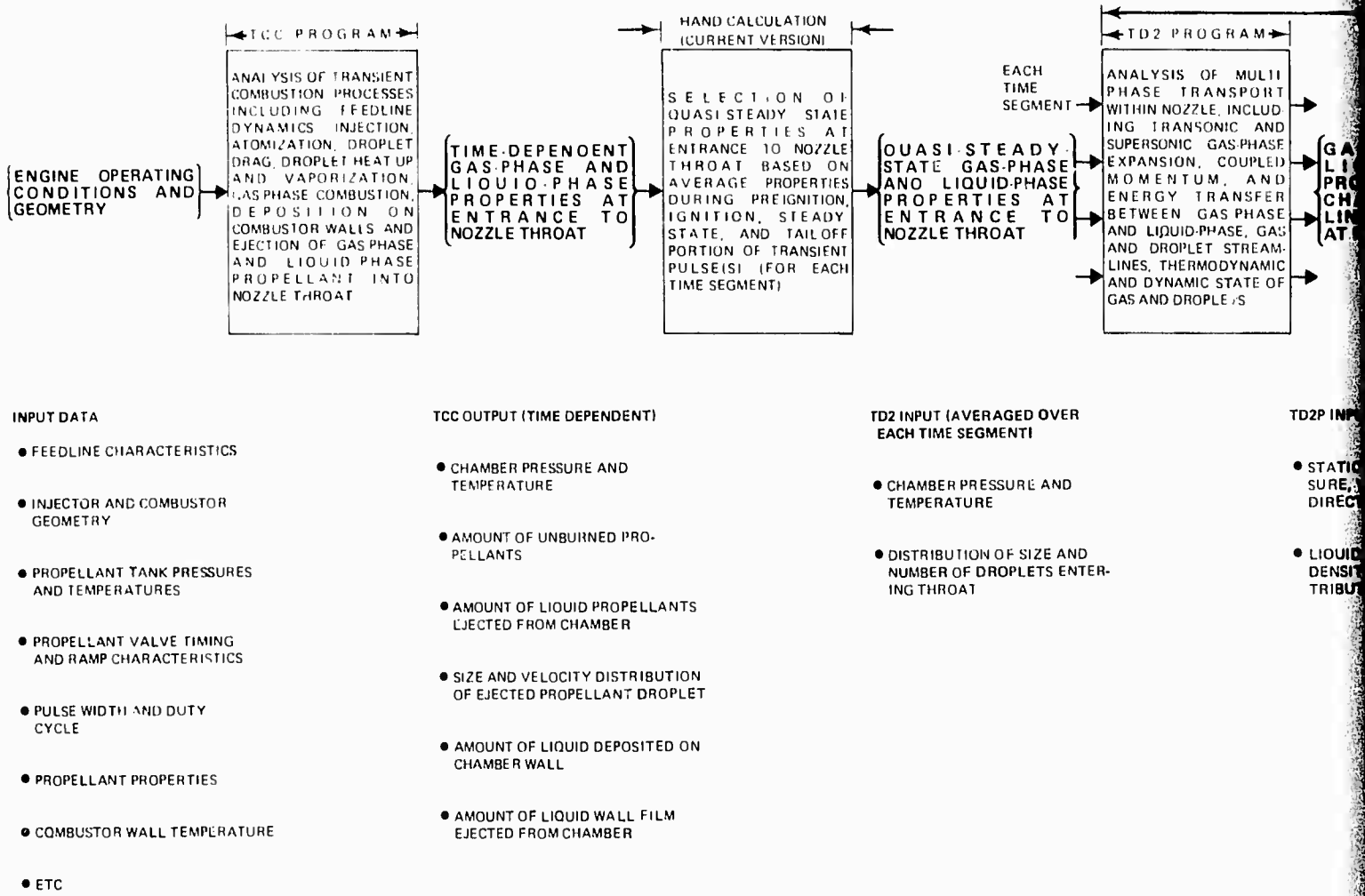
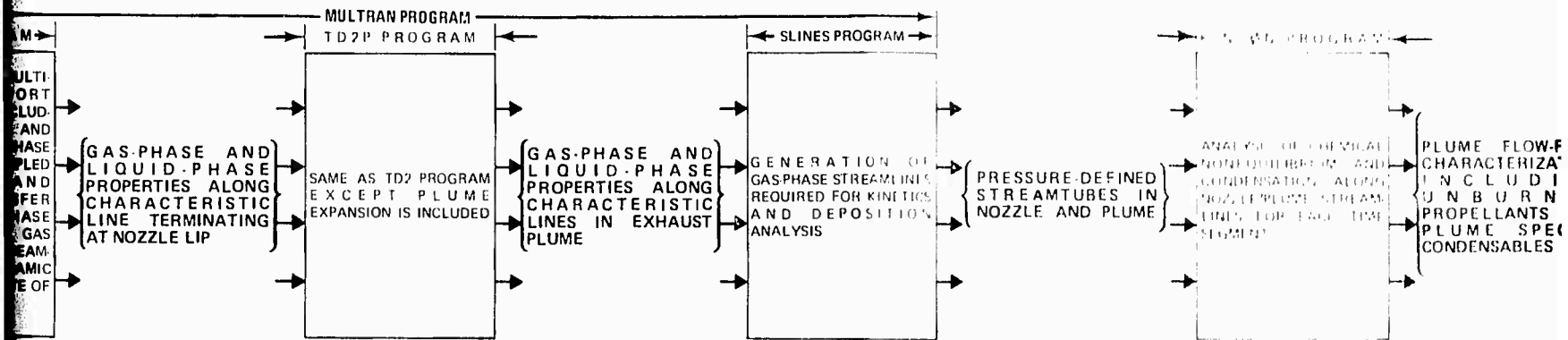


Figure 5. Schematic Diagram of Analytical Model Elements and Related Computer Programs



TD2P INPUT (FOR EACH TIME SEGMENT)

- STATIC GAS TEMPERATURE, PRESSURE, VELOCITY, AND FLOW DIRECTION
- LIQUID DROPLET TEMPERATURE, DENSITY, VELOCITY, SIZE DISTRIBUTION, AND FLOW DIRECTION

TD2P OUTPUT (FOR EACH TIME SEGMENT)

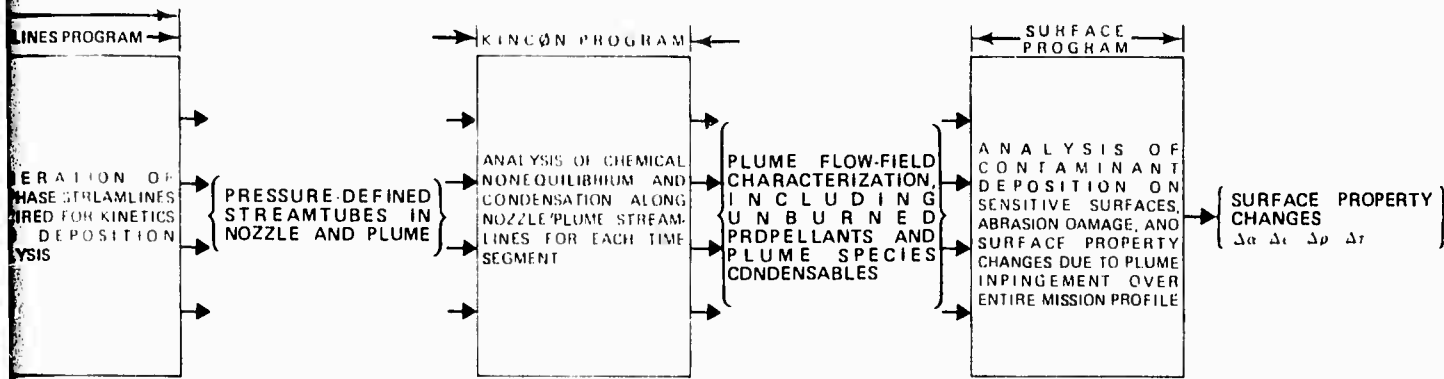
- STATIC GAS TEMPERATURE, PRESSURE, VELOCITY, AND FLOW DIRECTION
- LIQUID DROPLET TEMPERATURE, DENSITY, VELOCITY, SIZE DISTRIBUTION, AND FLOW DIRECTION

KINCDN INPUT (FOR EACH TIME SEGMENT AND EACH STREAMTUBE)

- AXIAL DISTANCE VS. PRESSURE ALONG EACH STREAMTUBE
- INITIAL COMPOSITION, TEMPERATURE, PRESSURE, VELOCITY

SURFACE INPUT

- PLUME STATE: PRESSURE, TEMPERATURE, VELOCITY, FLOW DIRECTION
- UNBURNED PROPELLANT DROPLET TEMPERATURE, VELOCITY, SIZE DISTRIBUTION
- NONEQUILIBRIUM PLUME
- CONDENSED PLUME SPECIES



KINCON INPUT (FOR EACH TIME SEGMENT AND EACH STREAM-TUBE)

- AXIAL DISTANCE VS. PRESSURE ALONG EACH STREAMTUBE
- INITIAL COMPOSITION, TEMPERATURE, PRESSURE, VELOCITY

SURFACE INPUT

- PLUME STATIC PRESSURE, TEMPERATURE, VELOCITY AND FLOW DIRECTION
- UNBURNED PROPELLANT LIQUID DROPLET TEMPERATURE, DENSITY, VELOCITY, SIZE DISTRIBUTION
- NONEQUILIBRIUM PLUME COMPOSITION
- CONDENSED PLUME SPECIES

Contaminant material is produced by the combustor of a bipropellant rocket engine when partially burned propellant droplets pass through the throat or when they strike a cold chamber wall to form a liquid film, which is moved downstream by chamber gas shear forces. When the unburned propellant or intermediate reaction products are ejected from a rocket engine, they may be transported in the plume and deposited on nearby sensitive spacecraft surfaces, changing their thermal or optical properties.

The sequence of combustion related events, in the rocket engine combustion chamber is calculated by numerically integrating the differential and algebraic equations which describe the basic processes of the feed system, injector, and combustion chamber. Figure A-1 in Appendix A is a drawing of the rocket system.

a. Feed Systems

The feed systems are approximated with single lumped parameters representing the inertial and resistive aspects of the feed system, the rate of acceleration of flow being proportional to the amount that the instantaneous pressure drop exceeds the instantaneous pressure losses in the system. The opening and closing of the valves are modeled by varying the feed system resistance as a function of time. Flow reversals or initial start conditions, which result in partially or fully gas-filled feed lines, are simulated by varying both the resistance and inertia of the feed system as functions of time.

b. Atomization

The atomization process is calculated for one of several modes, depending on the chamber pressure. If the injected propellant is sufficiently supersaturated, the stream is presumed to flash-atomize. The flash-atomization process resembles the gas-atomization process, with the gas being supplied by the explosive growth of bubbles in the supersaturated stream. The flash atomization process gives relatively fine droplets, on the order of 40 microns in diameter.

When the chamber pressure is sufficiently high that the injected propellant streams do not flash, the atomization occurs by the impingement of the fuel and oxidizer streams. The median droplet diameter is obtained from an equation based on the orifice diameters, injection velocities, relative momentum of the streams, and physical properties of the propellants.

When only one stream is being injected during a start transient, there can be no impingement and atomization is calculated based on single-stream breakup.

The injected propellant moves from the injection point to the impingement point along the direction of injection. After impingement, the stream moves in the direction of the resultant angle. The stream moves in this new direction until its atomization is complete, after which its two-dimensional trajectory is determined by the aerodynamic drag forces

c. Chamber Calculations

The vapors or gases that fill the combustion chamber are derived from several sources: vapor from flashing propellant streams; material evaporated from propellant droplets; evaporation of material deposited on the combustion chamber walls and from the ignitor if one is used. Fuel and oxidizer vapor from these sources are axially cumulated in the chamber at each time interval, while the amounts calculated to flow through the nozzle are subtracted. This gives current values for the chamber-gas mass and stoichiometry, and the axial addition rate of mass. These are used to calculate the pressure, temperature, molecular weight, and velocity distribution in the chamber. The simplifying assumption is made that at any instant the pressure is constant throughout the chamber, and the gas is well mixed.

d. Wall Calculations

When a computed propellant droplet moves radially to the location of the combustion chamber wall, its fuel or oxidizer mass is added to the axial distribution of fuel or oxidizer previously deposited on the chamber wall. The material on the wall experiences axial viscous flow under the influence of shear forces exerted by the chamber gas and is subject to boiloff from heat transferred from the chamber gas.

The boiloff from each axial segment of the wall is calculated from a heat-transfer coefficient, calculated from the Colburn equation corrected for counter-current mass transfer. Both the gas shear stress and heat transfer coefficients are correlated with the Reynolds number based on chamber diameter evaluated at each axial segment of the chamber.

e. Comparison with Experimental Results

The objective of the computer calculations is to predict the amounts and properties of contaminant material formed during the pulse-mode operation of small rocket engines. Since the quantitative experimental data on contaminant production is still rather scanty, the experimental confirmation of the model must be based, in part, on other experimental data, such as chamber pressure traces, which are more generally available. Two recent papers (3 and 4) have been published describing contaminant production from pulse-mode firings of the 22-pound Marquardt R1-E engine, which is very similar in design, but larger than the 5-pound Marquardt R6-C engine used for the parametric analysis at Appendix A. Many aspects of the experimental firings of the R1-E engine agree with the trends calculated for the R6-C engine, for example, see Figure 6.

Two modes of contaminant production were found experimentally (3). Large drops of MMH-Nitrate were blown from the lip of the nozzle, being directed approximately in the radial direction, i. e., at right angles to the engine centerline ± 45 degrees. Much smaller particles of MMH-Nitrate are carried downstream in the plume, being concentrated along the engine centerline, with the particles being directed a maximum of ± 10 degrees from the centerline. These findings are in agreement with the model, which

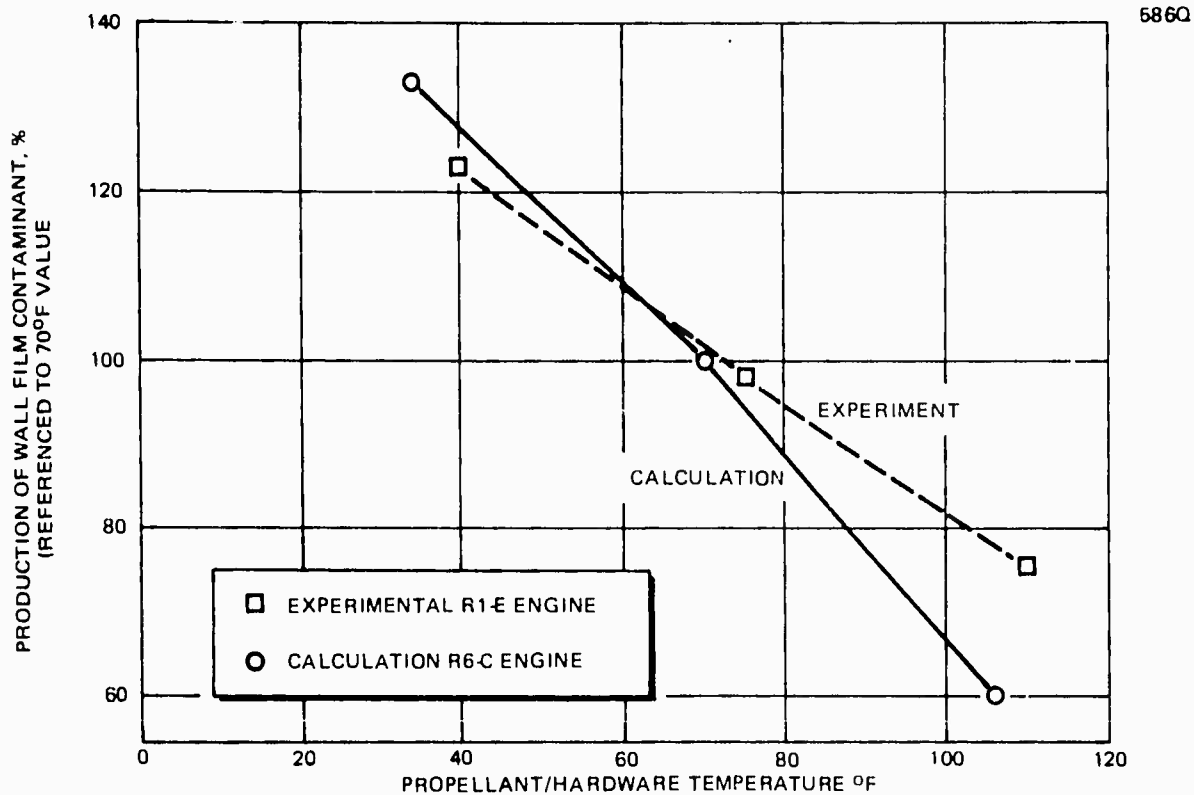


Figure 6. Comparison of Experimental and Calculated Wall-Film Contaminant Production as a Function of Propellant/Hardware Temperature

calculates contaminant production from material which flow down the chamber as wall-film and from propellant droplets which pass through the throat incompletely burned. According to the paper of Stechman and Thonet (4) contaminant production from a series of 17 ms. pulses is strongly dependent upon hardware temperature and upon the down-time between pulses, maximizing at about 80 milliseconds for the R1-E engine at an injector temperature of 60°F. The existence of a maximum is in agreement with the computer model, which calculates that the emptying of the dribble volumes is sequential at low temperatures, with the oxidizer side emptying completely before the fuel side starts to empty because of vapor pressure effects. According to the model calculations, the worst case for contaminant production is a down-time just sufficient to empty the oxidizer dribble volume, but not the fuel dribble volume.

The "worst down time" for the R6-C engine at 70°F is calculated to be 6 milliseconds, while the value for the larger R1-E engine at 60°F was experimentally found to be 80 milliseconds. The difference between the two values is probably a reflection of the steep vapor pressure vs temperature curve for NTO.

Martinkovic (3) found that contaminant production was a function of injector temperature. His measurements for the R1-F engine show fairly good agreement with our calculations for the R6-C engine as shown in Figure 6.

The absolute values for contaminant expelled as wall-film were also of the same order of magnitude. The Martinkovic 22-pound R1-E engine experimentally produced 0.772 milligrams of wall-film per 17 millisecond pulse at 75° F (about 1/1000 of total injected propellant). Our calculations for the 5-pound R6-C engine indicated that 0.161 milligrams of wall-film would be produced per 50-millisecond pulse at 70° F, excluding post-firing dribble (see Appendix A, Parametric Study).

Figure 7 compares a suitably documented experimental chamber pressure trace with a corresponding computed value. The two curves show surprisingly good agreement, especially in the prediction of events.

R202

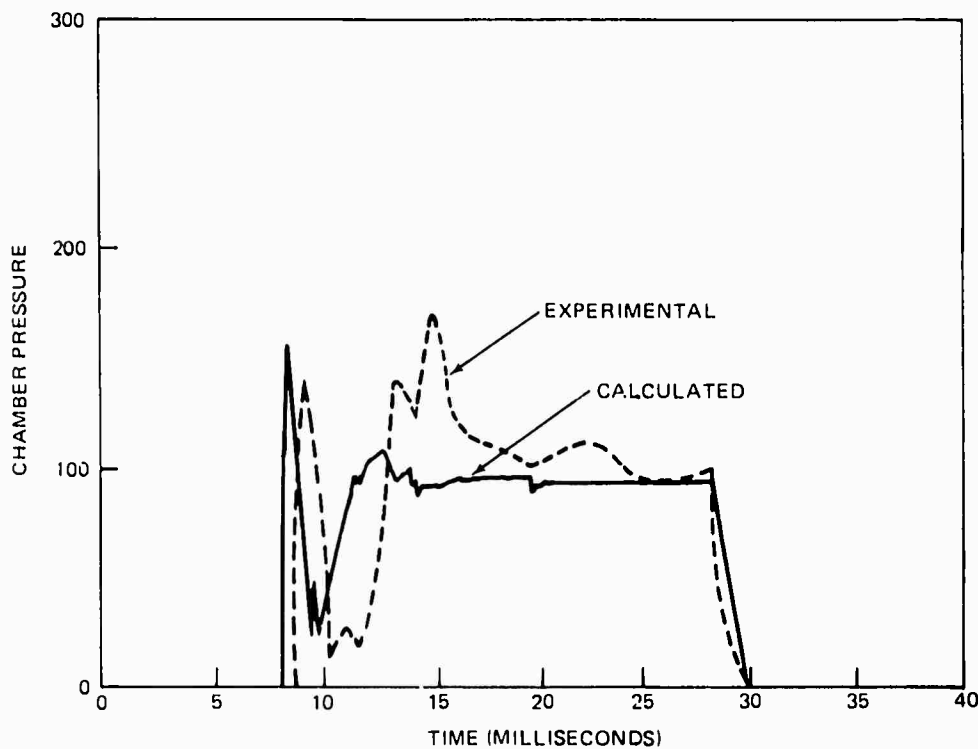


Figure 7. Comparison of Calculated and Experimental High Altitude Start

2. CONTAMINANT TRANSPORT (See Appendix B for further details).

Having defined the average amount of liquid phase contaminant ejected from the combustor for each pulse segment (see subsection III. 1) the two-phase nozzle and plume flow is then computed for transient and steady state pulse segments, using method-of-characteristics computer programs described by Nickerson and Kliegel in (5) and modified by Gabbert and Hoffman (6). In Figure 5, these programs are identified as TD2 and TD2P. Variations in chamber pressure, chamber temperature, droplet velocity, and droplet-size distribution produce considerably different two-phase flow fields for each of the pulse segments (preignition, ignition, steady state, and tail-off) and therefore require a unique analysis for each pulse segment.

Because several contaminant sources originate upstream of the nozzle exit plane (for example, unburned propellant and nonequilibrium condensed fuel nitrate species), it is necessary to obtain a complete characterization of the multiphase flow at the nozzle exit, including droplet/particle distributions (size, velocity, temperature, and species) as well as an axisymmetric distribution of the gas-phase flow. The extreme radial compression of droplet/particle laden regions indicates the need for accurate information concerning the combustor and nozzle transport of condensables as input to the plume analysis.

Starting at the convergent nozzle sections, up to 10 droplet groups are considered as an approximation to the distribution of condensed phase material produced in the combustion chamber. The concentrations, distribution, and trajectories of each droplet/particle group are considered at each mesh point in the axisymmetric method-of-characteristics flow analysis throughout the entire nozzle and plume. Fully coupled momentum exchange (drag) between the gas and droplet/particle phase is considered, including rarefaction effects. The results (output) of this program set provide the initial conditions (input) for the impingement model and subsequently, the surface effects analysis.

While the transport model will provide information about the dynamic condition and flux of species arriving in the vicinity of a functional surface submerged in an exhaust plume, the kinetic/condensation model and the deposition model are required to provide information regarding the chemical composition and amount of plume exhaust material actually deposited on the submerged surface.

3. CHEMICAL KINETICS AND CONDENSATION IN THE NOZZLE AND PLUM FLOW FIELD (See Appendix C for further details)

In addition to unburned propellant droplets, many liquid-bipropellant exhausts contain condensed phases as an important contaminant source. The primary condensables in bipropellant plumes are thought to be H_2O and nitrate salts of the fuel. One of the major study objectives was to review existing data on plume condensables and to model the mechanism of condensation analytically in rocket nozzles and exhaust plumes. A thermodynamic nonequilibrium nucleation and condensation model has been developed and is discussed in detail in Appendix C. The MDAC Streamtube Chemical Kinetics and Condensation Computer Program, identified in Figure 5 as KINCON, has provided the framework for development of this portion of the model. A preliminary study, using the combined chemical kinetics and condensation model, was performed to size condensation characteristics in the nozzle and plume, corresponding to typical engine operating regimes (both transient and steady state). The relative effect of condensation as a contaminant source, relative to combustion chamber sources, is yet to be determined, although it is thought to be an important factor in contamination of surfaces beyond the central core of the plume where heavy, unburned propellant droplets seem to dominate.

The modeling of this phase of the contaminant-production problem requires (1) the chemical kinetic analysis of the expanding exhaust gases and (2) a realistic analysis of the condensation process.

a. Chemical Kinetics Model

The chemical kinetic processes in the nozzle and plume are calculated along streamlines utilizing the MDAC KINCON computer program. The KINCON program possesses several unique features which make it well suited for analyzing the nozzle/plume chemical kinetics. These features include (1) a fully implicit numerical integration scheme that permits the rapid integration of the full set of kinetic equations (up to 40 species and 150 reactions) with complete numerical stability; (2) capability to treat the addition (or subtraction) of mass, momentum, and energy to the streamtube by specifying the specific rate as a function of streamtube distance; (3) reaction-rate screening capability, which identifies reactions and species that are unimportant and need not be considered in the calculation of a specific species concentration or fluid property in any particular application.

Principal assumptions inherent in the use of the streamtube kinetics model include the following: (1) the flow is one-dimensional, steady, and inviscid; (2) each component of the gas mixture is a perfect gas; and (3) internal degrees of freedom of each component are in equilibrium.

b. Condensation Model.

It is well known that condensation of a rapidly expanding supersonic flow does not occur at the point in the flow where the gas equilibrium temperature reaches the saturated vapor temperature of the particular species in question. Instead, condensation is delayed and eventually occurs as a "condensation shock" or condensation zone downstream of the equilibrium condensation point. Although this phenomenon is not thoroughly understood, it may be caused by a number of factors, including (1) lack of nuclear material on which condensables may form and (2) inability of the surrounding gas phase to readily remove heat from the condensing material.

To treat condensation effects in rapidly expanding gases, a kinetic model of the condensation process utilizing the classical liquid drop theory was adopted. The condensation phenomenon, as described by this model, occurs as a result of two distinct processes: (1) nucleation and (2) droplet growth.

As saturated vapor conditions are reached in a rapid expansion, sufficient surface area will not usually exist for the condensation required to maintain equilibrium ($P_v = P_{vs}$), and a supersaturated condition results ($P_v > P_{vs}$). The nucleation process (spontaneous self-nucleation) occurs in the expanding supersaturated vapor and involves the clustering of vapor molecules to give rise to very small nuclei (radius of 10 to 100 Å). Only nuclei reaching the critical drop radius r^* can exist and grow. The critical drop size is determined from thermodynamic equilibrium considerations and represents the size at which the drop has an equal probability of either evaporating or growing.

Figure 8 illustrates the effects of condensation on the flow static pressure and temperature. Following the saturation point, the vapor continues to expand along the frozen gas isentrope until a suitable number of nuclei are formed and the droplet growth process begins. At this point, the effects of condensation are observed. Both the static pressure and temperature increase rapidly with the temperature approaching the saturated-vapor temperature. The expansion then continues along a different isentrope corresponding to a new gas mixture.

4. DEPOSITION, ABRASION, AND SURFACE EFFECTS (See Appendix D for further details)

A simplified analytical model for the prediction of plume contaminant deposition, surface abrasion due to liquid and solid particle impingement, and changes in thermal and optical surface properties due to deposition or abrasion has been completed. Additional work is required to couple the resulting computer program, SURFACE (See Figure 5), to the total contamination prediction analysis and to extend the model to a general class of contaminants and surfaces. A brief outline of the model will be given.

Development of a surface effects model depends heavily upon experimental data relating plume species deposition and mechanical abrasion characteristics to changes in α and ϵ , in the case of thermal surfaces; and changes in transmissivity and reflectivity, in the case of optical surfaces. Such data are scarce for realistic plume-deposition products, such as MMH-Nitrate, although recent experiments have provided some data.

The first step in developing a model to predict surface property changes, based on a computed amount of abrasion or deposition, is to examine the possible interactions of plume material with spacecraft surfaces. The preliminary model developed accounts for plume-induced changes in α and ϵ on thermal control surfaces, such as heat-rejection radiators. This model will be extended to include optical surfaces in future studies.

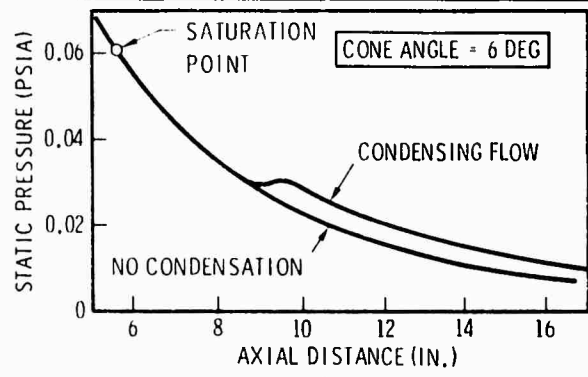
Figure 9 is a sketch of the possible interactions with both coated and uncoated portions of a radiator surface.

a. Solar Absorptivity

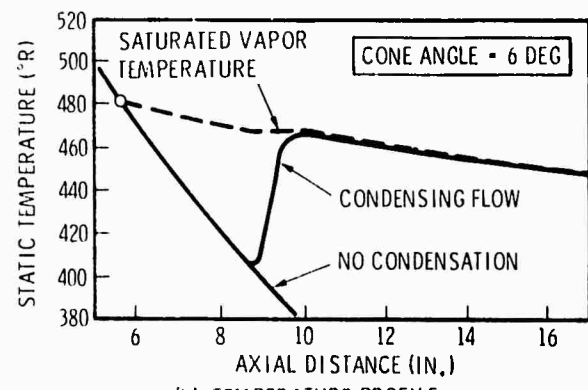
The absorptivity of the system is primarily determined by the characteristics of the external surface upon which the external radiation falls. The average or net absorptivity α_{net} of the radiator can be taken as the mean of the absorptivity of each type of absorptive surface α_i times the area of each type A_i . Generally, α_i is a simple term, easily determined or calculated, but in some instances, such as a transparent deposit, terms related to the thickness and internal parameters of the deposit become important.

b. Hemispherical Emissivity

When contaminant deposits are thin, it is assumed that they offer little resistance to heat flux through the layer. The emissivity of the surface is assumed to be that of the contaminant layer. For thick layers of deposits, the impedance to heat flow through the layer is also modeled.



(a) PRESSURE PROFILE



(b) TEMPERATURE PROFILE

Figure 8. Static Pressure and Temperature Profiles for Condensing Nozzle Flow (Sample Case 1:90% H₂O, 10% N₂ Mixture, P₀ = 1.25 Psia, T₀ = 1,300°R, Cone Angle = 6 Deg)

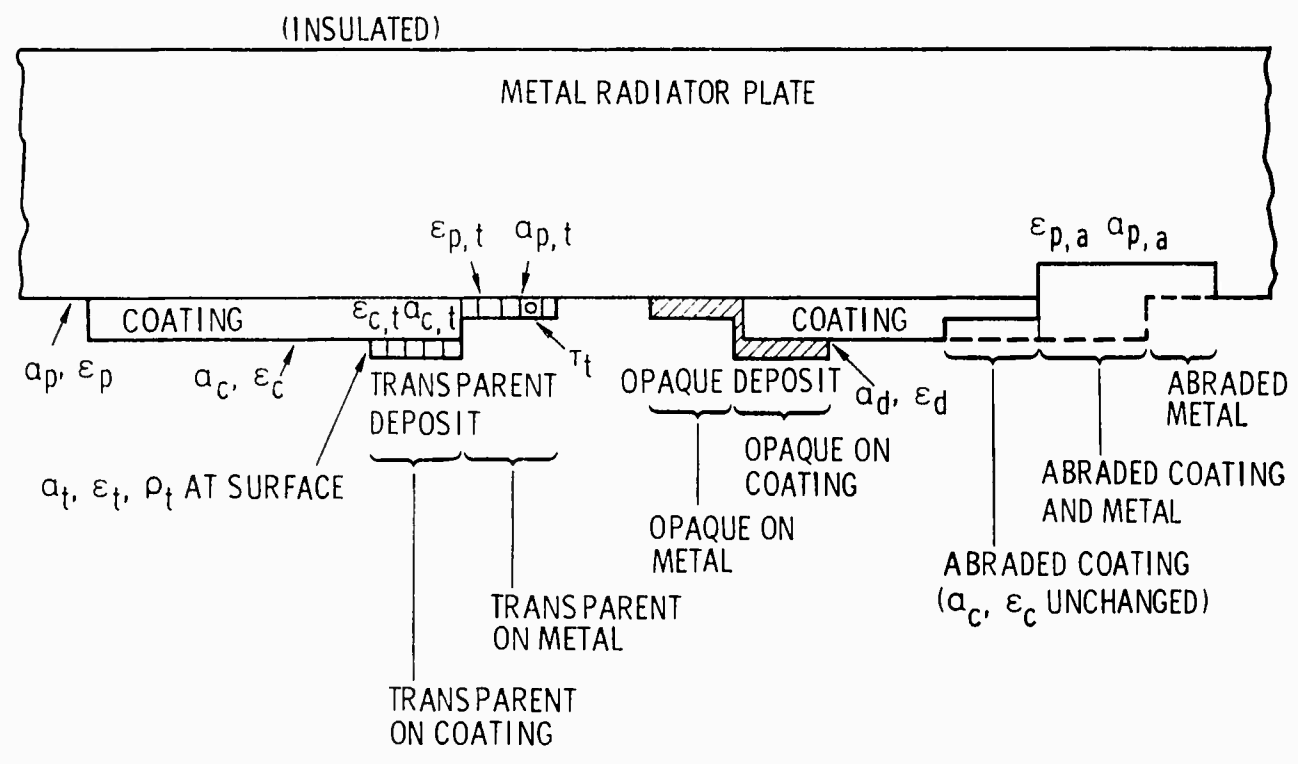


Figure 9. Contaminant Effects Physical Model-Heat Rejection Radiators

c. Surface Abrasion

Abrasion can occur on either or both of the coated or uncoated portions of the radiator surface. Abrasion of the radiator coating affects the heat flux in a step-function fashion. If only the thermal-control coating is abraded, the effect is simply that of decreasing the original coating thickness without affecting the absorptivity or the emissivity. If the abrasion proceeds far enough, it will penetrate through the coating and expose an area of the metal plate substrate. The abrasion of the metal surface, both that originally present and that exposed by removal of the coating, will alter its α_p and ϵ_p significantly. The abraded area of the metal will consist of two parts, the part that was originally bare and now abraded, plus all that was exposed when the coating is abraded away. It is assumed that in any area where the abrasion is sufficient to remove the coating, the flow field will attack the metal at once.

d. Material Deposition

A deposit of material from the plume, randomly located on the exterior of the spacecraft radiator, acts simply like an additional coating through which the heat must be transferred. The deposit may be transparent (crystalline, glassy, or liquid), or it may be opaque due to either its basic nature or to particle sizes.

Opaque deposits affect the heat flux in a manner identical to the thermal-control coating. The situation can become more complex if the deposit forms a transparent film. Such films are not completely transparent at all wavelengths, and therefore a complex interaction occurs.

Radiant energy impinging from the environment is partly reflected, partly absorbed, and partly transmitted into the film at the outer surface in accordance with the usual ρ , α , and τ coefficients. As the energy passes through the thickness of the film, more of it is absorbed. At the bottom surface with the opaque paint or metal, the energy is either absorbed or reflected. That portion of the radiation that is reflected from the substrate then passes outward through the film, and again, part is absorbed. When the energy again reaches the outer surface, the part that strikes the surface at less than the critical angle is radiated away; but the portion that strikes the surface at an angle equal to, or greater than, the critical angle cannot escape and is eventually absorbed. A similar process also occurs for the emission of energy from and through the transparent layer.

SECTION IV
THE CONTAM COMPUTER PROGRAM

1. GENERAL DESCRIPTION

This section describes the integrated computer program, CONTAM, which has been developed to provide an engineering design tool for the prediction of plume contaminant effects on sensitive spacecraft surfaces arising from direct plume impingement. Figure 10 illustrates the component subprograms of the CONTAM program. The CONTAM program is capable of independently running any of the subprograms or of running the entire analysis sequentially and automatically, subject to the restriction below. When run independently, the capabilities of each of the subprograms may be extended to solve problems associated with: combustion dynamics; nozzle and plume multiphase flow field characterization; nonequilibrium streamtube chemical kinetics and condensation; and impingement, deposition, abrasion, and surface property changes—not necessarily associated with plume contamination.

During the study effort, a bipropellant contaminant production model, contaminant transport model, nonequilibrium condensation model, and surface effects model were developed and coded. The surface effects model/development was deemphasized due to funding constraints, and therefore has not been completed to the level of sophistication of the other subprograms. At present, automatic interfacing of the contaminant production subprogram, TCC, with the contaminant transport subprogram, MULTRAN; and the kinetics and condensation subprogram, KINCON, with the surface effects subprogram, SURFACE, has not been provided. Provisions have been made, however, for easily interfacing these subprograms in the future.

Each of the major subprograms of CONTAM are described in detail in separate appendixes as follows:

Appendix A <u>TCC</u>	Transient Combustion Chamber Dynamics Computer Program (a bipropellant contaminant production model)
Appendix B <u>MULTRAN</u>	Multiphase Nozzle and Plume Transport Computer Program (a multiphase nozzle and plume flow field characterization model)
Appendix C <u>KINCON</u>	Nonequilibrium Chemical Kinetics and Condensation Computer Program (a multiphase reacting gas streamtube model)

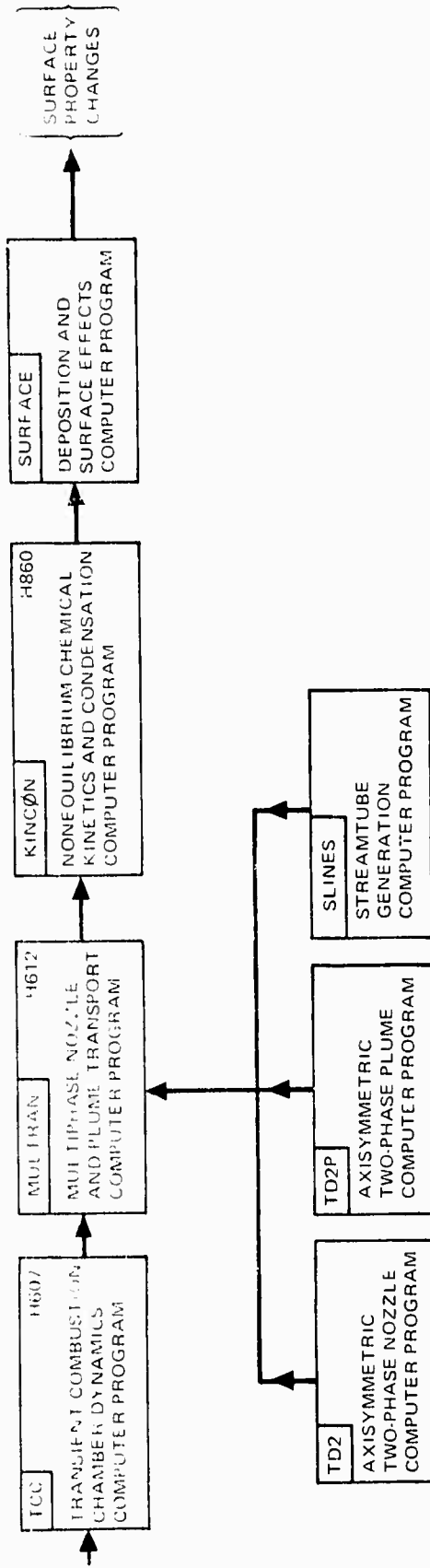


Figure 10. Schematic of the Plume Contamination Effects Prediction Computer Program C0NTAM

Appendix D SURFACE Deposition and Surface Effects Computer Program (a plume impingement, deposition, abrasion, and surface contamination effects model)

This section concentrates on describing the operation of the integrated program CONTAM, and the interfacing of the various subprograms. The reader is referred to the appropriate appendix for detailed information concerning the operation of the individual subprogram.

The CONTAM program is written in FORTRAN IV and requires 220,000⁸ core locations to load and execute in the automatic mode. The program contains 111 subroutines and is currently operational on the CDC 6500 and CDC 6600 computers.

a. Combustion Chamber Contaminant Production

Unburned propellant and intermediate products of combustion (gas and liquid phase) ejected from the combustion chamber are considered first as a source of contaminants. Referring to Figure 11, the Transient Combustion Chamber Dynamics (TCC) subprogram, is used to generate contaminant production data. The results of the TCC subprogram are time dependent and require interface manipulation for subsequent modeling and analyses since the transport model treats the flow as steady state. After examination of the production of contaminants during the entire transient pulse, representative "time slices" are chosen so that gas and liquid properties may be averaged over the time intervals for use as input to the MULTRAN subprogram. The required output from TCC includes: chamber pressure, chamber temperature, droplet size distribution, droplet velocity, and mass flux of gas and droplets.

b. Contaminant Transport

Having defined the average amount of gas and liquid phase ejected from the combustor for each pulse segment, the two-phase nozzle and plume flow is then computed for each steady state pulse segment, using method-of-characteristics computer subprogram MULTRAN (subprograms TD2, TD2P, and SLINES are included in MULTRAN).

Computer subprogram SLINES was developed to provide the necessary interface between the TD2, TD2P and the KINCON subprograms. Basically, SLINES interpolates between points on each characteristic line to provide exhaust gas properties for points on a streamline. A streamline is defined as that line which runs through the throat, nozzle, and plume, bounding a given constant percentage of the mass flow between it and the nozzle axis.

c. Chemical Kinetics and Condensation

In addition to unburned propellant droplets, many liquid-bipropellant exhausts contain condensed phase products of combustion as an important contaminant source. The formation of condensables in liquid propellant exhausts has been analytically modeled. The KINCON subprogram predicts

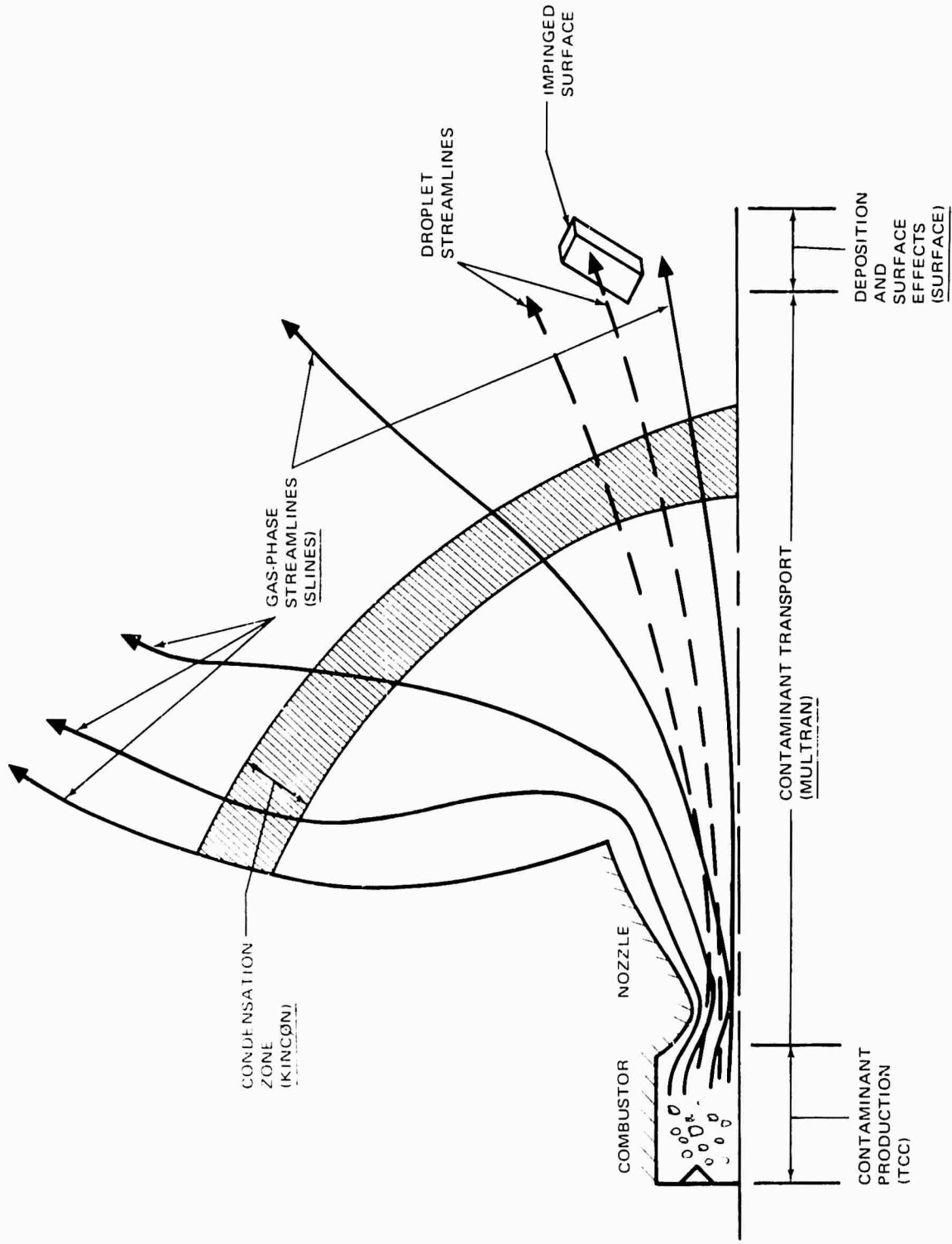


Figure 11. Schematic of Contamination Processes and Related Subprograms

the nozzle and plume condensation effects utilizing a classical nucleation and droplet growth model. It also provides the gas-phase chemical kinetics analysis along streamlines.

d. Deposition and Surface Property Effects

The flux of contaminants approaching a surface submerged in a bipropellant plume, as determined above, provides the starting point for the analysis of liquid and solid deposition on impinged surfaces. A model has been developed to account for the accommodation of momentum and energy upon impact of liquid and solid particles and to predict the amount and state (thin film, thick film, droplets, crystals, etc.) of the deposited materials. Damage and changes in surface properties due to mechanical abrasion and/or deposition are also treated in this subprogram, SURFACE. The surface property changes considered are absorptivity, emissivity, reflectivity, and transmissivity. Development of this subprogram is not complete and, therefore, is discussed only briefly in Appendix D.

2. PROGRAM DESCRIPTION

This section describes the structure and logic of the Plume Contaminant Effects Prediction Computer Program, CONTAM. Particular emphasis is placed on the description of the main program, the overlay structure, and the data interface between the various subprograms. Detailed descriptions of the subprograms may be found in the appropriate appendix.

The CONTAM program is structured so that any one subprogram may be run independently or any number of the subprograms may be run sequentially and automatically. Only the main program and the required subprogram reside in computer core during operation. In the sequential and automatic mode of operation, upon completion of operation by a particular subprogram, that subprogram is removed from the computer core and is replaced by the sequentially required subprogram.

The program runs on the CDC 6500 computer system. It is coded in FORTRAN IV and requires a field length of 220,000g. If TCC is not run on a particular submittal, the field length may be reduced to 135,000g. The conversion of the program to another third generation computer should be straight-forward.

The main program (EXEC) was coded to perform the required selection of the various subprograms. It initializes certain logical control variables, accepts control variables through input, and provides overall logic control for the program. It also provides overlay communication.

3. PROGRAM OVERLAY STRUCTURE

The program overlay structure is depicted in Figure 12. The program contains seven second-level overlays, each corresponding to a particular subprogram. The overlay structure extends to three levels.

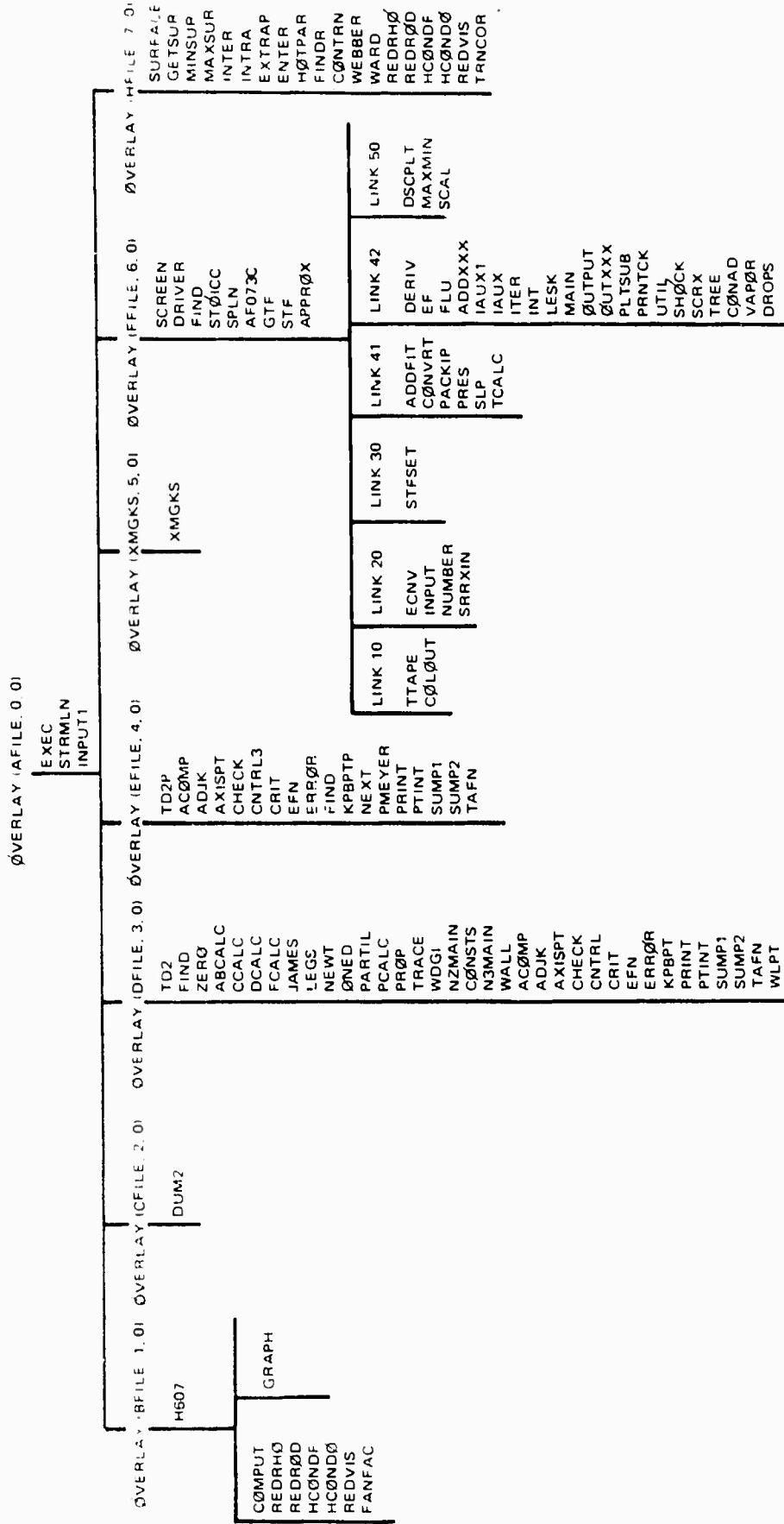


Figure 12. CONTAM Computer Program Overlay Structure

4. PROGRAM DATA INTERFACES

The resultant data from the various subprograms reside on magnetic tape or disc file for use by subsequent subprograms.

The data interface has been designed so that the input and output data to a particular subprogram are preserved subsequent to the running of that subprogram, while at the same time, the number of logical file units used are minimized by reusing logical files. This means that while the user may run each program independently but sequentially, if the data output from a particular subprogram is not acceptable for some reason, the input data file to that subprogram has been preserved so that the user has a "restart" capability without having to restart from the initial subprogram of the sequence.

a. TCC Data

Data output from TCC is written onto logical file 12 for use by the MULTRAN subprogram as input to TD2 subprogram. In addition, logical files 1, 16, and 48 are used internally by TCC. File 1 contains the variable data used by the plotting routine of TCC. Files 16 and 48 are required files for the system plotting package.

b. TD2 Data

The input logical file number for the TD2 program is 10. The TD2 subprogram provides data output on two logical files; 8 and 12. Logical file 8 contains data required to be input to the TD2P subprogram. Logical file 12 provides input data for the SLINES subprogram and the deposition and surface effects subprogram, SURFACE.

c. TD2P Data

Subprogram TD2P receives its input data from logical file 8. TD2P provides output data on logical files 9 and 12. File 9 contains radiation and force field data. File 12 contains the contaminant properties data. The subroutine which writes on file 12 is common to both TD2 and TD2P. It is located in the main overlay level so that it is accessible to both subprogram overlay levels.

d. SLINES Data

The SLINES subprogram reads data from logical file 12 which has been generated by subprograms TD2 and TD2P. It generates the streamline data and writes this data on logical file 8 for use by the KINCON subprogram.

e. KINCON

The KINCON subprogram uses six logical file units. The file unit numbers are 1, 4, 8, 10, 11, and 12. Files 1, 10, and 11 are scratch files used internally by the subprogram. File 1 contains the initial conditions and

area ratio table to be used in the condensation calculation. File 10 contains thermal data, only for the specific species being considered in the run, which has been packed in a data block. File 11 contains reaction tables. Files 4 and 8 are input files. File 4 is an optional input which contains a list of thermal properties in JANAF format. Since logical file 4 is an optional input, if it is not used as such, it will default to an internally used file by the subprogram. If the logical file 4 input is not exercised, the thermal properties data must be input by punched cards (see Appendix C). The subprogram will then write JANAF thermal properties on logical file 4 from the punched card input. Obviously, with the appropriate control cards, file 4 may then be saved for subsequent use. File 8 contains the streamline properties required by the KINCON subprogram. Logical file 12 is the output tape of the subprogram and contains the multiphase and kinetic results to be used by the deposition and surface effects subprogram, SURFACE. Since the surface effects subprogram has not been completely developed and amalgamated, the logical file 12 output from the KINCON subprogram has not been implemented yet.

5. PROGRAM USERS MANUAL

a. Input to CONTAM

Punched card input is required. Logical file 4 input is optional, but the option must be specified in the card input. The discussion pursued in this section pertains only to the sequential automatic mode of operation.

The punched card inputs required are of two types; NAMELISTS and other nonstandard format. Subsection 5.b describes the general nature of the data input through the various NAMELISTS and indicates the subprograms to which they apply. For a detailed description of the contents of the various NAMELISTS, the user should refer to the appropriate Appendix for each subprogram as listed in subsection of this section.

A detailed description of the nonstandard inputs will be found in Appendix C since they apply to the KINCON subprogram. Subsection 5.d describes the required stacking (organization) of the punched cards.

Section 5 presents a sample case which includes a data listing, the resulting output, and a "day file" from the CDC 6500 computer system. The "day file" is included to illustrate the required system control cards and their proper sequence.

In addition to the aforementioned inputs, there are the data interfaces which are required by the various subprograms and discussed in subsection 4 of this section. These interface data should be considered as inputs when running the subprograms independently.

b. Program NAMELISTS

Table I presents a list of the names of each NAMELIST and the subprograms to which they correspond. To determine the details and parameters contained in each NAMELIST, the user should refer to the appropriate Appendix as listed in subsection I of this section. NAMELISTS required by CONTAM (the main program) are described in the subsection 5. c.

Table I. NAMELIST AND SUBPROGRAM

<u>NAMELIST</u> Name	Subprogram
NCASE	CONTAM (EXEC)
IPATH	CONTAM (EXEC)
INPUT1	TCC
DATA	TD2
DATAP	TD2P
SID	SLINES
THERMO	KINCON
PROPEL	KINCON
IMPING	SURFACE

c. CONTAM NAMELISTS

Two NAMELISTS are required by the main program, CONTAM, to provide control of the overall program. They are:

- (1) NAMELIST/NCASE/
- (2) NAMELIST/IPATH/

There is only one parameter in the NAMELIST/NCASE/. It is ICASE. ICASE is an integer variable which tells the program how many pulse segments are to result from the transient pulse output of the TCC subprogram. Each pulse segment is considered a "case." Each subsequent subprogram in the sequence must operate on each pulse segment (case), one segment at a time.

NAMELIST/IPATH/ contains nine variables. However, only two of the variables are required per run (sequential-automatic mode). The variable list for NAMELIST/IPATH is:

- TCC
- SSCP
- TD2
- TD2P
- SLINES
- MGKS
- DUM7
- KMODE
- NSL

Each variable except KMODE and NSL is logical. For example:

$$TCC = T, TD2P = T,$$

The above example indicates that the first subprogram to be run will be TCC and the last will be TD2P. It is only necessary to input the first and last subprograms to be run. If only one subprogram is to be run, only that one variable need be input, unless the KINCON subprogram is to be run; then KMODE and NSL may also be required.

The variable KMODE is used only when the KINCON subprogram is run independently. If used, it is input as the integer variable "one." It indicates that certain options will be exercised in the operation of the KINCON subprogram. These options are described in Appendix C.

The variable NSL is required only when the KINCON subprogram is run independently. NSL indicates the number of streamlines that will be analyzed by the KINCON subprogram. If subprogram SLINES is run in conjunction with the KINCON subprogram, any NSL value input here will be overridden by the value of NSL input for the SLINES subprogram.

d. Nonstandard Format Inputs

All of the nonstandard format punched card inputs are used by the KINCON subprogram. The names of these inputs are:

- Thermodynamic Data (Optional)
- Title Card
- Species Cards
- Reaction Cards

The format for the data on these cards is detailed in Appendix C.

e. Input Card Stack

Figure 13 depicts the organization of the punched card deck required for automatic sequential operation of the entire program. For independent operation of subprogram(s), only the input data required for operation of the desired subprogram(s), in addition to the CONTAM input data, should be included in the data deck. For example: If only subprograms TD2 and TD2P are desired to be run, the data required for TCC, SLINES, and KINCON should be removed from the deck illustrated in Figure 13.

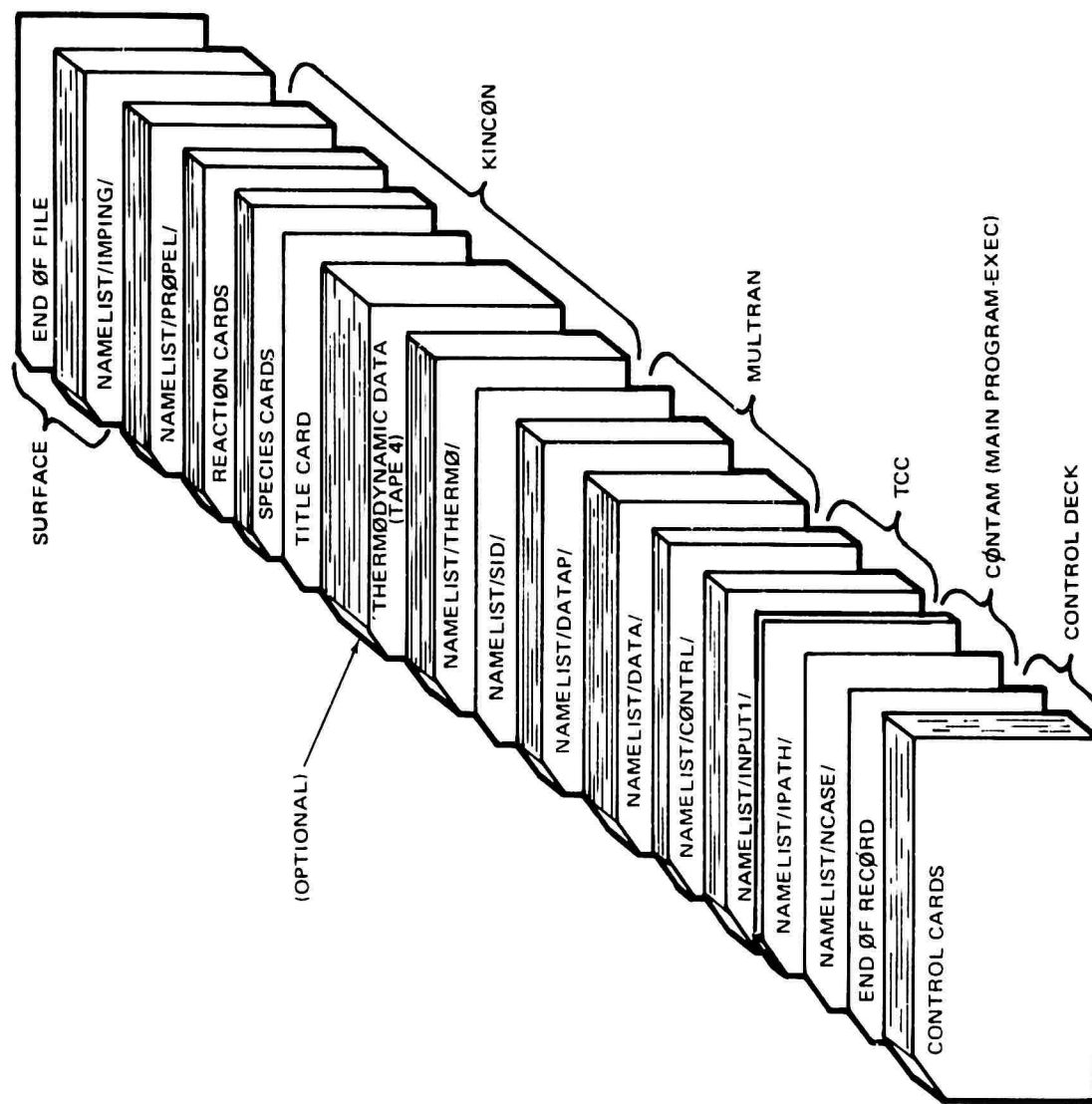


Figure 13. CØNTAM Input Card Stack

SECTION V

SAMPLE CASE

This section presents a data listing and printed output for a sample case run in the automatic sequential mode on the CDC 6500 computer system.

1. DEFINITION OF SAMPLE CASE

The sample case is chosen to illustrate the application of the successive subprograms of CONTAM for the prediction of the contamination effects resulting from a typical firing of a real rocket engine. The engine chosen for these computations is the Marquardt R-6C. The R-6C is a commercially available NTO-MMH rocket engine having a nominal thrust of five pounds and designed for pulse-mode operation. It is an excellent choice for experimental vacuum-chamber studies of contaminant production because of its small size, which makes it easier to maintain vacuum in the test chamber, and its short pulse capability which can be used to aggravate the production of contaminants. The effect of the small engine size, however, must be considered in designing the experiment. The R-6C is being used in an experimental contaminant effects study currently underway at NASA Lewis Research Center under the direction of Dr. Herman Mark. It is hoped that the computed values for contaminant production, transport, deposition, and surface effects can be experimentally verified by comparison with experiments such as those being run at NASA Lewis Research Center.

A pulse width of 50 milliseconds was chosen for our computations. This is short enough to show appreciable transient effects without being so short as to be unrealistic compared to actual duty cycles used with an engine of this type. In our calculations, the engine is fired with its walls initially clean and with its dribble volumes both initially empty, but with the lines full of propellant behind the valves. This initial condition would be easier to match experimentally than any prescribed axial accumulation of fuel and oxidizer on the wall or partially filled dribble volumes. The chamber, injector, and tankage were initially set to room temperature values, again for ease of experimental comparison. The line lengths, line diameters, tank pressures, and other installation and operational variables were chosen to agree with the NASA Lewis vacuum chamber installation, and the base case run parameters.

2. CONTAMINANT PRODUCTION - THE TCC PROGRAM

The TCC (transient combustion chamber) program calculates contaminant production by digital integration of the time-dependent engine processes, i. e., propellant flow, atomization, and combustion of the injected droplets. The calculated two-dimensional trajectories for the burning droplets determine how much propellant is deposited on the wall, and how much

passes through the throat unburned. The trajectories for the ejected unburned droplets are calculated up to the throat by the TCC subprogram, and in the nozzle and plume by the MULTRAN subprogram. The unburned propellant which is deposited on the combustion chamber wall is subjected to burnoff and axial flow from the action of the hot, fast-moving chamber gases. The amount of this wall film material which survives and passes through the throat is calculated by the TCC subprogram. Experimental firings of small pulsing engines show that much of this material accumulates on the nozzle lip during each firing, and is blown off during the succeeding start transient. The droplet size, initial direction of flight, and subsequent trajectory of this material may be defined statistically from experimental firings, but is outside of the present scope of the CONTAM program.

a. TCC Input-Sample Case (R-6C Engine)

Input data for the TCC program is broken down into several large blocks of related data. The block headings are: Chamber description, operating conditions, valve timing, ignition description, fuel feed system, oxidizer feed system, atomization parameters, fuel properties, oxidizer properties, combustion gas properties, contaminant properties, general instructions, flow rate overrides, and a thrust coefficient table. Obviously the values typifying each propellant constituent remain fixed for that constituent; consequently, the sub-decks of data for any given material such as UDMH or MMH or NTO can be retained for reuse whenever that particular propellant is to be used. In a similar way, the combustion gas properties remain constant for each particular propellant combination, such as WFNA and UDMH or LOX and RP-1. Again these sub-decks may be retained and reused whenever that particular propellant combination is called for. Having sub-decks on hand for the common propellants and propellant combinations greatly facilitates loading the input for the TCC subprogram. The engine hardware is described in the chamber description, fuel feed system, and oxidizer feed system sub-decks. When sub-decks are created for particular engines they may be incorporated into the input data with only such modifications as are required for feed system variables; i. e., line lengths and diameters, restrictor areas, etc. Again, retaining such data sub-decks for reuse greatly facilitates the loading of the program input.

(1) Origin of Engine and Propellant Data

The known physical properties of nitrogen tetroxide and monomethylhydrazine were taken from the Battelle "Liquid Propellant Handbook" (7) and the Aerojet publication "Performance and Properties of Liquid Propellants" (8). The burning-rate coefficient for monomethyl hydrazine was estimated to be halfway between the experimental values given for hydrazine and UDMH by Dykema and Greene (9). The burning-rate coefficient for NTO was calculated using Godsaves' equation. The equilibrium combustion gas properties of chamber temperature, mean molecular weight, gamma, and vacuum thrust coefficient for an expansion area ratio of 40 were calculated, using the MDAC thermochemistry program H099 and the JANNAF (10) values for heats of formation. The chamber dimensions, injector parameters, and valve ramp durations come from the manufacturer, while the feed system values were supplied by NASA Lewis Research Center.

The ignition parameters, activation energy, and frequency factor multiplied by heat of reaction are the experimental values measured for NTO and UDMH by Seamans, Vanpee, and Agosta (11). The fuel and oxidizer fan lengths are unknown and were set equal to zero. These values could be inferred by operating the engine at low tank pressures to obtain the chugging frequency and amplitude. The flash cone angle was taken from photographs of flashing streams in the thesis of Brown. The drop size distribution is from NACA TN 4222. The decomposition temperature for the MMH nitrate was taken from the paper of Perlee, Christos, Miron, and James (12). The values used for the density, vapor specific heat, latent heat and viscosity of the MMH nitrate and its solutions, and the accommodation coefficients for MMH and NTO are estimated values since no experimental values have ever been published. At the time that the first calculations were performed for the Marquardt R-6C engine, the calculated combustion efficiencies and calculated steady state chamber pressure were considerably lower than the experimental values. We felt that this might indicate that the correlations we were using for initial droplet diameter were in error when applied to the very small injector orifices of the Marquardt engine. In order to achieve agreement with experiment, we arbitrarily reduced the computational droplet diameter by a factor of two. This was done by entering one half the actual injector hole diameters in the input data. The actual fuel and oxidizer hole diameters are 0.0158 and 0.0186 inches, while 0.0079 and 0.0093 are the values used in the input data. Since this time, Rocketdyne has published droplet sizes obtained from small orifices (13). Below a threshold value for Reynolds number, laminar flow is obtained in long injector orifices, and the droplet sizes produced are about one-half the size predicted by the usual correlations for jets in turbulent flow. The orifices of the R-6C engine operate very close to the threshold value for Reynolds number quoted by Rocketdyne, therefore it is quite likely that they are in laminar flow and are actually producing droplets similar in size to those calculated using our biased orifice diameters.

(2) Input Data for TCC Subprogram (Marquardt R-6C Engine)

Input data for the Marquardt R-6C Engine are listed in Table II.

Table II. INPUT DATA FOR MARQUARDT R-6C ENGINE TCC

Item Number	Variable	Value	Comments/Source
1	Chamber length	1.07 in.	Manufacturer
2	Injector end area (A)	0.1368 in. ²	Manufacturer
3	Linear taper of chamber (B)	0.1427 in. ² /in.	Chamber area fitted by a parabola: Area = A + BX + CX ²
4	Parabolic taper of chamber (C)	-0.2268 in. ² /in. ²	
5	Throat area	0.0298 in. ²	Manufacturer
9	External pressure	1 x 10 ⁻⁶ psia	Estimated vacuum environment
10	Chamber wall temperature	294°K	Approximately room temperature
13	Fuel tank pressure	180 psia	NASA Lewis
14	Fuel Tank temperature	294°K	Approximately room temperature
15	Fuel injector temperature	294°K	Approximately room temperature
18	Fuel valve opening ramp duration	0.001 sec	Manufacturer
20	Fuel valve closing ramp duration	0.001 sec	Manufacturer
21	Oxidizer tank pressure	165 psia	NASA Lewis
22	Oxidizer tank temperature	294°K	Approximately room temperature
23	Oxidizer injector temperature	294°K	Approximately room temperature
26	Oxidizer valve opening ramp duration	0.001 sec	Manufacturer

Table II. INPUT DATA FOR MARQUARDT R-6C ENGINE TCC
(Continued)

Item Number	Variable	Value	Comments/Source
28	Oxidizer valve closing ramp duration	0.001 sec	Manufacturer
29	Fuel valve opening time	0.0 sec	Time of first motion opening
30	Oxidizer valve opening time	0.0 sec	Time of first motion opening
31	Fuel valve closing time	0.050 sec	Time of first motion closing
32	Oxidizer valve closing time	0.050 sec	Time of first motion closing
33	Assigned ignition delay	0.0 sec	Not used when chemical kinetic values are specified
34	Igniter port location	0.0 in. from injector	No igniter used
35	Igniter fuel flow rate	0.0 lb/sec	No igniter used
36	Igniter oxidizer flow rate	0.0 lb/sec	No igniter used
37	Activation energy	5200 cal/mole	Seamans, Vanpee, and Agosta
38	Frequency factor x heat of reaction	3.4×10^{14} (cc/mole sec) x (cal/mole)	Seamans, Vanpee, and Agosta
39	Perfect mixing flag	0.0	Use normal ignition calculations
40	No axial mixing flag	0.0	Use normal ignition calculations
41	Fuel line length	480 in.	NASA Lewis Research Center

Table II. INPUT DATA FOR MARQUARDT R-6C ENGINE TCC
(Continued)

Item Number	Variable	Value	Comments/Source
42	Fuel line area	0.0281 in. ²	NASA Lewis Research Center
43	Fuel restrictor area	0.00454 in. ²	NASA Lewis Research Center
44	Fuel venturi area	0.0281 in. ²	No venturi, use line area
45	Fuel valve port area	0.0281 in. ²	No valve restriction when open
46	Fuel injection area	0.000196 in. ²	Manufacturer
49	Fuel hole diameter	0.0079 in.	One half true diameter of 0.0158 in. to bias droplet size
50	Fuel hole length	0.0625 in.	Estimated from engine drawing
51	Axial location of fuel hole	0.0 in.	Approximately flush with injector face
52	Radial location of fuel hole	0.045 in.	Estimated from engine drawing
53	Fuel injection angle	-45 deg	Manufacturer
57	Fuel initial void volume	0.00113 in. ³	Set equal to dribble volume for initially empty condition
59	Fuel transition volume	0.0 in. ³	No hot fuel in injector
60	Fuel dribble volume	0.00113 in. ³	Manufacturer
61	Fuel check valve flag	0.0	Reverse flow in feed system is possible
65	Oxidizer line length	480 in.	NASA Lewis Research Center

Table II. INPUT DATA FOR MARQUARDT R-6C ENGINE TCC
(Continued)

Item Number	Variable	Value	Comments/Source
66	Oxidizer line area	0.0281 in. ²	NASA Lewis Research Center
67	Oxidizer restrictor area	0.00636 in. ²	NASA Lewis Research Center
68	Oxidizer venturi area	0.0281 in. ²	No venturi, use line area
69	Oxidizer valve port area	0.0281 in. ²	No valve restriction when open
70	Oxidizer injection area	0.000272 in. ²	Manufacturer
73	Oxidizer hole diameter	0.0093 in.	One-half true diameter of 0.0186 in. to bias droplet size
74	Oxidizer hole length	0.0625 in.	Estimated from engine drawing
75	Axial location of oxidizer hole	0.0 in.	Approximately flush with injector face
76	Radial location of oxidizer hole	-0.045 in.	Estimated from engine drawing
77	Oxidizer injection angle	45 deg	Manufacturer
81	Oxidizer initial void volume	0.000580 in. ³	Set equal to dribble volume for initially empty condition
83	Oxidizer transition volume	0.0 in. ³	No hot oxidizer in injector
84	Oxidizer dribble volume	0.000580 in. ³	Manufacturer
85	Oxidizer check valve flag	0.0	Reverse flow in oxidizer feed system is possible
89	Fuel fan length	0.0 in.	Strawman value, no data available

Table II. INPUT DATA FOR MARQUARDT R-6C ENGINE TCC
(Continued)

Item Number	Variable	Value	Comments/Source
90	Oxidizer fan length	0.0 in.	Strawman value, no data available
91	Single stream break-up distance given in stream diameters	10	Estimated from photographs of single-stream breakup. See NACA TN3835
93	Hold at triple point flag	0.0	Assume flashing propellant equilibrates with chamber pressure even though freezing occurs
94	No initial dribble flag	1.0	The quill-type Marquardt injector is not likely to dribble during start before the dribble volume fills completely
95	Flash cone angle	30 deg	Apex angle of flashing liquid spray taken from photographs of R. Brown
97-101	Drop size distribution table	0.198, 0.759, 1.0, 1.23, 2.3045	Taken from experimental values of NACA TN 4222
102	No wall breakup flag	0.0	Droplets and streams are assumed to atomize on wall impact
103	Drop rebound velocity ratio	1.0	Droplets which bounce off wall are assumed perfectly elastic
104	Fraction sticking	0.5	One-half the droplets impacting with the wall are assumed to bounce and the remainder stick. This is a "straw man" value. No data available

Table II. INPUT DATA FOR MARQUARDT R-6C ENGINE TCC
(Continued)

Item Number	Variable	Value	Comments/Source
105	No fuel flash flag	0.0	The fuel stream is permitted to flash atomize when the correlations indicate that it should
106	No oxidizer flash flag	0.0	The oxidizer stream is permitted to flash atomize when the correlations indicate that it should
107	No wall flow flag	0.0	The material on the wall is allowed to flow as the calculations say it should
108	No wall burnoff flag	0.0	The material on the wall is allowed to burn off as the calculations say it should
109	Fuel normal boiling point	360 °K	Aerojet compilation
110	Fuel freezing point	222 °K	Aerojet compilation
111	Fuel critical temperature	594 °K	Aerojet compilation
112	Fuel critical pressure	1195 psia	Aerojet compilation
113	Fuel vapor specific heat at film temperature	0.995 cal/gram °K	Value for propylene specific heat at 1500 °K extrapolated from NBS C461. Structure similar to MMH. No data for MMH
114	Fuel liquid specific heat at 300 °K	0.69 cal/gram °K	Aerojet compilation
116	Fuel vapor molecular weight	46.074 grams/gram mole	Aerojet compilation

Table II. INPUT DATA FOR MARQUARDT R-6C ENGINE TCC
(Continued)

Item Number	Variable	Value	Comments/Source
117	Fuel latent heat of vaporization (at normal boiling point)	210 cal/gram	Aerojet compilation
118	Fuel latent heat of fusion	67.5 cal/gram	Battelle handbook
119	Fuel liquid thermal conductivity	0.000545 cal/cm °K	Aerojet compilation
120	Fuel accommodation coefficient	1.0	Strawman value, no data available
121	Reference temperature for fuel properties	300 °K	Experimental values available at this temperature
122	Fuel density at reference temperature	0.88 gram/cc	Aerojet compilation
123	Fuel viscosity at reference temperature	0.0104 poise	Aerojet compilation
124	Fuel surface tension at reference temperature	47 dynes/cm	Battelle handbook
125	Fuel burning rate coefficient	0.0325 cm ² /sec	Dykema and Greene
126	Fuel monopropellant intercept (A)	0.0 cm/sec	Strand burning tests fitted $r = A + B P_c^n$ with r in cm/sec; P_c in psia
127	Fuel monopropellant coefficient (B)	0.0 cm/sec psi ⁿ	MMH does not burn in liquid strand tests
128	Fuel monopropellant exponent (n)	0.0	
129	Oxidizer normal boiling point	294 °K	Aerojet compilation

Table II. INPUT DATA FOR MARQUARDT R-6C ENGINE TCC
(Continued)

Item Number	Variable	Value	Comments/Source
130	Oxidizer freezing point	262 °K	Aerojet compilation
131	Oxidizer critical temperature	431 °K	Aerojet compilation
132	Oxidizer critical pressure	1,470 psia	Aerojet compilation
133	Oxidizer vapor specific heat at film temperature	0.298 cal/gram °K	JANNAF tables for NO ₂
134	Oxidizer liquid specific heat at 300 °K	0.36 cal/gram °K	Aerojet compilation
136	Oxidizer vapor molecular weight	46.008 gram/gram-mole	Vapor mostly NO ₂ at high temperature or low pressure
137	Oxidizer latent heat of vaporization (at normal boiling point)	99.0 cal/gram	Aerojet compilation
138	Oxidizer latent heat of fusion	39.2 cal/gram	Battelle handbook
139	Oxidizer liquid thermal conductivity	0.000306 cal/cm °K	Aerojet compilation
140	Oxidizer accommodation coefficient	1.0	Strawman value, no data available
141	Reference temperature for oxidizer properties	300 °K	Experimental values available at this temperature
142	Oxidizer density at reference temperature	1.45 gram/cc	Aerojet compilation
143	Oxidizer viscosity	0.00446 poise	Aerojet compilation

Table II. INPUT DATA FOR MARQUARDT R-6C ENGINE TCC
(Continued)

Item Number	Variable	Value	Comments/Source
144	Oxidizer surface tension	28 dyne/cm	Battelle handbook
145	Oxidizer burning rate coefficient	0.027 cm ² /sec	Calculated from Godsaves equation
146	Oxidizer mono-propellant intercept (A)	0.0 cm/sec	Strand burning rate fitted to: $r = A + B p_c^n$ with r in cm/sec and P_c in psia
147	Oxidizer mono-propellant coefficient (B)	0.0 cm/sec psia	NTO does not burn in liquid strand tests
148	Oxidizer mono-propellant exponent (n)	0.0	NTO does not burn in liquid strand tests
149-159	Equilibrium combustion gas temperature at fuel fractions 0.0, 0.1, 0.2, ... 1.0	300, 2, 103, 3, 084, 3, 397, 3, 061, 2, 368, 1, 705, 1, 433, 1, 344, 1, 266, 1, 190, in °K	From standard equilibrium thermochemistry calculations
161-171	Equilibrium combustion gas mean molecular weight at fuel fractions 0.0, 0.1, 0.2, ... 1.0	46.008, 28.79, 26.41, 23.39, 19.88, 16.75, 14.41, 13.91, 14.00, 14.10, 14.29	From standard equilibrium thermochemistry calculations
173-183	Equilibrium combustion gas gamma at fuel fractions 0.0, 0.1, 0.2, ... 1.0	1.120, 1.252, 1.220, 1.217, 1.235, 1.268, 1.309, 1.299, 1.270, 1.247, 1.228	From standard equilibrium thermochemistry calculations
185	Contaminant mixture density	1 gram/cc	Strawman value, no experimental data
186	Contaminant vapor specific heat	1 cal/gram °K	Strawman value, no experimental data

Table II. INPUT DATA FOR MARQUARDT R-6C ENGINE TCC
(Continued)

Item Number	Variable	Value	Comments/Source
187	Contaminant latent heat of vaporization	100 cal/gram	Strawman value, no experimental data
188	Contaminant decomposition temperature	500°K	Perlee, Christos, Miron, and James
189-199	Contaminant mixture viscosity at fuel fractions 0.0, 0.1, 0.2 - 1.0	0.00446, 0.024, 0.043, 0.068, 0.081, 0.100, 0.082, 0.064, 0.046, 0.029, 0.0104 poise	Experimental values for pure fuel and pure oxidizer. Strawman values for MMH nitrate mixtures
201	Model time at which computations are finished	0.060 sec	50 millisecc for pulse and 10 millisecc to drain oxidizer dribble volume
202	Integrating time interval	0.0001 sec	Chosen from experience running the program
203	Print one out of	10	A propellant disposition summary is printed for every tenth time interval
204	Plot one out of	30	A wall-film thickness profile is plotted for every thirtieth time interval
205	Delete graphics flag	0.0	The computer graphics will be produced
206	Delete droplet means flag	0.0	The D ₃₀ , D ₃₁ and D ₃₂ will be calculated for the chamber droplet population at each time interval
207	Delete summaries flag	0.0	The summaries will be printed for the intervals: preignition, start transient, steady-state, and tailoff

Table II. INPUT DATA FOR MARQUARDT R-6C ENGINE TCC
(Continued)

Item Number	Variable	Value	Comments/Source
208	Data review only flag	0.0	The program will compute the chamber processes instead of stopping after printing out the input data set for examination
209	Fuel trajectory group	3.0	A trajectory will be plotted for the third fuel size group
210	Oxidizer trajectory group	0.0	Only one droplet can be plotted per run. Either fuel or oxygen depending upon whether 209 or 210 is given a non-zero value (1, 2, 3, 4 or 5)
211	Trajectory start time	0.006/sec	The fuel droplet trajectory will be plotted for the fuel droplet injected when the model time is 6 milliseconds
212	Steady-state time	0.0125	The interval summary of item number 207 will be written assuming that steady-state conditions are attained 12.5 millisecond after start. This is based upon previous experience with this motor
213	Fuel flow-rate override	0.0 lb/sec	If the restrictor or valve port area are not known, but experimental flow rate vs. Δp curves are available, the line resistances are calculated from a consistent set of values for flow rate, Δp and injector orifice discharge coefficient. A non-zero value for discharge coefficient signals the program that this signal is being used

Table II. INPUT DATA FOR MARQUARDT R-6C ENGINE TCC
(Continued)

Item Number	Variable	Value	Comments/Source
214	Fuel pressure override drop	0.0 psi	This option is not being used
215	Fuel discharge coefficient	0.0	This signals the program that this option is not being used
216	No injector friction flag	1.0	No frictional pressure drop through the injector ports will be calculated because the correlation is for turbulent flow and these ports are in laminar flow. Set this flag 0.0 for large holes, 1.0 for small holes. If undecided, use 1.0
217	Oxidizer flow rate override	0.0 lb/sec	Oxidizer flow override not being used
218	Oxidizer pressure override drop	0.0 psi	Oxidizer flow override not being used
219	Oxidizer discharge coefficient	0.0	This signals program that oxidizer flow override is not being used
221-231	Vacuum thrust coefficients for the correct nozzle expansion area ratio of the motor, and fuel fractions of 0.0, 0.1, 0.2, ... 1.0	1.9240, 1.8028, 1.9082, 1.9617, 1.8470, 1.8122, 1.8680, 1.9331, 1.9294, 1.9224, 1.8959	These values were obtained from thermochemical calculations assuming equilibrium expansion. Values could be used from kinetics calculations or from steady-state experiments if they were available

Table II. INPUT DATA FOR MARQUARDT R-6C ENGINE TCC
(Continued)

Item Number	Variable	Value	Comments/Source
232	Nozzle expansion area ratio	+0	Manufacturer
233	Second-pulse, fuel-valve opening time	0.0 sec	No second-pulse calculations
234	Second-pulse, oxidizer-valve opening time	0.0 sec	No second-pulse calculations
235	Second-pulse, fuel valve closing time	0.0 sec	No second-pulse calculations
236	Second-pulse, oxidizer-valve closing time	0.0 sec	No second-pulse calculations
237-264	Valve timing for 3rd, 4th, 5th, 6th, 7th, 8th, and 9th pulses		Not being used

b. TCC Output-Sample Case (R-6C Engine)

The computer output is in the form of printout and computer graphics done on a Stromberg SD-4060 microfilm recorder operating in a SD-4020 emulation mode. Many of the output values are presented both in the form of printout and in the form of plots of variables versus time. It is generally easier to use the plots to follow the course of events in the chamber, but it is easier to use the printout to obtain exact numerical values, exact timing relationships, etc.

The computer printout includes a recapitulation of the input values and the derived fuel and oxidizer properties versus temperature, followed by the values of the major-system variables computed at each computing time interval. At each tenth-time interval, there is a summary print which gives the disposition of the total mass of each propellant constituent injected up till that time, i. e., how much has been ejected in the gas phase, as droplets, or as wall film and how much is being retained as gas, as droplets, or as wall film. Summary prints are also produced for the four major intervals of engine operation, i. e., the preignition interval, the start transient, the steady-state portion, and the tailoff including the post-firing dribble. These interval summaries also give mean values for ejected droplet diameter and axial velocity.

A more detailed summary is given at the end of the computation period, including mean values for the entire pulse. In the final summary, entire pulse values are also given for mixture ratio, C-Star, and specific impulse for three possible mass bases: propellant mass out of the tank, propellant mass through the injector, and propellant mass through the nozzle. The final summary also gives the propellant droplet size distribution for injected and ejected fuel and oxidizer.

(1) Computer Printout

The sequence of events in the chamber can be followed from the printout shown in Table III. The first action which can be detected in the time-interval printout is the increase in flow rates for the fuel and oxidizer after the valves start to open at time = 0. As time progresses, the fuel and oxidizer void volumes decrease (i. e., the dribble volumes fill up), but no propellant is injected into the chamber until the fuel dribble volume fills completely at time = 4.2 milliseconds. The first portion of injected fuel flashes, pressurizing the combustion chamber to 0.21 psia and producing some flash-atomized 55-micron fuel droplets. The oxidizer dribble volume fills in the succeeding time interval, flashing and increasing the chamber pressure to 0.90 psia. This is high enough to prevent any further flashing of the fuel, which now goes into a single-stream breakup mode, with a computed eventual drop size of 395 microns (unless wall impact occurs first). The chamber temperature is quite low at this time as a result of the low-pressure flashing, but slowly increases as the chamber pressure rises. Ignition occurs at 4.6 ms, increasing the chamber temperature from 230°K to 2,803°K and decreasing mean molecular weight from 46 to 27. The first fuel droplets impact upon the wall at 4.4 ms. While the first oxidizer deposit arrives at 4.6 ms, the first ejection of unburned fuel and oxidizer droplets occurs at 4.8 and 4.9 ms. While the first expulsion of fuel and

oxidizer derived wall film does not occur until 6.5 ms, the last wall-film to be ejected during the firing leaves at 16.7 ms., (however, much later, during the dribble period, oxidizer wall film begins to be ejected again at 57.2 ms.) The chamber walls dry up completely at 34 ms. The other values for the various mass accumulations and flow rates can be followed from the time interval prints. The interval summary for the entire ignition transient interval gives the amounts of fuel and oxidizer which have been ejected in the forms of unburned droplets and as wall-film in the interval 4.6 to 12.4 ms. Also given are the mean droplet diameters and mean axial velocity for the material ejected during this interval. Values from the interval summaries can be used to derive input values for the succeeding nozzle and plume programs.

The final summary print gives mean values for mixture ratio, C-star, specific impulse and amounts of propellant flow for the entire pulse. The mass of propellants out of tank differs from the mass through the injector by the filling or depletion of the dribble volumes. The mass of propellant through the nozzle differs from the mass through the injector by the amount of accumulation or depletion of propellant held in the chamber in the forms of gas, streams and droplets, or wall-film. For short pulse-widths, the accumulations in the dribble volumes and in the chamber can be an appreciable fraction of the total flow from the tank, and are important in reducing the apparent C-star and specific impulse, which are usually reported on a mass out-of-tank basis.

The second page of the final summary print indicates that for this pulse, 62 percent of injected propellant left the chamber as combustion gas or propellant vapors, 37 percent left as unburned droplets, and 0.2 percent left as wall film. At the 60 ms conclusion of these computations, 1.8 percent of injected oxidizer was on the motor wall, with no fuel being held on the wall. This is because of the short 10 ms dribble period which empties the oxidizer dribble volume, but barely starts to empty the fuel dribble volume. Only a small amount of material is ejected as wall film in this run because the engine started with clean walls, and because the pulse width was long enough to burn the walls clean again before cutoff. A subsequent start of this engine, with much of the material from the first pulse dribble still on the walls, would eject a larger amount of wall film. Pulse widths shorter than about 30 ms will not burn the walls clean before cutoff. Thus, the material will build up continuously over a series of pulses to form a thick film, which flows faster and leads to more wall film ejection.

The mean diameter, mean axial velocity, and droplet size distribution of ejected droplets are given as input to the nozzle and plume programs. In this case, the ejected fuel droplets have a D32 of 122 microns and an axial velocity of 270 ft/sec. The drop size distribution still shows major influence from the 5-size group approximation, but can show some real changes from flash atomization and preferential chamber burnoff of small droplets.

Table III. TCC OUTPUT

REFERENCE RUN NO.		U		CASE NO.		1	
THE INPUT DATA FOR THIS CASE ARE AS FOLLOWS							
CHAMBER DESCRIPTION							
CHAMBER LENGTH	INJECTOR AREA	LINEAR TAPER	PARABOLIC TAPER				
1.079300	.176900	.142700	.122600				
THROAT AREA							
.029300	0.000000	0.000000	0.000000				
OPERATING CONDITIONS							
EXTERNAL PRESSURE	WALL TEMPERATURE						
.000001	294.000000	0.000000	0.000000				
FUEL TANK PRESS	FUEL TANK TEMP	INJECTOR TEMP					
180.000000	294.000000	294.000000	0.000000				
	FUEL VALVE OPEN DT		FUEL VALVE CLOSE DT				
0.000000	.001000	0.000000	.001000				
OXID TANK PRESS	OXID TANK TEMP	INJECTOR TEMP					
165.000000	294.000000	294.000000	0.000000				
	OXID VALVE OPEN DT		OXID VALVE CLOSE DT				
0.000000	.001000	0.000000	.001000				
FIRST BURN VALVE TIMING							
FUEL VALVE OPEN	OXID VALVE OPEN	FUEL VALVE CLOSE	OXID VALVE CLOSE				
0.000000	0.000000	.050000	.000000				
IGNITION DESCRIPTION							
ASSIGNED DELAY	IGNITER PORT LOC.	FUEL FLOW RATE	OXID FLOW RATE				
0.000000	0.000000	0.000000	0.000000				
ACTIVATION ENERGY	FREQ. FACT. X 10	PERFECT MIXING	NO AXIAL MIXING				
9200.000000	3.400000E+14	0.000000	0.000000				

Table III-Continued

FUEL FEED SYSTEM			
LINE LENGTH 400.000000	LINE AREA .028100	RESTRICTOR AREA .004940	VENTURI AREA .028100
VALVE AREA .020100	INJECTION AREA .000190	0.000000	0.000000
MOLE DIAMETER .007900	MOLE LENGTH .042000	AXIAL LOCATION 0.000000	RADIAL LOCATION .045000
INJECTION ANGLE 45.000000	0.000000	0.000000	0.000000
INIT. VOID VOLUME .001130	0.000000	TRANSITION VOLUME 0.000000	DRIBBLE VOLUME 0.001130
CHECK VALVES 0.000000	0.000000	0.000000	0.000000
OXIDIZER FEED SYSTEM			
LINE LENGTH 400.000000	LINE AREA .028100	RESTRICTOR AREA .006360	VENTURI AREA 0.028100
VALVE AREA .028100	INJECTION AREA .000272	0.000000	0.000000
MOLE DIAMETER .009300	MOLE LENGTH .042500	AXIAL LOCATION 0.000000	RADIAL LOCATION .045000
INJECTION ANGLE 45.000000	0.000000	0.000000	0.000000
INIT. VOID VOLUME .000580	0.000000	TRANSITION VOLUME 0.000000	DRIBBLE VOLUME 0.000580
CHECK VALVES 0.000000	0.000000	0.000000	0.000000
ATOMIZATION PARAMETERS			
FUEL PIN LENGTH 0.000000	OXID PIN LENGTH 0.000000	SHOWERHEAD L/D 10.000000	0.000000
NO. HOLD AT TRIPLE PT 0.000000	NO. INIT. DRIBBLE 1.000000	FLASH CONE ANGLE 30.000000	0.000000
DROP SIZE 1 1.98000	DROP SIZE 2 1.759000	DROP SIZE 3 1.000000	DROP SIZE 4 1.230000
DROP SIZE 5 2.304500	NO WALL BREAKUP 0.000000	DROP RESTITUTION 1.000000	FRACTION STICKING 0.000000
NO FUEL FLASH 0.000000	NO OXID FLASH 0.000000	NO WALL FLOW 0.000000	NO WALL BURNOFF 0.000000

Table III-Continued

FUEL PROPERTIES			
BOILING POINT 380.000000	FREEZING POINT 222.000000	CRITICAL TEMP. 594.000000	CRITICAL PRESS. 1193.000000
VAPOR CP. .995000	LIQUID CP. .600000		MOL. WEIGHT 46.074000
LATENT HEAT VAP. 210.000000	LATENT HEAT FUS. 67.500000	LIC. THERM. COND. .000545	ACCOM. COEFF. 110.000000
REFERENCE TEMP. 300.000000	DENSITY .600000	VISCOSITY .010000	SURFACE TENSION 47.000000
BURNING RATE K .032500	MONO. INTERCEPT 0.000000	MONO. COEFFICIENT 0.000000	MONO. EXPONENT 0.000000
OXIDIZER PROPERTIES			
BOILING POINT 294.000000	FREEZING POINT 262.000000	CRITICAL TEMP. 431.000000	CRITICAL PRESS. 1470.000000
VAPOR CP. .298000	LIQUID CP. .340000		MOL. WEIGHT 46.038000
LATENT HEAT VAP. 99.000000	LATENT HEAT FUS. 19.200000	LIC. THERM. COND. .000306	ACCOM. COEFF. 110.000000
REFERENCE TEMP. 300.000000	DENSITY 1.400000	VISCOSITY .024460	SURFACE TENSION 28.000000
BURNING RATE K .027000	MONO. INTERCEPT 0.000000	MONO. COEFFICIENT 0.000000	MONO. EXPONENT 0.000000
COMBUSTION GAS PROPERTIES			
TEMP. 1 300.000000	TEMP. 2 2103.000000	TEMP. 3 3084.000000	TEMP. 4 3397.000000
TEMP. 5 3061.000000	TEMP. 6 2366.000000	TEMP. 7 1705.000000	TEMP. 8 1433.000000
TEMP. 9 1344.000000	TEMP. 10 1266.000000	TEMP. 11 1190.000000	0.000000
MOL. WT. 1 46.000000	MOL. WT. 2 28.790000	MOL. WT. 3 28.410000	MOL. WT. 4 23.390000
MOL. WT. 5 19.800000	MOL. WT. 6 18.750000	MOL. WT. 7 14.410000	MOL. WT. 8 13.910000
MOL. WT. 9 14.000000	MOL. WT. 10 14.100000	MOL. WT. 11 14.290000	0.000000
GAMMA 1 1.120000	GAMMA 2 1.252000	GAMMA 3 1.220000	GAMMA 4 1.217000
GAMMA 5 1.235000	GAMMA 6 1.248000	GAMMA 7 1.309000	GAMMA 8 1.299000
GAMMA 9 1.270000	GAMMA 10 1.247000	GAMMA 11 1.228000	0.000000
CONTAMINANT PROPERTIES			
DENSITY 1.000000	VAPOR CP. 1.000000	LATENT HEAT 100.000000	DECOMP. TEMP. 500.000000
VISCOSITY 1 .004460	VISCOSITY 2 .024000	VISCOSITY 3 .043000	VISCOSITY 4 .068000
VISCOSITY 5 .081000	VISCOSITY 6 .100000	VISCOSITY 7 .082000	VISCOSITY 8 .064000
VISCOSITY 9 .046000	VISCOSITY 10 .029000	VISCOSITY 11 .010400	0.000000

Table III-Continued

GENERAL INSTRUCTIONS				
STOP TIME	TIME INTERVAL	PRINT ONE OUT OF	PLOT ONE OUT OF	
0.000000	0.010100	10.000000	10.000000	
DELETE GRAPHICS	DELETE DROP MEANS	DELETE SUMMARIES	DATA REV. ONLY	
0.000000	0.000000	0.000000	0.000000	
FUEL TRAJ. GROUP	OXID TRAJ. GROUP	TRAJ. START TIME	STEADY-STATE TIME	
3.000000	0.000000	0.000000	10.125000	
FLOW RATE OVERRIDES				
FUEL FLOW RATE	FUEL PRESS. DROP	DISCHARGE COEFF.	NO INJ. FRICTION	
0.000000	0.000000	0.000000	1.000000	
OXID FLOW RATE	OXID PRESS. DROP	DISCHARGE COEFF.		
0.000000	0.000000	0.000000	0.000000	
THRUST COEFFICIENT TABLE				
CF VAC 1	CF VAC 2	CF VAC 3	CF VAC 4	
1.924000	1.872800	1.908200	1.961700	
CF VAC 5	CF VAC 6	CF VAC 7	CF VAC 8	
1.847000	1.812200	1.868000	1.933100	
CF VAC 9	CF VAC 10	CF VAC 11	EXP. AREA RATIO	
1.929400	1.922400	1.895900	40.000000	
SECOND PULSE TIMING				
FUEL VALVE OPEN	OXID VALVE OPEN	FUEL VALVE CLOSE	OXID VALVE CLOSE	
0.000000	0.000000	0.000000	0.000000	
THIRD PULSE TIMING				
FUEL VALVE OPEN	OXID VALVE OPEN	FUEL VALVE CLOSE	OXID VALVE CLOSE	
0.000000	0.000000	0.000000	0.000000	
FOURTH PULSE TIMING				
FUEL VALVE OPEN	OXID VALVE OPEN	FUEL VALVE CLOSE	OXID VALVE CLOSE	
0.000000	0.000000	0.000000	0.000000	
FIFTH PULSE TIMING				
FUEL VALVE OPEN	OXID VALVE OPEN	FUEL VALVE CLOSE	OXID VALVE CLOSE	
0.000000	0.000000	0.000000	0.000000	
SIXTH PULSE TIMING				
FUEL VALVE OPEN	OXID VALVE OPEN	FUEL VALVE CLOSE	OXID VALVE CLOSE	
0.000000	0.000000	0.000000	0.000000	
SEVENTH PULSE TIMING				
FUEL VALVE OPEN	OXID VALVE OPEN	FUEL VALVE CLOSE	OXID VALVE CLOSE	
0.000000	0.000000	0.000000	0.000000	
EIGHTH PULSE TIMING				
FUEL VALVE OPEN	OXID VALVE OPEN	FUEL VALVE CLOSE	OXID VALVE CLOSE	
0.000000	0.000000	0.000000	0.000000	
NINTH PULSE TIMING				
FUEL VALVE OPEN	OXID VALVE OPEN	FUEL VALVE CLOSE	OXID VALVE CLOSE	
0.000000	0.000000	0.000000	0.000000	
INPUT UNITS ARE INCHES, PSIA, SECONDS AND DEGREES KELVIN. PROPELLANT PROPERTIES ARE IN GRAMS/CC, POISE, DYNE/CM.				

Table III--Continued

DERIVED FUEL PROPERTIES							
REDUCED TEMP.	TEMPERATURE	LIQ. ENTHALPY	VAP. ENTHALPY	VAPOR PRESSURE LIO.	DENSITY	VISCOSITY	SURFACE TENSION
.30000	176,20000	122,956000	345,009000	.000013	.994678	.200413	76,710089
.40000	237,60000	231,444000	464,112000	.021783	.938751	.039109	60,869285
.50000	297,00000	272,430000	483,213000	1.120119	.862823	.011011	47,606846
.60000	356,40000	313,416000	522,318000	13,047653	.826698	.003909	36,641394
.70000	415,80000	354,402000	581,421000	69,232066	.770971	.002402	27,689749
.80000	475,20000	399,386000	640,524000	237,312266	.722244	.001377	20,467937
.90000	534,60000	436,374000	699,627000	281,695073	.624088	.001088	10,011953
1.00000	594,00000	477,360000	759,730000	1,95,00000	.292811	.000390	.000000
DERIVED OXID. PROPERTIES							
REDUCED TEMP.	TEMPERATURE	LIQ. ENTHALPY	VAP. ENTHALPY	V. P. P. PRESSURE LIO.	DENSITY	VISCOSITY	SURFACE TENSION
.30000	129,30000	46,548000	104,959400	.000000	1.065399	.365350	76,696121
.40000	182,40000	67,044000	247,932000	.000070	1.762515	.071334	69,847656
.50000	215,50000	77,580000	220,647000	.038852	1.655631	.020084	47,592715
.60000	258,60000	95,096000	233,405800	1,726303	1,552747	.007130	36,631102
.70000	301,70000	147,612000	249,334600	21,667967	1,442863	.004451	27,661520
.80000	344,80000	165,328000	258,178400	137,031787	1,340979	.002877	20,482071
.90000	387,90000	178,844000	272,022200	2,12,146110	1,172403	.001985	10,009366
1.00000	431,00000	194,360000	284,366000	1,007000	.549331	.001712	.000000

Table III-Continued

FUEL INJ RATE	OXID INJ RATE	FUEL FLOW RATE	OXID FLOW RATE	FUEL VOID VOL	OXID VOID VOL	FUEL INJ TEMP	OXID INJ TEMP
2.093330E+04	2.126206E+03	5.792374E+04	1.126206E+03	5.780739E+04	294,000	294,000	294,000
FUEL FLASH RATE	OXID FLASH RATE	FUEL FLASH RATE	OXID FLASH RATE	FUEL WALL BURN	OXID WALL BURN	FUEL WALL EVAP	OXID WALL EVAP
0.	0.	0.	0.	0.	0.	0.	0.
FUEL GAS MASS	OXID GAS MASS	FUEL DROPLETS	OXID DROPLETS	FUEL STREAMS	OXID STREAMS	FUEL ON WALL	OXID ON WALL
4.228900E+13	0.	0.	0.	0.	0.	0.	0.
FUEL GAS EFFLUX	OXID GAS EFFLUX	FUEL DROP RATE	OXID DROP RATE	FUEL FILM RATE	GAS FRACTION	THRUST * LRF	5.716490E+08
0.	0.	0.	0.	1.00000	0.	0.	0.
FUEL INJ. VEL.	OXID INJ. VEL.	RETA ANGLE	RETA ANGLE	MASS OUT OF TANK	INTEGRAL PC*DT	TOTAL IMPULSE	1.143298E+11
0.	0.	0.	0.	2.123127E+07	2.000000E+10	0.	0.
CHAMBER TEMP K	CHAMBER TEMP K	CHAMBER TEMP K	CHAMBER TEMP K	GAMMA	GAMMA	CF VAC	1.91829
300,000	300,000	300,000	300,000	1.16944	1.16944	0.	0.
FUEL INJ RATE	OXID FLOW RATE	FUEL FLOW RATE	OXID FLOW RATE	FUEL VOID VOL	OXID VOID VOL	FUEL INJ TEMP	OXID INJ TEMP
1.1213924E+03	1.161944E+03	1.161944E+03	1.122412E+03	5.761478E+04	294,000	294,000	294,000
FUEL FLASH RATE	OXID FLASH RATE	FUEL FLASH RATE	OXID FLASH RATE	FUEL WALL BURN	OXID WALL BURN	FUEL WALL EVAP	OXID WALL EVAP
0.	0.	0.	0.	0.	0.	0.	0.
FUEL GAS MASS	OXID GAS MASS	FUEL DROPLETS	OXID DROPLETS	FUEL STREAMS	OXID STREAMS	FUEL ON WALL	OXID ON WALL
4.228900E+13	0.	0.	0.	0.	0.	0.	0.
FUEL GAS EFFLUX	OXID GAS EFFLUX	FUEL DROP RATE	OXID DROP RATE	FUEL FILM RATE	GAS FRACTION	THRUST * LRF	5.716490E+08
0.	0.	0.	0.	1.00000	0.	0.	0.
FUEL INJ. VEL.	OXID INJ. VEL.	RETA ANGLE	RETA ANGLE	MASS OUT OF TANK	INTEGRAL PC*DT	TOTAL IMPULSE	1.143298E+11
0.	0.	0.	0.	4.456248E+07	3.000000E+10	0.	0.
CHAMBER TEMP K	CHAMBER TEMP K	CHAMBER TEMP K	CHAMBER TEMP K	GAMMA	GAMMA	CF VAC	1.91829
300,000	300,000	300,000	300,000	1.16944	1.16944	0.	0.
FUEL INJ RATE	OXID FLOW RATE	FUEL FLOW RATE	OXID FLOW RATE	FUEL VOID VOL	OXID VOID VOL	FUEL INJ TEMP	OXID INJ TEMP
1.1213924E+03	1.161944E+03	1.161944E+03	1.122412E+03	5.761478E+04	294,000	294,000	294,000
FUEL FLASH RATE	OXID FLASH RATE	FUEL FLASH RATE	OXID FLASH RATE	FUEL WALL BURN	OXID WALL BURN	FUEL WALL EVAP	OXID WALL EVAP
0.	0.	0.	0.	0.	0.	0.	0.
FUEL GAS MASS	OXID GAS MASS	FUEL DROPLETS	OXID DROPLETS	FUEL STREAMS	OXID STREAMS	FUEL ON WALL	OXID ON WALL
4.228900E+13	0.	0.	0.	0.	0.	0.	0.
FUEL GAS EFFLUX	OXID GAS EFFLUX	FUEL DROP RATE	OXID DROP RATE	FUEL FILM RATE	GAS FRACTION	THRUST * LRF	5.716490E+08
0.	0.	0.	0.	1.00000	0.	0.	0.
FUEL INJ. VEL.	OXID INJ. VEL.	RETA ANGLE	RETA ANGLE	MASS OUT OF TANK	INTEGRAL PC*DT	TOTAL IMPULSE	1.143298E+11
0.	0.	0.	0.	4.456248E+07	3.000000E+10	0.	0.
CHAMBER TEMP K	CHAMBER TEMP K	CHAMBER TEMP K	CHAMBER TEMP K	GAMMA	GAMMA	CF VAC	1.91829
300,000	300,000	300,000	300,000	1.16944	1.16944	0.	0.
FUEL INJ RATE	OXID FLOW RATE	FUEL FLOW RATE	OXID FLOW RATE	FUEL VOID VOL	OXID VOID VOL	FUEL INJ TEMP	OXID INJ TEMP
1.1213924E+03	1.161944E+03	1.161944E+03	1.122412E+03	5.761478E+04	294,000	294,000	294,000
FUEL FLASH RATE	OXID FLASH RATE	FUEL FLASH RATE	OXID FLASH RATE	FUEL WALL BURN	OXID WALL BURN	FUEL WALL EVAP	OXID WALL EVAP
0.	0.	0.	0.	0.	0.	0.	0.
FUEL GAS MASS	OXID GAS MASS	FUEL DROPLETS	OXID DROPLETS	FUEL STREAMS	OXID STREAMS	FUEL ON WALL	OXID ON WALL
4.228900E+13	0.	0.	0.	0.	0.	0.	0.
FUEL GAS EFFLUX	OXID GAS EFFLUX	FUEL DROP RATE	OXID DROP RATE	FUEL FILM RATE	GAS FRACTION	THRUST * LRF	5.716490E+08
0.	0.	0.	0.	1.00000	0.	0.	0.
FUEL INJ. VEL.	OXID INJ. VEL.	RETA ANGLE	RETA ANGLE	MASS OUT OF TANK	INTEGRAL PC*DT	TOTAL IMPULSE	1.143298E+11
0.	0.	0.	0.	4.456248E+07	3.000000E+10	0.	0.
CHAMBER TEMP K	CHAMBER TEMP K	CHAMBER TEMP K	CHAMBER TEMP K	GAMMA	GAMMA	CF VAC	1.91829
300,000	300,000	300,000	300,000	1.16944	1.16944	0.	0.

Table III-Continued

TIME MILLISEC	CHAMBER PRESS	IGNITION	FUEL FRACTION	CHAMBER TEMP K	MOL WT.	GAMMA	CF VAC
4.0000	1.000000000	0.	0.	300.000	46.1000	1.10994	1.91029
FUEL INJ RATE	OXID INJ RATE	FUEL FLOW RATE	OXID FLOW RATE	FUEL VOID VOL	OXID VOID VOL	FUEL INJ TEMP	OXID INJ TEMP
0.	0.	1.000000000	1.000000000	0.000000000	0.000000000	294.000	294.000
FUEL DROP BURN	OXID DROP BURN	FUEL FLASH RATE	OXID FLASH RATE	FUEL WALL BURN	OXID WALL BURN	FUEL WALL EVAP	OXID WALL EVAP
0.	0.	0.	0.	0.	0.	0.	0.
FUEL GAS MASS	OXID GAS MASS	FUEL DROPLETS	OXID DROPLETS	FUEL STREAMS	OXID STREAMS	FUEL ON WALL	OXID ON WALL
0.	0.	0.	0.	0.	0.	0.	0.
FUEL GAS EFFLUX	OXID GAS EFFLUX	FUEL DROP RATE	OXID DROP RATE	FUEL FILM RATE	OXID FILM RATE	GAS FRACTION	THRUST - LBF
0.	0.	0.	0.	0.	0.	1.00000	9.710000000
FUEL DROP DIAM	OXID DROP DIAM	FUEL INJ. VEL.	OXID INJ. VEL.	BETA ANGLE	MASS OUT OF TANK	INTEGRAL PCOUT	TOTAL IMPULSE
0.	0.	0.	0.	0.	0.000000000	0.000000000	2.200000000
INJECTED MASS	GAS EXPELLED	DROPS EXPELLED	WALL EXPELLED	GAS RETAINED	PROPS RETAINED	WALL RETAINED	
0.000000000	0.000000000	0.000000000	0.000000000	0.000000000	0.000000000	0.000000000	
OXID GRAMS	0.000000000	0.000000000	0.000000000	0.000000000	0.000000000	0.000000000	
0.000000000	0.000000000	0.000000000	0.000000000	0.000000000	0.000000000	0.000000000	
SUM 1	SUM 2	SUM 3	SUM 4	SUM 5	SUM 6	SUM 7	TOTAL MOMENTUM
0.	0.	0.	0.	0.	0.	0.	0.
FUEL DROPS INJECTED	0.	0.	0.	0.	0.	0.	0.
FUEL DROPS EJECTED	0.	0.	0.	0.	0.	0.	0.
OXID DROPS INJECTED	0.	0.	0.	0.	0.	0.	0.
OXID DROPS EJECTED	0.	0.	0.	0.	0.	0.	0.

TIME MILLISEC	CHAMBER PRESS	IGNITION	FUEL FRACTION	CHAMBER TEMP K	MOL WT.	GAMMA	CF VAC
4.1000	1.000000000	0.	0.	300.000	46.1000	1.10994	1.91029
FUEL INJ RATE	OXID INJ RATE	FUEL FLOW RATE	OXID FLOW RATE	FUEL VOID VOL	OXID VOID VOL	FUEL INJ TEMP	OXID INJ TEMP
0.	0.	1.000000000	1.000000000	0.000000000	0.000000000	294.000	294.000
FUEL DROP BURN	OXID DROP BURN	FUEL FLASH RATE	OXID FLASH RATE	FUEL WALL BURN	OXID WALL BURN	FUEL WALL EVAP	OXID WALL EVAP
0.	0.	0.	0.	0.	0.	0.	0.
FUEL GAS MASS	OXID GAS MASS	FUEL DROPLETS	OXID DROPLETS	FUEL STREAMS	OXID STREAMS	FUEL ON WALL	OXID ON WALL
0.	0.	0.	0.	0.	0.	0.	0.
FUEL GAS EFFLUX	OXID GAS EFFLUX	FUEL DROP RATE	OXID DROP RATE	FUEL FILM RATE	OXID FILM RATE	GAS FRACTION	THRUST - LBF
0.	0.	0.	0.	0.	0.	1.00000	9.710000000
FUEL DROP DIAM	OXID DROP DIAM	FUEL INJ. VEL.	OXID INJ. VEL.	BETA ANGLE	MASS OUT OF TANK	INTEGRAL PCOUT	TOTAL IMPULSE
0.	0.	0.	0.	0.	0.000000000	0.000000000	2.200000000
INJECTED MASS	GAS EXPELLED	DROPS EXPELLED	WALL EXPELLED	GAS RETAINED	PROPS RETAINED	WALL RETAINED	
0.000000000	0.000000000	0.000000000	0.000000000	0.000000000	0.000000000	0.000000000	
OXID GRAMS	0.000000000	0.000000000	0.000000000	0.000000000	0.000000000	0.000000000	
0.000000000	0.000000000	0.000000000	0.000000000	0.000000000	0.000000000	0.000000000	
SUM 1	SUM 2	SUM 3	SUM 4	SUM 5	SUM 6	SUM 7	TOTAL MOMENTUM
0.	0.	0.	0.	0.	0.	0.	0.
FUEL DROPS INJECTED	0.	0.	0.	0.	0.	0.	0.
FUEL DROPS EJECTED	0.	0.	0.	0.	0.	0.	0.
OXID DROPS INJECTED	0.	0.	0.	0.	0.	0.	0.
OXID DROPS EJECTED	0.	0.	0.	0.	0.	0.	0.

TIME MILLISEC	CHAMBER PRESS	IGNITION	FUEL FRACTION	CHAMBER TEMP K	MOL WT.	GAMMA	CF VAC
4.2000	1.000000000	0.	0.	300.000	46.1000	1.10994	1.91029
FUEL INJ RATE	OXID INJ RATE	FUEL FLOW RATE	OXID FLOW RATE	FUEL VOID VOL	OXID VOID VOL	FUEL INJ TEMP	OXID INJ TEMP
0.	0.	1.000000000	1.000000000	0.000000000	0.000000000	294.000	294.000
FUEL DROP BURN	OXID DROP BURN	FUEL FLASH RATE	OXID FLASH RATE	FUEL WALL BURN	OXID WALL BURN	FUEL WALL EVAP	OXID WALL EVAP
0.	0.	0.	0.	0.	0.	0.	0.
FUEL GAS MASS	OXID GAS MASS	FUEL DROPLETS	OXID DROPLETS	FUEL STREAMS	OXID STREAMS	FUEL ON WALL	OXID ON WALL
0.	0.	0.	0.	0.	0.	0.	0.
FUEL GAS EFFLUX	OXID GAS EFFLUX	FUEL DROP RATE	OXID DROP RATE	FUEL FILM RATE	OXID FILM RATE	GAS FRACTION	THRUST - LBF
0.	0.	0.	0.	0.	0.	1.00000	9.710000000
FUEL DROP DIAM	OXID DROP DIAM	FUEL INJ. VEL.	OXID INJ. VEL.	BETA ANGLE	MASS OUT OF TANK	INTEGRAL PCOUT	TOTAL IMPULSE
0.	0.	0.	0.	0.	0.000000000	0.000000000	2.200000000
INJECTED MASS	GAS EXPELLED	DROPS EXPELLED	WALL EXPELLED	GAS RETAINED	PROPS RETAINED	WALL RETAINED	
0.000000000	0.000000000	0.000000000	0.000000000	0.000000000	0.000000000	0.000000000	
OXID GRAMS	0.000000000	0.000000000	0.000000000	0.000000000	0.000000000	0.000000000	
0.000000000	0.000000000	0.000000000	0.000000000	0.000000000	0.000000000	0.000000000	
SUM 1	SUM 2	SUM 3	SUM 4	SUM 5	SUM 6	SUM 7	TOTAL MOMENTUM
0.	0.	0.	0.	0.	0.	0.	0.
FUEL DROPS INJECTED	0.	0.	0.	0.	0.	0.	0.
FUEL DROPS EJECTED	0.	0.	0.	0.	0.	0.	0.
OXID DROPS INJECTED	0.	0.	0.	0.	0.	0.	0.
OXID DROPS EJECTED	0.	0.	0.	0.	0.	0.	0.

Table III-Continued

TIME MILLISEC	CHAMBER PRESS	IGNITION	FUEL FRACTION	CHAMBER TEMP K	MOL WT,	GAMMA	CF VAC
4,3000	90237	0.	1284210	200,006	4610294	1.09832	2.01010
FUEL INJ RATE	OXID INJ RATE	FUEL FLOW RATE	OXID FLOW RATE	FUEL VOID VOL	OXID VOID VOL	FUEL INJ TEMP	OXID INJ TEMP
1.06793E+02	1.73208E+02	1.06793E+02	1.73208E+02	0.	0.	294,000	294,000
FUEL DROP BURN	OXID DROP BURN	FUEL FLASH RATE	OXID FLASH RATE	FUEL WALL BURN	OXID WALL BURN	FUEL WALL EVAP	OXID WALL EVAP
0.	0.	0.	0.	0.	0.	0.	0.
FUEL GAS MASS	OXID GAS MASS	FUEL DROPLETS	OXID DROPLETS	FUEL STREAMS	OXID STREAMS	FUEL ON WALL	OXID ON WALL
2.2393E+07	4.13099E+07	1.70000E+00	1.70000E+00	0.	0.	0.	0.
FUEL GAS EFFLUX	OXID GAS EFFLUX	FUEL DROP RATE	OXID DROP RATE	FUEL FILM RATE	OXID FILM RATE	GAS FRACTION	THROUST - LEF
2.2393E+04	5.17309E+04	0.	0.	0.	0.	1.00000	5.40469E+02
FUEL DROP DIA	OXID DROP DIA	FUEL INJ. VEL.	OXID INJ. VEL.	BETA ANGLE	MASS OUT OF TANK INTEGRAL PCOBT	TOTAL IMPULSE	TOTAL IMPULSE
364,845	364,436	224,036	92,164	-27,1973	7.02808E+05	1.34722E+02	1.34745E+04
TIME MILLISEC	CHAMBER PRESS	IGNITION	FUEL FRACTION	CHAMBER TEMP K	MOL WT,	GAMMA	CF VAC
4,4000	1,54297	0.	1,140565	219,084	461,179	1,12022	1,17994
FUEL INJ RATE	OXID INJ RATE	FUEL FLOW RATE	OXID FLOW RATE	FUEL VOID VOL	OXID VOID VOL	FUEL INJ TEMP	OXID INJ TEMP
1.64236E+02	2.14831E+02	1.64236E+02	2.14831E+02	0.	0.	294,000	294,000
FUEL DROP BURN	OXID DROP BURN	FUEL FLASH RATE	OXID FLASH RATE	FUEL WALL BURN	OXID WALL BURN	FUEL WALL EVAP	OXID WALL EVAP
0.	0.	0.	0.	0.	0.	2,977,592E+00	0.
FUEL GAS MASS	OXID GAS MASS	FUEL DROPLETS	OXID DROPLETS	FUEL STREAMS	OXID STREAMS	FUEL ON WALL	OXID ON WALL
1.09253E+07	1.11329E+07	1.75788E+00	1.75788E+00	0.	0.	0.	0.
FUEL GAS EFFLUX	OXID GAS EFFLUX	FUEL DROP RATE	OXID DROP RATE	FUEL FILM RATE	OXID FILM RATE	GAS FRACTION	THROUST - LEF
2.20021E+04	5.14001E+04	0.	0.	0.	0.	1.00000	5.12612E+02
FUEL DROP DIA	OXID DROP DIA	FUEL INJ. VEL.	OXID INJ. VEL.	BETA ANGLE	MASS OUT OF TANK INTEGRAL PCOBT	TOTAL IMPULSE	TOTAL IMPULSE
364,845	34,436	219,239	59,728	-25,5110	7.13485E+05	1.34722E+02	1.34733E+02
TIME MILLISEC	CHAMBER PRESS	IGNITION	FUEL FRACTION	CHAMBER TEMP K	MOL WT,	GAMMA	CF VAC
4,5000	2,15772	0.	1,101614	230,607	461,147	1,11257	1,18434
FUEL INJ RATE	OXID INJ RATE	FUEL FLOW RATE	OXID FLOW RATE	FUEL VOID VOL	OXID VOID VOL	FUEL INJ TEMP	OXID INJ TEMP
1.61803E+02	2.15003E+02	1.61803E+02	2.15003E+02	0.	0.	294,000	294,000
FUEL DROP BURN	OXID DROP BURN	FUEL FLASH RATE	OXID FLASH RATE	FUEL WALL BURN	OXID WALL BURN	FUEL WALL EVAP	OXID WALL EVAP
0.	0.	0.	0.	0.	0.	0.	0.
FUEL GAS MASS	OXID GAS MASS	FUEL DROPLETS	OXID DROPLETS	FUEL STREAMS	OXID STREAMS	FUEL ON WALL	OXID ON WALL
1.77533E+07	1.56959E+07	1.37033E+00	2.65832E+00	0.	0.	0.	0.
FUEL GAS EFFLUX	OXID GAS EFFLUX	FUEL DROP RATE	OXID DROP RATE	FUEL FILM RATE	OXID FILM RATE	GAS FRACTION	THROUST - LEF
2.17203E+04	1.23502E+04	0.	0.	0.	0.	1.00000	5.1262E+02
FUEL DROP DIA	OXID DROP DIA	FUEL INJ. VEL.	OXID INJ. VEL.	BETA ANGLE	MASS OUT OF TANK INTEGRAL PCOBT	TOTAL IMPULSE	TOTAL IMPULSE
364,845	34,436	219,085	56,1574	-24,4760	7.16274E+05	1.34722E+02	1.34733E+02

TABLE IV 4 AA. VII. 1560017C

Table III--Continued

IGNITE AT 4.60 MILLISECS

TIME MILLISECS	4.6000	FUEL FRACTION	17.402	CHAMBER TEMP K	2803.93	MCL HT.	27.10903	GAMMA	1.22915	CF VAC	1.87807
CHAMBER PRESS	45.9227	IGNITION	1.00000	FUEL VOID VOL	0.0	OXID VOID VOL	0.0	FUEL INJ TEMP	294.000	OXID INJ TEMP	294.000
FUEL INJ RATE	3.54558E-02	FUEL FLOW RATE	3.54558E-02	FUEL FLASH RATE	0.0	FUEL WALL BURN	0.0	FUEL WALL EVAP	0.0	OXID WALL EVAP	1.63208E-04
FUEL PROP RATE	4.23485E-04	OXID PROP RATE	4.23485E-04	FUEL DROPLETS	0.0	OXID DROPLETS	0.0	FUEL ON WALL	2.80135E-06	OXID ON WALL	1.62800E-07
FUEL INJ VELOCITY	1.49744E-05	FUEL INJ VELOCITY	1.49744E-05	FUEL FILM RATE	0.0	OXID FILM RATE	0.0	GAS FRACTION	1.00000	THRUST LRF	2.58957
FUEL MASS EFFICIENCY	1.70291E-03	OXID MASS EFFICIENCY	1.70291E-03	RET. ANGLE	-23.4512	MASS OUT OF TANK	7.904395E-05	INTEGRAL PC-DT	5.075194E-03	TOTAL IMPULSE	2.855556E-04
FUEL PROP VELOCITY	32.2581	OXID PROP VELOCITY	32.2581								

SUMMARY FOR TIME INTERVAL ENDING AT		4.60 MILLISECS	PRE-IGNITION
FUEL EJECTED THIS INTERVAL	0.00000	DROPLET MASS	0.00000
OXID EJECTED THIS INTERVAL	0.00000	WALL FILM	0.00000
PROP EJECTED THIS INTERVAL	0.00000	TOTAL MASS	0.00000
			0.00000
			0.00000
FUEL EJECTED THIS INTERVAL	0.00000	PROP. VELOCITY	0.00000
OXID EJECTED THIS INTERVAL	0.00000		0.00000
PROP EJECTED THIS INTERVAL	0.00000		0.00000

NOT REPRODUCIBLE

Table III-Continued

TIME MILLISEC	CHAMBER PRESS	IGNITION	FUEL FRACTION	CHAMBER TEMP K	MOL WT.	GAMMA	CF VAC
4,7000	40,6700	1,0000	122775	3179,68	29,5716	3,21917	1,92805
FUEL INJ RATE	FUEL FLOW RATE	FUEL FLASH RATE	OXID FLAME RATE	FUEL WALL BURN	OXID VOID VOL	FUEL INJ TEMP	OXID INJ TEMP
1,42000E+03	1,42000E+02	1,42000E+02	1,42000E+02	3,46433E+05	0	294,100	294,100
FUEL DROP RATE	FUEL DROP RATE	FUEL FLASH RATE	OXID FLASH RATE	FUEL WALL BURN	OXID VOID VOL	FUEL WALL EVAP	OXID WALL EVAP
1,42000E+03	1,42000E+02	1,42000E+02	1,42000E+02	3,46433E+05	0	0	0
FUEL GAS MASS	FUEL GAS MASS	FUEL DROPLETS	OXID DROPLETS	FUEL STREAMS	OXID STREAMS	FUEL ON WALL	OXID ON WALL
1,42000E+03	1,42000E+02	1,42000E+02	1,42000E+02	3,46433E+05	0	0	0
FUEL DROP RATE	FUEL DROP RATE	FUEL DROP RATE	OXID DROP RATE	FUEL FLOW RATE	OXID FLOW RATE	GAS FRACTION	THEORY LDF
1,42000E+03	1,42000E+02	1,42000E+02	1,42000E+02	3,46433E+05	0	1,00000	4,63444
FUEL INJ. VEL.	FUEL INJ. VEL.	BETA ANGLE	BETA ANGLE	MASS OUT OF TANK	INTEGRAL PCOD	TOTAL IMPULSE	TOTAL IMPULSE
203,424	203,424	89,437	89,437	8,158133E+05	2,1275593E+02	3,187719E+02	3,187719E+02
UNBURNED FUEL OUT OF ENGINE							
TIME MILLISEC	CHAMBER PRESS	IGNITION	FUEL FRACTION	CHAMBER TEMP K	MOL WT.	GAMMA	CF VAC
4,9000	91,9127	1,0000	1,44378	3742,18	25,1727	3,42529	1,92805
FUEL INJ RATE	OXID INJ RATE	FUEL FLOW RATE	OXID FLOW RATE	FUEL WALL BURN	OXID VOID VOL	FUEL INJ TEMP	OXID INJ TEMP
1,42000E+03	1,42000E+02	1,42000E+02	1,42000E+02	3,46433E+05	0	294,100	294,100
FUEL DROP RATE	FUEL DROP RATE	FUEL FLASH RATE	OXID FLASH RATE	FUEL WALL BURN	OXID VOID VOL	FUEL WALL EVAP	OXID WALL EVAP
1,42000E+03	1,42000E+02	1,42000E+02	1,42000E+02	3,46433E+05	0	0	0
FUEL GAS MASS	FUEL GAS MASS	FUEL DROPLETS	OXID DROPLETS	FUEL STREAMS	OXID STREAMS	FUEL ON WALL	OXID ON WALL
1,42000E+03	1,42000E+02	1,42000E+02	1,42000E+02	3,46433E+05	0	0	0
FUEL DROP RATE	FUEL DROP RATE	FUEL DROP RATE	OXID DROP RATE	FUEL FLOW RATE	OXID FLOW RATE	GAS FRACTION	THEORY LDF
1,42000E+03	1,42000E+02	1,42000E+02	1,42000E+02	3,46433E+05	0	1,00000	5,57000
FUEL INJ. VEL.	FUEL INJ. VEL.	BETA ANGLE	BETA ANGLE	MASS OUT OF TANK	INTEGRAL PCOD	TOTAL IMPULSE	TOTAL IMPULSE
203,424	203,424	89,437	89,437	8,158133E+05	2,1275593E+02	3,187719E+02	3,187719E+02
UNBURNED FUEL OUT OF ENGINE							
TIME MILLISEC	CHAMBER PRESS	IGNITION	FUEL FRACTION	CHAMBER TEMP K	MOL WT.	GAMMA	CF VAC
4,9000	91,9127	1,0000	1,44378	3742,18	25,1727	3,42529	1,92805
FUEL INJ RATE	OXID INJ RATE	FUEL FLOW RATE	OXID FLOW RATE	FUEL WALL BURN	OXID VOID VOL	FUEL INJ TEMP	OXID INJ TEMP
1,42000E+03	1,42000E+02	1,42000E+02	1,42000E+02	3,46433E+05	0	294,100	294,100
FUEL DROP RATE	FUEL DROP RATE	FUEL FLASH RATE	OXID FLASH RATE	FUEL WALL BURN	OXID VOID VOL	FUEL WALL EVAP	OXID WALL EVAP
1,42000E+03	1,42000E+02	1,42000E+02	1,42000E+02	3,46433E+05	0	0	0
FUEL GAS MASS	FUEL GAS MASS	FUEL DROPLETS	OXID DROPLETS	FUEL STREAMS	OXID STREAMS	FUEL ON WALL	OXID ON WALL
1,42000E+03	1,42000E+02	1,42000E+02	1,42000E+02	3,46433E+05	0	0	0
FUEL DROP RATE	FUEL DROP RATE	FUEL DROP RATE	OXID DROP RATE	FUEL FLOW RATE	OXID FLOW RATE	GAS FRACTION	THEORY LDF
1,42000E+03	1,42000E+02	1,42000E+02	1,42000E+02	3,46433E+05	0	1,00000	5,57000
FUEL INJ. VEL.	FUEL INJ. VEL.	BETA ANGLE	BETA ANGLE	MASS OUT OF TANK	INTEGRAL PCOD	TOTAL IMPULSE	TOTAL IMPULSE
203,424	203,424	89,437	89,437	8,158133E+05	2,1275593E+02	3,187719E+02	3,187719E+02
UNBURNED FUEL OUT OF ENGINE							

NOT REPRODUCIBLE

Table III-Continued

TIME MILLISEC	92.210	1.0000	360717	3192.99	21.2988	3.82793	3.89286
CHAMBER PRESS	92.210	1.0000	360717	3192.99	21.2988	3.82793	3.89286
OXID INJ RATE	9.268928E+03	1.480745E+02	9.268928E+03	1.480745E+02	0.	294.000	294.000
FUEL FLOW RATE	9.268928E+03	1.480745E+02	9.268928E+03	1.480745E+02	0.	294.000	294.000
OXID DROP BURN	9.268928E+03	1.480745E+02	9.268928E+03	1.480745E+02	0.	294.000	294.000
FUEL FLASH RATE	9.268928E+03	1.480745E+02	9.268928E+03	1.480745E+02	0.	294.000	294.000
OXID DROPLETS	9.268928E+03	1.480745E+02	9.268928E+03	1.480745E+02	0.	294.000	294.000
FUEL GAS MASS	9.268928E+03	1.480745E+02	9.268928E+03	1.480745E+02	0.	294.000	294.000
OXID GAS MASS	9.268928E+03	1.480745E+02	9.268928E+03	1.480745E+02	0.	294.000	294.000
FUEL DRDP RATE	9.268928E+03	1.480745E+02	9.268928E+03	1.480745E+02	0.	294.000	294.000
OXID DRDP RATE	9.268928E+03	1.480745E+02	9.268928E+03	1.480745E+02	0.	294.000	294.000
FUEL DRDP DIAM	92.206	123.166	95.7329	3.03731	2.726508E+04	1.70394	3.844650E+02
OXID DRDP DIAM	92.206	123.166	95.7329	3.03731	2.726508E+04	1.70394	3.844650E+02
CHAMBER PRESE	92.1911	1.00000	.564559	3193.52	21.2944	3.82790	1.89224
IGNITION	92.1911	1.00000	.564559	3193.52	21.2944	3.82790	1.89224
FUEL INJ RATE	9.268928E+03	1.480745E+02	9.268928E+03	1.480745E+02	0.	294.000	294.000
OXID INJ RATE	9.268928E+03	1.480745E+02	9.268928E+03	1.480745E+02	0.	294.000	294.000
FUEL DRDP BURN	9.268928E+03	1.480745E+02	9.268928E+03	1.480745E+02	0.	294.000	294.000
OXID DRDP BURN	9.268928E+03	1.480745E+02	9.268928E+03	1.480745E+02	0.	294.000	294.000
FUEL GAS MASS	9.268928E+03	1.480745E+02	9.268928E+03	1.480745E+02	0.	294.000	294.000
OXID GAS MASS	9.268928E+03	1.480745E+02	9.268928E+03	1.480745E+02	0.	294.000	294.000
FUEL DRDP RATE	9.268928E+03	1.480745E+02	9.268928E+03	1.480745E+02	0.	294.000	294.000
OXID DRDP RATE	9.268928E+03	1.480745E+02	9.268928E+03	1.480745E+02	0.	294.000	294.000
FUEL DRDP DIAM	92.203	123.074	95.7329	3.07488	2.750977E+04	1.72760	3.998741E+02
OXID DRDP DIAM	92.203	123.074	95.7329	3.07488	2.750977E+04	1.72760	3.998741E+02
CHAMBER PRESS	92.1214	1.00000	.560412	3194.01	21.2699	3.82787	1.89241
IGNITION	92.1214	1.00000	.560412	3194.01	21.2699	3.82787	1.89241
FUEL INJ RATE	9.268928E+03	1.480745E+02	9.268928E+03	1.480745E+02	0.	294.000	294.000
OXID INJ RATE	9.268928E+03	1.480745E+02	9.268928E+03	1.480745E+02	0.	294.000	294.000
FUEL DRDP BURN	9.268928E+03	1.480745E+02	9.268928E+03	1.480745E+02	0.	294.000	294.000
OXID DRDP BURN	9.268928E+03	1.480745E+02	9.268928E+03	1.480745E+02	0.	294.000	294.000
FUEL GAS MASS	9.268928E+03	1.480745E+02	9.268928E+03	1.480745E+02	0.	294.000	294.000
OXID GAS MASS	9.268928E+03	1.480745E+02	9.268928E+03	1.480745E+02	0.	294.000	294.000
FUEL DRDP RATE	9.268928E+03	1.480745E+02	9.268928E+03	1.480745E+02	0.	294.000	294.000
OXID DRDP RATE	9.268928E+03	1.480745E+02	9.268928E+03	1.480745E+02	0.	294.000	294.000
FUEL DRDP DIAM	92.3066	122.988	95.7329	3.11661	2.774739E+04	1.721973	4.050811E+02
OXID DRDP DIAM	92.3066	122.988	95.7329	3.11661	2.774739E+04	1.721973	4.050811E+02
CHAMBER PRESS	92.0580	1.00000	.560300	3194.39	21.2735	3.82785	1.89234
IGNITION	92.0580	1.00000	.560300	3194.39	21.2735	3.82785	1.89234
FUEL INJ RATE	9.268928E+03	1.480745E+02	9.268928E+03	1.480745E+02	0.	294.000	294.000
OXID INJ RATE	9.268928E+03	1.480745E+02	9.268928E+03	1.480745E+02	0.	294.000	294.000
FUEL DRDP BURN	9.268928E+03	1.480745E+02	9.268928E+03	1.480745E+02	0.	294.000	294.000
OXID DRDP BURN	9.268928E+03	1.480745E+02	9.268928E+03	1.480745E+02	0.	294.000	294.000
FUEL GAS MASS	9.268928E+03	1.480745E+02	9.268928E+03	1.480745E+02	0.	294.000	294.000
OXID GAS MASS	9.268928E+03	1.480745E+02	9.268928E+03	1.480745E+02	0.	294.000	294.000
FUEL DRDP RATE	9.268928E+03	1.480745E+02	9.268928E+03	1.480745E+02	0.	294.000	294.000
OXID DRDP RATE	9.268928E+03	1.480745E+02	9.268928E+03	1.480745E+02	0.	294.000	294.000
FUEL DRDP DIAM	92.3067	122.988	95.7329	3.11661	2.774739E+04	1.721973	4.050811E+02
OXID DRDP DIAM	92.3067	122.988	95.7329	3.11661	2.774739E+04	1.721973	4.050811E+02

Table III-Continued

FUEL WAX MASS	9.809787E-03	0.	FUEL WALL MASS	4.403097E-04	0.	FUEL MASS LAYER	0.	WAX MASS	2.892933E-04	0.
FUEL GAS MASS	1.591461E-06	5.767915E-06	FUEL DROPLETS	8.491492E-16	0.	FUEL ON WALL	6.386215E-06	OXID ON WALL	3.433804E-09	
FUEL OX EFFLUX	1.007817E-02	4.033885E-03	OXID DROP RATE	4.091556E-03	3.600709E-05	OXID FILM RATE	2.545173E-05	OXID FRACTION	1.433989	THROBT W LBT
FUEL DROP DIAM	92.3277	122.906	FUEL INJ. VEL.	85.7314	BETA ANGLE	3.35333	MASS OUT OF TANK	1.798795E-04	INTEGRAL PC=DT	1.731178
									TOTAL IMPULSE	4.102846E-02

SUMMARY FOR TIME INTERVAL ENDING AT 12.40 MILLISEC

		IGNITION TRANSIENT			
FUEL EJECTED THIS INTERVAL	0.03915	DROPLET MASS	1.00442	WALL FILM	1.014327
OXID EJECTED THIS INTERVAL	0.03581		0.00477		1.014037
PROP EJECTED THIS INTERVAL	0.027496		1.000889		1.028385
	DSO		DS1		DS2
FUEL EJECTED THIS INTERVAL	99.939016		109.714026		123.915942
OXID EJECTED THIS INTERVAL	63.951049		73.989981		87.1281831
PROP EJECTED THIS INTERVAL	38.731606		91.272920		107.072806
					MEAN VELOCITY
					250.791891
					252.450192
					256.071747

D₃₂ MEAN DROP DIAMETER (μ)

Table III-Continued

TIME MILLISEC 51.0000	CHAMBER PRESS 88.2414	IGNITION 1.00000	FUEL FRACTION .337750	CHAMBER TEMP K 3266.80	MOL WT. 22.10299	GAMMA 1.22397	CF VAC 1.91725
FUEL INJ RATE	OXID INJ RATE	FUEL FLOW RATE	OXID FLOW RATE	FUEL VOID VOL	OXID VOID VOL	FUEL INJ TEMP	OXID INJ TEMP
0.	0.	0.	0.	0.	0.	294.000	294.000
FUEL DROP BUR	OXID DROP BUR	FUEL FLASH RATE	OXID FLASH RATE	FUEL WALL BURN	OXID WALL BURN	FUEL WALL EVAP	OXID WALL EVAP
5.132241E+03	1.433806E+02	0.	0.	0.	0.	0.	0.
FUEL GAS MASS	OXID GAS MASS	FUEL DROPLETS	OXID DROPLETS	FUEL STREAMS	OXID STREAMS	FUEL ON WALL	OXID ON WALL
1.22222E+07	1.594745E+04	1.205345E+06	7.205345E+06	0.	0.	0.	0.
FUEL GAS EFFLUX	OXID GAS EFFLUX	FUEL DROP RATE	OXID DROP RATE	FUEL FILM RATE	OXID FILM RATE	GAS FRACTION	THRUST - LBF
5.114615E+03	1.003071E+02	4.173447E+03	5.150936E+03	0.	0.	1.619316	9.05554
FUEL DROP DIA	OXID DROP DIA	FUEL INJ. VEL.	OXID INJ. VEL.	BETA ANGLE	MASS OUT OF TANK	INTEGRAL PC*00	TOTAL IMPULSE
0.	0.	0.	0.	0.	1.214021E+03	1.17902	1.237444
FUEL GAS	INJECTED MASS	GAS EXPULSED	DROPS EXPULSED	WALL EXPULSED	GAS RETAINED	DROPS RETAINED	WALL RETAINED
1.22222E+07	1.22222E+07	1.00000E+00	1.00000E+00	1.00000E+00	1.00000E+00	1.00000E+00	1.00000E+00
OXID GAS	INJECTED MASS	GAS EXPULSED	DROPS EXPULSED	WALL EXPULSED	GAS RETAINED	DROPS RETAINED	WALL RETAINED
1.22222E+07	1.22222E+07	1.00000E+00	1.00000E+00	1.00000E+00	1.00000E+00	1.00000E+00	1.00000E+00
TOTAL CHARGE	INJECTED MASS	GAS EXPULSED	DROPS EXPULSED	WALL EXPULSED	GAS RETAINED	DROPS RETAINED	WALL RETAINED
1.22222E+07	1.22222E+07	1.00000E+00	1.00000E+00	1.00000E+00	1.00000E+00	1.00000E+00	1.00000E+00
FUEL DROPS INJECTED	SUM -	SUM D SQUARED	SUM D CUBED	TOTAL MOMENTUM			
1.078494E+06	1.078494E+06	1.161409E+12	1.22222E+18	1.078494E+06			
OXID DROPS INJECTED	SUM -	SUM D SQUARED	SUM D CUBED	TOTAL MOMENTUM			
1.078494E+06	1.078494E+06	1.161409E+12	1.22222E+18	1.078494E+06			
OXID DROPS INJECTED	SUM -	SUM D SQUARED	SUM D CUBED	TOTAL MOMENTUM			
1.078494E+06	1.078494E+06	1.161409E+12	1.22222E+18	1.078494E+06			
TIME MILLISEC 51.1000	CHAMBER PRESS 65.4845	IGNITION 1.00000	FUEL FRACTION .329429	CHAMBER TEMP K 3298.12	MOL WT. 22.13571	GAMMA 1.22230	CF VAC 2.12275
FUEL INJ RATE	OXID INJ RATE	FUEL FLOW RATE	OXID FLOW RATE	FUEL VOID VOL	OXID VOID VOL	FUEL INJ TEMP	OXID INJ TEMP
0.	0.	0.	0.	0.	0.	294.000	294.000
FUEL DROP BUR	OXID DROP BUR	FUEL FLASH RATE	OXID FLASH RATE	FUEL WALL BURN	OXID WALL BURN	FUEL WALL EVAP	OXID WALL EVAP
2.492595E+03	5.142073E+03	0.	0.	0.	0.	0.	0.
FUEL GAS MASS	OXID GAS MASS	FUEL DROPLETS	OXID DROPLETS	FUEL STREAMS	OXID STREAMS	FUEL ON WALL	OXID ON WALL
5.193411E+07	1.207923E+06	3.871832E+06	6.076428E+06	0.	0.	0.	0.
FUEL GAS EFFLUX	OXID GAS EFFLUX	FUEL DROP RATE	OXID DROP RATE	FUEL FILM RATE	OXID FILM RATE	GAS FRACTION	THRUST - LBF
5.133392E+03	1.003030E+02	4.173443E+03	5.150949E+03	0.	0.	1.619315	3.77621
FUEL DROP DIA	OXID DROP DIA	FUEL INJ. VEL.	OXID INJ. VEL.	BETA ANGLE	MASS OUT OF TANK	INTEGRAL PC*00	TOTAL IMPULSE
0.	0.	0.	0.	0.	1.214821E+03	4.16557	1.237672
FUEL GAS	INJECTED MASS	GAS EXPULSED	DROPS EXPULSED	WALL EXPULSED	GAS RETAINED	DROPS RETAINED	WALL RETAINED
1.22222E+07	1.22222E+07	1.00000E+00	1.00000E+00	1.00000E+00	1.00000E+00	1.00000E+00	1.00000E+00
OXID GAS	INJECTED MASS	GAS EXPULSED	DROPS EXPULSED	WALL EXPULSED	GAS RETAINED	DROPS RETAINED	WALL RETAINED
1.22222E+07	1.22222E+07	1.00000E+00	1.00000E+00	1.00000E+00	1.00000E+00	1.00000E+00	1.00000E+00
TOTAL CHARGE	INJECTED MASS	GAS EXPULSED	DROPS EXPULSED	WALL EXPULSED	GAS RETAINED	DROPS RETAINED	WALL RETAINED
1.22222E+07	1.22222E+07	1.00000E+00	1.00000E+00	1.00000E+00	1.00000E+00	1.00000E+00	1.00000E+00
FUEL DROPS INJECTED	SUM -	SUM D SQUARED	SUM D CUBED	TOTAL MOMENTUM			
1.078494E+06	1.078494E+06	1.161409E+12	1.22222E+18	1.078494E+06			
OXID DROPS INJECTED	SUM -	SUM D SQUARED	SUM D CUBED	TOTAL MOMENTUM			
1.078494E+06	1.078494E+06	1.161409E+12	1.22222E+18	1.078494E+06			
OXID DROPS INJECTED	SUM -	SUM D SQUARED	SUM D CUBED	TOTAL MOMENTUM			
1.078494E+06	1.078494E+06	1.161409E+12	1.22222E+18	1.078494E+06			
TIME MILLISEC 51.2000	CHAMBER PRESS 49.4208	IGNITION 1.00000	FUEL FRACTION .326585	CHAMBER TEMP K 3307.67	MOL WT. 22.14569	GAMMA 1.22379	CF VAC 1.93121
FUEL INJ RATE	OXID INJ RATE	FUEL FLOW RATE	OXID FLOW RATE	FUEL VOID VOL	OXID VOID VOL	FUEL INJ TEMP	OXID INJ TEMP
0.	0.	0.	0.	0.	0.	294.000	294.000
FUEL DROP BUR	OXID DROP BUR	FUEL FLASH RATE	OXID FLASH RATE	FUEL WALL BURN	OXID WALL BURN	FUEL WALL EVAP	OXID WALL EVAP
0.	0.	0.	0.	0.	0.	0.	0.
FUEL GAS MASS	OXID GAS MASS	FUEL DROPLETS	OXID DROPLETS	FUEL STREAMS	OXID STREAMS	FUEL ON WALL	OXID ON WALL
5.193411E+07	1.207923E+06	3.871832E+06	6.076428E+06	0.	0.	0.	0.
FUEL GAS EFFLUX	OXID GAS EFFLUX	FUEL DROP RATE	OXID DROP RATE	FUEL FILM RATE	OXID FILM RATE	GAS FRACTION	THRUST - LBF
5.133392E+03	1.003030E+02	4.173443E+03	5.150949E+03	0.	0.	1.619315	3.77621
FUEL DROP DIA	OXID DROP DIA	FUEL INJ. VEL.	OXID INJ. VEL.	BETA ANGLE	MASS OUT OF TANK	INTEGRAL PC*00	TOTAL IMPULSE
0.	0.	0.	0.	0.	1.214821E+03	4.16557	1.237672

Table III-Continued

TIME MILLISEC	CHAMBER PRESS	IGNITION	FUEL FRACTION	CHAMBER TEMP K	MOL WT.	GAMMA	CF VAC
2,226791E+03	4,654273E+03	0.	0.	3321,45	28,6000	3,222057	1,939991
FUEL GAS MASS	OXID GAS MASS	FUEL DROPLETS	OXID DROPLETS	FUEL STREAMS	OXID STREAMS	FUEL ON WALL	OXID ON WALL
4,446728E+07	9,169093E+07	3,231614E+06	5,095900E+06	0.	0.	0.	0.
FUEL GAS EFFLUX	OXID GAS EFFLUX	FUEL DROP RATE	OXID DROP RATE	FUEL FLM RATE	OXID FLM RATE	GAS FRACTION	TRUST - LBE
3,716136E+03	7,564409E+03	4,173440E+03	5,130964E+03	0.	0.	1,601393	2,86841
FUEL DROP DIA	OXID DROP DIA	FUEL INJ. VEL.	OXID INJ. VEL.	BETA ANGLE	MASS OUT OF TANK	INTEGRAL PC-DT	TOTAL IMPULSE
0.	0.	0.	0.	0.	1,214021E+03	4,19051	1,238596
TIME MILLISEC	CHAMBER PRESS	IGNITION	FUEL FRACTION	CHAMBER TEMP K	MOL WT.	GAMMA	CF VAC
31,3000	37,5508	1,00000	.322485	3323,07	28,6000	3,222057	1,939991
FUEL INJ RATE	OXID INJ RATE	FUEL FLOW RATE	OXID FLOW RATE	FUEL VOID VOL	OXID VOID VOL	FUEL INJ TEMP	OXID INJ TEMP
0.	0.	0.	0.	0.	0.	294,000	294,000
FUEL DROP BUR	OXID DROP BUR	FUEL FLASH RATE	OXID FLASH RATE	FUEL WALL BURN	OXID WALL BURN	FUEL WALL EVAP	OXID WALL EVAP
1,879107E+03	3,992745E+03	0.	0.	0.	0.	0.	0.
FUEL GAS MASS	OXID GAS MASS	FUEL DROPLETS	OXID DROPLETS	FUEL STREAMS	OXID STREAMS	FUEL ON WALL	OXID ON WALL
3,997388E+07	7,027210E+07	2,660138E+06	4,220225E+06	0.	0.	0.	0.
FUEL GAS EFFLUX	OXID GAS EFFLUX	FUEL DROP RATE	OXID DROP RATE	FUEL FLM RATE	OXID FLM RATE	GAS FRACTION	TRUST - LBE
2,923988E+03	5,736688E+03	4,174056E+03	5,132801E+03	0.	0.	1,970305	2,10074
FUEL DROP DIA	OXID DROP DIA	FUEL INJ. VEL.	OXID INJ. VEL.	BETA ANGLE	MASS OUT OF TANK	INTEGRAL PC-DT	TOTAL IMPULSE
0.	0.	0.	0.	0.	1,214021E+03	4,19427	1,238978
TIME MILLISEC	CHAMBER PRESS	IGNITION	FUEL FRACTION	CHAMBER TEMP K	MOL WT.	GAMMA	CF VAC
31,3000	28,7619	1,00000	.322002	3323,07	28,6177	3,222057	1,93846
FUEL INJ RATE	OXID INJ RATE	FUEL FLOW RATE	OXID FLOW RATE	FUEL VOID VOL	OXID VOID VOL	FUEL INJ TEMP	OXID INJ TEMP
0.	0.	0.	0.	0.	0.	294,000	294,000
FUEL DROP BUR	OXID DROP BUR	FUEL FLASH RATE	OXID FLASH RATE	FUEL WALL BURN	OXID WALL BURN	FUEL WALL EVAP	OXID WALL EVAP
1,303436E+03	2,750305E+03	0.	0.	0.	0.	0.	0.
FUEL GAS MASS	OXID GAS MASS	FUEL DROPLETS	OXID DROPLETS	FUEL STREAMS	OXID STREAMS	FUEL ON WALL	OXID ON WALL
2,557950E+07	5,188933E+07	2,248577E+06	3,418517E+06	0.	0.	0.	0.
FUEL GAS EFFLUX	OXID GAS EFFLUX	FUEL DROP RATE	OXID DROP RATE	FUEL FLM RATE	OXID FLM RATE	GAS FRACTION	TRUST - LBE
2,069228E+03	4,186293E+03	3,798221E+03	5,132788E+03	0.	0.	1,540022	1,67191
FUEL DROP DIA	OXID DROP DIA	FUEL INJ. VEL.	OXID INJ. VEL.	BETA ANGLE	MASS OUT OF TANK	INTEGRAL PC-DT	TOTAL IMPULSE
0.	0.	0.	0.	0.	1,214021E+03	4,19713	1,238543
TIME MILLISEC	CHAMBER PRESS	IGNITION	FUEL FRACTION	CHAMBER TEMP K	MOL WT.	GAMMA	CF VAC
31,3000	21,1898	1,00000	.319291	3332,18	22,7129	1,22047	1,93957
FUEL INJ RATE	OXID INJ RATE	FUEL FLOW RATE	OXID FLOW RATE	FUEL VOID VOL	OXID VOID VOL	FUEL INJ TEMP	OXID INJ TEMP
0.	0.	0.	0.	0.	0.	294,000	294,000
FUEL DROP BUR	OXID DROP BUR	FUEL FLASH RATE	OXID FLASH RATE	FUEL WALL BURN	OXID WALL BURN	FUEL WALL EVAP	OXID WALL EVAP
0,114450E+04	1,968462E+03	0.	0.	0.	0.	0.	0.
FUEL GAS MASS	OXID GAS MASS	FUEL DROPLETS	OXID DROPLETS	FUEL STREAMS	OXID STREAMS	FUEL ON WALL	OXID ON WALL
1,871392E+07	3,986695E+07	1,727848E+06	2,674384E+06	0.	0.	0.	0.
FUEL GAS EFFLUX	OXID GAS EFFLUX	FUEL DROP RATE	OXID DROP RATE	FUEL FLM RATE	OXID FLM RATE	GAS FRACTION	TRUST - LBE
0.	0.	0.	0.	0.	0.	0.	0.

Table III-Continued

CHAMBER PRESS	15.5899	ISOTIION	FUEL FRACTION	CHAMBER TEMP K	MCL WT.	GAMMA	CF VAC
FUEL INJ RATE	1.75515E-04	FUEL FLOW RATE	OXID FLOW RATE	FUEL VOID VOL	OXID VOID VOL	FUEL INJ TEMP	OXID INJ TEMP
FUEL GAS MASS	1.13366E-03	FUEL FLASH RATE	OXID FLASH RATE	FUEL WALL BURN	OXID WALL BURN	FUEL WALL EVAP	OXID WALL EVAP
FUEL GAS VELOCITY	1.3366E-03	FUEL PROPERTIES	OXID PROPERTIES	FUEL STREAMS	OXID STREAMS	FUEL ON WALL	OXID ON WALL
FUEL GAS PRESS	1.43834E-07	FUEL DROPLETS	OXID DROPLETS	FUEL FILM RATE	OXID FILM RATE	GAS FRACTION	MEASURED LFP
FUEL GAS TEMP	1.92285E-03	FUEL INJ. VEL.	OXID INJ. VEL.	BETA ANGLE	MASS OUT OF TANK	INTEGRAL PCOBT	TOTAL IMPULSE
FUEL INJ. VEL.	3.7647E-03	FUEL INJ. VEL.	OXID INJ. VEL.	BETA ANGLE	MASS OUT OF TANK	INTEGRAL PCOBT	TOTAL IMPULSE
CHAMBER PRESS	15.5899	ISOTIION	FUEL FRACTION	CHAMBER TEMP K	MCL WT.	GAMMA	CF VAC
FUEL INJ RATE	1.75515E-04	FUEL FLOW RATE	OXID FLOW RATE	FUEL VOID VOL	OXID VOID VOL	FUEL INJ TEMP	OXID INJ TEMP
FUEL GAS MASS	1.13366E-03	FUEL FLASH RATE	OXID FLASH RATE	FUEL WALL BURN	OXID WALL BURN	FUEL WALL EVAP	OXID WALL EVAP
FUEL GAS VELOCITY	1.3366E-03	FUEL PROPERTIES	OXID PROPERTIES	FUEL STREAMS	OXID STREAMS	FUEL ON WALL	OXID ON WALL
FUEL GAS PRESS	1.43834E-07	FUEL DROPLETS	OXID DROPLETS	FUEL FILM RATE	OXID FILM RATE	GAS FRACTION	MEASURED LFP
FUEL GAS TEMP	1.92285E-03	FUEL INJ. VEL.	OXID INJ. VEL.	BETA ANGLE	MASS OUT OF TANK	INTEGRAL PCOBT	TOTAL IMPULSE
FUEL INJ. VEL.	3.7647E-03	FUEL INJ. VEL.	OXID INJ. VEL.	BETA ANGLE	MASS OUT OF TANK	INTEGRAL PCOBT	TOTAL IMPULSE
CHAMBER PRESS	15.5899	ISOTIION	FUEL FRACTION	CHAMBER TEMP K	MCL WT.	GAMMA	CF VAC
FUEL INJ RATE	1.75515E-04	FUEL FLOW RATE	OXID FLOW RATE	FUEL VOID VOL	OXID VOID VOL	FUEL INJ TEMP	OXID INJ TEMP
FUEL GAS MASS	1.13366E-03	FUEL FLASH RATE	OXID FLASH RATE	FUEL WALL BURN	OXID WALL BURN	FUEL WALL EVAP	OXID WALL EVAP
FUEL GAS VELOCITY	1.3366E-03	FUEL PROPERTIES	OXID PROPERTIES	FUEL STREAMS	OXID STREAMS	FUEL ON WALL	OXID ON WALL
FUEL GAS PRESS	1.43834E-07	FUEL DROPLETS	OXID DROPLETS	FUEL FILM RATE	OXID FILM RATE	GAS FRACTION	MEASURED LFP
FUEL GAS TEMP	1.92285E-03	FUEL INJ. VEL.	OXID INJ. VEL.	BETA ANGLE	MASS OUT OF TANK	INTEGRAL PCOBT	TOTAL IMPULSE
FUEL INJ. VEL.	3.7647E-03	FUEL INJ. VEL.	OXID INJ. VEL.	BETA ANGLE	MASS OUT OF TANK	INTEGRAL PCOBT	TOTAL IMPULSE
CHAMBER PRESS	15.5899	ISOTIION	FUEL FRACTION	CHAMBER TEMP K	MCL WT.	GAMMA	CF VAC
FUEL INJ RATE	1.75515E-04	FUEL FLOW RATE	OXID FLOW RATE	FUEL VOID VOL	OXID VOID VOL	FUEL INJ TEMP	OXID INJ TEMP
FUEL GAS MASS	1.13366E-03	FUEL FLASH RATE	OXID FLASH RATE	FUEL WALL BURN	OXID WALL BURN	FUEL WALL EVAP	OXID WALL EVAP
FUEL GAS VELOCITY	1.3366E-03	FUEL PROPERTIES	OXID PROPERTIES	FUEL STREAMS	OXID STREAMS	FUEL ON WALL	OXID ON WALL
FUEL GAS PRESS	1.43834E-07	FUEL DROPLETS	OXID DROPLETS	FUEL FILM RATE	OXID FILM RATE	GAS FRACTION	MEASURED LFP
FUEL GAS TEMP	1.92285E-03	FUEL INJ. VEL.	OXID INJ. VEL.	BETA ANGLE	MASS OUT OF TANK	INTEGRAL PCOBT	TOTAL IMPULSE
FUEL INJ. VEL.	3.7647E-03	FUEL INJ. VEL.	OXID INJ. VEL.	BETA ANGLE	MASS OUT OF TANK	INTEGRAL PCOBT	TOTAL IMPULSE

OXIDIZER DRIBBLE

Table III-Continued

ORIBBLE		CHAMBER PRESS		IGNITION		FUEL FRACTION		CHAMBER TEMP K		MOL WT.		GAMMA		CF VAC	
TIME MILLISEC		.699720		.01		3.111210E-07		295.286		46.0080		3.16944		3.91829	
FUEL INJ RATE		2.084744E-24		FUEL FLOW RATE		7.733734E-06		OXID VOID VOL		5.000000E-04		FUEL INJ TEMP		204.000	
OXID INJ RATE		.01		FUEL FLOW RATE		7.733734E-06		OXID VOID VOL		5.000000E-04		FUEL INJ TEMP		204.000	
OXID DROP BURST		.01		FUEL FLASH RATE		.01		OXID WALL BURN		.01		FUEL WALL EVAP		9.203280E-04	
OXID DROP BURST		.01		FUEL FLASH RATE		.01		OXID WALL BURN		.01		FUEL WALL EVAP		9.203280E-04	
FUEL GAS MASS		5.117265E-07		FUEL DROPLETS		4.212496E-7		OXID STREAMS		.01		FUEL ON WALL		1.363843E-05	
OXID GAS MASS		.01		FUEL DROPLETS		4.212496E-7		OXID STREAMS		.01		FUEL ON WALL		1.363843E-05	
FUEL GAS EFFLUX		3.247132E-03		OXID DROP RATE		9.392101E-4		OXID FILM RATE		2.276496E-04		GAS FRACTION		.365555	
OXID GAS EFFLUX		3.247132E-03		OXID DROP RATE		9.392101E-4		OXID FILM RATE		2.276496E-04		GAS FRACTION		.365555	
FUEL DROP DIAM		3.97905		OXID INJ. VEL.		.01		BETA ANGLE		.49.0000		MASS OUT OF TANK		1.214821E-03	
OXID DROP DIAM		3.97905		OXID INJ. VEL.		.01		BETA ANGLE		.49.0000		MASS OUT OF TANK		1.214821E-03	
INJECTED MASS		.20262399		GAS EXPELLED		.00043371		WALL EXPELLED		.00000000		GAS RETAINED		.00000000	
FUEL DROPS		.20262399		GAS EXPELLED		.00043371		WALL EXPELLED		.00000000		GAS RETAINED		.00000000	
OXID DROPS		.33209992		GAS EXPELLED		.00070549		WALL EXPELLED		.00023212		GAS RETAINED		.00418429	
TOTAL GRAMS		.53474591		GAS EXPELLED		.00113920		WALL EXPELLED		.00023212		GAS RETAINED		.00618629	
FUEL DROPS INJECTED		6.594018E-06		SUM N		1.739172E-04		SUM D SQUARED		4.367972E-01		TOTAL MOMENTUM		5.608931E-02	
OXID DROPS INJECTED		1.999996E-05		SUM N		1.739172E-04		SUM D SQUARED		4.367972E-01		TOTAL MOMENTUM		5.608931E-02	
OXID DROPS EJECTED		1.434799E-07		SUM N		1.739172E-04		SUM D SQUARED		4.367972E-01		TOTAL MOMENTUM		5.608931E-02	
FUEL DROPS EJECTED		4.608800E-05		SUM N		1.739172E-04		SUM D SQUARED		4.367972E-01		TOTAL MOMENTUM		5.608931E-02	
SUMMARY FOR TIME INTERVAL ENDING AT 60.00 MILLISEC		CUTOFF TRANSIENT		DROPLET MASS		WALL FILM		TOTAL MASS		.001798		.009409		.007203	
FUEL EJECTED THIS INTERVAL		.001798		WALL FILM		.000000		TOTAL MASS		.001798		.009409		.007203	
OXID EJECTED THIS INTERVAL		.009409		WALL FILM		.000000		TOTAL MASS		.001798		.009409		.007203	
PROP EJECTED THIS INTERVAL		.006990		WALL FILM		.000000		TOTAL MASS		.001798		.009409		.007203	
FUEL EJECTED THIS INTERVAL		.006990		WALL FILM		.000000		TOTAL MASS		.001798		.009409		.007203	
OXID EJECTED THIS INTERVAL		.009409		WALL FILM		.000000		TOTAL MASS		.001798		.009409		.007203	
PROP EJECTED THIS INTERVAL		.006990		WALL FILM		.000000		TOTAL MASS		.001798		.009409		.007203	
MEAN VELOCITY		199.535615		MEAN VELOCITY		149.629700		MEAN VELOCITY		159.185060		MEAN VELOCITY		159.185060	

Table III-Continued

PERFORMANCE SUMMARY

PROPELLANT MASS BASIS	FUEL FLOW	OXID FLOW	MIXTURE RATIO	C STAR	SPECIFIC IMPULSE
MASS OUT OF TANK = POUNDS	.000483	.000732	1.516897	3326.345964	197.196698
MASS THROUGH INJECTOR = POUNDS	.000447	.000732	1.638818	3427.662731	203.203047
MASS THROUGH NOZZLE = POUNDS	.000447	.000718	1.609209	3471.141926	209.740612
PRESSURE INTEGRAL = PSIA*SEC.	4.2146				
TOTAL IMPULSE = POUND*SEC.	.2396				

	FUEL	OXID	TOTAL
FRACTION EXPELLED AS GAS	.566263	.652671	.7619926
FRACTION EXPELLED AS DROPS	.431043	.325374	.365418
FRACTION EXPELLED AS FILM	.002140	.002124	.002130
FRACTION RETAINED AS GAS	.000000	.000699	.000434
FRACTION RETAINED AS DROPS	.000431	.000575	.000521
FRACTION RETAINED AS FILM	0.000000	.018628	.011569

MEAN DROP DIAMETER	INJECTED FUEL	EJECTED FUEL	INJECTED OXID	EJECTED OXID
D30	40.4804	99.9489	312.0583	87.3884
D31	50.1128	108.9756	381.4416	76.7485
D32	70.3510	122.2178	531.8354	89.9753
MEAN VELOCITY FEET/SECOND	90.81	270.18	491.70	239.91

D MICRONS	LOG D	DROP SIZE DISTRIBUTION - CUMULATIVE MASS			
		FUEL	OXID	TOTAL	
10	1.0000	0.0000	0.0000	0.0000	0.0000
20	1.3010	0.0000	0.0000	.1919	.0001
30	1.4771	.1976	.0000	.1919	.0008
40	1.6021	.1976	.0000	.2042	.1018
50	1.6990	.1976	.0000	.2099	.1061
60	1.7782	.1979	.0002	.2099	.1147
70	1.8451	.1979	.1450	.3093	.3002
80	1.9031	.2002	.1466	.4118	.3832
90	1.9542	.2002	.1466	.4176	.3837
100	2.0000	.3978	.3572	.5936	.5557
110	2.0414	.3978	.3607	.6078	.5557
120	2.0792	.4787	.3607	.7855	.5557
130	2.1139	.5954	.6228	.7855	.5557
140	2.1461	.5954	.6277	.7855	.5557
150	2.1761	.7866	.6277	.7855	.5557
160	2.2041	.7931	.6277	.7855	.5557
170	2.2304	.7931	.6277	.7855	.5557
180	2.2553	.7931	.6277	.7855	.5627
190	2.2788	.7931	.6277	.7920	.5905
200	2.3010	.7931	.6277	.8000	.9926
210	2.3222	.7931	.6277	.8115	.9938
220	2.3424	.7931	.6277	.8230	.9938
230	2.3617	.7931	.6277	.8330	.9938
240	2.3802	.7931	.6277	.8430	.9938
250	2.3979	.7931	.6277	.8527	.9959
260	2.4159	.7931	.8207	.9887	.9959
270	2.4314	.7931	.9896	.9887	.9959
280	2.4472	.9830	.9936	.9887	.9959
290	2.4624	.9995	.9950	.9887	.9959
300	2.4771	.9930	.9963	.9887	.9959
310	2.4914	.9930	.9963	.9943	.9980
320	2.5054	.9930	.9963	.9943	.9980

Table III—Concluded

330	2,5185	.9930	.9963	.9943	.9980
340	2,5315	.9930	.9963	.9943	.9980
350	2,5441	.9930	.9963	.9943	.9980
360	2,5563	.9930	.9963	.9943	.9980
370	2,5682	.9930	.9963	.9943	.9980
380	2,5797	.9930	.9963	.9943	.9980
390	2,5911	.9930	.9967	.9943	.9980
400	2,6021	.9954	.9975	.9943	.9980
410	2,6128	.9954	.9975	.9943	.9980
420	2,6232	.9954	.9975	.9943	.9980
430	2,6335	.9954	.9975	.9943	.9980
440	2,6437	.9954	.9975	.9943	.9980
450	2,6532	.9954	.9975	.9943	.9980
460	2,6628	.9954	.9975	.9943	.9980
470	2,6721	.9954	.9975	.9943	.9980
480	2,6812	.9954	.9975	.9943	.9980
490	2,6902	.9977	.9987	.9943	.9980
500	2,6990	.9977	.9987	.9943	.9980
510	2,7076	.9977	.9987	.9943	.9980
520	2,7160	.9977	.9987	.9943	.9980
530	2,7243	.9977	.9987	.9943	.9980
540	2,7324	.9977	.9987	.9943	.9980
550	2,7404	.9977	.9987	.9943	.9980
560	2,7482	.9977	.9987	.9943	.9980
570	2,7559	.9977	.9987	1,0000	1,0000
580	2,7634	.9977	.9987	1,0000	1,0000
590	2,7709	.9977	.9987	1,0000	1,0000
600	2,7782	.9977	.9987	1,0000	1,0000
610	2,7853	.9977	.9987	1,0000	1,0000
620	2,7924	.9977	.9987	1,0000	1,0000
630	2,7993	.9977	.9987	1,0000	1,0000
640	2,8062	.9977	.9987	1,0000	1,0000
650	2,8129	.9977	.9987	1,0000	1,0000
660	2,8195	.9977	.9987	1,0000	1,0000
670	2,8261	.9977	.9987	1,0000	1,0000
680	2,8325	.9977	.9987	1,0000	1,0000
690	2,8388	.9977	.9987	1,0000	1,0000
700	2,8451	.9977	.9987	1,0000	1,0000
710	2,8513	.9977	.9987	1,0000	1,0000
720	2,8573	.9977	.9987	1,0000	1,0000
730	2,8633	.9977	.9987	1,0000	1,0000
740	2,8692	.9977	.9987	1,0000	1,0000
750	2,8751	.9977	.9987	1,0000	1,0000
760	2,8808	.9977	.9987	1,0000	1,0000
770	2,8865	.9977	.9987	1,0000	1,0000
780	2,8921	.9977	.9987	1,0000	1,0000
790	2,8976	.9977	.9987	1,0000	1,0000
800	2,9031	.9977	.9987	1,0000	1,0000
810	2,9085	.9977	.9987	1,0000	1,0000
820	2,9138	.9977	.9987	1,0000	1,0000
830	2,9191	.9977	.9987	1,0000	1,0000
840	2,9243	.9977	.9987	1,0000	1,0000
850	2,9294	.9977	.9987	1,0000	1,0000
860	2,9345	.9977	.9987	1,0000	1,0000
870	2,9395	.9977	.9987	1,0000	1,0000
880	2,9445	.9977	.9987	1,0000	1,0000
890	2,9494	.9977	.9987	1,0000	1,0000
900	2,9542	.9977	.9987	1,0000	1,0000
910	2,9590	1,0000	1,0000	1,0000	1,0000

(2) Computer Graphics

Only 13 of the 69 computer plots produced for this run are illustrated here for the sake of brevity. Plots for fuel behavior are produced which are completely analogous to the oxidizer plots shown here. The oxidizer plots have been presented for this particular firing because the entire oxidizer dribble period was included while the longer fuel dribble period was not. Figure 14 is the calculated chamber pressure trace for a 50 ms pulse on the Marquardt R-6C motor. It illustrates the broad features of the pulse, which is smooth, with only modest overshoot, but has some subtle features which will be discussed later.

Figure 15 shows the oxidizer valve trace. Opening starts at $T = 0.0$ ms and is full open at 1.0 ms. It starts to close at 50 ms and is full closed at 51 ms. The fuel valve trace is identical to the oxidizer. Figure 16 shows the volume of vapor in the oxidizer dribble volume. Flow starts at $T = 0.0$ ms accelerates rapidly and the oxidizer side of the injector primes at slightly after 4 ms. Dribbling can be seen to occur between 51.8 and 51.9 ms after the conclusion of the firing. The oxidizer injection rate is illustrated in Figure 17. The injection rate of oxidizer shows a slight initial overshoot, a slight depression between $T = 7.0$ and $T = 30$ and then a steady value until cutoff. The dribble injection rate is illustrated following valve closure. The fuel is much less dense than the oxidizer and consequently the fuel flow rate increases much faster than the oxidizer flow rate. This results in a very large initial overshoot in the fuel flow rate and injection rate. For this reason the impinged stream resultant angle is initially directed in the fuel-stream direction as shown on Figure 18. The angle of injection during the dribble periods are also illustrated. Obviously the periods when the stream is mal-directed can result in deposition of propellant on the chamber wall. The next two figures illustrate this. Figure 19 illustrates the mass of oxidizer contained in the chamber in the form of streams and droplets, while Figure 20 illustrates the mass of oxidizer deposited on the wall. The mass of propellant deposited on the chamber walls from the initial mismatch of stream momentum rate can be a significant source of contaminant production, but is not often considered in calculations on engine design or operation. The oxidizer on the wall is eventually removed by the flow of wall-film through the throat and by burnoff. The walls are dry within 35 ms after start. If the pulse width had been appreciably shorter than 30 ms, the wall deposit could build up continuously over a series of pulses and the flow of wall-film would be much larger under these conditions. The rate of burnoff of fuel and oxidizer from the wall is a significant fraction of the total combustion rate for the first 35 ms of the run and is the reason for higher-than-steady-state chamber pressure before $T = 35$ ms. (Figure 14) This elevated chamber pressure is the reason for the lower than steady value for oxidizer flow rate seen on Figure 17. The volume-area mean diameter (D_{32}) of the entire chamber population of oxidizer droplets is shown in Figure 21. The effect of flash atomization at the start of the run is obvious. The preferential burning of small drops immediately after cutoff is

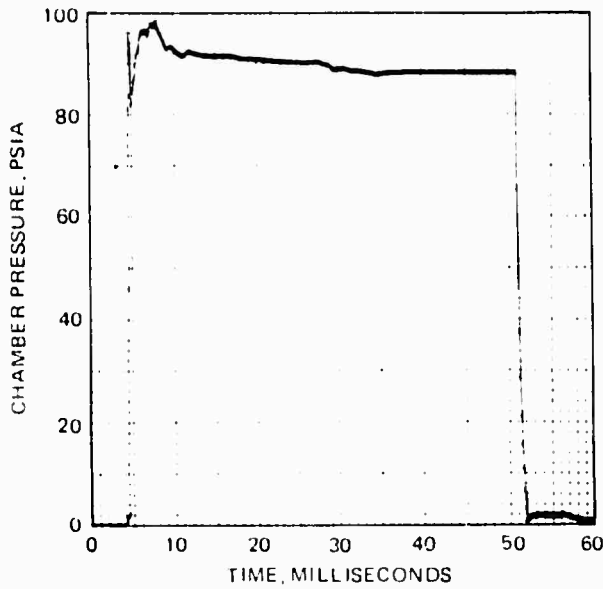


Figure 14. TCC Graphic Output - Chamber Pressure versus Time

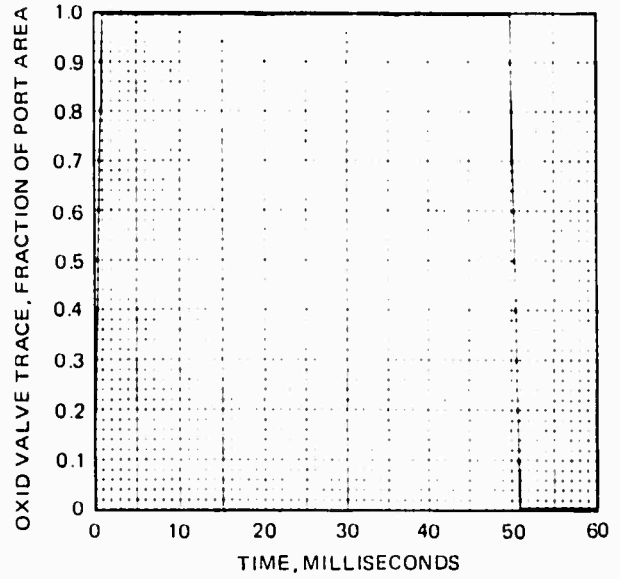


Figure 15. TCC Graphic Output - Oxidizer Valve Trace versus Time

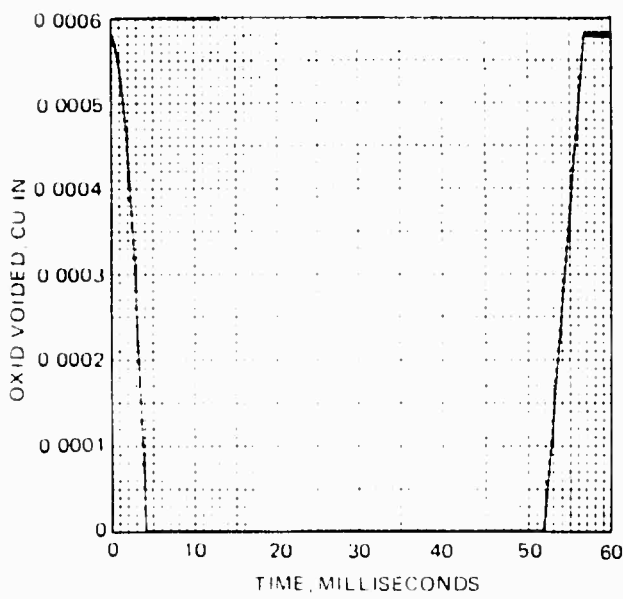


Figure 16. TCC Graphic Output - Oxidizer Voided Versus Time

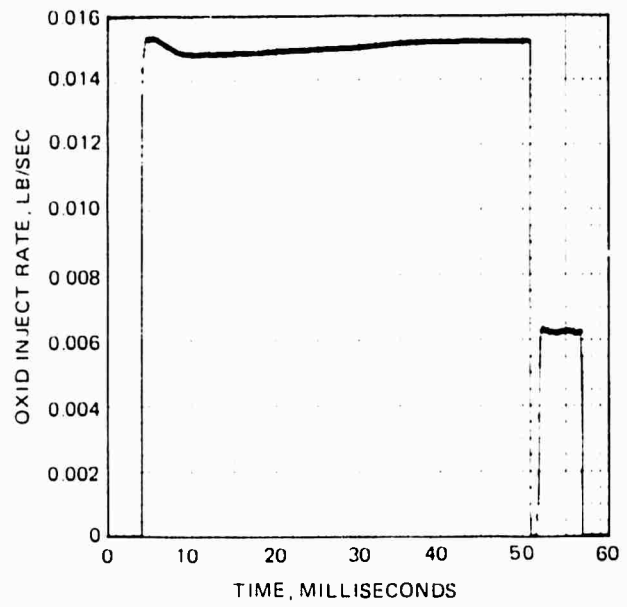


Figure 17. TCC Graphic Output - Oxidizer Injection Rate versus Time

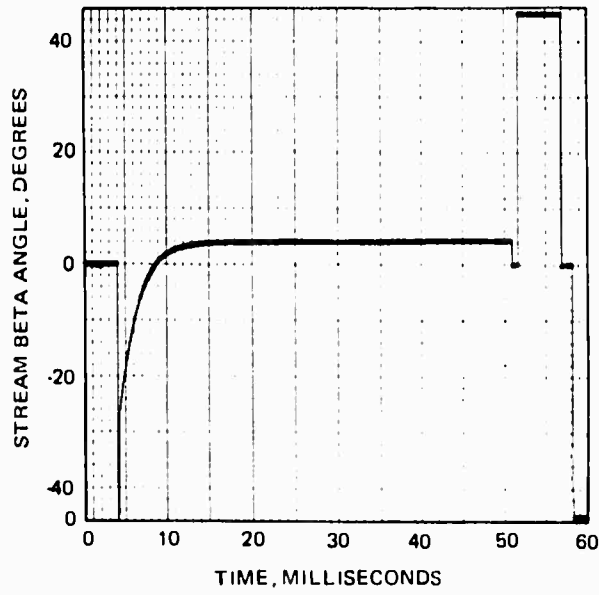


Figure 18. TCC Graphic Output - Stream Beta Angle versus Time

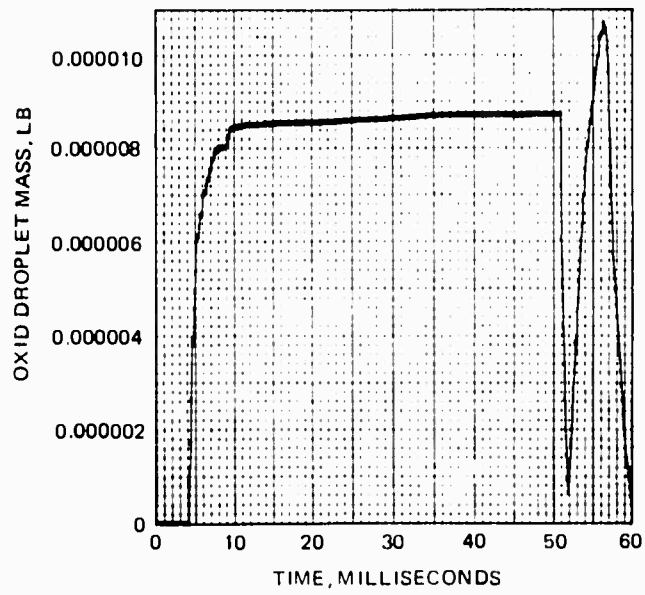


Figure 19. TCC Graphic Output - Oxidizer Droplet Mass versus Time

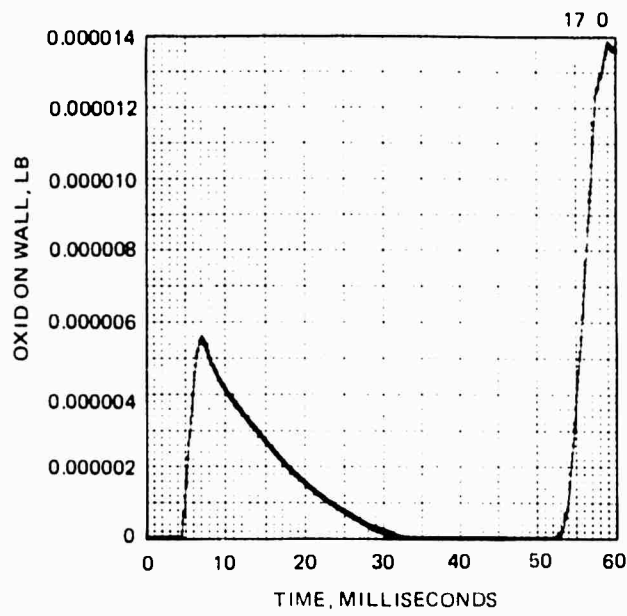


Figure 20. TCC Graphic Output - Oxidizer on Wall versus Time

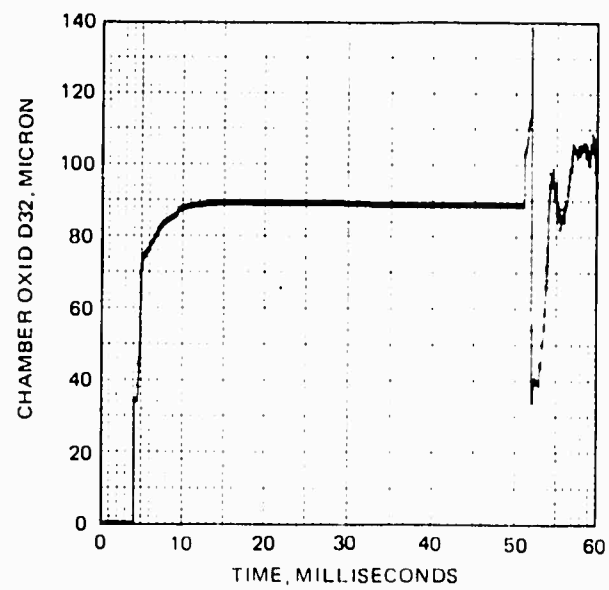


Figure 21. TCC Graphic Output - Chamber Oxidizer D32 versus Time

another prominent feature. The mean drop size in the dribble period is more complex, being composed of a mixture of small flash-atomized droplets and large single-stream-atomized droplets. The bimodal distribution of drops produced during the dribble periods can have important consequences for the ultimate droplet trajectories in the nozzle and plume for droplets which are ejected at this time. Figure 22 shows the mass flow rate for combustion gas and unburned propellant vapor leaving the motor. The chamber extinguishes at about 52 ms, so the vapor flow after this time is unburned propellant vapors. Figure 23 shows the mass flow rate for incompletely burned oxidizer droplets ejected through the throat. The ejection of incompletely burned droplets is one of the major sources of contaminant. Figure 24 shows the rate of outflow of unburned oxidizer-derived propellant in the form of wall film. It is instructive to compare this figure with the two following figures, which represent the axial distribution of wall-film material on the inside of the combustion chamber wall. When $T = 9.9$ ms, the wall-film flow is appreciable (Figure 25), and there is a coating of wall film about 1.4 thousandths of an inch thick which extends all the way through the throat. At $T = 18$ ms (Figure 26), there is no flow of wall film out of the engine although there is still an appreciable amount of unburned propellant on the wall. This is because the wall burnoff is so fast in the throat region, that no further flow of wall film through the throat is possible.

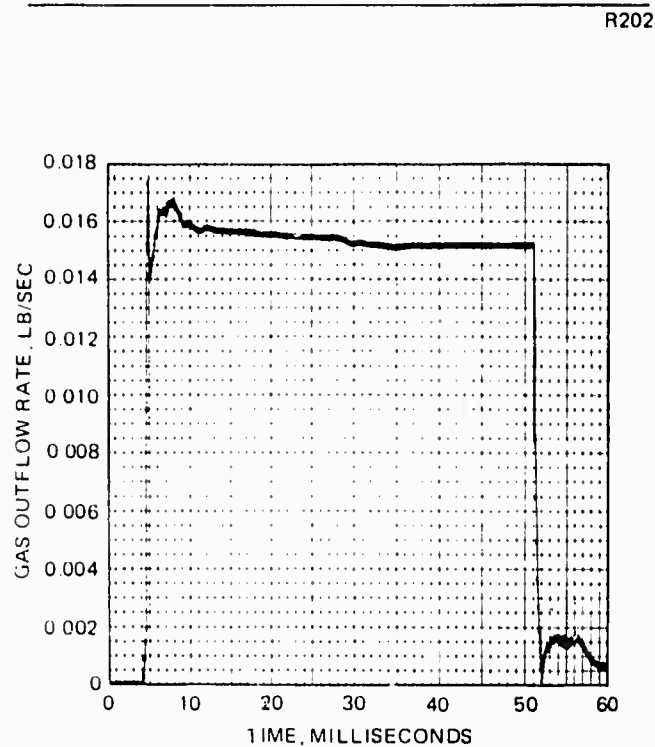


Figure 22. TCC Graphic Output - Gas Outflow Rate versus Time

R202

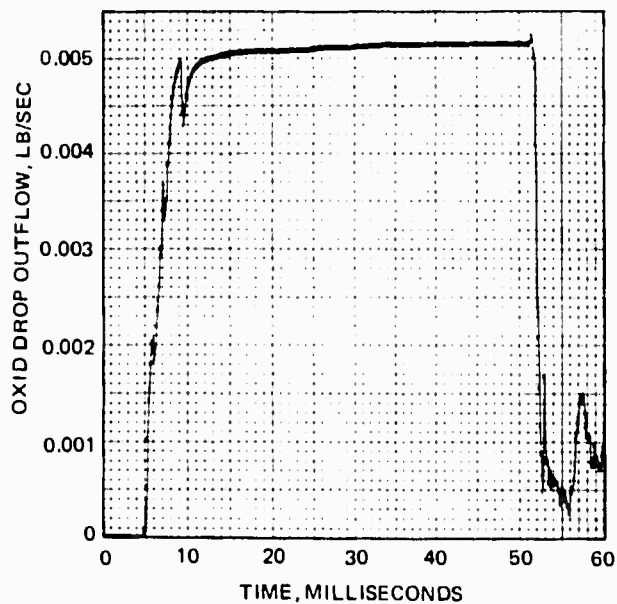


Figure 23. TCC Graphic Output - Oxidizer Droplet Outflow versus Time

R202

R202

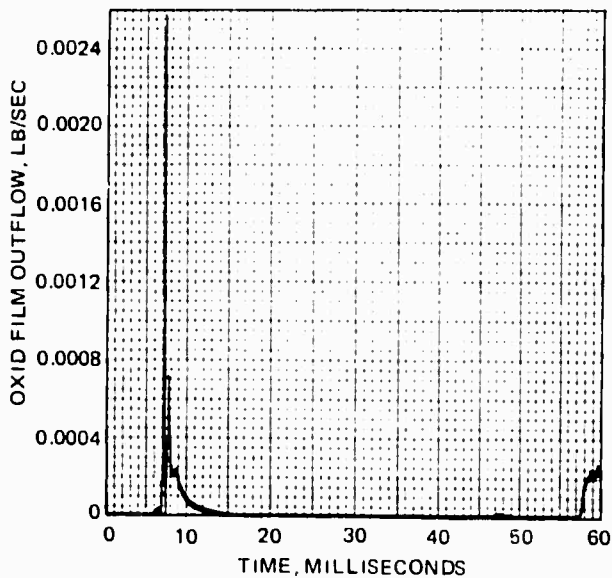


Figure 24. TCC Graphic Output - Oxidizer Film Outflow versus Time

R202

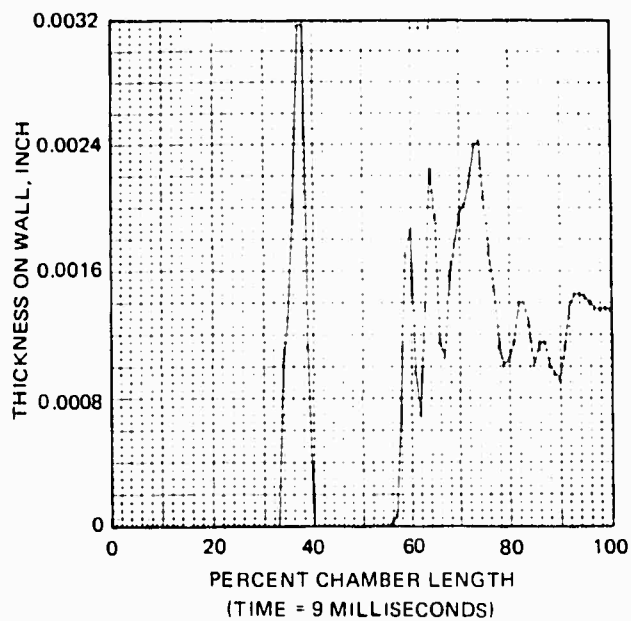


Figure 25. TCC Graphic Output - Film Thickness on Wall versus Percent Chamber Length at Time = 9 Milliseconds

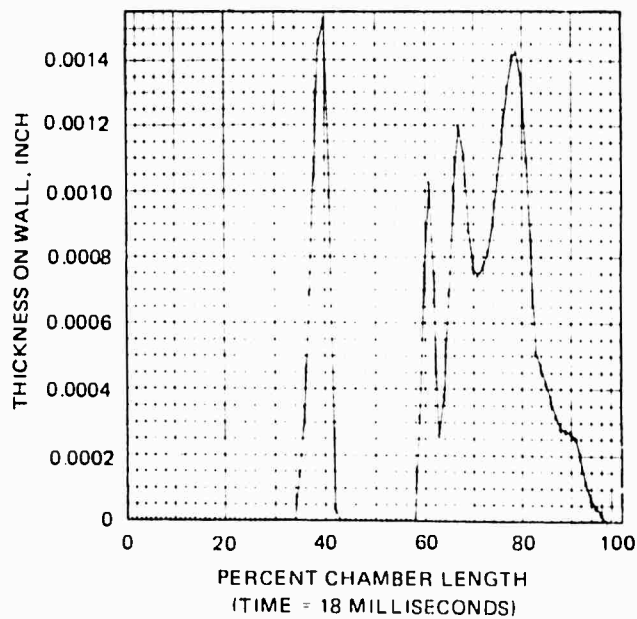


Figure 26. TCC Graphic Output - Film Thickness on Wall Versus Percent Chamber Length at Time = 18 Milliseconds

3. CONTAMINANT TRANSPORT—THE MULTRAN PROGRAM

The MULTRAN (multiphase nozzle and plume flow transport program) computes the steady-state transonic and supersonic flow field within the rocket nozzle and exhaust plume. Momentum and convective energy exchange between the gas-phase and unburned liquid droplets are completely coupled. Input to the MULTRAN analysis is derived from the TCC output by dividing the transient pulse into appropriate time "slices" and computing average values of contaminant production (droplets exiting the combustion chamber), and gas-phase properties for each time slice.

For the sample case (Marquardt R-6C engine used at NASA/LeRC), the 50 ms pulse (start of valves open to start of valves close) was divided into the following time slices:

Ignition transient	4.6 < t < 12.4 ms
Steady state	12.5 < t < 50.9 ms
Cutoff transient	51.0 < t < 60.0 ms
Post-pulse	60.1 < t < 100 ms

To demonstrate the computational procedure and results of the MULTRAN analysis, the ignition transient time segment was analyzed. The same procedure would be used to analyze the remaining three time segments, based on appropriate data from the TCC results.

a. Interpretation of TCC Results

Average properties during the ignition transient portion of the engine pulse were interpreted as follows, to be used as input to the transport analysis, MULTRAN:

<u>Variable</u>	<u>Definition</u>	<u>Value</u>
PC	Chamber pressure	90 (psia)
TGO	Chamber temperature	5750 (°R)
WPWGT	Weight fraction of unburned droplets in gas ejection from combustor	0.45
R(i)	Radius of the ith droplet group (fuel and oxidizer)	0.1, 0.3, 0.5, 1.0, 2.1, (10 ⁴ ft) (3, 9, 15, 30, 63μ)

<u>Variable</u>	<u>Definition</u>	<u>Value</u>
WPWT(I)	Weight fraction of ith droplet group in total droplet flow	0.01, 0.05, 0.10, 0.45, 0.35
GAMMA	C _p /C _v gas	1.23
PR	Prandtl number	0.7
RCAP	Gas constant	2,320 (ft ² / sec ² °R)
CPG	Specific heat of gas at constant pressure	11,350 (ft ² / sec ² °R)

The droplet groups are a composite of oxidizer drops ranging from 3 to 60 μ radius and fuel drops ranging from 15 to 80 μ radius. These values were inferred by examining the D₃₂ droplets for fuel and oxidizer over the 4.6 to 12.4 ms time increment (ignition transient).

b. MULTRAN Input—Sample Case (R-6C Engine)

Values for MULTRAN input are entered via Namelists DATA, and DATAP. Input data is printed immediately after being read in. The complete data for this case is shown in Table IV as it appeared as part of the program output. Asterisk (*) values indicate nominal data set internally. Refer to Appendix B for description of input data.

c. MULTRAN Output—Sample Case (R-6C Engine)

(1) Computer Output

A detailed description of the MULTRAN printout may be found in Appendix B. The extent of the printed output (several hundred pages) precludes presenting the entire output. Representative portions of the output are shown in Table V for the purpose of program checkout on other computer systems. The output is summarized in Figure 27.

The coordinates of the output are nondimensionalized by the nozzle throat radius which is 0.0973 inches. The nozzle has an area ratio of 40:1. The downstream limit for computations was set at 40.

Table IV. --CONTINUED

•	•	0.29E+01,
•	SI	0.3E+01,
•	SU	0.2E+01,
•	SZI	0.2E+02,
•	IORDER	3,
•	BOWCON	0.0,
•	YSW1	0,
•	ISW2	0,
•	ISW3	0,
•	VAN	0.3E+00, 0.0, 0.0, 3.1E+00, 0.1E+00, 0.0,
•	FLAG	0.0,
•	THJD	0.9E+01,
•	SAUR	0.19E+00, 0.1E+01, 0.9E+00, 0.3E+00, 0.1E+01, 0.0,
•	THFD	0.5E+01,
	EPS	0.4E+02,
•	RWPAX	0.0,
•	ZWPAX	0.0,
	IWALL	1,
	YTHW	0.12E+02,
	THJW	0.15E+02,
	NTAPE	3,
	SEND	

Table IV. -CONCLUDED

SDATAP	
ZMAX	= 0.4E+02,
PMA	= 0.45E+02,
NPM	= -1,
NPLOT	= 0,
NCASES	= 14031133549550850,
PCUT	= 0.1E-05,
EMIS	= 0.3E+00,
C1	= 0.1E+01,
C2	= 0.1E+01,
AREA	= 0.0,
DL	= 0.2E+01,
DR	= 0.2E+01,
N1	= 2,
N2	= 1,
GAMMA	= 0.123E+01,
END	

Table V-Continued

	P	H=PJ	RMO	HU=PJ	U	U=PJ	V	V=PJ	R	Z
	6.9774370E+04	7.3042904E+03	5.9946858E+03	1.2654104E+03	1.2189240E+00	1.2189240E+00	2.0791170E+00			
P	7.0845391E+04	7.3953435E+03	5.9610754E+03	1.1219500E+03	1.0966716E+00	1.0966716E+00	2.1990847E+00			
G	7.1607244E+04	7.4598973E+03	5.9697769E+03	9.4518688E+02	9.7481920E+01	9.7481920E+01	2.2306349E+00			
S	7.1933761E+04	7.4879271E+03	5.9751947E+03	9.0662037E+02	9.0257226E+01	9.0257226E+01	2.2691181E+00			
	7.187359E+07	5.71415E+07	4.35305E+03	7.81543E+02						
M	7.2549231E+04	7.5306504E+03	5.9920485E+03	4.8664415E+02	6.9247024E+01	6.9247024E+01	2.3640762E+00			
I	7.25339E+07	4.381804E+07	4.381804E+07	2.02512E+02						
I	7.1607244E+07	1.20532E+05	2.705237E+03	-4.649932E+01						
S	7.2867738E+04	7.5407787E+03	5.9977516E+03	4.706723E+02	6.271251E+01	6.271251E+01	2.3885186E+00			
I	7.168244E+07	4.32529E+07	4.32529E+07	2.12714E+02						
I	7.168244E+07	2.708145E+07	2.708145E+07	-4.11558E+01						
A	7.168244E+07	2.577346E+05	2.577346E+05	-8.725377E+01						
G	7.2751630E+04	7.5589297E+03	6.0222010E+03	5.4725929E+02	5.5494756E+01	5.5494756E+01	2.4127134E+00			
I	7.168244E+07	4.32529E+07	4.32529E+07	1.72276E+02						
I	7.168244E+07	1.227276E+05	2.711417E+07	-1.552113E+01						
I	7.168244E+07	3.91517E+07	2.577346E+05	-7.639846E+01						
I	7.168244E+07	3.774517E+04	1.342441E+07	-9.515517E+01						
	7.168244E+07	2.581418E+07	6.077630E+03	4.632247E+02	4.768544E+01	4.768544E+01	2.4371474E+00			
I	7.168244E+07	1.381100E+07	4.397761E+07	1.93111E+02						
I	7.168244E+07	1.20532E+05	4.716071E+07	-2.944425E+01						
I	7.168244E+07	3.91517E+07	4.154437E+07	-4.427485E+01						
I	7.168244E+07	2.708145E+07	1.342441E+07	-2.15212E+01						
I	7.168244E+07	5.758572E+04	5.846211E+07	-8.44313E+01						
	7.2890271E+04	7.5589297E+03	5.9977516E+03	4.587341E+02	4.768544E+01	4.768544E+01	2.4672134E+00			
I	7.168244E+07	4.32529E+07	4.32529E+07	1.590725E+02						
I	7.168244E+07	1.20532E+05	4.716071E+07	-2.434431E+01						
I	7.168244E+07	3.91517E+07	2.577346E+05	-4.95455E+01						
I	7.168244E+07	2.708145E+07	1.342441E+07	-2.15212E+01						
I	7.168244E+07	5.758572E+04	5.846211E+07	-8.44313E+01						
	7.294111E+04	7.577917E+03	6.086874E+03	2.707945E+02	2.4371474E+01	2.4371474E+01	2.5071474E+00			
I	7.168244E+07	4.32529E+07	4.32529E+07	1.41074E+02						
I	7.168244E+07	1.20532E+05	2.717031E+07	-3.47214E+01						
I	7.168244E+07	3.91517E+07	2.577346E+05	-7.23344E+01						
I	7.168244E+07	2.708145E+07	1.342441E+07	-1.72313E+01						
I	7.168244E+07	5.758572E+04	5.846211E+07	-8.44313E+01						
	7.294111E+04	7.577917E+03	6.086874E+03	1.82833E+02	2.4371474E+01	2.4371474E+01	2.5471474E+00			
I	7.168244E+07	4.32529E+07	4.32529E+07	1.174667E+02						
I	7.168244E+07	1.20532E+05	4.62437E+07	-1.46374E+01						
I	7.168244E+07	3.91517E+07	2.577346E+05	-7.24513E+01						
I	7.168244E+07	2.708145E+07	1.342441E+07	-1.54573E+01						
I	7.168244E+07	5.758572E+04	5.846211E+07	-8.44313E+01						
	7.294111E+04	7.577917E+03	6.086874E+03	1.82833E+02	2.4371474E+01	2.4371474E+01	2.5471474E+00			
I	7.168244E+07	4.32529E+07	4.32529E+07	1.174667E+02						
I	7.168244E+07	1.20532E+05	4.62437E+07	-1.46374E+01						
I	7.168244E+07	3.91517E+07	2.577346E+05	-7.24513E+01						
I	7.168244E+07	2.708145E+07	1.342441E+07	-1.54573E+01						
I	7.168244E+07	5.758572E+04	5.846211E+07	-8.44313E+01						

NOT REPRODUCIBLE

Table V-Continued

LRC ID	K	HEK	Z	R	MPC	P	ISP	MPK
			2.86913	.00000	.87406	19.38203		
			2.86727	.00000	.00000	14.78000		
			2.86864	.00000	.00000	14.00000		
			2.86784	.00000	.00000	13.00000		
			2.86813	.00000	.00000	11.37100		
			2.86833	.00000	.00000	9.90747		
			2.86853	.00000	.00000	9.59887		

TOTAL MASS FLOW = 1.2746367E=02 NO. POINTS = 7

LRC ID	K	HEK	Z	R	VG	YMETAG	IG/TOG	PG/PGG	DG/DCG	SDK/DG	CF	ISP	MPK
4	14	.69247	2.36408	1.7531	4147.6	8031.3	6.537	.72132	1.7389	.24121	.00012	0.0000	0.00
			1	6.05269E=01	4.38745E=03	2.88531E=00	5.33747E=03	1.16707E=04	6.25579E=05	1.00000E=00			
4	4	.92813	2.63216	1.8982	3989.1	8387.6	9.616	.89011	1.33726	.19890	.00013	0.0000	0.00
			1	5.84768E=01	4.53929E=03	4.30810E=00	5.31638E=03	1.26973E=04	5.61214E=05	1.00000E=00			
4	5	1.93128	3.29930	2.1864	3621.7	7028.9	15.000	.62986	.08407	.13347	0.00000	1.3767	249.33

LRC ID	K	HEK	Z	R	MPC	P	ISP	MPK
			2.86408	.87247	.34884	13.65904		
			2.86469	.79842	.41064	14.12137		
			2.86216	.92815	.49985	12.35341		
			2.86874	.97824	.57647	11.72334		
			2.84081	1.11383	.64072	10.17480		
			2.98932	1.28466	.75012	8.80404		
			3.06789	1.32958	.81076	8.25373		
			3.29530	1.53128	1.00000	7.56636		

TOTAL MASS FLOW = 1.2746367E=02 NO. POINTS = 5

LRC ID	K	HEK	Z	R	VG	YMETAG	IG/TOG	PG/PGG	DG/DCG	SDK/DG	CF	ISP	MPK
5	14	.62713	2.36852	1.7522	4148.8	8029.0	5.903	.72152	1.7426	.24151	.00172	0.0000	0.00
			1	6.05269E=01	4.38745E=03	2.88531E=00	5.33747E=03	1.16707E=04	6.25579E=05	1.00000E=00			
5	4	.92813	2.63216	1.8982	3989.1	8387.6	9.616	.89011	1.33726	.19890	.00013	0.0000	0.00
			1	5.84768E=01	4.53929E=03	4.30810E=00	5.31638E=03	1.26973E=04	5.61214E=05	1.00000E=00			
5	5	1.93128	3.29930	2.1864	3621.7	7028.9	15.000	.62986	.08407	.13347	0.00000	1.3767	249.33

LRC ID	K	HEK	Z	R	VG	YMETAG	IG/TOG	PG/PGG	DG/DCG	SDK/DG	CF	ISP	MPK
			2.86852	.62713	.28427	15.68311							
			2.82598	.65933	.30170	15.21737							
			2.86274	.69391	.31945	14.76351							
			2.85214	.76682	.36467	13.70337							
			2.70442	.80094	.40094	11.96259							
			2.74903	.83734	.43774	11.48845							
			2.76345	.84984	.46656	11.33734							
			2.92184	1.08810	.58846	9.81991							
			3.07780	1.22819	.69820	8.47892							
			3.15750	1.29842	.74492	8.19372							
			3.39474	1.51068	.93945	7.32459							
			3.48583	1.57666	1.00000	7.09844							

TOTAL MASS FLOW = 1.2746367E=02 NO. POINTS = 12

Table A-Continued

LRC TO	R	K	REK	Z	HACH	VG	THEYAG	TPK	WG/PGO	SG/DPO	CF	ISF
TOTAL PASS FLOW = 2.7942546E+02 NO. POINTS = 61												
					VPK	TPK	DPK/DO	DPK/DPO				RPK
31	3	0.00000	5.86850	2.7948	2957.6	0.000	0.000	0.000	0.000	0.000	0.000	0.00
1	2.59556E-01	5.57377E-03	0.1	5.190039E-03	0.000	0.000	0.000	0.000	0.000	0.000	0.000	0.00
2	1.38162E-00	3.46775E-03	0.1	5.448445E-03	6.20415E-02	3.000000E-03	5.172239E-03	2.982417E-03	1.000000E-03	3.000000E-03	1.000000E-03	0.00
3	2.70363E-00	2.65646E-03	0.1	5.825645E-03	2.19499E-02	2.633913E-01	5.000000E-03	2.19499E-02	2.633913E-01	5.000000E-03	2.633913E-01	5.000000E-03
4	4.29822E+00	1.73637E-03	0.1	5.602231E-03	3.032467E-01	3.637475E-00	1.000000E-04	3.032467E-01	3.637475E-00	1.000000E-04	3.637475E-00	1.000000E-04
5	1.460535E+01	1.02933E-03	0.1	5.60058E-03	1.491004E+00	1.752488E+01	2.100000E-04	1.491004E+00	1.752488E+01	2.100000E-04	1.752488E+01	2.100000E-04
31	4	1.7455	6.33984	2.922	2450.5	8277.3	1.676	1.49575	0.2263	0.4565	2.79768	0.000
1	2.236487E-01	5.46527E-03	1.742654E-00	5.1161003E-03	2.274815E-04	2.307864E-03	1.000000E-03	2.274815E-04	2.307864E-03	1.000000E-03	2.307864E-03	1.000000E-03
2	1.22712E+00	3.526430E-03	4.74040E-01	5.442948E-03	5.736828E-03	5.920174E-02	3.000000E-03	5.736828E-03	5.920174E-02	3.000000E-03	5.920174E-02	3.000000E-03
3	2.305193E+00	2.715307E-03	1.197293E-01	5.921149E-03	2.50070E-02	2.537031E-01	5.000000E-03	2.50070E-02	2.537031E-01	5.000000E-03	2.537031E-01	5.000000E-03
4	5.526273E+00	1.791546E-03	6.157333E-01	5.599753E-03	3.653820E-01	3.706904E+00	1.000000E-04	3.653820E-01	3.706904E+00	1.000000E-04	3.706904E+00	1.000000E-04
5	1.25774E+01	1.127322E-03	3.162248E-01	5.657415E-03	2.40330E+00	2.436217E+01	2.100000E-04	2.40330E+00	2.436217E+01	2.100000E-04	2.436217E+01	2.100000E-04
31	4	1.36423	6.83721	2.9745	2781.0	8381.1	2.952	1.48305	0.1999	0.4134	4.4562	0.000
1	2.46332E-01	5.76767E-03	2.16953E-00	5.171786E-03	2.233868E-04	2.333764E-03	1.000000E-03	2.233868E-04	2.333764E-03	1.000000E-03	2.333764E-03	1.000000E-03
2	1.12154E+00	3.58525E-03	1.59000E-01	5.437308E-03	5.805497E-03	4.33204E-02	3.000000E-03	5.805497E-03	4.33204E-02	3.000000E-03	4.33204E-02	3.000000E-03
3	2.21276E+00	2.785914E-03	3.26376E-01	5.516549E-03	2.586769E-02	2.376273E-01	5.000000E-03	2.586769E-02	2.376273E-01	5.000000E-03	2.376273E-01	5.000000E-03
4	5.15778E+00	1.82791E-03	1.129755E-01	5.595349E-03	4.137276E-01	3.80698E+00	1.000000E-04	4.137276E-01	3.80698E+00	1.000000E-04	3.80698E+00	1.000000E-04
31	4	1.57644	7.36646	3.1257	2733.7	8450.7	2.397	1.47842	0.1842	0.33674	4.1377	0.000
1	1.634137E-01	5.94867E-03	3.111640E-00	5.116292E-03	2.092764E-04	1.801756E-03	1.000000E-03	2.092764E-04	1.801756E-03	1.000000E-03	1.801756E-03	1.000000E-03
2	1.77114E+00	3.649284E-03	1.613044E-01	5.431761E-03	5.63897E-03	4.854873E-02	3.000000E-03	5.63897E-03	4.854873E-02	3.000000E-03	4.854873E-02	3.000000E-03
3	2.13359E+00	2.84939E-03	5.47165E-01	5.51222E-03	2.592496E-02	2.232002E-01	5.000000E-03	2.592496E-02	2.232002E-01	5.000000E-03	2.232002E-01	5.000000E-03
31	4	1.82035	7.92917	3.1913	2673.0	8536.4	3.251	1.46511	0.1645	0.33537	4.0541	0.000
1	1.76559E-01	5.94867E-03	4.12191E-00	5.153254E-03	2.092764E-04	1.801756E-03	1.000000E-03	2.092764E-04	1.801756E-03	1.000000E-03	1.801756E-03	1.000000E-03
2	1.78751E+00	3.76607E-03	2.174131E-01	5.424605E-03	5.595955E-03	4.395017E-02	3.000000E-03	5.595955E-03	4.395017E-02	3.000000E-03	4.395017E-02	3.000000E-03
31	4	1.87855	1.83723	3.4119	2461.6	8427.9	7.730	1.41753	0.1926	0.2219	4.0020	0.000
1	1.73407E-01	5.25188E-03	7.150126E-00	5.128273E-03	2.002044E-02	1.779321E-04	1.000000E-03	2.002044E-02	1.779321E-04	1.000000E-03	1.779321E-04	1.000000E-03
31	0	5.17727	1.87651	4.2965	1707.6	8735.5	13.070	1.31243	0.1596	0.0627	4.0000	1.4655
1	2.66850	5.97359	0.5116	0.00000	0.00000	0.00000	2.499E-1	2.499E-1	0.00000	0.00000	0.00000	0.00000
2	1.96464	2.4275	0.029	0.00000	0.00000	0.00000	2.3358E-1	2.3358E-1	0.00000	0.00000	0.00000	0.00000
3	6.14416	0.6706	0.0046	0.00000	0.00000	0.00000	2.3156E-1	2.3156E-1	0.00000	0.00000	0.00000	0.00000
4	6.11718	0.0335	0.0000	0.00000	0.00000	0.00000	2.2466E-1	2.2466E-1	0.00000	0.00000	0.00000	0.00000
5	6.15824	1.1291	0.0124	0.00000	0.00000	0.00000	2.19514E-1	2.19514E-1	0.00000	0.00000	0.00000	0.00000
6	6.21423	1.3463	0.0176	0.00000	0.00000	0.00000	2.3357E-1	2.3357E-1	0.00000	0.00000	0.00000	0.00000
7	5.27053	1.5697	0.0237	0.00000	0.00000	0.00000	2.7827E-1	2.7827E-1	0.00000	0.00000	0.00000	0.00000
8	6.31944	1.7455	0.0299	0.00000	0.00000	0.00000	2.3345E-1	2.3345E-1	0.00000	0.00000	0.00000	0.00000
9	6.37454	1.9233	0.0374	0.00000	0.00000	0.00000	1.86789E-1	1.86789E-1	0.00000	0.00000	0.00000	0.00000
10	6.44447	2.243R	0.0434	0.00000	0.00000	0.00000	1.82904E-1	1.82904E-1	0.00000	0.00000	0.00000	0.00000
11	6.51145	2.5329	0.0631	0.00000	0.00000	0.00000	1.86974E-1	1.86974E-1	0.00000	0.00000	0.00000	0.00000
12	6.57560	2.7341	0.0726	0.00000	0.00000	0.00000	1.96155E-1	1.96155E-1	0.00000	0.00000	0.00000	0.00000
13	6.64133	3.0846	0.0861	0.00000	0.00000	0.00000	1.83824E-1	1.83824E-1	0.00000	0.00000	0.00000	0.00000
14	6.71638	3.5192	0.1040	0.00000	0.00000	0.00000	1.82421E-1	1.82421E-1	0.00000	0.00000	0.00000	0.00000
15	6.77492	3.9931	0.1176	0.00000	0.00000	0.00000	1.81194E-1	1.81194E-1	0.00000	0.00000	0.00000	0.00000
16	6.83721	4.5413	0.1337	0.00000	0.00000	0.00000	1.79941E-1	1.79941E-1	0.00000	0.00000	0.00000	0.00000
17	6.89317	5.0942	0.1435	0.00000	0.00000	0.00000	1.79174E-1	1.79174E-1	0.00000	0.00000	0.00000	0.00000
18	6.95440	5.6303	0.1607	0.00000	0.00000	0.00000	1.77200E-1	1.77200E-1	0.00000	0.00000	0.00000	0.00000
19	7.01884	6.1632	0.1832	0.00000	0.00000	0.00000	1.75044E-1	1.75044E-1	0.00000	0.00000	0.00000	0.00000
20	7.08634	6.7168	0.2105	0.00000	0.00000	0.00000	1.72706E-1	1.72706E-1	0.00000	0.00000	0.00000	0.00000
21	7.15724	7.2971	0.2477	0.00000	0.00000	0.00000	1.70209E-1	1.70209E-1	0.00000	0.00000	0.00000	0.00000
22	7.23123	7.8944	0.2976	0.00000	0.00000	0.00000	1.67872E-1	1.67872E-1	0.00000	0.00000	0.00000	0.00000
23	7.30948	8.5046	0.3598	0.00000	0.00000	0.00000	1.6577E-1	1.6577E-1	0.00000	0.00000	0.00000	0.00000
24	7.39160	9.1478	0.4344	0.00000	0.00000	0.00000	1.63415E-1	1.63415E-1	0.00000	0.00000	0.00000	0.00000

NOT REPRODUCIBLE

Table V-Continued

7.51451	1.65061	0.3750	1.51127
7.65217	1.69091	0.4214	1.57839
7.78229	1.74004	0.4692	1.64457
7.90659	1.78780	0.5186	1.71034
8.02517	1.83529	0.5693	1.77574
8.13817	1.88251	0.6214	1.84077
8.24559	1.92946	0.6749	1.90544
8.34744	1.97614	0.7297	1.96977
8.44374	2.02256	0.7857	2.03377
8.53451	2.06872	0.8429	2.09734
8.61977	2.11463	0.9014	2.16049
8.70054	2.16029	0.9611	2.22324
8.77684	2.20571	1.0220	2.28559
8.84869	2.25089	1.0841	2.34754
8.91609	2.29584	1.1474	2.40909
8.97904	2.34056	1.2119	2.47024
9.03754	2.38505	1.2776	2.53099
9.09159	2.42932	1.3445	2.59134
9.14119	2.47337	1.4126	2.65129
9.18734	2.51721	1.4818	2.71084
9.23004	2.56084	1.5521	2.77009
9.26929	2.60427	1.6235	2.82894
9.30509	2.64750	1.6960	2.88739
9.33744	2.69053	1.7696	2.94544
9.36634	2.73337	1.8443	3.00309
9.39179	2.77602	1.9201	3.06034
9.41379	2.81849	1.9970	3.11719
9.43234	2.86078	2.0750	3.17364
9.44744	2.90289	2.1541	3.22969
9.45909	2.94482	2.2343	3.28534
9.46729	2.98658	2.3156	3.34059
9.47204	3.02817	2.3980	3.39544
9.47434	3.06959	2.4815	3.45009
9.47329	3.11085	2.5661	3.50444
9.46884	3.15196	2.6518	3.55849
9.46109	3.19293	2.7386	3.61224
9.45004	3.23377	2.8265	3.66569
9.43569	3.27449	2.9155	3.71884
9.41804	3.31509	3.0056	3.77169
9.39709	3.35558	3.0968	3.82424
9.37284	3.39597	3.1891	3.87649
9.34529	3.43727	3.2825	3.92834
9.31444	3.47848	3.3770	3.97979
9.28029	3.51961	3.4726	4.03084
9.24284	3.56066	3.5693	4.08149
9.20209	3.60163	3.6671	4.13174
9.15804	3.64253	3.7660	4.18159
9.11069	3.68336	3.8660	4.23104
9.06004	3.72413	3.9671	4.28009
9.00609	3.76484	4.0693	4.32874
8.94884	3.80550	4.1726	4.37709
8.88829	3.84611	4.2770	4.42514
8.82444	3.88668	4.3825	4.47289
8.75729	3.92721	4.4891	4.52034
8.68684	3.96770	4.5968	4.56749
8.61309	4.00816	4.7056	4.61434
8.53604	4.04859	4.8155	4.66089
8.45579	4.08899	4.9265	4.70714
8.37234	4.12936	5.0386	4.75309
8.28569	4.16971	5.1518	4.79874
8.19584	4.21004	5.2661	4.84409
8.10279	4.25035	5.3815	4.88914
8.00654	4.29064	5.4980	4.93389
7.90709	4.33091	5.6156	4.97834
7.80434	4.37116	5.7343	5.02249
7.69829	4.41139	5.8541	5.06634
7.58894	4.45160	5.9750	5.10989
7.47629	4.49179	6.0970	5.15314
7.36034	4.53196	6.2201	5.19609
7.24109	4.57211	6.3453	5.23874
7.11844	4.61224	6.4716	5.28109
6.99239	4.65235	6.5990	5.32314
6.86284	4.69244	6.7275	5.36489
6.72989	4.73251	6.8571	5.40634
6.59354	4.77256	6.9888	5.44749
6.45379	4.81259	7.1216	5.48834
6.31064	4.85260	7.2565	5.52889
6.16409	4.89259	7.3935	5.56914
6.01414	4.93256	7.5326	5.60909
5.86079	4.97251	7.6738	5.64874
5.70404	5.01244	7.8171	5.68809
5.54389	5.05235	7.9625	5.72714
5.38024	5.09224	8.1100	5.76589
5.21309	5.13211	8.2596	5.80434
5.04244	5.17196	8.4113	5.84249
4.86829	5.21179	8.5651	5.88034
4.69064	5.25160	8.7210	5.91789
4.50949	5.29139	8.8790	5.95514
4.32484	5.33116	9.0391	5.99209
4.13669	5.37091	9.2013	6.02874
3.94504	5.41064	9.3656	6.06509
3.75089	5.45035	9.5320	6.10114
3.55424	5.49004	9.7005	6.13689
3.35509	5.52971	9.8711	6.17224
3.15244	5.56936	10.0438	6.20729
2.94629	5.60899	10.2186	6.24204
2.73664	5.64860	10.3955	6.27649
2.52349	5.68819	10.5745	6.31064
2.30684	5.72776	10.7556	6.34449
2.08669	5.76731	10.9388	6.37794
1.86304	5.80684	11.1241	6.41109
1.63589	5.84635	11.3115	6.44394
1.40524	5.88584	11.5010	6.47649
1.17109	5.92531	11.6926	6.50874
0.93344	5.96476	11.8863	6.54069
0.69229	5.99419	12.0821	6.57234
0.44764	6.02360	12.2800	6.60369
0.20049	6.05299	12.4800	6.63474
0.00000	6.08236	12.6821	6.66549
	6.11171	12.8863	6.69584
	6.14104	13.0926	6.72589
	6.17035	13.3010	6.75564
	6.20064	13.5115	6.78509
	6.23091	13.7241	6.81424
	6.26116	13.9388	6.84309
	6.29139	14.1556	6.87164
	6.32160	14.3745	6.90009
	6.35179	14.5955	6.92824
	6.38196	14.8186	6.95609
	6.41211	15.0438	6.98364
	6.44224	15.2711	7.01099
	6.47235	15.5005	7.03814
	6.50244	15.7320	7.06509
	6.53251	15.9656	7.09184
	6.56256	16.2013	7.11839
	6.59259	16.4391	7.14474
	6.62260	16.6790	7.17089
	6.65260	16.9210	7.19684
	6.68259	17.1651	7.22259
	6.71256	17.4113	7.24814
	6.74251	17.6596	7.27349
	6.77244	17.9100	7.29864
	6.80235	18.1625	7.32359
	6.83224	18.4171	7.34834
	6.86211	18.6738	7.37289
	6.89196	18.9326	7.39724
	6.92179	19.1935	7.42139
	6.95160	19.4565	7.44534
	6.98139	19.7216	7.46909
	6.99999	19.9888	7.49264
	7.01850	20.2581	7.51609
	7.03691	20.5295	7.53934
	7.05522	20.8030	7.56239
	7.07353	21.0786	7.58524
	7.09174	21.3563	7.60789
	7.10985	21.6371	7.63034
	7.12786	21.9200	7.65259
	7.14577	22.2050	7.67464
	7.16358	22.4921	7.69649
	7.18129	22.7813	7.71814
	7.19890	23.0726	7.73959
	7.21641	23.3660	7.76084
	7.23382	23.6615	7.78189
	7.25113	23.9591	7.80274
	7.26834	24.2588	7.82339
	7.28545	24.5606	7.84384
	7.30246	24.8645	7.86409
	7.31937	25.1705	7.88414
	7.33618	25.4786	7.90399
	7.35289	25.7888	7.92464
	7.36950	26.0911	7.94509
	7.38601	26.3955	7.96534
	7.40242	26.7020	7.98539
	7.41873	27.0106	7.99999
	7.43494	27.3213	8.01424
	7.45105	27.6341	8.02829
	7.46706	27.9490	8.04204
	7.48297	28.2660	8.05559
	7.49878	28.5851	8.06894
	7.51449	28.9063	8.08209
	7.53010	29.2296	8.09504
	7.54561	29.5550	8.10779
	7.56102	29.8825	8.12034
	7.57633	30.2121	8.13269
	7.59154	30.5438	8.14484
	7.60665	30.8776	8.15679
	7.62166	31.2135	8.16854
	7.63657	31.5515	8.18009
	7.65138	31.8916	8.19144
	7.66609	32.2338	8.20259
	7.68070	32.5781	8.21354
	7.69521	32.9245	8.22429
	7.70962	33.2730	8.23484
	7.72393	33.6236	8.24519
	7.73814	33.9763	8.25534
	7.75225	34.3311	8.26539
	7.76626	34.6880	8.27524
	7.78017	35.0470	8.28489
	7.79398	35.4081	8.29434
	7.80769	35.7713	8.30359
	7.82130	36.1366	8.31264
	7.83481	36.5040	8.32149
	7.84822	36.8735	8.33014
	7.86153	37.2451	8.33859
	7.87474	37.6188	8.34684
	7.88785	37.9946	8.35489
	7.90086	38.3725	8.36274
	7.91377	38.7525	8.37039
	7.92658	39.1346	8.37784
	7.93929	39.5188	8.38509
	7.95190	39.9051	8.39214
	7.96441	40.2935	8.39909
	7.97682	40.6840	8.40584
	7.98913	41.0766	8.41239
	7.99999	41.4713	8.41874
	8.01030	41.8681	8.42489
	8.02011	42.2670	8.43084
	8.02942	42.6680	8.43659
	8.03823	43.0711	8.44214
	8.04654	43.4763	8.44749
	8.05435	43.8836	8.45264
	8.06166	44.2930	8.45759
	8.06847	44.7045	8.46234
	8.07478	45.1181	8.46689
	8.08059	45.5338	8.47134
	8.08590	45.9516	8.47559
	8.09071	46.3715	8.47964
	8.09502	46.7935	8.48349
	8.09883	47.2176	8.48714
	8.10214	47.6438	8.49059
	8.10595	48.0721	8.49384
	8.10926	48.5025	8.49689
	8.11207	48.9350	8.49974
	8.11438	49.3696	8.50239
	8.11619	49.8063	8.50484
	8.11750	50.2451	8.50709
	8.11831	50.6860	8.50914
	8.11872	51.1290	8.51099
	8.11873	51.5741	8.51264
	8.11834	52.0213	8.51409
	8.11755	52.4706	8.51534
	8.11636	52.9220	8.51639
	8.11477	53.3755	8.51724
	8.11278	53.8311	8.51789
	8.11039	54.2888	8.51834
	8.10760	54.7486	8.51859
	8.10441	55.2105	8.51864
	8.10082	55.6745	8.51849
	8.09683	56.1406	8.51814
	8.09244	56.6088	8.51759
	8.08765	57.0791	8.51684
	8.08246	57.5515	8.51589
	8.07687	58.0260	8.51474
	8.07088	58.5026	8.51339
	8.06449	58.9813	8.51184
	8.05770	59.4621	8.51009
	8.05051	59.9450	8.50814
	8.04292	60.4300	8.50599
	8.03493	60.9171	8.50364
	8.02654	61.4063	8.50109
	8.01775	61.8976	8.49834
	8.00856	62.3910	8.49539
	8.00000	62.8865	8.49224
	7.99101	63.3841	8.48889
	7.98152	63.8838	8.48534
	7.97163	64.3856	8.48159
</			

Table V-Continued

BEGINNING OF T-O-PHASE PLUME PROGRAM

CP TIME = 286.749 PP TIME = 133.692

3-5-5 PARTICLE FLOW

SIMPLE JET SPREADING

LINE NO	K	DEA	Z	WIND	VELOCITY	VELOCITY	TPK	DPK/DS	DPK/DS	DPK/DS	SRK/DS	RPK
1	5	5.7339	18.75349	4.4677	1772.1	9845.6	19.274	.29716	1.488553E-03	5.7110226E-03	0.03000	5
1	5	5.7339	19.75349	4.4551	1871.6	9472.5	22.490	.27958	1.778271E-03	1.849943E-03	0.03000	5
1	5	5.7339	20.75349	4.4664	1974.1	10094.3	25.775	.26245	7.574651E-04	2.924284E-03	0.03000	5
1	5	5.7339	21.75349	5.3862	1412.7	10212.1	26.921	.24563	5.392144E-04	2.194770E-03	0.03000	5
1	5	5.7339	22.75349	5.4233	1310.5	10329.9	28.177	.22931	3.723883E-04	1.626125E-03	0.03000	5
1	5	5.7339	23.75349	5.5776	1226.7	10432.9	29.353	.21354	2.534978E-04	1.105210E-03	0.03000	5
1	5	5.7339	24.75349	5.3511	1137.6	10542.2	30.566	.19751	1.691809E-04	7.552226E-04	0.03000	5
1	5	5.7339	25.75349	5.1449	1055.0	10642.0	31.784	.18272	1.106997E-04	5.197902E-04	0.03000	5
1	5	5.7339	26.75349	4.6671	969.0	10740.4	33.010	.16810	7.066293E-05	3.215905E-04	0.03000	5
2	7	7.5667	7.5667	1.0000	1000.0	10000.0	10.000	1.00000	1.48924	1.48924	1.48924	1.48924
2	7	7.5667	8.5667	1.0141	1014.1	10141.0	10.141	1.01410	1.48924	1.48924	1.48924	1.48924
2	7	7.5667	9.5667	1.0282	1028.2	10282.0	10.282	1.02820	1.48924	1.48924	1.48924	1.48924
2	7	7.5667	10.5667	1.0423	1042.3	10423.0	10.423	1.04230	1.48924	1.48924	1.48924	1.48924
2	7	7.5667	11.5667	1.0564	1056.4	10564.0	10.564	1.05640	1.48924	1.48924	1.48924	1.48924
2	7	7.5667	12.5667	1.0705	1070.5	10705.0	10.705	1.07050	1.48924	1.48924	1.48924	1.48924
2	7	7.5667	13.5667	1.0846	1084.6	10846.0	10.846	1.08460	1.48924	1.48924	1.48924	1.48924
2	7	7.5667	14.5667	1.0987	1098.7	10987.0	10.987	1.09870	1.48924	1.48924	1.48924	1.48924
2	7	7.5667	15.5667	1.1128	1112.8	11128.0	11.128	1.11280	1.48924	1.48924	1.48924	1.48924
2	7	7.5667	16.5667	1.1269	1126.9	11269.0	11.269	1.12690	1.48924	1.48924	1.48924	1.48924
2	7	7.5667	17.5667	1.1410	1141.0	11410.0	11.410	1.14100	1.48924	1.48924	1.48924	1.48924
2	7	7.5667	18.5667	1.1551	1155.1	11551.0	11.551	1.15510	1.48924	1.48924	1.48924	1.48924
2	7	7.5667	19.5667	1.1692	1169.2	11692.0	11.692	1.16920	1.48924	1.48924	1.48924	1.48924
2	7	7.5667	20.5667	1.1833	1183.3	11833.0	11.833	1.18330	1.48924	1.48924	1.48924	1.48924
2	7	7.5667	21.5667	1.1974	1197.4	11974.0	11.974	1.19740	1.48924	1.48924	1.48924	1.48924
2	7	7.5667	22.5667	1.2115	1211.5	12115.0	12.115	1.21150	1.48924	1.48924	1.48924	1.48924
2	7	7.5667	23.5667	1.2256	1225.6	12256.0	12.256	1.22560	1.48924	1.48924	1.48924	1.48924
2	7	7.5667	24.5667	1.2397	1239.7	12397.0	12.397	1.23970	1.48924	1.48924	1.48924	1.48924
2	7	7.5667	25.5667	1.2538	1253.8	12538.0	12.538	1.25380	1.48924	1.48924	1.48924	1.48924
2	7	7.5667	26.5667	1.2679	1267.9	12679.0	12.679	1.26790	1.48924	1.48924	1.48924	1.48924
2	7	7.5667	27.5667	1.2820	1282.0	12820.0	12.820	1.28200	1.48924	1.48924	1.48924	1.48924
2	7	7.5667	28.5667	1.2961	1296.1	12961.0	12.961	1.29610	1.48924	1.48924	1.48924	1.48924
2	7	7.5667	29.5667	1.3102	1310.2	13102.0	13.102	1.31020	1.48924	1.48924	1.48924	1.48924
2	7	7.5667	30.5667	1.3243	1324.3	13243.0	13.243	1.32430	1.48924	1.48924	1.48924	1.48924
2	7	7.5667	31.5667	1.3384	1338.4	13384.0	13.384	1.33840	1.48924	1.48924	1.48924	1.48924
2	7	7.5667	32.5667	1.3525	1352.5	13525.0	13.525	1.35250	1.48924	1.48924	1.48924	1.48924
2	7	7.5667	33.5667	1.3666	1366.6	13666.0	13.666	1.36660	1.48924	1.48924	1.48924	1.48924
2	7	7.5667	34.5667	1.3807	1380.7	13807.0	13.807	1.38070	1.48924	1.48924	1.48924	1.48924
2	7	7.5667	35.5667	1.3948	1394.8	13948.0	13.948	1.39480	1.48924	1.48924	1.48924	1.48924
2	7	7.5667	36.5667	1.4089	1408.9	14089.0	14.089	1.40890	1.48924	1.48924	1.48924	1.48924
2	7	7.5667	37.5667	1.4230	1423.0	14230.0	14.230	1.42300	1.48924	1.48924	1.48924	1.48924
2	7	7.5667	38.5667	1.4371	1437.1	14371.0	14.371	1.43710	1.48924	1.48924	1.48924	1.48924
2	7	7.5667	39.5667	1.4512	1451.2	14512.0	14.512	1.45120	1.48924	1.48924	1.48924	1.48924
2	7	7.5667	40.5667	1.4653	1465.3	14653.0	14.653	1.46530	1.48924	1.48924	1.48924	1.48924
2	7	7.5667	41.5667	1.4794	1479.4	14794.0	14.794	1.47940	1.48924	1.48924	1.48924	1.48924
2	7	7.5667	42.5667	1.4935	1493.5	14935.0	14.935	1.49350	1.48924	1.48924	1.48924	1.48924
2	7	7.5667	43.5667	1.5076	1507.6	15076.0	15.076	1.50760	1.48924	1.48924	1.48924	1.48924
2	7	7.5667	44.5667	1.5217	1521.7	15217.0	15.217	1.52170	1.48924	1.48924	1.48924	1.48924
2	7	7.5667	45.5667	1.5358	1535.8	15358.0	15.358	1.53580	1.48924	1.48924	1.48924	1.48924
2	7	7.5667	46.5667	1.5499	1549.9	15499.0	15.499	1.54990	1.48924	1.48924	1.48924	1.48924
2	7	7.5667	47.5667	1.5640	1564.0	15640.0	15.640	1.56400	1.48924	1.48924	1.48924	1.48924
2	7	7.5667	48.5667	1.5781	1578.1	15781.0	15.781	1.57810	1.48924	1.48924	1.48924	1.48924
2	7	7.5667	49.5667	1.5922	1592.2	15922.0	15.922	1.59220	1.48924	1.48924	1.48924	1.48924
2	7	7.5667	50.5667	1.6063	1606.3	16063.0	16.063	1.60630	1.48924	1.48924	1.48924	1.48924
2	7	7.5667	51.5667	1.6204	1620.4	16204.0	16.204	1.62040	1.48924	1.48924	1.48924	1.48924
2	7	7.5667	52.5667	1.6345	1634.5	16345.0	16.345	1.63450	1.48924	1.48924	1.48924	1.48924
2	7	7.5667	53.5667	1.6486	1648.6	16486.0	16.486	1.64860	1.48924	1.48924	1.48924	1.48924
2	7	7.5667	54.5667	1.6627	1662.7	16627.0	16.627	1.66270	1.48924	1.48924	1.48924	1.48924
2	7	7.5667	55.5667	1.6768	1676.8	16768.0	16.768	1.67680	1.48924	1.48924	1.48924	1.48924
2	7	7.5667	56.5667	1.6909	1690.9	16909.0	16.909	1.69090	1.48924	1.48924	1.48924	1.48924
2	7	7.5667	57.5667	1.7050	1705.0	17050.0	17.050	1.70500	1.48924	1.48924	1.48924	1.48924
2	7	7.5667	58.5667	1.7191	1719.1	17191.0	17.191	1.71910	1.48924	1.48924	1.48924	1.48924
2	7	7.5667	59.5667	1.7332	1733.2	17332.0	17.332	1.73320	1.48924	1.48924	1.48924	1.48924
2	7	7.5667	60.5667	1.7473	1747.3	17473.0	17.473	1.74730	1.48924	1.48924	1.48924	1.48924
2	7	7.5667	61.5667	1.7614	1761.4	17614.0	17.614	1.76140	1.48924	1.48924	1.48924	1.48924
2	7	7.5667	62.5667	1.7755	1775.5	17755.0	17.755	1.77550	1.48924	1.48924	1.48924	1.48924
2	7	7.5667	63.5667	1.7896	1789.6	17896.0	17.896	1.78960	1.48924	1.48924	1.48924	1.48924
2	7	7.5667	64.5667	1.8037	1803.7	18037.0	18.037	1.80370	1.48924	1.48924	1.48924	1.48924
2	7	7.5667	65.5667	1.8178	1817.8	18178.0	18.178	1.81780	1.48924	1.48924	1.48924	1.48924
2	7	7.5667	66.5667	1.8319	1831.9	18319.0	18.319	1.83190	1.48924	1.48924	1.48924	1.48924
2	7	7.5667	67.5667	1.8460	1846.0	18460.0	18.460	1.84600	1.48924	1.48924	1.48924	1.48924
2	7	7.5667	68.5667	1.8601	1860.1	18601.0	18.601	1.86010	1.48924	1.48924	1.48924	1.48924
2	7	7.5667	69.5667	1.8742	1874.2	18742.0	18.742	1.87420	1.48924	1.48924	1.48924	1.48924
2	7	7.5667	70.5667	1.8883	1888.3	18883.0	18.883	1.88830	1.48924	1.48924	1.48924	1.48924
2	7	7.5667	71.5667	1.9024	1902.4	19024.0	19.024	1.90240	1.48924	1.48924	1.48924	1.48924
2	7	7.5667	72.5667	1.9165	1916.5	19165.0	19.165	1.91650	1.48924	1.48924	1.48924	1.48924
2	7											

Table V-Continued

1.19885	0.2434	1.19885
1.19899	0.2572	1.19899
1.17760	0.2710	1.17760
1.16761	0.2847	1.16761
1.15747	0.2984	1.15747
1.13609	0.3302	1.13609
1.11614	0.3614	1.11614
1.09676	0.3935	1.09676
1.07754	0.4269	1.07754
1.06133	0.4669	1.06133
1.04948	0.4797	1.04948
1.03691	0.5045	1.03691
1.02421	0.5304	1.02421
1.01182	0.5523	1.01182
1.00091	0.5734	1.00091
0.99449	0.5953	0.99449
0.99490	0.6169	0.99490
0.96280	0.6469	0.96280
0.91377	0.6712	0.91377
0.86507	0.6925	0.86507
0.84471	0.7122	0.84471
0.82975	0.7366	0.82975
0.77644	0.7647	0.77644
0.74465	0.7954	0.74465
0.71377	0.8225	0.71377
0.68483	0.8471	0.68483
0.65792	0.8702	0.65792
0.63351	0.8950	0.63351
0.62038	0.9171	0.62038
0.60729	0.9384	0.60729
0.59689	0.9576	0.59689
0.57964	0.9848	0.57964
0.56584	1.0016	0.56584
0.54448	1.0207	0.54448
0.52557	1.0392	0.52557
0.50926	1.0571	0.50926
0.49444	1.0744	0.49444
0.48114	1.0911	0.48114
0.46932	1.1072	0.46932
0.45889	1.1228	0.45889
0.44977	1.1379	0.44977
0.44194	1.1525	0.44194
0.43531	1.1666	0.43531
0.42987	1.1802	0.42987
0.42562	1.1934	0.42562
0.42245	1.2061	0.42245
0.42027	1.2184	0.42027
0.41907	1.2302	0.41907
0.41884	1.2416	0.41884
0.41957	1.2525	0.41957
0.42124	1.2630	0.42124
0.42384	1.2731	0.42384
0.42736	1.2828	0.42736
0.43179	1.2922	0.43179
0.43703	1.3012	0.43703
0.44307	1.3098	0.44307
0.44991	1.3181	0.44991
0.45754	1.3260	0.45754
0.46595	1.3336	0.46595
0.47514	1.3409	0.47514
0.48510	1.3478	0.48510
0.49582	1.3544	0.49582
0.50730	1.3607	0.50730
0.51953	1.3667	0.51953
0.53251	1.3724	0.53251
0.54624	1.3778	0.54624
0.56071	1.3829	0.56071
0.57592	1.3877	0.57592
0.59187	1.3922	0.59187
0.60856	1.3964	0.60856
0.62599	1.4003	0.62599
0.64416	1.4039	0.64416
0.66307	1.4072	0.66307
0.68272	1.4102	0.68272
0.70311	1.4129	0.70311
0.72424	1.4153	0.72424
0.74611	1.4174	0.74611
0.76872	1.4192	0.76872
0.79207	1.4207	0.79207
0.81616	1.4219	0.81616
0.84099	1.4228	0.84099
0.86646	1.4234	0.86646
0.89257	1.4237	0.89257
0.91932	1.4237	0.91932
0.94671	1.4234	0.94671
0.97474	1.4228	0.97474
1.00341	1.4219	1.00341
1.03272	1.4207	1.03272
1.06267	1.4192	1.06267
1.09326	1.4174	1.09326
1.12449	1.4153	1.12449
1.15626	1.4129	1.15626
1.18857	1.4102	1.18857
1.22142	1.4072	1.22142
1.25481	1.4039	1.25481
1.28874	1.4003	1.28874
1.32321	1.3964	1.32321
1.35822	1.3922	1.35822
1.39377	1.3877	1.39377
1.42986	1.3829	1.42986
1.46649	1.3778	1.46649
1.50366	1.3724	1.50366
1.54137	1.3667	1.54137
1.57962	1.3607	1.57962
1.61841	1.3544	1.61841
1.65774	1.3478	1.65774
1.69761	1.3409	1.69761
1.73802	1.3336	1.73802
1.77897	1.3260	1.77897
1.82046	1.3181	1.82046
1.86249	1.3102	1.86249
1.90506	1.3022	1.90506
1.94817	1.2942	1.94817
1.99182	1.2861	1.99182
2.03601	1.2778	2.03601
2.08074	1.2694	2.08074
2.12601	1.2607	2.12601
2.17182	1.2518	2.17182
2.21817	1.2427	2.21817
2.26506	1.2334	2.26506
2.31249	1.2239	2.31249
2.36046	1.2142	2.36046
2.40897	1.2043	2.40897
2.45802	1.1942	2.45802
2.50761	1.1839	2.50761
2.55774	1.1734	2.55774
2.60841	1.1627	2.60841
2.65962	1.1518	2.65962
2.71137	1.1407	2.71137
2.76366	1.1294	2.76366
2.81649	1.1178	2.81649
2.86986	1.1060	2.86986
2.92377	1.0940	2.92377
2.97822	1.0817	2.97822
3.03321	1.0692	3.03321
3.08874	1.0565	3.08874
3.14481	1.0436	3.14481
3.20142	1.0305	3.20142
3.25857	1.0172	3.25857
3.31626	1.0037	3.31626
3.37449	0.9900	3.37449
3.43326	0.9761	3.43326
3.49257	0.9620	3.49257
3.55242	0.9477	3.55242
3.61281	0.9332	3.61281
3.67374	0.9185	3.67374
3.73521	0.9036	3.73521
3.79722	0.8885	3.79722
3.85977	0.8732	3.85977
3.92286	0.8577	3.92286
3.98649	0.8420	3.98649
4.05066	0.8261	4.05066
4.11537	0.8100	4.11537
4.18062	0.7937	4.18062
4.24641	0.7772	4.24641
4.31274	0.7605	4.31274
4.37961	0.7436	4.37961
4.44702	0.7265	4.44702
4.51497	0.7092	4.51497
4.58346	0.6917	4.58346
4.65249	0.6740	4.65249
4.72206	0.6561	4.72206
4.79217	0.6380	4.79217
4.86282	0.6197	4.86282
4.93401	0.6012	4.93401
5.00574	0.5825	5.00574
5.07801	0.5636	5.07801
5.15082	0.5445	5.15082
5.22417	0.5252	5.22417
5.29806	0.5057	5.29806
5.37249	0.4860	5.37249
5.44746	0.4661	5.44746
5.52297	0.4460	5.52297
5.59902	0.4257	5.59902
5.67561	0.4052	5.67561
5.75274	0.3845	5.75274
5.83041	0.3636	5.83041
5.90862	0.3425	5.90862
5.98737	0.3212	5.98737
6.06666	0.2997	6.06666
6.14649	0.2780	6.14649
6.22686	0.2561	6.22686
6.30777	0.2340	6.30777
6.38922	0.2117	6.38922
6.47121	0.1892	6.47121
6.55374	0.1665	6.55374
6.63681	0.1436	6.63681
6.72042	0.1205	6.72042
6.80457	0.0972	6.80457
6.88926	0.0737	6.88926
6.97449	0.0500	6.97449
7.06026	0.0261	7.06026
7.14657	0.0020	7.14657
7.23342	0.0000	7.23342
7.32081	0.0000	7.32081
7.40874	0.0000	7.40874
7.49721	0.0000	7.49721
7.58622	0.0000	7.58622
7.67577	0.0000	7.67577
7.76586	0.0000	7.76586
7.85649	0.0000	7.85649
7.94766	0.0000	7.94766
8.03937	0.0000	8.03937
8.13162	0.0000	8.13162
8.22441	0.0000	8.22441
8.31774	0.0000	8.31774
8.41161	0.0000	8.41161
8.50602	0.0000	8.50602
8.60097	0.0000	8.60097
8.69646	0.0000	8.69646
8.79249	0.0000	8.79249
8.88906	0.0000	8.88906
8.98617	0.0000	8.98617
9.08382	0.0000	9.08382
9.18201	0.0000	9.18201
9.28074	0.0000	9.28074
9.37999	0.0000	9.37999
9.47976	0.0000	9.47976
9.57999	0.0000	9.57999
9.68066	0.0000	9.68066
9.78177	0.0000	9.78177
9.88332	0.0000	9.88332
9.98541	0.0000	9.98541
10.08802	0.0000	10.08802
10.19117	0.0000	10.19117
10.29486	0.0000	10.29486
10.39909	0.0000	10.39909
10.50386	0.0000	10.50386
10.60917	0.0000	10.60917
10.71502	0.0000	10.71502
10.82141	0.0000	10.82141
10.92834	0.0000	10.92834
11.03581	0.0000	11.03581
11.14382	0.0000	11.14382
11.25237	0.0000	11.25237
11.36146	0.0000	11.36146
11.47109	0.0000	11.47109
11.58126	0.0000	11.58126
11.69197	0.0000	11.69197
11.80322	0.0000	11.80322
11.91501	0.0000	11.91501
12.02734	0.0000	12.02734
12.14021	0.0000	12.14021
12.25362	0.0000	12.25362
12.36757	0.0000	12.36757
12.48206	0.0000	12.48206
12.59709	0.0000	12.59709
12.71266	0.0000	12.71266
12.82877	0.0000	12.82877
12.94542	0.0000	12.94542
13.06261	0.0000	13.06261
13.18034	0.0000	13.18034
13.29861	0.0000	13.29861
13.41742	0.0000	13.41742
13.53677	0.0000	13.53677
13.65666	0.0000	13.65666
13.77709	0.0000	13.77709
13.89806	0.0000	13.89806
14.01957	0.0000	14.01957
14.14162	0.0000	14.14162
14.26421	0.0000	14.26421
14.38734	0.0000	14.38734
14.51101	0.0000	14.51101
14.63522	0.0000	14.63522
14.76006	0.0000	14.76006
14.88549	0.0000	14.88549
15.01152	0.0000	15.01152
15.13814	0.0000	15.13814
15.26535	0.0000	15.26535
15.39316	0.0000	15.39316
15.52157	0.0000	15.52157
15.65058	0.0000	15.65058
15.78019	0.0000	15.78019
15.91040	0.0000	15.91040
16.04121	0.0000	16.04121
16.17262	0.0000	16.17262
16.30463	0.0000	16.30463
16.43724	0.0000	16.43724
16.57045	0.0000	16.57045
16.70426	0.0000	16.70426
16.83867	0.0000	16.83867
16.97368	0.0000	16.97368
17.10929	0.0000	17.10929
17.24550	0.0000	17.24550
17.38231	0.0000	17.38231
17.51972	0.0000	17.51972
17.65773	0.0000	17.65773
17.79634	0.0000	17.79634
17.93555	0.0000	17.93555
18.07536	0.0000	18.07536
18.21577	0.0000	18.21577
18.35678	0.0000	18.35678
18.49829	0.0000	18.49829
18.64040	0.0000	18.64040
18.78311	0.0000	18.78311
18.92642	0.0000	18.92642
19.07033	0.0000	19.07033
19.21484	0.0000	19.21484
19.35995	0.0000	19.35995
19.50566	0.0000	19.50566
19.65197	0.0000	19.65197
19.79888	0.0000	19.79888
19.94639	0.0000	19.94639
20.09450	0.000	

Table V-Continued

3	1.774434E+02	2.610922E+03	1.515110E+03	5.135176E+02	2.774192E+01	5.1000000E+00
4	1.459749E+02	1.907392E+03	5.597946E+03	5.544717E+01	4.172432E+00	1.0000000E+04
5	1.113245E+02	1.151945E+03	5.153340E+03	8.248438E+03	4.215960E+01	2.1100000E+04
2 2	1.011027E+02	3.10712695E+01	1.00644572E+02	1.588726E+02	7.309493E+02	9.111925E+05
1	1.733506E+02	5.401111E+03	5.602081E+02	2.307741E+04	1.739745E+03	1.0000000E+05
2	9.553385E+01	3.503333E+03	2.946112E+02	5.433189E+03	6.628138E+02	1.0000000E+05
3	1.970425E+02	2.813244E+03	1.277629E+02	3.1149298E+03	2.371363E+01	5.0000000E+04
4	1.361292E+02	1.809922E+03	3.513119E+02	5.559516E+01	4.107746E+00	1.0000000E+04
5	1.123339E+02	1.163266E+03	3.407570E+01	8.324930E+03	4.421135E+01	2.1100000E+04
2 2	1.72208E+02	3.1082E+03	850000E+03	1.589596E+02	1.392025E+02	9.446649E+05
1	1.728272E+02	5.874039E+03	1.974248E+01	7.527777E+04	1.727330E+03	1.0000000E+05
2	9.83447E+01	3.608780E+03	6.254945E+02	5.990144E+03	4.971558E+02	3.0000000E+05
3	1.177359E+02	2.811105E+03	2.168134E+02	3.140836E+03	2.366260E+01	5.0000000E+05
4	4.75241E+01	1.870365E+03	7.44048E+02	5.872662E+01	4.194477E+00	1.0000000E+04
5	1.102203E+02	1.100147E+03	7.135738E+01	8.450970E+00	6.566134E+01	2.1100000E+04
2 2	1.12556E+02	3.1612E+03	26979E+03	1.591972E+02	3.397902E+02	9.79687E+04
1	1.74937E+02	5.877875E+03	1.792724E+01	2.276416E+04	1.715396E+03	1.0000000E+05
2	4.114412E+01	3.007246E+03	9.34376E+02	5.233593E+03	6.571079E+03	3.0000000E+05
3	1.124489E+02	2.815732E+03	3.26531E+02	5.123945E+03	3.133409E+02	2.361129E+01
4	4.75128E+01	1.870922E+03	1.117413E+02	5.583695E+01	4.207503E+00	1.0000000E+04
5	1.121129E+02	1.107745E+03	3.133548E+01	9.199770E+00	4.932338E+01	2.1100000E+04
2 2	1.74566E+02	3.1072E+03	26990E+03	1.593406E+02	3.383994E+02	9.79687E+04
1	1.73192E+02	5.882337E+03	2.153583E+01	2.259732E+04	1.742155E+03	1.0000000E+05
2	4.114412E+01	3.007246E+03	1.22062E+02	5.243133E+03	6.539044E+03	4.931914E+02
3	1.124489E+02	2.815732E+03	4.297449E+02	5.123622E+03	3.123444E+02	2.355782E+01
4	4.75128E+01	1.870922E+03	1.117413E+02	5.583695E+01	4.207503E+00	1.0000000E+04
5	1.121129E+02	1.107745E+03	3.133548E+01	9.199770E+00	4.932338E+01	2.1100000E+04
2 2	1.75476E+02	3.1072E+03	27019E+03	1.598300E+02	3.401486E+02	9.79687E+04
1	1.73550E+02	5.894485E+03	2.104106E+01	2.240051E+04	1.537223E+03	1.0000000E+05
2	4.114412E+01	3.007246E+03	1.22062E+02	5.243133E+03	6.539044E+03	4.931914E+02
3	1.124489E+02	2.815732E+03	4.297449E+02	5.123622E+03	3.123444E+02	2.355782E+01
4	4.75128E+01	1.870922E+03	1.117413E+02	5.583695E+01	4.207503E+00	1.0000000E+04
5	1.121129E+02	1.107745E+03	3.133548E+01	9.199770E+00	4.932338E+01	2.1100000E+04
2 2	1.77224E+02	3.1072E+03	27046E+03	1.615133E+02	3.412558E+02	9.79687E+04
1	1.73680E+02	5.894485E+03	2.104106E+01	2.240051E+04	1.537223E+03	1.0000000E+05
2	4.114412E+01	3.007246E+03	1.22062E+02	5.243133E+03	6.539044E+03	4.931914E+02
3	1.124489E+02	2.815732E+03	4.297449E+02	5.123622E+03	3.123444E+02	2.355782E+01
4	4.75128E+01	1.870922E+03	1.117413E+02	5.583695E+01	4.207503E+00	1.0000000E+04
5	1.121129E+02	1.107745E+03	3.133548E+01	9.199770E+00	4.932338E+01	2.1100000E+04
2 2	1.77224E+02	3.1072E+03	27062E+03	1.614779E+02	3.420287E+02	9.79687E+04
1	1.73680E+02	5.894485E+03	2.104106E+01	2.240051E+04	1.537223E+03	1.0000000E+05
2	4.114412E+01	3.007246E+03	1.22062E+02	5.243133E+03	6.539044E+03	4.931914E+02
3	1.124489E+02	2.815732E+03	4.297449E+02	5.123622E+03	3.123444E+02	2.355782E+01
4	4.75128E+01	1.870922E+03	1.117413E+02	5.583695E+01	4.207503E+00	1.0000000E+04
5	1.121129E+02	1.107745E+03	3.133548E+01	9.199770E+00	4.932338E+01	2.1100000E+04
2 2	1.77224E+02	3.1072E+03	27078E+03	1.613374E+02	3.428885E+02	9.79687E+04
1	1.73680E+02	5.894485E+03	2.104106E+01	2.240051E+04	1.537223E+03	1.0000000E+05
2	4.114412E+01	3.007246E+03	1.22062E+02	5.243133E+03	6.539044E+03	4.931914E+02
3	1.124489E+02	2.815732E+03	4.297449E+02	5.123622E+03	3.123444E+02	2.355782E+01
4	4.75128E+01	1.870922E+03	1.117413E+02	5.583695E+01	4.207503E+00	1.0000000E+04
5	1.121129E+02	1.107745E+03	3.133548E+01	9.199770E+00	4.932338E+01	2.1100000E+04
2 2	1.77224E+02	3.1072E+03	27094E+03	1.613374E+02	3.428885E+02	9.79687E+04
1	1.73680E+02	5.894485E+03	2.104106E+01	2.240051E+04	1.537223E+03	1.0000000E+05
2	4.114412E+01	3.007246E+03	1.22062E+02	5.243133E+03	6.539044E+03	4.931914E+02
3	1.124489E+02	2.815732E+03	4.297449E+02	5.123622E+03	3.123444E+02	2.355782E+01
4	4.75128E+01	1.870922E+03	1.117413E+02	5.583695E+01	4.207503E+00	1.0000000E+04
5	1.121129E+02	1.107745E+03	3.133548E+01	9.199770E+00	4.932338E+01	2.1100000E+04
2 2	1.77224E+02	3.1072E+03	27110E+03	1.613374E+02	3.428885E+02	9.79687E+04
1	1.73680E+02	5.894485E+03	2.104106E+01	2.240051E+04	1.537223E+03	1.0000000E+05
2	4.114412E+01	3.007246E+03	1.22062E+02	5.243133E+03	6.539044E+03	4.931914E+02
3	1.124489E+02	2.815732E+03	4.297449E+02	5.123622E+03	3.123444E+02	2.355782E+01
4	4.75128E+01	1.870922E+03	1.117413E+02	5.583695E+01	4.207503E+00	1.0000000E+04
5	1.121129E+02	1.107745E+03	3.133548E+01	9.199770E+00	4.932338E+01	2.1100000E+04
2 2	1.77224E+02	3.1072E+03	27126E+03	1.613374E+02	3.428885E+02	9.79687E+04
1	1.73680E+02	5.894485E+03	2.104106E+01	2.240051E+04	1.537223E+03	1.0000000E+05
2	4.114412E+01	3.007246E+03	1.22062E+02	5.243133E+03	6.539044E+03	4.931914E+02
3	1.124489E+02	2.815732E+03	4.297449E+02	5.123622E+03	3.123444E+02	2.355782E+01
4	4.75128E+01	1.870922E+03	1.117413E+02	5.583695E+01	4.207503E+00	1.0000000E+04
5	1.121129E+02	1.107745E+03	3.133548E+01	9.199770E+00	4.932338E+01	2.1100000E+04
2 2	1.77224E+02	3.1072E+03	27142E+03	1.613374E+02	3.428885E+02	9.79687E+04
1	1.73680E+02	5.894485E+03	2.104106E+01	2.240051E+04	1.537223E+03	1.0000000E+05
2	4.114412E+01	3.007246E+03	1.22062E+02	5.243133E+03	6.539044E+03	4.931914E+02
3	1.124489E+02	2.815732E+03	4.297449E+02	5.123622E+03	3.123444E+02	2.355782E+01
4	4.75128E+01	1.870922E+03	1.117413E+02	5.583695E+01	4.207503E+00	1.0000000E+04
5	1.121129E+02	1.107745E+03	3.133548E+01	9.199770E+00	4.932338E+01	2.1100000E+04
2 2	1.77224E+02	3.1072E+03	27158E+03	1.613374E+02	3.428885E+02	9.79687E+04
1	1.73680E+02	5.894485E+03	2.104106E+01	2.240051E+04	1.537223E+03	1.0000000E+05
2	4.114412E+01	3.007246E+03	1.22062E+02	5.243133E+03	6.539044E+03	4.931914E+02
3	1.124489E+02	2.815732E+03	4.297449E+02	5.123622E+03	3.123444E+02	2.355782E+01
4	4.75128E+01	1.870922E+03	1.117413E+02	5.583695E+01	4.207503E+00	1.0000000E+04
5	1.121129E+02	1.107745E+03	3.133548E+01	9.199770E+00	4.932338E+01	2.1100000E+04
2 2	1.77224E+02	3.1072E+03	27174E+03	1.613374E+02	3.428885E+02	9.79687E+04
1	1.73680E+02	5.894485E+03	2.104106E+01	2.240051E+04	1.537223E+03	1.0000000E+05
2	4.114412E+01	3.007246E+03	1.22062E+02	5.243133E+03	6.539044E+03	4.931914E+02
3	1.124489E+02	2.815732E+03	4.297449E+02	5.123622E+03	3.123444E+02	2.355782E+01
4	4.75128E+01	1.870922E+03	1.117413E+02	5.583695E+01	4.207503E+00	1.0000000E+04
5	1.121129E+02	1.107745E+03	3.133548E+01	9.199770E+00	4.932338E+01	2.1100000E+04
2 2	1.77224E+02	3.1072E+03	27190E+03	1.613374E+02	3.428885E+02	9.79687E+04
1	1.73680E+02	5.894485E+03	2.104106E+01	2.240051E+04	1.537223E+03	1.0000000E+05
2	4.114412E+01	3.007246E+03	1.22062E+02	5.243133E+03	6.539044E+03	4.931914E+02
3	1.124489E+02	2.815732E+03	4.297449E+02	5.123622E+03	3.123444E+02	2.355782E+01
4	4.75128E+01	1.870922E+03	1.117413E+02	5.583695E+01	4.207503E+00	1.0000000E+04
5	1.121129E+02	1.107745E+03	3.133548E+01	9.199770E+00	4.932338E+01	2.1100000E+04
2 2	1.77224E+02	3.1072E+03	27206E+03	1.613374E+02	3.428885E+02	9.79687E+04
1	1.73680E+02	5.894485E+03	2.104106E+01	2.240051E+04	1.537223E+03	1.0000000E+05
2	4.114412E+01	3.007246E+03	1.22062E+02	5.243133E+03	6.539044E+03	4.931914E+02
3	1.124489E+02	2.815732E+03	4.297449E+02	5.123622E+03	3.123444E+02	2.355782E+01
4	4.75128E+01	1.870922E+03	1.117413E+02	5.583695E+01	4.207503E+00	1.0000000E+04
5	1.121129E+02	1.107745E+03	3.133548E+01	9.199770E+00	4.932338E+01	2.1100000E+04
2 2	1.77224E+02	3.1072E+03	27222E+03	1.613374E+02	3.428885E+02	9.79687E+04
1	1.73680E+02	5.894485E+03	2.104106E+01	2.240051E+04	1.537223E+03	1.0000000E+05
2	4.114412E+01	3.007246E+0				

Table V--Continued

2	2	1.11289	7.67710	3.0374	2697.0	838.8	5.41771E+01	5.41771E+01	1.000000E-00
1	1	1.70796E-01	5.91060E-03	5.90749E-01	5.15732E+03	2.39770E+04	1.64037E+03	1.64037E+03	1.000000E-00
2	2	9.52224E-01	3.69026E-03	2.96533E-01	5.42808E+03	6.33480E+03	4.81378E+02	4.81378E+02	1.000000E-00
3	3	1.86949E-01	2.83737E-03	1.03750E-01	5.51071E+03	3.03771E+02	2.32830E+01	2.32830E+01	1.000000E-00
4	4	4.36849E-03	1.087140E+03	-3.71202E-01	5.591041E+03	5.596709E-01	4.250731E+00	4.250731E+00	1.000000E-00
2	2	1.3375	7.93736	3.0626	2693.0	849.0	5.42274E+02	5.42274E+02	1.000000E-00
1	1	1.70745E-01	5.91959E-03	6.55280E-01	5.15642E+03	2.311481E-04	1.621216E+03	1.621216E+03	1.000000E-00
2	2	9.54920E-01	3.69648E-03	3.495507E-01	5.429012E+03	6.275266E-02	4.773001E+02	4.773001E+02	1.000000E-00
3	3	1.87439E-01	2.84248E-03	1.22878E-01	5.51282E+03	3.03383E-02	2.307347E+01	2.307347E+01	1.000000E-00
4	4	4.39116E-03	1.090938E+03	-4.401617E-01	5.598662E+03	5.596663E-01	4.256822E+00	4.256822E+00	1.000000E-00
2	2	1.3344	7.99739	3.0671	2689.8	847.4	5.42577E+02	5.42577E+02	1.000000E-00
1	1	1.70745E-01	5.92536E-03	7.49105E-01	5.155529E+03	2.104991E-04	1.602473E+03	1.602473E+03	1.000000E-00
2	2	9.56822E-01	3.70282E-03	4.01552E-01	5.428463E+03	6.21932E-03	4.734702E+02	4.734702E+02	1.000000E-00
3	3	1.87873E-01	2.84757E-03	1.41769E-01	5.508809E+03	3.014173E-02	2.294622E+01	2.294622E+01	1.000000E-00
4	4	4.39116E-03	1.092471E+03	-5.084831E-01	5.598326E+03	5.597579E-01	4.261346E+00	4.261346E+00	1.000000E-00
2	2	1.3754	8.05745	3.0752	2683.4	850.7	5.42724E+02	5.42724E+02	1.000000E-00
1	1	1.70745E-01	5.93766E-03	6.43293E-01	5.154022E+03	2.091634E-02	1.587113E+03	1.587113E+03	1.000000E-00
2	2	9.54722E-01	3.70870E-03	4.54262E-01	5.42907E+03	6.201474E-03	4.695542E+02	4.695542E+02	1.000000E-00
3	3	1.87363E-01	2.85281E-03	1.43152E-01	5.500350E+03	3.012817E-02	2.261049E+01	2.261049E+01	1.000000E-00
4	4	4.37642E-03	1.098322E+03	-5.774663E-01	5.589967E+03	5.622332E-01	4.264363E+00	4.264363E+00	1.000000E-00
2	2	1.3723	8.11831	3.0816	2677.3	852.4	5.42765E+02	5.42765E+02	1.000000E-00
1	1	1.70745E-01	5.94684E-03	9.37131E-01	5.153718E+03	2.07940E-04	1.585139E+03	1.585139E+03	1.000000E-00
2	2	9.54722E-01	3.71519E-03	5.07297E-01	5.427353E+03	6.19587E-03	4.65998E+02	4.65998E+02	1.000000E-00
3	3	1.87673E-01	2.85747E-03	1.64171E-01	5.50894E+03	3.011024E-02	2.266941E+01	2.266941E+01	1.000000E-00
4	4	4.38442E-03	1.09231E+03	-6.44397E-01	5.58902E+03	5.569072E-01	4.267000E+00	4.267000E+00	1.000000E-00
2	2	1.3716	8.17991	3.0742	2671.3	854.5	5.42778E+02	5.42778E+02	1.000000E-00
1	1	1.70745E-01	5.95597E-03	1.43802E-01	5.152876E+03	2.06767E-04	1.584593E+03	1.584593E+03	1.000000E-00
2	2	9.54722E-01	3.72143E-03	5.63342E-01	5.427494E+03	6.171099E-03	4.651581E+02	4.651581E+02	1.000000E-00
3	3	1.87673E-01	2.86282E-03	2.2325E-01	5.508433E+03	3.01117E-02	2.252170E+01	2.252170E+01	1.000000E-00
4	4	4.38442E-03	1.09433E+03	-7.02243E-01	5.58986E+03	5.569144E-01	4.268442E+00	4.268442E+00	1.000000E-00
2	2	1.3717	8.24326	3.0725	2665.5	856.5	5.42787E+02	5.42787E+02	1.000000E-00
1	1	1.70745E-01	5.96597E-03	1.42606E-01	5.152030E+03	2.057549E-04	1.58333E+03	1.58333E+03	1.000000E-00
2	2	9.54722E-01	3.72697E-03	6.0900E-01	5.42753E+03	6.157743E-03	4.647552E+02	4.647552E+02	1.000000E-00
3	3	1.87673E-01	2.86731E-03	2.2112E-01	5.50829E+03	3.01157E-02	2.231541E+01	2.231541E+01	1.000000E-00
4	4	4.38442E-03	1.09657E+03	-7.77407E-01	5.58986E+03	5.56947E-01	4.27146E+00	4.27146E+00	1.000000E-00
2	2	1.3718	8.31729	3.0714	2659.2	858.7	5.42791E+02	5.42791E+02	1.000000E-00
1	1	1.70745E-01	5.97719E-03	1.7719E-01	5.151412E+03	2.05110E-04	1.58244E+03	1.58244E+03	1.000000E-00
2	2	9.54722E-01	3.73133E-03	6.4919E-01	5.42759E+03	6.147745E-03	4.645477E+02	4.645477E+02	1.000000E-00
3	3	1.87673E-01	2.87475E-03	2.24291E-01	5.50819E+03	3.01031E-02	2.22885E+01	2.22885E+01	1.000000E-00
4	4	4.38442E-03	1.09897E+03	-8.24107E-01	5.58971E+03	5.57132E-01	4.27377E+00	4.27377E+00	1.000000E-00
2	2	1.3719	8.39172	3.0702	2653.0	860.9	5.42795E+02	5.42795E+02	1.000000E-00
1	1	1.70745E-01	5.99071E-03	1.7449E-01	5.150719E+03	2.04510E-04	1.58154E+03	1.58154E+03	1.000000E-00
2	2	9.54722E-01	3.73582E-03	6.84374E-01	5.42765E+03	6.13443E-03	4.64382E+02	4.64382E+02	1.000000E-00
3	3	1.87673E-01	2.87921E-03	2.27147E-01	5.50809E+03	3.00903E-02	2.22747E+01	2.22747E+01	1.000000E-00
4	4	4.38442E-03	1.09846E+03	-8.74517E-01	5.58956E+03	5.56936E-01	4.27477E+00	4.27477E+00	1.000000E-00
2	2	1.3720	8.46615	3.0690	2646.5	863.1	5.42799E+02	5.42799E+02	1.000000E-00
1	1	1.70745E-01	5.99597E-03	1.71026E-01	5.150030E+03	2.03910E-04	1.58065E+03	1.58065E+03	1.000000E-00
2	2	9.54722E-01	3.74031E-03	7.2936E-01	5.42771E+03	6.12311E-03	4.64218E+02	4.64218E+02	1.000000E-00
3	3	1.87673E-01	2.88365E-03	2.3007E-01	5.50799E+03	3.00793E-02	2.22625E+01	2.22625E+01	1.000000E-00
4	4	4.38442E-03	1.09897E+03	-9.24051E-01	5.58941E+03	5.56921E-01	4.27577E+00	4.27577E+00	1.000000E-00
2	2	1.3721	8.54058	3.0678	2640.3	865.3	5.42803E+02	5.42803E+02	1.000000E-00
1	1	1.70745E-01	5.99597E-03	1.67565E-01	5.149341E+03	2.03399E-04	1.57976E+03	1.57976E+03	1.000000E-00
2	2	9.54722E-01	3.74480E-03	7.6869E-01	5.42777E+03	6.11209E-03	4.64053E+02	4.64053E+02	1.000000E-00
3	3	1.87673E-01	2.88814E-03	2.3295E-01	5.50789E+03	3.00685E-02	2.22503E+01	2.22503E+01	1.000000E-00
4	4	4.38442E-03	1.09897E+03	-9.74517E-01	5.58926E+03	5.56906E-01	4.27677E+00	4.27677E+00	1.000000E-00
2	2	1.3722	8.61501	3.0666	2634.1	867.5	5.42807E+02	5.42807E+02	1.000000E-00
1	1	1.70745E-01	5.99597E-03	1.64054E-01	5.148652E+03	2.02888E-04	1.57887E+03	1.57887E+03	1.000000E-00
2	2	9.54722E-01	3.74929E-03	8.0780E-01	5.42783E+03	6.10107E-03	4.63888E+02	4.63888E+02	1.000000E-00
3	3	1.87673E-01	2.89263E-03	2.3582E-01	5.50779E+03	3.00577E-02	2.22381E+01	2.22381E+01	1.000000E-00
4	4	4.38442E-03	1.09897E+03	-10.24051E-01	5.58911E+03	5.56886E-01	4.27777E+00	4.27777E+00	1.000000E-00
2	2	1.3723	8.68944	3.0654	2627.9	869.7	5.42811E+02	5.42811E+02	1.000000E-00
1	1	1.70745E-01	5.99597E-03	1.60543E-01	5.147963E+03	2.02377E-04	1.57798E+03	1.57798E+03	1.000000E-00
2	2	9.54722E-01	3.75373E-03	8.4691E-01	5.42789E+03	6.09005E-03	4.63723E+02	4.63723E+02	1.000000E-00
3	3	1.87673E-01	2.89712E-03	2.3870E-01	5.50769E+03	3.00467E-02	2.22259E+01	2.22259E+01	1.000000E-00
4	4	4.38442E-03	1.09897E+03	-10.74517E-01	5.58896E+03	5.56866E-01	4.27877E+00	4.27877E+00	1.000000E-00
2	2	1.3724	8.76387	3.0642	2621.7	871.9	5.42815E+02	5.42815E+02	1.000000E-00
1	1	1.70745E-01	5.99597E-03	1.57032E-01	5.147274E+03	2.01866E-04	1.57709E+03	1.57709E+03	1.000000E-00
2	2	9.54722E-01	3.75822E-03	8.8598E-01	5.42795E+03	6.07903E-03	4.63558E+02	4.63558E+02	1.000000E-00
3	3	1.87673E-01	2.90161E-03	2.4165E-01	5.50759E+03	3.00359E-02	2.22137E+01	2.22137E+01	1.000000E-00
4	4	4.38442E-03	1.09897E+03	-11.24051E-01	5.58881E+03	5.56846E-01	4.27977E+00	4.27977E+00	1.000000E-00
2	2	1.3725	8.83830	3.0630	2615.5	874.1	5.42819E+02	5.42819E+02	1.000000E-00
1	1	1.70745E-01	5.99597E-03	1.53521E-01	5.146585E+03	2.01365E-04	1.57620E+03	1.57620E+03	1.000000E-00
2	2	9.54722E-01	3.76271E-03	9.2505E-01	5.42801E+03	6.06741E-03	4.63393E+02	4.63393E+02	1.000000E-00
3	3	1.87673E-01	2.90610E-03	2.4454E-01	5.50749E+03	3.00251E-02	2.22015E+01	2.22015E+01	1.000000E-00
4	4	4.38442E-03	1.09897E+03	-11.74517E-01	5.58866E+03	5.56826E-01	4.28077E+00	4.28077E+00	1.000000E-00
2	2	1.3726	8.91273	3.0618	2609.3	876.3	5.42823E+02	5.42823E+02	1.000000E-00
1	1	1.70745E-01	5.99597E-03	1.50010E-01	5.145896E+03	2.00864E-04	1.57531E+03	1.57531E+03	1.000000E-00
2	2	9.54722E-01	3.76720E-03	9.6408E-01	5.42807E+03	6.05579E-03	4.63228E+02	4.63228E+02	1.000000E-00
3	3	1.87673E-01	2.91059E-03	2.4743E-01	5.50739E+03	3.00143E-02	2.21893E+01	2.21893E+01	1.000000E-00
4	4	4.38442E-03	1.09897E+03	-12.24051E-01	5.58851E+03	5.56806E-01	4.28177E+00	4.28177E+00	

Table V-Continued

2	3	1.697935E-01	2.922655E+03	5.67271E-1	1.67119E-3	3.873E-05	2	1.72753E-01	1.00000E-05
2	2	1.5564E-01	3.254E-05	2.571E-05	5.971E-07	1.447E-03	2	1.314663E-04	1.00000E-05
1	1	1.325445E-01	5.06774E-03	2.42913E-03	1.33292E-03	1.17722E-03	2	1.77222E-03	1.00000E-05
2	2	8.58458E-01	3.13348E+03	5.41171E-03	5.11411E-03	4.25E-04	2	1.17722E-03	1.00000E-05
3	3	1.688784E-01	2.93555E+03	5.78522E-01	1.17722E-03	1.17722E-03	2	1.17722E-03	1.00000E-05
2	2	5.7159E-01	9.17254E-01	1.546E-03	5.691E-07	1.447E-03	2	1.314663E-04	1.00000E-05
1	1	1.501067E-01	6.03781E-03	2.46237E-03	1.33292E-03	1.17722E-03	2	1.77222E-03	1.00000E-05
2	2	8.58458E-01	3.13348E+03	5.41171E-03	5.11411E-03	4.25E-04	2	1.17722E-03	1.00000E-05
3	3	1.679772E-01	2.93555E+03	5.65308E-01	1.17722E-03	1.17722E-03	2	1.17722E-03	1.00000E-05
2	2	5.6659E-01	9.21344E-01	1.217E-03	6.696E-07	1.447E-03	2	1.314663E-04	1.00000E-05
1	1	1.501067E-01	6.03781E-03	2.46237E-03	1.33292E-03	1.17722E-03	2	1.77222E-03	1.00000E-05
2	2	8.58458E-01	3.13348E+03	5.41171E-03	5.11411E-03	4.25E-04	2	1.17722E-03	1.00000E-05
3	3	1.671147E-01	2.94424E+03	5.13316E-01	1.17722E-03	1.17722E-03	2	1.17722E-03	1.00000E-05
2	2	6.0230E-01	9.2225E-01	1.2225E-03	6.717E-07	1.447E-03	2	1.314663E-04	1.00000E-05
1	1	1.501067E-01	6.03781E-03	2.46237E-03	1.33292E-03	1.17722E-03	2	1.77222E-03	1.00000E-05
2	2	8.58458E-01	3.13348E+03	5.41171E-03	5.11411E-03	4.25E-04	2	1.17722E-03	1.00000E-05
3	3	1.622342E-01	2.94424E+03	4.72744E-01	1.17722E-03	1.17722E-03	2	1.17722E-03	1.00000E-05
2	2	6.1509E-01	9.24914E-01	1.2269E-03	6.717E-07	1.447E-03	2	1.314663E-04	1.00000E-05
1	1	1.493861E-01	5.13348E-03	2.43223E-03	1.33292E-03	1.17722E-03	2	1.77222E-03	1.00000E-05
2	2	8.44857E-01	3.22616E+03	4.55249E-03	5.11411E-03	4.25E-04	2	1.17722E-03	1.00000E-05
3	3	1.654688E-01	2.94424E+03	4.492374E-01	1.17722E-03	1.17722E-03	2	1.17722E-03	1.00000E-05
2	2	6.3409E-01	9.2335E-01	1.2335E-03	6.717E-07	1.447E-03	2	1.314663E-04	1.00000E-05
1	1	1.46382E-01	4.11495E-03	2.73325E-03	1.33292E-03	1.17722E-03	2	1.77222E-03	1.00000E-05
2	2	8.33192E-01	3.2225E+03	4.55249E-03	5.11411E-03	4.25E-04	2	1.17722E-03	1.00000E-05
2	2	6.6411E-01	9.24276E-01	1.2442E-03	6.717E-07	1.447E-03	2	1.314663E-04	1.00000E-05
1	1	1.467143E-01	4.12527E-03	2.81793E-03	1.33292E-03	1.17722E-03	2	1.77222E-03	1.00000E-05
2	2	8.26130E-01	3.3332E+03	4.47612E-03	5.11411E-03	4.25E-04	2	1.17722E-03	1.00000E-05
2	2	5.9597E-01	9.2298E-01	1.2298E-03	6.717E-07	1.447E-03	2	1.314663E-04	1.00000E-05
1	1	1.49044E-01	5.13348E-03	2.43223E-03	1.33292E-03	1.17722E-03	2	1.77222E-03	1.00000E-05
2	2	8.1113E-01	3.2442E+03	4.55249E-03	5.11411E-03	4.25E-04	2	1.17722E-03	1.00000E-05
2	2	7.2743E-01	9.263E-01	1.263E-03	6.717E-07	1.447E-03	2	1.314663E-04	1.00000E-05
1	1	1.43335E-01	4.1347E-03	2.84352E-03	1.33292E-03	1.17722E-03	2	1.77222E-03	1.00000E-05
2	2	8.09261E-01	3.3332E+03	4.47612E-03	5.11411E-03	4.25E-04	2	1.17722E-03	1.00000E-05
2	2	7.5403E-01	9.2645E-01	1.2745E-03	6.717E-07	1.447E-03	2	1.314663E-04	1.00000E-05
1	1	1.42206E-01	4.1542E-03	2.8773E-03	1.33292E-03	1.17722E-03	2	1.77222E-03	1.00000E-05
2	2	8.16553E-01	3.3332E+03	4.47612E-03	5.11411E-03	4.25E-04	2	1.17722E-03	1.00000E-05
2	2	7.7478E-01	9.2717E-01	1.2717E-03	6.717E-07	1.447E-03	2	1.314663E-04	1.00000E-05
1	1	1.41075E-01	4.1655E-03	2.9273E-03	1.33292E-03	1.17722E-03	2	1.77222E-03	1.00000E-05
2	2	7.95564E-01	3.3332E+03	4.47612E-03	5.11411E-03	4.25E-04	2	1.17722E-03	1.00000E-05
2	2	7.844E-01	9.2742E-01	1.2742E-03	6.717E-07	1.447E-03	2	1.314663E-04	1.00000E-05
1	1	1.39945E-01	4.1671E-03	2.9273E-03	1.33292E-03	1.17722E-03	2	1.77222E-03	1.00000E-05
2	2	7.8117E-01	3.3332E+03	4.47612E-03	5.11411E-03	4.25E-04	2	1.17722E-03	1.00000E-05
2	2	8.1779E-01	9.282E-01	1.282E-03	6.717E-07	1.447E-03	2	1.314663E-04	1.00000E-05
1	1	1.36911E-01	4.1752E-03	2.9557E-03	1.33292E-03	1.17722E-03	2	1.77222E-03	1.00000E-05
2	2	7.8005E-01	3.3332E+03	4.47612E-03	5.11411E-03	4.25E-04	2	1.17722E-03	1.00000E-05
2	2	8.557E-01	9.287E-01	1.287E-03	6.717E-07	1.447E-03	2	1.314663E-04	1.00000E-05
1	1	1.35012E-01	4.1842E-03	2.988E-03	1.33292E-03	1.17722E-03	2	1.77222E-03	1.00000E-05
2	2	7.7505E-01	3.3332E+03	4.47612E-03	5.11411E-03	4.25E-04	2	1.17722E-03	1.00000E-05
2	2	8.827E-01	9.292E-01	1.292E-03	6.717E-07	1.447E-03	2	1.314663E-04	1.00000E-05
1	1	1.32012E-01	4.1932E-03	3.019E-03	1.33292E-03	1.17722E-03	2	1.77222E-03	1.00000E-05
2	2	7.6805E-01	3.3332E+03	4.47612E-03	5.11411E-03	4.25E-04	2	1.17722E-03	1.00000E-05
2	2	8.907E-01	9.297E-01	1.297E-03	6.717E-07	1.447E-03	2	1.314663E-04	1.00000E-05
1	1	1.28012E-01	4.2022E-03	3.049E-03	1.33292E-03	1.17722E-03	2	1.77222E-03	1.00000E-05
2	2	7.6105E-01	3.3332E+03	4.47612E-03	5.11411E-03	4.25E-04	2	1.17722E-03	1.00000E-05
2	2	9.037E-01	9.302E-01	1.302E-03	6.717E-07	1.447E-03	2	1.314663E-04	1.00000E-05
1	1	1.24012E-01	4.2112E-03	3.079E-03	1.33292E-03	1.17722E-03	2	1.77222E-03	1.00000E-05
2	2	7.5405E-01	3.3332E+03	4.47612E-03	5.11411E-03	4.25E-04	2	1.17722E-03	1.00000E-05
2	2	9.167E-01	9.307E-01	1.307E-03	6.717E-07	1.447E-03	2	1.314663E-04	1.00000E-05
1	1	1.20012E-01	4.2202E-03	3.109E-03	1.33292E-03	1.17722E-03	2	1.77222E-03	1.00000E-05
2	2	7.4705E-01	3.3332E+03	4.47612E-03	5.11411E-03	4.25E-04	2	1.17722E-03	1.00000E-05
2	2	9.297E-01	9.312E-01	1.312E-03	6.717E-07	1.447E-03	2	1.314663E-04	1.00000E-05
1	1	1.16012E-01	4.2292E-03	3.139E-03	1.33292E-03	1.17722E-03	2	1.77222E-03	1.00000E-05
2	2	7.3305E-01	3.3332E+03	4.47612E-03	5.11411E-03	4.25E-04	2	1.17722E-03	1.00000E-05
2	2	9.427E-01	9.317E-01	1.317E-03	6.717E-07	1.447E-03	2	1.314663E-04	1.00000E-05
1	1	1.12012E-01	4.2382E-03	3.169E-03	1.33292E-03	1.17722E-03	2	1.77222E-03	1.00000E-05
2	2	7.1905E-01	3.3332E+03	4.47612E-03	5.11411E-03	4.25E-04	2	1.17722E-03	1.00000E-05
2	2	9.517E-01	9.322E-01	1.322E-03	6.717E-07	1.447E-03	2	1.314663E-04	1.00000E-05
1	1	1.08012E-01	4.2472E-03	3.201E-03	1.33292E-03	1.17722E-03	2	1.77222E-03	1.00000E-05
2	2	7.0505E-01	3.3332E+03	4.47612E-03	5.11411E-03	4.25E-04	2	1.17722E-03	1.00000E-05
2	2	9.607E-01	9.327E-01	1.327E-03	6.717E-07	1.447E-03	2	1.314663E-04	1.00000E-05
1	1	1.04012E-01	4.2562E-03	3.231E-03	1.33292E-03	1.17722E-03	2	1.77222E-03	1.00000E-05
2	2	6.9105E-01	3.3332E+03	4.47612E-03	5.11411E-03	4.25E-04	2	1.17722E-03	1.00000E-05
2	2	9.707E-01	9.332E-01	1.332E-03	6.717E-07	1.447E-03	2	1.314663E-04	1.00000E-05
1	1	1.00012E-01	4.2652E-03	3.261E-03	1.33292E-03	1.17722E-03	2	1.77222E-03	1.00000E-05
2	2	6.7705E-01	3.3332E+03	4.47612E-03	5.11411E-03	4.25E-04	2	1.17722E-03	1.00000E-05
2	2	9.807E-01	9.337E-01	1.337E-03	6.717E-07	1.447E-03	2	1.314663E-04	1.00000E-05
1	1	0.96012E-01	4.2742E-03	3.291E-03	1.33292E-03	1.17722E-03	2	1.77222E-03	1.00000E-05
2	2	6.6305E-01	3.3332E+03	4.47612E-03	5.11411E-03	4.25E-04	2	1.17722E-03	1.00000E-05
2	2	9.907E-01	9.342E-01	1.342E-03	6.717E-07	1.447E-03	2	1.314663E-04	1.00000E-05
1	1	0.92012E-01	4.2832E-03	3.321E-03	1.33292E-03	1.17722E-03	2	1.77222E-03	1.00000E-05
2	2	6.5505E-01	3.3332E+03	4.47612E-03	5.11411E-03	4.25E-04	2	1.17722E-03	1.00000E-05
2	2	10.007E-01	9.347E-01	1.347E-03	6.717E-07	1.447E-03	2	1.314663E-04	1.00000E-05
1	1	0.88012E-01	4.2922E-03	3.351E-03	1.33292E-03	1.17722E-03	2	1.77222E-03	1.00000E-05
2	2	6.4705E-01	3.3332E+03	4.47612E-03	5.11411E-03	4.25E-04	2	1.17722E-03	1.00000E-05
2	2	10.107E-01	9.352E-01	1.352E-03	6.717E-07	1.447E-03	2	1.314663E-04	1.00000E-05
1	1	0.84012E-01	4.3012E-03	3.381E-03	1.33292E-03	1.17722E-03	2	1.77222E-03	1.00000E-05
2	2	6.41							

Table V—Continued

2	2	7,732275-01	3,077874E+00	2,133694E+00	7,413201E+03	6,190238E+03	3,935570E+02	3,000000E+00
2	2	1,97019	9,96922	3,3116	2491,7	43159	1,100000E+02	2,59561E+02
1	1	1,363146E-01	6,189951E+03	3,58919E+00	5,124275E+03	1,979974E+03	1,199974E+03	1,000000E+00
2	2	7,657082E-01	3,063116E+03	2,174419E+00	5,412936E+03	6,191027E+03	3,909479E+02	3,000000E+00
2	2	8,5738	10,5141E	3,3171	2477,1	43579	1,090142E+02	2,50544E+02
1	1	1,354734E-01	6,194013E+03	3,59717E+00	5,124275E+03	1,977480E+03	1,12022E+03	1,000000E+00
2	2	7,640429E-01	3,066501E+03	2,215998E+00	5,412670E+03	6,161988E+03	3,476397E+02	3,000000E+00
2	2	1,92233	1,1533E4	3,3221	2473,1	431010	1,080919E+02	2,513106E+02
1	1	1,374313E-01	6,189933E+03	3,58740E+00	5,124409E+03	1,978940E+03	1,105210E+03	1,000000E+00
2	2	7,599742E-01	3,069727E+03	2,225198E+00	5,412442E+03	6,173793E+03	3,47993E+02	3,000000E+00
2	2	1,92741	1,15218E5	3,3371	2449,3	42693	1,06552E+02	2,484241E+02
1	1	1,335253E-01	6,170423E+03	3,731192E+00	5,127765E+03	1,981431E+03	1,093656E+03	1,000000E+00
2	2	1,17161	1,1349E4	3,3551	2443,3	42492	1,013966E+02	2,384253E+02
1	1	1,293527E-01	6,173374E+03	4,22239E+00	5,127265E+03	1,987202E+03	1,059776E+03	1,000000E+00
2	2	1,20659	1,14277E5	3,3739	2422,0	42193	9,758543E+03	2,314364E+02
1	1	1,126244E-01	6,125029E+03	4,249473E+00	5,112343E+03	1,990051E+03	1,023303E+03	1,000000E+00
2	2	1,10533	1,11268E5	3,4345	2405,0	41537	9,343772E+03	2,213375E+02
1	1	1,224377E-01	6,127287E+03	4,195663E+00	5,112480E+03	1,994493E+03	1,049524E+03	1,000000E+00
2	2	1,24335	1,11205E5	3,4244	2380,4	40874	6,956033E+03	2,197979E+02
1	1	1,156446E-01	6,125379E+03	4,74181E+00	5,116644E+03	1,991144E+03	1,055192E+03	1,000000E+00
2	2	1,13200	1,11110E5	3,4922	2367,4	40172	5,566663E+03	2,065424E+02
1	1	1,116373E-01	6,117335E+03	4,87478E+00	5,111945E+03	2,033722E+03	1,042425E+03	1,000000E+00
2	2	1,19711	1,12165E5	3,5241	2311,0	39475	7,57175E+03	1,937151E+02
1	1	1,115527E-01	6,12430E+03	5,01705E+00	5,114332E+03	2,01950E+03	1,07774E+03	1,000000E+00
2	2	1,14258	1,14453E5	3,5345	233,5	39232	7,490174E+03	1,944495E+02
1	1	1,116373E-01	6,117335E+03	4,87478E+00	5,111945E+03	2,033722E+03	1,042425E+03	1,000000E+00
2	2	1,15094	1,14653E5	3,5241	2311,0	39475	7,57175E+03	1,937151E+02
1	1	1,177554E-01	6,135647E+03	5,46175E+00	5,114429E+03	2,028937E+03	1,049524E+03	1,000000E+00
2	2	1,14244	1,14045E5	3,5425	2290,1	38343	7,100446E+03	1,825271E+02
1	1	1,116373E-01	6,117335E+03	4,87478E+00	5,111945E+03	2,033722E+03	1,042425E+03	1,000000E+00
2	2	1,17908	1,12447E5	3,5310	2260,0	38314	6,710863E+03	1,744157E+02
1	1	1,105433E-01	6,139925E+03	6,18253E+00	5,107339E+03	2,01650E+03	1,052444E+03	1,000000E+00
2	2	1,18444	1,13718E5	3,6140	224E,3	38111	6,527277E+03	1,642444E+02
1	1	1,109119E-01	6,139954E+03	6,18253E+00	5,107339E+03	2,01650E+03	1,052444E+03	1,000000E+00
2	2	1,19201	1,12404E5	3,6214	2237,4	38112	6,360286E+03	1,634032E+02
1	1	1,062221E-01	6,144565E+03	6,140419E+00	5,110331E+03	2,075136E+03	1,054365E+03	1,000000E+00
2	2	1,19667	1,12614E5	3,6352	2220,9	37928	6,200426E+03	1,60422E+02
1	1	1,109119E-01	6,139954E+03	6,18253E+00	5,107339E+03	2,01650E+03	1,052444E+03	1,000000E+00
2	2	1,20104	1,12722E5	3,6439	2216,3	37945	6,044230E+03	1,560095E+02
1	1	1,109767E-01	6,143155E+03	6,147810E+00	5,110126E+03	2,095337E+03	1,05152E+03	1,000000E+00
2	2	1,20447	1,12632E5	3,6423	2207,3	37943	5,912446E+03	1,54177E+02

NOT REPRODUCIBLE

Table V--Continued

1	1.271125	1.434177	1.609134	1.804856	2.019257	2.250401	2.505401	2.781401	3.075401	3.385401	3.707401	4.049401	4.410401	4.789401	5.184401	5.594401	6.017401	6.451401	6.894401	7.345401	7.812401	8.294401	8.790401	9.299401	9.820401	10.352401	10.894401	11.446401	12.008401	12.580401	13.161401	13.751401	14.349401	14.954401	15.566401	16.184401	16.808401	17.437401	18.071401	18.709401	19.351401	19.997401	20.647401	21.300401	21.956401	22.615401	23.277401	23.941401	24.607401	25.275401	25.945401	26.617401	27.291401	27.967401	28.645401	29.325401	30.007401	30.691401	31.377401	32.064401	32.753401	33.443401	34.134401	34.826401	35.519401	36.213401	36.908401	37.604401	38.301401	39.000401	39.700401	40.401401	41.103401	41.806401	42.510401	43.215401	43.921401	44.628401	45.336401	46.045401	46.755401	47.466401	48.178401	48.891401	49.605401	50.320401	51.036401	51.753401	52.471401	53.190401	53.910401	54.631401	55.353401	56.076401	56.800401	57.525401	58.251401	58.978401	59.706401	60.435401	61.165401	61.896401	62.628401	63.361401	64.095401	64.830401	65.566401	66.303401	67.041401	67.780401	68.520401	69.261401	70.003401	70.746401	71.490401	72.235401	72.981401	73.728401	74.476401	75.225401	75.975401	76.726401	77.478401	78.231401	78.985401	79.740401	80.496401	81.253401	82.011401	82.770401	83.530401	84.291401	85.053401	85.816401	86.580401	87.345401	88.111401	88.878401	89.646401	90.415401	91.185401	91.956401	92.728401	93.501401	94.275401	95.050401	95.826401	96.603401	97.381401	98.160401	98.940401	99.721401	100.503401	101.286401	102.070401	102.855401	103.641401	104.428401	105.216401	106.005401	106.795401	107.586401	108.378401	109.171401	110.000401	110.830401	111.661401	112.493401	113.326401	114.160401	115.000401	115.841401	116.683401	117.526401	118.370401	119.215401	120.061401	120.908401	121.756401	122.605401	123.455401	124.306401	125.158401	126.011401	126.865401	127.720401	128.576401	129.433401	130.291401	131.150401	132.010401	132.871401	133.733401	134.596401	135.460401	136.325401	137.191401	138.058401	138.926401	139.795401	140.665401	141.536401	142.408401	143.281401	144.155401	145.030401	145.906401	146.783401	147.661401	148.540401	149.420401	150.301401	151.183401	152.066401	152.950401	153.835401	154.721401	155.608401	156.496401	157.385401	158.275401	159.166401	160.058401	160.951401	161.845401	162.740401	163.636401	164.533401	165.431401	166.330401	167.230401	168.131401	169.033401	170.000401	170.968401	171.937401	172.907401	173.878401	174.850401	175.823401	176.797401	177.772401	178.748401	179.725401	180.703401	181.682401	182.662401	183.643401	184.625401	185.608401	186.592401	187.577401	188.563401	189.550401	190.538401	191.527401	192.517401	193.508401	194.500401	195.493401	196.487401	197.482401	198.478401	199.475401	200.473401	201.471401	202.470401	203.469401	204.468401	205.468401	206.468401	207.468401	208.468401	209.468401	210.468401	211.468401	212.468401	213.468401	214.468401	215.468401	216.468401	217.468401	218.468401	219.468401	220.468401	221.468401	222.468401	223.468401	224.468401	225.468401	226.468401	227.468401	228.468401	229.468401	230.468401	231.468401	232.468401	233.468401	234.468401	235.468401	236.468401	237.468401	238.468401	239.468401	240.468401	241.468401	242.468401	243.468401	244.468401	245.468401	246.468401	247.468401	248.468401	249.468401	250.468401	251.468401	252.468401	253.468401	254.468401	255.468401	256.468401	257.468401	258.468401	259.468401	260.468401	261.468401	262.468401	263.468401	264.468401	265.468401	266.468401	267.468401	268.468401	269.468401	270.468401	271.468401	272.468401	273.468401	274.468401	275.468401	276.468401	277.468401	278.468401	279.468401	280.468401	281.468401	282.468401	283.468401	284.468401	285.468401	286.468401	287.468401	288.468401	289.468401	290.468401	291.468401	292.468401	293.468401	294.468401	295.468401	296.468401	297.468401	298.468401	299.468401	300.468401
---	----------	----------	----------	----------	----------	----------	----------	----------	----------	----------	----------	----------	----------	----------	----------	----------	----------	----------	----------	----------	----------	----------	----------	----------	----------	-----------	-----------	-----------	-----------	-----------	-----------	-----------	-----------	-----------	-----------	-----------	-----------	-----------	-----------	-----------	-----------	-----------	-----------	-----------	-----------	-----------	-----------	-----------	-----------	-----------	-----------	-----------	-----------	-----------	-----------	-----------	-----------	-----------	-----------	-----------	-----------	-----------	-----------	-----------	-----------	-----------	-----------	-----------	-----------	-----------	-----------	-----------	-----------	-----------	-----------	-----------	-----------	-----------	-----------	-----------	-----------	-----------	-----------	-----------	-----------	-----------	-----------	-----------	-----------	-----------	-----------	-----------	-----------	-----------	-----------	-----------	-----------	-----------	-----------	-----------	-----------	-----------	-----------	-----------	-----------	-----------	-----------	-----------	-----------	-----------	-----------	-----------	-----------	-----------	-----------	-----------	-----------	-----------	-----------	-----------	-----------	-----------	-----------	-----------	-----------	-----------	-----------	-----------	-----------	-----------	-----------	-----------	-----------	-----------	-----------	-----------	-----------	-----------	-----------	-----------	-----------	-----------	-----------	-----------	-----------	-----------	-----------	-----------	-----------	-----------	-----------	-----------	------------	------------	------------	------------	------------	------------	------------	------------	------------	------------	------------	------------	------------	------------	------------	------------	------------	------------	------------	------------	------------	------------	------------	------------	------------	------------	------------	------------	------------	------------	------------	------------	------------	------------	------------	------------	------------	------------	------------	------------	------------	------------	------------	------------	------------	------------	------------	------------	------------	------------	------------	------------	------------	------------	------------	------------	------------	------------	------------	------------	------------	------------	------------	------------	------------	------------	------------	------------	------------	------------	------------	------------	------------	------------	------------	------------	------------	------------	------------	------------	------------	------------	------------	------------	------------	------------	------------	------------	------------	------------	------------	------------	------------	------------	------------	------------	------------	------------	------------	------------	------------	------------	------------	------------	------------	------------	------------	------------	------------	------------	------------	------------	------------	------------	------------	------------	------------	------------	------------	------------	------------	------------	------------	------------	------------	------------	------------	------------	------------	------------	------------	------------	------------	------------	------------	------------	------------	------------	------------	------------	------------	------------	------------	------------	------------	------------	------------	------------	------------	------------	------------	------------	------------	------------	------------	------------	------------	------------	------------	------------	------------	------------	------------	------------	------------	------------	------------	------------	------------	------------	------------	------------	------------	------------	------------	------------	------------	------------	------------	------------	------------	------------	------------	------------	------------	------------	------------	------------	------------	------------	------------	------------	------------	------------	------------	------------	------------	------------	------------	------------	------------	------------	------------	------------	------------	------------	------------	------------	------------	------------	------------	------------	------------

NOT REPRODUCIBLE

2 2 5,12601 10,00007 0,4220 1149,3 10047,6 0,003 11,000 1,111111111 4 1,70 000000 0,00000

7.55052	0,00001	1,00000	1,4311
7.59198	0,0001	1,00000	1,42985
7.61682	0,0004	1,00001	1,43091
7.63083	0,0010	1,00003	1,43112
7.64271	0,0017	1,00006	1,43412
7.71432	0,0026	1,00012	1,43552
7.74671	0,0037	1,00018	1,44462
7.77952	0,0050	1,00025	1,45333
7.80910	0,0064	1,00033	1,46217
7.83640	0,0080	1,00042	1,47118
7.87710	0,0102	1,00053	1,48028
7.93736	0,0143	1,00067	1,48945
7.99719	0,0191	1,00083	1,49867
8.05765	0,0247	1,00101	1,50794
8.11831	0,0310	1,00121	1,51727
8.17991	0,0382	1,00143	1,52665
8.23428	0,0461	1,00167	1,53608
8.27529	0,0548	1,00193	1,54556
8.31992	0,0643	1,00221	1,55509
8.36379	0,0741	1,00251	1,56467
8.40303	0,0845	1,00282	1,57430
8.44174	0,0953	1,00315	1,58398
8.47933	0,1069	1,00350	1,59371
8.51759	0,1191	1,00387	1,60349
8.55122	0,1316	1,00426	1,61332
8.57855	0,1430	1,00467	1,62320
8.60294	0,1548	1,00509	1,63313
8.62688	0,1672	1,00553	1,64311
8.64959	0,1800	1,00599	1,65314
8.67285	0,1931	1,00647	1,66322
8.69872	0,2065	1,00696	1,67335
8.71427	0,2202	1,00747	1,68353
8.73531	0,2342	1,00799	1,69376
8.75634	0,2484	1,00853	1,70404
8.77999	0,2629	1,00908	1,71437
8.80344	0,2776	1,00964	1,72475
8.82759	0,2926	1,01021	1,73518
8.85224	0,3078	1,01079	1,74566
8.87729	0,3232	1,01138	1,75619
8.90274	0,3388	1,01198	1,76677
8.92859	0,3546	1,01259	1,77740
8.95484	0,3706	1,01321	1,78808
8.98149	0,3868	1,01384	1,79881
9.00854	0,4032	1,01448	1,80959
9.03599	0,4198	1,01513	1,82042
9.06384	0,4366	1,01579	1,83130
9.09209	0,4536	1,01646	1,84223
9.12074	0,4708	1,01714	1,85321
9.14979	0,4882	1,01783	1,86424
9.17924	0,5058	1,01853	1,87532
9.20909	0,5236	1,01924	1,88645
9.23934	0,5416	1,02000	1,89763
9.26999	0,5598	1,02077	1,90886
9.29114	0,5782	1,02156	1,92014
9.31269	0,5968	1,02236	1,93147
9.33464	0,6156	1,02317	1,94285
9.35699	0,6346	1,02399	1,95428
9.37974	0,6538	1,02482	1,96576
9.40289	0,6732	1,02567	1,97729
9.42644	0,6928	1,02653	1,98887
9.45039	0,7126	1,02740	1,99950
9.47474	0,7326	1,02829	2,01018
9.49949	0,7528	1,02919	2,02091
9.52464	0,7732	1,03010	2,03169
9.55019	0,7938	1,03102	2,04252
9.57614	0,8146	1,03196	2,05340
9.60249	0,8356	1,03291	2,06433
9.62924	0,8568	1,03387	2,07531
9.65639	0,8782	1,03484	2,08634
9.68394	0,8998	1,03582	2,09742
9.71189	0,9216	1,03681	2,10855
9.74024	0,9436	1,03781	2,11973
9.76899	0,9658	1,03882	2,13096
9.79814	0,9882	1,03984	2,14224
9.82769	1,0108	1,04087	2,15357
9.85764	1,0336	1,04191	2,16495
9.88799	1,0566	1,04296	2,17638
9.91874	1,0798	1,04402	2,18786
9.94989	1,1032	1,04509	2,19939
9.98144	1,1268	1,04617	2,21097
10.01339	1,1506	1,04726	2,22260
10.04574	1,1746	1,04836	2,23428
10.07849	1,1988	1,04947	2,24601
10.11164	1,2232	1,05059	2,25779
10.14519	1,2478	1,05172	2,26962
10.17914	1,2726	1,05286	2,28150
10.21349	1,2976	1,05401	2,29343
10.24824	1,3228	1,05517	2,30541
10.28339	1,3482	1,05634	2,31744
10.31894	1,3738	1,05752	2,32952
10.35489	1,4000	1,05871	2,34165
10.39124	1,4264	1,05991	2,35383
10.42799	1,4530	1,06112	2,36606
10.46514	1,4800	1,06234	2,37834
10.50269	1,5072	1,06357	2,39067
10.54064	1,5346	1,06481	2,40305
10.57899	1,5622	1,06606	2,41548
10.61774	1,5900	1,06732	2,42796
10.65689	1,6180	1,06859	2,44049
10.69644	1,6462	1,06987	2,45307
10.73639	1,6746	1,07116	2,46570
10.77674	1,7032	1,07246	2,47838
10.81749	1,7320	1,07377	2,49111
10.85864	1,7610	1,07509	2,50389
10.90019	1,7902	1,07642	2,51672
10.94214	1,8196	1,07776	2,52960
10.98449	1,8492	1,07911	2,54253
11.02724	1,8790	1,08047	2,55551
11.07039	1,9090	1,08184	2,56854
11.11394	1,9392	1,08322	2,58162
11.15789	1,9696	1,08461	2,59475
11.20224	1,9990	1,08601	2,60793
11.24709	2,0290	1,08742	2,62116
11.29234	2,0590	1,08884	2,63444
11.33809	2,0890	1,09027	2,64777
11.38424	2,1190	1,09171	2,66115
11.43079	2,1490	1,09316	2,67458
11.47774	2,1790	1,09462	2,68806
11.52509	2,2090	1,09609	2,70159
11.57284	2,2390	1,09757	2,71517
11.62109	2,2690	1,09906	2,72880
11.66974	2,2990	1,10056	2,74248
11.71889	2,3290	1,10207	2,75621
11.76844	2,3590	1,10359	2,77000
11.81839	2,3890	1,10512	2,78384
11.86874	2,4190	1,10666	2,79773
11.91949	2,4490	1,10821	2,81167
11.97064	2,4790	1,10977	2,82566
12.02219	2,5090	1,11134	2,83970
12.07414	2,5390	1,11292	2,85379
12.12649	2,5690	1,11451	2,86793
12.17924	2,5990	1,11611	2,88212
12.23239	2,6290	1,11772	2,89636
12.28594	2,6590	1,11934	2,91065
12.33989	2,6890	1,12097	2,92499
12.39424	2,7190	1,12261	2,93938
12.44909	2,7490	1,12426	2,95382
12.50434	2,7790	1,12592	2,96831
12.55999	2,8090	1,12759	2,98285
12.61604	2,8390	1,12927	2,99744
12.67249	2,8690	1,13096	3,01208
12.72934	2,8990	1,13266	3,02677
12.78659	2,9290	1,13437	3,04151
12.84424	2,9590	1,13609	3,05630
12.90229	2,9890	1,13782	3,07114
12.96074	3,0190	1,13956	3,08603
13.01959	3,0490	1,14131	3,10097
13.07884	3,0790	1,14307	3,11596
13.13849	3,1090	1,14484	3,13100
13.19854	3,1390	1,14662	3,14609
13.25899	3,1690	1,14841	3,16123
13.31984	3,1990	1,15021	3,17642
13.38109	3,2290	1,15202	3,19166
13.44274	3,2590	1,15384	3,20695
13.50479	3,2890	1,15567	3,22229
13.56724	3,3190	1,15751	3,23768
13.63009	3,3490	1,15936	3,25312
13.69334	3,3790	1,16122	3,26861
13.75709	3,4090	1,16309	3,28415
13.82124	3,4390	1,16497	3,29974
13.88579	3,4690	1,16686	3,31538
13.95074	3,4990	1,16876	3,33107
14.01609	3,5290	1,17067	3,34681
14.08184	3,5590	1,17259	3,36260
14.14799	3,5890	1,17452	3,37844
14.21454	3,6190	1,17646	3,39433
14.28149	3,6490	1,17841	3,41027
14.34884	3,6790	1,18037	3,42626
14.41659	3,7090	1,18234	3,44230
14.48474	3,7390	1,18431	3,45839
14.55329	3,7690	1,18629	3,47453
14.62224	3,7990	1,18828	3,49072
14.69159	3,8290	1,19028	3,50696
14.76134	3,8590	1,19229	3,52325
14.83149	3,8890	1,19431	3,53959
14.90194	3,9190	1,19634	3,55598
14.97279	3,9490	1,19838	3,57242
15.04404	3,9790	1,19990	3,58891
15.11569	4,0090	1,20143	3,60545
15.18774	4,0390	1,20297	3,62204
15.26019	4,0690	1,20452	3,63868
15.33304	4,0990	1,20608	3,65537
15.40629	4,1290	1,20764	3,67211
15.47994	4,1590	1,20921	3,68890
15.55399	4,1890	1,21079	3,70574
15.62844	4,2190	1,21237	3,72263
15.70329	4,2490	1,21396	3,73957
15.77854	4,2790	1,21556	3,75656
15.85419	4,3090	1,21716	3,77360
15.93024	4,3390	1,21877	3,79069
16.00669	4,3690	1,22038	3,80783
16.08354	4,3990	1,22199	3,82502
16.16079	4,4290	1,22361	3,84226
16.23844	4,4590	1,22524	3,85955
16.31649	4,4890	1,22687	3,87689
16.39494	4,5190	1,22851	3,89428
16.47379	4,5490	1,23016	3,91172
16.55304	4,5790	1,23181	3,92921
16.63269	4,6090	1,23347	3,94675
16.71274	4,6390	1,23513	3,96434
16.79319	4,6690	1,23680	3,98198
16.87404	4,6990	1,23847	3,99967
16.95529	4,7290	1,24015	4,01741
17.03694	4,7590	1,24183	4,03520
17.11899	4,7890	1,24352	4,05304
17.20144	4,8190	1,24521	4,07093
17.28429	4,8490	1,24691	4,08887
17.36754	4,8790	1,24861	4,10686
17.45119	4,9090	1,25032	4,12490
17.53524	4,9390	1,25203	4,14299
17.61969	4,9690	1,25375	4,16113
17.70454	4,9990	1,25547	4,17932
17.78979	5,0290	1,25720	4,19756
17.87544	5,0590	1,25893	4,21585
17.96149	5,0890	1,26067	4,23419
18.04794	5,1190	1,26241	4,25258
18.13479	5,1490	1,26416	4,27102
18.22204	5,1790	1,26591	4,28951
18.30969	5,2090	1,26766	4,30805
18.39774	5,2390	1,26942	4,32664
18.48619	5,2690	1,27118	4,34528
18.57504	5,2990	1,27294	4,36397
18.66429	5,3290	1,27471	4,38271
18.75394	5,3590	1,27648	4,40150
18.84399	5,3890	1,27825	4,42034
18.93444	5,4190	1,28003	4,43923
19.02529	5,4490	1,28181	4,45817
19.11654	5,4790	1,28359	4,47716
19.20819	5,5090	1,28538	4,49620
19.29924	5,5390	1,28717	4,51529
19.39069	5,5690	1,28896	4,53443
19.48244	5,5990	1,29076	4,55362

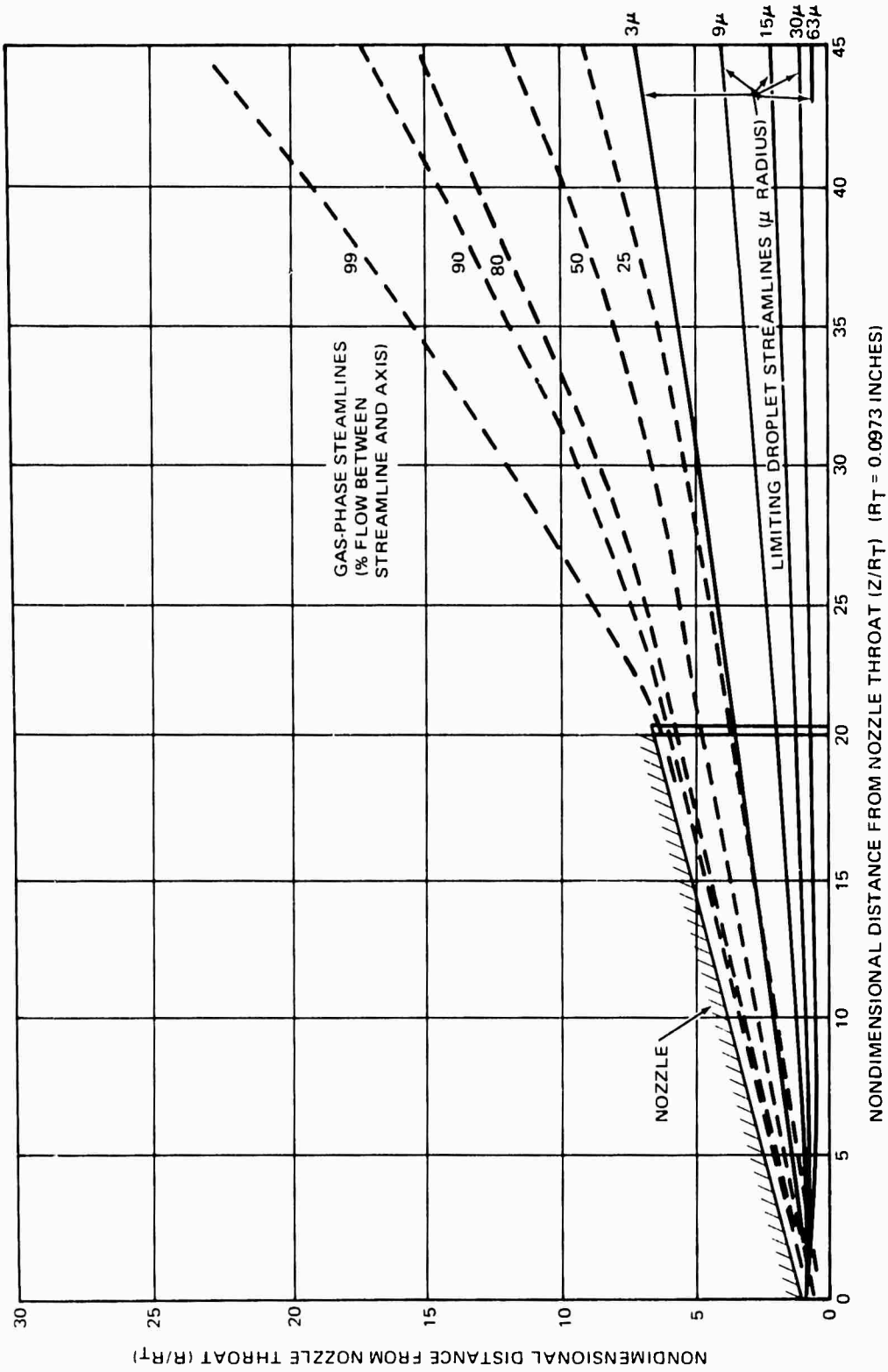


Figure 27. Marquardt R-6C Engine -- Contaminant Transport (MULTRAN Program)

(2) Interpretation of MULTRAN Output

Figure 27 shows the limiting droplet streamlines for the five droplet groups (3, 9, 15, 30, 63 μ radius) representing the unburned fuel and oxidizer droplets. The limiting droplet streamlines for each group are defined as the furthest radial position from the axis at which droplets of that particle size are found. Larger droplets are closer to the axis since they resist turning during the gas expansion due to their large mass. The gas-phase streamlines are also shown (dotted lines) representing the boundary of a streamtube containing a specified percent mass of the flow between the streamline and the axis.

The small size of this engine (5-lb thrust) and relatively large unburned droplets exiting the combustor tested the ability of the MULTRAN program in many unexpected ways. An assumption had to be made as to the initial flow angle of unburned droplets exiting the combustor—that is, in the convergent section of the nozzle throat.

The current program is set up to distribute the droplets uniformly across a radial section upstream of the throat and to assign uniformly increasing negative flow angles between the axis and the convergent wall point. The convergent inlet angle was set to a minimum value of 12 degrees presenting a very shallow inlet. The implication of this assumption is that droplets cannot turn to a greater angle than 12 degrees in the inlet due to their large mass. The 12-degree value represents a limitation of the current program, not an engineering judgement.

The results of the sample case show the difficulty with this assumption. It has originally been expected that the droplets would quickly turn and assume positive flow angles shortly downstream of the throat. The 3, 9, and 15 μ droplets did turn, although further downstream than expected. The heavier droplets, 30 and 63 μ , also turned, but only slightly, retaining a slightly negative flow angle.

The effect of this assumption (negative inlet angles for the droplets nearest the wall) on the results is very minor. Had the droplets been parallel to the axis (0 degree) at the throat, the droplet expansion "cones" would have been slightly larger. Numerical difficulty, however, had to be overcome, due to the extremely high droplet/gas weight flow ratios near the axis of the plume—sometimes exceeding 100:1—due to the negative initial angle of the heaviest particles. Future work will eliminate the necessity for this assumption.

(3) Summary of Results

The small size of the test engine, coupled with the relatively large unburned drop sizes and large area ratio of the nozzle, severely limits

the ability of the droplets to run away from the axial direction and expand into the plume. Residence times during which the droplets experience high radial drag forces in the nozzle and plume are extremely short, limited to approximately 0.2 ms (based on an average droplet velocity of approximately 2,000 ft/sec).

The droplet density profiles at any axial plane ($z = \text{constant}$) is practically uniform between the axis and limiting particle streamline for each particle group. This is due to the negligible influence that the ambient pressure has on the droplets in the plume. After exiting the nozzle, the droplets travel in almost radial paths.

Considering the initial droplet loadings and the total weight flow ratio of droplets to gas ($\Sigma \omega_p / \omega_g = 0.45$) approximately 51 percent of the total flow (gas + particles) is contained within the 3μ limiting particle streamline at the nozzle exit plane. Of this, 31 percent is liquid droplets and 20 percent is gas-phase. Further downstream, the gas expands radially while the particles are contained within a shallow cone. At 20 inches downstream of the nozzle throat (not shown in Figure 27) 42 percent of the flow is contained within the 3μ limiting droplet streamline, consisting of 31-percent liquid and 11-percent gas-phase.

Since the 3μ droplet group comprises only 1 percent of total droplet flow, a more significant result can be seen by examining the 15μ droplet limiting streamline which bounds 96 percent of the droplet flow (15μ , 30μ , and 63μ groups total). At the nozzle exit plane, 35 percent of the flow is bound by the 15μ limiting droplet streamline of which 30 percent is liquid droplets 15μ or greater and 5 percent is gas-phase. At 20-inches downstream of the nozzle throat, the flow composition bounded by the 15μ streamline is 30-percent liquid and 2-percent gas.

The impact of this result on any analysis or experiment involving direct impingement of the plume from this engine is obvious. Impingement of the shallow central cone of the plume will involve primarily liquid droplets while impingement by other portions of the plume will be practically entirely gaseous (aside from possible condensation of plume species).

4. KINETICS AND CONDENSATION—THE KINCON PROGRAM

The KINCON subprogram performs the chemical-kinetic and single-species condensation calculations along gas-phase streamlines as defined by the Multiphase Nozzle and Plume Transport program, MULTRAN. When operated in the automatic mode, KINCON accepts card input data

describing the initial gas-phase composition, chemical reactions with rate coefficients, and pertinent integration control parameters. The streamline definition including initial streamline conditions (pressure, temperature, and velocity) and the streamline pressure distribution are obtained from the MULTRAN program via TAPE 8.

a. Description of Input

Six streamlines (the axis, 25, 50, 80, 90, and 99 percent mass flow streamlines) were selected for analysis. The chemical system (12 species and 24 reactions) describing the kinetics of MMH/NTO combustion products is a commonly used set and was obtained from the ODK (the ICRPG One-Dimensional Kinetic Nozzle Analysis Computer Program) kinetics library (Reference C-1 and C-2 in Appendix C). The rate constants were updated whenever possible with the latest values from the literature. The initial gas-phase chemical composition was obtained from thermochemical equilibrium results corresponding to a chamber pressure of 67 psia and an oxidizer-to-fuel ratio (O/F) of 1.5. The chamber conditions represent averaged values over the segment of the engine pulse as calculated by the TCC subprogram.

A listing of the KINCON card input data for this sample case is presented in Table VI. Nothing is entered in the namelist \$THERMO since a master tape of thermodynamic data (in JANAF format) was attached to TAPE 4. The 12 chemical species with initial mass fractions follow the title card. The chemical reactions are specified in two groups; the three body dissociation and recombination reactions appearing before card END TBR REAX, and the binary exchange reactions following the END TBR REAX card. The rate constants for the reverse reaction are input on the same card as reaction, which is input in symbolic form. Integration control parameters and miscellaneous data follow the reaction cards in namelist \$PROPEL.

The normalizing factor for the streamline coordinate was taken as the throat radius, $RSTAR = 0.0972$ in. Initial step size (HI), minimum step size (HMIN), and maximum step size (HMAX) are input in values of the normalized streamline coordinate. DEL is the relative error criterion and represents a measure of the truncation error in the finite difference scheme. With JF = 0 all variables are considered for step size control. Every tenth integration step is output as specified by ND3. Inputs required for the condensation pass include: ICOND, the location of water vapor in the species list; AREPS, the relative convergence criterion for area ratio iteration.

b. Description of Output

Chemical kinetics calculation passes were performed for six streamlines corresponding to total mass flow percentages of 0 (axis streamline), 25., 50., 80., 90., and 99. Output samples from two of the streamlines (axis and 90-percent streamlines) are included here to illustrate the KINCON capabilities. Table VII and VIII present the properties for the two streamlines as computed by the SLINES portion of the MULTRAN subprogram.

Table VI. KINCON SAMPLE CASE-DATA LISTING

STHERMO S AUTOMATED KINCON TEST CASE				
SPECIES MASS FRACTIONS				
CO2	,0652			
H2O	,2738			
CO	,2017			
H2	,020			
N2	,42509761			
NO	,002			
OH	,00967			
O2	,000764			
C	1,69E-11			
H	,00115			
N	1,39E-6			
O	,000617			
REACTIONS				
O2 = 2*O,	A=3,3E17,	N=1,0,	B=0,0,	REACTION 1
N2 = 2*N,	A=9,6E17,	N=1,0,	B=0,0,	REACTION 2
NO = N + O,	A=7,2E15,	N=0,5,	B=0,0,	REACTION 3
H2 = 2*H,	A=5,0E18,	N=1,0,	B=0,0,	REACTION 4
H2O = H + OH,	A=1,17E17,	N=0,0,	B=0,0,	REACTION 5
OH = H + O,	A=2,3E16,	N=0,0,	B=0,0,	REACTION 6
CO2 = CO + O,	A=5,1E15,	N=0,0,	B=3,58,	REACTION 7
CO = C + O,	A=6,0E8,	N=0,0,	B=50,,	REACTION 8
END TBR REAX				
NO + O = N + O2,	A=3,0E11,	N=0,5,	B=7,13,	REACTION 9
NO + N = N2 + O,	A=9,0E13,	N=0,0,	B=75,5,	REACTION 10
N2 + O2 = 2*NO,	A=1,0E13,	N=0,0,	B=79,489,	REACTION 11
CO + O2 = CO2 + O,	A=1,9E13,	N=0,0,	B=54,15,	REACTION 12
CC + N = C + NO,	A=1,3E10,	N=0,1,	B=0,5,	REACTION 13
CO + O = C + O2,	A=2,4E13,	N=0,0,	B=1,99,	REACTION 14
CC + H = C + OH,	A=1,2E14,	N=0,0,	B=25,83,	REACTION 15
CO2 + H = CO + OH,	A=9,5E11,	N=0,0,	B=1,08,	REACTION 16
OH + O = H + O2,	A=2,24E14,	N=0,0,	B=16,9,	REACTION 17
OH + H2 = H2O + H,	A=8,41E13,	N=0,0,	B=20,1,	REACTION 18
2*OH = H2O + O,	A=9,75E13,	N=0,0,	B=18,1,	REACTION 19
H2 + O = OH + H,	A=7,33E12,	N=0,0,	B=0,0,	REACTION 20
H2 + O2 = 2*OH,	A=4,98E23,	N=2,5,	B=85,7,	REACTION 21
NO + CO = CO2 + N,	A=1,0E13,	N=0,0,	B=9,93,	REACTION 22
NO + H = OH + N,	A=3,4E13,	N=0,0,	B=1,38,	REACTION 23
CO + CO = CO2 + C,	A=1,0E13,	N=0,0,	B=9,93,	REACTION 24
LAST CARD				
SROPEL				
RSTAR=0,0972,JPFLAG=1, DEL=.01, ND3=10, HI=.0001, HMIN=.0001, HMAX=1,0,				
TCOND(1)=12*0,,				
AREPS=.001, ETA=0,1, TCOND(1)=12*0,, IDCOND=2,				
SEND				

Table VII. KINCON SAMPLE CASE-0% STREAMLINE

--- STREAMLINE (1) = 0.00000 PERCENT OF THE TOTAL MASS FLOW
 ZINIT = 0.00000 (NO DIMENSIONAL = 5/RC)
 PINIT = 79.663129 (PSIA)
 --- POINT = 3020.496393 (FEET) ---
 VINIT = 1714.578425 (FT/SFC)
 ZFINAL = 19.615868 (NO DIMENSIONAL = 2/RC)
 PWSK = 84 (NO. OF PRESSURE TABLE POINTS)

POINT NO.	AXIAL DISTANCE (Z/RC)	RADIAL DISTANCE (R/RC)	STREAMLINE DISTANCE (S/RC)	PRESSURE (PSIA)
1	2.079117E+00	0.	0.	7.966312E+01
2	1.871205E+00	0.	2.074117E+01	7.785458E+01
3	1.663294E+00	0.	4.148234E+01	7.578972E+01
4	1.455382E+00	0.	6.237351E+01	7.352600E+01
5	1.247471E+00	0.	8.316468E+01	7.094492E+01
6	1.039559E+00	0.	1.039559E+02	6.821332E+01
7	8.316468E+01	0.	1.247470E+02	6.535260E+01
8	6.237351E+01	0.	1.455382E+02	6.215614E+01
9	4.148234E+01	0.	1.663294E+02	5.877488E+01
10	2.079117E+01	0.	1.871205E+02	5.528007E+01
11	0.	0.	2.079117E+02	5.170037E+01
12	2.079117E+01	0.	2.287029E+02	4.805444E+01
13	4.158234E+01	0.	2.494940E+02	4.440632E+01
14	6.237351E+01	0.	2.702852E+02	4.072955E+01
15	8.316468E+01	0.	2.910764E+02	3.720222E+01
16	1.039559E+02	0.	3.118675E+02	3.394787E+01
17	1.247471E+02	0.	3.326587E+02	3.090433E+01
18	1.455382E+02	0.	3.534499E+02	2.795066E+01
19	1.663294E+02	0.	3.742411E+02	2.500373E+01
20	1.871205E+02	0.	3.950322E+02	2.237113E+01
21	2.079117E+02	0.	4.158234E+02	1.974853E+01
22	2.287029E+02	0.	4.366146E+02	1.716000E+01
23	2.494940E+02	0.	4.574058E+02	1.464886E+01
24	2.702852E+02	0.	4.781970E+02	1.220913E+01
25	2.910764E+02	0.	4.989882E+02	9.851113E+00
26	3.118675E+02	0.	5.197794E+02	8.397269E+00
27	3.326587E+02	0.	5.405706E+02	7.170444E+00
28	3.534499E+02	0.	5.613618E+02	6.273455E+00
29	3.742411E+02	0.	5.821530E+02	5.472446E+00
30	3.950322E+02	0.	6.029442E+02	4.779787E+00
31	4.158234E+02	0.	6.237354E+02	4.185716E+00
32	4.366146E+02	0.	6.445266E+02	3.680600E+00
33	4.574058E+02	0.	6.653178E+02	3.260070E+00
34	4.781970E+02	0.	6.861090E+02	2.900366E+00
35	4.989882E+02	0.	7.069002E+02	2.597160E+00
36	5.197794E+02	0.	7.276914E+02	2.324108E+00
37	5.405706E+02	0.	7.484826E+02	2.074453E+00
38	5.613618E+02	0.	7.692738E+02	1.840358E+00
39	5.821530E+02	0.	7.900650E+02	1.618537E+00
40	6.029442E+02	0.	8.108562E+02	1.415293E+00
41	6.237354E+02	0.	8.316474E+02	1.225131E+00
42	6.445266E+02	0.	8.524386E+02	1.043070E+00
43	6.653178E+02	0.	8.732298E+02	8.773700E-01
44	6.861090E+02	0.	8.940210E+02	7.250425E-01
45	7.069002E+02	0.	9.148122E+02	5.859531E-01
46	7.276914E+02	0.	9.356034E+02	4.586340E-01
47	7.484826E+02	0.	9.563946E+02	3.424777E-01
48	7.692738E+02	0.	9.771858E+02	2.376148E-01
49	7.900650E+02	0.	9.979770E+02	1.442216E-01
50	8.108562E+02	0.	1.018762E+03	8.626998E-02
51	8.316474E+02	0.	1.039754E+03	5.125414E-02
52	8.524386E+02	0.	1.060746E+03	2.940209E-02
53	8.732298E+02	0.	1.081738E+03	1.625024E-02
54	8.940210E+02	0.	1.102730E+03	8.559133E-03
55	9.148122E+02	0.	1.123722E+03	4.507105E-03
56	9.356034E+02	0.	1.144714E+03	2.147448E-03
57	9.563946E+02	0.	1.165706E+03	9.947601E-04
58	9.771858E+02	0.	1.186698E+03	4.947790E-04
59	9.979770E+02	0.	1.207690E+03	2.289161E-04
60	1.018762E+03	0.	1.228682E+03	1.068754E-04
61	1.039754E+03	0.	1.249674E+03	4.836233E-05
62	1.060746E+03	0.	1.270666E+03	1.403600E-05
63	1.081738E+03	0.	1.291658E+03	3.248000E-06
64	1.102730E+03	0.	1.312650E+03	5.966037E-07

Table VIII. KINCON SAMPLE CASE-90% STREAMLINE

- STREAMLINE(4) = 90.00005 PERCENT OF THE TOTAL MASS FLOW				
ZINIT =	0.000000	(NONDIMENSIONAL = S/RC)		
PINIT =	79.951810	(PSIA)		
<hr/>				
YINIT =	5619.029097	(DEG. W)		
VINIT =	1724.193862	(FT/SEC)		
ZFINAL =	24.405773	(NONDIMENSIONAL = Z/RC)		
MAXK =	50	(NO. OF PRESSURE TABLE POINTS)		
<hr/>				
POINT NO.	AXIAL DISTANCE (Z/RC)	RADIAL DISTANCE (R/RC)	STREAMLINE DISTANCE (S/RC)	PRESSURE (PSIA)
1	-2.079117E+00	1.155289E+00	0.	7.955181E+01
2	-1.971205E+00	1.115788E+00	2.116317E+01	7.763028E+01
3	-1.863294E+00	1.075388E+00	4.225094E+01	7.545083E+01
4	-1.755382E+00	1.035919E+00	6.327117E+01	7.295288E+01
5	-1.647470E+00	1.022811E+00	8.423410E+01	7.018117E+01
6	-1.539558E+00	1.000176E+00	1.051441E+02	6.713574E+01
7	-1.431646E+00	9.814667E+01	1.260215E+02	6.401010E+01
8	-1.323735E+00	9.672626E+01	1.469025E+02	6.051401E+01
9	-1.215824E+00	9.568440E+01	1.677935E+02	5.681435E+01
10	-1.107913E+00	9.506943E+01	1.886798E+02	5.304743E+01
11	-1.000002E+00	9.485110E+01	2.092722E+02	4.912345E+01
12	-8.92091E-01	9.503783E+01	2.300642E+02	4.515893E+01
13	-7.84182E-01	9.563013E+01	2.510618E+02	4.125753E+01
14	-6.76273E-01	9.662678E+01	2.715788E+02	3.737657E+01
15	-5.68364E-01	9.802880E+01	2.925172E+02	3.361944E+01
16	-4.60455E-01	9.983723E+01	3.133849E+02	3.003271E+01
17	-3.52546E-01	1.025534E+02	3.342956E+02	2.679429E+01
18	-2.44637E-01	1.044763E+02	3.552518E+02	2.386464E+01
19	-1.36728E-01	1.077189E+02	3.762699E+02	2.126729E+01
20	-2.28819E-01	1.111539E+02	3.973376E+02	1.890037E+01
21	-1.20910E-01	1.148399E+02	4.184970E+02	1.695590E+01
22	-1.13001E-01	1.174517E+02	4.344218E+02	1.540510E+01
23	-1.05092E-01	1.194118E+02	4.462149E+02	1.416195E+01
24	-9.7183E-02	1.211595E+02	4.537149E+02	1.315775E+01
25	-8.92743E-02	1.225578E+02	4.571711E+02	1.232233E+01
26	-8.13656E-02	1.236677E+02	4.574834E+02	1.155188E+01
27	-7.34569E-02	1.244495E+02	4.549543E+02	1.087877E+01
28	-6.55482E-02	1.249576E+02	4.492151E+02	1.033329E+01
29	-5.76395E-02	1.252049E+02	4.407904E+02	9.915891E+00
30	-4.97308E-02	1.252339E+02	4.292322E+02	9.619417E+00
31	-4.18221E-02	1.250380E+02	4.145277E+02	9.432350E+00
32	-3.39134E-02	1.246294E+02	3.964440E+02	9.350270E+00
33	-2.60047E-02	1.239855E+02	3.745332E+02	9.373010E+00
34	-1.80960E-02	1.231820E+02	3.482477E+02	9.419820E+00
35	-1.01873E-02	1.221970E+02	3.189470E+02	9.499740E+00
36	-2.22965E-02	1.212582E+02	2.851812E+02	9.748539E+00
37	-3.44058E-02	1.204492E+02	2.473119E+02	1.025555E+01
38	-4.65151E-02	1.197195E+02	2.046450E+02	1.092710E+01
39	-5.86244E-02	1.190370E+02	1.574780E+02	1.177300E+01
40	-7.07337E-02	1.184011E+02	1.060714E+02	1.289110E+01
41	-8.28430E-02	1.178125E+02	5.142590E+01	1.438240E+01
42	-9.49523E-02	1.172717E+02	0.000000E+00	1.619416E+01
43	-1.07061E-01	1.167781E+02	1.730259E+01	1.826333E+01
44	-1.19150E-01	1.163324E+02	1.812302E+01	2.034707E+01
45	-1.31239E-01	1.159362E+02	1.800820E+01	2.245002E+01
46	-1.43328E-01	1.155914E+02	1.704210E+01	2.457496E+01
47	-1.55417E-01	1.152980E+02	1.521431E+01	2.695800E+01
48	-1.67506E-01	1.150564E+02	1.255643E+01	2.970254E+01
49	-1.79595E-01	1.148664E+02	9.000000E+00	3.289970E+01
50	-1.91684E-01	1.147280E+02	0.000000E+00	3.654665E+01

Table IX identifies the first streamline (axis) and the calculation pass (kinetics). The pressure distribution as a function of the streamline coordinate is presented in Table X. Several pages listing input variables, species, and reactions have been omitted since all the input data have been presented in Tables VI, VII, and VIII.

Initial streamline conditions are shown in Table XI. The chemical composition corresponds to the input equilibrium chamber composition. The pressure, velocity, and temperature are the values obtained from TAPE 8 (MULTRAN analysis). Station output at several downstream positions is shown in Tables XII, XIII, and XIV. Output from all other stations has been omitted since it is of the same format. A summary of the maximum and minimum net production rates for each reaction is illustrated in Table XV.

A similar sampling of output for the 90-percent mass-flow streamline is included in Tables XVI through XXI. Over the region analyzed in the present sample case, water vapor did not reach saturation conditions and the condensation calculation pass was not performed. The characteristics of condensation calculation pass, including sample output, are illustrated by a sample case in Appendix C, subsection C. 7.

c. Discussion of Results

Results of the KINCON analysis are illustrated for the 99-percent mass-flow streamline and are typical of the other streamlines. Figures 28 through 30 present the static pressure, velocity, and mass fractions of several species as a function of the streamline coordinate which is zero at the upstream boundary of the transonic zone (nozzle throat). The streamline presented here extends just past the nozzle exit plane. Figure 29 presents the streamline static temperature as computed by the KINCON subprogram along with the gas-phase temperature predicted by the MULTRAN analysis (constant specific heat ratio). The error in static temperature, ignoring detailed kinetic effects, may be sizeable.

As can be seen by the distribution of species H_2O , H , and O in Figure 30, the chemistry is essentially frozen downstream of a streamline coordinate of 10. As would be expected, the constant specific heat ratio, which is an equilibrium value, results in a MULTRAN temperature prediction that is higher than the values predicted by KINCON which is essentially frozen.

Figure 29 presents the gas velocity along the streamline. The higher velocity predicted by the KINCON analysis is in keeping with the differences noted in the static temperature distributions. Again, ignoring the details of the streamline expansion could result in a significantly error in gas-phase properties. The analysis procedure utilizes the MULTRAN analysis to define only the coordinates and static pressure for the gas-phase streamlines.

Species compositions presented in Figure 30 are shown to indicate the region and extent of the chemistry. Some water vapor is formed from H , O , and OH ; however, the changes in composition in general were small with the composition essentially frozen downstream of a coordinate of 10.

Table IX. KINCON SAMPLE CASE—IDENTIFICATION (9" STREAMLINE)

.....
~~STREAMTUBE KINETICS/CONDENSATION CALCULATION~~
.....

~~STREAMTUBE NO. 1 CALCULATION PASS NO. 1~~

~~CHEMICAL KINETICS CALCULATION BEING PERFORMED~~
~~ON THIS PASS FOR PRESSURE DEFINED STREAMTUBE~~

Table X. KINCON SAMPLE CASE—PRESSURE TABLE (0% STREAMLINE)

I	Y	P	DP/CX
1	0.	7,96631295E+01	=8,6A903898E+00
2	2,07911696E+01	7,7A565766E+01	=9,32417296E+00
3	4,15823393E+01	7,57859202E+01	=1,04274885E+01
4	6,23735789E+01	7,35209958E+01	=1,19217098E+01
5	8,31646786E+01	7,09949234E+01	=1,27632943E+01
6	1,03955844E+02	6,82133171E+01	=1,35690466E+01
7	1,24747718E+02	6,53525948E+01	=1,45666596E+01
8	1,45538188E+02	6,23561593E+01	=1,54146296E+01
9	1,66329357E+02	5,97746422E+01	=1,65168314E+01
10	1,87120527E+02	5,52880744E+01	=1,77131289E+01
11	2,07911696E+02	5,17063727E+01	=1,73959388E+01
12	2,28702866E+02	4,80544741E+01	=1,75364100E+01
13	2,49494036E+02	4,44053232E+01	=1,73748823E+01
14	2,70285205E+02	4,08249536E+01	=1,70267047E+01
15	2,91076375E+02	3,73282270E+01	=1,65495445E+01
16	3,11867545E+02	3,39478498E+01	=1,54567425E+01
17	3,32658714E+02	3,06009342E+01	=1,46629711E+01
18	3,53449884E+02	2,75506594E+01	=1,41819510E+01
19	3,74241054E+02	2,50037708E+01	=1,31775515E+01
20	3,95032223E+02	2,23711253E+01	=1,17614475E+01
21	4,157911696E+02	1,97485426E+01	=1,01599422E+01
22	4,36582339E+02	1,71559944E+01	=8,43144740E+00
23	4,57373512E+02	1,46368576E+01	=7,57644669E+00
24	4,78164685E+02	1,22091758E+01	=6,65271310E+00
25	4,98955858E+02	9,85111300E+00	=5,75432583E+00
26	5,19747031E+02	8,39728842E+00	=4,97834342E+00
27	5,40538204E+02	7,17642419E+00	=4,23919753E+00
28	5,61329377E+02	6,27349754E+00	=3,57868797E+00
29	5,82120550E+02	5,47244418E+00	=3,06677410E+00
30	6,02911723E+02	4,77978746E+00	=2,61541063E+00

NOT REPRODUCIBLE

Table X.—Concluded

31	6,88265075E+00	4,128,1638E+00	-2,19522027E+00
32	7,14613471E+00	3,64069006E+00	-1,83478521E+00
33	7,42214157E+00	3,16806661E+00	-1,49560336E+00
34	7,7796987E+00	2,80036751E+00	-1,29356041E+00
35	8,01871704E+00	2,39716025E+00	-1,11209721E+00
36	8,4592439E+00	2,02410751E+00	-8,61140198E-01
37	8,7746596E+00	1,74452970E+00	-7,37791928E-01
38	9,11150120E+00	1,50358290E+00	-6,52082309E-01
39	9,45681705E+00	1,30153693E+00	1,17059658E-01
40	9,77395449E+00	1,15729393E+00	-1,05377273E-01
41	9,99209294E+00	1,24513123E+00	-2,45358634E-01
42	1,02836363E+01	1,43070936E+00	-2,81106185E-02
43	1,06239347E+01	1,22736971E+00	3,43856714E-01
44	1,09226209E+01	1,69042491E+00	-1,83890107E-01
45	1,11732701E+01	1,08958124E+00	-4,32903837E-01
46	1,14807802E+01	1,23543348E+00	-1,51333665E-01
47	1,24113572E+01	9,32477422E-01	-2,55210617E-01
48	1,25526707E+01	9,87614755E-01	-1,35423811E-01
49	1,32964711E+01	8,17621664E-01	-1,51554946E-01
50	1,35047111E+01	8,62699779E-01	-1,53499502E-01
51	1,39483716E+01	7,12541422E-01	-1,64767052E-01
52	1,41997744E+01	7,48402754E-01	-1,21526733E-01
53	1,46413114E+01	6,29024870E-01	-1,37682776E-01
54	1,4495559E+01	6,559F17,9E-01	-1,2290348E-01
55	1,54332584E+01	5,07105975E-01	-1,12186250E-01
56	1,61081764E+01	5,147E4770E-01	-8,63419434E-02
57	1,69112357E+01	3,94786089E-01	-9,45213436E-02
58	1,7377921E+01	3,94778976E-01	-6,23443531E-02
59	1,79995447E+01	3,28916102E-01	2,71174852E-02
60	1,81705077E+01	4,16275425E-01	-5,68597157E-02
61	1,87690489E+01	2,83623305E-01	-2,74240337E-03
62	1,89867993E+01	4,14036850E-01	-6,61713251E-02
63	1,96326952E+01	2,24480436E-01	-1,85188078E-02
64	1,98158485E+01	3,98683310E-01	9,39646721E-01

Table XI. KINCON SAMPLE CASE-INITIAL CONDITIONS (0% STREAMLINE)

FLOW PROPERTIES		KINETIC COUPLING TERMS							
MACH NUMBER	4.04856344E+01	COUPLING TERM A	-1.10170639E+00						
PRESSURE (PSIA)	7.96631295E+01	COUPLING TERM B	1.44649507E+00						
VELOCITY (FT/SEC)	1.71450042E+03	INTEGRATION PARAMETERS							
TEMPERATURE (DEGR)	5.77500000E+03	CURRENT STEP SIZE	1.00000000E+04						
DENSITY (LB/FT3)	2.54066357E+02	PERCENT ENTHALPY CHANGE	C1						
ENTHALPY (BTU/LB)	2.43513556E+03	1.0 = SUMMATION C(I)	-1.68540737E+11						
GAS MOLECULAR WEIGHT	1.96802243E+01	MAXIMUM RELATIVE ERROR	C1						
HEAT CAPACITY (BTU/LB-DEGR)	5.26014607E+01	GOVERNING EQUATION	0						
FROZEN GAMMA	1.23757914E+00								
ORIG CONST (FT2/SEC2)	2.52644534E+03								
SUM C(I)*H(I) (FT2/SEC2)	9.60574354E+06								
CHEMICAL COMPOSITION									
AC. SPECIES	MASS FRACTION	MOLE FRACTION	PCLEC/CC	NC. SPECIES	MASS FRACTION	MOLE FRACTION	PCLEC/CC		
1	CC2	6.52000E+02	2.915523E+02	3.6312E+17	2	H2O	2.738000E+01	2.990922E+01	3.7251E+18
3	CO	2.01700E+01	1.41712E+01	1.7650E+18	4	H2	2.00000E+02	1.952403E+01	2.4316E+18
5	N2	4.250976E+01	2.986157E+01	3.7161E+18	6	NC	2.00000E+03	1.311665E+03	1.6336E+16
7	O4	9.67000E+03	1.118931E+02	1.3636E+17	8	O2	7.64000E+04	4.698654E+04	5.8520E+15
9	C	1.68000E+11	2.76900E+11	3.4488E+08	10	H	1.15000E+03	2.245264E+02	2.7664E+17
11	N	1.39000E+06	1.952849E+06	2.4322E+13	12	O	6.17000E+04	7.589186E+04	9.4520E+15

Table XII. KINCON SAMPLE CASE-REPRESENTATIVE PRINTOUT (AXIAL POSITION 0.9767, 0" STRFAMLINE)

FLOW PROPERTIES		KINETIC COUPLING TERMS							
MACH NUMBER	6.36289070E+01	COUPLING TERM A	1.01344076E+02						
PRESSURE (PSIA)	6.90682690E+01	COUPLING TERM B	1.35059228E+02						
VELOCITY (FT/SEC)	2.6315936E+03	INTEGRATION PARAMETERS							
TEMPERATURE (DEGR)	5.5977995E+03	CURRENT STEP SIZE	2.56000000E+02						
DENSITY (LB/FT3)	2.32356349E+02	PERCENT ENTHALPY CHANGE	1.00734896E+01						
ENTHALPY (BTU/LB)	2.25481021E+03	1.0 = SUMMATION C(I)	1.54045665E+11						
GAS MOLECULAR WEIGHT	1.94933558E+01	MAXIMUM RELATIVE ERROR	3.57798693E+03						
HEAT CAPACITY (BTU/LB-DEGR)	5.22505438E+01	GOVERNING EQUATION							
FROZEN GAMMA	1.24241015E+00								
GAS CONST (FT2/SEC2/DEGR)	2.5506093E+03								
SUM C(I)*H(I) (FT2/SEC2)	7.60180386E+06								
CHEMICAL COMPOSITION									
NO. SPECIES	MASS FRACTION	MOLE FRACTION	MOLEC/CC	NO. SPECIES	MASS FRACTION	MOLE FRACTION	MOLEC/CC		
1	CO2	6.535699E+02	2.894792E+02	3.3299E+17	4	H2O	2.670061E+01	2.889013E+01	3.3233E+18
3	CO	2.016001E+01	1.462971E+01	1.6139E+18	4	H2	1.993428E+02	1.927510E+01	2.2172E+18
5	N2	4.250905E+01	2.957753E+01	3.4024E+18	6	NO	2.014667E+03	1.308738E+03	1.5055E+16
7	OH	1.420937E+02	1.628976E+02	1.8734E+17	8	O2	1.692076E+03	1.030757E+03	1.1857E+16
9	C	2.917598E+11	4.735141E+11	5.4469E+08	10	H	1.706924E+03	3.309959E+02	3.7972E+17
11	N	1.632962E+06	2.271852E+06	2.6134E+13	12	O	1.387342E+03	1.692247E+03	1.9443E+16
STEP SIZE HALVED AT Z #		1.13990000E+00							

Table XIII. KINCON SAMPLE CASE-REPRESENTATIVE PRINTOUT (AXIAL POSITION = 10.0839, 0% STREAMLINE)

FLOW PROPERTIES		KINETIC COUPLING TERMS							
MACH NUMBER	3.20929483E+00	COUPLING TERM A	3.906646627E+04						
PRESSURE (PSIA)	1.27873262E+00	COUPLING TERM B	-3.95097870E+04						
VELOCITY (FT/SEC)	9.21646935E+03	INITIATION PARAMETERS							
TEMPERATURE (DEGR)	2.55623153E+03	CURRENT STEP SIZE	2.56000000E+02						
DENSITY (LB/FT3)	9.53733571E+04	PERCENT ENTHALPY CHANGE	6.81121435E+01						
ENTHALPY (BTU/LB)	8.36392354E+02	1.0 * SUMMATION C(I)	0.45305999E+11						
GAS MOLECULAR WEIGHT	1.97212260E+01	MAXIMUM RELATIVE ERROR	6.28938666E+04						
HEAT CAPACITY (BTU/LB*DEGR)	4.61063763E+01	GOVERNING EQUATION	3						
FROZEN GAMMA	1.27968684E+00								
GAS CONDUCTIVITY (BTU/SEC*FT*DEGR)	2.52119270E+03								
SUM C(I)*L(I) (FT2/SEC2)	-3.13207029E+07								
CHEMICAL COMPOSITION									
NO. SPECIES	MASS FRACTION	MOLE FRACTION	MOL: C/CC	NO. SPECIES	MASS FRACTION	MOLE FRACTION	MOLEC/CC		
1	O2	7.285035E+02	3.264405E+02	1.4640E+14	2	H2O	2.801757E+01	3.066945E+01	1.3792E+17
3	CO	1.968309E+01	1.385794E+01	6.2318E+16	4	H2	1.943505E+02	1.961293E+01	8.5500E+16
5	N2	4.250888E+01	2.992316E+01	1.3456E+17	6	NO	2.021532E+03	1.322546E+03	5.9744E+14
7	OH	1.314295E+03	1.523960E+03	6.6532E+14	8	O2	5.544177E+04	3.663327E+04	1.6474E+14
9	O	1.979182E+12	3.249674E+12	1.4614E+04	10	H	1.495619E+03	2.924827E+02	1.3160E+16
11	N	1.681934E+07	2.367918E+07	1.0648E+11	12	O	1.921197E+04	2.366022E+04	1.0649E+14
STEP SIZE HALVED AT 2 *		1.02631000E+01							

Table XIV. KINCON SAMPLE CASE-REPRESENTATIVE PRINTOUT (AXIAL POSITION = 19.8159, 0" STREAMLINE)

FLOW PROPERTIES		KINETIC COUPLING TERMS					
MACH NUMBER	3.93740277E+00	COUPLING TERM A	8.29980084E+05				
PRESSURE (PSIA)	3.98483310E+01	COUPLING TERM B	8.34816406E+05				
VELOCITY (FT/SEC)	9.96228505E+03	INTEGRATION PARAMETERS					
TEMPERATURE (DEGR)	1.95060311E+03	CURRENT STEP SIZE	6.40000000E+03				
DENSITY (LB/FT3)	3.73068923E+04	PERCENT ENTHALPY CHANGE	3.53267138E+00				
ENTHALPY (BTU/LB)	5.64890807E+02	PERCENT ENTHALPY CHANGE	1.35642608E+11				
GAS MOLECULAR WEIGHT	1.97215288E+01	MAXIMUM RELATIVE ERROR	4.99283676E+04				
HEAT CAPACITY (BTU/LB-DEGR)	4.34705472E+01	GOVERNING EQUATION	15				
FROZEN GAMMA	1.30175711E+00						
GAS CONST (FT2/SEC2)	2.52153998E+03						
SUM C(I)*M(I) (FT2/SEC2)	-3.81567871E+07						
CHEMICAL COMPOSITION							
NO. SPECIES	MASS FRACTION	MOLE FRACTION	MOLEC/CC	NO. SPECIES	MASS FRACTION	MOLE FRACTION	MOLEC/CC
1 CO2	7.322452E+02	3.281224E+02	6.0248E+15	2 H2O	2.809615E+01	3.075813E+01	5.6514E+16
3 CO	1.965928E+01	1.384138E+01	2.5432E+16	4 H2	1.933559E+02	1.891505E+01	3.4754E+16
5 N2	4.250888E+01	2.992362E+01	5.4641E+16	6 NC	2.021550E+03	1.328581E+03	2.4411E+14
7 OH	5.115695E+04	5.931875E+04	1.0999E+14	6 O2	5.879731E+04	3.623665E+04	6.658CE+13
9 C	1.901369E+12	3.121964E+12	5.7362E+05	10 H	1.553583E+03	3.038586E+02	5.5649E+15
11 N	1.442689E+07	2.031127E+07	3.7319E+10	12 O	1.720332E+04	1.257656E+04	2.310EE+13

Table XV. KINCON SAMPLE CASE—MAXIMUM AND MINIMUM FOR REACTION PRODUCTION RATES (0% STREAMLINE)

1	2,0793266E+01	0,	11,7042821E+05	2,0230000E+01
2	2,73413081E+05	0,	3,90131497E+10	1,96647000E+01
3	1,46944879E+03	0,	5,93911283E+08	1,96647000E+01
4	3,10603690E+03	0,	1,79374564E+02	2,11960000E+01
5	1,3970543E+05	0,	1,59415316E+00	2,11500000E+01
6	1,64323358E+03	3,1000000E+03	7,50082804E+02	2,12300000E+01
7	1,51943309E+03	0,	2,70916262E+02	2,12300000E+01
8	1,71708455E+16	0,	4,73926434E+29	1,96647000E+01
9	1,38115166E+01	1,5100000E+02	5,75311574E+04	9,3900000E+02
10	3,19297067E+00	1,3230000E+01	2,13705462E+03	2,49990000E+00
11	3,34265564E+03	1,5470000E+01	6,85405356E+15	1,96647000E+01
12	1,22071772E+00	2,5970000E+02	2,30407552E+07	1,96647000E+01
13	1,31500623E+07	0,	2,157164665E+12	5,75400000E+01
14	5,14359542E+05	0,	6,06529744E+16	1,35500000E+01
15	1,74120971E+04	0,	2,70983643E+11	1,96647000E+01
16	5,02997618E+03	0,	2,01489145E+01	2,07100000E+01
17	3,65221416E+03	3,2300000E+02	1,19122009E+02	1,96655000E+01
18	1,43798471E+05	0,	7,17103980E+01	2,9500000E+01
19	4,4789910E+03	0,	2,12952225E+01	2,32300000E+01
20	7,10799026E+03	4,0000000E+03	1,67637433E+01	2,25100000E+01
21	2,69604019E+00	2,1100000E+02	8,76716204E+15	1,97543000E+01
22	2,50863933E+00	0,	4,0876013E+03	2,9500000E+02
23	1,96081139E+01	0,	2,30534907E+02	2,9500000E+02
24	3,78390189E+04	0,	8,6609949E+06	1,16300000E+01

Table XVI. KINCON SAMPLE OUTPUT-IDENTIFICATION (90° STREAMLINE)

S T R E A M T U B E K I N E T I C S / C O N D E N S A T I O N C A L C U L A T I O N

S T R E A M T U B E N O . 5 C A L C U L A T I O N P A S S N O . 1

C H E M I C A L K I N E T I C S C A L C U L A T I O N B E I N G P E R F O R M E D
O N T H I S P A S S F O R P R E S S U R E D E F I N E D S T R E A M T U B E .

Table XVII. KINGON SAMPLE CASE.—PRESSURE TABLE (90° STREAMLINE)

1	0.	7,9551809E+01	-9,87962011E+00
2	2,11631705E-01	7,76302834E+01	-9,70623941E+00
3	4,22509407E-01	7,54508322E+01	-1,11048806E+01
4	6,32711699E-01	7,29528818E+01	-1,25518579E+01
5	8,42341025E-01	7,01913683E+01	-1,38917464E+01
6	1,05148118E+00	6,71357359E+01	-1,47677737E+01
7	1,26221517E+00	6,40100975E+01	-1,58739559E+01
8	1,46862523E+00	6,05148092E+01	-1,72734937E+01
9	1,67679282E+00	5,68143461E+01	-1,79417498E+01
10	1,88479137E+00	5,30474263E+01	-1,84908916E+01
11	2,09272155E+00	4,91234531E+01	-1,89698732E+01
12	2,30064163E+00	4,51589323E+01	-1,89122760E+01
13	2,50763768E+00	4,12575325E+01	-1,87010098E+01
14	2,71678811E+00	3,73765728E+01	-1,83362942E+01
15	2,92517204E+00	3,36198356E+01	-1,76277797E+01
16	3,13386868E+00	3,00327101E+01	-1,63374111E+01
17	3,34295621E+00	2,67942915E+01	-1,53543131E+01
18	3,55251780E+00	2,36246404E+01	-1,45995219E+01
19	3,76262950E+00	2,06672913E+01	-1,33162964E+01
20	3,97337509E+00	1,80003620E+01	-1,17533633E+01
21	4,22996985E+00	1,51255006E+01	-1,06495393E+01
22	4,34421878E+00	1,40510520E+01	-9,16475187E+00
23	4,62743900E+00	1,16169478E+01	-7,85863842E+00
24	4,91214896E+00	9,58777483E+00	-5,32891537E+00
25	5,21713105E+00	8,43723254E+00	-3,53336018E+00
26	5,48534132E+00	7,55187966E+00	-3,00187650E+00

Table XVII.—Concluded

27	5,76953976E+00	4,47877551E+00	-2,61095081E+00
28	6,22315053E+00	5,63332896E+00	-2,20039266E+00
29	6,59799365E+00	4,87589092E+00	-1,85669501E+00
30	6,99828178E+00	4,19414663E+00	-1,55568209E+00
31	7,42827652E+00	3,58423472E+00	-1,29790457E+00
32	7,89843995E+00	3,02582723E+00	-1,08813711E+00
33	8,42533234E+00	2,49930128E+00	-8,91167045E-01
34	9,0243664E+00	2,04198177E+00	-6,97108415E-01
35	9,65946952E+00	1,63897387E+00	-5,23437055E-01
36	1,05181247E+01	1,24853865E+00	-3,91364943E-01
37	1,14310855E+01	9,45625460E-01	-2,86883480E-01
38	1,22464524E+01	7,52710026E-01	-2,05638094E-01
39	1,31547568E+01	5,91172991E-01	-1,53620618E-01
40	1,40873446E+01	4,69911024E-01	-1,13254262E-01
41	1,51425932E+01	3,65982366E-01	-8,35529436E-02
42	1,60976799E+01	3,01941592E-01	-6,00551747E-02
43	1,73025912E+01	2,36263314E-01	-4,37313885E-02
44	1,81230195E+01	2,13370681E-01	-3,29956234E-02
45	2,00341997E+01	1,46000206E-01	-2,98124943E-02
46	2,10621071E+01	1,25749622E-01	-1,97256126E-02
47	2,23143113E+01	1,02495787E-01	-1,55641547E-02
48	2,33664334E+01	8,21025440E-02	-1,04510280E-02
49	2,41824349E+01	6,31699734E-02	6,25607242E-03

NOT REPRODUCIBLE

Table XVIII. KINCON SAMPLE CASE-INITIAL CONDITIONS (90% STREAMLINE)

INITIAL CONDITIONS KINETIC STREAMTUBE CALCULATION AXIAL POSITION = 0.

INPUT NORMALIZING AXIAL SCALE FACTOR (FT) 8.10000E+03

FLOW PROPERTIES		KINETIC COUPLING TERMS	
MACH NUMBER	4.11323034E-01	COUPLING TERM A	-6.84304163E-01
PRESSURE (PSIA)	7.75518098E+01	COUPLING TERM B	8.88718546E-01
VELOCITY (FT/SEC)	1.72419386E+03	INTEGRATION PARAMETERS	
TEMPERATURE (DEG-R)	5.61402910E+03	CURRENT STEP SIZE	1.00000000E-03
DENSITY (LB/FT3)	2.59624950E-02	PERCENT ENTHALPY CHANGE	-1.92471122E-02
ENTHALPY-HR (BTU/LB)	2.34432955E+03	INITIAL SUBSTITUTION	-1.68545737E-11
GAS MOLECULAR WEIGHT	1.96572243E+01	MAXIMUM RELATIVE ERROR	0.
HEAT CAPACITY (BTU/LB-DEG-R)	5.24626236E-01	CHEMICAL COMPOSITION	
FROZEN GAMMA	1.23135777E+00	1	2.715701E-11
GAS CONST(FI2/DEG-R)	2.52644534E+03	2	2.715701E-11
SURFACE AREA (FT2/SEC2)	7.6442367E+06	3	2.715701E-11
		4	2.715701E-11
		5	2.715701E-11
		6	2.715701E-11
		7	2.715701E-11
		8	2.715701E-11
		9	2.715701E-11
		10	2.715701E-11
		11	2.715701E-11
		12	2.715701E-11
		13	2.715701E-11
		14	2.715701E-11
		15	2.715701E-11

NOT REPRODUCIBLE

Table XIX. KINCON SAMPLE CASE--REPRESENTATIVE PRINTOUT
(AXIAL POSITION 0.974875, 90% STREAMLINE)

FLOW PROPERTIES		KINETIC COUPLING TERMS	
MASS NUMBER	6.51332026E-01	COUPLING TERM A	1.02810708E-02
PRESSURE (PSIA)	6.022095152E+01	COUPLING TERM B	-1.36541490E-02
VELOCITY (FT/SEC)	6.07944415E+03	INTEGRATION PARAMETERS	
TEMPERATURE (KELVIN)	5.05720516E+03	INTEGRATION STEP SIZE	3.20000000E-02
DENSITY (G/CM ³)	2.33319105E-02	PERCENT ENTHALPY CHANGE	-5.55944700E-02
ENTHALPY (BT/LB)	6.26718978E+03	RELATIVE SUMMATION ERROR	-1.56743724E-11
GAS MOLECULAR WEIGHT	5.93074028E+01	RELATIVE ERROR	2.05931537E-02
HEAT CAPACITY (BT/LB-DEG F)	5.26745350E-01	CONVERGENCE ADJUSTING	7
PRONER JA ²	1.6319101E+02		
CAN COEFF (BT/SEC/IN ²)	2.026231195E+03		
COEFFICIENT (BT/SEC/IN ²)	5.7770337E+06		
CHEMICAL COMPOSITION			
NO. SPECIES	MOLECULAR WEIGHT	NO. SPECIES	MASS FRACTION
1	CO ₂	2.692517E-01	2.722794E-01
3	H ₂ O	1.976209E-04	1.76518E-01
2	H ₂	2.00819E-03	1.87425E-03
7	N ₂	1.349542E-03	6.21779E-03
4	CH ₄	1.5311622E-03	2.77101E-02
11	C ₂ H ₆	1.093455E-03	1.37761E-03

NOT REPRODUCIBLE

Table XX. KINCON SAMPLE CASE-REPRESENTATIVE PRINTOUT
(AXIAL POSITION - 24.4058, 90% STREAMLINE)

FLOW PROPERTIES		KINETIC COUPLING TERMS							
MACH NUMBER	5.06634318E+00	COUPLING TERM A	1.96474408E+05						
PRESSURE (PSIA)	8.5478639E+02	COUPLING TERM B	-1.96918325E+05						
VELOCITY (FT/SEC)	1.05264249E+04	INTEGRATION PARAMETERS							
TEMPERATURE (DEGR)	1.28360469E+03	CURRENT STEP SIZE	1.28000000E+01						
DENSITY (LB/FT3)	1.09705443E+04	PERCENT ENTHALPY CHANGE	5.91663000E+00						
ENTHALPY-HD (BTU/LB)	2.86031494E+02	I,J - SUPMATION C(I)	-1.46229695E+11						
GAS MOLECULAR WEIGHT	1.97494481E+01	MAXIMUM RELATIVE ERROR	5.69247817E+01						
HEAT CAPACITY(BTU/LB-DEGR)	4.00243999E+01	GOVERNING EQUATION	3						
FROZEN GAMMA	1.33584505E+00								
GAS CONST(FT2/SEC2/DEGR)	2.51758989E+03								
SUP C(I)*RH(I) (FT2/SEC2)	-4.54758120E+07								
CHEMICAL COMPOSITION									
NO, SPECIES	MASS FRACTION	MOLE FRACTION	MOLEC/CC	NO, SPECIES	MASS FRACTION	MOLE FRACTION	MOLEC/CC		
1	CO2	7.344764E+02	3.295881E-02	1.9730E+15	2	H2O	2.810704E+01	3.081142E-01	1.8444E+16
3	CO	1.964508E+01	1.385097E-01	6.2915E+15	4	H2	1.946279E+02	1.906644E-01	1.1414E+16
5	N2	4.250932E+01	2.996629E-01	1.7939E+16	6	NO	2.012062E+03	1.324217E-03	7.9271E+13
7	OH	4.637928E+04	5.385997E-04	3.2239E+13	8	O2	4.794933E+04	2.759290E-04	1.7715E+13
9	C	1.663973E+12	2.736037E-12	1.6379E+05	10	H	1.419261E+03	2.780717E-02	1.6646E+15
11	N	1.278041E+07	1.601870E-07	1.0786E+10	12	O	1.004162E+04	1.239478E-04	7.4198E+12

Table XXI. KINCON SAMPLE CASE--MAXIMUM AND MINIMUM FOR REACTION PRODUCTION RATES (90% STREAMLINE)

1	1.72726829E+01	0.	-2.58466694E+05	2.40628750E+01
2	1.16803868E+05	0.	-1.59510406E+10	2.40628750E+01
3	7.87084322E+04	0.	-2.19112225E+08	2.40628750E+01
4	1.93923472E+03	0.	-1.20726840E+01	2.22375000E+01
5	8.13979729E+04	0.	-1.74638735E+00	2.22375000E+01
6	9.90253322E+02	2.62500000E+03	6.82117378E+03	2.22875000E+01
7	8.65115913E+02	0.	-2.53048149E+02	2.40628750E+01
8	5.37645590E+17	0.	-3.26730671E+34	2.40628750E+01
9	8.24636049E+02	1.48750000E+02	9.15174370E+05	1.09875000E+01
10	-1.89393873E+01	1.43875000E+01	-4.75045631E+03	1.96687500E+00
11	1.03317535E+03	1.69875000E+01	-2.80038967E+22	2.40628750E+01
12	-6.68065127E+01	2.93750000E+02	8.75744250E+12	2.40628750E+01
13	7.55869024E+08	0.	2.78472214E+11	1.73875000E+01
14	2.69123450E+05	0.	-2.71040189E+09	1.43875000E+01
15	7.96575386E+05	0.	-8.52443760E+14	2.40628750E+01
16	-3.53422055E+03	4.99087500E+00	-3.82129988E+00	5.62500000E+03
17	2.17701528E+03	3.58750000E+02	9.44846181E+02	2.54375000E+01
18	-9.22810310E+04	0.	-3.49746947E+00	2.06375000E+01
19	-2.65271384E+03	0.	1.85092812E+01	2.34875000E+01
20	-4.20455118E+03	4.37500000E+03	-2.33498159E+01	2.12468750E+01
21	-1.39438197E+00	2.48750000E+02	-2.10023032E+21	2.40628750E+01
22	1.69291846E+00	0.	-1.35021951E+03	2.41487500E+00
23	1.24412163E+01	0.	2.94273258E+02	3.16750000E+02
24	1.95464349E+04	0.	-3.30507898E+08	2.40628750E+01

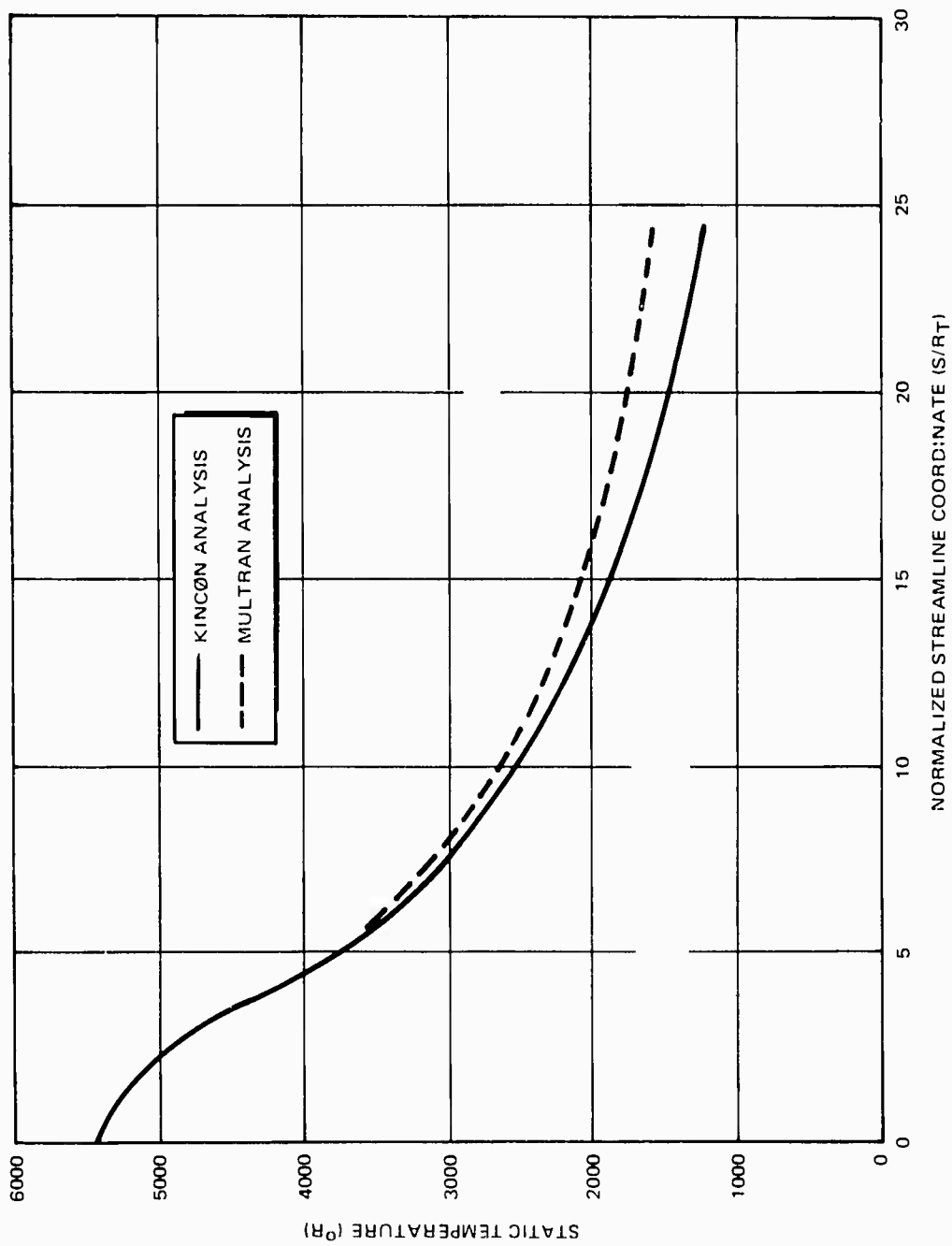


Figure 28. Static Temperature Distribution for 99% Streamline

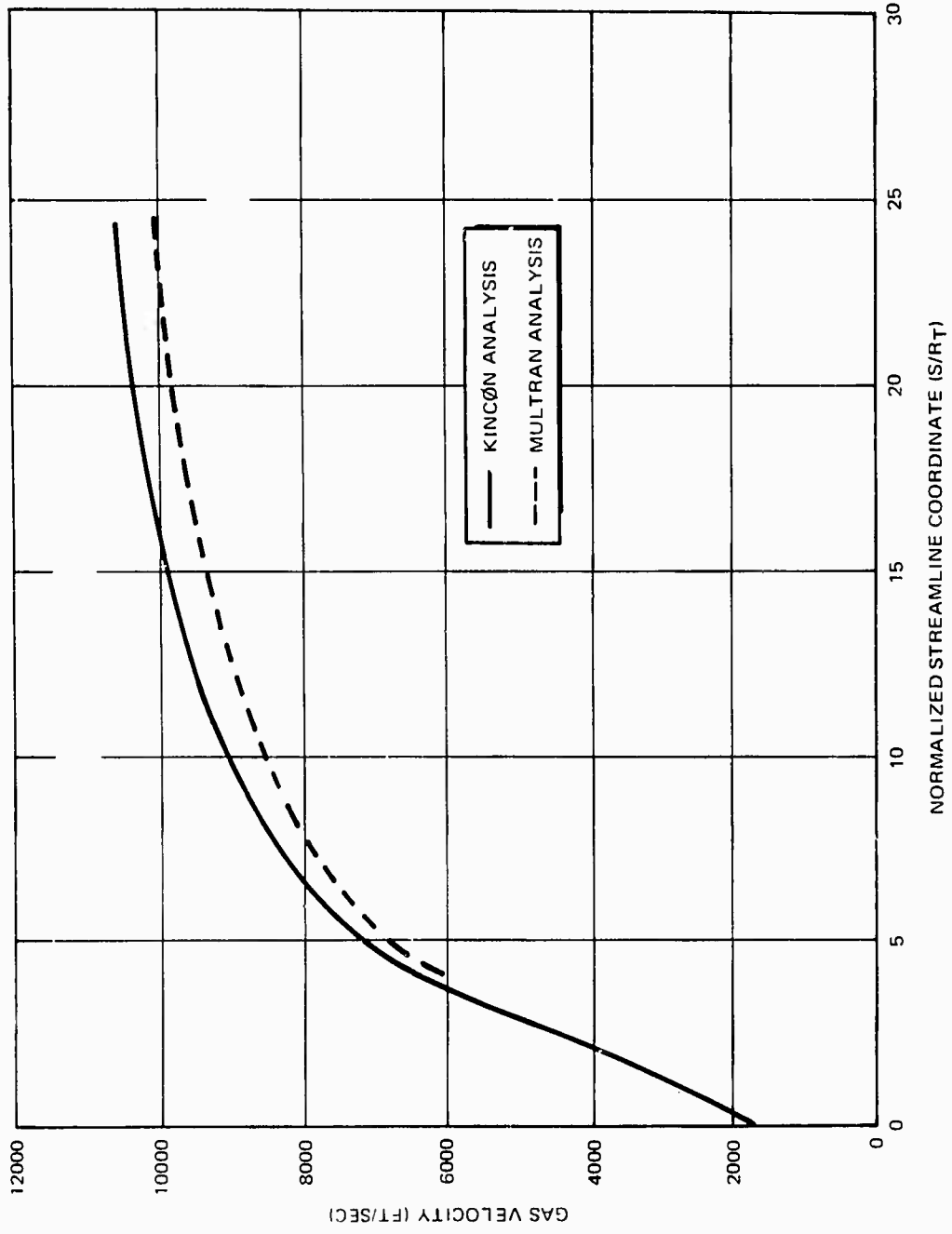
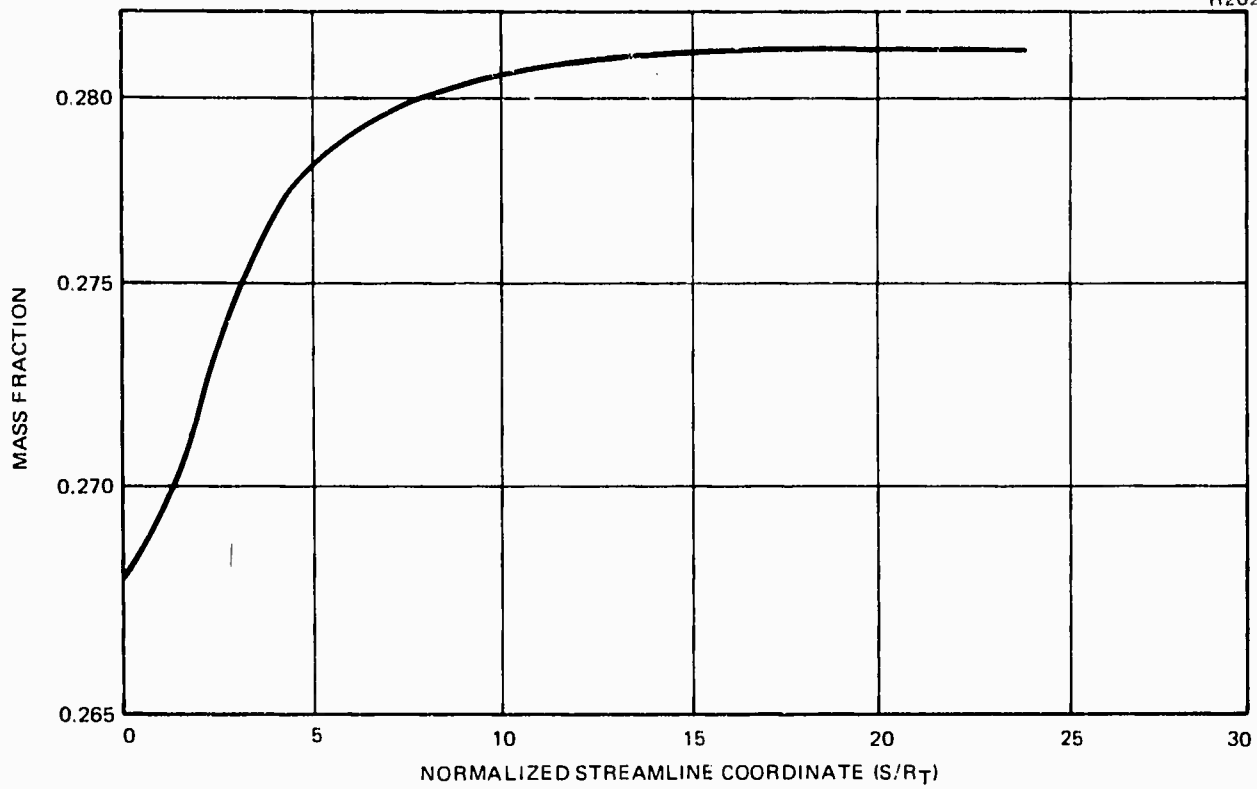
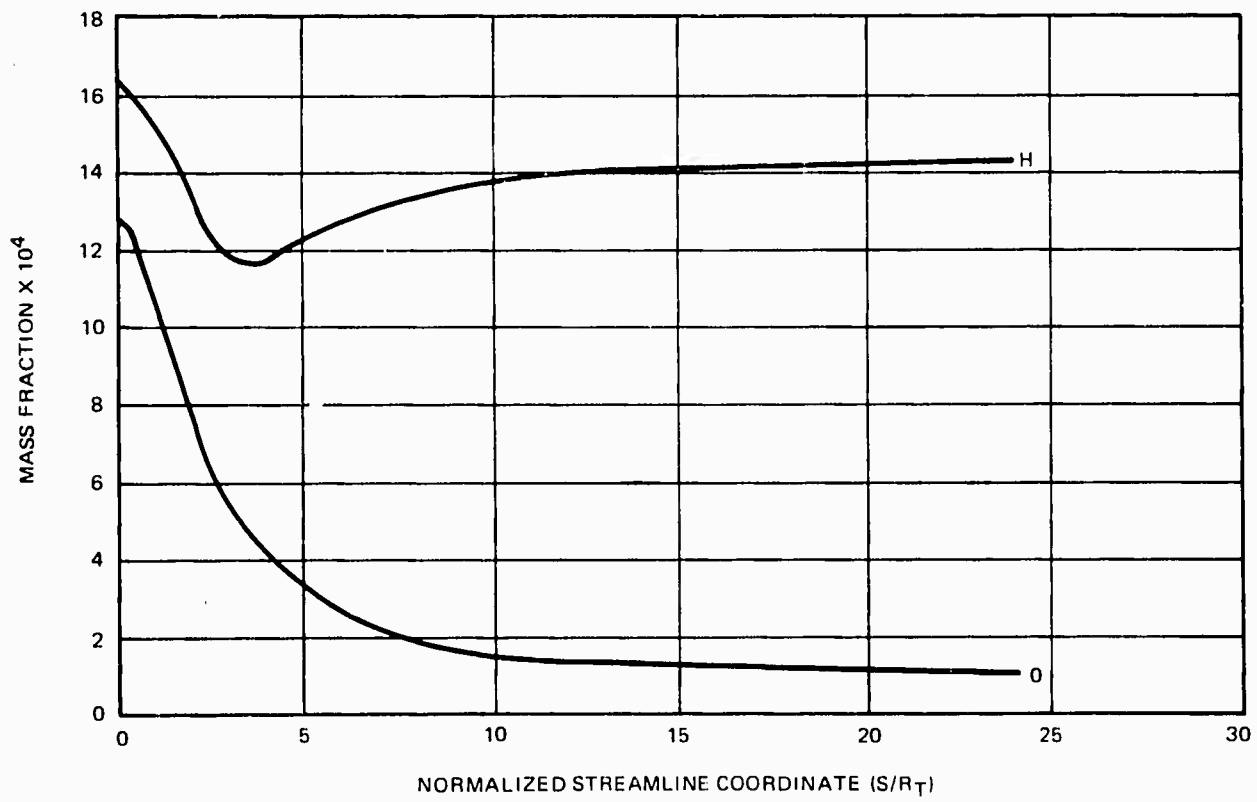


Figure 29. Gas Velocity Distribution for 99% Streamline



a. MASS FRACTION H₂O FOR 99% STREAMLINE



b. MASS FRACTION H AND O FOR 99% STREAMLINE

Figure 30. H₂O, H and O Composition for 99% Streamline

SECTION VI

CONCLUSIONS AND RECOMMENDATIONS

1. CONCLUSIONS

A computer program has been developed to predict the sensitivity to engine operating parameters and impingement geometry for the production and transport of bipropellant engine contaminants. A subprogram to analyze the effect of plume impingement on sensitive thermal and optical surfaces in terms of changes in surface properties has been initiated but not completed. The contaminant production and contaminant transport models and subprograms have been checked out and seem to be working correctly, although verification with experimental data has not been attempted due to a lack of detailed experimental data relating engine operation to contaminant effects on surfaces.

Based on the analysis of a single engine, the Marquardt R-6C MMH/NTO 5-lb thruster, it appears that significant amounts of unburned fuel and oxidizer will be ejected from the engine during the transient portion of the pulse and that this contaminant may cause damage to sensitive thermal and optical surfaces if they are impinged upon by the central core of the plume.

2. RECOMMENDATIONS

The contaminant effects model is incomplete. It is recommended that the additional effort be undertaken to improve this portion of the analysis by: (1) experimentally determining the rate of deposition of plume material on thermal and optical surfaces as a function of surface temperature, impingement flux, and type of material, and (2) extending the analytical model to include a sufficient number of surface materials and contaminant species.

Additional programming work is required to complete the development of the Transient Combustion Chamber Dynamics Program (TCC) as an operational program.

It is further recommended that the CONTAM analysis be extended to include contamination resulting from hydrazine monopropellant thrusters.

Preceding page blank

SECTION VII

REFERENCES

1. W. T. Webber and W. A. Gaubatz. Calculation of the Ignition and Start Transient of Liquid Propellant Rocket Engines. MDAC Paper 1439, presented at the 1970 Fall Meeting, Western States Section, The Combustion Institute, Pasadena, California, October 26-27, 1970 (WSS/CI Paper 70-23).
2. W. T. Webber, W. A. Gaubatz, and R. J. Hoffman. Calculation of Contaminant Production in Liquid Bipropellant Rocket Engines. MDAC Paper WD 1513, presented at the JANNAF Sixth Plume Technology Meeting, March 9, 1971.
3. P. J. Martinkovic. Bipropellant Attitude Control engine exhaust contamination and its effect on Space borne equipment. 12th JANNAF Liquid Propulsion Meeting, Nov. 17-19, 1970, Las Vegas, Nevada. CPIA publication No. 201, Vol. 2, page 315.
4. R. C. Stechman and T. A. Thonet. The Effect of Rocket Exhaust Impingement on Spacecraft Surfaces During Pulsing Engine Duty Cycles. 12th JANNAF Liquid Propulsion Meeting, Nov. 17-19, 1970, Las Vegas, Nevada. CPIA publication No. 201, Vol. I, page 869.
5. J. R. Kliegel and G. R. Nickerson. Axisymmetric Two-Phase Perfect Gas Performance Program. TRW 02874-6006-R000, April 3, 1967.
6. C. Gabbert and R. J. Hoffman. Reacting, Multiphase Plume Characterization and Plume Effects: Including Gas-Particle Impingement Heating. AIAA Paper No. 70-845. AIAA Fifth Thermophysics Conference, Los Angeles, California, June 29 to July 1, 1970.
7. A. W. Lemman, et al., Eds. Liquid Propellants Handbook. Battelle Memorial Institute, Columbus, Ohio, October 1955.
8. C. M. Beighley and W. R. Fish Ed., Performance and Properties of Liquid Propellants, Aerojet General Corporation.
9. O. W. Dykema and S. A. Greene. An Experimental Study of RP-1, UDMH and N₂H₄ Single-Droplet Burning in Air and in Oxygen. Research Report No. 59-41, Rocketdyne, Canoga Park, Calif., 1960.
10. D. R. Stull, et al., Eds. JANAF Thermochemical Tables. Thermal Research Laboratory, Dow Chemical Company, Midland, Michigan, August 1965.

Preceding page blank

11. T.F. Seamans, M. Vanpee, and V.D. Agosta. Development of a Fundamental Model of Hypergolic Ignition in Space-ambient Engines, AIAA Journal, Vol. 5, No. 9, September 1967.

12. H.E. Perlee, T. Christos, Y. Miron, and H.K. James. Pre-ignition Phenomena in Small A-50/NTO Pulsed Rocket Engines, Journal of Spacecraft and Rockets, Vol. 5, No. 2, February 1968.

13. J. Zajac and W.H. Nurick. Correlation of Spray Droplet Distribution and Injector Variables, 8th JANNAF Liquid Propellant Combustion Instability Meeting, Los Angeles, Calif., October 1971.

Appendix A

TCC

TRANSIENT COMBUSTION CHAMBER DYNAMICS
COMPUTER PROGRAM

A Bipropellant Contaminant Production Model

Program Number H607

TABLE OF CONTENTS

Section		
A. 1	INTRODUCTION	141
	a. The <u>TCC</u> Program	141
	b. Previous Combustion Dynamics Models	142
	c. The MDAC Transient Combustion Chamber Program	146
A. 2	ANALYSIS	148
	a. Scope	148
	b. Limitations and Assumptions	151
	c. Modeling of System Processes	155
	d. Contaminant Production in the Combustion Chamber	191
	e. Contaminant Production Parametric Study	194
A. 3	NUMERICAL INTEGRATION METHOD	222
	a. Computational Methods for Droplet Arrays	224
	b. Integrating Time Interval	226
A. 4	PROGRAM OVERLAY STRUCTURE	228
A. 5	SUBROUTINES	228
	a. Subroutine REDRHO (TRED)	228
	b. Subroutine REDROD (TRED)	229
	c. Subroutine HCONDF (TEMP)	229
	d. Subroutine HCONDO (TEMP)	229
	e. Subroutine REDVIS (TRED)	230
	f. Subroutine FANFAC (RENCH)	230
A. 6	PROGRAM USERS MANUAL	231
	a. Input	231
	b. Program Output	244
A. 7	SAMPLE CASE	250
A. 8	REFERENCES	280

ILLUSTRATIONS

Figure		Page
A-1.	Rocket System Schematic	149
A-2.	Feed System Schematic	157
A-3.	Injection Temperature Profile vs Flow from Tank	159
A-4.	Approximate Enthalpy of Monomethyl Hydrazine	161
A-5.	Preimpingement Trajectory of Propellant	172
A-6.	Droplet Circulation Criterion	177
A-7.	Burning Rate vs Reynolds Number	178
A-8.	Temperature vs Stoichiometry	180
A-9.	Molecular Weight vs Stoichiometry	185
A-10.	Gamma vs Stoichiometry	185
A-11.	The Effect of Throat Area on Material Ejected from the Motor	198
A-12.	The Effect of Chamber Length on Material Ejected from Motor	201
A-13.	The Effect of Chamber Diameter on Material Ejected from Motor	202
A-14.	Disposition of Material on Chamber Wall as a Function of Chamber Diameter	203
A-15.	The Effect of Chamber Wall Temperature on Material Ejected from the Motor	204
A-16.	Material Ejected with One Valve Open	206
A-17.	The Effect of Valve Opening on Material Ejected from Motor	207
A-18.	The Effect of Valve Operation on Propellant Ejected Before Ignition	208

Figure		Page
A-19.	The Effect of Valve Opening on Exhaust Composition	209
A-20.	Disposition of Material on Chamber Wall as a Function of Valve Operation	210
A-21.	The Effect of Valve Closing on Material Ejected from Motor	211
A-22.	The Effect of Fuel Tank Pressure on Material Ejected from Motor	213
A-23.	The Effect of Fuel Tank Pressure on Material Deposited on Wall	214
A-24.	The Effect of Oxidizer Tank Pressure on Material Ejected from Motor	215
A-25.	The Effect of Oxidizer Tank Pressure on Material Deposited on Chamber Wall	216
A-26.	The Effect of Bulk Fuel Temperature on Material Ejected from Motor	218
A-27.	The Effect of Draining Dribble Volume Between Pulses	220
A-28.	The Effect of Heat Transfer to Propellant Remaining in Dribble Volumes Between Pulses on Material Ejected from the Motor	221

TABLES

Table		Page
A-I	Droplet Diameter Distributions Mid-Quintile Diameter/Median Diameter	171
A-II	Droplet Parameters	173
A-III	Disposition of Propellant Injected Into Chamber	199
A-IV	The Effect of Tank Pressure on Chamber Conditions	212
A-V	Sample Case For TCC Program	251

LIST OF ABBREVIATIONS AND SYMBOLS

A	Area, Acceleration, Molecular collision frequency
a	Acoustic velocity
B	Coefficient in vapor pressure equation
C	Specific heat, Coefficient
D	Diameter
E	Activation Energy, Accommodation Coefficient
F	Stoichiometry (mass fraction which is fuel)
f	Fanning fraction factor
H	Enthalpy
K	Drop size distribution coefficient, Thermal conductivity
L	Length
M	Mass
N	Dimensionless modulus, Number of droplets
P	Pressure
Q	Heat of reaction
q	Volumetric flow rate, Heat flow rate, Quenching distance
R	Axial location where impingement occurs, Universal gas constant, Coefficient for resistance to flow
S	Axial location where atomization is complete
T	Temperature
t	Time
U	Chamber volume, Gas velocity
V	Velocity, Any time-dependent variable, Chamber volume
W _m	Molecular weight
X	Mass fraction which flashes, Axial location
Y	Radial location
β	Resultant stream angle
γ	Ratio of specific heats
Δ	Difference
ϵ	Expansion area ratio

μ	Viscosity
ρ	Density
σ	Surface tension

SUBSCRIPTS

c	Chamber
cond.	Condensed phase
d	Drag, Difference
e	External, Effusion correction
F	Fuel, Thrust coefficient
flash	Flash threshold
fuel	Fuel
g	Gas
gas	Gas
i	Droplet group identifier, Chamber axial segment identifier
inj	Injection conditions
j	Jet conditions
L	At axial location L
l	Liquid
m	Wall film material
mn	Droplet mean $D_{mn} = \left[\frac{\sum Ni Di^n}{\sum Ni Di^m} \right]^{\frac{1}{m-n}}$
n	Injection group identifier
Nu	Nusselt number
O	Oxidizer, Orifice, Stagnant
Oxid	Oxidizer
P	Propellant p, At constant pressure
R	Resultant after impingement
r	Reduced variable (ratio to critical value)
rel.	Relative
Re	Reynolds number
S	Surface
Sat	Saturation conditions
Stream	Stream conditions

T	Throat, Total of fuel plus oxidizer
t	Tank
Vap.	Vapor
We	Weber number
x	Component in the x direction
y	Component in the y direction

Appendix A

TCC

TRANSIENT COMBUSTION CHAMBER DYNAMICS COMPUTER PROGRAM

A Bipropellant Contaminant Production Model

A. 1 INTRODUCTION

a. The TCC Program

The computer program described in this appendix is a subprogram to the Plume Contamination Effects Prediction Computer Program, CONTAM, and performs the time-varying analysis of the chemical and physical processes occurring in the feed system, injector, combustion chamber, and nozzle-throat inlet of a bipropellant rocket-engine system operating under unsteady conditions. As a subprogram to CONTAM, the TCC program is the first link in the analysis of contamination effects, providing information about production of contaminants in the combustion chamber and the dynamic and thermodynamic state of combustion gases entering the nozzle throat. Unburned propellant droplet distributions and liquid wall film flow are computed for the entire transient pulse as well as gas-phase properties. TCC may also be used as an independent computer program on any third-generation computer with a core exceeding 135,000 words and a Fortran IV processor.

Development of the TCC program has been supported by MDAC Independent Research and Development over a period of approximately five years with additional modification supported by the current Air Force Rocket Propulsion Laboratory study. References A-1 through A-3 discuss the detailed modeling of the combustion processes included in the basic TCC program. Reference A-4 discusses extensions of the TCC program to predict contaminant production. As far as is practical, this appendix will cover all aspects of the modeling and computer program. If detailed information is desired, see References A-1 through A-4.

The program is based upon a finite-difference computer solution for the large set of differential and algebraic equations describing the physical and chemical processes which occur during the preignition, start transient, steady operation, cutoff transient, and between-firing intervals

Preceding page blank

of rocket engine operation. The intent has been to use the simplest acceptable mathematical approximation for each process, but to model all of the processes which are known to be important. Thus the program is sufficiently general to calculate steady and unsteady combustion efficiency; vacuum-hypergolic starts, sea-level ignited starts, low-frequency combustion instability, pulse-mode impulse, and contaminant production, without requiring any special assumptions for any of the special cases.

b. Previous Combustion Dynamics Models

The earliest calculations of rocket-engine behavior treated the rocket engine system as a simple thermodynamic device. In 1949, Sutton described methods adequate to calculate steady flow rates (Reference A-5), pressures, and performance, assuming isenthalpic combustion followed by an isentropic expansion.

Unfortunately, the major problems encountered in the actual operation of rocket engines were not described by nor amenable to solution using the assumption of steady equilibrium processes. The most important operational problems included destructive hard starts, both at sea level and high altitude, and for both hypergolic and ignited propellants. Oscillatory cutoffs contributed large but irreproducible impulse increments after the engine cutoff command. Incomplete combustion led to lower than ideal specific impulse and the existence of nonequilibrium contaminant products in the engine exhaust. System instabilities were damaging to engine hardware, propulsion-system performance, and vehicle effectiveness. Transient operations, such as pulse-mode operation with short pulse widths were not described adequately by idealized steady-state assumptions; therefore, actual realized specific impulse, mixture ratio, response times, chamber pressure peak values, and rate of pressure rise had to be obtained experimentally.

The analysis of steady rocket-engine combustion and the analysis of rocket system transients were sufficiently complex to require two decades of study and contributions from a large number of investigators in order to arrive at the present degree of understanding. Unfortunately, the studies of the steady processes and the studies of transients took quite divergent paths, and it is only in the most recent work that the droplet evaporation approach to combustion and the time-dependent system simulation by digital integration have been combined. The TCC program described here is based upon both of these classic approaches to rocket-engine analysis. Although the digital system model with droplet combustion has not yet incorporated all of the refinements from either of its antecedent lines, it has shown a considerable capability to explain rocket engine phenomena which were previously beyond analysis.

(1) Steady State Engine Analysis

The mathematical analysis of the rocket combustion chamber operating under steady conditions was developed over an extended period of time.

In 1953 Penner approximated the lifetime of droplets in a rocket combustion chamber assuming simultaneous Knudsen-Langmuir evaporation and nonconvective heat transfer with no effusion correction (Reference A-6).

In 1954 Meisse calculated one-dimensional trajectories and combustion rates for monodisperse droplets in a chamber (Reference A-7). One case arbitrarily assumed axial gas velocity to be constant, while another assumed gas velocity to be proportional to the distance from the injector. Stokes Law was used for drag and Frossling's correlation of heat transfer rate with droplet Reynolds number, but no correction was made for effusion.

The droplet approach to combustion chamber analysis was greatly advanced between 1957 and 1960 by Priem and his associates (Reference A-8 and A-9) who developed methods for the numerical integration of the equations determining heat transfer, evaporation rate, and aerodynamic drag of propellant droplets; and who tied the combustion gas velocity at each axial point to the total droplet evaporation upstream of that point. Priem's method handles ensembles of droplets having arbitrary droplet size distributions and uses accurate empirical correlations for the simultaneous transport processes and for temperature-dependent physical properties.

The droplet approach to combustion chamber analysis received detailed experimental confirmation through the combined experimental and theoretical studies of Lambiris, Combs, and Levine in the period 1961 to 1962 (Reference A-10). Experimental droplet and gas trajectories were obtained from streak photographs using a windowed rocket combustion chamber. These experimental trajectories were compared with trajectories calculated using a wide variety of conflicting correlations for the transport processes, size distributions, and physical properties. The variation study determined the correlations most appropriate for the rocket-engine environment.

In 1965 and 1966, the Dynamic Science Corporation further refined the droplet method by simultaneously computing the combustion of fuel and oxidizer droplets, instead of assuming—as previously—that oxidizer vaporization was "fast" (Reference A-11). This leads to an axial composition and temperature profile for the combustion gas. The overlapping bipropellant-monopropellant behavior of the hydrazine fuels was also considered.

The most recent advance in the droplet approach has been to break down the thrust chamber into separate streamtubes or zones to reflect the uneven transverse distribution of fuel and oxidizer from the injection elements. Each zone is separately analyzed, using a droplet analysis upstream of the chamber throat and an equilibrium or chemical kinetic expansion downstream of the throat. Overall specific impulse is obtained by summing the mass flow rate and thrust over the ensemble of zones (References A-12 and A-13).

(2) Unsteady System Behavior

The problems related to transient behavior of rocket engine systems have been attacked in a very fragmented way. The approaches to low-frequency instability, vacuum hypergolic ignition and spiking, pulse-mode operation, and cutoff impulse have been quite independent of each other, and generally totally unrelated to the analyses of steady combustion.

(a) Stability Boundary Analyses

Low-frequency combustion instability was first analyzed in the period 1949 to 1951 by a variety of investigators (References A-14, A-15, and A-16). Generally, however, they all considered the equations of flow through a single feed system having lumped resistance and inertia terms, and considered the accumulation and efflux of combustion gas from the chamber. In all cases, the combustion process was approximated as a fixed time delay. The equations were not integrated to give the chamber pressure history, but were attacked with control system theory to give criteria for stability or instability of the system as a function of frequency.

In 1951 Crocco performed a similar analysis in which the combustion time delay was elaborated by being regarded as a variable function of chamber pressure (Reference A-17).

In 1956 Barrere and Bernard extended this approach to make the combustion time delay a function of both chamber pressure and time-varying primary atomization droplet size (dependent upon injection pressure drop) (Reference A-18).

Calculations of combustion instability boundaries with a combustion time delay dependent upon both chamber pressure and primary atomization droplet size, were pursued further by Hurrell in 1959 (Reference A-19).

"Klystron effect," or bunching of the injected propellant streams in the preimpingement region as the result of injection velocity modulation, was observed in experimental chugging motor firings and was described by Lawhead, Levine, and Webber in 1956 (Reference A-20). Theoretical and experimental investigations of this phenomena were reported by McCormack in 1964 (Reference A-21) and Fenwick and Bugler in 1966 (Reference A-22).

(b) Time-Dependent Solutions

There were several early attempts to integrate the equations describing the system processes, so as to obtain a calculated transient combustion chamber history; however, close agreement with experiment was not obtained.

In 1956, Lawhead, Levine, and Webber (Reference A-20) digitally integrated the system equations for a square-law resistive feed

system, accumulation and efflux of gas from the chamber, and a pressure-dependent Vieille's law combustion rate assuming a fixed mean droplet diameter. The computed starts and low-frequency combustion instability agreed with experiment only in general trends.

In 1957 Gore and Carroll obtained time-dependent solutions for a complicated rocket-engine system, using an analogue computer (Reference A-23). The system model included turbopumps, controllers, inertial-resistive feed systems, and a fixed time-delay approximation for combustion. This analysis was basically intended to calculate start and cutoff transients and throttle control response, but one of the published calculations included what was apparently chugging instability. Scales were omitted from the plotted results, and no comparison with experiment was made.

In 1958, Kluger and Farrell described a very detailed transient system analysis which was solved on a digital computer (Reference A-24). It included resistive-inertial-compressible feed systems calculated by the method of characteristics and the effects of valve opening, injector priming, a bootstrap gas generator, and turbopumps. The combustion was approximated as a pressure-dependent time delay. The calculated and experimental chamber pressure histories agreed within 10 percent during a smooth-start transient and most of a cutoff transient. However, the calculations did not model the low-frequency combustion instability which occurred on cutoff.

(c) Closed Form Mathematical Solutions

There have been a number of efforts to obtain mathematical closed form solutions to steady and transient combustion-chamber phenomena. In several cases these have followed after more general solutions had been obtained by numerical methods. The approximate solutions to the steady combustion chamber by Mayer (Reference A-25) and Spalding (Reference A-26) are in this category. Rodeau (Reference A-27) has offered an analytic solution for the cutoff transient and Peterson (Reference A-28) for the start transient. All of these methods are so over-simplified for mathematical convenience that the results are of very restricted utility.

(d) Hypergolic Ignition

The vacuum hypergolic ignition process was analyzed by Seamans, Vanpee, and Agosta in the period 1964 to 1967 (Reference A-29). Their approach was a droplet-analysis of the chamber transient during the preignition interval. The propellant droplets were presumed to vaporize by a Knudsen-Langmuir evaporation, with adiabatic cooling of the droplet-vapor system. A portion of the propellant vapor flows through the nozzle, with the remainder accumulating to pressurize the chamber. Although droplet

trajectories were not calculated, the evaporation from each droplet could be terminated after a prescribed droplet residence time. The walls could be presumed to be wetted. Evaporation from the walls and condensation on the walls were both modeled. The size distribution of the injected droplets was simulated by three discrete initial size groups; however, the mean size and distribution used were typical of impinging-stream atomization rather than vacuum-flashing atomization, which would be the expected mode for the earliest propellant injected. The injection flow rate and initial droplet size were not varied with time. The global chemical kinetics of the vapor phase ignition reactions were experimentally investigated. They did not calculate any of the combustion events subsequent to ignition.

Spiking—or explosive hard starts in hypergolic vacuum ignition—was examined experimentally and theoretically by Martens in 1966 (Reference A-30). Based upon his experimental studies, he ascribed great importance to the propellant deposited on the chamber walls during the preignition interval.

The postfiring vacuum evaporation from the wetted chamber walls and the postfiring deposit of new propellant on the walls by injector dribble were described by Juran and Stechman in 1968 (Reference A-31). They emphasized the possibility of continued buildup of combustible material on the wall over a series of closely spaced short pulses.

In addition to the above chamber and system studies, there has been a large volume of experimental and theoretical work describing the individual processes occurring in the chamber, such as flash atomization, impinging stream atomization, aerodynamic droplet drag, droplet combustion rates, etc.

c. The MDAC Transient Combustion Chamber Program

The present transient combustion chamber program, TCC, is based upon and extended from these previous studies (Reference A-1 through A-4). The TCC program was started at MDAC in 1967 under IRAD funding as a general method for solving transient problems in liquid rocket engines, and in particular as a basis for aiding in the development of very fast response control engines. It very quickly became evident that the program had the capability to model low-frequency combustion instability with great precision, that it had a considerable potential for assisting in the analysis of hard starts in both hypergolic and externally ignited engines, and that it offered a feasible approach to the study of contaminant production in pulse-mode rocket engines.

Since 1970 the AFRPL has supported the extension of the program to model contaminant production in liquid bipropellant rocket engines.

The TCC program differs from any earlier combustion chamber analysis by having a greater scope and generality. The analysis attempts to model all of the relevant system processes starting with the propellant in the tank and following it until it eventually passes through the throat. As a result, the program has the capability to calculate a wide variety of engine problems without the introduction of any special assumptions for particular cases. To obtain information on chugging instability, vacuum hypergolic starts, or pulse-mode performance, it is only necessary to specify low tank pressures, low ambient pressure, or short valve durations. It is just as simple to obtain steady state combustion efficiency by specifying a stable operating point.

This program is presently capable of calculating all the sequential events in a nine-pulse series of vacuum hypergolicly ignited firings. This is done in one continuous calculation, with the buildup of wall material and the extent of injector dribbling being carried over continuously from one pulse to the next.

The transient combustion chamber program resembles earlier transient systems analysis programs in that the time-varying flows through the lines and valves, the injector priming, accumulation of vapors or gas in the chamber, and efflux through the nozzle are solved through digital integration. In contrast with previous systems analyses, the combustion process has been calculated using the droplet approach. To adequately model wall deposition, two-dimensional droplet trajectories are calculated. The primary atomization calculations give droplets which are time varying in initial diameter, initial velocity vector and point of primary breakup. Vacuum-flashing atomization is calculated instead of impinging-stream atomization when the conditions warrant it. The "Klystron effect" is modeled using the normal droplet trajectory calculations. The times of ignition and extinguishment are calculated using global vapor phase kinetics and a quenching distance correlation. The combustion rates of the droplets, the combustion rate of the material on the walls, the droplet aerodynamic drag, and viscous axial flow of the material on the wall are all calculated using empirical correlations with the appropriate time-varying local Reynolds number. The stoichiometry-dependent properties for equilibrium combustion product gases or for unreacted propellant vapors are used at the appropriate times. Aftercutoff, the "dribbling" of the injector is simulated by inertial-resistive flow through the injector orifices, driven by the

difference between vapor pressure and chamber pressure. Between pulses, the material on the walls simultaneously undergoes vacuum evaporation and heat transfer from the chamber wall.

The present program, however, is still incomplete, in that there are some important processes which are not yet represented, i. e., axial and radial variation in gas stoichiometry, secondary atomization of droplets, wave formation and stripping of liquid from the wetted wall, pressure waves in the propellant feed systems, heat transfer to and through the walls, etc. It is also obvious that the present experimental correlations for stream breakup distance and primary atomization droplet size which were all obtained with large orifice sizes, are not sufficiently accurate to form a good basis for design or prediction when extrapolated to the very small injection orifice sizes found in pulse-mode engines. The complexities of very reactive impingement or stream blow-apart have not been modelled. No attempt has been made to model either gas-phase or mixed-phase detonations in the combustion chamber.

Although the current program has not yet been developed to its ultimate limit, it is already of great value in offering theoretical guidance for correcting hard starts, improving inefficient operation, avoiding contaminant production, improving response time, eliminating system instabilities, etc.

A. 2 ANALYSIS

a. Scope

The transient combustion chamber program uses numerical integration of the detailed system processes to calculate the events in a rocket engine system operating under unsteady conditions. The system which is modeled consists of a pressure-fed bipropellant feed system, an injector, a combustion chamber, and a nozzle (Figure A-1).

The initial flow of propellant is calculated as the valves open, the fluids accelerate through the resistive-inertial feed lines, and the injector primes.

If the vapor pressure of the first injected propellant is sufficiently above the initial chamber pressure, the atomization will commence by vacuum-flashing of the stream. If one stream is injected before the other and does not flash, it will undergo single stream breakup if there is sufficient distance for it to do so; alternatively, it will impinge upon the chamber wall, where part of it will stick as wall film and the rest will be atomized by the wall impact. Later in the firing, atomization occurs by the impingement of the two unlike streams. The time-varying initial mean droplet size, the droplet size distribution, the initial droplet velocity vector, initial velocity distribution, and the distance traveled before the breakup process is completed—all depend upon the details of the atomization process.

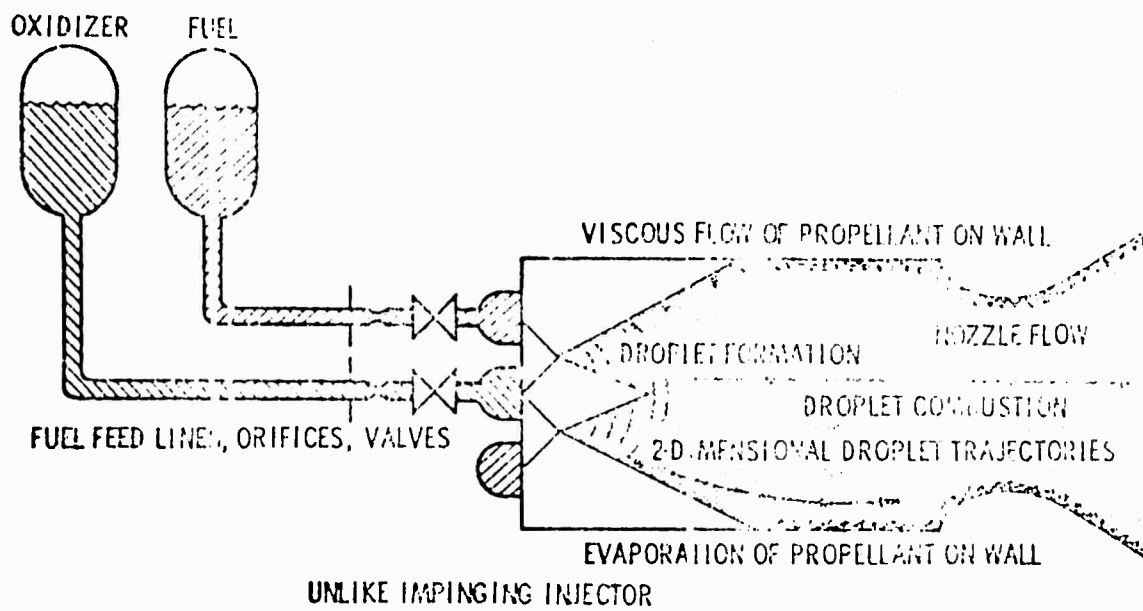


Figure A-1. Rocket System Schematic

The two-dimensional trajectories of the injected droplets are followed until the droplets either burn completely, pass through the nozzle incompletely burned, or impact upon the wall.

The hypergolic vacuum ignition is calculated in the vapor phase, based upon global chemical kinetics. Various locations are examined to determine where ignition will occur first; the well-mixed vapors in the chamber, the most-recently formed vapor mixture from the flashing streams, the boundary layer around the fuel droplets, or the boundary layer around the oxidizer droplets. Once ignition occurs anywhere, the entire chamber contents are presumed to ignite and will continue to burn until the criterion for extinguishment is met. Before ignition, the values for the temperature, molecular weight, and specific heat of the chamber gas are calculated assuming well-mixed but unreacted fuel and oxidizer vapors. After ignition, properties appropriate for equilibrium combustion products are used. After extinguishment, a distinction is drawn between quenched combustion gas and newly formed propellant vapors, so as to properly calculate reignition, if it occurs.

The film of material which builds up on the wall is partially burned off by the heat transfer from the hot combustion gases flowing past it and undergoes viscous flow under the influence of the shear forces from the combustion gas.

The axial variation in thickness of the wall-deposited material is approximated by dividing the chamber wall into one hundred discrete axial slices. The deposition, flow, burnoff, and vacuum evaporation from each slice is treated separately, so as to give an approximate wall thickness profile and to correctly reflect the influence of unevenly distributed propellant. If the amount and rate of flow of the material on the wall are sufficiently high, some of the wall film material will be carried through the throat and ejected.

After the valves have closed, the pressure in the chamber decays, most of the droplets leave the chamber, and the combustion in the chamber is extinguished if the calculated quenching distance exceeds the chamber diameter.

If the chamber pressure falls below the vapor pressure of the propellant in the injector dribble volumes, this material will flow out of the injector. The same technique is used to compute flow rate, atomization, and droplet trajectory as was used during the rest of the firing, with the exception that injector vapor pressure is now used instead of tank pressure to produce flow, and the flow impedances of the injector orifices are used instead of the whole system flow impedances. This dribbled material will burn, be expelled through the throat unburned, or be deposited upon the chamber walls, depending upon the injector and chamber conditions.

When the chamber pressure falls below the vapor pressure of the material on the walls, it will start to evaporate, absorbing heat from the chamber walls (presently assumed to be isothermal).

At any time, the propellant valves may be reopened to initiate a second pulse of firing. The propellant dribbled from the injector following the first pulse will constitute the injector void volume which must be filled to prime the injector for the second pulse; the propellant buildup on the walls will continue from the values attained during the vacuum evaporation following the first pulse, etc. Up to nine sequential pulses of varied interval, pulse width, and propellant lead may be made in a single, continuous calculation.

The information obtained from the calculation includes a chamber pressure history, flow rate histories, the thrust history, and plots of some fifty other variables which could be of value in interpreting operational problems or motor performance. The specific impulse, C-Star, total impulse, pressure-time integral, and eventual disposition of all the propellant that flowed from the tanks is given to define the engine performance.

The amounts and stoichiometry of the wall film material that was ejected unburned is given, and the amounts, stoichiometry, mean axial velocity, mean droplet size, and droplet size distribution of the droplets that were ejected unburned is given to define the contamination-production characteristics of the engine.

Details of the ignition, start, and cutoff transients are given, as well as any low-frequency combustion instability which might occur either during the run or during the transients.

The weight, distribution, and stoichiometry of the material left on the wall are given as an indication of possible future explosion hazards.

b. Limitations and Assumptions

The particular processes which have been emphasized in the current program have been dependent upon the immediate interests or problems of the users. Thus many aspects of the start transient and contaminant production are well represented, while pressure wave action in the propellant feed lines, heat transfer in the chamber walls, and sophistication in the dynamics of the combustion gas are conspicuously absent. There are several obvious places where the precision or generality of the present program could be extended if there was a sufficient requirement for the added capability to justify the expense of programming and the longer computing time which goes with greater sophistication.

(1) Feed System

Compressibility of the propellant and the resulting wave action in the lines could be modeled using the method of characteristics. The pressure waves in the lines are important in determining the response of attitude control engines which have very fast valves and extended lines. The two-phase flow in the injector may be important during injector priming and during postrun dribbling under vacuum ambient conditions. Neither wave action nor two-phase flow is modeled at present.

(2) Chamber Gas Dynamics

The gas flow in the chamber is presently assumed to be purely in the axial direction, even where this is not reasonable, as in the converging portion of the nozzle. The gas flow could easily be computed to follow a path at a fixed fraction of the local chamber radius. This would yield a more nearly correct value for the number of small droplets impinging upon the chamber wall in the vicinity of the converging portion of the nozzle. This modification is already complete in an advanced version of the program.

The axial and transverse variation in gas stoichiometry could be modeled to replace the current assumption of well-mixed gas. This

could be done by following discrete "slugs" of chamber gas along streamtubes and summing the additions of fuel and oxidant vapor from the passage of the "slug" of gas through the droplet array. Doing this would permit calculation of performance losses due to composition striations and would also permit calculation of system instabilities of the entropy wave variety.

At present the combustion chamber gas state is imperfectly modeled. It is assumed that the chamber gas pressure, temperature, and density at the nozzle throat and at the injector end of the chamber are equal. No consideration is made of the fall in gas temperature associated with the large gas expansions at cutoff or during chugging. To model the expansion or compression of hot thermochemically equilibrated gas with concurrent arbitrary additions of fuel or oxidizer will probably require that equilibrium thermochemistry calculations be performed at each time step. There are current thermochemistry programs which possess sufficient speed and reliability to make this feasible, but it is not warranted for the present uses of the program.

(3) Droplet Evaporation

There are two conflicting assumptions which are commonly made regarding droplet evaporation rate. The droplet calculations of Priem et al, assume temperature equilibration between the surface and interior of the droplet. The evaporation and heat-transfer equations are linked together through the time-varying temperature of the liquid droplet interior, and thus the warmup transient of the droplet is described.

The other conflicting assumption which is commonly used is that heat from the droplet surface does not penetrate into the interior of the droplet, and that evaporation from the surface proceeds at a rate proportional to the instantaneous heat transfer into the surface. This assumption was used in the droplet calculations of Lambiris et al. To physically justify the first assumption, there must be considerable internal circulation of the droplet, since conduction alone is insufficient to heat the interior of the droplet appreciably. Droplet circulation, in turn, depends upon exceeding a threshold value for droplet surface stress sufficient to develop new liquid surface while working against the effects of surface tension hysteresis. Thus, circulation is probably present in large droplets with large relative velocity and absent in small droplets with small relative velocity. The present program treats all droplets as noncirculating instead of properly treating droplet circulation as a time-varying function for each droplet. Since the combustion efficiency of an engine depends markedly upon the evaporation of the large droplets, an extension of the program to handle circulating droplets would be advantageous.

When the temperature of the liquid droplet is such that the vapor pressure of the liquid is below the total pressure of the chamber, then

it is correct to use the equations for molecular diffusion to calculate the evaporation rate of the droplet. When the vapor pressure of the droplet is above the total pressure of the chamber, as would be the case when warm propellant is injected into an initially evacuated chamber or when large heated droplets remain in the chamber during the cutoff transient or during the pressure-decay phase of a cycle of low-frequency combustion instability, then it is appropriate to use the Langmuir-Knudsen evaporation Law. The program at present does not provide for Langmuir-Knudsen evaporation from the propellant droplets, but adding this capability would give a more accurate description of the vacuum hypergolic ignition process, the cutoff transient, and low-frequency combustion instability.

The present program treats droplet trajectories as being only two-dimensional (axisymmetric). This means that the lateral spreading of the propellant fans is not modeled. Instead, all the propellant droplets are regarded as being initially directed down the centerline of the fan. This leads to predictions of wall deposition more localized than would be the case with a correct description of the fan. Changing the droplet trajectories to be fully three-dimensional would require only minor program changes but would give more precise results, at the expense of longer computing time.

It is well known that when droplets are subjected to sufficiently high relative gas velocities, they undergo secondary atomization, and that this can have an important effect in increasing the combustion efficiency of the chamber. This phenomenon is not presently modeled, but it should be considered if it ever became desirable to better approximate the actual delivered impulse of the engine.

(4) Wall Effects

When droplets of propellant are impinged upon the chamber wall, a layer of liquid is built up which is then subjected to axial flow, to burnoff by heat transferred from the combustion gas, and to vacuum evaporation by heat transfer from the wall. All of these processes are oversimplified in the present program.

Propellant deposited on the wall is presumed to lose its axial velocity upon impact, but the loss of axial momentum of the droplets, which should produce an axial force on the wall film, is at present not accounted for. The wall film is treated as being in steady motion, following Poiseuille's Law. This is an adequate approximation for very thin layers; however, there are situations where thick layers are formed and where inertial effects become important. In this case, each axial element of liquid must be treated with an unsteady analysis which conserves axial momentum. A modification to do this is already complete on an advanced version of the program.

When gas moves rapidly over the surface of a sufficiently thick layer of fluid, ripples are formed due to Rayleigh instability (i. e., the diminution of static pressure where the peaks are highest). This can affect the drag and heat transfer rate. If sufficient ripple amplitudes are reached they can lead to stripping of the crests, i. e., secondary atomization from the liquid wall film. These phenomena could be modeled if they prove to be important.

The heat transfer to the nonwetted portions of the chamber walls is not presently calculated. This is a very interesting possibility, since the axial gas velocity profile, temperature, density, heat capacity, Reynolds number, and even heat transfer coefficients are already calculated for other uses. A simple two-dimensional mesh for unsteady heat transfer into the chamber walls would permit rather sophisticated calculations to be made, such as internal-regenerative cooling, and the effects of thermal soakback on the evaporation of deposited propellant and on subsequent hypergolic starts. Thermal histories for multiple-pulse firings could be calculated, including effects of quenching from propellant leads, from injector dribbling, etc.

The thermochemical effects of the bipropellant impingement on the wall could be treated in greater detail. At present, the viscosity of the wall layer is specified in the program input as a function of stoichiometry. The least volatile wall film constituent is hydrazinium nitrate, which is generally found mixed with fuel and water to form a viscous solution. The heat of neutralization which is evolved when hydrazinium nitrate is formed is well known, and the associated adiabatic temperature rise for the newly formed mixture can be calculated. This temperature rise, along with dilution effects are used to estimate the viscosity values currently used as program input. Since heat losses to the wall, or cooling by evaporation of excess fuel, would change the temperature and composition of the wall film, these viscosity effects should be modeled in a time-dependent way.

During the vacuum evaporation of the wall material, the evaporation is treated as though the propellants were two immiscible phases. This is an adequate approximation for small asymmetric engines having a single injection element, or for the case where pure fuel or oxidizer is deposited on the wall unmixed during a propellant lead. For situations in which the propellants are actually mixed and reacted, it would be preferable to calculate vapor pressures based upon a physical system containing hydrazinium nitrate and the excess propellant, whose vapor pressure is appropriately depressed by solution effects.

(5) Experimental Uncertainties

In addition to the computational limitations of the program, there are some important processes and physical properties which are inadequately known.

The droplet sizes resulting from primary atomization of reactive unlike streams have never been investigated. There have been no experimental determinations of droplet size for the small orifice sizes and extremes of momentum imbalance which can be found in pulse-mode engines. Comparison of calculated and experimental firings of small engines indicates that the actual droplet sizes must be smaller than the value predicted using the current correlations, that a different drop size distribution must be used, or that the fuel burning rate is in error. This uncertainty as to correct droplet size is one of the greatest restrictions on the present use of the program. Very little is known about the droplet sizes produced when either an unatomized stream or large droplets impact upon the wall.

The breakup distances for impinging-stream and single-stream atomization have been determined for only a very limited range of liquid velocities, gas densities, and orifice diameters. Further investigations are badly needed for smaller orifice diameters. Along with the inadequate knowledge of droplet sizes, this is one of the most severe restrictions on the utility of the program.

Very little is known about the impingement of droplets against the chamber wall. The fraction of impinging droplets which will stick to either a cold chamber wall or to a hot chamber wall is not known.

The effects of droplet size or velocity of approach is not known. The velocity of rebound from the wall and the amount of heat transfer between a bouncing droplet and a hot wall are unknown.

The physical properties of the hydrazinium nitrates and their solutions are completely unknown. Accommodation coefficients for the hydrazines, for nitrogen tetroxide, and for the hydrazinium nitrates are unknown, but because of the highly polar, highly associated nature of the molecules, they are certainly very far from unity.

c. Modeling of System Processes

(1) Feed System

The feed systems are approximated with single lumped parameters representing the inertial and resistive aspects of the feed systems:

$$\frac{dq}{dt} = \frac{P_t - P_c - \frac{1}{2} \rho R q |q|}{\rho \Sigma L/A} \quad (A-1)$$

where

q = volumetric flow rate through the line

P_t = tank pressure

P_c = chamber pressure

R = a coefficient representing the steady-flow pressure drop through the feed system

$\Sigma L/A$ = the summation of segment length divided by cross-sectional area for the series of segments which make up the feed system

Opening and closing of the valves are modeled by varying the value of R as a function of time. Flow reversals or initial start conditions which result in partially or fully gas-filled feed lines are simulated by varying both R and $\Sigma L/A$ as functions of time, so as to delete the resistive and inertial contribution of components which are not liquid filled at any particular instant. Equation A-1 does not model the compressibility of the propellant or the pressure waves in the lines. For cases in which wave action is important, a method of characteristics solution for a distributed parameter resistive-inertial-compressible feed system would be more accurate; however, the present approximation is quite adequate to model flow events which take longer than five or six acoustic periods of the feed system (see Reference A-32).

After the valves close at the end of a firing, the chamber pressure decays, approaching the external pressure. When the chamber pressure falls below the vapor pressure of either propellant, it will start to flow from the dribble volume (the liquid-filled volume between the valve and the injector face). The flow rate out of the dribble volume is calculated using Equation A-1, but with R and $\Sigma L/A$ now restricted to the injector orifice values and with P_t replaced with the propellant vapor pressure evaluated at the injector temperature. As soon as the dribble volume is emptied, the dribble flow rate is set to zero.

There are two optional assumptions which may be used to describe the injector priming process (Figure A-2). If a ring-type injector is being filled in a vacuum environment, some of the orifices will be wetted

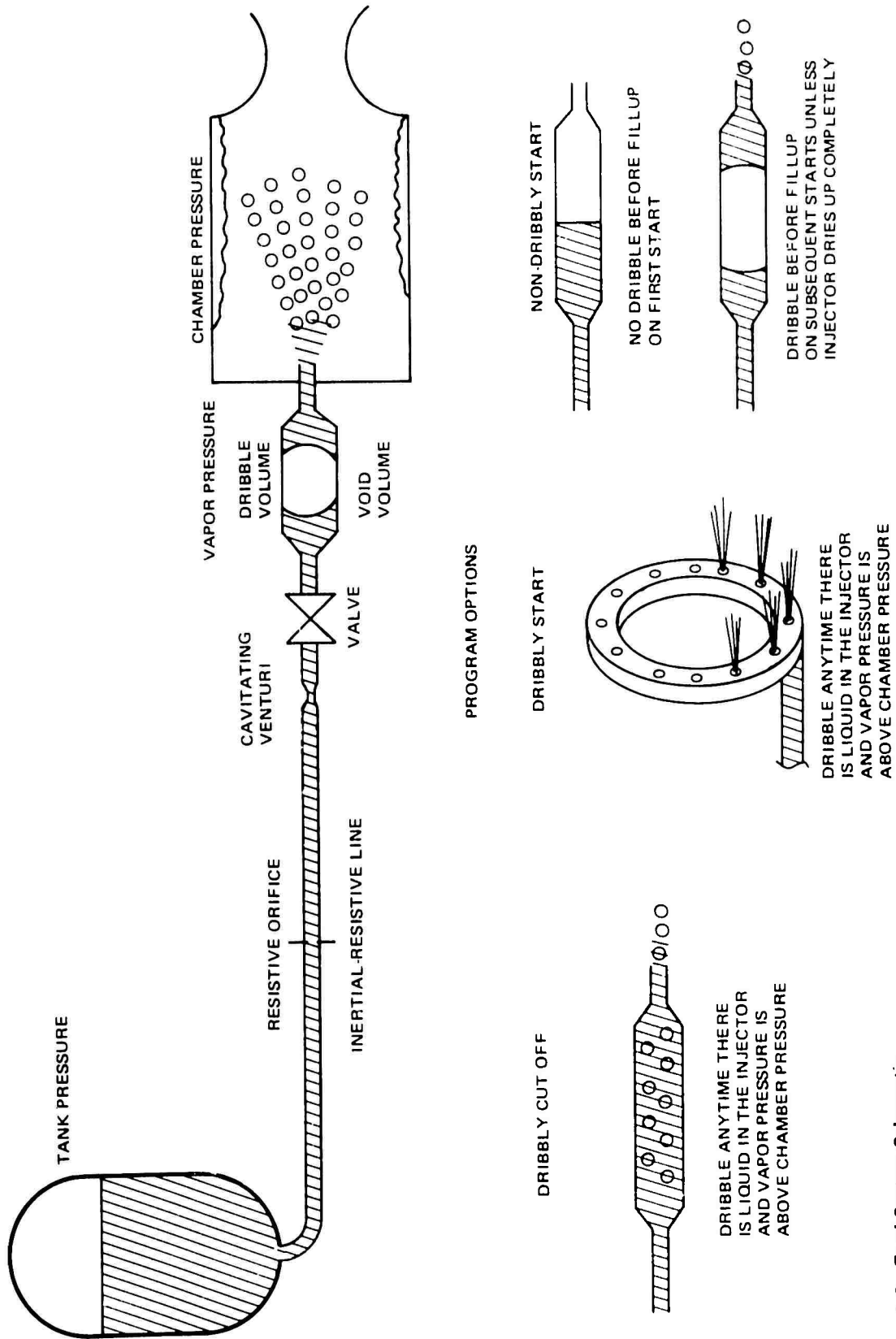


Figure A-2. Feed System Schematic

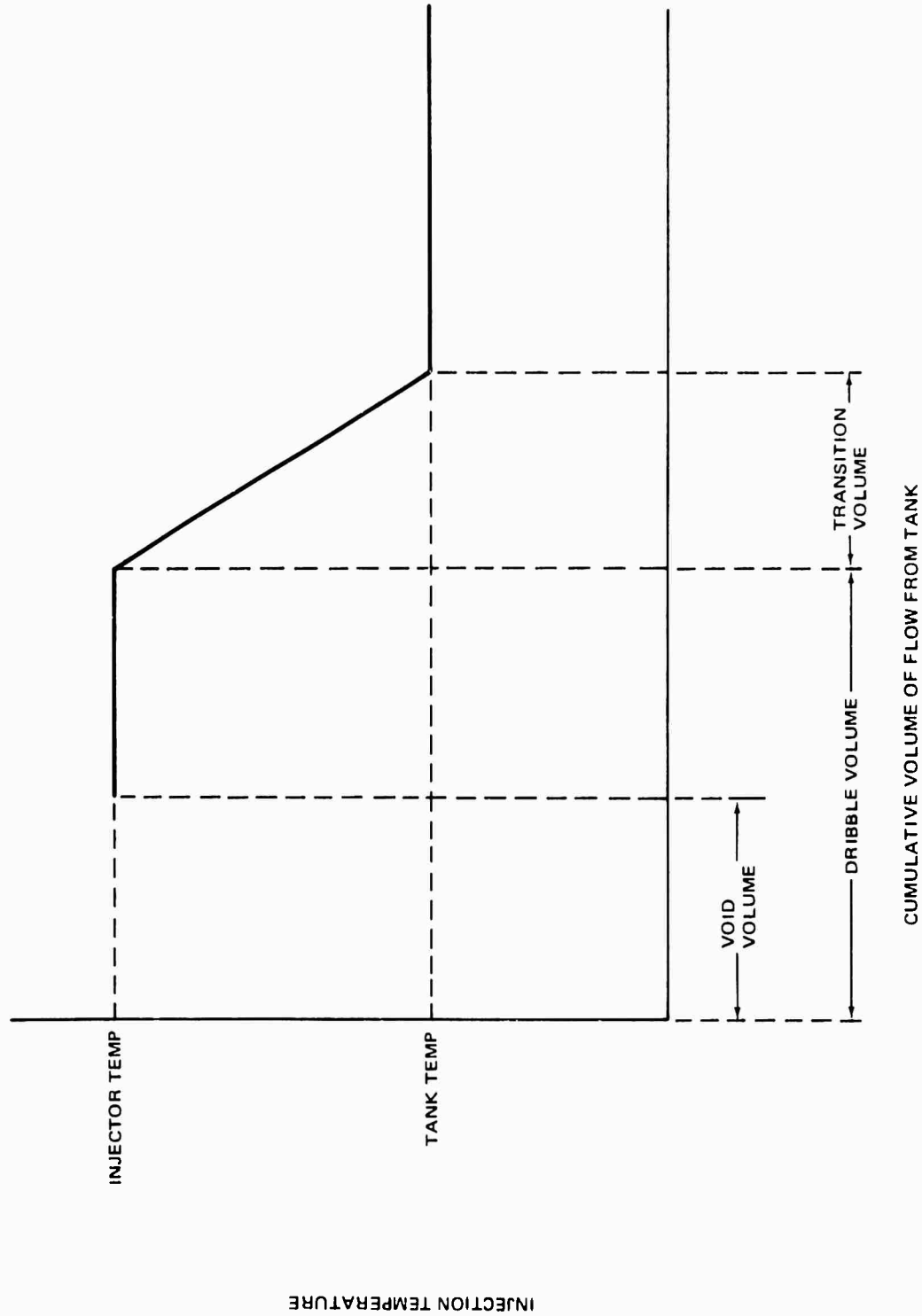
even before the ring volume is filled, and flow will be expected through these wetted orifices under the influence of the propellant vapor pressure. The initial dribble option is for this situation, and the initial dribble flowrate is calculated the same as a postfiring dribble. The flow from the propellant tank into the dribble volume is calculated according to Equation A-1 but with R and $\Sigma L/A$ restricted to the values for the upstream hardware and with P_c replaced with the vapor pressure evaluated at the injector temperature. As soon as the injector is primed, the flow follows Equation A-1 as written.

The other injector priming option which may be used is appropriate for a smooth unbranched injector passage which would be expected to fill progressively from the valve out to the injector orifices without any dribbling of propellant before the passages are completely filled.

If high-amplitude combustion instability or high-amplitude pressure spikes temporarily reverse the flow in the propellant feed lines, the reverse flow is time-integrated to give the time-varying gas volume behind the injector. So long as there is gas behind the injector, the injection rate is set equal to zero, and the inertial and resistive contributions of the injector orifices are deleted from Equation A-1.

The static pressure in the throat of the cavitating venturi is monitored, and if it falls below the vapor pressure of the propellant, Equation A-1 is evaluated for the impedance of the upstream hardware only, with the venturi throat pressure set to the vapor pressure.

The heating of the portions of propellant held in the dribble volumes by thermal soakback has been modeled. The propellant injection temperature is taken as the prescribed injector temperature until an amount has flowed from the tank equal to the dribble volume. Following this the injection temperature varies linearly with flowed volume from the injector temperature to the tank temperature, where it remains for the remainder of the firing. (Figure A-3). The density, viscosity, surface tension, vapor pressure, and liquid enthalpy are evaluated at the injection temperature, and are important in determining the dribble flowrates, the onset and extent of stream flashing, the flashing or impinging stream atomization droplet size, and the ignition delay time. The propellant in the injector is presumed to warm up to injector temperature whenever the valves are closed, so repeated firings will all start with propellant initially at injector temperature.



INJECTION TEMPERATURE

Figure A-3. Injection Temperature Profile vs Flow from Tank

There are several complex modes that flow from the injector could take which have not been programmed in the current model. The propellant in the dribble volume could boil in a vacuum environment, with the well-mixed foam flowing through the orifice. Chugging or popping during the dribble periods could force noncondensable combustion gases into the dribble volumes to form foam at a pressure higher than the vapor pressure. If these modes of flow were found to be important they could be modeled.

(2) Physical Properties

The densities of the liquid propellants are obtained from a mathematical approximation to a general correlation of reduced density versus reduced temperature along the saturation line (Reference A-33). The critical density is obtained from the propellant density given at a reference temperature.

The viscosity is approximated from a mathematical approximation to a generalized correlation of reduced viscosity versus reduced temperature. The critical viscosity is obtained from the propellant viscosity given at a reference temperature.

The surface tension is approximated using the parachor and a mathematical approximation to a generalized correlation of reduced density difference (liquid density-vapor density) versus reduced temperature along the saturation line. The parachor is a parameter which is closely related to the critical properties of a fluid. It is defined as the molecular weight multiplied by the surface tension raised to the one-quarter power and divided by the difference between liquid density and vapor density. The parachor may be regarded as a measurement of the molar volume of the liquid at a standard value for surface tension. For most materials it varies by no more than a few percent over the entire liquid range. The parachor for each propellant constituent is calculated from the propellant surface tension given at a reference temperature, and is used to calculate surface tension at other temperatures.

The vapor pressures of the propellants are obtained from the equation of Calingaert and Davis (Reference A-34):

$$\ln P = A - \frac{B}{T-43} \quad (A-2)$$

where A and B are evaluated for the fuel and oxidizer using the pressures and temperatures corresponding to the normal boiling point and the critical point.

Because of the scarcity of thermodynamic data for many propellants, the specific heats of vapor, liquid, and the solid form of each propellant are assumed to be constants which are neither temperature- nor pressure-dependent. When these values are supplemented by the melting point, heat of fusion, normal boiling point, latent heat of vaporization at the boiling point, and critical temperature, the straight-line relationship of Figure A-4 is obtained. This relationship is used to approximate the enthalpy of the vapor or condensed phases as a function of temperature.

(3) Atomization

The atomization process is calculated for one of several modes, depending upon the chamber pressure, the propellant injection temperature, and the propellant injection rates. If the chamber pressure is sufficiently below the vapor pressure of the propellant at its injection temperature, the stream is presumed to flash atomize. If streams of both propellants are being injected and are not flashing, then impinging stream atomization is calculated. If only one stream is being injected, and it does not flash, the stream breaks up in a single-stream mode unless it hits the wall first, in which case it is calculated to break up by wall impact. If both streams are being injected, and only one of them flashes, the other stream is presumed to be unaffected by passing through the spray of small flashed droplets and behaves as though the other stream were absent.

R202

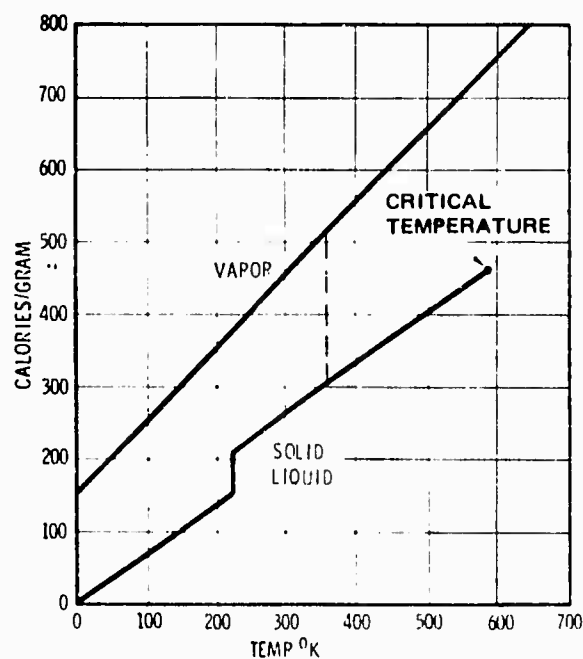


Figure A-4. Approximate Enthalpy of Monomethyl Hydrazine

(a) Flash Atomization Threshold

Bushnell and Gooderum (Reference A-35) investigated the flashing of streams of water over a range of subatmospheric pressures, and found that the ratio of stream temperature to saturation temperature was almost a constant at the onset of flashing (with temperature measured on an absolute scale). Brown (Reference A-36) investigated the flashing of streams of superheated water at atmospheric pressure, varying temperature, orifice diameter, and stream velocity, and found that the temperature at the onset of flashing was a function of the stream Weber number. If these findings may be combined, the supersaturation temperature ratio at the onset of flashing may be represented as a function of stream Weber number. The following correlation is taken from the experimental data of Brown, but does not disagree with the data of Bushnell and Gooderum.

$$\begin{aligned} 0 < N_{we} < 12.5 \quad \frac{T_{flash}}{T_{sat}} &= 1.138 - 0.005 N_{we} \\ 12.5 < N_{we} < 24 \quad \frac{T_{flash}}{T_{sat}} &= 1.085 - 0.00353 N_{we} \\ 24 < N_{we} \quad \frac{T_{flash}}{T_{sat}} &= 1.0 \end{aligned} \tag{A-3}$$

Where the Weber Number is

$$N_{we} = \frac{\rho_g V_j D_o}{2\sigma}$$

There is a discontinuity in the function at a Weber number of 12.5 corresponding to some unknown change in the mechanism. The supersaturation temperature ratio is known to depend upon the surface roughness of the orifice; however, this effect has not been modeled in the TCC Computer Program, and the above relationship is for ordinary drilled holes.

(b) Flash Atomization Droplet Size

Brown has investigated the mean droplet diameter and droplet size distribution obtained when superheated water is flash-atomized at atmospheric pressure. The experimental data obtained for flow through ordinary drilled holes shows that the mean drop size depends strongly upon nozzle pressure drop (stream velocity) and the degree of superheat of the liquid, but not upon the nozzle orifice diameter. The correlation for his data is:

$$D_{32} = \frac{18.9}{V^{1.28} \left(\frac{T_{\text{stream}} - T_{\text{sat}}}{T_{\text{sat}}} \right)} \quad (\text{A-4})$$

where

D_{32} = Sauter mean diameter in centimeters

V = stream velocity in cm/sec, based upon the orifice pressure drop and the upstream liquid density

T = temperature measured on an absolute temperature scale.

Gooderum and Bushnell (Reference A-37) flashed water through drilled holes into a vacuum (~2 mm Hg) under otherwise comparable conditions and found mean droplet diameter was proportional to orifice diameter, did not depend upon stream velocity, but did depend upon the temperature of the stream. Their data can be correlated:

$$\ln \left(\frac{D_{32}}{D_o} \right) = 6.4 - 0.0244 T \quad (\text{A-5})$$

where

D_{32} = Sauter mean diameter

D_o = orifice diameter

T = stream temperature in degrees K

The large disagreement between the two relationships is probably due to the large differences in Weber number. Until the relationships are better understood, we will take 40 microns as a typical mean droplet diameter for the flash atomization of water, with reasonable values for orifice diameter, stream velocity, and degree of superheat. Brown described the flash atomization process as resembling the gas atomization process, with the gas being supplied by the explosive growth of bubbles in the superheated stream. For this reason we have applied a physical properties correction which would be suitable for the gas atomization process. The equation used in the program to describe flash atomization droplet size is:

$$\bar{D}_p = 0.0065 \left(\frac{\sigma_p \mu_p}{\rho_p} \right)^{0.25} \quad (A-6)$$

where

\bar{D}_p = median droplet diameter of propellant P, in centimeters

σ = surface tension of propellant, P

μ = viscosity of propellant, P

ρ = density of propellant, P

The drop size distribution obtained by flash atomization is much narrower than that obtained by impinging stream atomization.

(c) Vacuum Vaporization of Propellant

When a stream of propellant is injected into a combustion chamber having a total pressure lower than the vapor pressure of the propellant, and if the Weber number is sufficiently high, then flash atomization will take place from explosive growth of vapor bubbles at nucleation sites in the stream. A certain amount of evaporation of propellant will occur during the flash atomization process. Following this, evaporation from the droplets will proceed, initially following the Langmuir-Knudsen Law. If the chamber pressure increases to a value above the vapor pressure of one or both of the constituents, the evaporation can continue by molecular diffusion. Molecular-diffusion-evaporation can continue until the droplets have either equilibrated with the chamber vapors, are expelled through the throat, or impact upon the chamber wall. There are large areas of uncertainty in this complex

process. One unknown is the amount of evaporation which takes place during the atomization process, before the droplets are completely formed. Another is the chemical processes which could occur on the surface of a cold droplet of nitrogen tetroxide which is cryopumping vapors of hydrazine onto its surface.

Scamans, Vanpee and Agosta (Reference A-29) have calculated the preignition chamber pressure history for the injection of one propellant component, based upon Langmuir-Knudsen evaporation of droplets having a mean diameter of 100 microns in a chamber one-in. long. They found that the droplets had nearly equilibrated by the end of a time period (1.5 to 5.5 msec) corresponding to a nominal droplet residence time. Since their droplets were quite large for flash-atomized propellant, and since their chamber was quite small, it is not unreasonable to assume that phase equilibrium is generally attained, and to use this asymptotic value to describe the preignition evaporation.

The TCC program tests each portion of injected propellant by Equations (A-3) to determine whether flashing occurs. If it does, the program calculates the fraction of the propellant which will vaporize to obtain local phase equilibrium at the instantaneous chamber pressure. The vapor formed is added to the vapors already in the chamber, the addition being made at the propellant injection point. The liquid which is unvaporized is assigned droplet properties, and the droplets are entered into the chamber droplet array. No further evaporation from or condensation on the droplets is calculated until they either impact upon the wall or until the ignition of the chamber contents occurs.

When liquid propellant is injected at a prescribed injection temperature, the relationships shown in Figure A-4 fix the injection enthalpy. The value of the chamber pressure at the time of injection is used in Equation (A-2) to determine the equilibrium temperature of the flashing propellant. When the enthalpies of the vapor and condensed-phase propellant are evaluated at the equilibrium flashing temperature, the fraction of the propellant which evaporates may be obtained:

$$H_{inj} = X \cdot H_{vap} + (1-X)H_{cond} \quad (A-7)$$

or

$$X = \frac{H_{inj} - H_{cond}}{H_{vap} - H_{cond}} \quad (A-8)$$

Since internal boiling and convective heat transfer inside the droplet both cease after freezing, the program has the option of terminating the evaporation process once the droplets have frozen.

(d) Impinging Stream Atomization

When the chamber pressure is sufficiently high that the injected propellant streams do not flash, atomization occurs by either the impinging stream or single stream mode of breakup. The expression for droplet diameter used in our program is based upon the work of Ingebo (Reference A-38), who examined the atomization of two identical streams of heptane, impinging at 90-degree included angle in air streams having velocities typical of rocket-engine thrust chambers. Ingebo correlated his data:

$$D_{30} = \frac{D_j}{0.30 \sqrt{D_j V_j} + 0.0125 D_j \Delta V} \quad (\text{A-9})$$

where

D_{30} = volume-number-mean droplet diameter

D_j = injector orifice diameter

V_j = injection velocity

ΔV = velocity difference between the injected streams and the gas flow at the atomization point.

Preim et al. reported (Reference A-5) that for rocket-engine conditions, where ΔV varies with axial distance from the injector, that 4,560 cm/sec (150 ft/sec) is an appropriate average value to use for ΔV .

Preim also offers a correction for liquid physical properties:

$$\frac{D_A}{D_B} = \left(\frac{\rho_B \sigma_A^{\mu_A}}{\rho_A \sigma_B^{\mu_B}} \right)^{1/4} \quad (\text{A-10})$$

where

D_A = mean diameter obtained with fluid A

ρ = density

σ = surface tension

μ = viscosity

Equations (A-9) and (A-10) are combined, along with the above value for ΔV , the physical properties of heptane and the multiplier need to convert from volume-number-mean diameter to mass median diameter. This yields a more general expression for initial median droplet diameter expected from a symmetrical self-impinging doublet injecting a fluid of specified properties.

$$\bar{D} = \left[\frac{D_j}{0.20 \sqrt{D_j} V_j + 39 D_j} \right] \left[1.725 \left(\frac{\sigma \mu}{\rho} \right)^{1/4} \right] \quad (\text{A-11})$$

This expression is still insufficiently general for the analysis of unlike impinging streams during transients, where the momenta of the two streams may be very different, or where one stream may be missing completely. In the absence of experimental data, a simplifying assumption is used to estimate the effects of relative stream momenta. The simplifying assumption is that a small element of liquid in the stream approaching the impingement point is not affected by the condition of the other stream except through the formation of a quasi-stationary planar stagnation surface which acts to redirect the stream into the initial planar flow pattern leading to the formation of the fan. This leads to the conclusion that stream velocity is not the variable controlling fan formation in Equation A-11, but rather the component of stream velocity relative to the resultant direction of the combined stream. This leads to the generalization:

$$\bar{D}_p = \left[\frac{D_p}{0.24 \sqrt{D_p} V_p \sin |\beta_p - \beta_R| + 39 D_p} \right] \left[1.725 \left(\frac{\sigma_p \mu_p}{\rho_p} \right)^{0.25} \right] \quad (\text{A-12})$$

where

\bar{D}_p = median droplet diameter for propellant p

D_p = orifice diameter of the injector for propellant p

V_p = velocity of the jet of propellant p along its own centerline

β_p = angle of the stream of propellant p relative to the engine centerline

β_R = angle of the resultant stream relative to the engine centerline

The resultant angle of the combined fuel plus oxidizer stream is calculated assuming conservation of momentum in the axial and radial directions. When a stream which has not flashed intersects a stream which has flash atomized, it is assumed that there is no momentum interaction; i. e., each stream continues in its original direction instead of being redirected to the "resultant" direction.

If a single stream impacts against the wall before it has travelled a sufficient distance to atomize in the single stream mode, then atomization is presumed to take place by wall impact. Atomization by wall impact is based upon equation A-12, however the value used for relative velocity is simply the absolute value of the radial velocity of the stream, $|V_y|$ which is substituted for the term $V_p \sin |\beta_p - \beta_R|$.

Experimental verification of equation (A-12) is still rather sketchy. It is obviously as correct as Ingebo's expression for the special case (symmetrical 90-degree impingement of heptane) from which it was derived. When only one stream is being injected, the stream angle and resultant angle are identical, and the following special case is obtained:

$$\bar{D}_p = \frac{1}{39} \left[1.725 \left(\frac{\sigma_p \mu_p}{\rho_p} \right)^{0.25} \right] \quad (A-13)$$

This is an expression for single-stream breakup (with an assumed value for mean gas velocity) and was compared with the findings of Weiss and Worsham (Reference A-39) for this special case. The functional relationships appear to be in approximate agreement and the values predicted for mean droplet diameter under typical rocket conditions were in adequate agreement.

Since Equation (A-12) should account for stream impingement angle, it was compared with the findings of Heidmann and Foster (Reference A-40), who measured mean drop size as a function of impingement angle for symmetrical impinging streams. Again the predictions were in reasonable accord with the data. The droplet sizes obtained from the unlike impingement of streams of water and molten wax have been reported by Rocketdyne. Unfortunately, their three published expressions for median droplet diameter from an unlike doublet disagree with each other. It was presumed that the latest published value (Reference A-41) is correct. Evaluated at several points, the Rocketdyne droplet diameter values differed from the values of Equation (A-12) by no more than 5 percent.

This droplet size correlation and the Ingebo experimental drop size distribution have been adequate to accurately predict the chugging frequencies and amplitudes of a small research motor and the start transients of several motors having quite different characteristics; however, it does not give correct predictions for the combustion efficiency of the Marquardt 5-pound R-6C rocket engine which was used for the parametric studies of this report. To force the calculations to agree with experiment, it was necessary to reduce the computational droplet sizes to one half the values given by Equation (A-12). We do not yet know whether the problem of droplet size prediction is associated with the extremely small injection orifices of the R-6C engine, with the very reactive nature of the propellants, or with some other cause, such as the drop size distribution. The Rocketdyne experiments with unlike doublets show a significantly narrower size distribution than the Ingebo experiments and should give a higher combustion efficiency, but calculations have not yet been performed using the Rocketdyne distribution (Table A-1). It is also possible that the droplet size prediction is accurate, but that the combustion rate of NTO-MMH is higher in the rocket engine than would be expected from droplet burning rate experiments. Further experimental testing will be required to clear up this uncertainty. (Reference A-56, presented as this report goes to press, indicates that the low orifice Reynolds numbers of the Marquardt Engine could result in anomalously small droplets.)

(e) Distributed Parameters

The droplets injected into a real combustion chamber are distributed in droplet size, initial direction, initial speed, in point of origin as newly formed drops, and possibly in composition, if the fuel and oxidizer are miscible and not excessively reactive. It is possible to model these distributed parameters by adding more than two droplet groups (one fuel, one oxidizer) to the droplet array during each computational time interval; however, the more droplet groups that are added, the more time-consuming the calculations become. If M values are used to approximate the distribution of each parameter and if N properties are treated as distributed, then the number of droplet groups per propellant is M^N . If M and N were each

taken equal to five, then 6,250 droplet groups would have to be added to the computational array during each time interval, instead of the ten which are presently added. The storage location requirement for the droplet array would increase from 15,000 to 9,375,000 and the computing time on a high-speed computer would increase from about two minutes to about 20 hours. Obviously great restraint must be exercised in "improving" the calculations by this particular approach.

In the present computer program, the initial droplet diameter is the only parameter which is treated as distributed during "normal" operation; five values are used to approximate the experimental size distribution. For impinging stream atomization, the fifth mass quintile of the propellant has a droplet diameter approximately nine times that of the first quintile. This distribution is so wide that the distribution must be modeled if meaningful results are to be obtained.

During the periods that flash atomization is occurring, the droplet size distribution is much narrower, the fifth quintile diameter being only about twice the first quintile value (Reference A-36). However, at this time the initial directions of the droplets from the flashing stream are distributed over a cone having an apex angle of about 30 degrees. This distributed initial direction must be modeled in order to adequately describe the thickness profile of the propellant which is deposited on the chamber wall during the pre-ignition period.

For these reasons, only the droplet size distribution is modeled for impinging stream atomization, while only the initial direction distribution is modeled for flash atomization.

(f) Droplet Size Distribution for Impinging Stream Atomization

The droplet size distribution about the median value is approximated by dividing the injected mass of each propellant into five equal portions. Each of these portions is converted to a group of droplets having a diameter which is a prescribed multiple of the mean droplet diameter. The droplet group size ratios come from a table of coefficients chosen to approximate the experimental droplet size distribution. The droplet diameter of the nth group is:

$$D_n = \bar{D} K_n \quad (A-14)$$

The coefficients used to represent Ingebo's experimental distribution, a Rocketdyne experimental distribution and a widely used analytical approximation are given in Table A-I.

Table A-I. DROPLET DIAMETER DISTRIBUTIONS
MID-QUINTILE DIAMETER/MEDIAN DIAMETER

	Ingebo Experimental (like doublets)	Log-Probability $\sigma = 2, 4$	Rocketdyne Experimental (unlike doublets)
K_1	0.198	0.333	0.60
K_2	0.759	0.645	0.81
K_3	1.00	1.00	1.00
K_4	1.23	1.55	1.22
K_5	2.30	3.00	1.55

After the droplet diameters of the fuel or oxidizer size groups are calculated, the mass per droplet and number of droplets in the group can be computed. The mass of each droplet in the nth group is:

$$M_n = \frac{\pi}{6} D_n^3 \quad (A-15)$$

The number of droplets in the nth group is:

$$N_n = \frac{0.2 \rho g \Delta t}{M_n} \quad (A-16)$$

(g) Atomization Distance

The distance which the impinged streams travel before the atomization is complete is calculated based upon investigations performed at NASA (References A-40 and A-42). The calculations used in this study presume that the distance to breakup is a prescribed number of orifice diameters in the absence of impingement (i. e., when $\beta_p - \beta_R = 0$ degrees), is as specified in Reference A-42 for impingement when $\beta_p - \beta_R = 45$ degrees, and is linearly interpolated with $\sin(\beta_p - \beta_R)$ for intermediate values.

$$L_p = L_{45p} + \left(L_{op} - L_{45p} \right) \left(1 - \frac{\sin |\beta_p - \beta_R|}{\sin 45^\circ} \right) \quad (A-17)$$

L_p = fan length for complete atomization of propellant p

L_{45p} = experimental fan length for symmetrical 90° impingement

L_{op} = distance for single stream breakup of propellant p

β_p = injection angle of propellant p

β_R = resultant angle of the fuel plus oxidizer fan

When $\beta_p - \beta_R$ is greater than 45 degrees, L_p is taken equal to L_{45} degrees. When the injected streams are flash-atomized, the droplets are presumed to be formed immediately at the injection point.

(h) Pre-Atomization Trajectory

The atomization is completed at an axial location in the chamber equal to the impingement distance plus the breakup distance multiplied by the cosine of the resultant angle. This axial location is a droplet group property called S_i in the TCC program.

To approximate the relatively inert condition of the propellants prior to breakup, we assume that there are no combustion, aerodynamic drag, or momentum interaction between particles of injected propellant in the interval between the injection point and the point of droplet formation, i. e., when $X_i < S_i$. Since the injection velocity is time-varying, this implies propellant bunching in this region. This behavior may be visualized from a plot of particle location versus time (Figure A-5). When the first propellant is injected, it is moving quite slowly due to the restriction of the partly opened valve and the inertia of the fluid in the lines. The propellant, which is injected a few milliseconds later, is moving much faster and overtakes the previously injected material.

R202

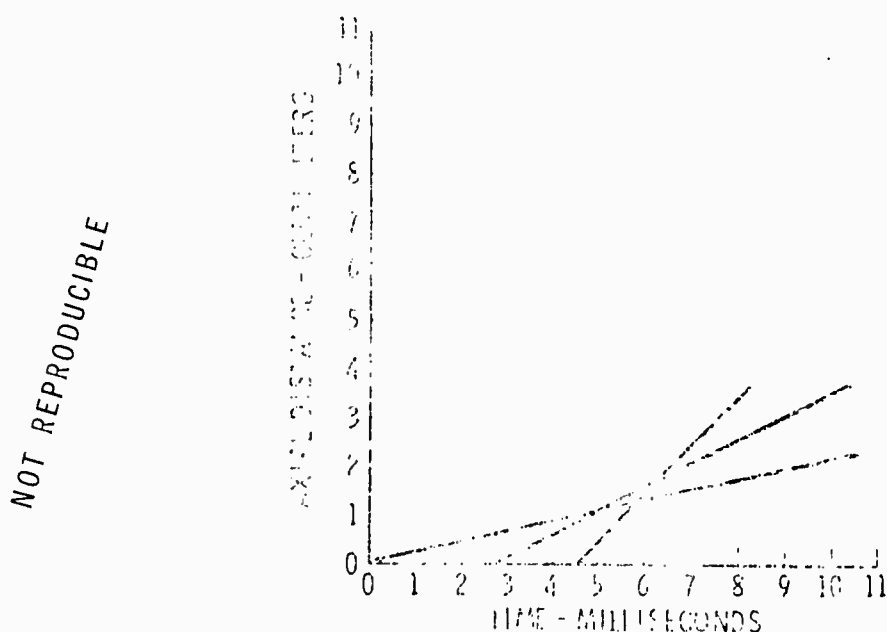


Figure A-5. Preimpingement Trajectory of Propellant

Where the world-lines are close together, the bunching is most extreme, and the effects of velocity modulation produce the maximum effect in varying the arrival rate of propellant. In many rocket engines, this point of least-stable propellant flow is close to the location where droplets are formed and become available for combustion, i. e., S_1 . The injected propellant moves from the injection point to the impingement point along the direction of injection. After impingement, the stream moves in the direction of the resultant angle. It moves in this new direction until its atomization is complete, after which its two-dimensional trajectory is determined by the aerodynamic drag forces exerted by the chamber combustion gases. At the present time, the spreading of the fan is not modeled. When droplets are formed by flash-atomization, they are presumed to be formed at the injection point, and they are presumed to be immediately subject to aerodynamic forces and available for combustion.

(i) Droplet Array Calculations

The feed system and atomization calculations provide values for the mass, mean droplet diameter, initial velocity, etc., for the propellant which is injected into the combustion chamber at each time interval. The group of droplets injected at each time interval is described by fifteen variables, shown in Table A-II.

Table A-II. DROPLET PARAMETERS

M	Mass per droplet
N	Number of droplets in the group
V_X	Axial velocity
V_Y	Radial velocity
X	Axial position of the group
Y	Radial position of the group
F	Fraction of the droplet mass which is fuel
ρ	Droplet liquid density
$\left(\frac{\pi K}{c_p}\right)$	Burning rate parameter A
$\left(\frac{c_p}{\Delta H}\right)$	Burning rate parameter B
S	Axial location where atomization is complete
R	Axial location where impingement occurs
V_{XR}	Axial velocity immediately after impingement
V_{YR}	Radial velocity immediately after impingement
\dot{M}	Calculated evaporation rate per droplet this time interval

This data array has ten new droplet groups added to it each integrating time interval, and has droplet groups deleted when the mass of the droplet falls to zero, the axial location exceeds the chamber length, or the radial distance exceeds the chamber radius. This data array grows to represent the entire droplet population of the combustion chamber.

Each droplet group has the mathematical character of a vector in that fifteen independent values are required for its description. The total droplet population of the chamber is then an array of droplet vectors or a matrix. The droplet population of the chamber can usually be adequately described using no more than 1,000 droplet groups or 15,000 computer storage locations. (The number is determined by the size of the integrating time interval.) The combustion chamber calculations consist of working on the array of droplet groups at each computational time interval to obtain the succeeding new value for droplet mass, droplet axial velocity, droplet radial velocity, droplet axial position, droplet radial position, and droplet evaporation rate.

(4) Droplet Drag and Motion Equations

The aerodynamic drag, heat transfer, and diffusion rates associated with the droplets depend upon a number of dimensionless groups which characterize the regime of flow; thus, the Reynolds number, Mach number, and Knudsen number must be considered. The Reynolds number is of great importance to all of the transport processes. Drag coefficients and heat transfer coefficients are correlated with droplet Reynolds number. The Mach number of the flow about the droplets is generally less than 0.1 and its effects are ignored. The Knudsen numbers associated with the chamber processes have been calculated for a large number of conditions. The Knudsen numbers may be large for the first computational time interval, when the chamber pressure is taken equal to space ambient pressure; however, the Knudsen numbers have always been well into the continuum flow regime as soon as the first portion of either propellant is injected. Thus, free molecular flow effects should be negligible and are not considered in the correlations for vaporization rate, aerodynamic drag, and nozzle flow.

The velocity of the chamber gas relative to each droplet group must be calculated at each time interval in order to obtain the droplet aerodynamic drag and droplet combustion rate. The simplifying assumption is made that the chamber gas moves in the axial direction only. Hence:

$$V_{rel} = \sqrt{(V_{gas} - V_X)^2 + V_Y^2} \quad (A-18)$$

V_X and V_Y are the axial and radial components of the droplet velocity. The direction cosines of the relative wind are calculated:

$$C_X = \frac{V_{gas} - V_X}{V_{rel}} \quad (A-19)$$

$$C_Y = \frac{-V_Y}{V_{rel}} \quad (A-20)$$

The Reynolds number is calculated for each droplet group at each time interval based upon the droplet diameter (obtained from the droplet mass, presuming spherical geometry) and the velocity difference between the droplet and the gas.

$$D = \left(\frac{6M_i}{\pi \rho_i} \right)^{1/3} \quad (\text{A-21})$$

$$N_{\text{Re}} = \frac{\rho_{\text{gas}} D_{\text{drop}} V_{\text{rel}}}{\mu_{\text{gas}}} \quad (\text{A-22})$$

If the Reynolds number is less than 0.5, Stokes-law acceleration is calculated:

$$A = \frac{18\mu_{\text{gas}} V_{\text{rel}}}{\rho_{\text{drop}} D^2} \quad (\text{A-23})$$

If the Reynolds number is greater than 0.5, the acceleration is calculated from the Newtonian drag law:

$$A = \frac{0.75 C_d \rho_{\text{gas}} V_{\text{rel}}^2}{\rho_{\text{drop}}} \quad (\text{A-24})$$

The drag coefficient data of Rabin (Reference A-43) is approximated by the functions:

$$\begin{aligned} 0.5 < N_{\text{Re}} < 70 & \quad C_d = 27 N_{\text{Re}}^{-0.84} \\ 70 < N_{\text{Re}} < 59,200 & \quad C_d = 0.414 N_{\text{Re}}^{0.1433} \\ 59,200 < N_{\text{Re}} & \quad C_d = 2.0 \end{aligned} \quad (\text{A-25})$$

After the droplet acceleration has been calculated, the new velocity and location of the droplet group are calculated

$$V_{X(t+\Delta t)} = V_{X(t)} + A C_X \Delta t \quad (\text{A-26})$$

$$V_{Y(t+\Delta t)} = V_{Y(t)} + A C_Y \Delta t \quad (\text{A-27})$$

$$X_{(t+\Delta t)} = X_{(t)} + V_{x(t)} \Delta t + 0.5 A C_x \Delta t^2 \quad (\text{A-28})$$

$$Y_{(t+\Delta t)} = Y_{(t)} + V_{Y(t)} \Delta t + 0.5 A C_Y \Delta t^2 \quad (\text{A-29})$$

When the axial position of a droplet group exceeds the length of the chamber the droplet group is removed from the array and its mass is added to the summation of unburned droplets that escape from the chamber. When the radial position of a droplet group exceeds the radial dimensions of the chamber—and certain other conditions are satisfied—the droplet group is removed from the array and its mass is added to the summation of propellant mass which is coating the chamber wall at that particular axial location.

(5) Droplet Evaporation Rate Calculations

The evaporation rate (combustion rate) of a stable fuel or oxidizer droplet is determined by the heat transport to the droplet surface and diffusional mass transport away from it. In the regime encountered in a rocket combustion chamber, the vapor effusion from the droplet has a very large effect on the heat transport process, and the effect of the forced convective flow about the droplet is also of great importance. An additional, important factor in determining the droplet life history is the transport of heat from the surface of the droplet to its interior.

(a) Droplet Circulation

If the droplet has appreciable internal circulation, the convective transport of heat to the interior of the droplet will be large, and there will be a considerable unsteady period when the droplet is warming from its initial injection temperature to the final steady temperature at which it evaporates. The unsteady droplet evaporation problem may be solved by simultaneous calculation of the heat and mass transport about the droplet together with the droplet state (Reference A-44).

If the droplet lacks internal circulation, then heat transport into the interior of the droplet is negligible (Reference A-45), and all the heat which reaches the droplet surface is used in vaporizing the outermost layer of fluid. When this is the case, the droplet state and vapor diffusion equations need not be solved.

According to Bond and Newton (Reference A-46) as cited by Hughes and Gilliland (Reference A-47), droplets will only circulate when the surface shear forces are sufficient to overcome the surface tension forces. An approximate criterion for the onset of circulation is

$$\Delta V = \sqrt[3]{\frac{\sigma^2}{\mu_{\text{gas}} \rho_{\text{gas}} D}} \quad (\text{A-30})$$

Where ΔV is the difference in velocity between droplet and combustion gas at which circulation will start. This threshold is illustrated in Figure A-6. According to this figure, circulation is expected in large droplets even at low relative velocity, but is not expected during most of the lifetime of the smallest droplets found in a rocket combustion chamber. In order to accurately model the evaporation of both large and small droplets in a time-varying environment, the presence or absence of circulation should be determined for each droplet group at each integration time interval, with heat transport into the droplet permitted only when circulation is present.

For the present calculations, the simplifying assumption is made that there is no heat transfer into the interior of any of the droplets. This permits accurate calculations for the small droplets responsible for much of rocket transient behavior, at the expense of accuracy in modeling the large droplets which largely determine combustion efficiency.

(b) Heat Transfer Calculations

Heat transfer is correlated in terms of a Nusselt number.

For a sphere

$$q = N_{NU} \pi K D \Delta T \tag{A-31}$$

where q is heat transfer rate and K is thermal conductivity of the vapor film.

R202

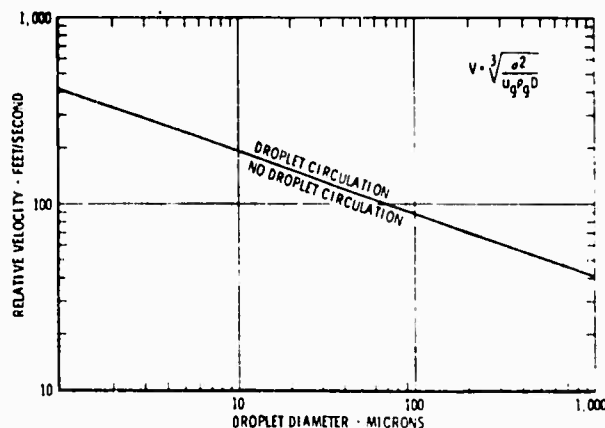


Figure A-6. Droplet Circulation Criterion

From the assumption that all heat reaching the surface of the droplet goes to evaporate liquid

$$\dot{M} = \frac{q}{\Delta H} = \frac{N_{NU} \pi K D \Delta T}{\Delta H} \quad (A-32)$$

Where \dot{M} is the rate of evaporation and ΔH is the sum of the latent heat of the liquid and the sensible heat required to raise it from the injection temperature.

A noneffusing sphere in a nonconvecting environment has a Nusselt number of 2.0, but the value for a droplet evaporating into a high-temperature environment is much lower. Godsave (Reference A-48) gives a simple but adequate estimate for the heat transfer to a burning droplet, assuming that thermal conductivity and specific heat of the vapor film are constant. His equation may be rearranged

$$N_{NU} = 2.0 \left[\frac{\Delta H}{C_p \Delta T} \ln \left(1 + \frac{C_p \Delta T}{\Delta H} \right) \right] \quad (A-33)$$

The rate of fuel consumption from burning fuel-wetted spheres has been determined experimentally under forced convective conditions by several investigators (References A-49, A-50, and A-51). These experimental values are correlated (Figure A-7) by the equation

$$\frac{\dot{M} - \dot{M}_0}{\dot{M}_0} = 0.25 N_{Re}^{0.50} \quad (A-34)$$

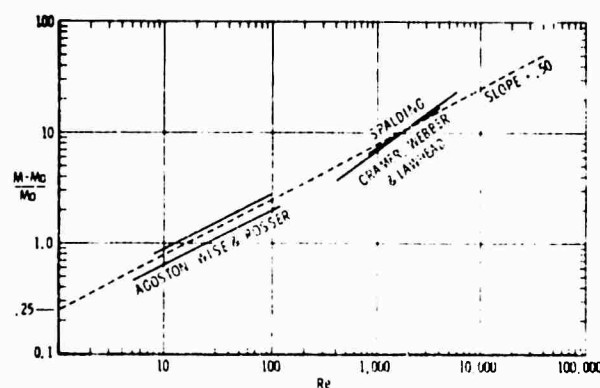


Figure A-7. Burning Rate vs Reynolds Number

where \dot{M}_0 and \dot{M} are nonconvective and convective consumption rates. This is rearranged and combined with Equations (A-32) and (A-33) to give

$$N_{NU} = \left[2.0 + 0.5 N_{Re}^{0.5} \right] \times \left[\frac{\Delta H}{C_p \Delta T} \ln \left(1 + \frac{C_p \Delta T}{\Delta H} \right) \right] \quad (A-35)$$

The term containing Reynolds number represents the effect of forced convection on a burning sphere. It is very similar in value to the correlation of Ranz and Marshall (Reference A-52) for the rate of evaporation from wetted spheres, but is preferred for this application because it was obtained in the presence of combustion and with temperature differences up to 3,000°K and Reynolds numbers up to 6,000. The Ranz and Marshall experiments were limited to temperature differences of 100°K and Reynolds numbers of 200.

Equations (A-32) and (A-35) may be combined to give

$$\dot{M} = \left(\frac{\pi K}{C_p} \right) D \left[2.0 + 0.5 N_{Re}^{0.5} \right] \times \ln \left[1 + \left(\frac{C_p}{\Delta H} \right) \Delta T \right] \quad (A-36)$$

which is the expression used to calculate the burning rate of a single droplet. In the computer calculations, $(\pi K/C_p)$ and $(C_p/\Delta H)$ are two of the subscripted variables characterizing the combustion properties of the material in each droplet group. These values are not treated as time-varying in the analysis in order to simplify the calculations. To obtain agreement with experimental burning rate values, C_p and K are evaluated at the arithmetic mean of the expected droplet surface and hot gas temperatures.

The temperature difference used in the burning-rate equation is the difference between the instantaneous droplet boiling temperature obtained from equation A-2, and the flame temperature or gas temperature surrounding the droplet.

The flame or gas temperature used in the burning-rate equation is obtained from the curve of chamber temperature vs composition (Figure A-8), the calculated composition of the chamber gas, and the known composition of the droplet which is carried as a subscripted variable. It is presumed that when a droplet of a given stoichiometry is evaporating into chamber gas having a different stoichiometry, every intermediate stoichiometry will be found in the diffusion zone surrounding the droplet and that the local temperature in the diffusion zone will correspond to the local stoichiometry. Thus the flame temperature used in the burning-rate equation is the highest temperature found on the temperature vs composition curve in the interval between the chamber gas stoichiometry and the droplet stoichiometry.

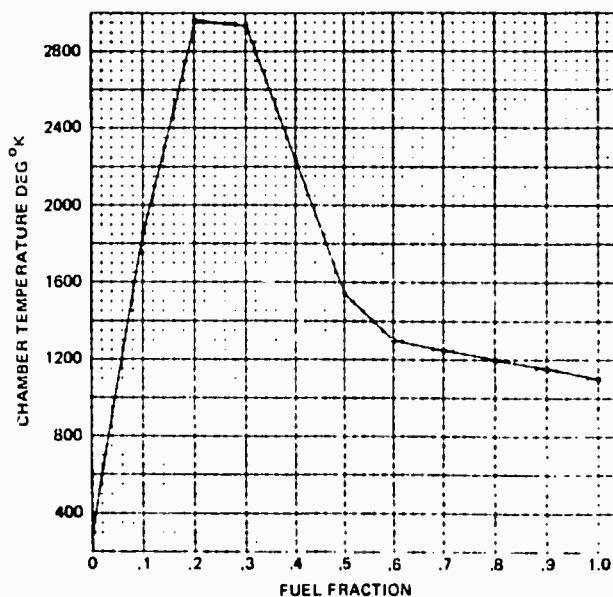


Figure A-8. Temperature vs Stoichiometry

Each time that the burning rate of a droplet is calculated from Equation (A-36), the value is stored temporarily as a subscripted variable until it can be used in the summations which give the velocity profile in the chamber and the total burning rate for the chamber.

(6) Use of Experimental Burning Rate Data

There are many common propellant materials for which the vapor thermal conductivity is unknown in the 1,500 to 2,000°K temperature range. Nitric acid and UDMH are good examples. Experimental droplet burning rates have been obtained for these materials, and these burning rates may be used to infer this necessary information. Normally experimental burning rate data are given in terms of a burning rate constant, K'

$$\frac{dD^2}{dt} = -K' \quad (\text{A-37})$$

in terms of our droplet burning rate expression

$$K' = \frac{8K \Delta T}{\rho \Delta H} \left[\frac{\Delta H}{C_p \Delta T} \ln \left(1 + \frac{C_p \Delta T}{\Delta H} \right) \right] \quad (\text{A-38})$$

This expression is solved for K using the experimental value for K'. When the mean value for thermal conductivity is obtained this way, the droplet combustion equations are no longer being used to derive the burning rates from basic principles, but merely become functions for extending a burning rate measurement to a different flame temperature.

Some propellant materials have the capability of burning as a monopropellant. Examples are hydrazine, propyl nitrate, and hydrogen peroxide. When the monopropellant burning rate is known as a function of chamber pressure from liquid strand tests, the burning rate may be entered, correlated in the form $r = A + BP^n$, where r is the burning rate in cm/sec and P is pressure in psia. The corresponding mass burning rate of a droplet is $\dot{M} = r\pi\rho D^2$. When propellant droplets can burn as either a bipropellant or as a monopropellant, the computer program calculates the burning rate for each droplet group in both ways at each time interval, and the larger of the two values is used.

(7) Ignition and Extinguishment

Several types of ignition are modeled by the computer program. Calculations may be performed for sea-level or high-altitude ambient conditions, and for hypergolic or nonhypergolic propellants.

When a motor is being started at atmospheric pressure, using a liquid propellant igniter, it is assumed that droplets of the main propellants ignite instantaneously. When the fuel and oxidizer flow rates to the igniter and the axial location of the igniter port are specified, the initial composition, temperature, and axial velocity profile of the chamber gas are established. Although droplet ignition is presumed to be instantaneous, it would be erroneous to presume that the calculated start transient will necessarily be either smooth or simple, as experience has frequently shown it to be otherwise.

When nonvolatile hypergols are injected at atmospheric pressure, the ignition results from complex liquid and vapor phase processes and it is necessary to obtain ignition delay values from the published literature based on experimental tests. When such an ignition delay time is prescribed, the droplet burning rates are set to zero during the preignition period. The delay time is counted as starting only after both fuel and oxidizer streams have reached the impingement point in the chamber.

When volatile hypergolic pairs are injected under near-vacuum conditions, the ignition depends upon the physical processes which contribute to the production of reactive vapors in the chamber. The calculation of the ignition delay time in the vapor phase is based on an equation given by Seamans, Vanpee, and Agosta (Reference A-29):

$$\tau_{\text{ignition}} = \frac{RT^2 \rho_{\text{gas}} C_p}{EAQ C_{\text{fuel}} C_{\text{oxidizer}}} \text{Exp} \left(\frac{E}{RT} \right) \quad (\text{A-39})$$

where E , A and Q are the activation energy, frequency factor, and heat of reaction for the vapor phase reaction responsible for ignition. C_p is the specific heat of the vapor mixture in the combustion chamber and C_{fuel} or $C_{oxidizer}$ are the concentrations of fuel and oxidizer vapor in the chamber gases.

This function may be evaluated in either of three ways. One option is to assume that there is no axial mixing of vapors. In this mode, the relative concentrations of fuel vapor and oxidizer vapor come from the relative amounts flashed at each instant. A second option is to assume that all the vapors in the chamber are well-mixed. In this mode, the values for fuel and oxidizer vapor concentration used in Equation (A-39) are derived from a mass balance on the chamber considering the entire previous history of vapor generation and outflow. The third option presumes that at any instant there will be some location in the chamber which has the optimum stoichiometry for the quickest possible ignition. This optimum stoichiometry is found by examining the well-mixed vapor composition in the chamber, as well as the most advantageous composition in the boundary layers surrounding fuel droplets and oxidizer droplets (where they are present), the composition having the greatest value for $(C_{fuel} \times C_{oxidizer})$ is the one used in the ignition calculations. Any ignition delay time longer than the gas residence time is discarded, as external ignition is ineffective. Because of the necessity of calculating repeated ignitions and extinguishments, unreacted fuel and oxidizer vapors are distinguished from residual quenched combustion product gases in calculating the concentrations used in Equation (A-39).

The vapor-phase ignition delay time is recalculated at each time interval, and the chemical delay time is added to the model time at which the calculation is made to obtain a projected time of ignition. The smallest value for the projected time of ignition is retained. Ignition is presumed to occur when the model time exceeds the smallest value for projected ignition time.

Since the droplet population of the chamber declines very rapidly after the propellant valves are closed, the vacuum evaporation of fuel and oxidizer film on the wall becomes the major source of fuel and oxidizer vapors very shortly after valve closure. For this reason the criterion for extinguishment is based upon the combustion chamber gas state rather than upon the conditions in the droplet boundary layers. Extinguishment in the gas is predicted from experimental quenching distance values taken from data on the combustion of premixed gases (Reference A-53). Quenching distance of premixed gases is a function of the pressure, and of the initial temperature and stoichiometry of the combustible mixture. For the present purposes, the effects of stoichiometry and initial temperature can be lumped together in terms of the corresponding final gas temperature. The data on propane-air quenching distance are correlated adequately by:

$$q = 3.6 \times 10^{17} p^{-1.0} T^{-4.0} \quad (A-40)$$

Where q is quenching distance in cm, P is pressure in dyne/cm², and T is equilibrium final gas temperature in °K. When the calculated value of q becomes larger than the chamber diameter, extinguishment is presumed to occur.

(8) Chamber Calculations

The vapors or gases which fill the combustion chamber are derived from the following five sources: vapor from flashing propellant streams; material evaporated from propellant droplets; burnoff of material on the chamber walls; vacuum evaporation of material on the chamber walls; and igniter combustion products, if any. Fuel and oxidizer vapors from these five sources are axially cumulated in the chamber each time interval, while the amounts calculated to flow through the nozzle are subtracted. This gives current values for the chamber gas mass and stoichiometry and for axial addition rate of mass. These are used to calculate the pressure, temperature, molecular weight, and the velocity distribution in the chamber. The simplifying assumption is made that at any instant the pressure is constant throughout the chamber and the gas is well mixed. Since the computation time interval is typically of the order of 1 to 10 times the longitudinal acoustic period of the engine, the uniform chamber pressure assumption seems justified for engines with large contraction ratios. If ignition has occurred, the temperature and molecular weight are interpolated from tables of these variables versus stoichiometry. The table values are calculated assuming isenthalpic combustion to give reaction products in thermochemical equilibrium. If ignition has not occurred, the gas properties are calculated for the unreacted fuel and oxidizer vapors, assuming ideal gas behavior.

(a) Gas State

At each integration time interval, the expressions for flashing of the propellant streams, evaporation of droplets, burnoff of propellant on the walls, vacuum evaporation of propellant on the walls, and the assigned igniter flows are used to calculate the amounts of fuel-derived mass and oxidizer-derived mass which have been added to the chamber. Nozzle flow equations are used to calculate the amount of gas leaving the chamber, with the assumption being made that the material flowing through the nozzle has the same composition as the well-mixed material in the chamber. The new amounts of fuel-derived gas mass and oxidizer-derived gas mass contained in the chamber are then calculated:

$$M_{F(t+\Delta t)} = M_{f(t)} + \text{fuel evaporated} - \text{fuel exhausted} \quad (\text{A-41})$$

$$M_{O(t+\Delta t)} = M_{O(t)} + \text{oxidizer evaporated} - \text{oxidizer exhausted} \quad (\text{A-42})$$

The total mass of gas in the chamber is the sum of the fuel-derived and oxidizer-derived mass

$$M_T = M_F + M_O \quad (\text{A-43})$$

The stoichiometry of the chamber gas is expressed in terms of the fraction of the total gas mass which is fuel-derived

$$F = \frac{M_F}{M_F + M_O} \quad (\text{A-44})$$

When combustion is taking place in the chamber, the temperature, molecular weight, and thermal properties of the chamber gas are functions of the elemental compositions and heats of formation of the fuel and oxidizer, the stoichiometry and the chamber pressure. Since the composition and heat of formation of the fuel and oxidizer are fixed for a given set of propellants, and since the product composition is only a weak function of pressure, the temperature, molecular weight and thermal properties of the chamber gas are approximated as a function of F alone with only small error. Temperature, molecular weight and gamma are stored as 11-point tables with linear interpolation being used to obtain values for intermediate values of F . Figures A-8, A-9, and A-10 illustrate the values used for the white fuming nitric acid - UDMH propellant combination.

After chamber temperature and molecular weight are estimated as functions of the gas stoichiometry, the chamber pressure is calculated

$$P_c = \frac{\rho R T}{W_m} \quad (\text{A-45})$$

The density is obtained from the known total gas mass and total chamber volume, where U_c is chamber volume

$$\rho = \frac{M_T}{U_c} \quad (\text{A-46})$$

(b) Nozzle Throat Flow

Conventional steady flow, compressible gas, nozzle flow equations are used to calculate the instantaneous mass flow rate through the nozzle throat. The use of these equations together with the assumption of constant pressure throughout the chamber restricts the validity of these calculations to cases where the rate of change of pressure is sufficiently slow that only a small change in pressure occurs during a single acoustic time period of the chamber or nozzle.

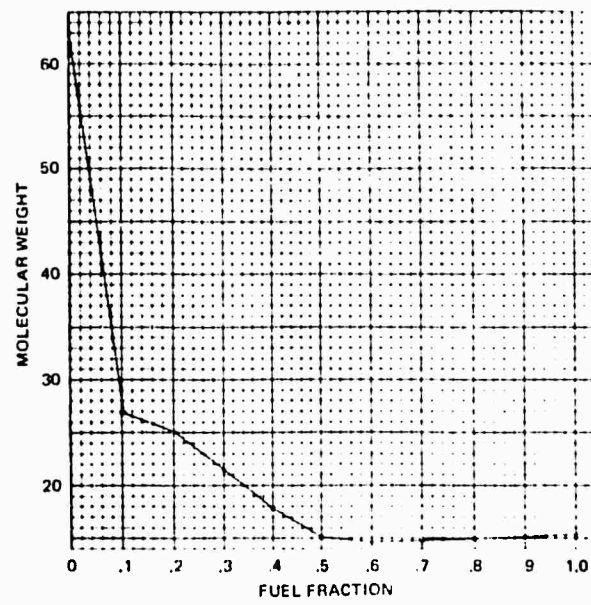


Figure A-9. Molecular Weight vs Stoichiometry

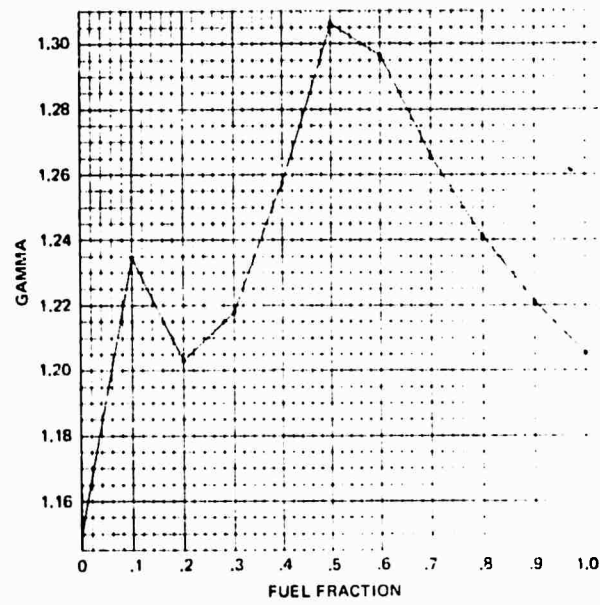


Figure A-10. Gamma vs Stoichiometry

The nozzle is sonic when

$$\frac{P_e}{P_c} = \left(\frac{2.0}{\gamma+1} \right)^{\gamma/(\gamma-1)} \quad (\text{A-47})$$

Subsonic mass flow rate is calculated

$$\dot{M}_T = A_T P_C \sqrt{\frac{2.0 \gamma W_m}{(\gamma-1) RT_c}} \sqrt{\left[\left(\frac{P_e}{P_c} \right)^{2/\gamma} - \left(\frac{P_e}{P_c} \right)^{(\gamma+1)/\gamma} \right]} \quad (\text{A-48})$$

Sonic flow rate is calculated

$$\dot{M}_T = A_T P_C \sqrt{\frac{\gamma W_m}{RT_c} \left(\frac{2.0}{\gamma+1} \right)^{(\gamma+1)/(\gamma-1)}} \quad (\text{A-49})$$

The rates at which fuel- and oxidizer-derived mass leave the chamber are

$$\dot{M}_F = \dot{M}_T \times F \quad (\text{A-50})$$

$$\dot{M}_O = \dot{M}_T \times (1 - F) \quad (\text{A-51})$$

(c) Axial Gas Velocity

The axial gas velocity is calculated at 100 equally spaced axial locations at each integrating time interval to give the gas velocities used in the droplet drag and evaporation rate calculations, the wall burnoff calculations and the wall-film viscous flow calculations during the next time interval. When velocities are required at intermediate locations, linear interpolation is used.

The axial gas velocity at any axial location L may be obtained through the continuity equation, a mass balance on the chamber

volume upstream of location L, and the assumption of uniform density throughout the chamber. The axial velocity at L is

$$V_L = \frac{\dot{M}_L}{\rho_{\text{gas}} A_L} \quad (\text{A-52})$$

where \dot{M}_L is the rate at which gas mass is flowing past the section at L and A_L is the cross-sectional area at L. The value for \dot{M}_L is obtained from a mass balance on the chamber volume upstream of L.

$$\dot{M}_L = \text{Evaporation rate upstream of L} - \text{accumulation rate upstream of L}$$

$$\dot{M}_L = \sum_{\substack{\text{All droplet groups} \\ \text{upstream of L}}} \dot{M}_i N_i - \frac{U_L}{U_C} \left[\sum_{\substack{\text{All droplet groups} \\ \text{in chamber}}} \dot{M}_i N_i - \dot{M}_T \right] \quad (\text{A-53})$$

where \dot{M}_i and N_i are the mass evaporation rates per drop in the i th group and the number of droplets in the i th group. U_L is the chamber volume upstream of L, and \dot{M}_T is the mass flow rate through the nozzle. U_C is total chamber volume.

(9) Wall Calculations

When a droplet group moves radially to the location of the combustion chamber wall, its fuel or oxidizer mass is deleted from the droplet array and is added to the appropriate location in a 100-member array which represents the axial distribution of fuel or oxidizer deposited on the chamber wall. The material on the wall experiences axial viscous flow under the influence of shear forces exerted by the chamber gas and is subjected to burnoff from heat transferred from the chamber gas. When the chamber pressure falls below the vapor pressure of the fuel and oxidizer deposited on the wall, they undergo Knudsen-Langmuir evaporation, with heat simultaneously being transferred from the chamber wall.

(a) Viscous Flow Rate

The viscous flow rate for each axial portion of the wall is calculated.

$$\dot{M}_i = \frac{M_i^2 f_i \rho_{\text{gas}} V_{i \text{ gas}} |V_{i \text{ gas}}|}{4\pi \mu_{m_i} \rho_{m_i} D_i \Delta X^2} \quad (\text{A-54})$$

Where \dot{M}_i is the mass flow rate at the i th segment of the chamber wall; M_i is the mass of deposited propellant on this segment of wall; f_i is the Fanning friction factor, a function of chamber Reynolds number, evaluated at the i th segment, μ_{m_i} is the viscosity of the contaminant mixture on the i th segment of wall, interpolated from a table of viscosity vs stoichiometry; ρ_{m_i} is the density of the contaminant mixture; and ΔX is the length of the wall segment. The Fanning friction factor is calculated (Reference A-54):

$$\begin{aligned} N_{\text{Re}_i} < 16.0 & \quad f_i = 1.0 \\ 16 < N_{\text{Re}_i} < 2,000 & \quad f_i = 16. N_{\text{Re}_i}^{-1.0} \\ 2,000 \leq N_{\text{Re}_i} & \quad f_i = 0.06028 N_{\text{Re}_i}^{-0.2113} \end{aligned} \quad (\text{A-55})$$

N_{Re_i} is the Reynolds number, based on chamber diameter evaluated at the i th wall segment.

(b) Wall Burnoff Rate

The burnoff from each axial segment of the wall is calculated from a heat transfer coefficient calculated from the Colburn Equation (Reference A-55) corrected for Counter-Current mass transfer:

$$\dot{M}_i = \frac{H_i A_i C_e \Delta T}{\Delta H} \quad (\text{A-56})$$

\dot{M}_i is the rate of burnoff of propellant from the i th wall segment. H_i and A_i are the heat transfer coefficient evaluated for the conditions at i and the chamber wall surface area of the i th segment. The value for H_i is calculated:

$$\begin{aligned} 0. < N_{Re_i} < 500,000 & \quad H_i = 2.23 C_{p_{gas}} \rho_{gas} V_{i, gas} N_{Re_i}^{-0.66} (D_i/L_i)^{0.33} \\ 500,000 \leq N_{Re_i} & \quad H_i = 0.027 C_{p_{gas}} \rho_{gas} V_{i, gas} N_{Re_i}^{-0.2} \end{aligned} \quad (A-57)$$

N_{Re_i} is the Reynolds number based on chamber diameter evaluated at the i th segment.

The correction for simultaneous heat and mass transfer is calculated:

$$C_e = \left(\frac{\Delta H_m}{C_{p_m} \Delta T} \right) \ln \left(1.0 + \frac{C_{p_m} \Delta T}{\Delta H_m} \right) \quad (A-58)$$

Where ΔH_m is the heat required to evaporate or pyrolyze unit mass of the propellant mixture, C_{p_m} is the specific heat of the vapor produced and ΔT is the difference between the chamber gas temperature and the surface temperature of the evaporating propellant.

(10) Vacuum Evaporation Rate

The evaporating wall film is treated as being locally thermally quasi-steady (Reference A-27) and the local vacuum evaporation rate from

each of the 100 axial segments of wall is presumed to balance the local heat transfer rate from the chamber wall to the evaporating surface. The expression for Knudsen-Langmuir evaporation is:

$$\dot{M}_{pi} = A_{pi} E_p (P_{vap p}(T_{si}) - P_c) \left(\frac{M_w p}{2 \pi R T_{si}} \right)^{1/2} \quad (A-59)$$

Where \dot{M}_{pi} is the evaporation rate of constituent p from the i th axial segment of the chamber wall, A_{pi} is the exposed surface area of constituent p on the i th segment. E_p is the accommodation coefficient of constituent p . $P_{vap p}(T_{si})$ is the vapor pressure of constituent p at the local surface temperature T_s . P_c is the chamber pressure. $M_w p$ is the vapor molecular weight of constituent p , and R is the gas constant. The effects of the neutralization reaction removing fuel or oxidizer from the mixed layer with the consequent formation of hydrazinium nitrate, and the vapor pressure reduction from solution effects are not considered. This expression is correct only when the fuel and oxidizer on the wall are unmixed. The expression for heat transfer through the wall film is:

$$\dot{M}_{pi} = \frac{A_{pi} K_p (T_{wi} - T_{si})}{S_i \Delta H_p} \quad (A-60)$$

Where K_p is thermal conductivity of constituent p , T_{wi} is the chamber wall temperature at segment i , S_i is the thickness of coating on segment i , ΔH_p is the latent heat of evaporation of constituent p .

Equations (A-59) and (A-60) must be simultaneously solved to obtain the values of \dot{M}_{pi} and T_{si} . This is done by Newton iteration. The solutions are obtained separately for the fuel and for oxidizer on each segment, as though they occupied separate patches of the total wall surface area. The exposed surface area of each propellant constituent is presumed to be proportional to its volume fraction on the particular segment.

(11) Thrust Calculation

The vacuum thrust is calculated as the sum of the momentum rate of the ejected droplets and the theoretical vacuum thrust of the gas:

$$F = P_c A_t C_F + \frac{1}{\Delta t} \sum V_i M_i \quad (\text{A-61})$$

droplets ejected

When the chamber contents are ignited, the C_F is interpolated from a table of C_F vs stoichiometry of the chamber gas. When the chamber products are not ignited, C_F is calculated for the mixture of unburned vapors. In calculating the C_F for the vapors, first the ratio of exit pressure to throat pressure must be obtained from the exit area ratio:

$$\frac{1}{\epsilon} = \left(\frac{\gamma+1}{2}\right)^{\frac{1}{\gamma-1}} \left(\frac{P_e}{P_t}\right)^{\frac{1}{\gamma}} \sqrt{\frac{\gamma+1}{\gamma-1} \left[1 - \left(\frac{P_e}{P_c}\right)^{\frac{\gamma-1}{\gamma}}\right]} \quad (\text{A-62})$$

This is solved for the time-varying γ using a Newton iteration. After the pressure ratio is obtained, the thrust coefficient is obtained:

$$C_F = \sqrt{\frac{2\gamma^2}{\gamma-1} \left(\frac{2}{\gamma+1}\right)^{\frac{\gamma+1}{\gamma-1}} \left[1 - \left(\frac{P_e}{P_t}\right)^{\frac{\gamma-1}{\gamma}}\right]} + \frac{P_e}{P_t} \epsilon \quad (\text{A-63})$$

d. Contaminant Production in the Combustion Chamber

(1) Definition of Contaminant Production

In the present context a contaminant is any material ejected from the rocket engine which can degrade any part of the vehicle surface. Abrasive, corrosive or otherwise physically damaging materials or persistent materials which cause significant optical changes to impinged surfaces are all included in the class of contaminants. The theoretical equilibrium combustion products, such as gaseous CO_2 , H_2O , N_2 , etc. are not normally regarded as contaminants, although condensed phases are potential contaminants. The most undesirable materials are raw unreacted fuel or oxidizer, or the mixtures of cold-reaction intermediate products containing hydrazine nitrates, water, fuel, polymeric materials, etc. The latter materials can be produced whenever local conditions are inadequate to initiate or

carry the combustion reactions to completion. For transport limited processes, such as droplet evaporation, incomplete combustion arises from excessive drop sizes, inadequate chamber dimensions, low pressure or low temperature (which, in turn can result from incorrect stoichiometry or lack of ignition). For chemical rate limited processes, such as in a film of well-mixed fuel and oxidizer on the wall, incomplete combustion arises from chilling by the wall or from the vacuum evaporation of excess reactants or by quenching in a large excess of one or the other of the reactants.

(2) Application of the TCC Computer Program to the Prediction of Contaminant Production

The transient combustion chamber program can predict the amounts and characteristics (film stoichiometry, droplet size, droplet velocity) of contaminant produced during an engine firing by mathematically modelling the injection rates, combustion and trajectory of droplets and the rates of accretion, evaporation, and axial flow of propellant deposited on the chamber wall. These processes depend in very complex ways upon the details of chamber geometry, injector geometry, tank pressures, valve timing, propellant properties, etc.

The contaminant production from a single pulse of a clean engine may be calculated by inputting the necessary data and performing the system calculations for the single pulse. The contamination from one pulse in a series of successive firings, however, will depend upon the accumulation of material on the walls from previous firings, the extent of injector dribbling between firings, the vacuum evaporation of material from the walls between firings, and the cumulative heating or cooling of chamber and injector over the series of firings. Thus it may be necessary to model an entire duty cycle to obtain representative values for contaminant production. Such calculations may be of value in assisting in the design, development, or modification of an engine, in optimizing the engine size and duty cycle for a particular vehicle mission, in modifying the duty cycle of an existing vehicle, or in choosing between alternate engine choices for a particular vehicle, where contamination is an important consideration.

(3) Assumptions, Limitations and Validity

The production of contaminants can be in any of several modes even for a single firing of a particular engine. If fuel injection commences before oxidizer injection, and if the trajectory of the streams or droplets takes them directly through the engine throat, very few simplifying assumptions or approximations are involved. If the same fuel impinges on the chamber wall and later is dragged downstream by shear forces developed by the relative velocity of the hot combustion chamber gases, the fluid flow and heat transfer processes are so complex as to defy analysis without the most drastic simplification. In our analysis the liquid flow on the wall is essentially quasi-steady, one-dimensional, and viscous. Instabilities leading to ripple formation or secondary atomization of wave crests are ignored and

the effects of such instabilities upon heat transfer and drag are ignored. The gas shear stress correlations are for fully developed pipe flow, and ignore the boundary layer growth process in the short combustion chamber. The evolution of gas from the liquid surface by evaporation or pyrolysis is considered in the heat transfer calculation, but ignored in the shear stress calculation. The shear stress produced from stagnation of the axial momentum of the impinging propellant droplets is ignored. It is obvious that experimental examination of the wall-film flow process is necessary if reliable approximations to this process are required. On the other hand, the axial mass flow rate down the wall increases rapidly with the film thickness, so the process is strongly self-regulating, with increased deposition rates leading to increased axial flow rates; hence, after a certain period of accumulation, the axial flow rates should be nearly correct even though the value calculated for the mass held on the wall is in error.

The values for the physical properties of wall-film material containing both fuel and oxidizer have a high order of uncertainty. Combustion intermediate mixtures from motors using NTO-MMH propellant have been observed by eye and described as honey-like. This would imply a viscosity in the range of 1,000 to 100,000 centipoise; however, the temperature and gross composition (i. e., mass fraction of fuel in the mixture) were not reported, so the uncertainty in the value to use for viscosity must be at least a factor of 100. The viscosity of mixtures of this sort would be expected to vary strongly with temperature and with dilution by fuel, but no measurements have yet been made. The axial mass flow rate of wall-film material is, unfortunately, inversely proportional to viscosity. The viscosity function used for our calculation is a linear interpretation with composition, from the viscosities of pure fuel and oxidizer to a value of 10 centipoise at the composition of pure monomethyl hydrazinium nitrate. The low value used comes from the assumption that freshly produced MMH nitrate will still retain most of its heat of neutralization, which will heat it about 240°C above the reactant temperature.

The vacuum evaporation rates of NTO, MMH and monomethyl hydrazinium nitrate should be proportional to the accommodation coefficients of these materials; however none of these has even been measured. Accommodation coefficients for nonassociated materials such as hydrocarbons or perhalocarbons are approximately 1.0; however, materials which undergo dissociation or bonding changes during evaporation generally have values far less than 1.0. The accommodation coefficient for water, which is hydrogen bonded in the liquid phase, has been reported as low as 0.02, and the accommodation coefficient for ammonium chloride which dissociates upon evaporation has been reported as low as 4×10^{-4} . Liquid monomethyl hydrazine is certainly hydrogen bonded. Liquid NTO exists largely as the dimer N_2O_4 , which dissociates to the monomer NO_2 under evaporation. Monomethyl hydrazinium nitrate probably dissociates into nitric acid and monomethyl hydrazine upon evaporation. Hence the values for the accommodation coefficients might be expected to differ from unity by a factor of 50 to 5000; however, the values are not known, and a value of 1.0 is used in our calculations. Because of the absence of experimental values for the physical

properties, there has been no attempt to treat the vacuum evaporation from the wall in a sophisticated manner; instead, the fuel and oxidizer are treated as though they were immiscible phases. The exposed area of each phase on a particular segment of chamber wall is taken to be proportional to the volume fraction of the material on that segment of wall. Vacuum evaporation rates are then calculated based upon the exposed area of each phase and the estimated physical properties of the pure material. When properties of the materials are well known enough to warrant, it will be feasible to calculate reaction stoichiometry in the film, vapor pressure depression from dilution, and a heat balance considering the neutralization reaction, dilution, evaporation of excess reactants, and heat transfer to the wall or from the gas.

The injector hole diameters of the Marquardt R-6C engine are 0.0158 inch for the fuel and 0.0186 inch for the oxidizer. These are much smaller than have been employed in experimental investigations of primary atomization. In order to force agreement between calculated and experimental combustion efficiencies and steady-state chamber pressures, the computational initial mean droplet sizes were arbitrarily reduced by a factor of two from the value obtained using equation A-12. This probably indicates the inadequacy of the present mean drop size correlation and drop size distribution to describe the droplet sizes produced by the impingement of unlike hypergolic streams from very small orifices.

In the absence of any reliable data for breakup distances of fans produced by small streams of unlike materials, the fan lengths were arbitrarily set to zero for the calculations for the Marquardt R-6C engine. If the chugging frequencies and amplitudes had been known for this engine, the correct values for fan breakup distance could have been deduced from these values.

In the absence of any experimental data on the behavior of droplets or streams impinging on the chamber wall, it was assumed that half the impinging droplets stuck to the chamber wall and half rebounded back into the chamber. It was assumed that the bouncing drops rebounded from the wall with 100 percent of their speed of approach.

At present, the inadequate knowledge of propellant and cold-reaction-product physical properties must rank in importance with uncertainty of primary atomization droplet size, stream or fan breakup distance, and the unknown behavior of droplets and streams impinging on the wall, as the major unknowns limiting the confidence in the calculated predictions. It should be obvious that the above values are important to the calculations, and that some experimental work would be desirable to eliminate the necessity for guess-work in these values.

e. Contaminant Production Parametric Study

(1) Reasons for Parametric Study

The original reason for doing the parametric study was to develop a simplified mathematical correlation to characterize the behavior

of a rocket engine in terms of its response to variation of its most important variables, including hardware dimensions, operating conditions and duty cycle. Preim (Reference A-9) has correlated droplet combustion efficiency as a function of engine parameters for steady operation, and it was hoped that pulse-mode operation could be correlated in a similar manner. Such a mathematical correlation would be desirable in that it would eliminate the need for further computer calculations and would permit easy multivariate optimizations. A second reason for the parametric study was to publish theoretical predictions for engine behavior in the hope that this might encourage corresponding experimental tests, which could serve to verify the calculations or point out errors in the method. A third obvious reason for the study was to further our general understanding of the processes by identifying the most important variables, by establishing the general shapes of the functional relationships, by obtaining a more detailed understanding of the sequence of events which take place during transients, and by pointing up where necessary input values or correlations are inadequate or missing entirely.

It soon became obvious that no simple, general mathematical correlation of our calculations would be possible, because of the complex time-dependent character of the solutions. If each pulse of given duration in an extended duty cycle were identical to every other similar pulse, then simple correlations would be possible; however the accumulation of wall-film mass takes place on a time-scale which can extend over a considerable number of short pulses, making the average rate of wall-film efflux different for each otherwise-identical pulse in the series. The injector temperature and chamber wall temperature also show variations which can extend over a considerable number of pulses. The postcutoff and preignition behavior turned out to be more complex than had been supposed, with important changes in behavior occurring at threshold values of the variables, as the following example will illustrate.

According to our calculations, the fuel and oxidizer passages of the 5-pound thrust Marquardt engine will dribble sequentially after propellant cutoff, for a 300°K injector temperature. This is because the chamber pressure generated by the flash-vaporization of the dribbling oxidizer stream is higher than the vapor pressure of the fuel in the injector. Thus the fuel does not begin to dribble until the oxidizer has dribbled to exhaustion. When the dribbling is sequential, our calculations show that there are one or two brief periods of reignition during the oxidizer dribble period, which consume any fuel in the chamber available for combustion, and are followed by extinguishment.

When the fuel injector temperature is higher, however, the higher fuel vapor pressure can result in simultaneous dribbling of the oxidizer and fuel. This leads to reignition with enough of each propellant present to produce a rise in chamber pressure to a value above the vapor pressure of one or both propellants, which in turn cuts off the dribbling flow, which leads to a decay in chamber pressure. The decay in chamber pressure leads to the reestablishment of dribbling flow of the propellants and another rise in chamber pressure. This vapor-pressure driven chugging cycle can continue until one of the dribble volumes is drained.

The injector temperature follows a slow temperature rise extending over a series of pulses; hence, the early pulses in the series will show smooth cutoffs with little postcutoff impulse. When the injector temperature gets high enough, the subsequent pulses will show chugging cutoffs with greater postcutoff impulse, better combustion of the propellant in the dribble volumes, different amounts and axial distributions of the dribbled propellant deposited on the chamber wall, and a higher degree of voiding of the dribble volumes before the initiation of the next pulse.

This is a good example of the complex threshold-sensitive behavior which makes a simple mathematical correlation of the calculations impractical.

(2) Scope of the Parametric Study

The parametric study was based on the dimensions and operating values of the Marquardt 5-pound thrust R-6C rocket engine using NTO and MMH as propellants. The variables were chamber length, chamber diameter, throat area, leads and lags in opening and closing the propellant valves, fuel and oxidizer tank pressure, bulk propellant temperature, chamber wall temperature, and pulse length. Several arbitrary assumptions were made for the initial condition of the dribble volumes. Calculations were made with both dribble volumes initially full, both initially empty, and with the fuel volume full but the oxidizer volume empty. The temperatures of the dribble volume contents were normally set equal to the propellant tank temperature; but for one series, they were set to a much higher temperature.

The postfiring and prefiring dribbling of the injector and the between pulse evaporation from the chamber walls were not calculated in this parametric study, because these portions of the program were not completely checked out at the time the parametric series was performed. A further reason for not including these phenomena in the parametric study is the great expense of calculating the extended pulse trains necessary to categorize the dribble, wall accumulation, and wall evaporation behavior, and the almost endless number of possible variations to a duty cycle. The calculations of the present parametric study are all terminated very shortly after engine cutoff (three milliseconds after the last valve closed), and do not include any postfiring dribble effects.

(3) Results

The TCC computer program parametric study yielded a substantial amount of information about the motor selected as a basis for the investigation.

The basis for this part of the study is a 5-pound-thrust rocket engine using NTO and MMH as propellants. This engine was developed by Marquardt and presently is being used by NASA-Lewis for contamination

studies. The engine has a chamber 0.4 inches in diameter by 1.07 inches long; i. e., a volume of 1/8 cubic inch. It is operated with fuel and oxidizer tank pressures of 180 and 165 psia, respectively, producing a chamber pressure of approximately 100 psia. The engine can be operated from pulses of a few milliseconds to durations of many seconds. A 50 millisecond pulse was selected as the base for the investigation. The following sections contain the results of the parametric study in the form of graphs and tables, as well as discussion of these results.

(a) The Effects of Geometry

Throat area, chamber diameter, and chamber length were investigated with the TCC program. The importance of these variables will vary greatly with motor size. With very small thrusters of the type used as a basis for these calculations, the duration that droplets remain in the combustion chamber is a critical parameter. This droplet residence time is an inverse function of droplet velocity, a direct function of chamber length and droplet trajectory, as well as a more complex function of the result of propellant hitting the inner surface of the chamber. Droplet velocities are dependent upon the momentum of the injected streams of propellant and the drag forces of the chamber gases upon individual droplets. Therefore, any change in geometry which causes a change in gas velocity within the chamber, causes a change in the fraction of droplets hitting the wall, or a change in the distance traveled by the average droplet before leaving the chamber and thus will affect the amount of contamination produced by the motor. For the thruster being investigated, the following results were observed.

Variation in Throat Area

When the throat size is changed with no other changes made to the system, several system variables are affected. Chamber pressure and propellant flow rates are two of the major variables that change. In investigating the effect of throat area, two runs were made with one 50-percent larger and one 50-percent smaller than the base case. The history of the cumulative propellant ejected is shown in Figure A-11. The results are somewhat deceptive in that direct comparisons between the cases must consider the difference in the amount of propellant injected. For the large throat, 19 percent of the injected propellant is ejected unburned, compared with 18 percent in the base case, and 15 percent for the small throat (Table A-III). Therefore, the greater amount of propellant ejected from the motor with the larger throat is almost entirely due to the greater amount of propellant injected into the chamber. Two factors contribute to the remaining differences between throat sizes when compared for the same amount injected. First, when the throat is enlarged, the velocity of gas in the chamber is increased significantly. This, in turn, increases the velocity of the droplets traveling toward the throat. Second, when the throat area is larger, there is a greater area through which droplets may escape. Third, the momentum of the stream of propellant into the lower pressure chamber is greater, and the droplets have a greater resultant velocity after impingement of the propellant streams.

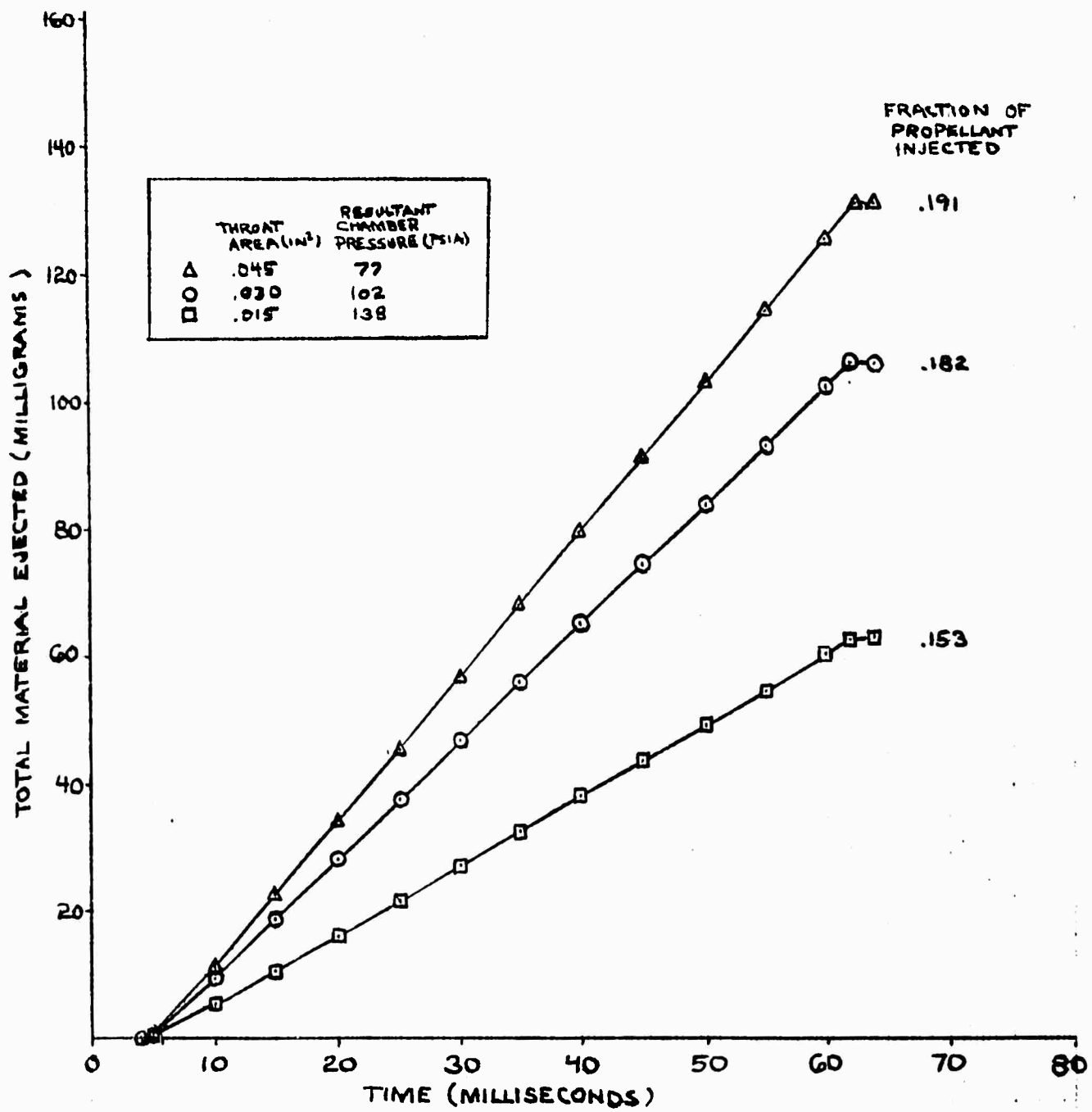


Figure A-11. The Effect of Throat Area on Material Ejected from the Motor

Table A-III. DISPOSITION OF PROPELLANT INJECTED INTO CHAMBER

Variation from Base Case	Fraction Ejected Unburned	Fraction Remaining in Motor at 60 ms
None	0.182	0.0
Larger throat (1.5x)	0.191	0.0
Smaller Throat (0.5x)	0.152	0.0
Longer chamber (2x)	0.081	0.0
Larger chamber (3.6x)	0.168	0.0
Smaller chamber (0.75x)	0.187	0.0
Fuel Valve		
Lag in opening (4ms)	0.184	0.0
Lag in opening (9ms)	0.217	0.009
Lag in closing (4ms)	0.181	0.044
Oxidizer Valve		
Lag in opening (4ms)	0.180	0.004
Lag in opening (9ms)	0.181	0.023
Lag in closing (4ms)	0.181	0.050
Tank Pressure		
Higher fuel (+35 psi)	0.191	0.0
Lower fuel (-35 psi)	0.148	0.001
Higher oxidizer (+30 psi)	0.158	0.002
Lower oxidizer (-30 psi)	0.197	0.001
Bulk Propellant Temperature		
Higher (+20°K)	0.151	0.0
Lower (-20°K)	0.191	0.0
Chamber Wall		
Hotter than decom- position Temperature	0.187	0.0
Pulse Length		
20 ms (0.4x)	0.177	0.001
100 ms (2x)	0.184	0.0

Variation in Chamber Length

A change in chamber length directly affects the droplet residence time, both in the distance droplets have to travel to leave the chamber, and in the amount of the spray that hits the wall. One run was made with a chamber twice as long as with the base case (Figure A-12). Only 8 percent of the propellant was ejected unburned, which is the lowest amount of any of the situations investigated. Less than 1 percent of the total propellant flow is retained by the chamber wall in either case, with all of the deposition occurring in the first 8 milliseconds of the start transient. Slightly less was retained with the longer chamber.

Variation in Chamber Diameter

A change in chamber inside diameter affects gas velocity in the chamber, and the resultant Reynolds Numbers and heat transfer coefficients along the surface. The change in gas velocity will influence droplet velocity and the resultant droplet residence time. Two runs were made in which chamber diameter was varied, using values of 0.3 and 0.76 inches compared with 0.4 inches for the base case. Figure A-13 shows that contamination is relatively insensitive to variations in chamber diameter. An increase of 75 percent in gas velocity in the chamber causes an additional 3 percent of the injected propellant to be ejected unburned. These runs are computed for the conditions of a first pulse. In Figure A-14, the disposition of material on the chamber wall is shown as a function of chamber diameter. Of particular interest, this figure shows that the time at which the wall is clear of propellant is a strong function of chamber diameter, with the wall clear of propellant at 26 milliseconds with the small diameter chamber, and 60 milliseconds with the large diameter chamber. Furthermore, the amount of film expelled is considerably less with the smaller chamber indicating that propellant on the wall is being removed as it flows towards the throat.

(b) Chamber Wall Temperature

One effect of chamber wall temperature on material ejected from the motor is shown in Figure A-15. This figure shows the variation anticipated from the motor when surface temperature of the chamber walls is greater than decomposition temperature of the propellant. For this condition, the program assumes that all droplets hitting the walls of the chamber bounce unbroken and unvaporized back into the chamber. The difference between the material ejected for hot wall and cold wall (base case) is not appreciable with this small motor because very small amounts of propellant hit the wall in relation to the amounts of propellant injected at base case conditions.

(c) The Effect of Valve Operation

Valve operation was examined in more detail than any other variable with 4 runs made with variations in opening the valves, and two runs made to investigate variations in closing the valves. When one propellant, but not the other, is flowing through the injector; the stream of

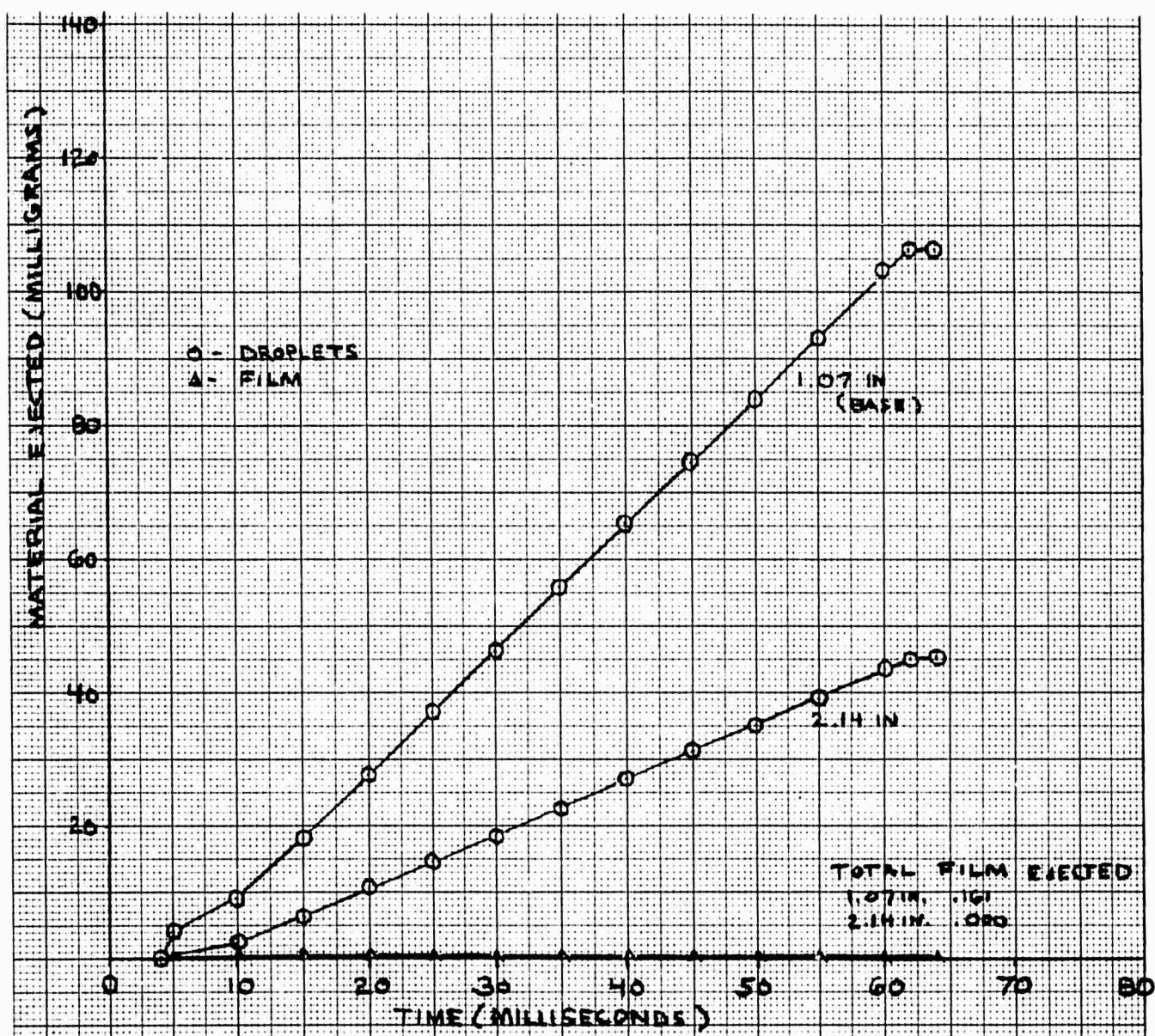


Figure A-12. The Effect of Chamber Length on Material Ejected from Motor

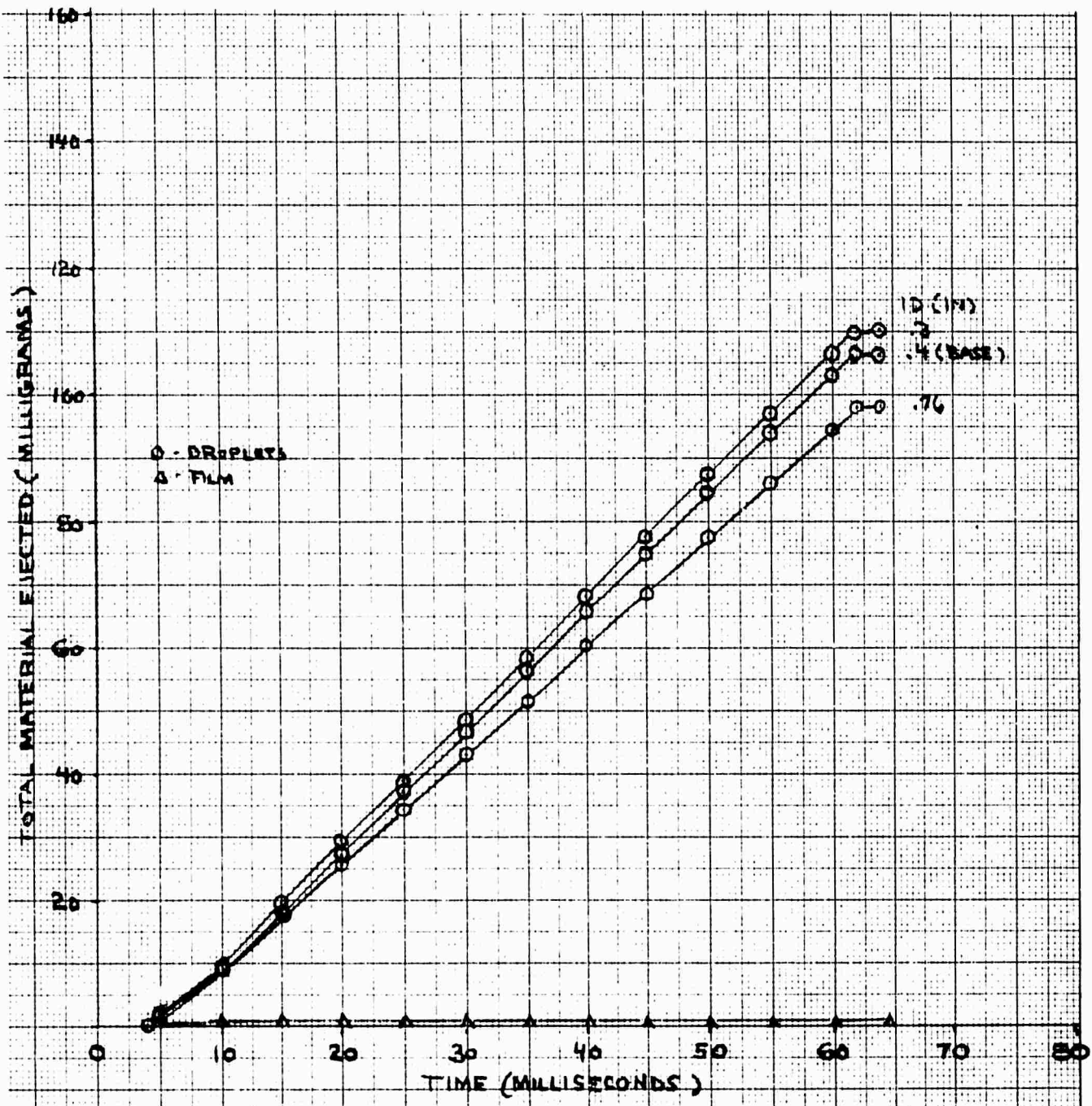


Figure A-13. The Effect of Chamber Diameter on Material Ejected from Motor

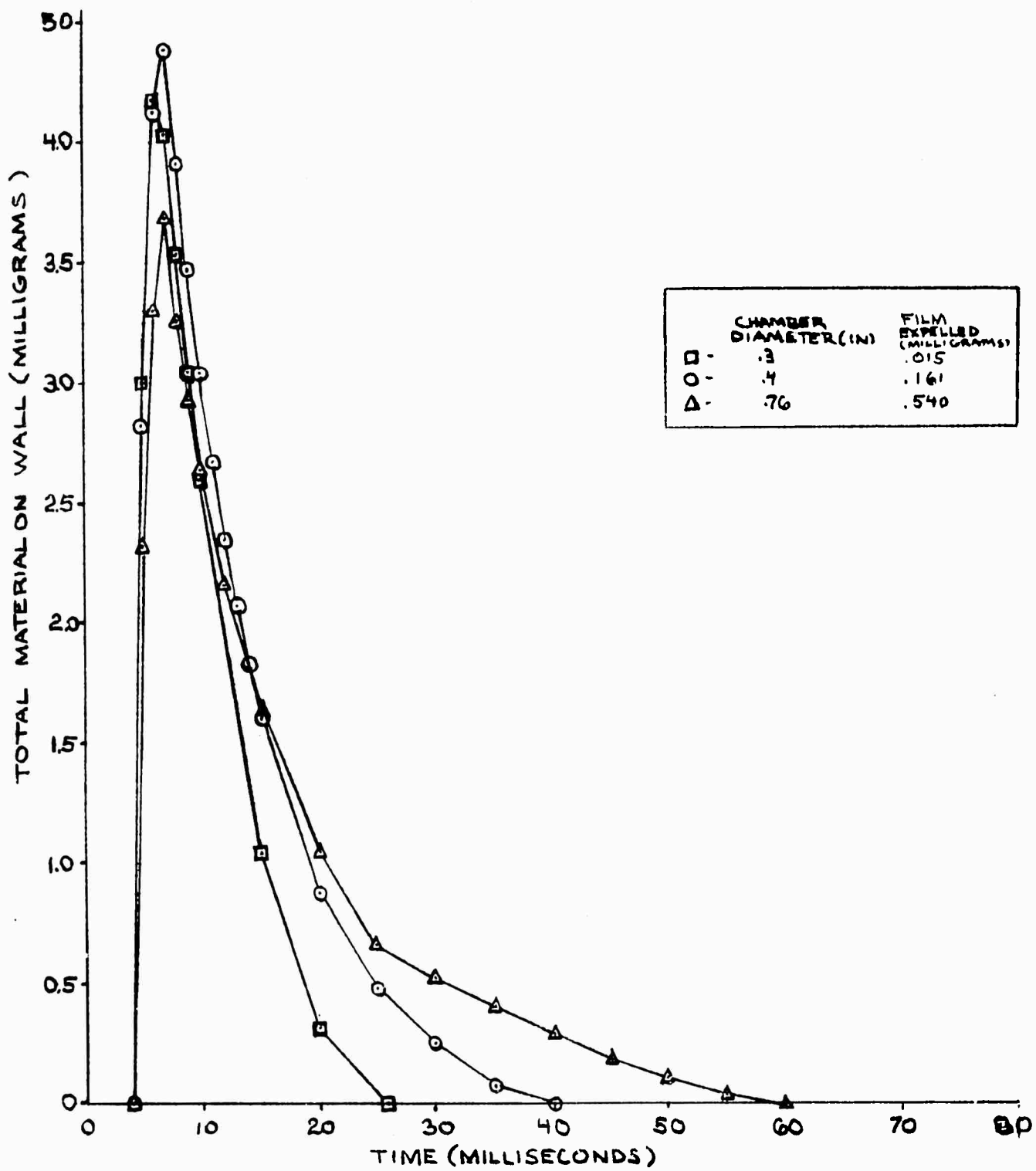


Figure A-14. Disposition of Material on Chamber Wall as a Function of Chamber Diameter

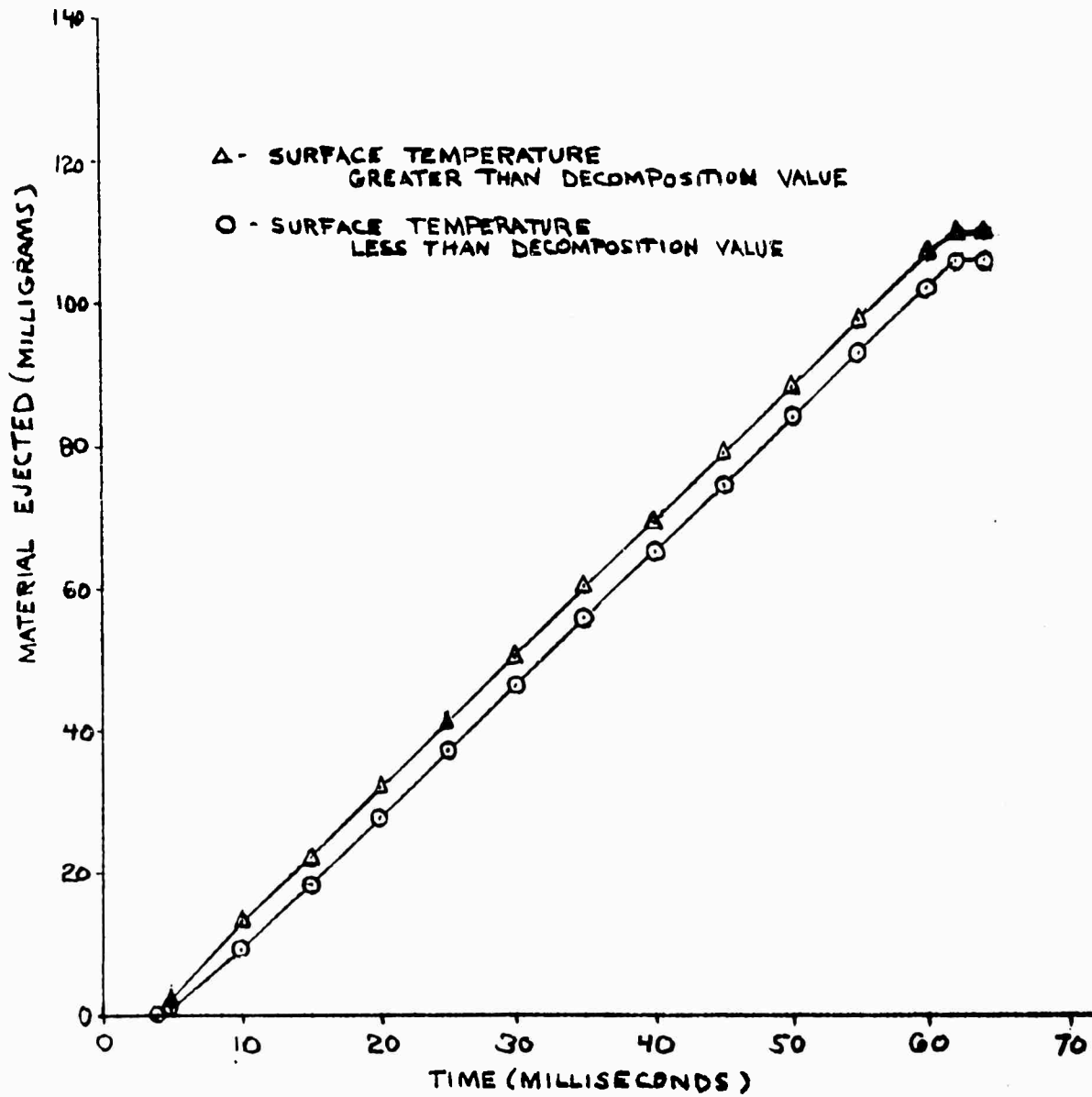


Figure A-15. The Effect of Chamber Wall Temperature on Material Ejected from the Motor

propellant impinges directly upon the wall. A fraction of this propellant remains on the surface, with the remainder rebounding. One of the weaknesses of the present model is in the detailed description of the disposition of propellant hitting the chamber wall, but the results should be qualitatively correct.

With one valve is opened in advance of the other, liquid propellant is ejected from the motor at a rate corresponding to the rate into the chamber less the amount that flash vaporizes or sticks to the chamber walls (Figure A-16). At ignition, the amount of droplets expelled from the motor changes (approximately) to the amount of propellant unburned during the combustion process (Figure A-17). The rate of expulsion of droplets after ignition is approximately the same for all cases; therefore, the contamination before ignition is of prime importance. Figure A-18 shows the amount of contamination before ignition. The best case is obviously a simultaneous operation of the valves. A fuel lead produces a lower mass of contaminant than the corresponding oxidizer lead because of the lower injection rate. In Figure A-19, the percentage of droplets in the exhaust is shown for different valve operating conditions. This figure shows that, before ignition, a substantial amount of the propellant vaporizes in the chamber; and after ignition, approximately 18 percent of the propellant is ejected unburned.

The disposition of material on the chamber wall is shown in Figure A-20. With a lead in opening either valve, a substantial quantity of propellant is deposited on the walls of the chamber. Even with the relatively long (9 millisecond) lead, the chamber walls are nearly clear by the end of the pulse, but significant amounts of the propellant sprayed on the wall is removed by flowing out the nozzle. (With the 9 millisecond oxidizer lead, nearly 50 percent of the propellant on the wall at the end of the ignition period is ejected through the nozzle.)

The effect of valve closing sequence is shown in Figure A-21. The amount of contaminant produced is identical until the first valve is closed, and then an additional amount of propellant is ejected according to the injection rate and lag time.

(d) The Effect of Tank Pressure

A variation in either fuel or oxidizer tank pressure causes a shift in the relative injection rates. This affects the system in two major ways. First, the change in the momentum of one of the injected propellant streams occurs, causing a shift in the beta angle. A change in tank pressure can, therefore, cause a significant change in the fraction of propellant hitting the chamber walls. The second major change is in the oxidizer-fuel ratio and the resultant chamber temperature. Four runs were made in which tank pressure was varied.

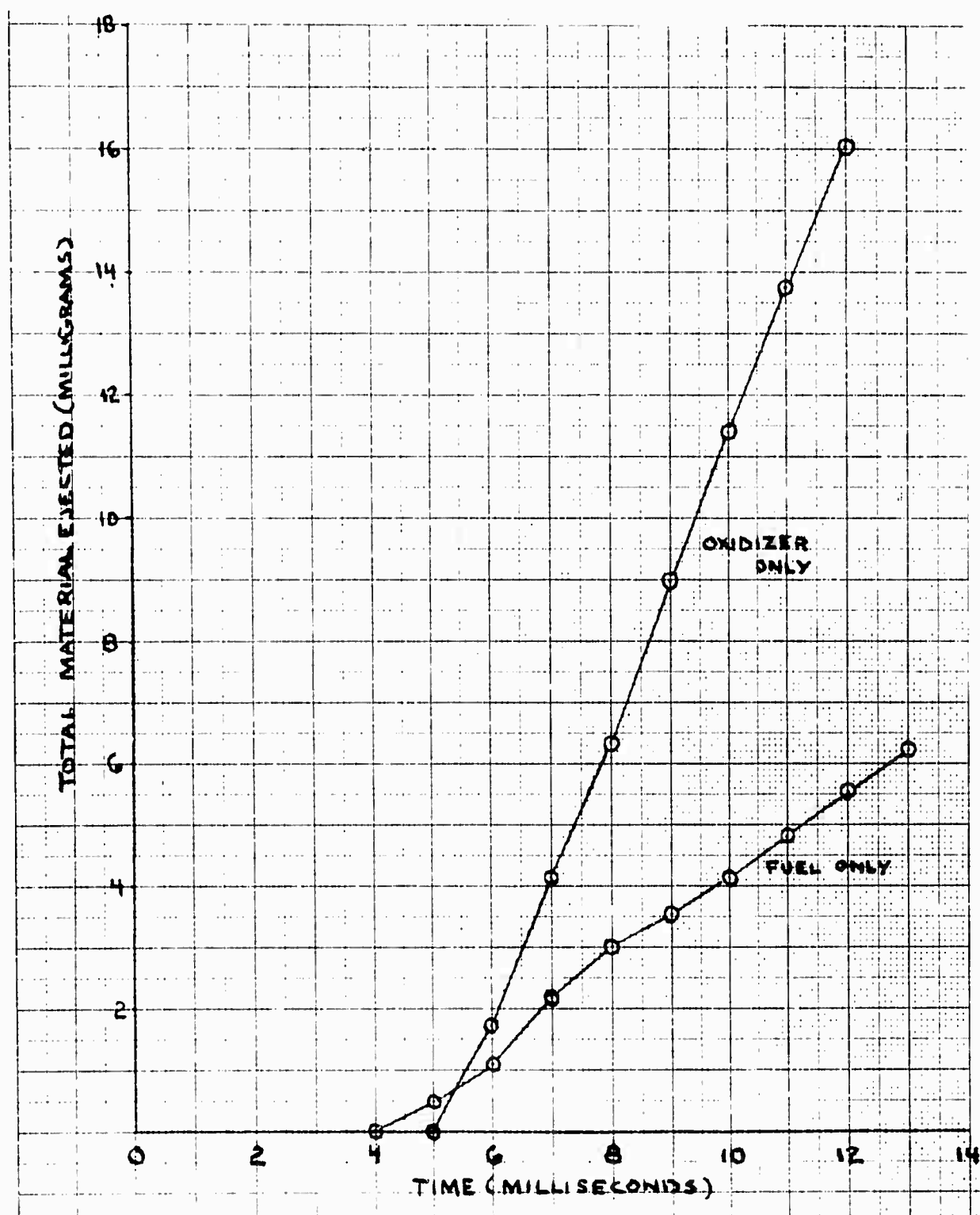


Figure A-16. Material Ejected with One Valve Open

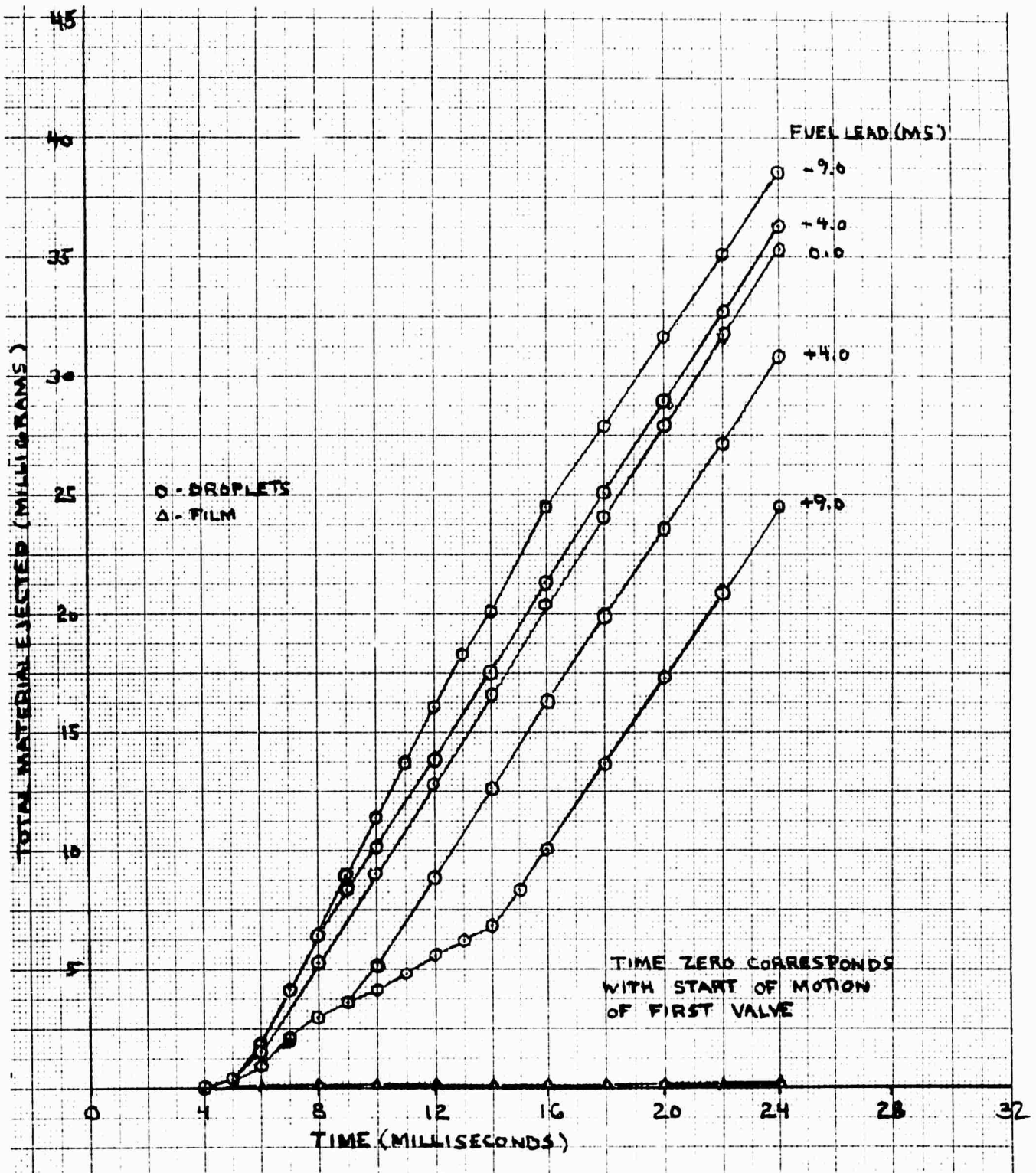


Figure A-17. The Effect of Valve Opening on Material Ejected from Motor

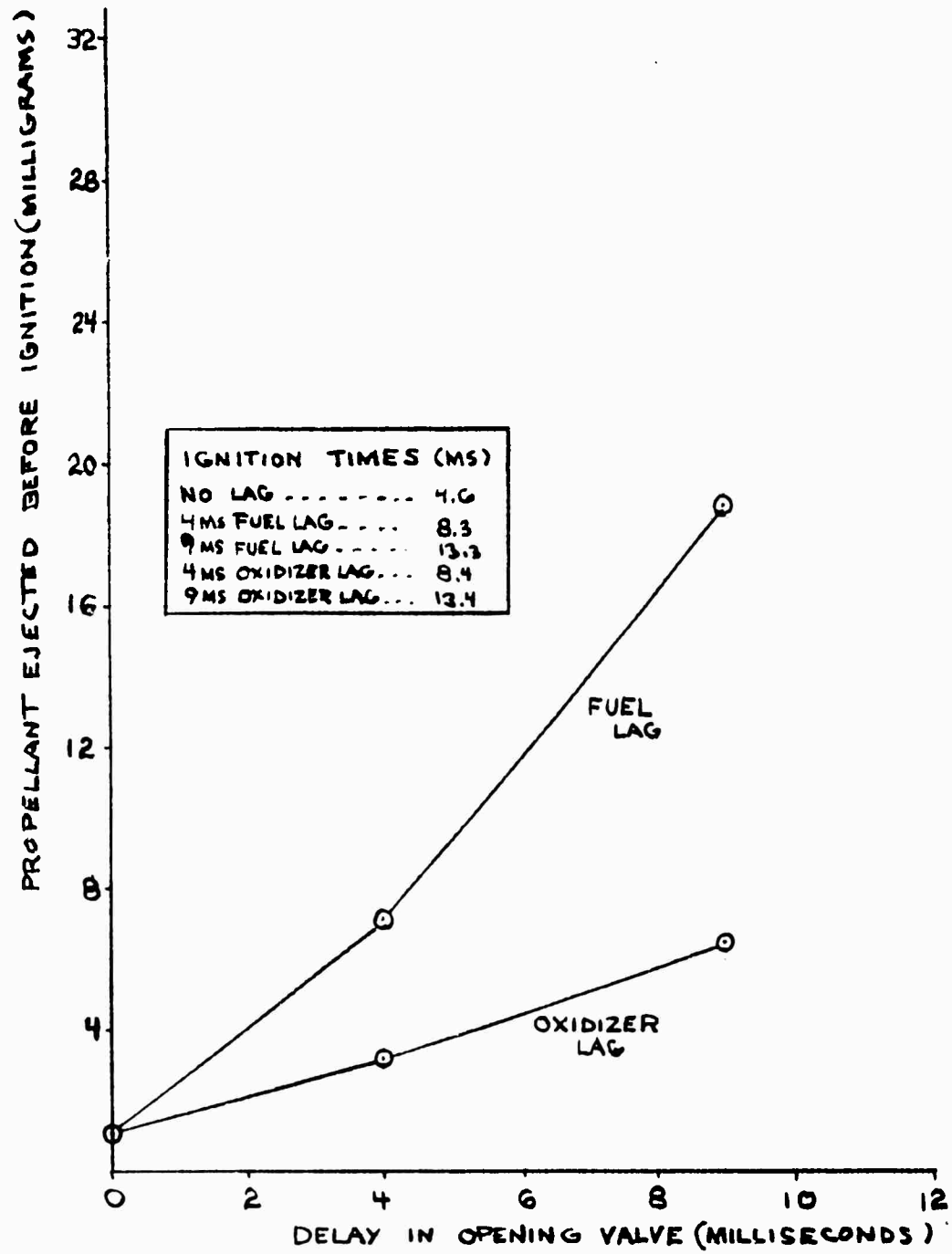


Figure A-18. The Effect of Valve Operation on Propellant Ejected Before Ignition

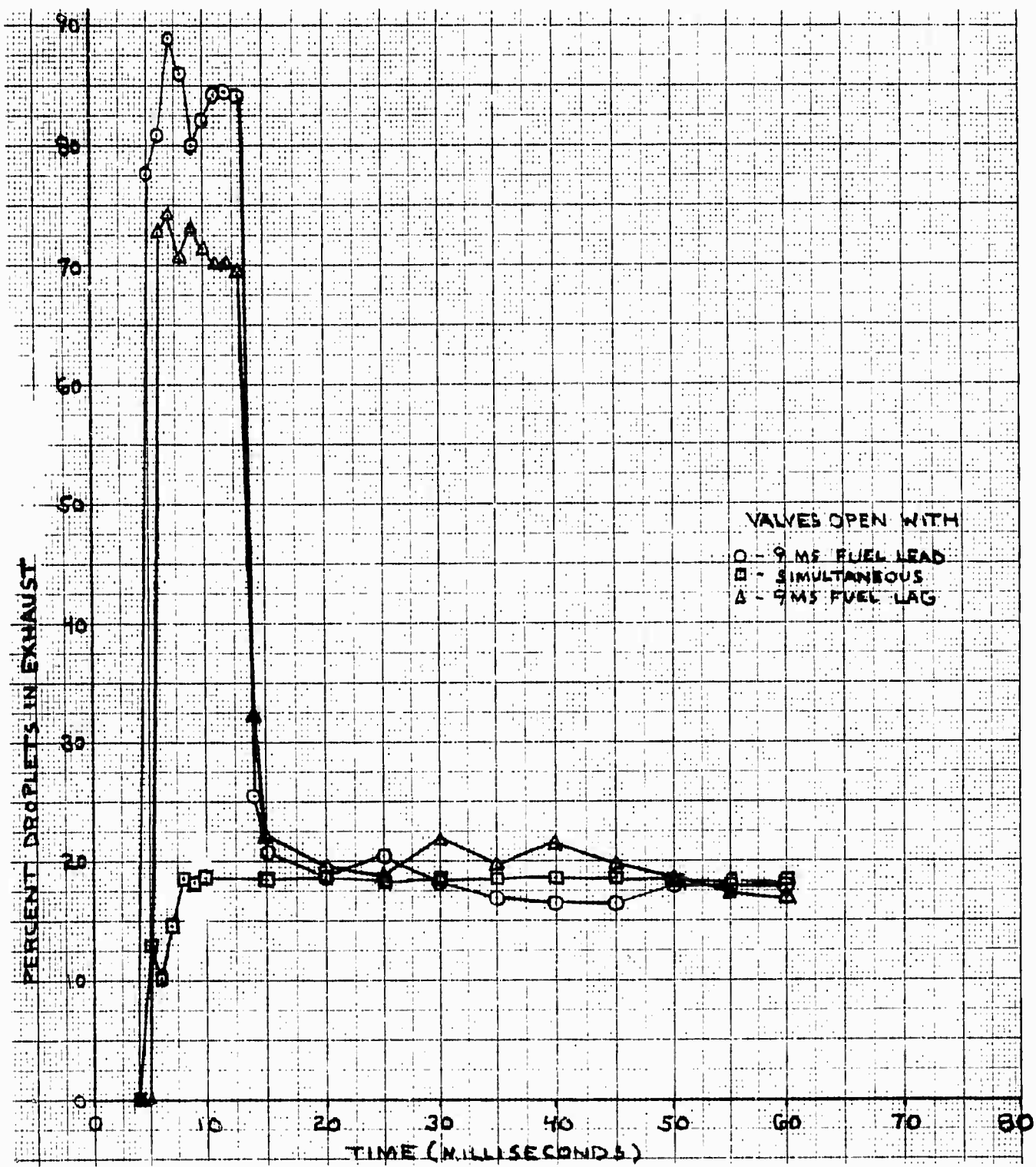


Figure A-19. The Effect of Valve Opening on Exhaust Composition

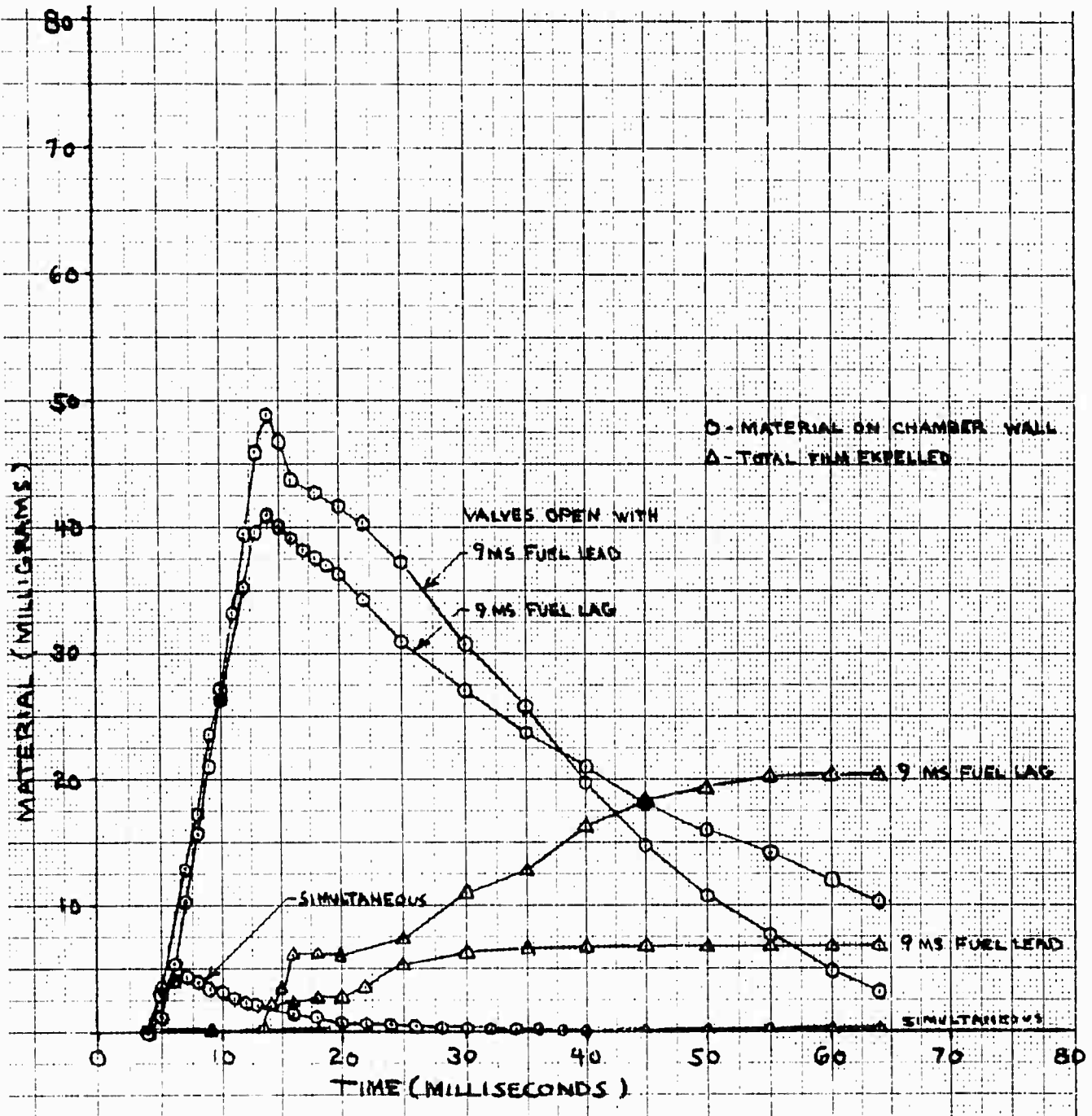


Figure A-20. Disposition of Material on Chamber Wall as a Function of Valve Operation

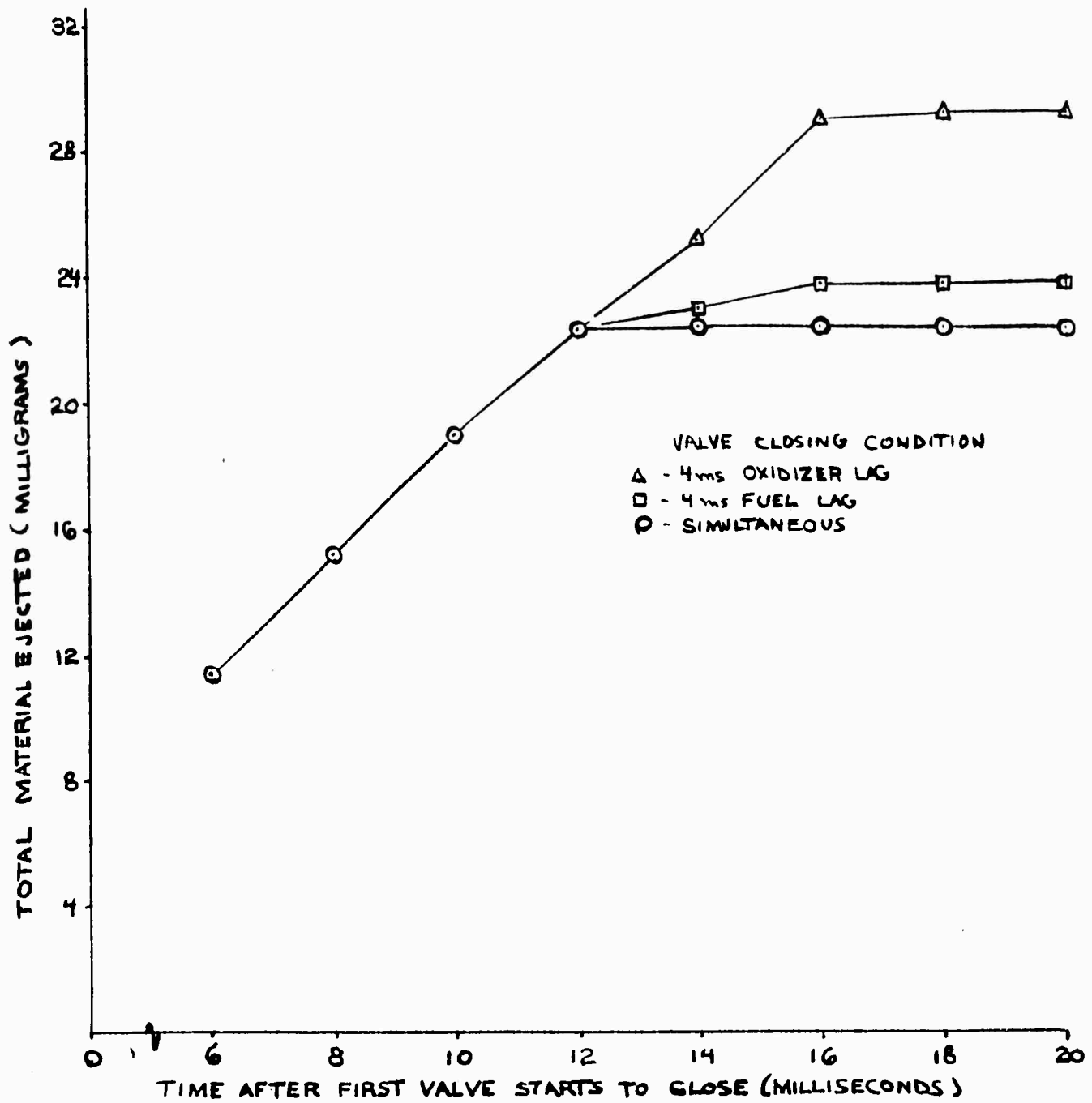


Figure A-21. The Effect of Valve Closing on Material Ejected from Motor

Figure A-22 shows the effect of fuel tank pressure. The expulsion mechanism changes at low fuel tank pressure where a substantial fraction of the material ejected from the nozzle is material that flows along the chamber walls to the throat. This is shown more clearly in Figure A-23. In the low pressure case, the propellant on the walls of the chamber builds up to an equilibrium value after 30 milliseconds. In both the overpressurized and under pressurized case, propellant is sprayed on the chamber walls at the end of the pulse.

Figure A-24 shows the effect of oxidizer tank pressure on material ejected from the motor. Either a higher or lower pressure causes a smaller amount of propellant to be ejected from the motor, but the reason differs. With the smaller tank pressure, less propellant is injected into the chamber, and although a higher fraction of the injected propellant is ejected unburned, (Table A-III), the absolute amount decreases. With higher oxidizer tank pressure, more propellant is injected into the chamber but, (1) combustion is improved and (2) less fuel is injected. These two factors apparently produce the observed result. Inside the motor, material is deposited upon the chamber walls at a greater rate with the higher or lower tank pressure as compared to the base case. Figure A-25 shows that propellant is sprayed on the wall at the beginning and end of a pulse for both the higher and lower oxidizer tank pressure. The propellant on the chamber wall appears to approach an equilibrium thickness after a period of several milliseconds, with propellant spraying on the wall at the same rate as material burns off and dribbles out the throat.

The oxidizer-fuel ratio is a strong function of tank pressure. Table A-IV shows O/F ratio for the various tank pressure conditions. This table also illustrates the variation between the O/F ratio based on injected propellant and one based on propellant vaporized in the chamber.

Table A-IV. THE EFFECT OF TANK PRESSURE ON CHAMBER CONDITIONS

Fuel Tank Pressure	Oxidizer Tank Pressure	Maximum Chamber Pressure	Equilibrium Chamber Pressure	Mixture Ratio Based on Injected Propellant	Mixture Ratio Based on Vaporized Propellant
145	165	148	96	2.10	3.02
180	165	134	103	1.59	2.45
215	165	139	107	1.30	2.00
180	135	123	94	1.23	1.88
180	195	160	111	1.96	2.87

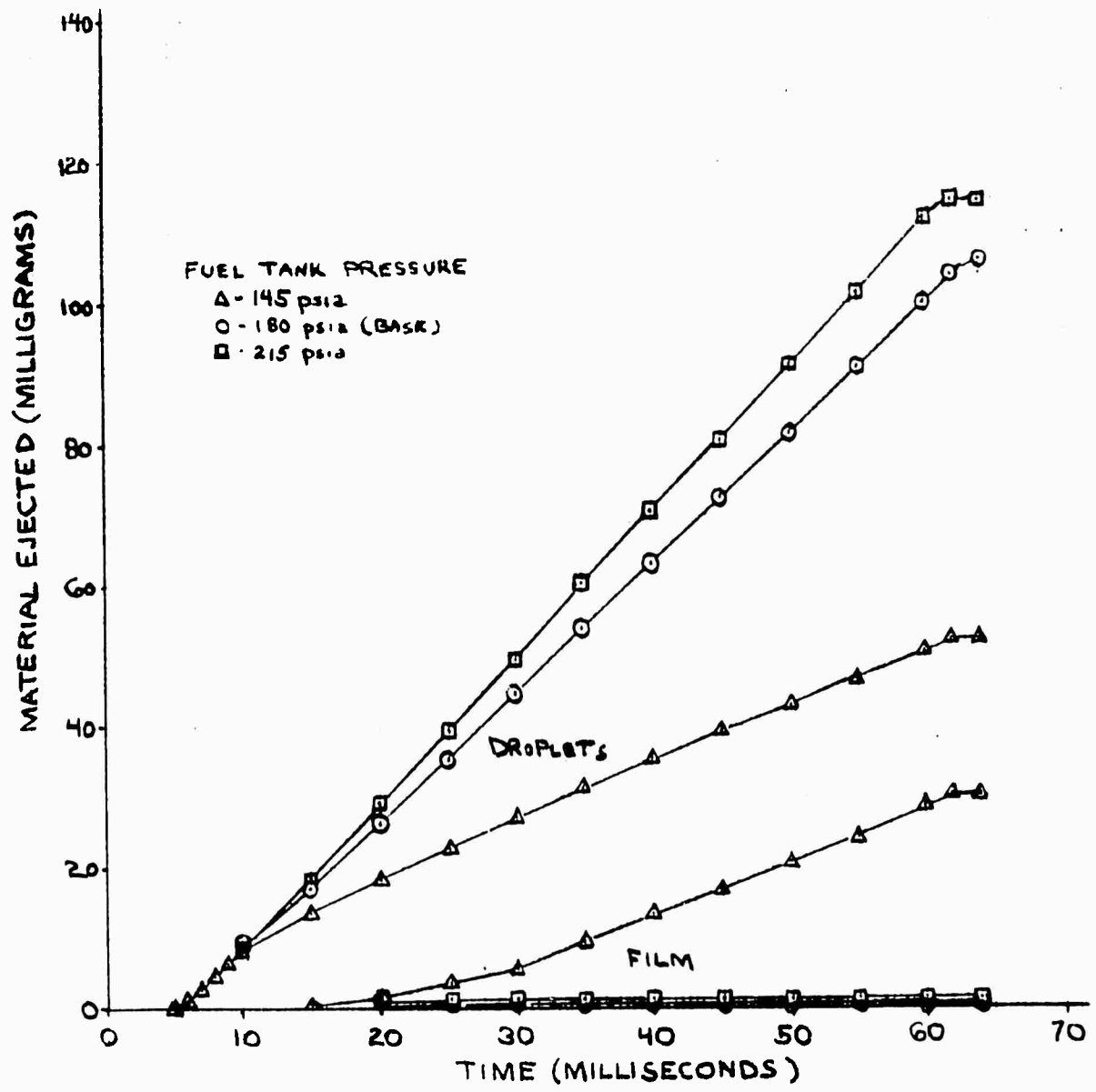
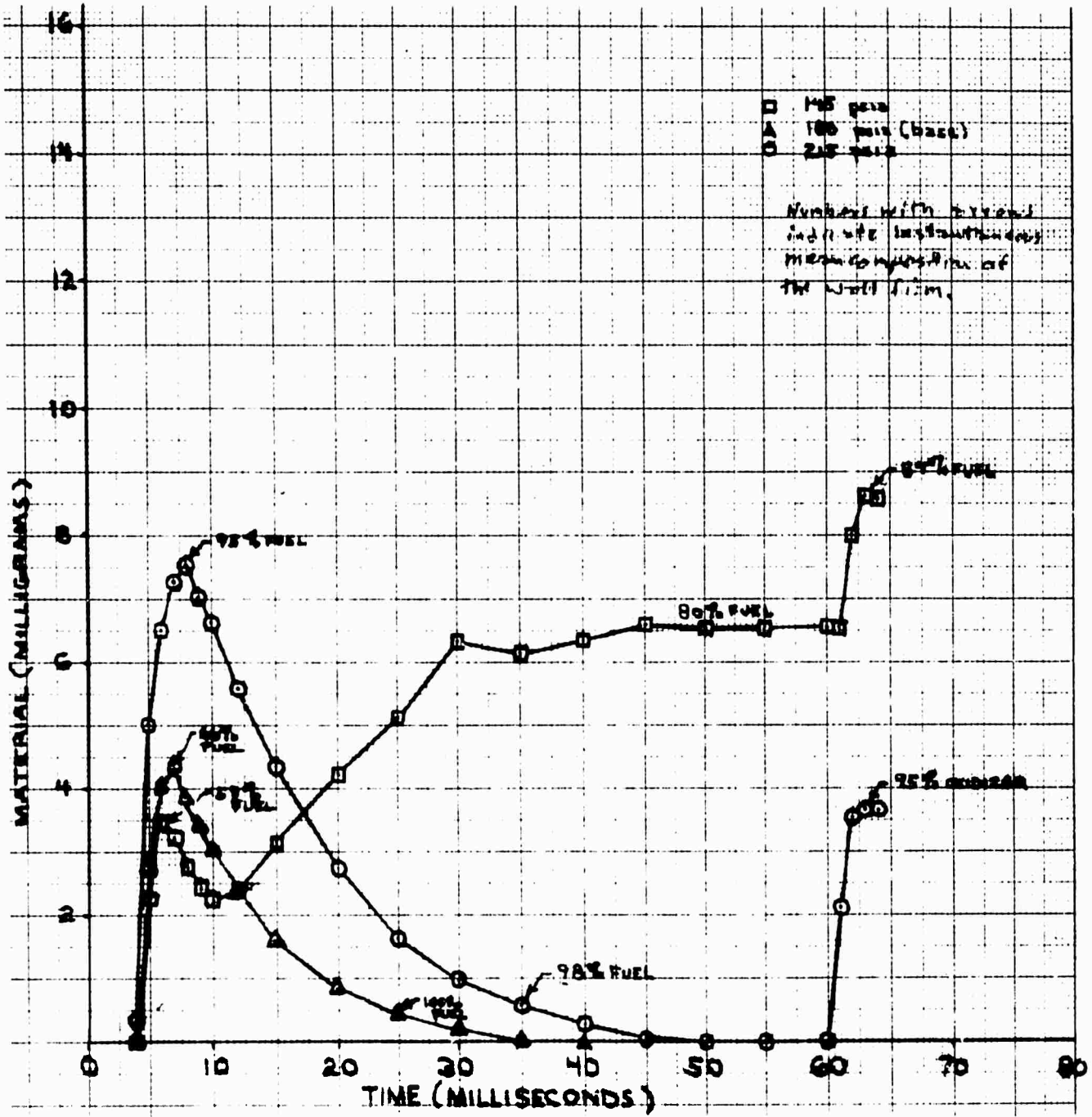


Figure A-22. The Effect of Fuel Tank Pressure on Material Ejected from Motor



NOT REPRODUCIBLE

Figure A-23. The Effect of Fuel Tank Pressure on Material Deposited on Wall

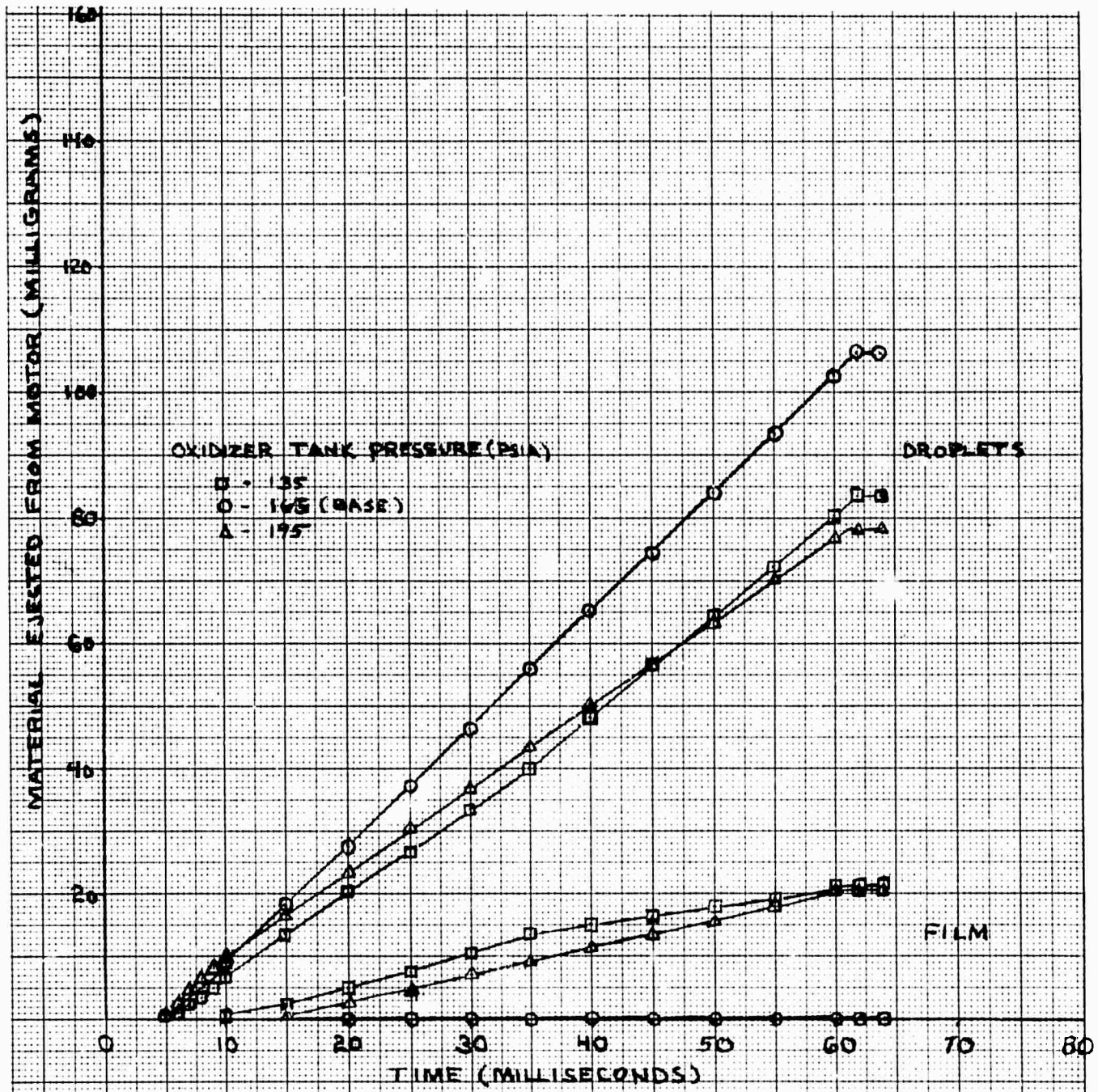
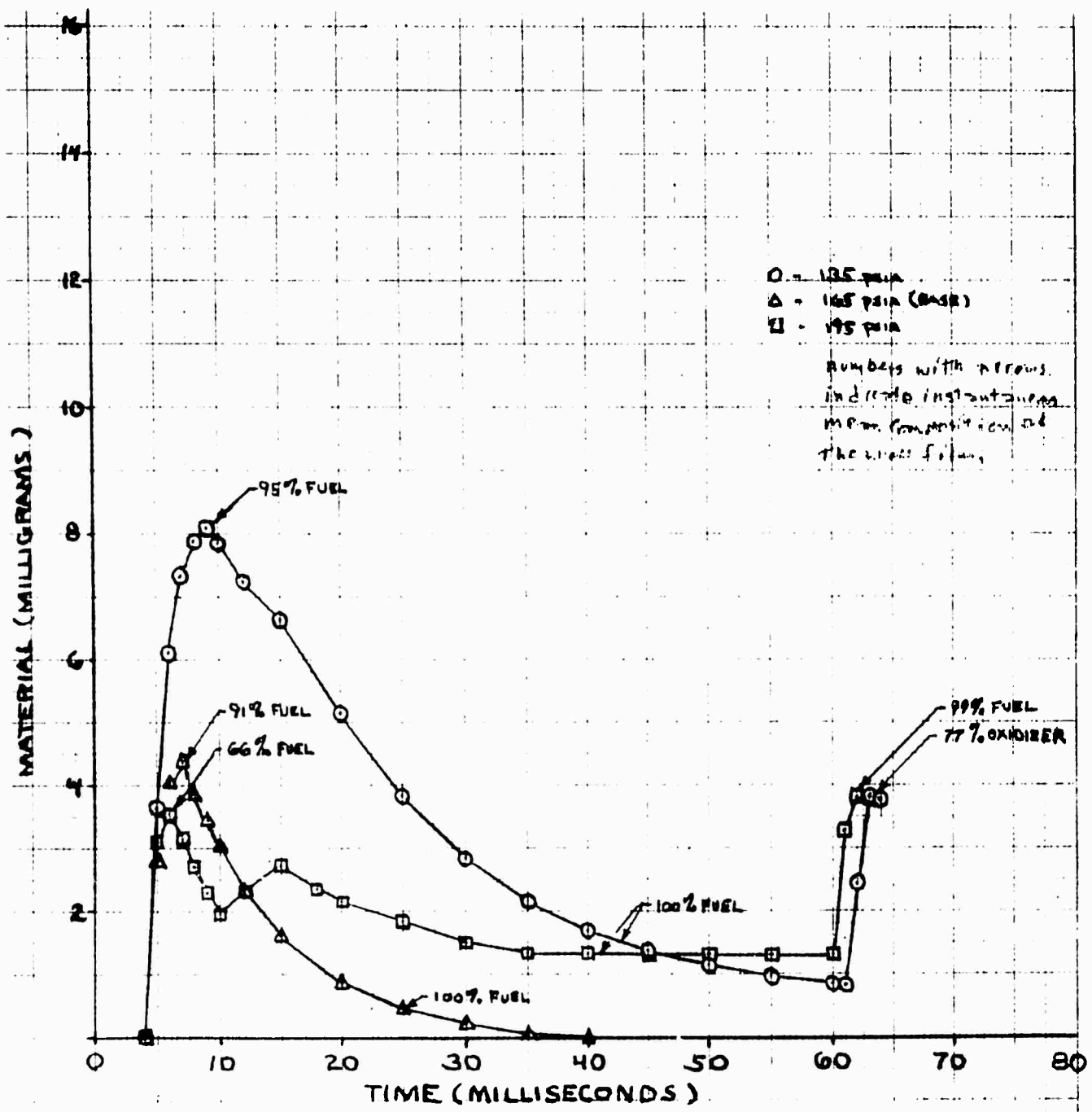


Figure A-24. The Effect of Oxidizer Tank Pressure on Material Ejected from Motor



NOT REPRODUCIBLE

Figure A-25. The Effect of Oxidizer Tank Pressure on Material Deposited on Chamber Wall

An O/F ratio determined experimentally is based on injected propellant rates, but the O/F ratio based on the amount of propellant vaporized in the chamber is the value of importance in performance calculations. The variation between the two bases is quite substantial in this motor. For the base case, the experimental O/F ratio is 1.6, but the O/F ratio of the vapor in the chamber is 2.45, almost exactly the theoretical O/F ratio for maximum ISP. Peak pressures are also indicated in Table A-IV. Higher oxidizer tank pressure in relation to fuel tank pressure produces a higher spike at ignition. Tables A-III and A-IV show that the same conditions that produce a higher peak pressure, cause a smaller fraction of injected propellant to be ejected unburned.

(e) The Effect of Propellant Temperature

The propellant temperature effects the steady operation of the engine by changing the propellant density, viscosity, and surface tension, which are all important in determining impinging-stream atomization droplet size. Propellant temperature also strongly affects the pre-ignition conditions in the chamber. The flashing-atomization threshold of the injected streams, the amount flashed when stream flashing does occur, and the combustion chamber vapor temperature and pressure are strongly sensitive to propellant temperature. The most important effects illustrated in Figure A-26 are those of impinging stream droplet size. A 20° C increase in propellant temperature decreases ejected droplet mass by 21 percent, while a 20° C decrease in propellant temperature increases the ejected droplet mass by 7 percent compared to the base case. The masses of wall film expelled are decreased 33 percent or increased 40 percent, respectively, by the same changes. Although postfiring dribble calculations are not shown here, propellant temperature is quite important in determining dribble rates through the effect on vapor pressure.

(f) The Effect of Pulsing

From the single pulse runs made in this study, some information concerning multiple pulses have been obtained. Major differences of a second pulse following the first include (1) propellant left on the chamber wall from the first pulse, and (2) the condition of dribble volumes. The dribble volumes can drain during the time between pulses so that the second pulse can start with (1) both dribble volumes full of propellant for very short down times, (2) the fuel dribble volume full and the oxidizer dribble volume empty for some longer down time, or (3) both dribble volumes empty at some still longer down time. Furthermore, the engine hardware may be hot and the propellant in the dribble volumes for the second pulse can be at a temperature substantially greater than bulk propellant temperature.

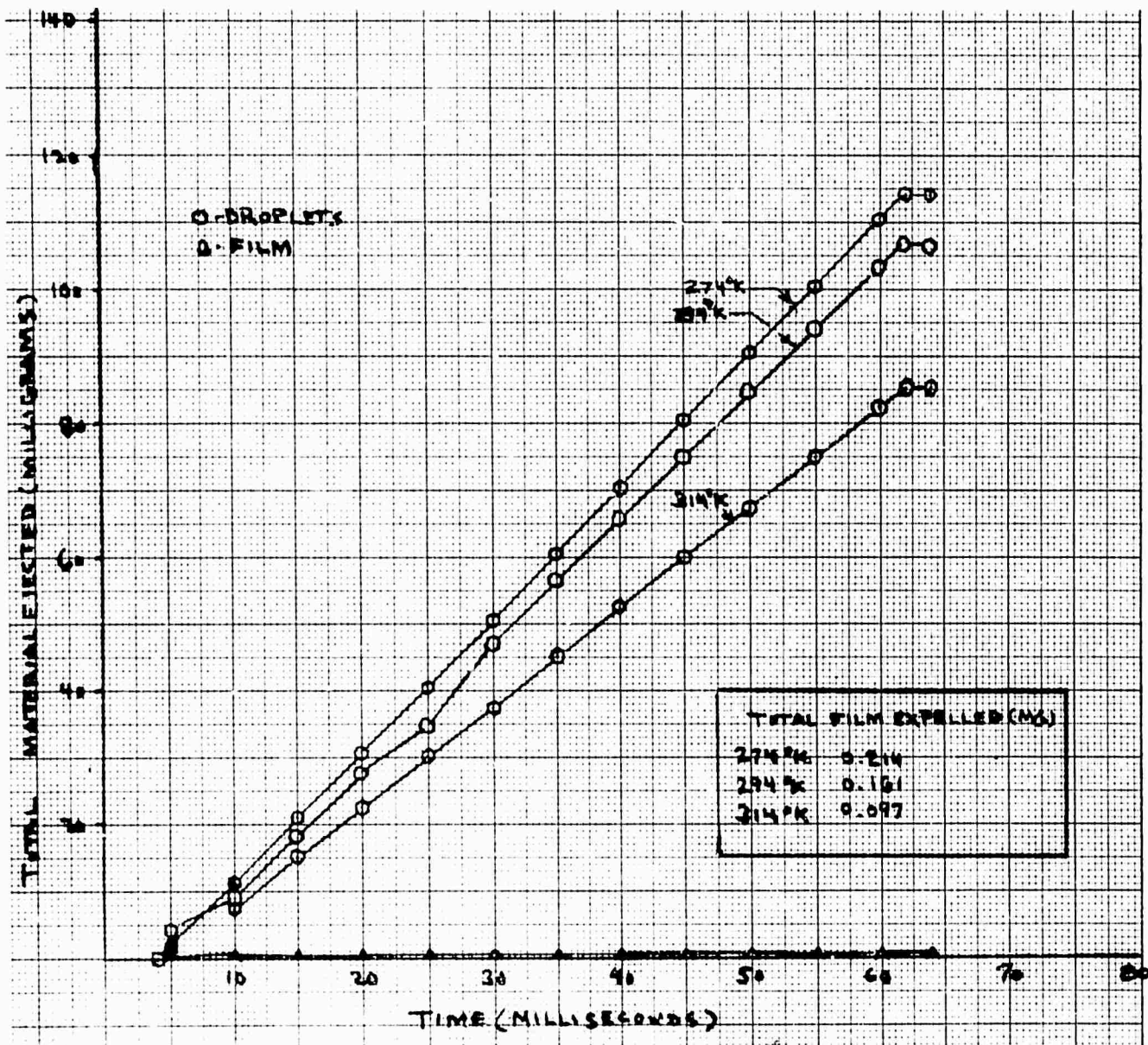


Figure A-26. The Effect of Bulk Fuel Temperature on Material Ejected from Motor

(g) The Effect of Dribble Volume

The effect of propellant in the dribble volume is illustrated in Figure A-27. When both dribble volumes are full, propellant enters the chamber immediately after the valves open and ignition occurs in less than one millisecond, compared with ignition times of 4.4 and 4.6 milliseconds in the other cases. Comparison of contamination (droplets ejected) should be made as a function of time after ignition rather than on the absolute time scale used in Figure A-27. On this basis, both dribble volumes full or both empty produce lower contamination than fuel full and oxidizer empty. The differences, however, are not substantial for this particular engine, because of its very small dribble volumes. In Figure A-28, the effect of heating the propellant in the dribble volumes has been illustrated. Although previous work has found this parameter to be important in motors with substantial dribble volumes, very little effect is found for this engine design.

The amount of material left on the chamber wall at the end of a pulse is a function of many variables, and this condition is discussed at other locations in this section. Generally, the propellant sprayed on the wall during the start transient burns off within 40 milliseconds with this motor. Variations from this norm occur when tank pressures are varied from normal (Figures A-23 and A-25 or geometry is changed (Figure A-14). Furthermore, a lag in closing either oxidizer or fuel valve leaves propellant on the chamber wall at the end of the pulse (Figure A-20). If the heat transfer to the chamber wall is sufficient to heat the surface to temperature greater than decomposition temperatures of the propellant, the surface remains clear of propellant (Figure A-15).

(4) Conclusions

The conclusions are drawn from the results discussed in the last section which are based on a relatively small engine. Careful interpretation of the results has been emphasized in the discussion of the results presented in Subsection A.2e(3). The following conclusions are noted:

1. Geometry—Contamination resulting from propellant ejected unburned from an engine is affected by chamber geometry. This is particularly true for chamber length where an increase significantly reduces the amount of propellant ejected unburned. This is attributed to the longer residence time of droplets in the chamber. An increase in chamber diameter causes some reduction in propellant ejected due to lower gas velocities in the chamber, but the velocity of droplets large enough to be ejected is apparently a stronger function of initial momentum

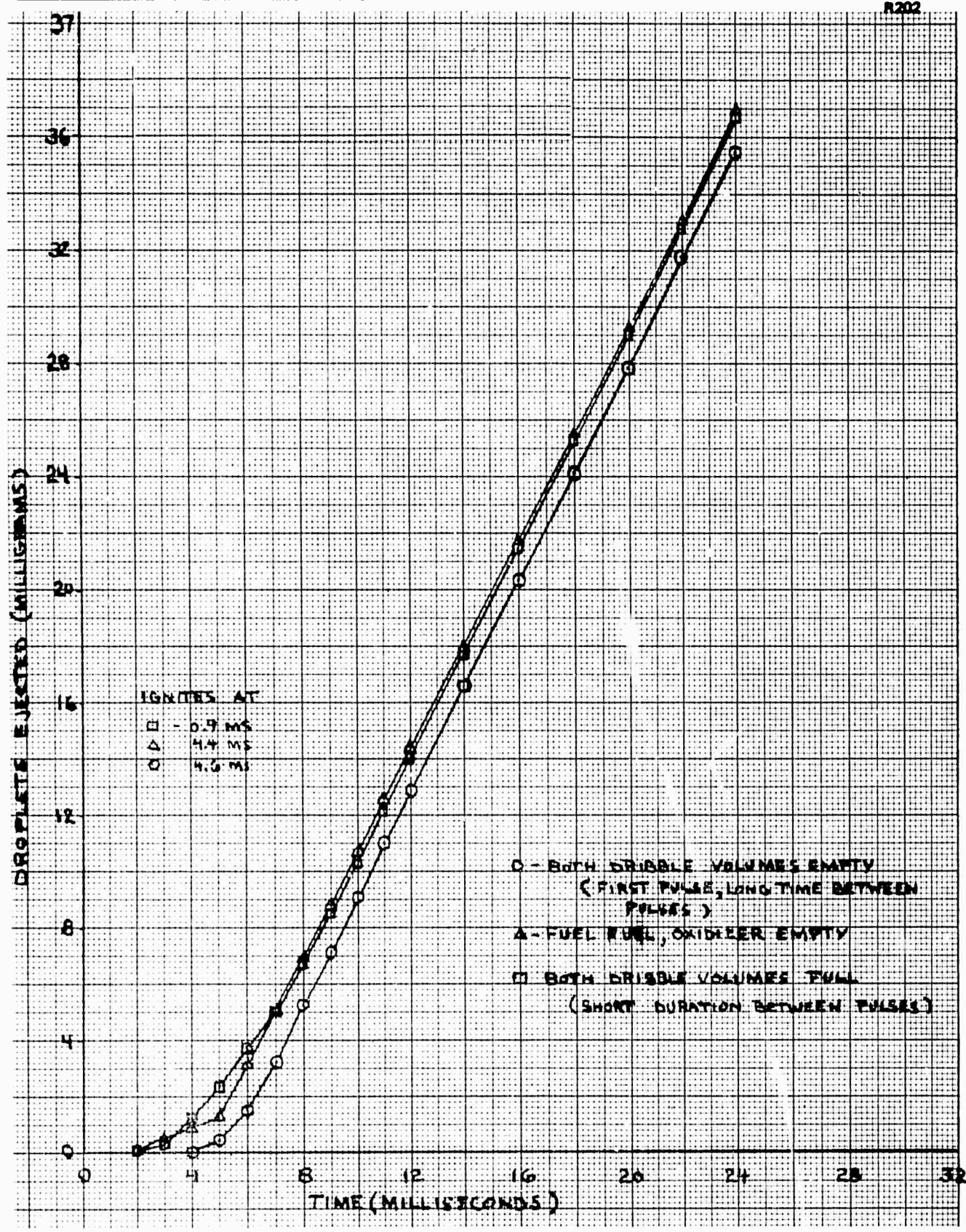


Figure A-27. The Effect of Draining Dribble Volume Between Pulses

NOT REPRODUCIBLE

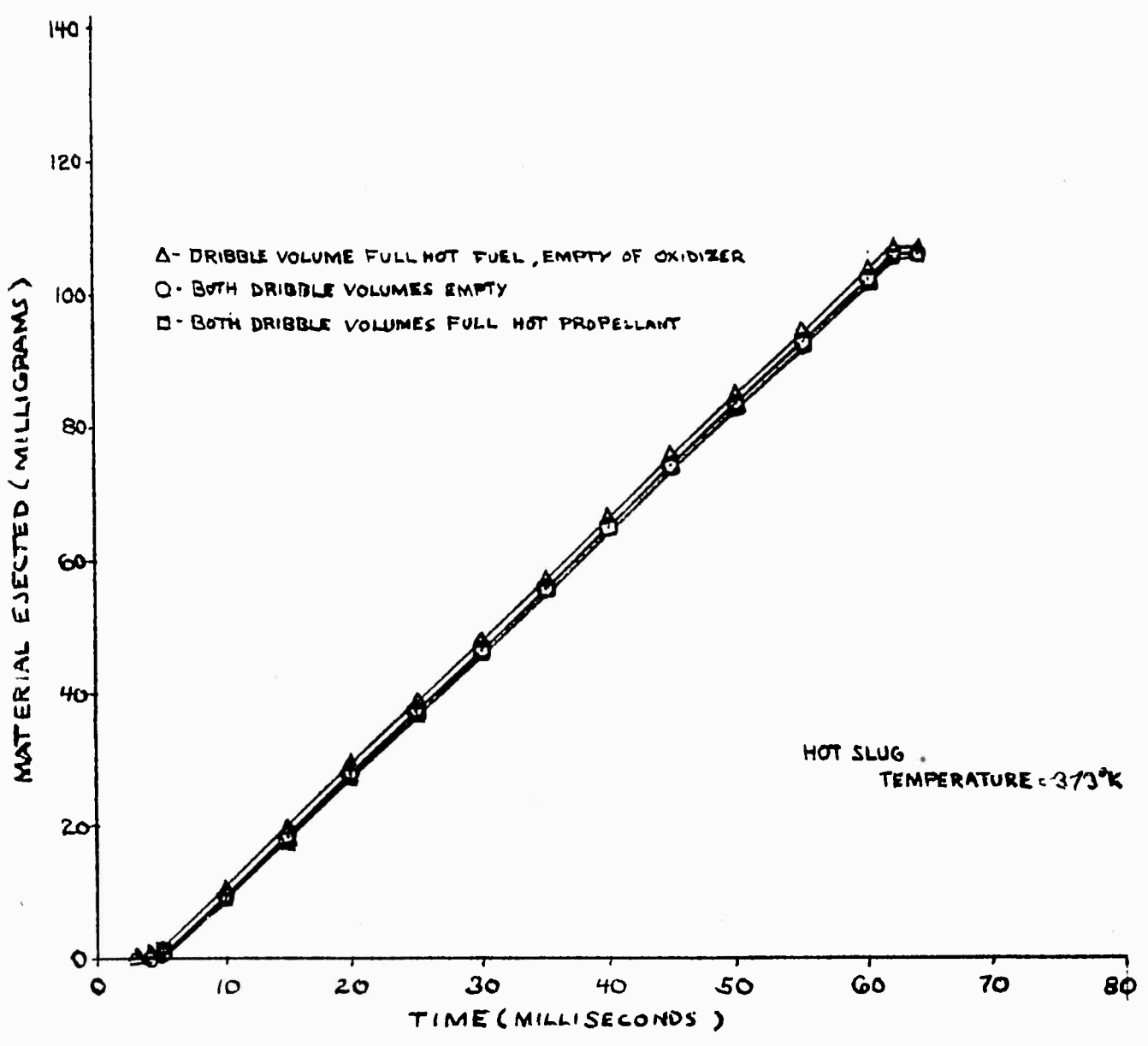


Figure A-28. The Effect of Heat Transfer to Propellant Remaining in Dribble Volumes Between Pulses on Material Ejected from the Motor

than gas drag. A reduction in throat area results in less propellant being ejected unburned from the motor, but not significantly less, and in view of the other changes on the system, a variation of this parameter for contamination control is unlikely.

2. Valve Operations—To expel a minimum mass of droplets during delivery of a specified total impulse, both valves should operate as nearly simultaneously as possible. Less droplet mass is expelled when valves open with a fuel lead than with an oxidizer lead of the same duration, mainly due to the lower injection rate. With an oxidizer lead, significant amounts of the propellant flow out of the nozzle. With a fuel lead less flows out the nozzle and more burns off the chamber wall. The effect of a non-simultaneous valve closing is to leave substantial amounts of propellant on the wall at the end of the pulse, as well as ejecting propellant as long as the valve is open.
3. Tank Pressure—A variation in either oxidizer or fuel pressure from the norm causes an increased amount of propellant to be sprayed on the chamber walls. If the shift in beta angle is sufficiently great, propellant is sprayed on the chamber walls throughout the pulse and the amount on the wall establishes an equilibrium value where the amount of propellant sprayed on the wall equals the amount vaporizing or burning off plus the amount flowing out the nozzle. Tank pressure variation also causes a shift in oxidizer-fuel ratio and the resultant temperature of the gas in the chamber which affects the vaporization rate of the propellant. The maximum or peak pressure at ignition is also a function of tank pressure. Propellant is sprayed on the wall at the end of the pulse when tank pressure is varied from the norm.
4. Pulsing—Major differences between the start of a second pulse and the start of the first pulse are (1) propellant may be left on the chamber walls from the first pulse, and (2) the dribble volumes may be full or partially full of propellant. Furthermore, the propellant left in the dribble volumes may absorb some of the heat from the system between pulses. For the conditions investigated, for this engine, very little effect was observed for the variation of initial conditions of the dribble volumes.

A. 3 NUMERICAL INTEGRATION METHOD

The numerical solution of sets of differential equations can be accomplished using a number of different techniques. The simplest technique is Euler's method. In this method, the next value for each dependent variable

is obtained by linear extrapolation of the present value using the first derivative calculated at the present value. For a time-dependent function:

$$V(t + \Delta t) = V(t) + \frac{dV}{dt}(t) \Delta t \quad (A-64)$$

where V may be any variable value defined by a differential equation.

Other methods of numerical integration are available in which higher order derivatives are calculated and used:

$$V(t + \Delta t) = V(t) + \frac{dV}{dt} \Delta t + \frac{1}{2} \frac{d^2V}{dt^2} \Delta t^2 + \dots + \frac{1}{n!} \frac{d^n V}{dt^n} \Delta t^n \quad (A-65)$$

The use of higher order derivatives often allows larger values for Δt to be used without introducing excessive error or instability. A penalty must be paid for the use of the higher order derivatives. In the present calculations, any higher order derivatives would have to be estimated numerically by taking differences between previous values for the variables. Since 15,000 computer storage locations are required to contain the current values for the droplet array, the requirement that previous values be kept also would drastically increase the already large computer storage requirement. A further argument against the use of a higher-order integrating scheme is that many of the physical processes which are modeled do not have continuous derivatives. The feed system flow rates vary discontinuously when the dribble volumes fill up. The chamber gas properties and droplet burning rates vary discontinuously when the chamber contents ignite. The propellant primary atomization droplet size varies discontinuously when a decrease in chamber pressure or an increase in Weber number causes flashing to commence. When even the first derivative is not continuous, it is pointless to think of approximating higher order derivatives.

One way that the Euler method can be improved in the solution of certain physical problems is by limiting variables to their physically defined asymptotic values. The time interval chosen for the calculations is based mostly upon the response time of the chamber pressure. If a fuel droplet is injected which is so small that it would burn up completely in less than one computing time interval, then Equation A-64 would predict that it would burn to a negative diameter in one time interval and contribute more than one hundred percent of its mass to the gas phase. Obviously a real burning droplet has an asymptotic value of zero for its diameter and mass. Hence it is appropriate to limit the derivative to a value which will just consume the droplet completely in one computational time interval. Doing this will obviously assign an incorrect value to the droplet burning rate, but will yield a value for chamber pressure at the end of the interval which is correct. Several other derivatives are limited to known asymptotic values. Droplets being accelerated by aerodynamic drag forces will not exceed the local velocity of the gas which is accelerating them, feed system flow rates will not accelerate past the steady-state flow rate corresponding to the current pressure

drop. The instructions for limiting the value of the derivatives are all written so as to properly consider flow rates and velocities approaching from either side of the asymptotic value. It should be emphasized that this derivative-limiting procedure is to stabilize the calculations for exceptional conditions, and that most of the calculations are made according to Equation A-64.

a. Computational Methods for Droplet Arrays

The methods used for the calculation of droplet combustion and trajectories differ according to the generality or restriction of the particular case. Three methods will be described to illustrate the similarities and differences. The first two methods illustrate the historical development of droplet analysis of rocket engine combustion chambers.

(1) Steady-State Chamber with Monodisperse Droplets

The simplest case is that of axially directed monodisperse droplets in a steady chamber. All of the droplets injected as a group at any particular time will behave alike, and the droplet group injected at any particular time will behave the same as any other group introduced at any other time. Thus, knowing the mass, velocity and position history for any one droplet yields a general solution for the entire combustion chamber. The aerodynamic drag force and evaporation rate for a droplet may be computed, and the successive values for mass, velocity and location may be calculated for a sequence of time steps in a very straightforward manner:

$$M_{(t + \Delta t)} = M_{(t)} - \dot{M}_{(t)} \Delta t \quad (\text{A-66})$$

$$V_{(t + \Delta t)} = V_{(t)} + \frac{F_{(t)}}{M_{(t)}} \Delta t \quad (\text{A-67})$$

$$X_{(t + \Delta t)} = X_{(t)} + V_{(t)} \Delta t \quad (\text{A-68})$$

$$U_{(t + \Delta t)} = U_{(t)} + \frac{1}{\rho A} N \dot{M}_{(t)} \Delta t \quad (\text{A-69})$$

Where M is the mass of a droplet, \dot{M} is the evaporation rate of the droplet, V is the velocity of the droplet, F is the aerodynamic drag force acting on the droplet, X is the axial location of the droplet, U is the combustion gas velocity, N is the number of droplets in the group, ρ is the density of the combustion gas, and A is the cross-sectional area of the chamber. Since U and X are both functions of t , $U(X)$ is defined. This was the method used by Priem to evaluate chamber conditions with uniform droplets (Reference 8).

(2) Steady-State Chamber with Distributed Droplet Sizes

When the droplets produced by the injector are distributed in initial diameter, the calculations are less straightforward. The small droplets are accelerated by aerodynamic forces much more rapidly than the large droplets, hence, if the droplets are initially together at some particular place and time, they will be separated a short interval of time later. For this reason, the same time interval cannot be used by all the different sized droplet groups to progress from one axial location to the next. In the steady-stage chamber, no generality is lost by summing up combustion gas contributions from large, medium and small droplet groups which originated at different times, but which happen to be at the desired axial location in the chamber at the time the gas velocity summation is made. In marching down the chamber to develop the gas velocity profile, an axial distance interval is chosen, and then the time interval required for each different droplet size group to traverse the distance is calculated. The evaporation and acceleration effects for each droplet size group must be evaluated using its own correct time interval.

$$\Delta t_i = \frac{\Delta x}{V_{i(x)}} \quad (\text{A-70})$$

$$M_{i(x + \Delta x)} = M_{i(x)} - \dot{M}_{i(x)} \Delta t_i \quad (\text{A-71})$$

$$V_{i(x + \Delta x)} = V_{i(x)} + \frac{F_{i(x)}}{M_{i(x)}} \Delta t_i \quad (\text{A-72})$$

$$U_{(x + \Delta x)} = U_{(x)} + \frac{1}{\rho A} \sum N_i \dot{M}_{i(x)} \Delta t_i \quad (\text{A-73})$$

The subscript i is used to distinguish between the various groups of different sized droplets. This is the method used by Priem⁹ and later by Lambiris¹⁰ to calculate chamber profiles with distributed droplet sizes. The Dynamic Science approach¹¹ differed only in having groups of oxidizer droplets as well as fuel droplets.

It is apparent that the previous methods depend very strongly upon the assumption of steady conditions in the chamber and cannot be used to calculate the unsteady state. There are other more subtle restrictions, the methods cannot be used for droplets injected in the reverse direction, etc.

(3) Unsteady-State Chamber with Distributed Droplets

The method used in the present program differs from the earlier methods. Instead of following one or a few droplet groups progressively down the length of the chamber, the entire chamber population of droplets is represented simultaneously and reexamined at each time interval. When this method is used, a larger computer memory is required in order to store the description of the entire droplet population of the chamber, and more

computing time is required since all of the droplet groups constituting the entire population are examined at each time interval, however it is now possible to calculate time-varying behavior and it is simple to calculate droplet motion in one, two or three dimensions with no arbitrary restrictions. The mass, velocity and location for each droplet group in the chamber is recalculated at each time interval:

$$M_i(t + \Delta t) = M_i(t) - \dot{M}_i(t) \Delta t \quad (\text{A-74})$$

$$V_i(t + \Delta t) = V_i(t) + \frac{F_i(t)}{M_i(t)} \Delta t \quad (\text{A-75})$$

$$X_i(t + \Delta t) = X_i(t) + V_i(t) \Delta t \quad (\text{A-76})$$

The forces, velocities and locations may be treated as being one, two or three dimensional with no difficulty.

The axial gas velocity may be calculated at any axial chamber location, based upon a mass balance on the upstream region. In its present form, this calculation depends upon the assumption that the gas in the chamber is well mixed and has a constant density (i. e. , no gradients in composition, temperature or pressure).

$$U_x = \frac{\dot{M}_x}{\rho A} \quad (\text{A-77})$$

\dot{M}_x = Evaporation rate upstream of X - Accumulation Rate Upstream of x

$$\dot{M}_x = \sum_{\text{All groups upstream of x}} N_i \dot{M}_i - \frac{V_x}{V_c} \left[\sum_{\text{All groups in chamber}} N_i \dot{M}_i - \dot{M}_{\text{Nozzle}} \right] \quad (\text{A-78})$$

Where V_x is volume upstream of x and V_c is total chamber volume. In the present program the axial gas velocity is calculated at each of one hundred equally spaced intervals and interpolated between these points.

b. Integrating Time Interval

When gas is flowing from a chamber through a sonic throat, the mass flow rate is:

$$\dot{M}_t = A_t P_c \sqrt{\frac{\gamma W m}{RT} \left(\frac{2}{\gamma + 1} \right)^{(\gamma+1)/(\gamma-1)}} \quad (\text{A-79})$$

The mass stored in the chamber is:

$$M = \frac{P_c V_c W_m}{RT} \quad (A-80)$$

The ratio of M/\dot{M} is often referred to as "gas residence time" and is a rough measure of how fast the chamber pressure can fall by flow through the nozzle. When equations A-79 and A-80 are combined and simplified:

$$\text{gas residence time} = \frac{\frac{A_c}{L_c A_t}}{a_c \sqrt{\left(\frac{2}{\gamma + 1}\right)^{(\gamma + 1)/(\gamma - 1)}}} \quad (A-81)$$

When this is evaluated using the values $\gamma = 1.25$, $(A_c/A_t) = 4$, $a_c = 3600$ feet/second and $L_c = 1.0$ inch, a value of 0.17 millisecond is obtained for gas residence time. It is obvious that if normal pressure changes are to be modeled with sufficient accuracy, the integrating time interval must be considerably less than the gas residence time of the particular chamber.

Fuel and oxidizer droplets are introduced at the injector end of the chamber and move downstream with a velocity which depends upon the axial injection velocity and the subsequent aerodynamic drag. To maintain sufficient accuracy in the calculation of the droplet trajectory and mass history, a sufficient number of calculations must be made during the stay time of a droplet in the chamber. Droplet staytime may be estimated as chamber length divided by average droplet axial velocity. A reasonable estimate for axial velocity is 100 feet/second. Hence, for a chamber one inch long the droplet stay time is on the order of 0.8 millisecond.

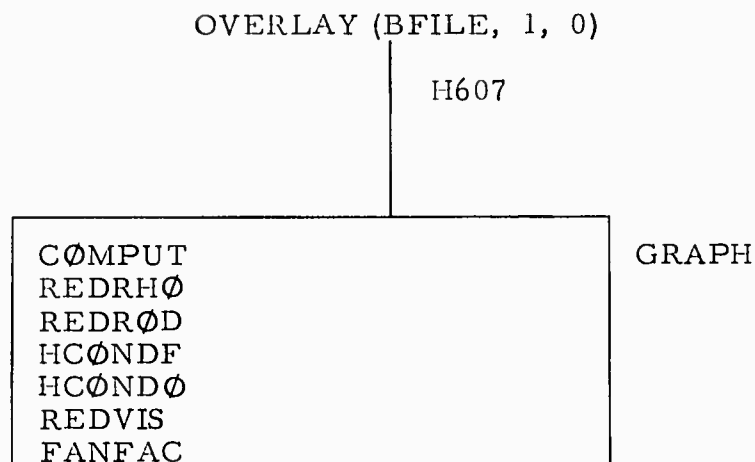
In addition to the obvious restraints on maximum integrating time interval, there is a more subtle restraint on minimum time interval. At each time interval the axial gas velocity profile in the chamber is calculated based upon the mass of newly formed combustion gas which must be moved to restore the chamber to a uniform density and pressure. If an extremely short time interval is taken, it is possible that in some unusual cases, gas velocities will be calculated which are higher than are physically possible. This would introduce error in the velocity-sensitive functions such as droplet burning rate, drag, wall film flow and wall film burnoff. If the chamber is viewed as a closed-closed organ pipe a pressure relaxation physically requires one quarter of an acoustic period, i. e. ,

$$\Delta t = \frac{L_c}{2 a_c} \quad (A-82)$$

This sets 0.012 millisecond as a minimum time interval for a combustion chamber one-inch long.

Since the maximum and minimum permissible time intervals often differ considerably, there is leeway to trade off computer expense against precision of calculation. Most of the computations reported here were done near the maximum acceptable value for time interval to reduce the computation expense.

A. 4 PROGRAM OVERLAY STRUCTURE



A. 5 SUBROUTINES

There are six subroutines used in COMPUT to calculate physical properties of the propellants and to calculate chamber wall shear stresses associated with the combustion chamber gas flow.

a. Subroutine REDRHO (TRED)

Approximates the reduced density of a liquid as a function of reduced temperature along the saturation line, based upon the curves of Hougen and Watson:

$$0.8 > T_r \quad \rho_{r(l)} = 3.97 - 1.91T_r$$

$$1.0 > T_r > 0.8 \quad \rho_{r(l)} = 1 + \sqrt{34.7T_r - 25T_r^2 - 9.7}$$

$$T_r > 1.0 \quad \rho_{r(l)} = 1$$

b. Subroutine REDROD (TRED)

Approximates the reduced density difference (reduced density of the liquid minus reduced density of the vapor) as a function of reduced temperature, along the saturation line. Based upon the curves of Hougen and Watson, the law of rectilinear diameters, and some supplementary physical property data:

$$0.8 > T_r \quad \rho_d = 3.97 - 1.91 T_r$$

$$1.0 > T_r > 0.8 \quad \rho_d = -2.21 + 2.21 T_r + 2 \sqrt{34.7 T_r - 25. T_r^2 - 9.7}$$

$$1.0 > T_r \quad \rho_d = 0.0$$

c. Subroutine HCONDF (TEMP)

Approximates the enthalpy of the condensed phase fuel as a function of temperature:

$$T_{\text{freeze}} > T \quad H_F = C_{P_F} T$$

$$T \geq T_{\text{freeze}} \quad H_F = C_{P_F} T + \Delta H_{\text{fusion}}$$

d. Subroutine HCONDO (TEMP)

Approximates the enthalpy of the condensed phase oxidizer as a function of temperature. Same as HCONDF except with correct C_P and heat of fusion for the oxidizer.

e. Subroutine REDVIS (TRED)

Approximates the reduced viscosity of the liquid as a function of reduced temperature along the saturation line up to the critical temperature, and the reduced viscosity of the gas along the $P = 0$ line above the critical temperature.

$$0.6 > T_r \quad \mu_r = 0.55 T_r^{-5.68}$$

$$1.0 > T_r \geq 0.6 \quad \mu_r = 2.0 T_r^{-3.15}$$

$$T_r = 1.0 \quad \mu_r = 1.0$$

$$2.0 > T_r > 1.0 \quad \mu_r = 0.45 T_r$$

$$T_r > 2.0 \quad \mu_r = 0.572 T_r^{0.655}$$

f. Subroutine FANFAC (RENCH)

Approximates the Fanning Friction Factor as a function of Reynolds number based upon chamber diameter:

$$16 > Re \quad f = 1.0$$

$$2,000 > Re > 16 \quad f = 16 Re^{-1.0}$$

$$Re > 2000 \quad f = 0.06028 Re^{-0.2113}$$

A.6 PROGRAM USERS MANUAL

The TCC program is the first link of the CONTAM computer program. It may be run as a subprogram to CONTAM under control of subroutine EXEC (Link 0, 0) or as an independent program. The TCC program requires 150,000 words of core and is written in Fortran IV.

a. Input

A data set consists of 264 data values. These are normally punched four to a card on 64 cards. These numbers describe the engine, propellants, operating conditions and a number of general instructions or choices of program options.

The data is loaded using the INPUT 1 input editor (included as a subroutine in Link 0, 0). The Input 1 data cards are each punched with the values of four items of data and with the item numbers which identify what the particular data entries are, i.e., Data Item number 1 is the chamber length, data item number 2 is the chamber cross-sectional area at the injector end, etc. In punching cards to be read by INPUT 1, Card Column 1 is punched with a 1 to indicate that Input 1 is being used. Card columns 2 through 6 are punched with a data item number, card columns 7 through 15 and 16 through 17 are punched with a data value in scientific notation, i.e., a decimal value less than one and the exponent of 10 required to give the correct magnitude. If a minus sign is required for either the decimal fraction or the exponent it is overpunched over the number in columns 7 or 16. The other three data fields on the card are each treated the same way as the first, with 5 columns used for the data item number and 11 columns used for the fraction and exponent representing the data value. The case number should be punched in card columns 71 through 73 and card columns 66 through 70 should be punched with zeros unless the data editor capabilities are to be used. The use of the data editor will not be described here. The program is written to run only one case at a time.

The first step in the program reads the data and then prints it along with descriptive headings. This makes it easy to review the data to insure that all the values have been written, punched and entered correctly. The first program option is to terminate the run at this point, to permit a new set of data to be examined thoroughly before time is spent on calculations. The input data to this program is sufficiently complicated that occasional mistakes in entering the data may be expected and careful periodic examination of the contents of the data deck is highly recommended.

Certain of the data entries are not required for particular calculations and may be omitted (set to zero by the data editor). For a chamber of constant cross-section items, 3 and 4 may be omitted. For a computed vacuum hypergolic ignition, items 33, 34, 35, and 36 are omitted. When an igniter is used, items 33, 37, 38, 39 and 40 are omitted. When sea-level hypergolic ignition is being simulated by assigning a value for ignition delay, items 34, 35, 36, 37, 38, 39, and 40 are omitted. If injector heating of propellant and post-firing dribble are unimportant, the transition volumes (59 and 83) and the dribble volumes (60 and 84) may be omitted. The mono propellant, burning-rate constants (126, 127, 128, 146, 147, 148) are omitted for materials which do not burn in a mono propellant mode. When droplet trajectories are not desired, items 209, 210, and 211 are omitted. When flow rate overrides are not desired, 213, 214, 215, 217, 218, and 219 are omitted. When multiple pulses are not desired, 233 to 264 are omitted. The option flags are all set to zero for "normal" calculations, so they may all be omitted unless an option is specifically desired.

The data is printed out four numbers to a line, so that each line printed represents one card of input (Table A-29). Occasional unused data entries have been retained so as to separate the data deck into discrete sections which can be replaced or exchanged as a unit. The sections have the descriptive headings: CHAMBER DESCRIPTION, OPERATING CONDITIONS, FIRST BURN VALVE TIMING, IGNITION DESCRIPTION, etc.

The data entries are as follows:

<u>Item Number</u>	<u>Description</u>	<u>Units</u>
1.	Chamber Length	Inches
2.	A	Square Inches
3.	B	Square Inches/ Inch
4.	C	Square Inches/ Inch Squared

[The Chamber Cross-Sectional Area is Curve-fitted as a polynomial, $S = A + BX + CX^2$]

<u>Item Number</u>	<u>Description</u>	<u>Units</u>
5.	Throat Area	Square Inches
6.	Blank	
7.	Blank	
8.	Blank	
9.	External Pressure	psia
10.	Chamber Wall Temperature (Used for Vacuum Evaporation of Propellant deposited on walls)	°K
11.	Blank	
12.	Blank	
13.	Fuel Tank Pressure	psia
14.	Fuel Tank Temperature	Degrees K
15.	Injector Temperature (Fuel Side)	Degrees K
16.	Blank	
17.	Blank	
18.	Fuel Valve Opening Time (Mechanical Ramp Duration, not Electrical Time)	Seconds
19.	Blank	
20.	Fuel Valve Closing Time (Mechanical Ramp Duration, not Electrical Time)	Seconds
21.	Oxidizer Tank Pressure	psia
22.	Oxidizer Tank Temperature	Degrees K
23.	Injector Temperature (Oxidizer Side)	Degrees K

<u>Item Number</u>	<u>Description</u>	<u>Units</u>
24.	Blank	
25.	Blank	
26.	Oxidizer Valve Opening Time (Mechanical Ramp Duration, not Electrical Time)	Seconds
27.	Blank	
28.	Oxidizer Valve Closing Time (Mechanical Ramp Duration, not Electrical Time)	Seconds
29.	Fuel Valve Opening Time (Time First Valve Motion Occurs Opening for First Firing)	Seconds
30.	Oxidizer Valve Opening Time (Time First Valve Motion Occurs Opening for First Firing)	Seconds
31.	Fuel Valve Closing Time (Time First Valve Motion Occurs Closing for First Firing)	Seconds
32.	Oxidizer Valve Closing Time (Time First Valve Motion Occurs Closing for First Firing)	Seconds
33.	Assigned Ignition Delay (For Sea-Level Hypergolic Starts an Experimental Value for Ignition Delay Time is Entered)	Seconds
34.	Igniter Port Location (If an External Igniter is being Used, the Location, Downstream of the Injector, Where the Hot Gases enter the Chamber)	Inches
35.	Igniter Fuel Flow Rate (Flow Rate of Fuel Through the Igniter)	Pounds/Second

<u>Item Number</u>	<u>Description</u>	<u>Units</u>
36.	Igniter Oxidizer Flow Rate (Flow Rate of Oxidizer Through the Igniter)	Pounds/Second
37.	Activation Energy (Activation Energy of the Global Gas-Phase Ignition Reaction)	(Calories/Mole)
38.	Frequency Factor X Q (Molar Collision Frequency Multiplied by the Heat of Reaction of the Initiating Reaction)	(Cubic cm/Mole/Sec) X (Calories/Mole)
39.	Perfect Mixing Option (If This Flag is Set to 1.0, Ignition will Be calculated Only for the Well-mixed Free-stream gases, Ignoring the Possibility of Ignition in the Boundary Layers Around Droplets or on the Wetted Chamber Walls)	(0.0 or 1.0)
40.	No Axial Mixing Option (If This is Marked with a 1.0, Ignition will be Calculated Only for the New Flashed Fuel and Oxidizer Vapors Presuming no Axial Mixing of Vapor and Ignoring Ignition in the Boundary Layer)	(0.0 or 1.0)
41.	Fuel Line Length (Fuel Feed System Line Length)	Inches
42.	Fuel Line Area (Fuel Feed Line Inside Cross-Sectional Area)	Square Inches
43.	Fuel Restrictor Area (Area X Discharge Coefficient)	Square Inches
44.	Fuel Venturi Area (Cavitating Venturi Throat Area)	Square Inches

<u>Item Number</u>	<u>Description</u>	<u>Units</u>
45.	Fuel Valve Area (Port Area X Discharge Coefficient)	Square Inches
46.	Fuel Injection Area (Summation of (Port Area X Discharge Coefficient) of Injector Holes)	Square Inches
47.	Blank	
48.	Blank	
49.	Fuel Hole Diameter (Injector Hole Size)	Inches
50.	Fuel Hole Length (Injector Hole Length)	Inches
51.	Axial Location (Axial Location of Fuel Injection Point)	Inches
52.	Radial Location (Radial Location of Fuel Injection Point)	Inches
53.	Injection Angle (Outward Angles Counted as Positive)	Degrees
54.	Blank	
55.	Blank	
56.	Blank	
57.	Initial Void Volume (Initial Empty Volume in the Fuel Feed System)	Cubic Inches
58.	Blank	

<u>Item Number</u>	<u>Description</u>	<u>Units</u>
59.	Transition Volume (Volume of fuel that flows while the injection temperature decreases from the injector temperature to the tank temperature. (See Figure A-3.))	Cubic Inches
60.	Dribble Volume (Volume between the closed valve and the injector face)	Cubic Inches
61.	Check Valve Option (If this is marked 1.0 no reverse flow will be permitted in the fuel feed line)	(0.0 or 1.0)
62.	Blank	
63.	Blank	
64.	Blank (Entries 65-88 are identical to 41-64 except that they describe the oxidizer feed system instead of the fuel feed system.)	

<u>Item Number</u>	<u>Description</u>	<u>Units</u>
89.	Fuel Fan Length (Distance between the impingement point and the point at which the fuel is atomized when the stream turns 45 degrees at impingement)	Inches
90.	Oxidizer Fan Length	Inches
91.	Showerhead length/orifice diameter ratio (The distance, in orifice diameters, that an unimpinged stream travels from the injection point to atomize completely.)	
92.	Blank	
93.	Hold at triple point option (When this flag is set to 1.0 a propellant stream flashing in a low pressure environment will not freeze, but will stop as triple-point liquid)	(0.0 or 1.0)
94.	No initial dribble option (When this flag is set to 1.0, no liquid will be injected until the void volume is filled, even when the injector-temperature vapor pressure is higher than the chamber pressure)	(0.0 or 1.0)
95.	Flash cone angle (This is the included apex angle of the cone of spray formed by a flashing stream)	Degrees
96.	Blank	
97-101.	Drop Size 1-Drop Size 5 (These are the diameter ratios of the droplet groups to the mass-median droplet)	
102.	No wall breakup option (When this flag is set to 1.0 an unatomized stream hitting the wall is not atomized by the impact)	(0.0 or 1.0)

<u>Item Number</u>	<u>Description</u>	<u>Units</u>
103.	Drop Restitution Coefficient (The normal-velocity ratio for a droplet which hits the wall and bounces off)	
104.	Fraction sticking (The fraction of the droplets hitting the wall which stick to the wall instead of bouncing)	
105.	No Fuel Flash Option (When this flag is set to 1. the injected fuel stream will not flash even when it is highly superheated)	(0.0 or 1.0)
106.	No Oxidizer Flash Option (When this flag is set to 1.0 the injected oxidizer stream will not flash even when it is highly superheated)	(0.0 or 1.0)
107.	No Wall Flow Option (When this flag is set to 1.0 the propellant film on the wall will not flow axially under the influence of chamber gas shear forces)	(0.0 or 1.0)
108.	No Wall Burnoff Option (When this flag is set to 1.0 the propellant film on the wall will not burn off by heat transfer from the hot chamber gas)	(0.0 or 1.0)
109.	Fuel Boiling Point (The normal boiling point of the fuel)	Degrees K
110.	Fuel Freezing Point	Degrees K
111.	Fuel Critical Temperature	Degrees K
112.	Fuel Critical Pressure	psia
113.	Fuel Vapor specific heat (Fuel vapor specific heat at a temperature midway between the combustion gas and the droplet surface)	Calories / Gram / °K

<u>Item Number</u>	<u>Description</u>	<u>Units</u>
114.	Fuel Liquid Specific Heat (Liquid Fuel specific heat at the injection temperature)	Calories/ Gram/°K
115.	Blank	
116.	Fuel Molecular Weight (Molecular weight of fuel in the vapor phase)	Grams/Gram Mole
117.	Fuel Latent Heat of Vaporization (Latent heat of vaporization of fuel at the normal boiling point)	Calories/Gram
118.	Fuel Latent Heat of Fusion (Latent heat of fusion of the fuel at the freezing point)	Calories/Gram
119.	Fuel Liquid Thermal Conductivity	Calories/Sec/ Gm/°K
120.	Fuel Accommodation Coefficient (Coefficient for Langmuir-Knudsen vacuum evaporation rate)	
121.	Fuel Reference Temperature (Temperature at which values for density, viscosity and surface tension are given)	Degrees K
122.	Fuel Density (Density of liquid fuel at the reference temperature)	Grams/Cm ³
123.	Fuel Viscosity (Viscosity of liquid fuel at the reference temperature)	Poises
124.	Fuel Surface Tension (Surface tension of fuel at the reference temperature)	dynes/cm

<u>Item Number</u>	<u>Description</u>	<u>Units</u>
125.	Fuel Burning Rate Coefficient from droplet burning experiments ($-dD^2/dt$ for a burning fuel droplet in pure oxidizer vapor)	cm^2/sec
126.	Fuel Monopropellant Burning Rate Intercept	cm/sec
127.	Fuel Monopropellant Burning Rate Coefficient	$\text{cm}/\text{sec}/(\text{psia})^n$
128.	Fuel Monopropellant Burning Rate Exponent (Monopropellant burning rate values from liquid-strand experiments correlated by $r = A + BP^n$ where r is in centimeters per second and P is in psia)	
129-148	are identical to 109-128 except that they describe the oxidizer instead of the fuel	
149-159	Are the thermochemical equilibrium combustion product temperatures corresponding to fuel fractions of 0, 0.1, 0.2, ... 1.0	$^{\circ}\text{K}$
160.	Blank	
161-171	Are the mean molecular weights of the combustion products in thermochemical equilibrium at fuel fractions 0, 0.1, 0.2, ... 1.0	
172.	Blank	
173-183	Are the values for frozen Gamma of the equilibrium combustion products at fuel fractions 0, 0.1, 0.2, ... 1.0	
184.	Blank	
185.	Density of the contaminant material produced on the chamber wall	gm/cm^3
186.	Specific heat of the gases produced by the evaporation or pyrolysis of the wall-film material	$\text{Cal}/\text{gm}/^{\circ}\text{k}$
187.	Latent heat of evaporation or heat of ablation of the wall-film material	Cal/gm
188.	Surface temperature of the wall-film material during evaporation or pyrolysis	Degrees K

<u>Item Number</u>	<u>Description</u>	<u>Units</u>
189-199	Viscosity of the wall-film material at the temperature to be expected on the wall at fuel fractions 0, 0.1, 0.2, ... 1.0	
200.	Blank	
201.	Model time at which the calculations should be terminated	Seconds
202.	Integrating Time Interval	Seconds
203.	Number of time intervals between printing of a propellant mass disposition print	
204.	Number at time intervals between plotting of contaminant thickness profiles	
205.	Delete Graphics Option	(0.0 or 1.0)
	When this flag is set to 1.0 no graphics will be produced	
206	Delete Droplet Means Option	(0.0 or 1.0)
	(When this flag is set to 1.0 the mean diameters (D30, D31, D32) of the fuel and oxidizer droplets in the chamber are not calculated at each time interval.)	
207.	Delete Summaries Option	(0.0 or 1.0)
	(When this flag is set to 1.0 summaries are not printed to show the amounts, drop sizes and velocities of contaminant expelled during the four time intervals making up the pulse, i. e., the pre-ignition interval, the post-ignition start transient, the steady portion of the firing and the cutoff and dribbling after the valves close.)	
208.	Data Review Option	(0.0 or 1.0)
	(When this flag is set to 1.0 the data is read, certain checks and initializing steps are made and the raw data and some derived information is printed out with headings, however the chamber calculations are not performed. This makes it possible to check a new data deck for errors before proceeding with expensive calculations.)	

<u>Item Number</u>	<u>Description</u>	<u>Units</u>
209.	Fuel Trajectory Group (The chamber trajectory of one selected fuel or droplet group may be plotted each run. The chosen fuel size group is entered.)	(1.0 through 5.0)
210.	Oxid Trajectory Group (If a trajectory plot is wanted for an oxidizer droplet instead of a fuel droplet, the size group desired should be entered.)	(1.0 through 5.0)
211.	Trajectory Start Time (The trajectory is plotted for a fuel or oxidizer droplet which is injected at some chosen time. The time chosen should be entered.)	Seconds
212.	Steady State Time (The time points needed to print the interval summaries mentioned in item 207 are the ignition time, the time steady operation is attained, and the time the last valve closes. It is difficult to define the time steady operation is first attained, so the desired time is entered as an input value, based upon previous experience.) Flow rate overrides are provided for propellant feed systems where the internal dimensions are inadequately known, but where experimental values are available for flow rate versus pressure drop. To define the feed system resistances, it is necessary to specify a propellant flow rate, the associated pressure drop, and the discharge coefficient of the injector orifices.	Seconds
213.	Fuel Flow Rate	Pounds/Sec
214.	Fuel pressure drop	psi
215.	Fuel Injector Discharge Coefficient	
217-219	are corresponding values for the oxidizer feed system	

<u>Item Number</u>	<u>Description</u>	<u>Units</u>
216.	No Injector Friction Option (When this flag is set to 1.0 no frictional losses are calculated for the flow through the injector passages. The frictional loss correlation is correct only for the turbulent flow regime and gives excessively large values for small orifices which are in the laminar flow regime. This flag should be set to 1.0 for very small injector holes.)	(0.0 or 1.0)
221-231	Vacuum thrust coefficients are entered for combustion product gases having fuel fractions of 0., 0.1, 0.2, ... 1.0	
232.	Nozzle expansion area ratio	
233-264	Valve timing for the second through ninth pulses of engine operation	
233	Fuel valve, time of first motion opening on second pulse	(seconds)
234.	Oxidizer valve, time of first motion opening on second pulse	(seconds)
235.	Fuel Valve, time of first motion closing on second pulse	(seconds)
236.	Oxidizer valve, time of first motion closing on second pulse	(seconds)

b. Program Output

(1) Input Print

The first print which is produced by the program is a recapitulation of the program input.

(2) Propellant Property Print

The second print produced is a table of calculated propellant properties versus temperature. These values can be compared with known experimental values to assure that the program physical properties sub-routines are giving an adequate representation of the true values. The values printed are liquid enthalpy, vapor enthalpy, vapor pressure, liquid density, liquid viscosity, and surface tension. These are given for evenly spaced

intervals of reduced temperature, with the corresponding absolute temperature also given. The units are calories/gram, psia, grams/cc, poise, dyne/cm and degrees K.

(3) Print of Time-Varying Rocket System Parameters

At each integrating time interval, values are printed for 48 of the more important system variables. This print consists of six lines containing eight values per line.

The first line contains the model time in milliseconds, the chamber pressure in psia, the ignition state of the chamber (1.0 for ignited, 0.0 for unignited), the mass fraction of the gas or vapor in the chamber which is fuel-derived, the chamber temperature in degrees K, the mean molecular weight of the gases or vapors in the chamber, the specific heat ratio for the gases or vapors in the chamber and the vacuum thrust coefficient for the gas or vapor phase flowing from the chamber.

The second line contains the fuel and oxidizer injection rates in pounds per second, and the fuel and oxidizer feed line flow rates in pounds per second. The injection flowrate and feed-line flowrate will differ when the injector is dribbling into a vacuum after the propellant valves close, or when a partially empty dribble volume is being filled before the injector primes. The void volumes on fuel and oxidizer sides of the injector are given in cubic inches. The dribble injection rate will decrease to zero when the dribble volume is emptied. The fuel and oxidizer injection temperatures are given in degrees Kelvin. The injection temperatures are equal to the injector temperature, until a volume of propellant has flowed out of the tank equal to the dribble volume, then the temperature linearly decreases to the tank temperature, with the decrease spread out over the prescribed transition volume.

The third line contains the evaporation rates of the fuel drop ensemble and the oxidizer drop ensemble in pounds per second. The fuel flash rate and oxidizer flash rate are given in pounds per second of vapor produced by the vacuum flashing of the injected streams. The rates of propellant burnoff from the wall is given for fuel and oxidizer in pounds per second. The heat for wall burnoff comes from heat transferred from the chamber gases. The rates of vacuum evaporation from the wall are given for fuel and oxidizer in pounds per second. The heat for vacuum evaporation is transferred from the chamber wall through the propellant film to the evaporating surface.

The fourth line contains the mass of fuel-derived combustion gas or vapor in the chamber in pounds. The mass of oxidizer-derived gas or vapor is given similarly. The masses of fuel droplets and oxidizer droplets in the chamber are given in pounds. The masses of injected, but not yet atomized fuel and oxidizer are given under the headings Fuel Streams and Oxidizer Streams. The mass of fuel and oxidizer deposited on the walls are the final entries of the fourth line.

The first and second entries of the fifth line give the mass rate of efflux for fuel and oxidizer-derived vapors or combustion-product gases

in pounds per second, the third and fourth entries are the mass rate of ejection through the throat for incompletely burned fuel drops and oxidizer drops in pounds per second. The rate at which propellant film on the wall is being flowed through the throat is given next in pounds per second. "Gas Fraction" is the instantaneous value for the fraction of the total mass efflux which is in the gas phase. The final entry on this line is thrust, in pounds force. The thrust includes the axial momentum rate of the expelled droplets, and the thrust from the gas phase products.

The sixth line starts with the mass-median droplet diameter for the fuel and oxidizer spray being produced this time interval. The next two entries give fuel and oxidizer stream injection velocities. The Beta angle is the resultant angle after the fuel and oxidizer streams have impinged. It is measured in degrees, with positive values being taken outward from the centerline. The mass out of tank is total mass of propellant flowed from the propellant tanks from the start of the run, in pounds. The integral $PC \times DT$ is the area under the curve of chamber-pressure-versus time, in psia x seconds. Total impulse is the time integral of thrust in pound-force x seconds.

(4) Summary Prints and Special Messages

Other prints which may occur interspersed with the normal six line prints are summary prints and special messages. The most frequent special messages specify when ignition or extinguishment occurs in the combustion chamber. Other special messages indicate minor errors, such as failure to converge to within 2 percent of the correct surface temperature during vacuum evaporation, or catastrophic errors such as calculation of a negative chamber pressure.

The propellant disposition summary, whose frequency is specified in data item 203 consists of seven lines of numbers. The first four lines give a mass balance for all fuel and oxidizer injected up to the present time. The masses, in grams, are given for total injected fuel, oxidizer and sum of fuel plus oxidizer, and the amounts expelled as gas, as droplets and as wall-film. Also given are the masses currently retained as gas, as droplets and as wall film. The last five lines gives the numbers of fuel drops and oxidizer drops injected and ejected up to the present time. The summation of droplet diameters, diameters squared, diameters cubed and axial momentum is also given, which makes it possible to calculate the mean diameters and mean axial velocities of expelled droplets for the interval between any two summary prints.

Another type of summary which may be printed gives values for four time intervals of motor operation, i. e., the pre-ignition interval, the ignition transient, the steady operation interval and the cutoff interval. The time and description of the interval is given, and the masses are given in grams of fuel, oxidizer and sum of fuel plus oxidizer expelled during the time interval in the form of droplets and in the form of wall film. The droplet diameter means, D_{30} , D_{31} , and D_{32} as well as mean axial velocity are given for the droplets expelled during the interval. Droplet diameters are given in microns, axial velocity in feet per second.

(5) Final Performance Summary

After the last of the time-steps is printed, a performance summary is printed. The mass flowed out of tank is given, the mass flowed through the injector is given and the mass flowed through the nozzle is given. These values are not generally the same, because of filling or voiding of the injector dribble volumes, and because of increase or depletion of propellant mass stored in the combustion chamber in the forms of gas, droplets or streams, and wall-film. The mixture ratio, C-Star and specific impulse are calculated on each of these propellant mass bases. The pressure time integral for the entire pulse and the total impulse are also printed. The final print also gives the disposition of injected propellant for the entire firing. The fractions of injected fuel, oxidizer and total propellant expelled in the form of gas, droplets and as wall-film are given, and the fraction retained in the chamber as gas, droplets and wall film are given. The mean diameters for injected and ejected fuel and oxidizer are given, in microns. The mean axial velocity for injected and ejected fuel and oxidizer droplets are given in feet per second. The calculated size distribution for injected and ejected fuel and oxidizer is given. When this is plotted, it very strongly shows the five-group approximation for injected droplet size, which is a computational artifact, however, also apparent are the real effects of flashing versus impinging stream atomization, the preferential burning of small droplets, the segregation by drag versus momentum effects, etc.

(6) Computer Graphics

The computer graphics include the trajectory of the specified fuel or oxidizer droplet, forty-four time-varying system parameters plotted versus time, and a specified number of instantaneous profile plots of wall deposit thickness versus chamber length. The wall deposit plots may be eliminated by making input item 204 a large number. All graphics may be eliminated by setting input item 205 equal to 1. The plots are as follows: (all variables are plotted versus time in milliseconds except where specifically stated otherwise).

1. Droplet Trajectory—Axial position in inches.
2. Droplet Trajectory—Radial position in inches.
3. Droplet Trajectory—Axial position in inches versus radial position in inches.
4. Chamber pressure in psia.
5. Fuel Valve Trace—Fraction of full-open port area.
6. Oxidizer Valve Trace—Same as for fuel.
7. Fuel Flow Rate from the Tank in Pounds per Second.
8. Oxidizer Flowrate—Same as for fuel.
9. Flowrate of Fuel Plus Oxidizer—Same as for fuel.
10. Fuel Injection Rate in Pounds per Second.
11. Oxidizer Injection Rate—Same as for fuel.

12. Fuel Droplet Mass—Pounds (total mass of fuel in-flight in the chamber, sum of streams and droplets).
13. Oxidizer Droplet Mass—Same as for fuel.
14. Total Droplet Mass—Fuel plus oxidizer.
15. Fuel on the Wall—Pounds.
16. Oxidizer on the Wall—Pounds.
17. Propellant on the Wall—Fuel Plus Oxidizer, in pounds.
18. Gas Mass—Pounds (mass of vapors or gas-phase combustion products in the chamber).
19. Gas Fuel Fraction—Fraction of the chamber gas which is derived from fuel.
20. Chamber Temperature—Degrees Kelvin (temperature of the gaseous combustion products).
21. Fuel Evaporation Rate—Pounds per second (rate at which fuel vapors are entering the chamber from all sources, vacuum flashing of streams, droplet evaporation, wall film burnoff and wall film vacuum evaporation).
22. Oxidizer Evaporation Rate—Same as for fuel.
23. Total Evaporation Rate—Fuel plus oxidizer.
24. Gas Outflow Rate—Pounds per second (sonic or subsonic throat flow of gas or vapor).
25. Fuel Droplet Outflow Rate—Pounds per second. (Mass of unburned droplets ejected each interval divided by length of the time interval. To reduce random fluctuation, this value is time-averaged over four time intervals and has some lag.)
26. Oxidizer Droplet Outflow Rate—Same as fuel.
27. Total Droplet Outflow Rate—Fuel plus oxidizer.
28. Fuel Film Outflow Rate—Pounds per second (rate of flow of fuel-derived wall-film through the throat).
29. Oxidizer Film Outflow Rate—Same as fuel.
30. Total Film Outflow—Fuel plus oxidizer.
31. Fraction Vaporized—The fraction of the total material expelled each time interval which is in the gas phase. The total material expelled is gas plus unburned droplets plus wall film. To reduce random fluctuation, this value is time-averaged over four time intervals, and has some lag.

32. Stream Beta Angle—Degrees outward from the chamber center-line. Angle of the resultant stream from the impingement of fuel and oxidizer.
33. Fuel Fan length—Inches. (Axial distance from the injector face where atomization is complete. Longest when other stream is absent or is flash atomized; depends upon momentum ratio when both streams are present; zero when the stream is flash atomizing.)
34. Oxidizer Fan Length—Same as fuel.
35. Fuel Droplet Diameter—Microns (mass-median atomization droplet diameter for fuel being injected this time interval).
36. Oxidizer Droplet Diameter—Microns (same as fuel).
37. Fuel Flash Quality—Mass fraction of the fuel injected this time interval which flashes to vapor.
38. Oxidizer Flash Quality—Same as fuel.
39. Chamber Fuel D30 (Mass-Number Mean Diameter for Entire Chamber Population of Fuel Droplets).
40. Chamber Fuel D31 (Mass-Diameter Mean diameter for Entire Chamber Population of Fuel Droplets).
41. Chamber Fuel D32 (Mass-Surface Mean diameter for Entire Chamber Population of Fuel Droplets).
42. Chamber Oxidizer D30 (Same as Fuel).
43. Chamber Oxidizer D31 (Same as Fuel).
44. Chamber Oxidizer D32 (Same as Fuel).
45. Fuel Voided—Cubic inches (volume of injector fuel passages unfilled with liquid).
46. Oxidizer Voided—Cubic inches (same as fuel).
47. Thrust-Pounds (Calculated Engine Thrust).
48. To End—Thickness on wall versus percent of chamber length.

The number of prints depends upon the value specified for data item 204. The thickness of the deposit of fuel plus oxidizer on the chamber wall is plotted for each of the one hundred axial segments into which the chamber is divided. The thickness profile is plotted for every n^{th} computational time interval, where n is input as data item 204.

A. 7 SAMPLE CASE

Table A-V consists of a sample case for the TCC program. Illustrated in the following order are (1) the load sheets used to punch the data, (2) a listing of the control cards, (3) the data deck used, and (4) a representative sample of the prints and graphics produced.

Only 150,000 storage locations are called for (compared to 220,000 to run the complete CONTAM program) because of the overlay structure and the LIBLIST system routine which avoids calling subroutines which are not required by the particular portion of the program being run.

The printer output consists of the input data print, the derived property print, the print of time-varying system parameters (abbreviated), summary prints, ignition and extinguishment prints, the performance summary, and the disposition of propellant print.

A sampling of computer graphics includes a valve trace, chamber pressure, flow rate of oxidizer in the feedline and injector (illustrating the injector priming and the large dribble flowrate of oxidizer). The droplet mass plot shows that there is a large mass of oxidizer droplets in the chamber during the dribble period. The wall-mass plot shows accumulation of propellant on the wall during the start transient and dribble period, and its removal by burnoff and by vacuum evaporation.

Table A-V. SAMPLE CASE FOR TCC PROGRAM

60-115 19-611

7090 DATA LOAD SHEET
DATA INPUT 1

PROBLEM H-607 PAGE 1 OF 4
PREPARED BY W.T. WEBBER DATE _____

MUST BE FILLED IN FOR
PROPER PROCESSING

66-0889-7071 7174-76
000 00001
BD RR CASE

QUAN	LOC	+	VALUE	E	QUAN	LOC	+	VALUE	E
	1		107	1		33		0	0
	2		1368	0		34		0	0
	3		1427	0		35		0	0
	4		-2268	0		36		0	0
	5		0298	0		37		5200	4
	6		0	0		38		34	15
	7		0	0		39		0	0
	8		0	0		40		0	0
	9		000001	0		41		480	3
	10		294	3		42		0281	0
	11		0	0		43		00454	0
	12		0	0		44		0281	0
	13		180	3		45		0281	0
	14		294	3		46		000196	0
	15		294	3		47		0	0
	16		0	0		48		0	0
	17		0	0		49		0079	0
	18		001	0		50		0625	0
	19		0	0		51		0	0
	20		001	0		52		045	0
	21		165	3		53		-45	2
	22		294	3		54		0	0
	23		294	3		55		0	0
	24		0	0		56		0	0
	25		0	0		57		00113	0
	26		001	0		58		0	0
	27		0	0		59		0	0
	28		001	0		60		00113	0
	29		0	0		61		0	0
	30		0	0		62		0	0
	31		01	0		63		0	0
	32		01	0		64		0	0

KEY PUNCH: STANDARD DATA INPUT 1

Table A-V-Continued

00 00 0 0 0 0

7090 DATA LOAD SHEET
DATA INPUT 1

PROBLEM H-607 PAGE 2 OF 4
PREPARED BY W.T. WEBBER DATE _____

MUST BE FILLED IN FOR
PROG. PROCESSING

66	6869	7071	7374	76
000	0000	001	<input checked="" type="checkbox"/>	
BD	RR	CASE		

QUAN	LOC	+	VALUE	-	E
	65		480		3
	66		0281		0
	67		00636		0
	68		0281		0
	69		0281		0
	70		000272		0
	71		0		0
	72		0		0
	73		0093		0
	74		0625		0
	75		0		0
	76		045		0
	77		45		2
	78		0		0
	79		0		0
	80		0		0
	81		00058		0
	82		0		0
	83		0		0
	84		00058		0
	85		0		0
	86		0		0
	87		0		0
	88		0		0
	89		024		0
	90		027		0
	91		10		2
	92		0		0
	93		0		0
	94		1		1
	95		30		2
	96		0		0

QUAN	LOC	+	VALUE	-	E
	97		198		0
	98		759		0
	99		1		1
	100		123		1
	101		23045		1
	102		0		0
	103		1		1
	104		5		0
	105		0		0
	106		0		0
	107		0		0
	108		0		0
	109		360		3
	110		222		3
	111		594		3
	112		1195		4
	113		995		0
	114		69		0
	115		0		0
	116		46074		2
	117		210		3
	118		675		2
	119		000545		0
	120		1		1
	121		300		3
	122		88		0
	123		0104		0
	124		47		2
	125		0325		0
	126		0		0
	127		0		0
	128		0		0

KEY PUNCH: STANDARD DATA INPUT 1

Table A-V-Continued

DD FORM 19 611

7090 DATA LOAD SHEET
DATA INPUT 1

PROBLEM H-607 PAGE 3 OF 4
PREPARED BY W.T. WEBBER DATE _____

MUST BE FILLED IN FOR
PROPER PROCESSING

66 6869 7071 7374 76
000 0000
BD RR CASE

QUAN	LOC	+	VALUE	+	E	QUAN	LOC	+	VALUE	+	E
	129		294		3		161		46,008		2
	130		362		3		162		2879		2
	131		431		3		163		2641		2
	132		1470		4		164		2339		2
	133		298		0		165		1988		2
	134		360		0		166		1675		2
	135		0		0		167		1441		2
	136		46,008		2		168		1391		2
	137		99		2		169		1400		2
	138		392		2		170		1410		2
	139		000306		0		171		1429		2
	140		1		1		172		0		0
	141		300		3		173		112		1
	142		145		1		174		1252		1
	143		00446		0		175		1220		1
	144		28		2		176		1217		1
	145		027		0		177		1235		1
	146		0		0		178		1268		1
	147		0		0		179		1309		1
	148		0		0		180		1299		1
	149		300		3		181		1270		1
	150		2103		4		182		1247		1
	151		3084		4		183		1228		1
	152		3397		4		184		0		0
	153		3061		4		185		1		1
	154		2368		4		186		1		1
	155		1705		4		187		100		3
	156		1433		4		188		500		3
	157		1344		4		189		00446		0
	158		1266		4		190		024		0
	159		1190		4		191		043		0
	160		0		0		192		068		0

KEY PUNCH: STANDARD DATA INPUT 1

Table A-V-Continued

4612,2.500,800,000,120000,220000,
 ID HOFFMAN 403833PBR047612 404612 9660400010
 REQUEST,CONTAM,RY, (14640)
 RELIND(CONTAM)
 COPYHF(CONTAM,REL)
 RELIND(REL)
 RETURN(CONTAM)
 RFL,100,
 RFL,220000,
 SETCORE,
 LOAD(REL)
 *
 \$NCASE ICASE=13
 \$IPATH TCC=T,5

100001107000000001000021368000000000000314970000000000042680000000	00001
100005029800000000000600000000000000070000000000000008000000000000	00001
10000900000001000000001029400000000300001100000000000001200000000000	00001
10001318000000000300014294000000003000152940000000000016000000000000	00001
100017000000000000000180010000000000019000000000000002000000000000	00001
1000211650000000030002229400000000300023294000000003000240000000000	00001
1000250000000000000002600100000000000270000000000000028001000000000	00001
100029000000000000000300000000000000310100000000000032010000000000	00001
100033000000000000000340000000000000350000000000000360000000000000	00001
100037520000000004000383400000000150003900000000000040000000000000	00001
100041460000000003000420281000000000043004540000000004402810000000	00001
10004502810000000004600019600000000470000000000048000000000000	00001
10004900790000000000050062500000000005100000000000052045000000000	00001
10005305000000000002000540000000000005500000000000056000000000000	00001
100057001130000000000580000000000005900000000000060001130000000	00001
100061000000000000000620000000000006300000000000064000000000000	00001
100065480000000003000660281000000000067006836000000006802810000000	00001
100069028100000000007000027200000000710000000000072000000000000	00001
100073009300000000007406250000000007500000000000076045000000000	00001
10007745000000000200078000000000007900000000000080000000000000	00001
1000810005800000000082000000000008300000000000084000580000000	00001
1000850000000000000086000000000008700000000000088000000000000	00001
10008902400000000000900270000000000910000000000092000000000000	00001
1000930000000000000094100000000001000953000000000200096000000000	00001
100097190000000000009875900000000099100000000010010012300000001	00001
1001012304500000010010200000000000103100000000010410450000000000	00001
100105000000000000010600000000000107000000000000108000000000000	00001
1001093600000000030011022000000003001115940000000030011211950000004	00001
10011399500000000001146900000000000115000000000000116460740000002	00001
100117210000000003001186750000000200119000545000000012010000000001	00001
1001213000000000030012280000000000123010400000000012447000000002	00001
10012503250000000000126000000000000127000000000000128000000000000	00001
10012929400000000300130262000000003001314310000000030013214700000004	00001
1001332900000000000134360000000000013500000000000013646000000002	00001
10013709000000000001383000000000000139000000000000140000000000001	00001
100141300000000003001421450000000100143004460000000014426000000002	00001
10014502700000000000146000000000000147000000000000148000000000000	00001
100149300000000003001502103000000400151300400000040015233970000004	00001
100153306100000040015423680000004001551705000000400156143300000004	00001
10015713440000004001581266000000400159119000000040016000000000000	00001
100161460080000002001622879000000200163264100000020016423390000002	00001
10016519880000002001661675000000200167144100000020016813910000002	00001
1001691400000000200170141000000200171142900000020017200000000000	00001
100173000000000000017400000000000175000000000000176000000000000	00001
10017712350000001001781268000000100179130900000010018012990000001	00001
10018112700000001001821247000000010018312280000001001840000000000	00001

Table A-V-Continued

10018510000000000100186100000000010018710000000000300110850000000003	00001
1001890044600000000190024000000000019104300000000019206000000000	00001
100193081000000000019410000000000001950820000000000196064000000000	00001
100197046000000000019802900000000001990104000000000200000000000000	00001
1002010200000000000202000100000000002031000000000020420430000000002	00001
1002050000000000000206000000000000020710000000000100208000000000000	00001
100209300000000000021000000000000002110000000000000212000000000000	00001
100213000000000000021400000000000002150000000000000216100000000001	00001
10021700000000000002180000000000000219000000000000022000000000000	00001
100221192400000001002221802800000100223190820000010022419617000001	00001
10022518470000000100226181220000010022718480000010022819331000001	00001
100229197940000001002301922400000100231189590000010023240000000002	00001
10023300000000000002340000000000000235000000000000023600000000000	00001

NOT REPRODUCIBLE

Table A-V-Continued

REFERENCE NUMBER, 1 CASE NO, 300

THE INPUT DATA FOR THIS CASE ARE AS FOLLOWS

CHAMBER DESCRIPTION

CHAMBER LENGTH	INJECTOR AREA	LINEAR TAPER	PARABOLIC TAPER
1,070000	,136000	,142700	-,226800
THROAT AREA	0,000000	0,000000	0,000000
,029500			

OPERATING CONDITIONS

EXTERNAL PRESSURE	WALL TEMPERATURE	0,000000	0,000000
,000000	294,000000		
FUEL TANK PRESS	FUEL TANK TEMP	INJECTOR TEMP	0,000000
180,000000	294,000000	294,000000	
0,000000	FUEL VALVE OPEN DT	0,000000	FUEL VALVE CLOSE DT
	,001000		,001000
OXID TANK PRESS	OXID. TANK TEMP	INJECTOR TEMP	0,000000
160,000000	294,000000	294,000000	
0,000000	OXID. VALVE OPEN DT	0,000000	OXID VALVE CLOSE DT
	,001000		,001000

FIRST BURST VALVE TIMING

FUEL VALVE OPEN	OXID VALVE OPEN	FUEL VALVE CLOSE	OXID VALVE CLOSE
0,000000	0,000000	,010000	,010000

IGNITION DESCRIPTION

ASSIGNED DELAY	IGNITER PORT LOC,	FUEL FLOW RATE	OXID FLOW RATE
0,000000	0,000000	0,000000	0,000000
ACTIVATION ENERGY	FREQ. FACT, X 10	PERFECT MIXING	NO AXIAL MIXING
5200,000000	3,400000E+14	0,000000	0,000000

NOT REPRODUCIBLE

Table A-V-Continued

FUEL FEED SYSTEM			
LINE LENGTH 489.000000	LINE AREA .028100	RESTRICTOR AREA .004540	VENTURI AREA .026100
VALVE AREA .028100	INJECTION AREA .000196	0.000000	0.000000
HOLE DIAMETER .007900	HOLE LENGTH .042500	AXIAL LOCATION 0.000000	RADIAL LOCATION .045000
INJECTION ANGLE 45.000000	0.000000	0.000000	0.000000
INIT. VOID VOLUME .001130	0.000000	TRANSITION VOLUME 0.000000	DRIPPLE VOLUME .001130
CHECK VALVES 0.000000	0.000000	0.000000	0.000000
OXIDIZER FEED SYSTEM			
LINE LENGTH 489.000000	LINE AREA .028100	RESTRICTOR AREA .006360	VENTURI AREA .026100
VALVE AREA .028100	INJECTION AREA .000272	0.000000	0.000000
HOLE DIAMETER .008300	HOLE LENGTH .042500	AXIAL LOCATION 0.000000	RADIAL LOCATION -.045000
INJECTION ANGLE 45.000000	0.000000	0.000000	0.000000
INIT. VOID VOLUME .006580	0.000000	TRANSITION VOLUME 0.000000	DRIPPLE VOLUME .006580
CHECK VALVES 0.000000	0.000000	0.000000	0.000000
ATOMIZATION PARAMETERS			
FUEL FAN LENGTH 1.000000	OXID FAN LENGTH 1.000000	SHOWERHEAD L/D 10.000000	0.000000

NOT REPRODUCIBLE

Table A-V—Continued

HOLD AT TRIPLE PT 1.000000	NO INIT. DRIBBLE 1.000000	FLASH CONE ANGLE 30.000000	0.000000
DROP SIZE 1 .198000	DROP SIZE 2 .759000	DROP SIZE 3 1.000000	DROP SIZE 4 1.240000
DROP SIZE 5 2.304500	NO WALL BREAKUP 0.000000	DROP RESTITUTION 1.000000	FRACTION STICKING .500000
NO FUEL FLASH 0.000000	NO OXID FLASH 0.000000	NO WALL FLOW 0.000000	NO WALL RUNOFF 0.000000

FUEL PROPERTIES

BOILING POINT 360.000000	FREEZING POINT 222.000000	CRITICAL TEMP. 594.000000	CRITICAL PRESS. 1195.000000
VAPOR CP. .895000	LIQUID CP. .690000	0.000000	MOL. WEIGHT 46.074000
LATENT HEAT VAP. 210.000000	LATENT HEAT FUS. LIQ. THERM. COND. 67.500000	.000545	ACCOM. COEFF. 1.000000
REFERENCE TEMP. 300.000000	DENSITY .850000	VISCOSITY .016400	SURFACE TENSION 47.000000
BURNING RATE K .032500	MONO. INTERCEPT MONO. COEFFICIENT 0.000000	0.000000	MONO. EXPONENT 0.000000

OXIDIZER PROPERTIES

BOILING POINT 294.000000	FREEZING POINT 262.000000	CRITICAL TEMP. 431.000000	CRITICAL PRESS. 1470.000000
VAPOR CP. .298000	LIQUID CP. .360000	0.000000	MOL. WEIGHT 46.000000
LATENT HEAT VAP. 99.000000	LATENT HEAT FUS. LIQ. THERM. COND. 39.200000	.000306	ACCOM. COEFF. 1.000000
REFERENCE TEMP. 300.000000	DENSITY 1.450000	VISCOSITY .004460	SURFACE TENSION 28.000000
BURNING RATE K .027000	MONO. INTERCEPT MONO. COEFFICIENT 0.000000	0.000000	MONO. EXPONENT 0.000000

NOT REPRODUCIBLE

Table A-V—Continued

COMBUSTION GAS PROPERTIES

TEMP, 1 300.00000	TEMP, 2 2103.00000	TEMP, 3 3094.00000	TEMP, 4 3397.00000
TEMP, 5 3061.00000	TEMP, 6 2368.00000	TEMP, 7 1705.00000	TEMP, 8 1433.00000
TEMP, 9 1344.00000	TEMP, 10 1266.00000	TEMP, 11 1190.00000	0.00000
MOL. WT, 1 46.00000	MOL. WT, 2 28.79000	MOL. WT, 3 26.41000	MOL. WT, 4 23.39000
MOL. WT, 5 19.86000	MOL. WT, 6 16.75000	MOL. WT, 7 14.41000	MOL. WT, 8 13.91000
MOL. WT, 9 14.00000	MOL. WT, 10 14.10000	MOL. WT, 11 14.29000	0.00000
GAMMA 1 1.12000	GAMMA 2 1.25200	GAMMA 3 1.22000	GAMMA 4 1.21700
GAMMA 5 1.23500	GAMMA 6 1.26800	GAMMA 7 1.30900	GAMMA 8 1.29900
GAMMA 9 1.27000	GAMMA 10 1.24700	GAMMA 11 1.22800	0.00000

CONTAMINANT PROPERTIES

DENSITY 1.00000	VAPOR CP, 1.00000	LATENT HEAT 100.00000	DECOMP. TEMP, 500.00000
VISCOSITY 1 .04400	VISCOSITY 2 .05000	VISCOSITY 3 .05600	VISCOSITY 4 .06200
VISCOSITY 5 .06800	VISCOSITY 6 .07400	VISCOSITY 7 .08000	VISCOSITY 8 .08600
VISCOSITY 9 .09200	VISCOSITY 10 .09800	VISCOSITY 11 .10400	0.00000

Table A-V—Continued

GENERAL INSTRUCTIONS

STOP TIME .020000	TIME INTERVAL .000100	PRINT ONE OUT OF 10,000000	PLOT ONE OUT OF 30,000000
DELETE GRAPHICS 0.000000	DELETE DROP MEANS 0.000000	DELETE SUMMARIES 1,000000	DATA REVIEW ONLY 0,000000
FUEL TRAJ. GROUP 3,000000	OXID TRAJ. GROUP 0,000000	TRAJ. START TIME .006000	STEADY-STATE TIME 0,000000

FLOW RATE OVERRIDES

FUEL FLOW RATE 0,000000	FUEL PRESS. DROP 0,000000	DISCHARGE COEFF. 0,000000	NO INJ. FRICTION 1,000000
OXID FLOW RATE 0,000000	OXID PRESS. DROP 0,000000	DISCHARGE COEFF. 0,000000	0,000000

THRUST COEFFICIENT TABLE

CF VAC 1 1,924000	CF VAC 2 1,812000	CF VAC 3 1,908200	CF VAC 4 1,941700
CF VAC 5 1,847000	CF VAC 6 1,812200	CF VAC 7 1,868000	CF VAC 8 1,933100
CF VAC 9 1,922400	CF VAC 10 1,922400	CF VAC 11 1,895900	EXP. AREA RATIO 40,000000

NOT REPRODUCIBLE

Table A-V--Continued

SECOND PULSE TIMING			
FUEL VALVE OPEN .020000	OXID VALVE OPEN .020000	FUEL VALVE CLOSE .030000	OXID VALVE CLOSE .030000
THIRD PULSE TIMING			
FUEL VALVE OPEN 0,000000	OXID VALVE OPEN 0,000000	FUEL VALVE CLOSE 0,000000	OXID VALVE CLOSE 0,000000
FOURTH PULSE TIMING			
FUEL VALVE OPEN 0,000000	OXID VALVE OPEN 0,000000	FUEL VALVE CLOSE 0,000000	OXID VALVE CLOSE 0,000000
FIFTH PULSE TIMING			
FUEL VALVE OPEN 0,000000	OXID VALVE OPEN 0,000000	FUEL VALVE CLOSE 0,000000	OXID VALVE CLOSE 0,000000
SIXTH PULSE TIMING			
FUEL VALVE OPEN 0,000000	OXID VALVE OPEN 0,000000	FUEL VALVE CLOSE 0,000000	OXID VALVE CLOSE 0,000000
SEVENTH PULSE TIMING			
FUEL VALVE OPEN 0,000000	OXID VALVE OPEN 0,000000	FUEL VALVE CLOSE 0,000000	OXID VALVE CLOSE 0,000000
EIGHTH PULSE TIMING			
FUEL VALVE OPEN 0,000000	OXID VALVE OPEN 0,000000	FUEL VALVE CLOSE 0,000000	OXID VALVE CLOSE 0,000000
NINTH PULSE TIMING			
FUEL VALVE OPEN 0,000000	OXID VALVE OPEN 0,000000	FUEL VALVE CLOSE 0,000000	OXID VALVE CLOSE 0,000000

INPUT UNITS ARE INCHES, PSIA, SECONDS AND DEGREES KELVIN,
PROPELLANT PROPERTIES ARE IN GRAMS/CC, POISE, DYNE/CM²,

NOT REPRODUCIBLE

Table A-V--Continued

DERIVED FUEL PROPERTIES							
REDUCED TEMP.	TEMPERATURE	LIQ. ENTHALPY	VAP. ENTHALPY	VAPOR PRESSURE LIQ.	DENSITY	VISCOSITY	SURFACE TENSION
.30000	175.20000	122.58900	345.88900	.001013	.994673	.206413	76.718089
.40000	237.60000	231.44400	404.11200	.021783	.936721	.339109	60.845285
.50000	297.00000	272.43000	463.21500	1.126119	.862625	.511011	47.606346
.60000	355.40000	313.41600	522.31600	13.047653	.826893	.603909	36.641594
.70000	413.80000	354.40200	581.42100	69.252066	.773971	.602402	27.609749
.80000	475.20000	395.38800	640.52400	232.315246	.715044	.601577	20.487937
.90000	534.60000	436.37400	699.62700	581.695073	.624003	.601088	19.011953
1.00000	594.00000	477.36000	758.73000	1195.000000	.292811	.600390	.000000
DERIVED TAJ PROPERTIES							
REDUCED TEMP.	TEMPERATURE	LIQ. ENTHALPY	VAP. ENTHALPY	VAPOR PRESSURE LIQ.	DENSITY	VISCOSITY	SURFACE TENSION
.30000	174.30000	46.54500	194.95940	.000000	1.865399	.365550	76.696121
.40000	172.40000	62.16400	207.53320	.000070	1.763515	.671334	60.847856
.50000	215.50000	77.59000	220.64700	.035892	1.655691	.620094	47.592715
.60000	251.40000	93.19600	233.49090	1.724303	1.550747	.607130	36.631102
.70000	301.70000	147.81200	246.33450	21.667087	1.445903	.604381	27.631823
.80000	344.50000	193.32300	259.17840	132.031787	1.340979	.602877	20.482070
.90000	387.90000	174.54400	272.02220	512.146110	1.170403	.601955	19.019084
1.00000	431.00000	194.35000	284.86600	1470.000000	.549151	.600712	.000000

NOT REPRODUCIBLE

Table A-V-Continued

THE CALCULATED RUN PARAMETERS ARE PRINTED FOR EACH INTERVAL OF TIME FOLLOWING START

TIME MILLISEC	CHAMBER PRESS	IGNITION	FUEL FRACTION	CHAMBER TEMP K	MOL WT.	GAMMA	CF VAC
0.	5.00000E-08	0.	0.	300,000	46.0050	1.16944	0.
FUEL INJ RATE	OXID INJ RATE	FUEL FLOW RATE	OXID FLOW RATE	FUEL VOID VOL	OXID VOID VOL	FUEL INJ TEMP	OXID INJ TEMP
0.	0.	0.	0.	1.13000E-03	5.17935E-04	0.	0.
FUEL DROP BURN	OXID DROP BURN	FUEL FLASH RATE	OXID FLASH RATE	FUEL WALL BURN	OXID WALL BURN	FUEL WALL EVAP	OXID WALL EVAP
0.	0.	0.	0.	0.	0.	0.	0.
FUEL GAS MASS	OXID GAS MASS	FUEL DROPLETS	OXID DROPLETS	FUEL STREAMS	OXID STREAMS	FUEL ON WALL	OXID ON WALL
0.	3.11164E-14	0.	0.	0.	0.	0.	0.
FUEL GAS EFFLUX	OXID GAS EFFLUX	FUEL DROP RATE	OXID DROP RATE	FUEL FILM RATE	OXID FILM RATE	GAS FRACTION	THRUST - LBF
0.	0.	0.	0.	0.	0.	1.00000	0.
FUEL DROP DIAM	OXID DROP DIAM	FUEL INJ. VEL.	OXID INJ. VEL.	BETA ANGLE	MASS OUT OF TANK	INTEGRAL PC=0T	TOTAL IMPULSE
0.	0.	0.	0.	0.	0.	0.	0.
FUEL GRAMS	INJECTED MASS	GAS EXPELLED	ORCS EXPELLED	WALL EXPELLED	GAS RETAINED	ORCS RETAINED	WALL RETAINED
0.	0.000000	0.000000	0.000000	0.000000	0.000000	0.000000	0.000000
OXID GRAMS	0.000000	0.000000	0.000000	0.000000	0.000000	0.000000	0.000000
TOTAL GRAMS	0.000000	0.000000	0.000000	0.000000	0.000000	0.000000	0.000000
	SUM *	SUM †	SUM ‡	SUM §	SUM ¶	SUM ††	TOTAL MOMENTUM
FUEL DROPS INJECTED	0.	0.	0.	0.	0.	0.	0.
FUEL DROPS EJECTED	0.	0.	0.	0.	0.	0.	0.
OXID DROPS INJECTED	0.	0.	0.	0.	0.	0.	0.
OXID DROPS EJECTED	0.	0.	0.	0.	0.	0.	0.
TIME MILLISEC	CHAMBER PRESS	IGNITION	FUEL FRACTION	CHAMBER TEMP K	MOL WT.	GAMMA	CF VAC
1.00000E-01	5.00000E-08	0.	0.	300,000	46.0050	1.16944	1.91829
FUEL INJ RATE	OXID INJ RATE	FUEL FLOW RATE	OXID FLOW RATE	FUEL VOID VOL	OXID VOID VOL	FUEL INJ TEMP	OXID INJ TEMP
0.	0.	4.34657E-04	3.39719E-04	1.12873E-03	5.17935E-04	294,000	294,000
FUEL DROP BURN	OXID DROP BURN	FUEL FLASH RATE	OXID FLASH RATE	FUEL WALL BURN	OXID WALL BURN	FUEL WALL EVAP	OXID WALL EVAP
0.	0.	0.	0.	0.	0.	0.	0.
FUEL GAS MASS	OXID GAS MASS	FUEL DROPLETS	OXID DROPLETS	FUEL STREAMS	OXID STREAMS	FUEL ON WALL	OXID ON WALL
0.	3.11164E-14	0.	0.	0.	0.	0.	0.
FUEL GAS EFFLUX	OXID GAS EFFLUX	FUEL DROP RATE	OXID DROP RATE	FUEL FILM RATE	OXID FILM RATE	GAS FRACTION	THRUST - LBF
0.	0.	0.	0.	0.	0.	1.00000	2.85024E-09
FUEL DROP DIAM	OXID DROP DIAM	FUEL INJ. VEL.	OXID INJ. VEL.	BETA ANGLE	MASS OUT OF TANK	INTEGRAL PC=0T	TOTAL IMPULSE
0.	0.	0.	0.	0.	7.44376E-08	5.00000E-12	2.85024E-13
TIME MILLISEC	CHAMBER PRESS	IGNITION	FUEL FRACTION	CHAMBER TEMP K	MOL WT.	GAMMA	CF VAC
2.00000	5.00000E-08	0.	0.	300,000	46.0050	1.16944	1.91829

Table A-V-Continued

TIME MILLISEC	CHAMBER PRESS	IGNITION	FUEL FRACTION	CHAMBER TEMP K	MOL WT.	GAMMA	CF VAC
4,0000	5,00000E-08	0.	0.	3707000	45,0080	1,16944	1,91829
FUEL INJ RATE	OXID INJ RATE	FUEL FLOW RATE	OXID FLOW RATE	FUEL VOID VOL	OXID VOID VOL	FUEL INJ TEMP	OXID INJ TEMP
0.	0.	1,615167E-02	1,357710E-02	9,406947E-05	5,375548E-05	294,000	294,000
FUEL DROP BURN	OXID DROP BURN	FUEL FLASH RATE	OXID FLASH RATE	FUEL WALL BURN	OXID WALL BURN	FUEL WALL EVAP	OXID WALL EVAP
0.	0.	0.	0.	0.	0.	0.	0.
FUEL GAS MASS	OXID GAS MASS	FUEL DROPLETS	OXID DROPLETS	FUEL STREAMS	OXID STREAMS	FUEL ON WALL	OXID ON WALL
0.	0.	3,111645E-14	0.	0.	0.	0.	0.
FUEL GAS EFFLUX	OXID GAS EFFLUX	FUEL DROP RATE	OXID DROP RATE	FUEL FILM RATE	OXID FILM RATE	GAS FRACTION	THRUST - LBF
0.	0.	0.	0.	0.	0.	1,00000	2,558245E-09
FUEL DROP DIAM	OXID DROP DIAM	FUEL INJ. VEL.	OXID INJ. VEL.	BETA ANGLE	MASS OUT OF TANK	INTEGRAL PC-DT	TOTAL IMPULSE
0.	0.	0.	0.	0.	0,099079E-05	2,000000E-10	1,143298E-11
FUEL GRAMS	OXID GRAMS	INJECTED MASS	GAS EXPELLED	WALL EXPELLED	DROPS RETAINED	WALL RETAINED	
0.	0.	0,0000000	0,0000000	0,0000000	0,0000000	0,0000000	
TOTAL GRAMS		0,0000000	0,0000000	0,0000000	0,0000000	0,0000000	
		0,0000000	0,0000000	0,0000000	0,0000000	0,0000000	
		0,0000000	0,0000000	0,0000000	0,0000000	0,0000000	
FUEL DROPS INJECTED	FUEL DROPS EJECTED	OXID DROPS INJECTED	OXID DROPS EJECTED	SUM D	SUM D CUSED	TOTAL MOMENTUM	
0.	0.	0.	0.	0.	0.	0.	

TIME MILLISEC	CHAMBER PRESS	IGNITION	FUEL FRACTION	CHAMBER TEMP K	MOL WT.	GAMMA	CF VAC
4,1000	5,00000E-08	0.	0.	3001000	45,0080	1,16944	1,91829
FUEL INJ RATE	OXID INJ RATE	FUEL FLOW RATE	OXID FLOW RATE	FUEL VOID VOL	OXID VOID VOL	FUEL INJ TEMP	OXID INJ TEMP
0.	0.	1,655354E-02	1,391991E-02	2,745555E-05	294,000	294,000	294,000
FUEL DROP BURN	OXID DROP BURN	FUEL FLASH RATE	OXID FLASH RATE	FUEL WALL BURN	OXID WALL BURN	FUEL WALL EVAP	OXID WALL EVAP
0.	0.	0.	0.	0.	0.	0.	0.
FUEL GAS MASS	OXID GAS MASS	FUEL DROPLETS	OXID DROPLETS	FUEL STREAMS	OXID STREAMS	FUEL ON WALL	OXID ON WALL
0.	0.	3,111645E-14	0.	0.	0.	0.	0.
FUEL GAS EFFLUX	OXID GAS EFFLUX	FUEL DROP RATE	OXID DROP RATE	FUEL FILM RATE	OXID FILM RATE	GAS FRACTION	THRUST - LBF
0.	0.	0.	0.	0.	0.	1,00000	2,558245E-09
FUEL DROP DIAM	OXID DROP DIAM	FUEL INJ. VEL.	OXID INJ. VEL.	BETA ANGLE	MASS OUT OF TANK	INTEGRAL PC-DT	TOTAL IMPULSE
0.	0.	0.	0.	0.	0,403775E-05	2,000000E-10	1,171860E-11
FUEL GRAMS	OXID GRAMS	INJECTED MASS	GAS EXPELLED	WALL EXPELLED	DROPS RETAINED	WALL RETAINED	
0.	0.	0,0000000	0,0000000	0,0000000	0,0000000	0,0000000	
TOTAL GRAMS		0,0000000	0,0000000	0,0000000	0,0000000	0,0000000	
		0,0000000	0,0000000	0,0000000	0,0000000	0,0000000	
		0,0000000	0,0000000	0,0000000	0,0000000	0,0000000	
FUEL DROPS INJECTED	FUEL DROPS EJECTED	OXID DROPS INJECTED	OXID DROPS EJECTED	SUM D	SUM D CUSED	TOTAL MOMENTUM	
0.	0.	0.	0.	0.	0.	0.	

TIME MILLISEC	CHAMBER PRESS	IGNITION	FUEL FRACTION	CHAMBER TEMP K	MOL WT.	GAMMA	CF VAC
4,2000	5,00000E-08	0.	0.	1521000	45,0740	1,04529	2,59238
FUEL INJ RATE	OXID INJ RATE	FUEL FLOW RATE	OXID FLOW RATE	FUEL VOID VOL	OXID VOID VOL	FUEL INJ TEMP	OXID INJ TEMP
0.	0.	1,69587E-02	1,42848E-02	5,15406E-07	294,000	294,000	294,000
FUEL DROP BURN	OXID DROP BURN	FUEL FLASH RATE	OXID FLASH RATE	FUEL WALL BURN	OXID WALL BURN	FUEL WALL EVAP	OXID WALL EVAP
0.	0.	0.	0.	0.	0.	0.	0.
FUEL GAS MASS	OXID GAS MASS	FUEL DROPLETS	OXID DROPLETS	FUEL STREAMS	OXID STREAMS	FUEL ON WALL	OXID ON WALL
0.	0.	3,111645E-14	0.	0.	0.	0.	0.
FUEL GAS EFFLUX	OXID GAS EFFLUX	FUEL DROP RATE	OXID DROP RATE	FUEL FILM RATE	OXID FILM RATE	GAS FRACTION	THRUST - LBF
0.	0.	0.	0.	0.	0.	1,00000	2,558245E-09
FUEL DROP DIAM	OXID DROP DIAM	FUEL INJ. VEL.	OXID INJ. VEL.	BETA ANGLE	MASS OUT OF TANK	INTEGRAL PC-DT	TOTAL IMPULSE
0.	0.	0.	0.	0.	0,403775E-05	2,000000E-10	1,171860E-11
FUEL GRAMS	OXID GRAMS	INJECTED MASS	GAS EXPELLED	WALL EXPELLED	DROPS RETAINED	WALL RETAINED	
0.	0.	0,0000000	0,0000000	0,0000000	0,0000000	0,0000000	
TOTAL GRAMS		0,0000000	0,0000000	0,0000000	0,0000000	0,0000000	
		0,0000000	0,0000000	0,0000000	0,0000000	0,0000000	
		0,0000000	0,0000000	0,0000000	0,0000000	0,0000000	
FUEL DROPS INJECTED	FUEL DROPS EJECTED	OXID DROPS INJECTED	OXID DROPS EJECTED	SUM D	SUM D CUSED	TOTAL MOMENTUM	
0.	0.	0.	0.	0.	0.	0.	

Table A-V-Continued

TIME MILLISEC	CHAMBER PRESS	IGNITION	FUEL FRACTION	CHAMBER TEMP	MOL AT	GAMMA	CF VAC
4.47000	46.9200	1.00000	.175015	2838.90	27.0046	1.22800	1.88187
FUEL INJ RATE	OXID INJ RATE	FUEL FLOW RATE	OXID FLOW RATE	FUEL VOID VOL	OXID VOID VOL	FUEL INJ TEMP	OXID INJ TEMP
1.506595E-02	1.519321E-02	1.594595E-02	1.519921E-02	0.	0.	294.000	294.000
FUEL DROP BURN	OXID DROP BURN	FUEL FLASH RATE	OXID FLASH RATE	FUEL WALL BURN	OXID WALL BURN	FUEL WALL EVAP	OXID WALL EVAP
1.455273E-03	8.202122E-04	0.	0.	0.	0.	0.	1.381165E-04
FUEL GAS MASS	OXID GAS MASS	FUEL DROPLETS	OXID DROPLETS	FUEL STREAMS	OXID STREAMS	FUEL ON WALL	OXID ON WALL
3.174560E-07	1.494429E-06	3.577569E-06	3.927948E-06	0.	0.	2.879975E-06	1.627475E-07
FUEL GAS EFFLUX	OXID GAS EFFLUX	FUEL DROP RATE	OXID DROP RATE	FUEL FILM RATE	OXID FILM RATE	GAS FRACTION	THRUST - LBF
2.142174E-04	1.747486E-03	0.	0.	0.	0.	1.00000	2.63522
FUEL DROP DIAM	OXID DROP DIAM	FUEL INJ. VEL.	OXID INJ. VEL.	RETA ANGLE	MASS OUT OF TANK	INTEGRAL PC-DT	TOTAL IMPULSE
117.244	72.4062	212.157	84.0062	-23.4512	7.964481E-05	5.176124E-03	2.917548E-04
TIME MILLISEC	CHAMBER PRESS	IGNITION	FUEL FRACTION	CHAMBER TEMP	MOL AT	GAMMA	CF VAC
4.47000	82.4436	1.00000	.229893	3177.56	25.15073	1.21910	1.92419
FUEL INJ RATE	OXID INJ RATE	FUEL FLOW RATE	OXID FLOW RATE	FUEL VOID VOL	OXID VOID VOL	FUEL INJ TEMP	OXID INJ TEMP
1.546261E-02	1.529764E-02	1.566261E-02	1.529764E-02	0.	0.	294.000	294.000
FUEL DROP BURN	OXID DROP BURN	FUEL FLASH RATE	OXID FLASH RATE	FUEL WALL BURN	OXID WALL BURN	FUEL WALL EVAP	OXID WALL EVAP
4.633375E-03	1.651425E-02	0.	0.	2.842931E-05	3.027534E-05	0.	0.
FUEL GAS MASS	OXID GAS MASS	FUEL DROPLETS	OXID DROPLETS	FUEL STREAMS	OXID STREAMS	FUEL ON WALL	OXID ON WALL
5.175357E-07	2.164563E-06	4.297569E-06	3.754335E-06	0.	0.	3.264558E-06	4.777765E-07
FUEL GAS EFFLUX	OXID GAS EFFLUX	FUEL DROP RATE	OXID DROP RATE	FUEL FILM RATE	OXID FILM RATE	GAS FRACTION	THRUST - LBF
1.651137E-03	7.923943E-03	0.	0.	0.	0.	1.00000	4.72852
FUEL DROP DIAM	OXID DROP DIAM	FUEL INJ. VEL.	OXID INJ. VEL.	RETA ANGLE	MASS OUT OF TANK	INTEGRAL PC-DT	TOTAL IMPULSE
111.272	72.4341	204.126	86.5369	-22.4468	8.273936E-05	1.342248E-02	7.646964E-04
TIME MILLISEC	CHAMBER PRESS	IGNITION	FUEL FRACTION	CHAMBER TEMP	MOL AT	GAMMA	CF VAC
4.47000	109.174	1.00000	.277954	3306.18	24.2663	1.21787	1.94618
FUEL INJ RATE	OXID INJ RATE	FUEL FLOW RATE	OXID FLOW RATE	FUEL VOID VOL	OXID VOID VOL	FUEL INJ TEMP	OXID INJ TEMP
1.530305E-02	1.530129E-02	1.530305E-02	1.530129E-02	0.	0.	294.000	294.000
FUEL DROP BURN	OXID DROP BURN	FUEL FLASH RATE	OXID FLASH RATE	FUEL WALL BURN	OXID WALL BURN	FUEL WALL EVAP	OXID WALL EVAP
5.372595E-03	1.204775E-02	0.	0.	8.335585E-05	1.932654E-04	0.	0.
FUEL GAS MASS	OXID GAS MASS	FUEL DROPLETS	OXID DROPLETS	FUEL STREAMS	OXID STREAMS	FUEL ON WALL	OXID ON WALL
1.111905E-07	2.176429E-06	4.582599E-06	3.780413E-06	0.	0.	3.575058E-06	7.014237E-07
FUEL GAS EFFLUX	OXID GAS EFFLUX	FUEL DROP RATE	OXID DROP RATE	FUEL FILM RATE	OXID FILM RATE	GAS FRACTION	THRUST - LBF
3.956010E-03	1.100355E-02	0.	0.	0.	0.	1.950618	5.82539
FUEL DROP DIAM	OXID DROP DIAM	FUEL INJ. VEL.	OXID INJ. VEL.	RETA ANGLE	MASS OUT OF TANK	INTEGRAL PC-DT	TOTAL IMPULSE
117.591	72.4040	203.349	88.5073	-21.4601	8.579930E-05	2.345987E-02	1.347146E-03
TIME MILLISEC	CHAMBER PRESS	IGNITION	FUEL FRACTION	CHAMBER TEMP	MOL AT	GAMMA	CF VAC
4.47000	95.8512	1.00000	.347183	3238.47	21.7339	1.22549	1.90758

NOT REPRODUCIBLE

Table A-V-Continued

FUEL GAS EFFLUX	OXID GAS EFFLUX	FUEL DROP RATE	OXID DROP RATE	FUEL FILM RATE	OXID FILM RATE	OXID FLY RATE	GAS FRACTION	THRUST - LBF
3.36557E-04	4.463064E-04	1.255864E-03	1.707491E-03	3.569164E-04	2.485270E-06	2.485270E-06	.900694	.165268
FUEL DROP DIAM	OXID DROP DIAM	FUEL I-J, VEL.	OXID I-J, VEL.	BETA ANGLE	MASS OUT OF TANK	INTEGRAL PC*DT	TOTAL IMPULSE	
0.	245.289	0.	31.7873	45.0000	2.400255E-04	.679448	3.903006E-02	
TIME MILLISEC	CHAMBER PRESS	IGNITION	FUEL FRACTION	CHAMBER TEMP K	MOL WT.	GAMMA	CF VAC	
12.6000	2.71490	1.00000	.167417	2692.69	27.3521	1.23267	1.85648	
FUEL INJ RATE	OXID INJ RATE	FUEL FLOW RATE	OXID FLOW RATE	FUEL VOID VOL	OXID VOID VOL	FUEL INJ TEMP	OXID INJ TEMP	
0.	5.792599E-03	0.	0.	0.	4.395701E-05	294.000	294.000	
FUEL DROP BUR.	OXID DROP BURN	FUEL FLASH RATE	OXID FLASH RATE	FUEL WALL BURN	OXID WALL BURN	FUEL WALL EVAP	OXID WALL EVAP	
0.	0.	0.	0.	4.862659E-05	6.224612E-05	0.	4.984243E-04	
FUEL GAS MASS	OXID GAS MASS	FUEL DROPLETS	OXID DROPLETS	FUEL STREAMS	OXID STREAMS	FUEL ON WALL	OXID ON WALL	
1.783214E-06	9.382210E-08	0.	6.537676E-07	0.	1.481042E-06	6.031612E-06	2.341038E-06	
FUEL GAS EFFLUX	OXID GAS EFFLUX	FUEL DROP RATE	OXID DROP RATE	FUEL FILM RATE	OXID FILM RATE	GAS FRACTION	THRUST - LBF	
1.17412E-04	4.614508E-04	9.419930E-04	1.281368E-03	3.028420E-06	2.023799E-06	.698336	.131002	
FUEL DROP DIAM	OXID DROP DIAM	FUEL I-J, VEL.	OXID I-J, VEL.	BETA ANGLE	MASS OUT OF TANK	INTEGRAL PC*DT	TOTAL IMPULSE	
0.	245.289	0.	33.5402	45.0000	2.400255E-04	.679719	3.904515E-02	

EXTINGUISH AT 12.50 MILLISECONDS

TIME MILLISEC	CHAMBER PRESS	IGNITION	FUEL FRACTION	CHAMBER TEMP K	MOL WT.	GAMMA	CF VAC
12.5000	1.79734	0.	.167325	2184.67	46.9131	1.13069	1.94998
FUEL INJ RATE	OXID INJ RATE	FUEL FLOW RATE	OXID FLOW RATE	FUEL VOID VOL	OXID VOID VOL	FUEL INJ TEMP	OXID INJ TEMP
0.	5.940758E-03	0.	0.	0.	5.516455E-05	294.000	294.000
FUEL DROP BUR.	OXID DROP BURN	FUEL FLASH RATE	OXID FLASH RATE	FUEL WALL BURN	OXID WALL BURN	FUEL WALL EVAP	OXID WALL EVAP
0.	3.305667E-04	0.	0.	7.915419E-05	5.250120E-05	0.	5.908539E-04
FUEL GAS MASS	OXID GAS MASS	FUEL DROPLETS	OXID DROPLETS	FUEL STREAMS	OXID STREAMS	FUEL ON WALL	OXID ON WALL
1.664109E-06	1.369602E-07	0.	1.615008E-06	0.	1.269980E-06	6.023453E-06	2.285789E-06
FUEL GAS EFFLUX	OXID GAS EFFLUX	FUEL DROP RATE	OXID DROP RATE	FUEL FILM RATE	OXID FILM RATE	GAS FRACTION	THRUST - LBF
9.266468E-05	4.819423E-04	7.064235E-04	9.610263E-04	2.432752E-06	1.562337E-06	.772023	.105298
FUEL DROP DIAM	OXID DROP DIAM	FUEL I-J, VEL.	OXID I-J, VEL.	BETA ANGLE	MASS OUT OF TANK	INTEGRAL PC*DT	TOTAL IMPULSE
0.	245.289	0.	34.3951	45.0000	2.400255E-04	.679899	3.905569E-02

TIME MILLISEC	CHAMBER PRESS	IGNITION	FUEL FRACTION	CHAMBER TEMP K	MOL WT.	GAMMA	CF VAC
12.6000	1.34563	0.	7.551722E-02	1741.88	46.9130	1.14042	1.95350
FUEL INJ RATE	OXID INJ RATE	FUEL FLOW RATE	OXID FLOW RATE	FUEL VOID VOL	OXID VOID VOL	FUEL INJ TEMP	OXID INJ TEMP
0.	6.144469E-03	0.	0.	0.	6.680086E-05	294.000	294.000
FUEL DROP BUR.	OXID DROP BURN	FUEL FLASH RATE	OXID FLASH RATE	FUEL WALL BURN	OXID WALL BURN	FUEL WALL EVAP	OXID WALL EVAP
0.	0.	0.	0.	0.	0.	0.	4.368746E-04
FUEL GAS MASS	OXID GAS MASS	FUEL DROPLETS	OXID DROPLETS	FUEL STREAMS	OXID STREAMS	FUEL ON WALL	OXID ON WALL
1.049309E-08	1.333534E-07	0.	2.195268E-06	0.	1.305357E-06	6.023267E-06	2.232670E-06
FUEL GAS EFFLUX	OXID GAS EFFLUX	FUEL DROP RATE	OXID DROP RATE	FUEL FILM RATE	OXID FILM RATE	GAS FRACTION	THRUST - LBF
5.747994E-05	4.731432E-04	5.299176E-04	7.207695E-04	1.862188E-06	1.142166E-06	.827610	7.833449E-02

Table A-V-Continued

PERFORMANCE SUMMARY						
PROPELLANT MASS BASIS	FUEL FLOW	OXID FLOW	MIXTURE RATIO	C STAR	SPECIFIC IMPULSE	
MASS OUT OF TANK - POUNDS	.000111	.000129	1.162090	2765.022741	161.657111	
MASS THROUGH INJECTOR - POUNDS	.000075	.000129	1.721204	3257.400170	197.242236	
MASS THROUGH NOZZLE - POUNDS	.000069	.000112	1.619648	3678.296479	214.818605	
PRESSURE INTEGRAL - PSIA*SEC.	.6939					
TOTAL IMPULSE - POUND*SEC.	.0388					

Table A-V-Continued

DISPOSITION OF INJECTED PROPELLANT

	FUEL	OXID	TOTAL
FRACTION EXPELLED AS GAS	.579169	.638936	.616972
FRACTION EXPELLED AS DROPS	.328669	.219171	.259497
FRACTION EXPELLED AS FILM	.011669	.007542	.009132
FRACTION RETAINED AS GAS	.000067	.001587	.001654
FRACTION RETAINED AS DROPS	.000925	.001733	.002658
FRACTION RETAINED AS FILM	.078749	.131377	.112056

MEAN DROP DIAMETER	INJECTED FUEL	EJECTED FUEL	INJECTED OXID	EJECTED OXID
D30	36,8171	85,7081	28,3380	50,5210
D31	45,9424	95,7369	35,4348	60,3431
D32	65,5011	110,0485	50,0263	74,5905
MEAN VELOCITY FEET/SECOND	107.95	267.94	50.13	221.01

D MICRONS	LOG D	DROP SIZE DISTRIBUTION	CUMULATIVE MASS
10	1.0000	0.0000	0.0000
20	1.3010	0.0000	.0000
30	1.4771	.1663	.1663
40	1.6021	.1563	.3226
50	1.6990	.1863	.5089
60	1.7762	.1174	.6263
70	1.8451	.1774	.8037
80	1.9031	.2809	.1081
90	1.9542	.3472	.4937
100	2.0000	.3256	.8193
110	2.0414	.5570	.3727
120	2.0792	.5735	.7157
130	2.1139	.5909	.7157
140	2.1461	.7599	.7157
150	2.1761	.7599	.7157
160	2.2041	.7599	.7157
170	2.2304	.7599	.7157
180	2.2553	.7599	.7157
190	2.2768	.7599	.7157
200	2.3010	.7599	.7157
210	2.3222	.7599	.7157
220	2.3424	.7599	.7157
230	2.3617	.7599	.7157
240	2.3802	.7599	.7157
250	2.3979	.9462	.7157
260	2.4150	.9462	.7157
270	2.4314	.9462	.7157
280	2.4472	.9462	.7157
290	2.4624	.9462	.7157
300	2.4771	.9462	.7157
310	2.4914	.9462	.7157
320	2.5051	.9462	.7157

Table A-V-Continued

330	2.5145	9497	9707	9470	9827
340	2.5315	9597	9707	9470	9827
350	2.5441	9597	9707	9470	9827
360	2.5543	9597	9707	9470	9827
370	2.5622	9597	9707	9470	9827
380	2.5795	9597	9707	9470	9827
390	2.5911	9597	9771	9470	9827
400	2.6021	9731	9804	9470	9827
410	2.6124	9731	9804	9470	9827
420	2.6232	9731	9804	9470	9827
430	2.6335	9731	9804	9470	9827
440	2.6435	9731	9804	9470	9827
450	2.6532	9731	9804	9470	9827
460	2.6628	9731	9804	9470	9827
470	2.6721	9731	9804	9470	9827
480	2.6812	9731	9804	9470	9827
490	2.6902	9496	9801	9470	9827
500	2.6990	9496	9801	9470	9827
510	2.7076	9496	9801	9470	9827
520	2.7160	9496	9801	9470	9827
530	2.7243	9496	9801	9470	9827
540	2.7324	9496	9801	9470	9827
550	2.7404	9496	9801	9470	9827
560	2.7482	9496	9801	9470	9827
570	2.7559	9496	9801	9470	9827
580	2.7634	9496	9801	9470	9827
590	2.7709	9496	9801	9470	9827
600	2.7782	9496	9801	9470	9827
610	2.7853	9496	9801	9470	9827
620	2.7924	9496	9801	9470	9827
630	2.7993	9496	9801	9470	9827
640	2.8062	9496	9801	9470	9827
650	2.8129	9496	9801	9470	9827
660	2.8194	9496	9801	9470	9827
670	2.8261	9496	9801	9470	9827
680	2.8325	9496	9801	9470	9827
690	2.8388	9496	9801	9470	9827
700	2.8450	9496	9801	9470	9827
710	2.8513	9496	9801	9470	9827
720	2.8573	9496	9801	9470	9827
730	2.8633	9496	9801	9470	9827
740	2.8692	9496	9801	9470	9827
750	2.8751	9496	9801	9470	9827
760	2.8810	9496	9801	9470	9827
770	2.8865	9496	9801	9470	9827
780	2.8921	9496	9801	9470	9827
790	2.8976	9496	9801	9470	9827
800	2.9031	9496	9801	9470	9827
810	2.9085	9496	9801	9470	9827
820	2.9139	9496	9801	9470	9827
830	2.9191	9496	9801	9470	9827
840	2.9247	9496	9801	9470	9827
850	2.9294	9496	9801	9470	9827
860	2.9345	9496	9801	9470	9827
870	2.9395	9496	9801	9470	9827
880	2.9445	9496	9801	9470	9827
890	2.9494	9496	9801	9470	9827
900	2.9542	9496	9801	9470	9827
910	2.9589	14000	14000	14000	14000

Table A-V-Continued

SERIAL 817464

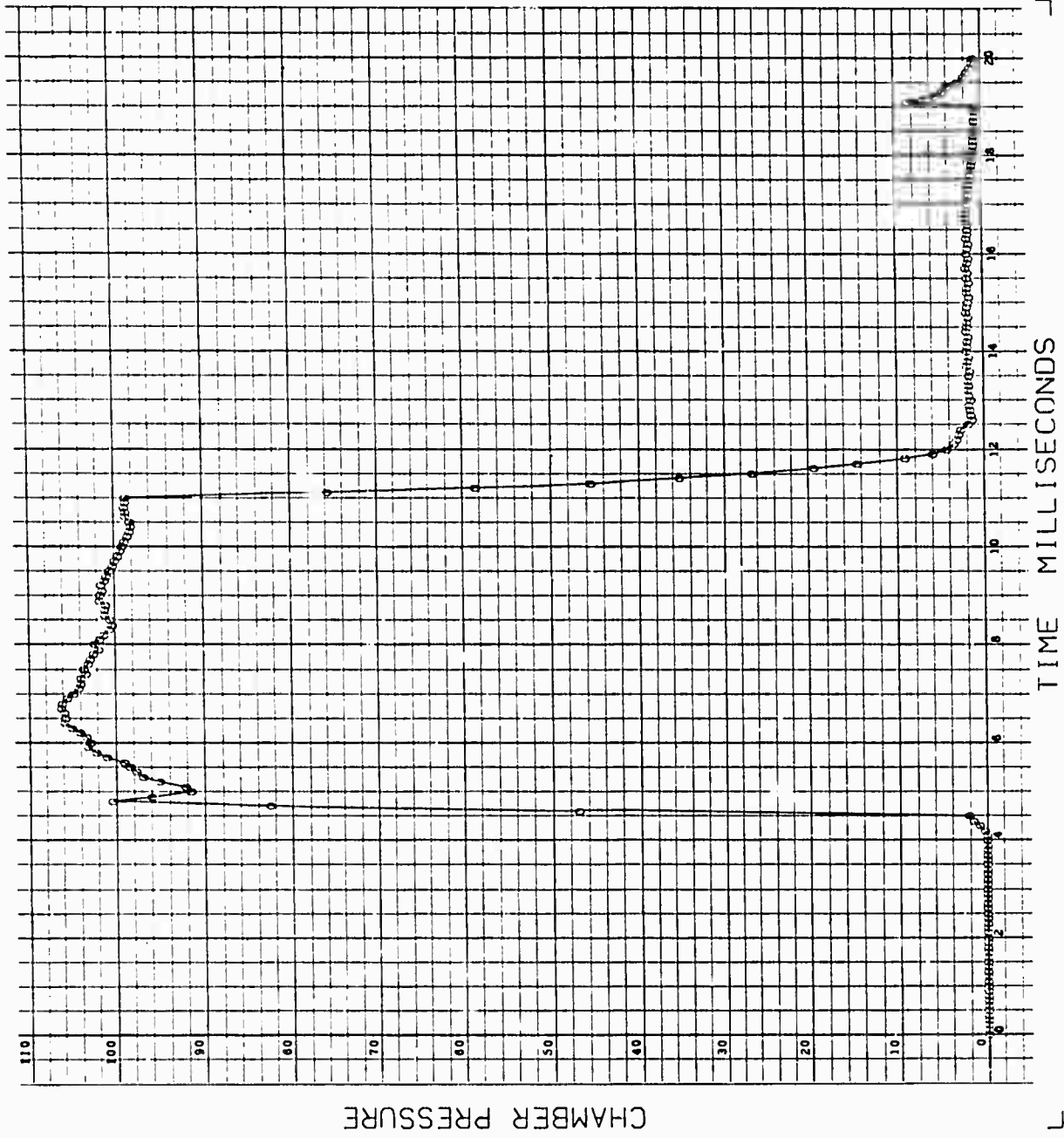


Table A-V-Continued

SERIAL 817400

7 6

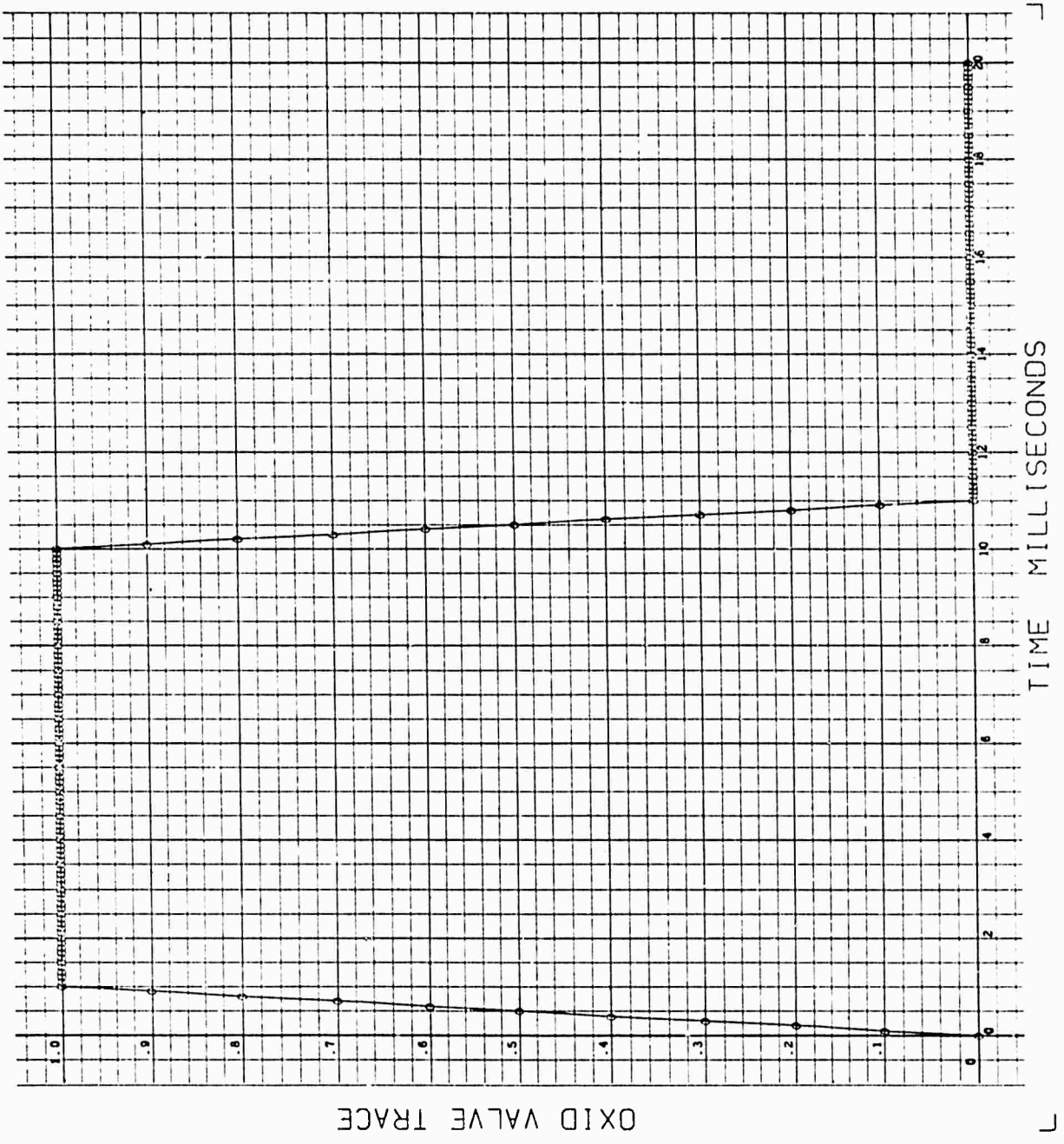


Table A-V-Continued

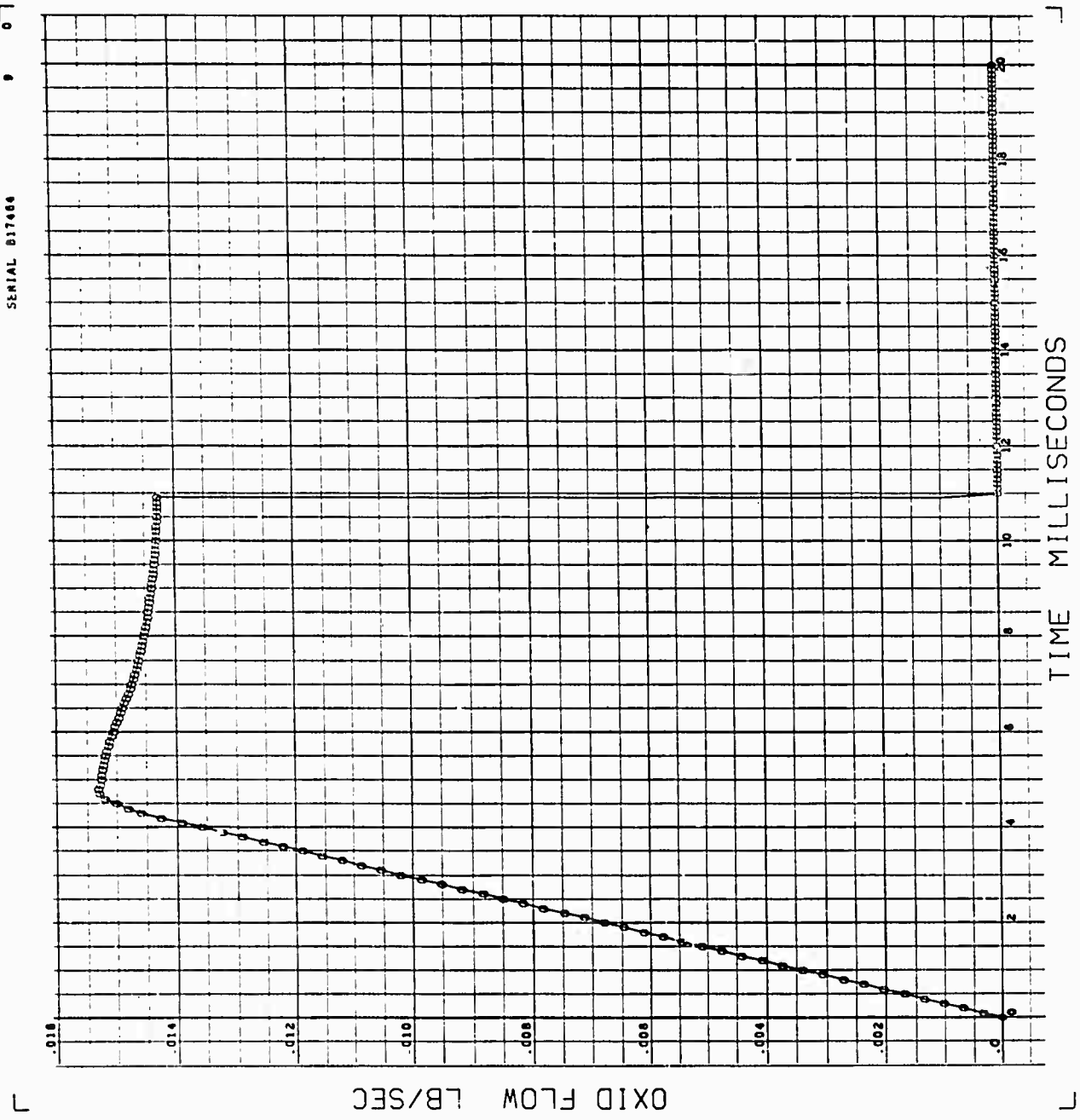


Table A-V-Continued

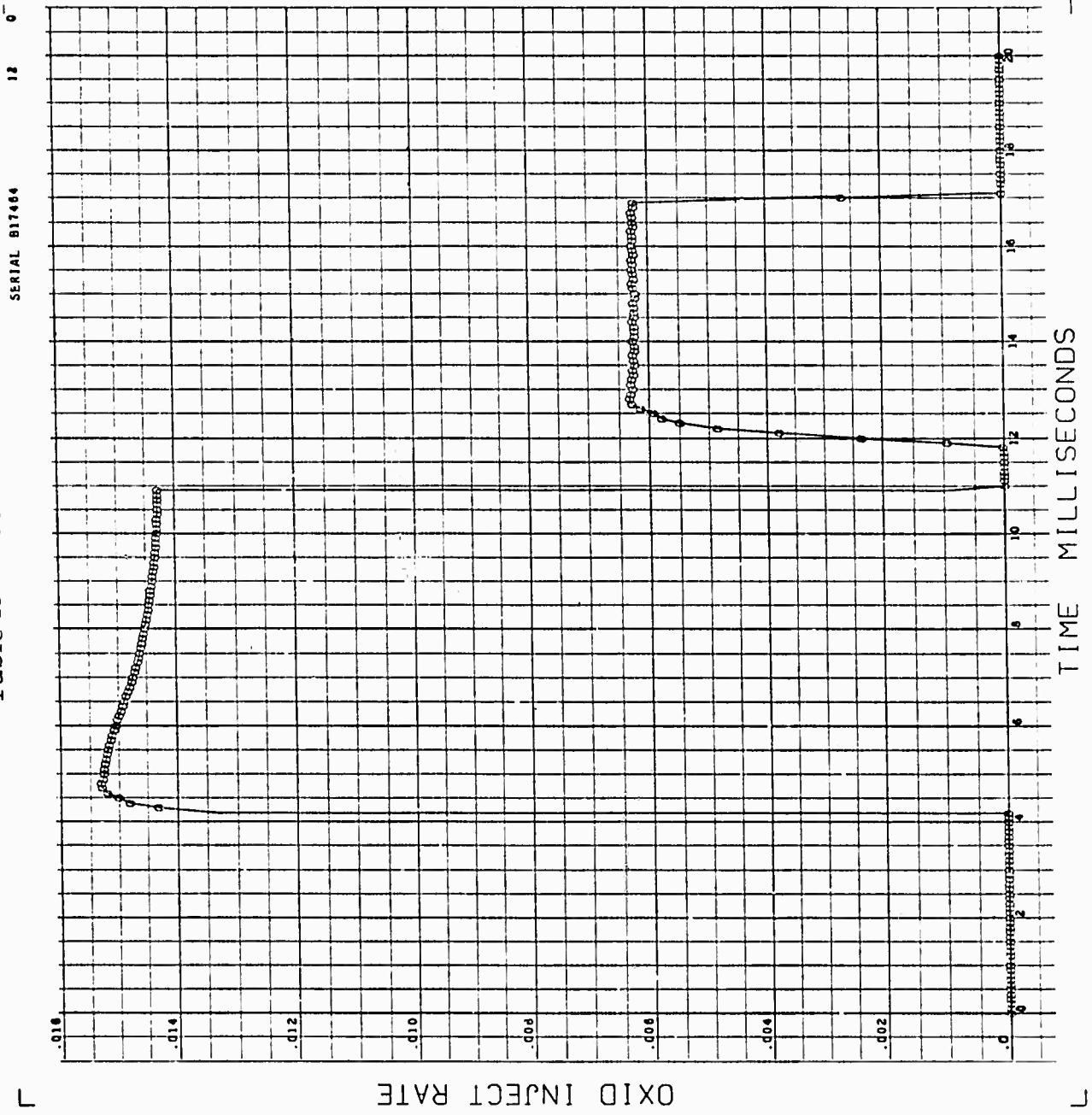


Table A-V-Continued

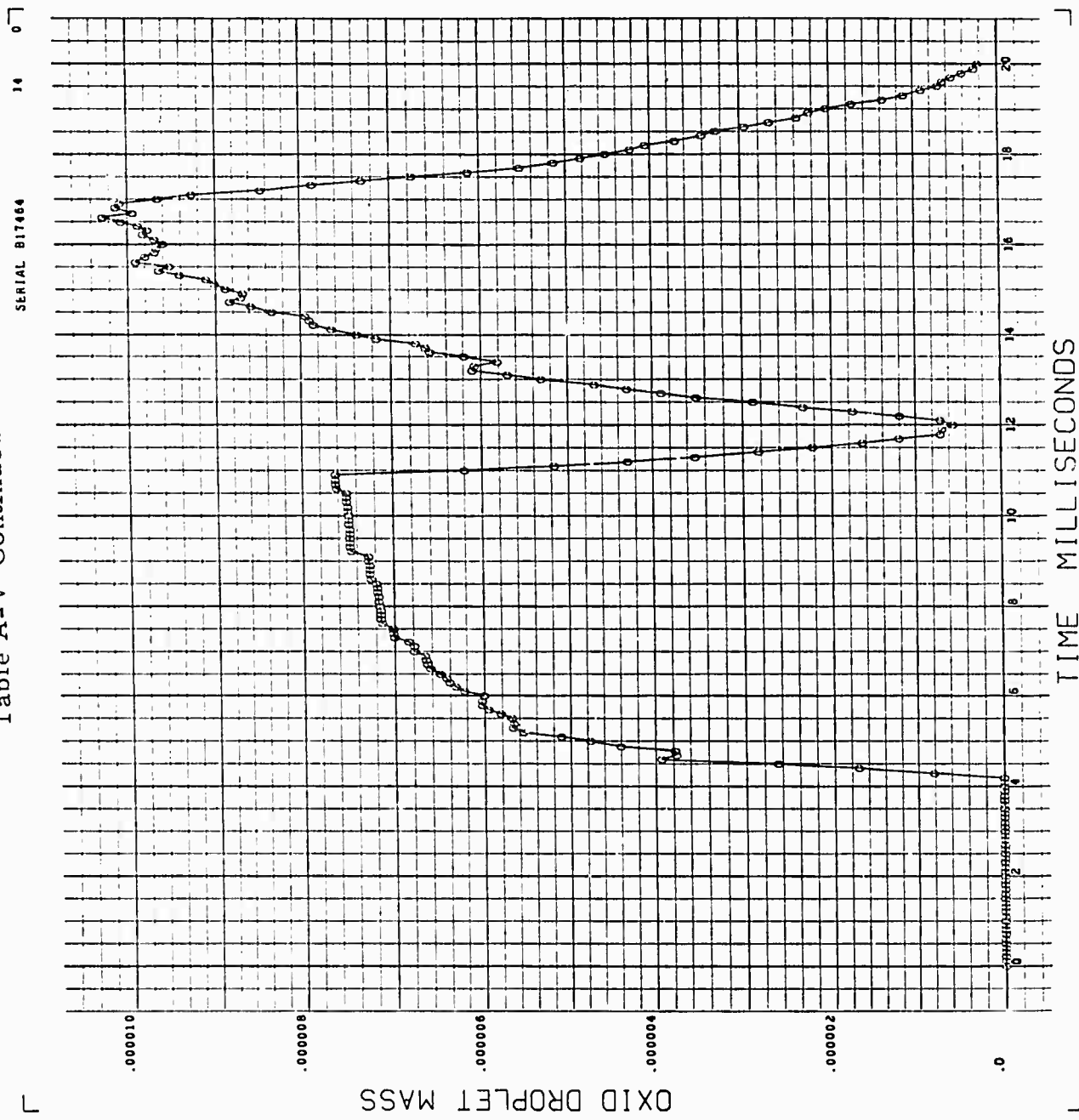
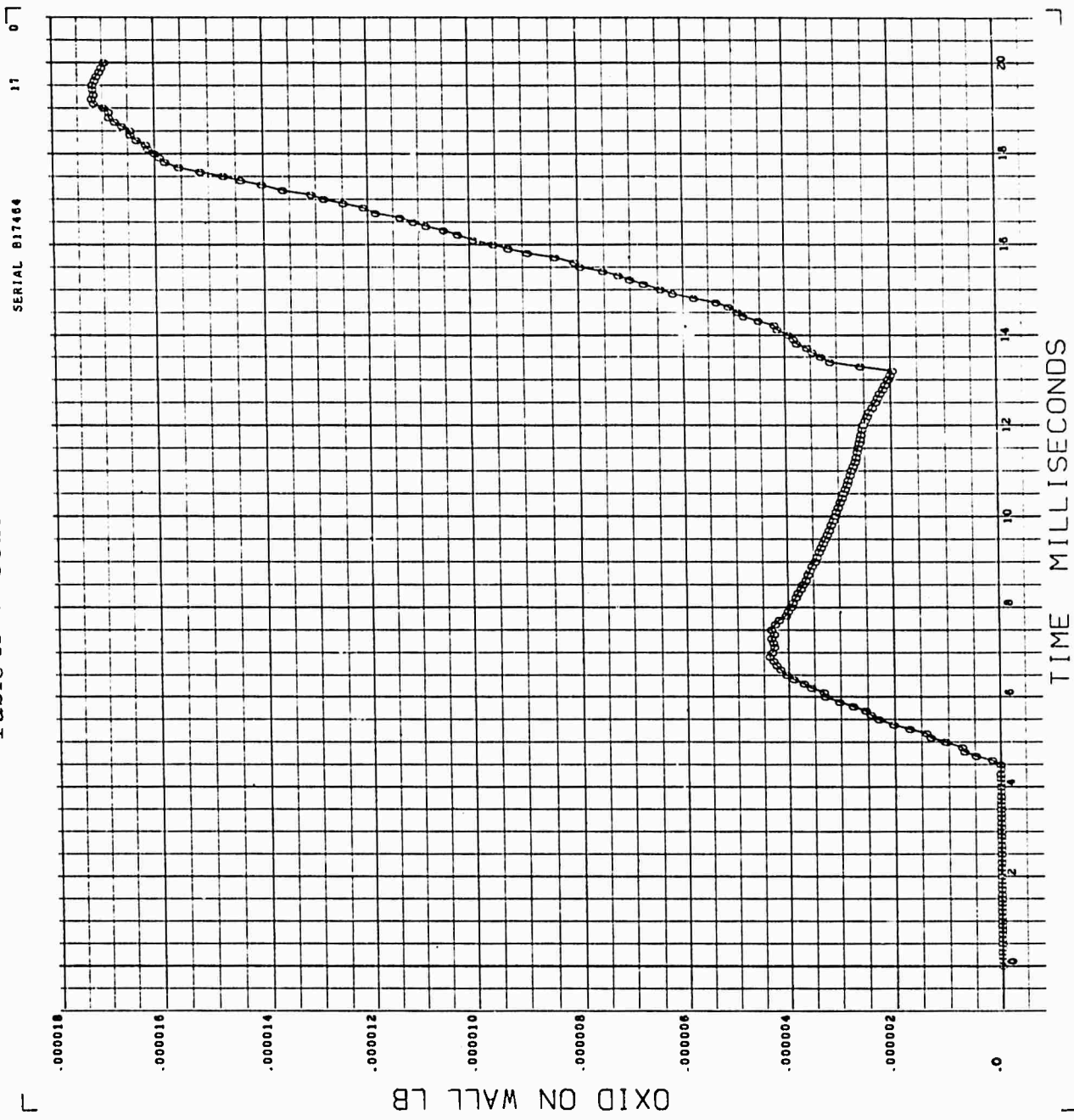


Table A-V-Conclusion



A. 8 REFERENCES

- A-1. W. T. Webber. "Calculation of Low-Frequency Unsteady Behavior of Liquid Rockets from Droplet Combustion Parameters." AIAA 6th Propulsion Joint Specialist Conference, San Diego, Calif, June 15, 1970, AIAA Paper No. 70-620.
- A-2. W. T. Webber, and W. A. Gaubatz. "Calculation of the Ignition and Start Transient of Liquid Propellant Rocket Engines." Western States Section, The Combustion Institute, Pasadena, Calif., Oct. 26, 1970, Paper No. 70-23, also published as McDonnell Douglas Astronautics Company Paper, MDAC WD-1439.
- A-3. W. T. Webber and W. A. Gaubatz. "Calculation of Low-Frequency Combustion Instability in Liquid-Propellant Rocket Engines." 7th JANNAF Liquid Propellant Combustion Instability Meeting, Pasadena, Calif., Oct. 27, 1970.
- A-4. W. T. Webber, W. A. Gaubatz, and R. J. Hoffman. "Calculation of Contaminant Production in Liquid Bipropellant Rocket Engines." JANNAF Sixth Plume Technology Meeting. March 1971. Also published as McDonnell Douglas Astronautics Company Paper, MDAC WD1513, April 1971.
- A-5. G. P. Sutton. Rocket Propulsion Elements. John Wiley & Sons, Inc., 1949.
- A-6. S. S. Penner. On Maximum Evaporation Rates of Liquid Droplets in Rocket Motors. American Rocket Society Journal, Vol. 23, No. 2 March 1953.
- A-7. C. C. Miesse. "Ballistics of an Evaporating Droplet." Jet Propulsion, Vol. 24, No. 4, July 1954.
- A-8. R. J. Priem. Propellant Vaporization as a Criterion for Rocket Engine Design; Calculations of Chamber Length to Vaporize a Single n-Heptane Drop, NACA TN3985 July 1957.
- A-9. R. J. Priem and M. F. Heidmann. Propellant Vaporization as a Design Consideration for Rocket Engine Combustion Chambers. NASA TR R-67, 1970.
- A-10. S. Lambiris, L. P. Combs, and R. S. Levine. "Stable Combustion Processes in Liquid Propellant Rocket Engines." Combustion and Propulsion. Fifth AGARD Colloquium: High Temperature Phenomena, the MacMillan Co., 1962.

- A-11. M. R. Beltran, B. P. Breen, T. C. Kosvic, C. F. Sanders, R. J. Hoffman, and R. O. Wright. Analysis of Liquid Rocket Engine Combustion Instability. AFRPL-TR-65-254, January 1966.
- A-12. D. L. Kors, L. B. Bassham, and R. E. Walker. "A Liquid Rocket Performance Model Based on Vaporization Interactions." *Journal of Spacecraft and Rockets*, Vol. 6, No. 10, October 1969.
- A-13. L. P. Combs, W. D. Chadwick, and D. T. Campbell. Liquid Rocket Performance Analysis with Distributed Energy Release. CPIA Publication No. 204, February 1971.
- A-14. M. Yachter and H. V. Waldinger. Dynamic Analysis of a Rocket Motor. Rep. SPD-241, M. W. Kellogg Co., October 1949.
- A-15. D. F. Gunder and D. R. Friant. "Stability of Flow in a Rocket Motor." *Journal of Applied Mechanics*, Vol. 17, 1950.
- A-16. M. Summerfield. "A Theory of Unstable Combustion in Liquid Propellant Rocket Systems." *Journal of the American Rocket Society*, Vol. 21, No. 5, September 1951.
- A-17. L. Crocco and S. Cheng. Theory of Combustion Instability in Liquid Propellant Rocket Motors. AGARDograph No. 8, Butterworths, 1956.
- A-18. M. Barrere and J. J. Bernard. "Influence of the Injector pressure Drop on Low Frequency Instability in Liquid Propellant Rockets." Sixth Symposium on Combustion, Reinhold Publishing Corp, 1956.
- A-19. H. G. Hurrell. Analysis of Injection-Velocity Effects on Rocket Motor Dynamics and Stability. NACA TR R-43, September 1959.
- A-20. R. B. Lawhead, R. S. Levine, and W. T. Webber. Liquid-propellant Rocket Combustion Instability Studies-Final Summary Report Covering the Period 1 June 1954 to 30 November 1955. Rocketdyne Report R-122, 1956.
- A-21. P. McCormack. "A Driving Mechanism for High Frequency Combustion Instability in Liquid Fuel Rocket Engines." *Journal of the Royal Aeronautical Society*, September 1964.
- A-22. J. R. Fenwick and G. J. Bugler. "Oscillatory Flame Front Flowrate Amplification through Propellant Injection Ballistics (The Klystron Effect)." CPIA Publication No. 138, Vol. 1, February 1967.
- A-23. M. R. Gore and J. L. Carroll. "Dynamics of a Variable Thrust, Pump Fed, Bipropellant, Liquid Rocket Engine System." *Jet Propulsion*, Vol. 27, No. 1, January 1957.

- A-24. P. Kluger and E. C. Farrell. "Digital Computer Analysis of Transients in Liquid Rocket Engines." *Jet Propulsion*, Vol. 28, No. 12, December 1958.
- A-25. E. Mayer. "Vaporization Limited Combustion in Bipropellant Rocket Chambers." *Journal of the American Rocket Society*, Vol. 29, No. 7, July 1959.
- A-26. D. B. Spalding. "A One-Dimensional Theory of Liquid-Fuel Rocket Combustion," A. R. C. 20, 175, May 1958.
- A-27. H. C. Rodean. "Rocket Thrust Termination Transients." *Journal of the American Rocket Society*, Vol. 29, No. 6, June 1959.
- A-28. J. A. Peterson. "Starting Transients of Hypergolic Bipropellant Rockets." *Liquid Rockets and Propellants (Progress in Astronautics and Rocketry Vol. 2)* Academic Press, 1960.
- A-29. T. F. Seamans, M. Vanpee, and V. D. Agosta. "Development of a Fundamental Model of Hypergolic Ignition in Space-Ambient Engines." *AIAA Journal*, Vol. 5, No. 9, September 1967.
- A-30. R. E. Martens. "Investigation of Hypergolic Ignition Spike Phenomena." 8th Liquid Propulsion Symposium, CPIA Publication No. 121, Vol. 1, October 1966.
- A-31. W. Juran and R. C. Stechman. "Ignition Transients in Small Hypergolic Rockets." *Journal of Spacecraft and Rockets*, Vol. 5, No. 3, March 1968.
- A-32. H. M. Paynter. "Fluid Transients in Engineering Systems." *Handbook of Fluid Dynamics*, McGraw-Hill Book Company, 1961.
- A-33. O. A. Hougen and K. M. Watson. Chemical Process Principles John Wiley & Sons, 1950.
- A-34. Calingaert and Davis. *Industrial and Engineering Chemistry*, Vol. 17, page 1287, 1925.
- A-35. D. M. Bushnell and P. B. Gooderum. "Atomization of Superheated Water Jets at Low Ambient Pressures." *Journal of Spacecraft and Rockets*, Vol. 5, No. 2, February 1968.
- A-36. R. Brown. Sprays Formed by Flashing Liquid Jets. Ph. D. Thesis, University of Michigan, 1961.
- A-37. P. B. Gooderum and D. M. Bushnell. "Measurement of Mean Drop Sizes for Sprays from Superheated Water Jets." *Journal of Spacecraft and Rockets*, Vol. 6, No. 2, February 1969.

- A-38. R. D. Ingebo. Drop-Size Distributions for Impinging-Jet Breakup in Airstreams Simulating the Velocity Conditions in Rocket Combustors. NACA TN 4222, 1950.
- A-39. M. A. Weiss and C. H. Worsham. "Atomization in High Velocity Airstreams." *Journal of the American Rocket Society*, Vol. 29, No. 4, April 1959.
- A-40. M. F. Heidmann and H. H. Foster. Effect of Impingement Angle on Drop-Size Distribution and Spray Pattern of Two Impinging Water Jets. NASA TN D-872, 1961.
- A-41. R. A. Dickerson. "Like and Unlike Impinging Injection Element Droplet Sizes." *Journal of Spacecraft and Rockets*, Vol. 6, No. 11, November 1969.
- A-42. M. E. Heidmann, R. J. Priem, and J. C. Humphrey. A Study of Sprays Formed by Two Impinging Jets. NACA TN 3835, 1957.
- A-43. E. Rabin, A. R. Schallennueller, and R. B. Lawhead. Displacement and Shattering of Propellant Droplets. AFOSR TR 60-75, 1960.
- A-44. M. M. El Wakil, et al. Experimental and Calculated Temperature and Mass Histories of Vaporizing Fuel Drops. NACA TN 3490, 1956.
- A-45. J. G. Sotter. Nonsteady Evaporation of Liquid Propellant Drops. The Grossman Model JPL TR 32-1061, 1968.
- A-46. W. N. Bond and D. A. Newton. *Phil. Mag.* (7), 5, 794, 1928.
- A-47. R. R. Hughes and E. R. Gilliland. "The Mechanics of Drops." *Chem. Eng. Prog.*, Vol. 28, No. 10, 1952.
- A-48. G. A. E. Godsave. "Studies of the Combustion of Drops in a Fuel Spray - The Burning of Single Drops of Fuel." *Fourth Symposium on Combustion*, Williams and Wilkins, 1953.
- A-49. D. B. Spalding. "The Combustion of Liquid Fuels." *Fourth Symposium on Combustion*, Williams and Wilkins, 1953.
- A-50. G. A. Agoston, H. Wise, and W. A. Rosser. "Dynamic Factors Affecting the Combustion of Liquid Spheres." *Sixth Symposium on Combustion*, Reinhold, 1956.
- A-51. W. T. Webber. Effects of Gas Motion on Heterogeneous Combustion etc. WADC TR 59-50, 1959.
- A-52. W. E. Ranz and W. R. Marshall. "Evaporation from Drops." *Chem. Eng. Prog.*, Vol. 48, No. 4, 1952.

- A-53. H. C. Barnett and R. B. Hibbard, Ed. Basic Considerations in the Combustion of Hydro Carbon Fuels with Air. NACA Report 1300, 1957.
- A-54. W. H. Walker, W. K. Lewis, W. H. McAdams, and E. R. Gilliland, Principles of Chemical Engineering. McGraw-Hill Book Company, 1937.
- A-55. G. G. Brown, Unit Operations. John Wiley & Sons, New York, 1950.
- A-56. L. J. Zajac and W. H. Nurick. "Correlation of Spray Droplet Distribution and Injector Variables." 8th JANNAF Liquid Propellant Combustion Instability Meeting, Oct. 1971.

Appendix B

MULTRAN

MULTIPHASE NOZZLE AND PLUME TRANSPORT
COMPUTER PROGRAM

A Multiphase Nozzle and Plume Flow Field
Characterization Model

Program Number H612

TABLE OF CONTENTS

Section		
B. 1	INTRODUCTION	289
B. 2	ANALYSIS, INTEGRATION METHOD, AND SUBROUTINE STRUCTURE	290
B. 3	PROGRAM OVERLAY STRUCTURE	290
B. 4	PROGRAM USER'S MANUAL	291
	a. TD2 Program Input	291
	b. TD2P Program Input	296
	c. TD2/TD2P Output Description	298
	d. SLINES Subprogram	303
B. 5	SAMPLE CASE	309

Appendix B

MULTRAN

MULTIPHASE NOZZLE AND PLUME TRANSPORT COMPUTER PROGRAM

A Multiphase Nozzle and Plume Flow Field Characterization Model

B.1 INTRODUCTION

The computer program described in this appendix is a subprogram to the Plume Contamination Effects Prediction Computer Program, CONTAM, and performs the subsonic, transonic, and supersonic computations required to define the steady-state multiphase flow field within a rocket nozzle and exhaust plume. The TCC program (Appendix A) provides the input to MULTRAN in terms of quasi-steady values of droplet distributions, and gas properties, averaged over specified portions of a transient engine pulse. The nozzle and plume flow field defined by MULTRAN provides the input data for the kinetics and condensation computation, KINCON (Appendix C), and subsequently for the deposition and surface effects computations, SURFACE (Appendix D). MULTRAN may also be used as an independent computer program on any third generation computer with a core exceeding 135,000g words and a Fortran IV processor.

The MULTRAN program combines three previously independent programs:

- a. TD2, Axisymmetric Two-Phase Perfect Gas Performance Computer Program (developed by TRW for NASA/MSFC, reference B-1)
- b. TD2P, Axisymmetric Two-Phase Perfect Gas Plume Analysis Computer Program (developed by Dynamic Science and MDAC)
- c. SLINES, Streamline Generation Computer Program (developed by MDAC)

(B-1) G. R. Nickerson and J. R. Kliegel. Axisymmetric Two-Phase Perfect Gas Performance Program, TRW Systems Report No. 02874-6006-R000, Vol. I and II, April 1967.

B. 2 ANALYSIS, INTEGRATION METHOD, AND SUBROUTINE STRUCTURE

The axisymmetric two-phase analysis, numerical methods, and subroutine structure used in TD2, which also forms the basis for TD2P, is discussed in detail in Reference B-1 and will not be repeated here.

B. 3 PROGRAM OVERLAY STRUCTURE

OVERLAY
(DFILE, 3, 0)

TD2
FIND
ZERØ
ABCALC
CCALC
DCALC
FCALC
JAMES
LEGS
NEWT
ØNED
PARTIL
PCALC
PRØP
TRACE
WDGI
NZMAIN
CØNSTS
N3MAIN
WALL
ACØMP
ADJK
AXISPT
CHECK
CNTRL
CRIT
EFN
ERRØR
KPBPT
PRINT
PTINT
SUMPI
SUMP2
TAFN
WLPT

OVERLAY
(EFILE, 4, 0)

TD2P
ACØMP
ADJK
AXISPT
CHECK
CNTRL3
CRIT
EFN
ERRØR
FIND
KPBPTP
NEXT
PMEYER
PRINT
PTINT
SUMPI
SUMP2
TAFN

OVERLAY
(XMGKS, 5, 0)

XMGKS

B.4 PROGRAM USER'S MANUAL

This program was developed on the CDC 6500 computer using the FORTRAN IV language. Conversion to another computer system should be straight forward provided sufficient core storage (135,000 words) is available. Program overlay extends two levels deep including the executive level, when used as a subprogram to CONTAM:

The description of the input to and output from the computer program is divided into the following four subsections:

- B.4.a TD2 INPUT
- B.4.b TD2P INPUT
- B.4.c TD2/TD2P OUTPUT DESCRIPTION
- B.4.d SLINES Subprogram

A card listing for the complete input for the sample case is given in Subsection B.5.

a. TD2 Program Input

The program input for the Axisymmetric Two-Phase Perfect Gas Performance Subprogram TD2 conforms to the I. B. M. NAMELIST format. All input items are read under control of the name \$DATA. The input items are divided into five types 1) Propellant Data, 2) Particle Data, 3) Inlet and Throat Parameters, 4) Characteristics mesh control data, 5) Nozzle Wall Contour Data.

For some input items, values are assumed by the program. These items need not be input to the program.

\$ DATA

(1) Propellant Data

<u>Item Name</u>	<u>Input Quantity</u>	<u>Units</u>
CAPN =	N, Viscosity temperature exponent.	none
CPG =	C_{gp} , specific heat of gas at constant pressure.	$\text{ft}^2/\text{sec}^2 \cdot \text{R}$
CPL =	C_{pl} , particle heat capacity ($T_p > T_{pm}$).	$\text{ft}^2/\text{sec}^2 \cdot \text{R}$
CPS =	C_{ps} , particle heat capacity ($T_p < T_{pm}$).	$\text{ft}^2/\text{sec}^2 \cdot \text{R}$
GAMMA =	γ , specific heat ratio, C_{gp}/C_{gv} .	none
GMG0 =	μ_{go} , chamber gas viscosity coefficient.	lb/ft sec
HPL =	h_{pl} , liquid particle enthalpy ($T_p = T_{pm}$).	ft^2/sec^2
HPS =	h_{ps} , solid particle enthalpy ($T_p = T_{pm}$).	ft^2/sec^2

<u>Item Name</u>	<u>Input Quantity</u>	<u>Units</u>
PC =	P_{g_0} , chamber pressure.	PSIA
PR =	P_r , Prandtl number.	none
RCAP =	R, gas constant.	$\text{ft}^2/\text{sec}^2 \cdot \text{R}$
SMP =	m_p , particle density.	lb/ft^3
TG0 =	T_{g_0} , chamber temperature	$^{\circ}\text{R}$
TPM =	T_{p_m} , particle solidification temperature.	$^{\circ}\text{R}$

(2) Particle Data

<u>Item</u>	<u>Input Quantity</u>	<u>Units</u>
R(1) =	r_{p_j} , the radius of each of n particles is to be input so that $r_{p_1} < r_{p_2} \dots < r_{p_n}$ set $r_{p_{n+1}} = 0$. n < 10 is required.	ft
WPWGT =	$\Sigma \dot{w}_{p_j} / \dot{w}_g$, ratio of particle to gas weight flow.	none
WPWT(1) =	$\dot{w}_{p_j} / \Sigma \dot{w}_{p_j}$, particle weight flow fractions corresponding to each of the above particle radii, r_{p_j} .	none

(3) Inlet and Throat Parameters (Figure B-1)

<u>Item Name</u>	<u>Input Quantity</u>	<u>Units</u>	<u>Assumed Value</u>
DZI =	Δz , particle trajectory integration step size.	none	0.002
DZMIN =	Δz_{min} , inlet step size parameter.	none	0.002
NILP =	N_i , number of initial line points.	none	15
RRT =	R_c , throat radius of curvature. A value $R_c > 1$ is required.	none	

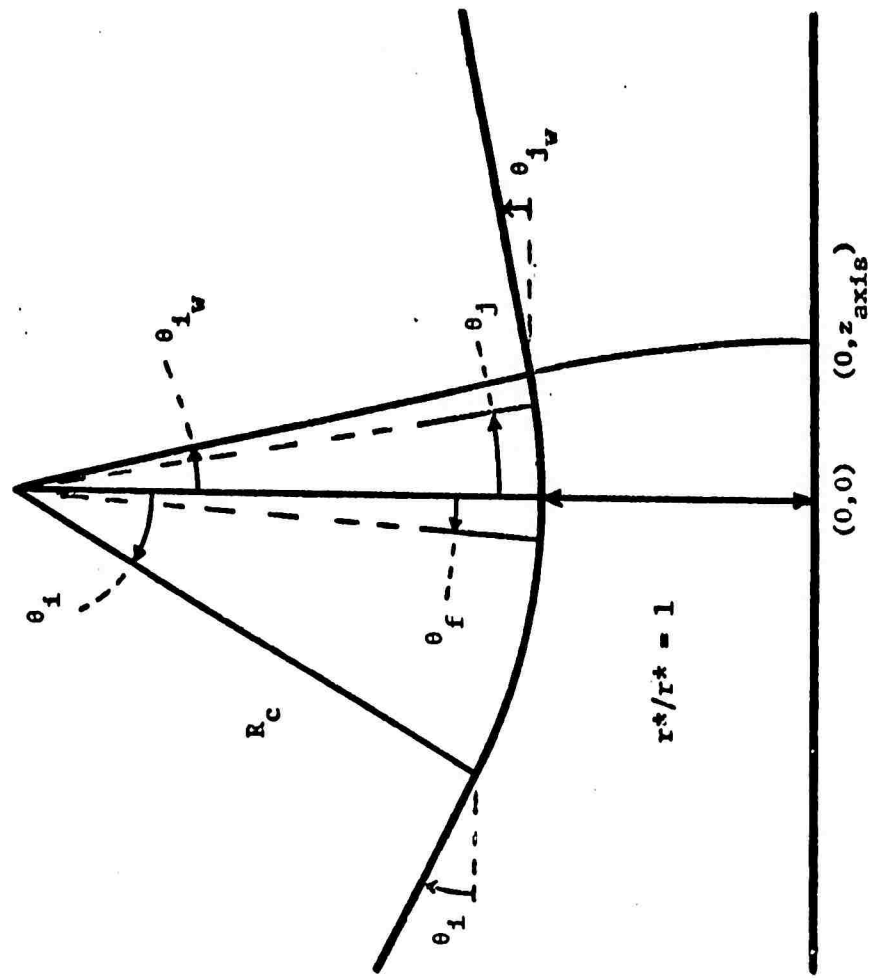


Figure B-1. Inlet and Throat Parameters

<u>Item Name</u>	<u>Input Quantity</u>	<u>Units</u>	<u>Assumed Value</u>
RT =	r^* , throat radius.	ft	
SAUR(1) =	First estimates of x_o , u_o , α , β , and γ for the special throat expansion. Required only if $\theta_i > \theta_f$.	none	-0.15, 1, 0.5, 0.3, -1
THFD =	θ_f , faring angle ($\theta_f > \theta_i \Rightarrow$ no faring).	degrees	5.0
THID =	θ_i , inlet angle.	degrees	
THIW =	θ_{iw} , intersection of initial line and wall.	degrees	12.0
THJD =	θ_j , angle defining the zone farthest downstream	degrees	9.0
VAR(1) =	First estimates of x_o , u_o , α , β , and γ for the zone farthest upstream	none	0.3, 0, 0, 0.1, 0.1
ZAX =	z_{axis} , intersection of initial line and axis.	none	
ZI =	n_i , number of upstream zones.	none	3.0
ZJ =	n_j , number of downstream zones.	none	2.0

(4) Characteristics Mesh Control Data

<u>Item Name</u>	<u>Input Quantity</u>	<u>Units</u>	<u>Assumed Value</u>
DL =	Δl , maximum LRC mesh width.	none	0.2
DTWI =	$\Delta \theta_w$, maximum flow angle change along the wall.	degrees	3.0
DR =	Δr , maximum RRC mesh width.	none	0.2
EW =	ϵ_w , end of nozzle wall criterion.	none	0.001
IMAX =	i_{max} , maximum number of iterations per mesh point.	none	5.0
N1 =	n_1 , select each n_1^{th} LRC for print.	none	1,000
N2 =	n_2 , print each n_2^{th} point on selected characteristics.	none	1.0

(5) Nozzle Wall Contour Data

<u>Item Name</u>	<u>Input Quantity</u>	<u>Units</u>
IWALL =	Option flag.	none
	0=> tabular input	
	1=> cone	
	2=> circular arc	
	3=> parabola	

If the wall is to be input in tabular form (IWALL = 0):

PW(1) = (r_i, z_i) , wall coordinates $i = 1, 2, \dots, n$ points. none
viz.: PW(1) = $r_1, z_1, r_2, z_2, \dots, r_n, z_n, 0, 0$.

Note:

(a) always mark the end of the table with two zeros.

(b) $n \leq 79$ is required.

If a cone, parabola, or circular arc contour is to be specified then:

THJW = θ_j , attachment angle for the contour; e.g., for a degrees
cone, the conical half angle.

EPS = ϵ , nozzle expansion ratio (cone only). none

RWMAX = r_{\max} , nozzle exit radius (parabola or arc only). none

ZWMAX = z_{\max} , nozzle length from throat to exit (parabola or arc only). none

\$ END OF CASE.

NOTE:

A case is defined as the data included or implied between the \$DATA card and the \$ signifying the end of case. Whenever a value is input as data for a case, that value will remain set for succeeding cases until a new value is input. The values indicated as assumed by the program hold only until a different value is input. If more than one value is input for a given quantity within a case, the last value given will be used.

b. TD2P Program Input

The program input for the Axisymmetric Two-Phase Perfect Gas Plume Analysis computer subprogram is an extension of the input to the TD2 computer subprogram. Input to the TD2P computer subprogram consists of a binary start tape ((TAPE 8) or an extend disc storage file (TAPE 8) generated by the TD2 computer subprogram. The same NAMELIST data deck used for the TD2 calculation must be used for the TD2P calculation and is read from TAPE 8 automatically. The following input items must be inserted into the data deck following the TD2 data. Additional data for the TD2P subprogram is read under control of the name DATAP.

\$ DATAP

<u>Item Name</u>	<u>Input Quantity</u>	<u>Units</u>
PMA =	θ_{PM} , The Prandtl-Meyer expansion angle to be used at the nozzle lip.	degrees
NPM =	The number of Prandtl-Meyer points to be generated.	none
	NPM < 0 The maximum number (98-IP) of points will be generated.	
	NPM = 0 Points will be generated one degree apart unless less than 5 points would result.	
	NPM > 0 This number of points will be generated unless the maximum would be exceeded. If the maximum would be exceeded, points are placed one degree apart unless this would again exceed the maximum or would result in less than 5 points.	
ZMAX =	This item defines a cutoff plane for the calculations. The run will be terminated when an axis point is calculated located downstream of $Z = ZMAX$.	none
PCUT =	If a Pressure, P_g , is calculated such that the ratio P_g/P_{g0} drops below this value, no more points will be calculated on the characteristic.	none

<u>Item Name</u>	<u>Input Quantity</u>	<u>Units</u>
NPLOT =	Flag for auxiliary radiation output on tape unit 9, (see Description of Program Output). NPLOT = 0 deletes this output. NPLOT = 1 requests this output.	none
AREA =	Flag for auxiliary force field output on tape unit 9. This item is also used to represent the frontal surface area of a body in the plume, (see Description of Program Output). AREA = 0 deletes this output. AREA > 0 requests this output e. g., AREA = 1.	in. ²
EMIS =	ϵ_p , particle emissivity used for the radiation printout.	none
C1 =	C_1 , force coefficient used for the force printout.	none
C2 =	C_2 , force coefficient used for the force printout.	none

REMARKS

If the mesh width control items DL and DR have been input as part of the NAMELIST DATA deck, these items should be deleted for the plume calculation. The TD2P computer program will then assume large values for these variables and avoid the generation of many mesh points.

The last item printed at the end of a complete TD2 calculation is the item IP = nm, where nm is number of points used along the last running characteristic. Reference should be made to this number to determine if sufficient space is available (98-IP) for the Prandtl-Meyer expansion.

The TD2P computer subprogram is not suitable for running consecutive cases.

c. TD2/TD2P Output Description

Program output may be viewed in detail by examining the sample case in Section B. 5. The program output follows the sequence listed below:

For the one-dimensional inlet and the axisymmetric transonic throat calculations

- (1) The values k and \dot{m}_g for gas-particle equilibrium.
- (2) Initial and final conditions for the one-dimensional inlet integration.
- (3) Converged values for x_0 , u_0 , α , β , γ and f_1 , f_2 , f_3 , f_4 , f_5 for each transonic flow zone.
- (4) The corrected estimate for k , corrected values for x_0 , u_0 , α , β , and γ in the transonic zone containing the initial supersonic data line, corrected values for \dot{m}_g and \dot{m}_{pj} .
- (5) Items 2, 3, and 4 are iterated twice.
- (6) The gas-particle flow properties P_g , ρ_g , u_g , v_g , r , z , h_{pj} , ρ_{pj} , u_{pj} and v_{pj} along the initial supersonic data line.

For the supersonic method of characteristics calculations for the nozzle and plume, printout may occur after the completion of each mesh point calculation. Points for print are selected as follows:

The following points are always printed:

axis points.

Kth particle boundary points.

initial line points.

wall points.

Interior points are selected for print only along every n_1^{th} left running characteristic and only at every n_2^{th} position along these characteristics.

Inserted points are printed if all points are to be printed ($n_1 = n_2 = 1$).

The items printed are listed below in the order they appear, left to right, on the output sheet. A header is printed for identification purposes above each characteristic.

Row One:

<u>Item</u>	<u>Header</u>	<u>Meaning</u>	<u>Units</u>
LRC number	LRC	Left running characteristic number.	none
Ident. number	ID	Type of point (see below).	none
r	R	r position coordinate.	none
z	Z	z position coordinate.	none
M	MACH	Mach number.	none
T_g	TG	Gas temperature.	°R
V_g	VG	Gas velocity (scalar).	ft/sec
θ_g	THETA-G	Streamline angle	degrees
T_g/T_{g_0}	TG/TG0	Ratio of gas temperature to chamber temperature.	none
P_g/P_{g_0}	PG/PG0	Ratio of gas pressure to chamber pressure.	none
ρ_g/ρ_{g_0}	DG/DG0	Ratio of gas density to chamber density.	none
$\frac{\sum \rho_{pj}^k}{\rho_g}$	SDK/DG	Ratio of total particle density to gas density.	none
C_F	CF	Thrust coefficient.	none
I_{sp}	ISP	Specific impulse.	sec.
interaction no.	IT	Number of interactions required.	none

Rows Two through K+1

A row is printed for each particle size, $k=1, \dots, K$.

<u>Item</u>	<u>Header</u>	<u>Meaning</u>	<u>Units</u>
k	K	Particle size number.	none
Re_k	REK	Particle Reynolds number	none
V_{p_k}	VPK	Particle velocity (scalar).	ft/sec

<u>Item</u>	<u>Header</u>	<u>Meaning</u>	<u>Units</u>
θ_{pk}	THETA-K	Particle streamline angle,	degrees
T_{pk}	TPK	Particle temperature,	°R
ρ_{pk} / ρ_g	DPK/DG	Ratio of particle density to gas density,	none
ρ_{pk} / ρ_{p0}	DPK/DP0	Ratio of particle density to chamber particle density,	none
r_{pk}	RPK	Particle radius	ft

d. Additional Output

Table B-1 illustrates additional output options as discussed below.

(1) Force Field Print

If the force field auxiliary output is requested (AREA > 0) the following items will be computed and written on tape unit 9.

	<u>Item</u>	<u>Units</u>
$F_g =$	$\frac{C_1 A}{144g} \frac{\gamma}{2} P_g M^2$	lb _f
$F_{pk} =$	$\frac{C_2 A}{144g} \rho_{pk} V_{pk}^2$	lb _f
$F_p =$	$\sum_{k=1}^{k_{max}} F_{pk}$	lb _f
$F =$	$F_g + F_p$	lb _f
F_p / F_g		None

The quantities C_1 and C_2 (which are nondimensional force coefficients) and A (which is surface area in square inches) are input as C_1 , C_2 , and AREA.

(2) Radiation Print

If the radiation auxiliary output is requested (NPLØT = 1) the following items will be computed and written on tape unit 9.

Table B-I. OPTIONAL OUTPUT - RADIATION AND FORCEFIELD PROPERTIES

LMC ID	R	Z	K	FKP	NPK	MAN PK	MAN PK	TP4 4
4 3	11.67444	31.741521E-01	12.005487E-01	12.006750E+09	71.648925E-11	56.627119E-01	29.376589E+13	
			2	27.531414E-01	22.013422E+08	26.937847E-10	11.533647E+00	29.726099E+13
			3	36.749444E-01	14.223337E+08	69.188494E-10	13.027043E+00	33.768048E+13
			4	73.217735E-01	17.774416E+08	13.531111E-09	24.053446E+00	37.337741E+13
			5	95.471431E-01	13.11152E+08	23.068425E-09	30.245363E+00	40.580945E+13
			6	74.632752E-01	51.273753E+07	35.572877E-09	18.239549E+00	43.430402E+13
			7	33.234366E-01	14.981786E+07	50.497593E-09	10.190230E+00	45.843655E+13
				F SUM P	F SUM G	F	F/FG	TMAP 4
				33.644307E+00	27.589356E+01	30.957787E+01	12.204147E-02	37.403884E+13
4 4	11.67444	34.107407E-01	75.217008E-02	26.037919E+08	44.637826E-11	25.906866E-01	18.301439E+13	
			2	17.873304E-01	20.463396E+08	26.621120E-10	55.546698E-01	29.376589E+13
			3	25.514093E-01	45.987393E+07	60.190645E-10	57.727317E-01	29.376589E+13
			4	55.240016E-01	76.793414E+07	10.646008E-09	10.304635E+00	29.376589E+13
			5	74.474996E-01	77.879995E+07	16.699257E-09	13.005381E+00	29.376589E+13
			6	54.360571E-01	33.714843E+07	24.723572E-09	83.355136E-01	30.184785E+13
			7	34.672392E-01	14.787049E+07	36.419576E-09	53.453806E-01	32.738927E+13
				F SUM P	F SUM G	F	F/FG	TMAP 4
				27.466106E+00	16.148356E+01	18.934967E+01	16.966581E-02	29.927252E+13
4 4	12.67444	34.472155E-01	73.371945E-02	25.531599E+08	40.622931E-11	22.558563E-01	16.655702E+13	
			2	17.449455E-01	20.013153E+08	26.621120E-10	53.277255E-01	29.376589E+13
			3	25.042487E-01	42.085539E+07	60.190645E-10	55.426917E-01	29.376589E+13
			4	54.476350E-01	73.262512E+07	10.646008E-09	99.266053E-01	29.376589E+13
			5	79.015371E-01	75.560781E+07	16.699257E-09	12.614089E+00	29.376589E+13
			6	54.550009E-01	33.013352E+07	24.061600E-09	79.435407E-01	29.376589E+13
				F SUM P	F SUM G	F	F/FG	TMAP 4
				23.741284E+00	15.532782E+01	17.911911E+01	15.316221E-02	29.260213E+13
4 4	14.64444	34.554267E-01	71.120493E-02	22.407795E+08	34.515105E-11	19.136761E-01	14.971463E+13	
			2	16.947033E-01	18.932293E+08	26.621120E-10	50.399883E-01	29.376589E+13
			3	24.372366E-01	37.117995E+07	60.190645E-10	52.439918E-01	29.376589E+13
			4	53.365172E-01	28.645204E+07	10.646008E-09	96.374951E-01	29.376589E+13
			5	78.140420E-01	72.515560E+07	16.699257E-09	12.109560E+00	29.376589E+13
				F SUM P	F SUM G	F	F/FG	TMAP 4
				14.001704E+00	14.732367E+01	16.532537E+01	12.219152E-02	27.856576E+13

NOT REPRODUCIBLE

<u>Item</u>	<u>Header</u>	<u>Meaning</u>	<u>Units</u>
<u>Row 1:</u>			
LRC number	LRC	Left characteristic number.	none
Ident. number	ID	Identification code.	none
r	R	r, radial coordinate	none
z	Z	z, axial coordinate	none
Rows 1 through k_{\max} (i. e., for each particle size $k = 1, \dots, k_{\max}$):			
N_{Pk}	NPK	Particle number density	number of particles/ft ³
q_1	RAD PK		BTU/sec
q_2	RAD BAR PK		BTU-number of particles/sec
\bar{T}_{Pk}^4	TPK 4		°R ⁴
Row $k_{\max} + 1$:			
\bar{T}_p^4	TBAR 4	Effective particle temperature	°R ⁴

where:

$$N_{Pk} = \frac{\rho_{Pk}}{\frac{4}{3} \pi r_{Pk}^3 m_p}$$

$$q_1 = \epsilon_p \sigma T_{Pk}^4 r_{Pk}^2$$

$$q_2 = \epsilon_p \sigma T_{Pk}^4 r_{Pk}^2 N_{Pk}$$

$$\sigma = 0.475834 \times 10^{-12} \text{ BTU/ft}^2\text{-sec-}^\circ\text{R}^4$$

$$\bar{T}_p^4 = \frac{\sum_{k=1}^{k_{\max}} T_{Pk}^4 N_{Pk} r_{Pk}^2}{\sum_{k=1}^{k_{\max}} N_{Pk} r_{Pk}^2}$$

d. SLINES Subprogram

This computer subprogram, SLINES, was developed to provide the necessary interface between the TD2 and TD2P subprograms and the KINCON subprogram. Basically, the program interpolates from data points on the characteristic lines (TD2 and TD2P results) to determine points of constant percentage of mass flow running through the throat, nozzle, and plume.

Subsection (1) lists the program variables FORTRAN names, symbols, and definitions. Subsection (2) discusses the program logic interpolation equations and editing technique. Subsection (3) provides the user with the necessary operating information. Subsection B.5 provides input and output for a sample case of the MULTRAN program, which includes the output from SLINES (last portion).

(1) FORTRAN Variables

The FORTRAN names given are the names used throughout the program. The symbols are used in the text of this document.

<u>FORTTRAN NAME</u>	<u>SYMBOL</u>	<u>DEFINITION</u>
Z	Z	The axial distance of a point on a streamline.
R	R	The radial distance of a point on a streamline.
P	P	The pressure at a point on a streamline.
S	S	The distance from the initial point on a streamline to a given point on a streamline.
T	T	The temperature at a point on a streamline.
V	V	The velocity of the gas at a point on a streamline.
KD	i	The i^{th} point along a streamline. ($1 \leq i \leq n$)
JD	n	The total number of points along a streamline before editing.
ID	j	The streamline identification number. ($1 \leq j \leq m$)
NSL	m	The total number of streamlines.
K	k	A given point on a characteristic line. ($1 \leq k \leq \text{NPTS}$)

<u>FORTTRAN NAME</u>	<u>SYMBOL</u>	<u>DEFINITION</u>
NPTS	-	Total number of points on a given characteristic line.
N	N	The number of points on a streamline in the throat only.
PCM	η	The percentage of normalized integrated total mass pertaining to the point on a characteristic line.
PCS	ϵ	The percentage of normalized integrated total mass criteria for a streamline.
Z, R, P, S, T, V ZMGKS, RMGKS, PMGKS, TMGKS, VMGKS	X	The class of parameters pertaining to the properties of a point on a streamline or characteristic line. Each parameter is defined elsewhere in this glossary.
DSK	ΔS	The streamline distance criteria used in editing.
SX	S^{np}	The distance of the streamline from the supersonic start line through the nozzle and plume.
SID	-	The name of the namelist through which the user input data is provided.
TØTM	-	The integrated total mass along a characteristic line.
ZMGKS	-	The axial distance at a point on a characteristic line.
RMGKS	-	The radial distance at a point on a characteristic line.
PMGKS	-	The pressure at a point on a characteristic line.
TMGKS	-	The temperature at a point on a characteristic line.
ZINIT	-	The distance of the initial point on a streamline (ZINIT = S (j, 1) = 0).
PINIT	-	The pressure at the initial point of a streamline.

<u>FORTTRAN NAME</u>	<u>SYMBOL</u>	<u>DEFINITION</u>
TINIT	-	The temperature at the initial point of a streamline.
VINIT	-	The gas velocity at the initial point of a streamline.
MGKSK	-	The total number of points on a streamline after editing.
EXIT	-	The streamline distance of the last point on a streamline [EXIT = S(j, MGKSK)].

(2) Program Description

The program runs on the CDC 6500 computer system. It is written in FORTRAN IV and requires a field length less than 40,000g. A nominal case providing ten streamlines will require less than 7 central processor seconds and less than 20 peripheral processor seconds to execute.

The program includes five distinct functions:

1. Input
2. Streamline Location
3. Data Interpolation
4. Data Editing
5. Output

Each function is discussed in the subsequent paragraphs.

(a) Data Input

Two sources are required for data input: cards via NAME-LIST which is user data allowing the program to know how many streamlines are desired and the percent mass flowing within a torroid bounded by each streamline; and logical file TAPE 12 (tape or disc) which provides the program with data from the TD2 and TD2P subprograms on which to operate.

The data from the TD2 and TD2P subprograms consists of two records for each characteristic line. The first record tells how many points are on the characteristic line and the total integrated mass associated with the characteristic line. The second record contains the data designating the location, pressure and percentage of the normalized integrated total mass for each point on the characteristic line. The first requirements of the program is to provide initial temperature and velocity properties of each streamline. Therefore, the initial characteristic line has an additional record of data associated with it which gives the temperature and velocity properties associated with each point on the initial characteristic line. This

record follows the first two records, in order. The last record of both the TD2 and the TD2P subprograms contain a one word, negative number, record. This permits the program to know when there are no more characteristic lines provided by the respective programs.

(b) Streamline Location

The definition of a streamline is that line which runs through the throat, nozzle, and plume bounding a given constant percentage of the mass flow between it and the nozzle axis.

There are a discrete number of points on a characteristic line. The properties at any point usually will not meet the criteria for a point on the desired streamline, therefore, interpolation must be performed between the two input data points which bound the desired point on the streamline in order to obtain the necessary properties (location and pressure) on the streamline.

The initial point, with regard to distance along a streamline, is designated as the interpolated point on the initial TD2 subsonic start line. Each subsequent streamline point has a distance corresponding to:

$$S_i = S_{i-1} + \left[(Z_i - Z_{i-1})^2 + (R_i - R_{i-1})^2 \right]^{1/2}$$

where

S = the distance along the streamline

Z = axial distance along the streamline

R = radial distance along the streamline

i = the i^{th} point along the streamline ($1 \leq i \leq n$)

n = the total number of points along the streamline

As previously stated, $S_1 = 0$.

(c) Data Interpolation

Linear interpolation is used to locate a streamline point as follows:

$$X_{ji} = X_{k-1} + \left[\frac{\epsilon_j - \eta_{k-1}}{\eta_k - \eta_{k-1}} \right] \left[X_k - X_{k-1} \right]$$

where:

- X = the required streamline property (location, pressure, mass, etc.)
- ϵ = the percentage of normalized integrated total mass criteria for the streamline
- η = the percentage of normalized integrated total mass pertaining to the points on the characteristic line
- k = the point on the characteristic line having the greater value and bounding the streamline value
- k-1 = the point on the characteristic line having the lesser value and bounding the streamline value
- i = the i^{th} point along the streamline ($1 \leq i \leq n$)
- n = the total number of points along the streamline
- j = the streamline identification number ($1 \leq j \leq m$)
- m = the total number of streamlines

(d) Data Editing

There exists two reasons for editing the streamline data before output:

1. Due to the change in the nature of the characteristic lines at the supersonic start line in conjunction with the logic used previously in the program, there exists a redundant point along the axis streamline at the supersonic start line. This redundant point must be removed.
2. The KINCON program will accept a maximum of 101 data points for each streamline.

To locate the redundant point along the axial streamline, the points along that streamline are searched until two points are found which have no separation distance. The redundant point and its associated properties are removed from that streamline. In addition, the location of that point provides information as to the location of the supersonic start line and the number of points in the throat, along the streamline, which will be required for use in subsequent editing.

It is desirable that each point and its relevant properties along each streamline in the throat be provided as input to the KINCON program. Therefore these data are not edited. The remaining points along

the streamline, in the nozzle and plume, must be edited by some criteria which will limit the total number of points along the streamline to not more than 101. The criteria chosen is such that each point (exclusive of the last two points) in the nozzle and plume shall be separated by at least some distance determined by:

$$\Delta S_j = \frac{S_j^{np}}{100 - N_j}$$

where

ΔS = the distance criteria for editing

S^{np} = the distance of the streamline from the supersonic start line through the nozzle and plume

N = the number of points along the streamline through the throat to the supersonic start line

j = the streamline identification number

The last point along the streamline is always made available for output regardless of its distance from the previous point.

(e) Output

The output of this program is both printed and written onto a logical file (TAPE 8). The printed output is provided for the scrutiny of the user. The TAPE 8 file output is for use as input to the KINCON program. The written data contains only that information which is necessary for the operation of the KINCON program. The printed output provides the same data as the TAPE 8 file output but also contains other pertinent data which allows the user to determine the validity of the data. A sample of the printed output may be found in Subsection B. 5.

(3) Program User's Manual

Input to the computer program is divided into two subsections:

(a) NAMELIST/SID

(b) Logical File

Written output from the computer program is on logical file unit number 8. The sample case provided in Subsection B. 5 details the loadsheets for the NAMELIST card, and computer output.

(a) NAMELIST/SID

The NAMELIST feature permits the input of parameters without a format specification. The NAMELIST/SID contains two parameters:

1. NSL; the number of streamlines for which the program is to provide data.
2. PCS; an array of up to ten mass % values which provide the criteria for the streamline definition. The variable NSL determines the number of values which must be input.

The two permissible formats for PCS are:

1. PCS(1) = a, b, c,, j where a through j are the quantities corresponding to the PCS criteria.
2. PCS(2) = b, PCS(1) = a, PCS(4) = d, PCS(5) = e, PCS(7) = g, PCS(3) = c, and so on.

(b) Logical Files

The logical file input may be either tape or disc file. The unit number for the logical file is 12. This means that the logical file name used on the REQUEST or ATTACH card must be TAPE 12. The data on the logical file is provided from the TD2 and TD2P programs. The data is binary (unformatted).

B. 5 SAMPLE CASE

Included in the section are the computer input and output for a sample case using the MULTRAN program as an independent program. The subprograms to MULTRAN, which are called sequentially are TD2, TD2P and SLINES. The use of MULTRAN as a subprogram to CONTAM for the analysis of contaminant transport is illustrated in Section 4 at the main text. To illustrate the use of MULTRAN as an independent program for other than bipropellant contaminant transport analysis, the sample case in this section is for a solid rocket motor nozzle and plume.

(B-2) H. H. Radke, L. J. Delaney, and Lt. P. Smith. Exhaust Particle Size Data from Small and Large Solid Rocket Motors. San Bernardino Operations, Aerospace Corporation, Report No. TOR-1001 (S2951-18)-3, July, 1967.

The calculation is performed for a typical solid propellant engine operating at a chamber pressure of 2,250 psia whose exhaust contains 13.6% Al_2O_3 by weight. The particle size distribution was obtained from experimental data of Radke, Delaney and Smith (Reference B-2). Six particle sizes are assumed with radius yielding weight flows as follows:

<u>Particle Size (ft x 10⁶)</u>	<u>Weight Fraction of Total Particles</u>
4.92	0.0214
9.84	0.1180
16.32	0.2390
22.90	0.3260
29.40	0.2344
36.20	<u>0.0612</u>
	1.0000

A complete set of Control Cards and Data Cards for the sample case are listed preceding the sample case. The use of the LIBLIST system routine is illustrated in Table B-II, showing the control cards which allows the user to select the appropriate overlay structure for a particular case, thereby reducing core requirements (in this case from 220,000 for the complete CONTAM program, to 135,000 for MULTRAN)

Table B-II. MULTRAN SAMPLE CASE OUTPUT

CATALOG OF FILE LG1

RECORD NO.	LEVEL NO.	LENGTH	PACKAGE	CHKSUM
	OCTAL	DECIMAL	OCTAL(B)	
1			<CARD IMAGE><OVERLAY(AF,0,0) >	
2	0	348	534 H612	5203
3			<CARD IMAGE><OVERLAY(CFILE,2,0) >	
4	0	46	56 DUM2	4404
5			<CARD IMAGE><OVERLAY(DFILE,3,0) >	
6	0	964	1704 TD2	1730
7	0	1425	2621 BLKDATA	5026
8	0	1274	2372 PARTIL	7452
9	0	62	76 N2MAIN	1266
10	0	529	1021 ONED	53
11	0	311	467 JAMES	5165
12	0	390	606 PROP	4412
13	0	128	200 FIND	2045
14	0	163	243 WDG1	4423
15	0	485	745 STRMLN	4042
16	0	326	506 TRACE	5610
17	0	41	51 N3MAIN	4126
18	0	840	1510 CNTRL	5066
19	0	292	444 NEWT	6600
20	0	424	650 FCALC	1425
21	0	246	366 CONSTS	2663
22	0	263	407 WALL	3162
23	0	448	700 PRINT	3772
24	0	1307	2433 PTINT	5115
25	0	242	362 ERROR	2410
26	0	640	1200 AXISPT	1063
27	0	422	646 WLPT	1776
28	0	1434	2632 KPBPT	4263
29	0	673	1241 LEGS	3540
30	0	219	333 ABCALC	1711
31	0	489	751 CCALC	1305
32	0	36	44 DCALC	752
33	0	1292	2414 PCALC	5746
34	0	181	255 ACOMP	1200
35	0	107	153 SUMP1	4267
36	0	59	73 TAFN	1476
37	0	99	143 EFN	3303
38	0	79	117 CHECK	6143
39	0	55	67 CRIT	6146
40	0	127	177 ADJK	7316
41	0	122	172 SUMP2	2423
42			<CARD IMAGE><OVERLAY(EFILE,4,0) >	
43	0	829	1475 TD2P	2227
44	0	624	1160 CNTRL3	7300
45	0	323	503 PMEYER	676

Table B-II-Continued

46	0	448	700	PRINT	3772
47	0	485	745	STRMLN	4042
48	0	640	1,100	AXISPT	1063
49	0	242	362	ERRUR	2410
50	0	1388	2554	KPBPTP	2422
51	0	1307	2433	PTINT	5115
52	0	38	46	NEXT	5473
53	0	55	67	CRIT	6146
54	0	181	265	ACOMP	1200
55	0	107	153	SUMP1	4267
56	0	59	73	TAFN	1476
57	0	99	143	EFN	3303
58	0	79	117	CHECK	6143
59	0	127	177	ADJK	7316
60	0	122	172	SUMP2	2423
61	0	128	200	FIND	2045
62	<CARD IMAGE><OVERLAY(XMGKS,5,0) >				
63	0	697	1271	XMGKS	5713
64	<CARD IMAGE><OVERLAY(FFILE,6,0) >				
65	0	417	641	SCREEN	4305
66	0	109	155	GTF	7305
67	0	293	445	STF	2315
68	0	129	201	APPROX	647
69	0	128	200	FIND	2045
70	0	73	111	STOICC	4367
71	0	93	135	SPLN	6613
72	0	119	167	DRIVER	2407
73	0	72	110	AF073C	2034
74	<CARD IMAGE><OVERLAY(FFILE,6,1) >				
75	0	48	60	LINK10	3673
76	0	573	1075	TTAPE	2507
77	0	142	216	COLOUR	4242
78	<CARD IMAGE><OVERLAY(FFILE,6,2) >				
79	0	48	60	LINK20	4316
80	0	1322	2452	INPUT	7270
81	0	1085	2075	SPRXIN	2545
82	0	274	422	ECNV	4014
83	0	84	124	NUMBER	6521
84	<CARD IMAGE><OVERLAY(FFILE,6,3) >				
85	0	48	60	LINK30	7777
86	0	474	732	STFSET	757
87	<CARD IMAGE><OVERLAY(FFILE,6,4) >				
88	0	48	60	LINK41	4625
89	0	488	750	PACK1P	6516
90	0	299	453	CONVRT	6407
91	0	455	707	PRES	1213
92	0	674	1242	ADDFIT	5561
93	0	597	1125	SLP	2727
94	0	50	62	TCALC	1022
95	<CARD IMAGE><OVERLAY(FFILE,6,5) >				
96	0	48	60	LINK42	6501

Table B-II-Continued

97	0	599	1127	DERIV	3665
98	0	1096	2110	MAIN	5346
99	0	197	535	EF	4655
100	0	536	1030	SCRX	1612
101	0	410	632	FLU	6066
102	0	95	137	UTIL	7731
103	0	825	1471	OUTPUT	4212
104	0	424	650	INT	7206
105	0	585	1111	IAUX	7141
106	0	67	103	PRNTCK	6136
107	0	700	1274	SHOCK	4730
108	0	103	147	TREE	3566
109	0	717	1315	ADDXXX	2512
110	0	183	267	PLTSUB	3375
111	0	435	663	IAUX1	6200
112	0	178	262	VAPOR	2006
113	0	95	137	ITER	6300
114	0	95	137	OUTXXX	4157
115	0	632	1170	CONAD	3070
116	0	298	452	LESK	4332
117	0	151	227	DROPS	7733
118		<CARD IMAGE><OVERLAY(FILE,6,6) >			
119	0	140	214	LINKSO	6172
120	0	189	275	DSCPLY	6736
121	0	71	107	MAXMIN	4453
122	0	118	166	SCAL	3562
123	17	0	0		0
LEVEL 17GROUP LENGTH IS 41695 121337					
***** END FILE *****					

Table B-II-Continued

CONTROL CARD AND DATA LISTING

```

M612,2,1500,800,600,12000,135000,
ID          HOFFMAN      A03833RBRO47612 40H612 9615780010
-----
REQUEST,CONTAM,HY,      (14640)
REQUEST,TAPE9,HY,      (RESERVE)
COPYBF (CONTAM,REL)
COPYBF (CONTAM,TAPE4)
COPYBF (CONTAM,UCONT)
REWIND(REL)
-----
REWIND(TAPE4)
REWIND(UCONT)
RETURN(CONTAM)
RFL,100,
RFL,60000,
UPDATE(P=UCONT)
-----
RUN(S,,1001,COMPILE)
REWIND(LGO)
RFL,100,
RFL,135000,
COPYLIB(LG1,LGO,REL)
REWIND(LG1)
-----
LISTIT(LG1)
SETCORE,
LOAD(LG1)
NOOD,
RFL,115000,
AFILE,
-----
REWIND(TAPE9)
COPYCF (TAPE9,OUTPUT)
RETURN(TAPE9)
-----
EXIT,
REWIND(TAPE9)
COPYCF (TAPE9,OUTPUT)
RETURN(TAPE9)
-----
•IDENT,SEPT14
•DELETE,TD2,134
  CALL MAXTP(NPG,NPPS,NCPS,N4,N5)
•DELETE,TD2,164
  CALL MAXTP(NPG,NPPS,NCPS,N4,N5)
•DELETE,TD2P,91
  CALL MAXTP(NPG,NPPS,NCPS,N4,N5)
•DELETE,TD2P,127
  CALL MAXTP(NPG,NPPS,NCPS,N4,N5)
•DELETE,XMGKS,10
  CALL MAXTP(NPG,NPPS,NCPS,N4,N5)
•DELETE,XMGKS,134
  CALL MAXTP(NPG,NPPS,NCPS,N4,N5)
-----

```

180

Table B-II-Continued

*DELETE,SCREEN,67
CALL MAXTP(NPG,NPPS,NCPS,N4,N5)

OVERLAY(AFILF,0,0)
M612
OVERLAY(CFILE,2,0)
DUM2
OVERLAY(DFILE,3,0)
TD2

RLKDATA
OVERLAY(EFILF,4,0)
TD2P
OVERLAY(XMGKS,5,0)

XMGKS
OVERLAY(FFILE,6,0)
SCREEN
GTF

STF
APPROX
FIND
STCICC
SPLN
OVERLAY(FFILE,6,1)

LINK10
OVERLAY(FFILE,6,2)
LINK20
OVERLAY(FFILE,6,3)
LINK30
OVERLAY(FFILE,6,4)

LINK41
OVERLAY(FFILE,6,5)
LINK42
DERIV
OVERLAY(FFILE,6,6)
LINK50

*
\$NCASE ICASE=1\$
\$IPATH NOZZLE=T,PLUME=T,SLINES=T\$
\$DATA CAPN=0,6, CPG=15750,0, CPL=8500,0, CPS=6700,0, GAMMA=1,210,
QMG0=5,08E-5, HPL=4,03606E7, HPS=2,78606E7, PR=0,822, RCAP=1917,0,
PC=2250,0, TGD=6250,0,
SMP=250,0, TPM=4170,0,
R(1)=4,92E-6,9,84E-6,16,32E-6,22,9E-6,29,4E-6,36,2E-6, 0,0,
WPMGT=0.136,
WPWT(1)=0,0214,0,1180,0,2390,0,3260,0,2344,0,0612,
RRT=2,5,
RT=0,697,

Table B-II-Continued

ZAX=0.0,
N1=5,
IWALL=1, THJW=21.0, EPS=7.44, THID=30.0, NYAPE=8 \$
SDATAP PMA=50.0, NPM=-1, ZMAX=80.0, PCUT=0.00653, NPLOT=1,
N1=5,
AREA=1.0, EMIS=0.3, C1=1.0, C2=1.0, DL=5.0, DR=5.0 \$
SSID NSL=5, PCS(1)=0.0, PCS(2)=0.2, PCS(3)=0.4, PCS(4)=0.6, PCS(5)=0.8 \$

Table B-II-Continued

SDATA	TD2 (NOZZLE - NAMELIST/DATA PRINTOUT)
CAPN	0.6E+00,
CPL	0.85E+04,
CPS	0.67E+04,
PR	0.822E+00,
DL	0.2E+00,
DR	0.2E+00,
DTWI	0.3E+01,
EW	0.1E+02,
FA	0.0, 0.0, 0.1E+01, 0.125E+01, 0.1E+01, 0.125E+01, 0.1E+01, 0.126E+01, 0.1001E+01, 0.126E+01, 0.1002E+01, 0.1582E+01, 0.1063E+01, 0.1995E+01, 0.1141E+01, 0.251E+01, 0.1224E+01, 0.316E+01, 0.1315E+01, 0.398E+01, 0.1412E+01, 0.501E+01, 0.1517E+01, 0.631E+01, 0.1625E+01, 0.795E+01, 0.1745E+01, 0.1E+02, 0.1874E+01, 0.126E+02, 0.2026E+01, 0.1582E+02, 0.2186E+01, 0.1995E+02, 0.2364E+01, 0.251E+02, 0.2555E+01, 0.316E+02, 0.276E+01, 0.398E+02, 0.3E+01, 0.501E+02, 0.325E+01, 0.631E+02, 0.3534E+01, 0.795E+02, 0.3825E+01, 0.1E+03, 0.4155E+01, 0.316E+03, 0.79E+01, 0.1E+04, 0.2E+02, 0.1001E+04, 0.2002E+02, 0.1E+06, 0.2E+04, 0.0,
GAMMA	0.121E+01,
GMGO	0.50E+04,
HPL	0.403606E+08,
HPS	0.278606E+08,
IMAX	5,
N1	5,
N2	1,

Table B-II-Continued

ZAX	=	0.8E+00,
ZI	=	-.3E+01,
ZJ	=	0.2E+01,
DZ1	=	0.2E+02,
IORDER	=	3,
SOLCON	=	0.0,
ISW1	=	0,
ISW2	=	0,
ISW3	=	0,
VAR	=	0.3E+00, 0.0, 0.0, 0.1E+00, 0.1E+00, 0.0,
FLAG	=	0.0,
THJD	=	0.9E+01,
SAUR	=	0.15E+00, 0.1E+01, 0.5E+00, 0.3E+00, 0.1E+01, 0.0,
THFD	=	0.5E+01,
BPS	=	0.744E+01,
RHMAX	=	0.0,
ZHMAX	=	0.0,
IWALL	=	1,
THIH	=	0.12E+02,
THJH	=	0.21E+02,
NTAPE	=	6,
SEND		

Table B-II--Continued

BEGINNING OF TWO PHASE NOZZLE PROGRAM

CP TIME = 33.945 PP TIME = 206.557

GAS=PARTICLE FLOW (THROAT)

K BAR=1.1928711 WDG= 3332.513 EQUILIBRIUM CONDITIONS.
 ONE DIMENSIONAL FLOW
 ZD= -4.7154 MAX= -2.66987 STEP SIZE= .002000 UO= 423.346 TPIO= 6243.979 AU= 9.0928
 Z= -2.66987 A/YAT= 1.91000 UG= 1410.955 UP(I) TP(I) K(I) L(I) I=1... 6
 1377.957 6186.164 .97748 1330.710 6189.122 .93913 .92071
 1271.853 6192.766 .89760 1219.674 6195.915 .86077 .81797
 1179.875 6198.249 .83268 1146.391 6200.179 .80905 .75349

ITERATION NUMBER 3

1 VAR(I) F(I)
 1 -1.4296234E=01 8.1630957E=02
 2 1.0000000E=00 -1.5680209E=07
 3 4.8352448E=01 -1.1943964E=06
 4 1.8099247E=01 -2.4972899E=06
 5 -8.3384005E=01 -6.4296273E=06

NEXT 2 PAGES OMITTED

ITERATION NUMBER 3

1 VAR(I) F(I)
 1 2.6813848E=01 1.3138703E=08
 2 3.7442189E=01 4.8020254E=09
 3 3.1366425E=01 -9.8832160E=09
 4 1.9353962E=01 0
 5 4.9625531E=01 0

ITERATION NUMBER 3

1 VAR(I) F(I)
 1 1.1992486E=01 4.4576320E=07
 2 5.5201790E=01 -3.0355539E=07
 3 3.4369217E=01 -1.87033331E=08
 4 3.8178315E=01 0
 5 1.9142396E=01 0

ITERATION NUMBER 3

1 VAR(I) F(I)
 1 -7.1181256E=02 2.6235800E=07
 2 7.7892708E=01 -1.6745772E=07
 3 4.0214494E=01 4.3875653E=08
 4 4.4853039E=01 0
 5 -9.4098445E=01 0

Table B-II-Continued

	3	4,9539044E=01	1,3017406E=06
	4	2,8957743E=02	6,1723970E=08
	5	5,8361681E=01	6,050125E=06
ITERATION NUMBER	4		
	1	VAR(I)	F(I)
	1	-4,6130382E=01	2,1752895E=08
	2	1,3437841E=00	-1,4953303E=07
	3	4,8115801E=01	-1,3543688E=07
	4	-3,7311429E=02	-2,3196490E=07
	5	-4,4061143E=01	-4,7520581E=07
← BAR=1,1924398			
ITERATION NUMBER	0		
	1	VAR(I)	F(I)
	1	-4,6130382E=01	-9,8154769E=08
	2	1,3437841E=00	-9,8016217E=09
	3	4,8115801E=01	3,6394933E=07
	4	-3,7311429E=02	8,9702167E=07
	5	-4,4061143E=01	2,3906601E=06

WDG= 3346,204 WDP(1)= 9,73879 53,69988108,76500148,35728106,67162 27,85112
 ***** CHANGE ZONES *****

Z	R	MPC	P
1,25000	0,00000	0,00000	1992,76431
1,25000	,04603	,06137	1992,84691
1,25000	,09206	,00549	1993,09643
1,25000	,13810	,01235	1993,51797
1,25000	,18413	,02194	1994,11993
1,25000	,23016	,03426	1994,91387
1,25000	,27619	,04928	1995,91429
1,25000	,32223	,06699	1997,13837
1,25000	,36826	,08736	1998,60564
1,25000	,41429	,11037	2000,33755
1,25000	,46032	,13599	2002,35708
1,25000	,50636	,16417	2004,66812
1,25000	,55239	,19487	2007,35491
1,25000	,59842	,22803	2010,38133
1,25000	,64445	,26358	2013,79013
1,25000	,69048	,30147	2017,60202
1,25000	,73652	,34159	2021,83473
1,25000	,78255	,38365	2026,50188
1,25000	,82858	,42815	2031,61175
1,25000	,87461	,47436	2037,16591
1,25000	,92065	,52234	2043,15769
1,25000	,96668	,57192	2049,57048
1,25000	1,01271	,62293	2056,37582
1,25000	1,05874	,67516	2063,53136
1,25000	1,10478	,72840	2070,97852
1,25000	1,15081	,78240	2078,64002
1,25000	1,19684	,83687	2086,41717
1,25000	1,24287	,89152	2094,18695

Table B-II-Continued

=1,25000 1,28890 ,94602 2101,79895
 =1,25000 1,33494 1,00000 2109,07218
 TOTAL MASS FLOW = 3,5544769E+03 NO. POINTS = 30

VEL	T
1918,29121	6128,73483
1917,96691	6128,77583
1916,98702	6128,89967
1915,33069	6129,10884
1912,96348	6129,40749
1909,83775	6129,80125
1905,89329	6130,29724
1901,05812	6130,90383
1895,24940	6131,63052
1888,37457	6132,48771
1880,33268	6133,48646
1871,01586	6134,63823
1860,31110	6135,95450
1848,10221	6137,44651
1834,27212	6139,12477
1818,70556	6140,99867
1801,29216	6143,07597
1781,93018	6145,36226
1760,53096	6147,86036
1737,02428	6150,56970
1711,36497	6153,48557
1683,54102	6156,59838
1653,58369	6159,89283
1621,58012	6163,34896
1587,68906	6166,93121
1552,16054	6170,60736
1515,36013	6174,32739
1477,79873	6178,03231
1440,16790	6181,65083
1403,38026	6185,09805

Z	R	MPC	P
=1,16151	0,00000	0,00000	1968,19768
=1,16151	,04435	,00133	1968,27290
=1,16151	,08870	,00532	1968,49977
=1,16151	,13306	,01196	1968,88190
=1,16151	,17741	,02125	1969,42523
=1,16151	,22176	,03318	1970,13792
=1,16151	,26611	,04773	1971,03020
=1,16151	,31046	,06490	1972,11416
=1,16151	,35481	,08466	1973,40350
=1,16151	,39917	,10698	1974,91323
=1,16151	,44352	,13186	1976,65932
=1,16151	,48787	,15924	1978,65831
=1,16151	,53222	,18910	1980,92683

Table B-II--Continued

-1,16151	,57657	,22140	1983,48108
-1,16151	,62093	,07607	1986,33626
-1,16151	,66528	,1308	1989,50589
-1,16151	,70963	,33235	1993,00110
-1,16151	,75398	,37381	1996,82982
-1,16151	,79833	,41738	2000,99583
-1,16151	,84269	,46297	2005,49784
-1,16151	,88704	,51048	2010,32831
-1,16151	,93139	,55978	2015,47229
-1,16151	,97574	,61075	2020,90604
-1,16151	1,02009	,66324	2024,59563
-1,16151	1,06444	,71709	2032,49532
-1,16151	1,10880	,77213	2038,54585
-1,16151	1,15315	,82817	2044,67263
-1,16151	1,19750	,88498	2050,78378
-1,16151	1,24185	,94235	2056,76806
-1,16151	1,28620	1,00000	2062,49282

TOTAL MASS FLOW = 3,5393880E+03

NO. POINTS = 30

Z	R	MPC	P
-1,07302	0,00000	0,00000	1939,71774
-1,07302	,04263	,00129	1939,78092
-1,07302	,08565	,00517	1939,97127
-1,07302	,12848	,01163	1940,29126
-1,07302	,17131	,02067	1940,74492
-1,07302	,21414	,03227	1941,33778
-1,07302	,25696	,04644	1942,07675
-1,07302	,29979	,06315	1942,96995
-1,07302	,34262	,08240	1944,02655
-1,07302	,38544	,10416	1945,25651
-1,07302	,42827	,12842	1946,67034
-1,07302	,47110	,15516	1948,27875
-1,07302	,51393	,18433	1950,09236
-1,07302	,55675	,21592	1952,12127
-1,07302	,59958	,24989	1954,37463
-1,07302	,64241	,28620	1956,86012
-1,07302	,68523	,32479	1959,58345
-1,07302	,72806	,36562	1962,54775
-1,07302	,77089	,40862	1965,75286
-1,07302	,81372	,45374	1969,19465
-1,07302	,85654	,50089	1972,86423
-1,07302	,89937	,54999	1976,74703
-1,07302	,94220	,60096	1980,82192
-1,07302	,98502	,65369	1985,06015
-1,07302	1,02785	,70807	1989,42426
-1,07302	1,07068	,76397	1993,86693
-1,07302	1,11351	,82127	1998,32971
-1,07302	1,15633	,87982	2002,74175
-1,07302	1,19916	,93945	2007,01840
-1,07302	1,24199	1,00000	2011,05985

SEVERL PAGES OMITTED

Table B-II-Continued

P	H=PJ	RHO	RHO=PJ	U	U=PJ	V	V=PJ	R	Z
2.882720E+06	2.9608847E+01	5.8305280E+03	5.8305280E+03	1.2393285E+03	1.2393285E+03	1.0546310E+00	1.0546310E+00	5.1977924E+01	
2.9643068E+06	3.0307963E+01	5.7862526E+03	5.7862526E+03	1.1638050E+03	1.1638050E+03	1.0167727E+00	1.0167727E+00	5.3953641E+01	
J# 1	4.891017E+07	1.059494E+03	5.552314E+03	9.296124E+02	9.296124E+02				
3.0480674E+06	3.1624529E+01	5.7412270E+03	5.7412270E+03	1.0842898E+03	1.0842898E+03	9.7428587E+01	9.7428587E+01	5.6084909E+01	
J# 1	4.908613E+07	1.080837E+03	5.509294E+03	8.664181E+02	8.664181E+02				
J# 2	4.970401E+07	6.965846E+03	5.245389E+03	6.579170E+02	6.579170E+02				
3.1293497E+06	3.1682859E+01	5.7000117E+03	5.7000117E+03	1.0087308E+03	1.0087308E+03	9.3112202E+01	9.3112202E+01	5.8156992E+01	
J# 1	4.924124E+07	1.095333E+03	5.471106E+03	8.073476E+02	8.073476E+02				
J# 2	4.981520E+07	7.057630E+03	5.218683E+03	6.195405E+02	6.195405E+02				
J# 3	5.040200E+07	1.673803E+02	4.947993E+03	4.449407E+02	4.449407E+02				
3.1730410E+06	3.2087804E+01	5.674730E+03	5.674730E+03	9.6083287E+02	9.6083287E+02	9.0220892E+01	9.0220892E+01	5.9492464E+01	
J# 1	4.932372E+07	1.101647E+03	5.448210E+03	7.702462E+02	7.702462E+02				
J# 2	4.988628E+07	7.093915E+03	5.201268E+03	5.939962E+02	5.939962E+02				
J# 3	5.045922E+07	1.687666E+02	4.934801E+03	4.285754E+02	4.285754E+02				
J# 4	5.085724E+07	2.570532E+02	4.743014E+03	3.209399E+02	3.209399E+02				
3.2052655E+06	3.2360865E+01	5.6576702E+03	5.6576702E+03	9.2782988E+02	9.2782988E+02	8.8153400E+01	8.8153400E+01	6.0421592E+01	
J# 1	4.939488E+07	1.105241E+03	5.433011E+03	7.447858E+02	7.447858E+02				
J# 2	4.993530E+07	7.109662E+03	5.189111E+03	5.759173E+02	5.759173E+02				
J# 3	5.049462E+07	1.693670E+02	4.925149E+03	4.166560E+02	4.166560E+02				
J# 4	5.086864E+07	2.586455E+02	4.735327E+03	3.130196E+02	3.130196E+02				
J# 5	5.116843E+07	2.013121E+02	4.595521E+03	2.401332E+02	2.401332E+02				
3.2304882E+06	3.2574285E+01	5.6443569E+03	5.6443569E+03	9.0159717E+02	9.0159717E+02	8.6464039E+01	8.6464039E+01	6.1164798E+01	
J# 1	4.944205E+07	1.107356E+03	5.421256E+03	7.245885E+02	7.245885E+02				
J# 2	4.997419E+07	7.117311E+03	5.179382E+03	5.612966E+02	5.612966E+02				
J# 3	5.052614E+07	1.694539E+02	4.917188E+03	4.068452E+02	4.068452E+02				
J# 4	5.091493E+07	2.594831E+02	4.728759E+03	3.063501E+02	3.063501E+02				
J# 5	5.119942E+07	2.025661E+02	4.587300E+03	2.348879E+02	2.348879E+02				
J# 6	5.143193E+07	5.654945E+03	4.466610E+03	1.767800E+02	1.767800E+02				
3.3510296E+06	3.3590570E+01	5.5809939E+03	5.5809939E+03	7.7023584E+02	7.7023584E+02	7.7339607E+01	7.7339607E+01	6.4930350E+01	
J# 1	4.965977E+07	1.111787E+03	5.466582E+03	6.235237E+02	6.235237E+02				
J# 2	5.016548E+07	7.103559E+03	5.130517E+03	4.853657E+02	4.853657E+02				
J# 3	5.069039E+07	1.690243E+02	4.874519E+03	3.540901E+02	3.540901E+02				
J# 4	5.105964E+07	2.589719E+02	4.691089E+03	2.689124E+02	2.689124E+02				
J# 5	5.135064E+07	2.034862E+02	4.546919E+03	2.068986E+02	2.068986E+02				
J# 6	5.154679E+07	5.707947E+03	4.440168E+03	1.600251E+02	1.600251E+02				
3.4280784E+06	3.4237071E+01	5.540625E+03	5.540625E+03	6.7927510E+02	6.7927510E+02	7.0308733E+01	7.0308733E+01	6.7545744E+01	
J# 1	4.979345E+07	1.111270E+03	5.332591E+03	5.530829E+02	5.530829E+02				
J# 2	5.029109E+07	7.062941E+03	5.197590E+03	4.308420E+02	4.308420E+02				

Table B-II-Continued

J# 3	5.08046E+07	1.672680E+02	4.843750E+03	3.150167E+02		
J# 4	1.16593E+07	2.555382E+02	4.662252E+03	2.401440E+02		
J# 5	1.44958E+07	2.004876E+02	4.520220E+03	1.859611E+02		
J# 6	5.164094E+07	5.620423E+03	4.415105E+03	1.451019E+02		
J# 1	3.4935173E+06	3.4784314E+01	5.5064715E+03	5.9557316E+02	6.3277660E+01	6.9912053E+01
J# 2	4.990479E+07	1.110631E+03	5.039598E+03	4.875458E+02		
J# 3	5.039842E+07	7.023248E+03	5.069034E+03	3.797711E+02		
J# 4	5.090560E+07	1.654850E+02	4.918091E+03	2.779630E+02		
J# 5	5.126167E+07	2.517019E+02	4.635646E+03	2.124428E+02		
J# 6	5.153458E+07	1.967394E+02	4.497088E+03	1.657134E+02		
J# 1	5.173003E+07	5.503277E+03	4.390619E+03	1.297843E+02		
J# 2	3.5489481E+06	3.5246570E+01	5.4775371E+03	5.1779512E+02	5.6246967E+01	7.2029276E+01
J# 3	4.999839E+07	1.111558E+03	5.279599E+03	4.258605E+02		
J# 4	5.048869E+07	6.998640E+03	5.044700E+03	3.317702E+02		
J# 5	5.099211E+07	1.641606E+02	4.792067E+03	2.429667E+02		
J# 6	5.134498E+07	2.486786E+02	4.612286E+03	1.960587E+02		
J# 1	5.160691E+07	1.935968E+02	4.477253E+03	1.461231E+02		
J# 2	5.180919E+07	5.401805E+03	4.368473E+03	1.146204E+02		
J# 3	3.5996503E+06	3.5635131E+01	5.4531695E+03	4.4477700E+02	4.9216113E+01	7.3897415E+01
J# 4	5.007744E+07	1.114747E+03	5.256786E+03	3.672141E+02		
J# 5	5.056339E+07	6.995269E+03	5.024458E+03	2.863091E+02		
J# 6	5.106433E+07	1.635633E+02	4.771870E+03	2.097641E+02		
J# 1	5.141451E+07	2.470618E+02	4.592610E+03	1.609136E+02		
J# 2	5.166778E+07	1.917433E+02	4.469452E+03	1.270363E+02		
J# 3	5.187617E+07	5.339590E+03	4.349579E+03	9.979370E+01		
J# 4	3.6346196E+06	3.5958731E+01	5.432841E+03	3.7551863E+02	4.2185240E+01	7.5516468E+01
J# 5	5.014400E+07	1.120136E+03	5.241058E+03	3.109648E+02		
J# 6	5.062413E+07	7.013056E+03	5.007960E+03	2.428252E+02		
J# 1	5.112307E+07	1.637646E+02	4.752388E+03	1.779954E+02		
J# 2	5.147083E+07	2.469630E+02	4.576650E+03	1.367729E+02		
J# 3	5.171829E+07	1.913583E+02	4.446436E+03	1.084720E+02		
J# 4	5.193051E+07	5.323427E+03	4.334237E+03	8.529219E+01		
J# 5	3.666107E+06	3.6223966E+01	5.4161564E+03	3.0917237E+02	3.5154367E+01	7.6886436E+01
J# 6	5.019998E+07	1.127136E+03	5.228154E+03	2.565952E+02		
J# 1	5.062245E+07	7.047537E+03	4.994838E+03	2.007950E+02		
J# 2	5.116958E+07	1.645248E+02	4.742348E+03	1.472786E+02		
J# 3	5.151500E+07	2.481495E+02	4.564174E+03	1.233557E+02		
J# 4	5.175939E+07	1.922433E+02	4.434978E+03	9.015073E+01		
J# 5	5.197288E+07	5.348089E+03	4.322341E+03	7.101776E+01		
J# 6	3.6921797E+06	3.6435688E+01	5.4028236E+03	2.4502811E+02	2.8123493E+01	7.8007319E+01
J# 1	5.024431E+07	1.134845E+03	5.213952E+03	2.036792E+02		
J# 2	5.070982E+07	7.091590E+03	4.984720E+03	1.597719E+02		
J# 3	5.120522E+07	1.657044E+02	4.732390E+03	1.172720E+02		
J# 4	5.154841E+07	2.501773E+02	4.554802E+03	9.039992E+01		
J# 5	5.179190E+07	1.939929E+02	4.428881E+03	7.1201160E+01		

Table B-II-Continued

JR 6	5,200458E+07	5,400803E+03	4,313539E+03	5,685455E+01	2,1092620E+01	7,887911E+01
3,711723E+06	3,16597359E+01	5,3926349E+03	5,204420E+03	1,8249521E+02		
JR 1	5,027915E+07	1,142238E+03	5,204420E+03	1,518576E+02		
JR 2	5,073749E+07	7,137056E+03	4,972258E+03	1,194032E+02		
JR 3	5,123132E+07	1,670059E+02	4,729135E+03	8,770288E+01		
JR 4	5,157253E+07	2,525104E+02	4,548100E+03	6,769771E+01		
JR 5	5,181650E+07	1,960914E+02	4,418980E+03	5,397045E+01		
JR 6	5,202713E+07	5,465339E+03	4,307309E+03	4,270755E+01		
3,7255139E+06	3,16711353E+01	5,3854473E+03	1,2108172E+02		1,4061747E+01	7,9501830E+01
JR 1	5,030403E+07	1,148338E+03	5,197573E+03	1,008192E+02		
JR 2	5,075649E+07	7,176105E+03	4,972155E+03	7,942882E+01		
JR 3	5,124905E+07	1,681579E+02	4,720235E+03	5,837581E+01		
JR 4	5,158869E+07	2,546231E+02	4,543655E+03	4,510775E+01		
JR 5	5,183371E+07	1,960279E+02	4,414145E+03	3,597171E+01		
JR 6	5,204200E+07	5,525417E+03	4,303363E+03	2,852054E+01		
3,7337243E+06	3,1677919E+01	5,381168E+03	6,0371529E+01		7,0308733E+02	7,9875457E+01
JR 1	5,031898E+07	1,152346E+03	5,193445E+03	5,028583E+01		
JR 2	5,076759E+07	7,202324E+03	4,969187E+03	3,966851E+01		
JR 3	5,125931E+07	1,689444E+02	4,717413E+03	2,916568E+01		
JR 4	5,159793E+07	2,560610E+02	4,541133E+03	2,255164E+01		
JR 5	5,184388E+07	1,993770E+02	4,411282E+03	1,798529E+01		
JR 6	5,205040E+07	5,567447E+03	4,301131E+03	1,427858E+01		
3,7364809E+06	3,16801712E+01	5,3797481E+03	0.		0.	8,0000000E+01
JR 1	5,032396E+07	1,153742E+03	5,192066E+03	0.		
JR 2	5,077123E+07	7,211545E+03	4,968214E+03	0.		
JR 3	5,126266E+07	1,692230E+02	4,716492E+03	0.		
JR 4	5,160094E+07	2,565999E+02	4,540318E+03	0.		
JR 5	5,184725E+07	1,998591E+02	4,410334E+03	0.		
JR 6	5,205311E+07	5,582493E+03	4,300417E+03	0.		

Table B-II-Continued

G...-PARTICLE FLOW(NOZZLE)

CP TIME = 127.427 PP TIME = 211.937

CHARACTERISTIC CALCULATION

Z	R	MPC	P
.80000	0.00000	0.00000	806.47652
.79675	.07031	.00495	805.88801
.79502	.14062	.01976	804.11588
.78879	.21093	.04437	801.13938
.78007	.28123	.07868	796.92102
.76886	.35154	.12251	791.40219
.75516	.42185	.17565	784.49723
.73897	.49216	.23784	776.08608
.72029	.56247	.30874	766.00586
.69912	.63278	.38792	754.04167
.67546	.70309	.47490	739.91732
.64930	.77340	.56905	723.28710
.61165	.84364	.67070	697.26940
.56422	.91393	.78610	691.82534
.59492	.98421	.91759	684.37000
.58157	.03112	.80229	674.57629
.55082	.97429	.67030	657.89566
.53954	1.01677	.93848	639.81674
.51978	1.05463	1.00000	622.20708

TOTAL MASS FLOW = 3.0237958E+03

NO. POINTS = 19

LRC	IU	K	P	REK	Z	MACH	VPK	TG	VG	THETA=K	THETA=G	TPK	TPG	PG/PGO	DG/DGO	SDK/DGO	DPK/DPO	CF	ISP	IT
0	15	1.05463	.51978	1.7366	5079.1	5960.8	12.000	.81266	.27654	.34029	0.00000	1.6663	216.77	0						
1	14	1.01677	.53954	1.7157	5102.0	5902.1	11.372	.81633	.28436	.34834	0.00000	0.0000	0.00	0						
1	5	1.07043	.58921	1.7986	4992.0	6120.3	13.707	.79873	.25029	.31336	0.00000	1.6752	217.92	4						

Z	R	MPC	P
.53954	1.01677	.93848	639.81674
.55915	1.03785	.9262	615.91232
.58921	1.07043	1.00000	563.15344

TOTAL MASS FLOW = 3.0237958E+03

NO. POINTS = 3

Table B-II-Continued

LRC ID	K	R	REK	Z	MACH	TG	VG	THETA=K	TG/TGO	TPK	PG/PGO	DG/DGO	SDK/DG	DPK/DPO	CF	ISP	IT																																																								
2	14	.97429	.56005	1.6946	5125.0	5842.7	10.695	.82001	.29240	.35658	.00348	0.0000	0.00	0																																																											
1		2.154109E+01	5.577006E+03	8.937410E+00	5.196533E+03				3.483814E+03	9.134260E+03	4.920000E+06																																																														
2	4	1.03361	.61624	1.7713	5024.7	6047.0	12.750	.80395	.26011	.32354	.00277	0.0000	0.00	5																																																											
1		1.782435E+01	5.824357E+03	1.100549E+01	5.094579E+03				2.771356E+03	6.592978E+03	4.920000E+06																																																														
2	5	1.09118	.66899	1.8701	4691.6	6299.3	15.569	.78266	.22261	.28442	0.00000	1.6858	219.30	4																																																											
<table border="0" style="width:100%"> <tr> <td>Z</td> <td></td> <td>R</td> <td></td> <td>MPC</td> <td></td> <td>P</td> </tr> <tr> <td>.56085</td> <td>.97429</td> <td>.67030</td> <td></td> <td></td> <td>657.89566</td> <td></td> </tr> <tr> <td>.58254</td> <td>.99745</td> <td>.89584</td> <td></td> <td></td> <td>631.82628</td> <td></td> </tr> <tr> <td>.61624</td> <td>1.03361</td> <td>.93606</td> <td></td> <td></td> <td>585.24707</td> <td></td> </tr> <tr> <td>.63491</td> <td>1.05381</td> <td>.95858</td> <td></td> <td></td> <td>555.16911</td> <td></td> </tr> <tr> <td>.66899</td> <td>1.09118</td> <td>1.00000</td> <td></td> <td></td> <td>500.86451</td> <td></td> </tr> </table>																		Z		R		MPC		P	.56085	.97429	.67030			657.89566		.58254	.99745	.89584			631.82628		.61624	1.03361	.93606			585.24707		.63491	1.05381	.95858			555.16911		.66899	1.09118	1.00000			500.86451															
Z		R		MPC		P																																																																			
.56085	.97429	.67030			657.89566																																																																				
.58254	.99745	.89584			631.82628																																																																				
.61624	1.03361	.93606			585.24707																																																																				
.63491	1.05381	.95858			555.16911																																																																				
.66899	1.09118	1.00000			500.86451																																																																				
TOTAL MASS FLOW = 3.023795AE+03 NO. POINTS = 5																																																																									
LRC ID	K	R	REK	Z	MACH	TG	VG	THETA=K	TG/TGO	TPK	PG/PGO	DG/DGO	SDK/DG	DPK/DPO	CF	ISP	IT																																																								
3	14	.93112	.58157	1.6755	5145.8	5788.6	10.036	.82333	.29981	.36415	.02573	0.0000	0.00	0																																																											
1		2.102542E+01	5.530353E+03	8.394312E+00	5.214781E+03				3.457179E+03	9.256769E+03	4.920000E+06																																																														
2		8.5337389E+01	5.255329E+03	6.770233F+00	5.282330E+03				2.227649E+02	5.964641E+02	9.840000E+06																																																														
3	4	.98980	.63678	1.7432	5057.4	5970.5	11.821	.80919	.27052	.33431	.01622	0.0000	0.00	5																																																											
1		1.701336E+01	5.756699E+03	1.027487E+01	5.123380E+03				3.456625E+03	8.497030E+03	4.920000E+06																																																														
2		7.867566E+01	5.458343E+03	8.404042E+00	5.202525E+03				1.476396E+02	3.629256E+02	9.840000E+06																																																														
3	4	1.05365	.69616	1.8401	4928.8	6221.7	14.497	.78861	.23252	.29485	.00205	0.0000	0.00	5																																																											
1		1.781902E+01	5.995079E+03	1.249938E+01	5.013775E+03				2.048869E+03	4.441979E+03	4.920000E+06																																																														
3	5	1.11593	.75243	1.9444	4787.6	6479.5	17.431	.76601	.19664	.25671	0.00000	1.6972	220.79	4																																																											
<table border="0" style="width:100%"> <tr> <td>Z</td> <td></td> <td>R</td> <td></td> <td>MPC</td> <td></td> <td>P</td> </tr> <tr> <td>.58157</td> <td>.93112</td> <td>.80229</td> <td></td> <td></td> <td>674.57629</td> <td></td> </tr> <tr> <td>.60326</td> <td>.95414</td> <td>.82626</td> <td></td> <td></td> <td>649.68767</td> <td></td> </tr> <tr> <td>.63678</td> <td>.98980</td> <td>.66467</td> <td></td> <td></td> <td>608.67466</td> <td></td> </tr> <tr> <td>.66117</td> <td>1.01587</td> <td>.69279</td> <td></td> <td></td> <td>576.76224</td> <td></td> </tr> <tr> <td>.69616</td> <td>1.05365</td> <td>.93357</td> <td></td> <td></td> <td>523.17357</td> <td></td> </tr> <tr> <td>.71724</td> <td>1.07673</td> <td>.95836</td> <td></td> <td></td> <td>492.61980</td> <td></td> </tr> <tr> <td>.75243</td> <td>1.11593</td> <td>1.00000</td> <td></td> <td></td> <td>442.44339</td> <td></td> </tr> </table>																		Z		R		MPC		P	.58157	.93112	.80229			674.57629		.60326	.95414	.82626			649.68767		.63678	.98980	.66467			608.67466		.66117	1.01587	.69279			576.76224		.69616	1.05365	.93357			523.17357		.71724	1.07673	.95836			492.61980		.75243	1.11593	1.00000			442.44339	
Z		R		MPC		P																																																																			
.58157	.93112	.80229			674.57629																																																																				
.60326	.95414	.82626			649.68767																																																																				
.63678	.98980	.66467			608.67466																																																																				
.66117	1.01587	.69279			576.76224																																																																				
.69616	1.05365	.93357			523.17357																																																																				
.71724	1.07673	.95836			492.61980																																																																				
.75243	1.11593	1.00000			442.44339																																																																				
TOTAL MASS FLOW = 3.023795AE+03 NO. POINTS = 7																																																																									
LRC ID	K	R	REK	Z	MACH	TG	VG	THETA=K	TG/TGO	TPK	PG/PGO	DG/DGO	SDK/DG	DPK/DPO	CF	ISP	IT																																																								
4	14	.90221	.59492	1.6639	5158.4	5755.5	9.610	.82534	.30439	.36880	.07814	0.0000	0.00	0																																																											

Table B-II-Continued

LRC ID	K	R	REK	Z	MACH	VG	TPK	NO, PRINTS	IT
1	2	064474E+01	5.502388E+03	8.046919E+00	5.225661E+03	3.433850E+03	9.311819E+03	4.920000E+06	0
2	P	354075E+01	5.235076E+03	6.515077E+00	5.290669E+03	2.210782E+02	5.995137E+02	9.400000E+06	5
3	L	108561E+02	4.953376E+03	4.963544E+00	5.357885E+03	5.259526E+02	1.426263E+01	1.320000E+05	0
4	4	94028	1.7030	5107.0	5861.3	10.666	81712	0.000	0.00
1	1	730271E+01	5.647076E+03	9.210188E+00	5.169045E+03	3.43381E+03	8.856717E+03	4.920000E+06	5
2	7	741710E+01	5.367240E+03	7.558273E+00	5.239913E+03	2.220796E+02	5.727077E+02	9.840000E+06	0
3	2	025482E+02	5.068449E+03	5.857997E+00	5.314047E+03	3.014628E+02	7.774242E+02	1.632000E+05	0
4	4	100117	1.7783	5008.2	6061.1	12.663	80131	0.000	0.00
1	1	611454E+01	5.856666E+03	1.107661E+01	5.077365E+03	3.460946E+03	8.110913E+03	4.920000E+06	5
2	7	498451E+01	5.561576E+03	6.167609E+00	5.152106E+03	8.744620E+03	2.049349E+02	9.840000E+06	0
4	4	106861	1.8862	4864.3	6335.7	15.646	77829	0.000	0.00
1	1	749179E+01	6.106456E+03	1.355415E+01	4.954019E+03	1.406578E+03	2.862432E+03	4.920000E+06	5
4	4	113473	2.0031	4705.7	6617.8	19.983	75292	1.7052	221.82

TOTAL MASS FLOW = 3.0237958E+03 NO, PRINTS = 11

LRC ID	K	R	REK	Z	MACH	VG	TPK	NO, PRINTS	IT
5	14	88153	1.6561	5166.8	5733.2	9.313	82669	0.000	0.00
1	2	036230E+01	5.483823E+03	7.805755E+00	5.232857E+03	3.415363E+03	9.340500E+03	4.920000E+06	0
2	8	235127E+01	5.220973E+03	4.333056E+00	5.298436E+03	2.198994E+02	6.008445E+02	9.840000E+06	0
3	2	061958E+02	4.942742E+03	4.835574E+00	5.362238E+03	5.233697E+02	1.431337E+01	1.632000E+05	0
4	3	625279E+02	4.745661E+03	3.781924E+00	5.408593E+03	7.992539E+02	2.185636E+01	2.290000E+05	0
5	4	90826	1.6805	5134.5	5799.4	10.016	82152	0.000	0.00
1	1	755455E+01	5.583992E+03	6.599281E+00	5.194347E+03	3.413782E+03	9.033221E+03	4.920000E+06	5
2	7	726334E+01	5.312079E+03	7.040433E+00	5.267016E+03	2.203784E+02	5.83140E+02	9.840000E+06	0
3	2	000694E+02	5.025943E+03	5.473488E+00	5.331073E+03	5.124620E+02	1.388199E+01	1.632000E+05	0
4	3	527925E+02	4.819628E+03	4.341250E+00	5.381085E+03	4.152464E+02	1.098785E+01	2.290000E+05	0
5	4	94721	1.6664	5078.0	5915.7	11.168	81248	0.000	0.00
1	1	609321E+01	5.715786E+03	9.731145E+00	5.139577E+03	3.431668E+03	8.596759E+03	4.920000E+06	5
2	7	362066E+01	5.439098E+03	8.084098E+00	5.211179E+03	2.1216136E+02	5.551700E+02	9.840000E+06	0

Table B-II-Continued

LRC ID	K	R	REK	Z	MACH	VPK	TG	VG	THETA	TPK	IG/TG	PG/DG	DG/DGU	SDK/DG	CF	ISP	IT
3	1	1.958464E+02	5.135411E+03	6.343370E+00	5.284230E+03	1.363087E+02	3.414705E+02	1.632000E+05									
5	4	1.1988	.72536	1.8069	4968.6	6134.1	13.87	.79496									
1	1	1.624295E+01	5.926414E+03	1.168859E+01	5.142684E+03	3.468501E+03	7.817289E+03	4.920000E+06									
2	7	4.11313E+01	5.632533E+03	9.749841E+00	5.127516E+03	4.075807E+03	9.184033E+03	9.840000E+06									
5	4	1.0800R	.76949	1.9187	4819.2	6415.2	16.462	.77108									
1	1	1.721911E+01	6.184201E+03	1.431179E+01	4.911060E+03	8.808955E+04	1.713229E+03	4.920000E+06									
5	5	1.14932	.85102	2.0394	4655.3	6701.5	19.934	.74484									

TOTAL MASS FLOW # 3.0237958E+03																	
NO. POINTS = 14																	
LRC ID	K	R	REK	Z	MACH	VPK	TG	VG	THETA	TPK	IG/TG	PG/DG	DG/DGU	SDK/DG	CF	ISP	IT
6	14	.86464	.61165	1.6503	5173.3	5715.9	9.075	.82773									
1	2	0.12787E+01	5.469465E+03	7.612859E+00	5.1238406E+03	3.399480E+03	9.358377E+03	4.920000E+06									
2	8	1.44686E+01	5.209708E+03	6.185082E+00	5.301011E+03	2.184948E+02	6.014910E+02	9.840000E+06									
3	2	0.61420E+02	4.933991E+03	4.728844E+00	5.1365946E+03	5.208215E+02	1.433762E+01	1.632000E+05									
4	3	5.922497E+02	4.738672E+03	3.704696E+00	5.411686E+03	7.965887E+02	2.192917E+01	2.290000E+05									
5	5	2.78061E+02	4.593331E+03	2.931334E+00	5.445156E+03	6.218589E+02	1.711906E+01	2.940000E+05									
6	4	.88623	.63219	1.6672	5150.4	5762.5	9.608	.82406									
1	1	1.747337E+01	5.548936E+03	8.236763E+00	5.1208179E+03	3.396169E+03	9.118455E+03	4.920000E+06									
2	7	6.58453E+01	5.282109E+03	6.740794E+00	5.1273925E+03	2.189408E+02	5.878394E+02	9.840000E+06									
3	1	9.64038E+02	5.000325E+03	5.1230886E+00	5.341328E+03	5.224900E+02	1.402846E+01	1.632000E+05									
4	3	4.85265E+02	4.800782E+03	4.170550E+00	5.1388721E+03	7.922982E+02	2.127260E+01	2.290000E+05									
5	5	1.46152E+02	4.651940E+03	3.351130E+00	5.423670E+03	3.000998E+02	8.057450E+02	2.940000E+05									
6	4	.91342	.65799	1.6947	5114.0	5837.0	10.376	.81825									
1	1	1.610998E+01	5.639700E+03	9.003073E+00	5.1171688E+03	3.407422E+03	8.826133E+03	4.920000E+06									
2	7	3.38216E+01	5.369777E+03	7.446151E+00	5.1239788E+03	2.202065E+02	5.703937E+02	9.840000E+06									
3	1	9.51199E+02	5.080632E+03	5.563840E+00	5.1310466E+03	5.211858E+02	1.350011E+01	1.632000E+05									
4	3	4.31433E+02	4.870951E+03	4.707475E+00	5.162239E+03	1.476635E+02	3.824680E+02	2.290000E+05									

NOT REPRODUCIBLE

Table B-II-Continued

6	4	1	12	69555	1,7408	5053,9	5960,1	11,77	80962	26902	33269	102768	0,0000	0,00	5
1	1	543488E+01	5,767736E+03	1,013647E+01	5,116242E+03	3,431019E+03	8,393224E+03	4,20000E+06							
2	7	101974E+01	5,495032E+03	8,497877E+00	5,18187E+03	2,211970E+02	5,41102E+02	9,84000E+06							
3	1	910444E+02	5,187786E+03	6,728728E+00	5,267438E+03	2,130733E+03	5,212363E+03	1,63200E+05							
6	4	1,01740	75588	1,9309	4935,1	6194,5	13,994	78962	23420	29659	100406	0,0000	0,00	5	
1	1	635716E+01	5,983610E+03	1,220480E+01	5,013182E+03	3,472920E+03	7,573886E+03	4,92000E+06							
2	7	333228E+01	5,168987E+03	1,022143E+01	5,100889E+03	5,854019E+04	1,276668E+03	9,84000E+06							
6	4	1,06994	82223	1,9455	4781,9	6479,5	17,122	76510	19495	25481	100046	0,0000	0,00	5	
1	1	697053E+01	6,246802E+03	1,493318E+01	4,975929E+03	4,563659E+04	8,550399E+04	4,92000E+06							
6	5	1,16198	8523	2,0748	4606,2	6781,9	20,845	73700	15740	21357	0,00000	1,7157	223,18	3	

Z	R	MPC	P
.61165	.86464	.70070	697,26940
.61986	.87327	.70908	689,60509
.63219	.88623	.72177	677,03476
.64555	.90030	.73566	662,54424
.65799	.91342	.74871	648,56098
.66721	.92315	.75846	638,37194
.68293	.93976	.77520	619,84509
.69555	.95312	.78875	605,30445
.70338	.96141	.79720	596,39580
.72660	.98607	.82246	567,80075
.74287	1,00344	.84033	545,15611
.75588	1,01740	.85470	526,94229
.76759	1,03003	.86769	510,78300
.79195	1,05653	.89485	477,89690
.80879	1,07504	.91373	455,85803
.82223	1,08994	.92864	438,64367
.82917	1,09767	.93665	430,09684
.85433	1,12614	.96506	394,13543
.87150	1,14592	.98447	373,77052
.88523	1,16198	1,00000	354,14719

CHARACTERISTICS 7 THROUGH 25
ARE OMITTED

TOTAL MASS FLOW = 3,0237958E+03												NO, POINTS = 20					
LHC ID	R	REX	Z	MACH	TG	VG	THETA=K	THETA=K	TPK	IG/TGO	PG/DG	DG/DGO	SDK/DG	CF	ISP	IT	
7	1	77340	164930	1,6216	5204,0	5633,9	7,858	83264	32146	38607	22944	0,0000	0,00	0			
1	1	886754E+01	5,402683E+03	6,627274E+00	5,264020E+03	3,309820E+03	9,395824E+03	4,92000E+06									
2	7	741484E+01	5,153425E+03	5,404306E+00	5,323515E+03	2,114748E+02	6,005286E+02	9,84000E+06									
3	1	975173E+02	4,887363E+03	4,154727E+00	5,385246E+03	5,031697E+02	1,428441E+01	1,63200E+05									
4	3	422545E+02	4,698790E+03	3,280838E+00	5,428710E+03	7,709662E+02	2,18597E+01	2,29000E+05									
5	1	10231E+02	4,151924E+03	2,695334E+00	5,1462946E+03	6,057638E+02	1,719882E+01	2,94000E+05									
6	6	913119E+02	4,443051E+03	2,064065E+00	5,486023E+03	1,699270E+02	4,823842E+02	3,62000E+05									
7	4	87075	164879	1,6636	5153,1	5751,5	9,432	16249	130136	36551	122587	0,0000	0,00	5			

Table B-II--Continued

LRC ID	K	R	Z	MACH VPK	TG	VG THETA=K	IG/TSO TPK	PG/PGO DPK/DGO	SUK/DG DPK/DGO	GF	ISP RPK	IT		
26	5	0.00000	1.56317	1.8106	4900.0	6104.1	0.000	179400	.21456	.27368	.22576	0.0000	5	
1	7.78668E+00	5.95818E+03	0.	4.959165E+03	3.186279E-03	6.411845E-03	3.186279E-03	6.411845E-03	4.920000E-06			0.00	5	
2	3.481298E+01	5.777955E+03	0.	5.026831E+03	2.029617E-02	4.064259E-02	2.029617E-02	4.064259E-02	9.840000E-06				06	
3	1.006642E+02	5.535386E+03	0.	5.1068234E+03	4.897507E-02	9.855401E-02	4.897507E-02	9.855401E-02	1.632000E-05				05	
4	1.887670E+02	5.344149E+03	0.	5.164153E+03	7.599317E-02	1.529233E-01	7.599317E-02	1.529233E-01	2.290000E-05				05	
5	2.887494E+02	5.198741E+03	0.	5.208389E+03	6.023506E-02	1.212128E-01	6.023506E-02	1.212128E-01	2.940000E-05				05	
6	4.036068E+02	5.076331E+03	0.	5.240618E+03	1.707106E-02	3.435261E-02	1.707106E-02	3.435261E-02	3.620000E-05				05	
26	4	1.98030	4.06594	2.8247	3615.3	6179.9	18.091	.57845	.63448	.05960	.03060	0.0000	5	
1	1.829019E+00	5.048131E+03	1.922940E+01	3.740429E+03	3.395874E-03	1.488259E-03	3.395874E-03	1.488259E-03	4.920000E-06				06	
2	8.18910E+00	7.866992E+03	1.840801E+01	4.170000E+03	2.273492E-02	9.963693E-03	2.273492E-02	9.963693E-03	9.840000E-06				06	
3	2.646353E+01	7.608881E+03	1.832673E+01	4.170000E+03	4.505801E-03	2.000485E-03	4.505801E-03	2.000485E-03	1.632000E-05				05	
4	5.443408E+01	7.342124E+03	1.787431E+01	4.170000E+03	2.101312E-04	-9.120910E-05	2.101312E-04	-9.120910E-05	2.290000E-05				05	
5	9.047523E+01	7.100106E+03	1.727095E+01	4.170000E+03	1.101292E-04	4.826467E-05	1.101292E-04	4.826467E-05	2.940000E-05				05	
6	1.340874E+02	5.887883E+03	1.662009E+01	4.213695E+03	7.530572E-08	-3.300311E-08	7.530572E-08	-3.300311E-08	3.620000E-05				05	
26	4	2.04147	4.14193	2.8536	3584.7	8228.5	18.329	.57356	.63332	.05808	.01367	0.0000	4	
1	1.819688E+00	8.096384E+03	1.844776E+01	3.683931E+03	3.434970E-03	1.467060E-03	3.434970E-03	1.467060E-03	4.920000E-06				06	
2	6.1638237E+00	7.914616E+03	1.860636E+01	4.170000E+03	2.220267E-02	9.48194E-03	2.220267E-02	9.48194E-03	9.840000E-06				06	
3	2.595847E+01	7.656416E+03	1.852428E+01	4.170000E+03	1.509238E-02	-7.727170E-03	1.509238E-02	-7.727170E-03	1.632000E-05				05	
4	5.354959E+01	7.387292E+03	1.806498E+01	4.170000E+03	6.203023E-03	2.649282E-03	6.203023E-03	2.649282E-03	2.290000E-05				05	
5	8.932744E+01	7.140957E+03	1.744266E+01	4.170000E+03	7.872126E-05	-3.404858E-05	7.872126E-05	-3.404858E-05	2.940000E-05				05	
26	4	2.11723	4.23594	2.8879	3546.3	8285.2	18.625	.56773	.63194	.05625	.02454	0.0000	5	
1	1.766376E+00	8.153312E+03	1.872295E+01	3.628830E+03	3.421158E-03	1.415012E-03	3.421158E-03	1.415012E-03	4.920000E-06				06	
2	8.395027E+00	7.971699E+03	1.865682E+01	4.170000E+03	2.175546E-02	8.998190E-03	2.175546E-02	8.998190E-03	9.840000E-06				06	
3	2.526696E+01	7.713477E+03	1.876881E+01	4.170000E+03	1.768566E-03	7.314897E-04	1.768566E-03	7.314897E-04	1.632000E-05				05	
4	5.236347E+01	7.441497E+03	1.829285E+01	4.170000E+03	2.403964E-03	-9.9433026E-04	2.403964E-03	-9.9433026E-04	2.290000E-05				05	
26	4	2.22637	4.37106	2.9364	3496.3	8382.4	19.056	.55941	.63006	.05373	.02333	0.0000	5	
1	1.699167E+00	8.230338E+03	1.912380E+01	3.566236E+03	3.442544E-03	1.360170E-03	3.442544E-03	1.360170E-03	4.920000E-06				06	
2	8.056636E+00	8.049380E+03	1.922437E+01	4.170000E+03	1.200786E-02	4.744375E-03	1.200786E-02	4.744375E-03	9.840000E-06				06	
3	2.422479E+01	7.793342E+03	1.912413E+01	4.170000E+03	1.312345E-02	-5.185152E-03	1.312345E-02	-5.185152E-03	1.632000E-05				05	
26	4	2.39667	4.58103	3.0065	3422.2	8476.8	19.713	.54755	.62737	.04999	.00620	0.0000	5	
1	1.587525E+00	8.339571E+03	1.974946E+01	3.486180E+03	3.089166E-03	1.135477E-03	3.089166E-03	1.135477E-03	4.920000E-06				06	
2	7.448424E+00	8.163071E+03	1.980850E+01	4.066354E+03	3.109173E-03	1.142824E-03	3.109173E-03	1.142824E-03	9.840000E-06				06	
26	4	2.57624	4.80073	3.0741	3353.0	8573.1	20.401	.53648	.62484	.04631	.00260	0.0000	5	
1	1.439545E+00	8.446140E+03	2.040069E+01	3.413824E+03	2.402709E-03	-2.862294E-04	2.402709E-03	-2.862294E-04	4.920000E-06				06	
26	5	2.70566	4.90673	3.1149	3313.3	8635.4	21.000	.53013	.62356	.04444	0.0000	2.0672	268.92	2
26	5	2.72396	4.95442	3.1240	3302.7	8648.9	21.000	.52643	.62313	.04377	0.0000	2.0696	265.22	2
26	5	2.72855	4.96636	3.1273	3300.0	8652.4	21.000	.52300	.62302	.04360	0.0000	2.0701	269.29	2

1P= 78

NOT REPRODUCIBLE

Table B-II--Continued

TWO-PHASE NOZZLE PROGRAM HAS BEEN COMPLETED.

UP TIME = 278.218 PP TIME = 223.239

Table B-II-Continued

T02P (PLUME) - NAMELIST/DATA PRINT JT
(READ FROM TAPE 8)

```

SDATA
CAPV  = 0.0E+00,
CPL   = 0.05E+04,
CPS   = 0.07E+04,
PR    = 0.022E+00,
DL    = 0.2E+00,
DR    = 0.2E+00,
DTLJ  = 0.3E+01,
EW    = 0.1E-02,
FA    = 0.0, 0.0, 0.1E+01, 0.125E+01, 0.1E+01, 0.125E+01, 0.1E+01,
      0.120E+01, 0.1001E+01, 0.126E+01, 0.1002E+01, 0.1582E+01,
      0.1063E+01, 0.1995E+01, 0.1141E+01, 0.251E+01, 0.1224E+01,
      0.310E+01, 0.1315E+01, 0.39E+01, 0.1412E+01, 0.501E+01,
      0.1517E+01, 0.631E+01, 0.1025E+01, 0.795E+01, 0.1745E+01,
      0.1E+02, 0.1874E+01, 0.126E+02, 0.2026E+01, 0.1582E+02,
      0.2166E+01, 0.1995E+02, 0.2304E+01, 0.251E+02, 0.2555E+01,
      0.310E+02, 0.276E+01, 0.39E+02, 0.3E+01, 0.501E+02,
      0.3252E+01, 0.631E+02, 0.3534E+01, 0.795E+02, 0.3825E+01,
      0.1E+03, 0.4155E+01, 0.316E+03, 0.79E+01, 0.1E+04, 0.2E+02,
      0.1001E+04, 0.2002E+02, 0.1E+06, 0.2E+04, 0.0, 0.0, 0.0, 0.0,
      0.0, 0.0, 0.0, 0.0, 0.0, 0.0, 0.0, 0.0, 0.0, 0.0,
      0.0, 0.0, 0.0, 0.0, 0.0, 0.0, 0.0, 0.0, 0.0, 0.0,
      0.0, 0.0, 0.0, 0.0, 0.0, 0.0,
GAMMA = 0.121E+01,
GMGO  = 0.506E+04,
HPL   = 0.403606E+08,
HPS   = 0.276606E+08,
IMAX  = 5,
N1    = 5,
N2    = 1,

```

NOT REPRODUCIBLE

Table B-II-Continued

ZAX = 0,8E+00,
 ZI = 0,3E+01,
 ZJ = 0,2E+01,
 DZI = 0,2E+02,
 IORDER = 3,
 SORCON = 0,0,
 ISK1 = 0,
 ISK2 = 0,
 ISK3 = 0,
 VAR = 0,3E+00, 0,0, 0,0, 0,1E+00, 0,1E+00, 0,0,
 FLAG = 0,0,
 THJD = 0,9E+01,
 SAUR = 0,15E+00, 0,1E+01, 0,5E+00, 0,3E+00, 0,1E+01, 0,0,
 THFD = 0,5E+01,
 IPS = 0,744E+01,
 RWPAX = 0,0,
 ZWPAX = 0,0,
 IWALL = 1,
 THIW = 0,12E+02,
 THJW = 0,21E+02,
 NTAPE = 0,
 SEND

NOT REPRODUCIBLE

Table B-II-Continued

SDATAP
ZMAX = 0,8E+02,
PMA = 0,5E+02,
NPM = -1,
NPLOT = 1,
NGASES = 18031133649550850,
PCUT = 0,053E+02,
EMIS = 0,3E+00,
C1 = 0,1E+01,
C2 = 0,1E+01,
AREA = 0,1E+01,
DL = 0,5E+01,
DH = 0,5E+01,
N1 = 5,
N2 = 1,
GAMMA = 0,121E+01,
SEND

NOT REPRODUCIBLE

Table B-II-Continued

BEGINNING OF THROPHASE PLUME PROGRAM

CP TIME = 264.079 PP TIME = 222.234

SIMPLE JET SPREADING		GAS-PARTICLE FLOW												
LRC ID	R	Z	MACH	TG	VG	THETA=K	THETA=K	TG/TKO	PG/PGO	DG/DGO	SDK/DGO	CF	ISP	IT
K	REK		VPK		THETA=K	TPK	DPK/DG	DPK/DGO	DPK/DGO	DPK/DGO	DPK/DGO	DPK/DGO	RPK	
1	5	2,72855	4,96638	3,1819	3242,1	8725,9	22,450	.51874	.02079	.04006	0,00000	0,0000	0,00	4
1	5	2,72855	4,96638	3,2374	3184,4	8798,7	23,900	.50951	.01875	.03679	0,00000	0,0000	0,00	4
1	5	2,72855	4,96638	3,2936	3126,9	8870,6	25,350	.50030	.01888	.03373	0,00000	0,0000	0,00	4
1	5	2,72855	4,96638	3,3511	3069,5	8941,8	26,800	.49112	.01517	.03088	0,00000	0,0000	0,00	4
1	5	2,72855	4,96638	3,4094	3012,3	9012,2	28,250	.48196	.01361	.02823	0,00000	0,0000	0,00	4
1	5	2,72855	4,96638	3,4688	2955,2	9081,0	29,700	.47284	.01219	.02576	0,00000	0,0000	0,00	4
1	5	2,72855	4,96638	3,5292	2898,4	9150,7	31,150	.46375	.01090	.02350	0,00000	0,0000	0,00	4
1	5	2,72855	4,96638	3,5906	2841,8	9218,8	32,600	.45469	.00973	.02139	0,00000	0,0000	0,00	4
1	5	2,72855	4,96638	3,6533	2785,4	9286,1	34,050	.44567	.00867	.01945	0,00000	0,0000	0,00	4
1	5	2,72855	4,96638	3,7171	2729,3	9352,6	35,500	.43668	.00771	.01765	0,00000	0,0000	0,00	4
1	5	2,72855	4,96638	3,7822	2673,4	9418,4	36,950	.42774	.00684	.01599	0,00000	0,0000	0,00	4
1	5	2,72855	4,96638	3,8485	2617,7	9483,4	38,400	.41884	.00600	.01447	0,00000	0,0000	0,00	4
1	5	2,72855	4,96638	3,9162	2562,4	9547,7	39,850	.40998	.00536	.01307	0,00000	0,0000	0,00	4
1	5	2,72855	4,96638	3,9853	2507,3	9611,1	41,300	.40118	.00473	.01179	0,00000	0,0000	0,00	4
1	5	2,72855	4,96638	4,0559	2452,6	9673,9	42,750	.39241	.00416	.01061	0,00000	0,0000	0,00	4
1	5	2,72855	4,96638	4,1279	2398,2	9735,8	44,200	.38371	.00366	.00953	0,00000	0,0000	0,00	4
1	5	2,72855	4,96638	4,2015	2344,0	9797,0	45,650	.37505	.00321	.00855	0,00000	0,0000	0,00	4
1	5	2,72855	4,96638	4,2768	2290,3	9857,5	47,100	.36645	.00281	.00766	0,00000	0,0000	0,00	4

Table B-II-Continued

1	5	2,72P55	4,96636	4,3537	2236,9	9917,1	46,550	.35790	.00245	.00684	0,00000	0,0000	0,000	0,00	4
1	2	.855	4,96638	4,4325	2183,6	9976,0	50,000	.34941	.00213	.00610	0,00000	0,0000	0,000	0,00	4
1	4	2,02452	4,21350	2,8541	35P1,3	8226,2	18,012	.57302	.03244	.05661	.03000	0,0000	0,000	0,00	4
1	1	1,70334E+00	8,094763E+03	1,814750E+01	3,675666E+03	1,632515E+01	4,170000E+03	4,170000E+03	3,390873E-03	1,411491E-03	9,279173E-03	9,840000E-06	4,920000E-06	0,00	4
2	1	8,401092E+00	7,914081E+03	1,832515E+01	4,170000E+03	1,632515E+01	4,170000E+03	4,170000E+03	2,229168E-02	9,279173E-03	9,840000E-06	4,920000E-06	0,00	4	
3	2	2,522953E+01	7,656591E+03	1,827492E+01	4,170000E+03	1,632515E+01	4,170000E+03	4,170000E+03	2,7612R3E-03	1,149410E-03	1,632000E-05	1,632000E-05	0,00	4	
4	5	1,85625E+01	7,390376E+03	1,766454E+01	4,170000E+03	1,632515E+01	4,170000E+03	4,170000E+03	1,527607E-03	6,356645E-04	2,290000E-05	2,290000E-05	0,00	4	
5	8,624009E+01	7,147428E+03	1,729592E+01	4,170000E+03	4,170000E+03	1,632515E+01	4,170000E+03	4,170000E+03	2,476805E-05	1,030999E-05	2,940000E-05	2,940000E-05	0,00	4	
6	1,277659E+02	6,934756E+03	1,668055E+01	4,170000E+03	4,170000E+03	1,668055E+01	4,170000E+03	4,170000E+03	7,625895E-08	-3,174368E-08	3,620000E-05	3,620000E-05	0,00	4	
1	4	2,06992	4,29592	2,8547	3549,2	8276,8	18,266	.56788	.03128	.05509	.02379	0,0000	0,000	0,00	4
1	1	1,731096E+00	8,145121E+03	1,832992E+01	3,629400E+03	1,632515E+01	4,170000E+03	4,170000E+03	3,413829E-03	1,382847E-03	4,920000E-06	4,920000E-06	0,00	4	
2	1	8,218301E+00	7,964044E+03	1,83915E+01	4,170000E+03	1,632515E+01	4,170000E+03	4,170000E+03	2,210194E-02	8,952883E-03	9,840000E-06	9,840000E-06	0,00	4	
3	2,4/1348E+01	7,706203E+03	1,848540E+01	4,170000E+03	4,170000E+03	1,632515E+01	4,170000E+03	4,170000E+03	-2,931200E-03	-1,187348E-03	1,632000E-05	1,632000E-05	0,00	4	
4	5,094460E+01	7,437766E+03	1,80686E+01	4,170000E+03	4,170000E+03	1,632515E+01	4,170000E+03	4,170000E+03	1,283133E-03	5,197617E-04	2,290000E-05	2,290000E-05	0,00	4	
5	8,495652E+01	7,191393E+03	1,748719E+01	4,170000E+03	4,170000E+03	1,748719E+01	4,170000E+03	4,170000E+03	-8,053272E-05	-3,262160E-05	2,940000E-05	2,940000E-05	0,00	4	
1	4	2,17048	4,39092	2,9209	3511,2	8335,6	18,581	.56178	.02992	.05326	.02419	0,0000	0,000	0,00	4
1	1	1,676303E+00	8,204222E+03	1,867622E+01	3,581364E+03	1,632515E+01	4,170000E+03	4,170000E+03	3,424150E-03	1,341083E-03	4,920000E-06	4,920000E-06	0,00	4	
2	7,971158E+00	8,023168E+03	1,880676E+01	4,170000E+03	4,170000E+03	1,632515E+01	4,170000E+03	4,170000E+03	3,039564E-02	7,988041E-03	9,840000E-06	9,840000E-06	0,00	4	
3	2,401186E+01	7,765260E+03	1,874461E+01	4,170000E+03	4,170000E+03	1,632515E+01	4,170000E+03	4,170000E+03	2,788868E-03	1,092272E-03	1,632000E-05	1,632000E-05	0,00	4	
4	4,969443E+01	7,494943E+03	1,831402E+01	4,170000E+03	4,170000E+03	1,831402E+01	4,170000E+03	4,170000E+03	-2,421224E-03	-9,482828E-04	2,290000E-05	2,290000E-05	0,00	4	
1	4	2,28496	4,54008	2,9715	3456,9	8414,6	19,030	.55311	.02809	.05079	.00461	0,0000	0,000	0,00	4
1	1	1,612906E+00	8,282848E+03	1,909617E+01	3,522320E+03	1,632515E+01	4,170000E+03	4,170000E+03	3,448250E-03	1,287737E-03	4,920000E-06	4,920000E-06	0,00	4	
2	7,641931E+00	8,102560E+03	1,919331E+01	4,170000E+03	4,170000E+03	1,632515E+01	4,170000E+03	4,170000E+03	5,124849E-03	1,913857E-03	9,840000E-06	9,840000E-06	0,00	4	
3	2,298213E+01	7,847330E+03	1,911629E+01	4,170000E+03	4,170000E+03	1,911629E+01	4,170000E+03	4,170000E+03	-1,317678E-02	-4,921372E-03	1,632000E-05	1,632000E-05	0,00	4	
1	4	2,46065	4,75872	3,0430	3382,1	8523,0	19,700	.54113	.02554	.04719	.00666	0,0000	0,000	0,00	5
1	1	1,502631E+00	8,392383E+03	1,973646E+01	3,44913E+03	1,632515E+01	4,170000E+03	4,170000E+03	3,345351E-03	1,160051E-03	4,920000E-06	4,920000E-06	0,00	4	
2	7,050805E+00	8,216636E+03	1,979169E+01	4,170000E+03	4,170000E+03	1,979169E+01	4,170000E+03	4,170000E+03	3,116252E-03	1,081052E-03	9,840000E-06	9,840000E-06	0,00	4	
1	4	2,64549	4,96690	3,1118	3312,3	8625,3	20,399	.52997	.02314	.04367	.00261	0,0000	0,000	0,00	4
1	1	1,357754E+00	8,499236E+03	2,040423E+01	3,373058E+03	1,632515E+01	4,170000E+03	4,170000E+03	-2,606063E-03	-8,367703E-04	4,920000E-06	4,920000E-06	0,00	4	
Z		1,56317	0,00000	0,00000	0,00000	0,00000	0,00000	0,00000	492,76554						
		1,62449	.04068	.00053	.00053	.00053	.00053	.00053	460,69742						
		1,68915	.06368	.08223	.08223	.08223	.08223	.08223	437,85400						
		1,75798	.12961	.00528	.00528	.00528	.00528	.00528	414,15061						
		1,85514	.19481	.01172	.01172	.01172	.01172	.01172	381,99492						
		1,89492	.22166	.01504	.01504	.01504	.01504	.01504	368,58457						
		1,92613	.24281	.01793	.01793	.01793	.01793	.01793	357,96717						
		1,97400	.27542	.02282	.02282	.02282	.02282	.02282	341,90644						
		1,99837	.29210	.02552	.02552	.02552	.02552	.02552	333,80484						
		2,02276	.30885	.02836	.02836	.02836	.02836	.02836	325,87229						
		2,05803	.33180	.03246	.03246	.03246	.03246	.03246	315,20745						
		2,10652	.36684	.03917	.03917	.03917	.03917	.03917	299,46743						
		2,13220	.38477	.04280	.04280	.04280	.04280	.04280	291,57886						

NOT REPRODUCIBLE

Table B-II-Continued

2,15809	,40294	,04660	283,78112
2,19333	,42779	,05201	273,23414
2,24021	,46665	,06094	257,08744
2,27580	,48665	,06566	249,22253
2,30344	,50660	,07054	241,57583
2,37706	,56034	,08423	222,19645
2,41360	,56738	,09139	213,06793
2,45040	,61473	,09880	204,27810
2,52446	,67059	,11442	167,46460
2,56217	,69942	,12269	179,28431
2,60014	,72872	,13122	171,36860
2,67660	,78857	,14897	156,40278
2,75301	,84956	,16742	142,68412
2,81641	,90097	,18320	133,63092
2,86652	,94193	,19599	128,61275
2,90966	,97726	,20722	125,74909
2,95094	1,01101	,21817	123,56070
2,99285	1,04521	,22949	121,48852
3,03505	1,07957	,24110	119,46831
3,07828	1,11469	,25320	117,49159
3,12184	1,15002	,26562	115,51223
3,16660	1,18626	,27859	113,50851
3,21159	1,22264	,29185	111,52440
3,25795	1,26008	,30574	109,50731
3,30460	1,29773	,31995	107,48011
3,35286	1,33664	,33490	105,38523
3,40127	1,37563	,35013	103,31407
3,45152	1,41606	,36621	101,20875
3,50186	1,45651	,38258	99,13500
3,55416	1,49850	,39986	97,01203
3,60654	1,54049	,41745	94,91669
3,66142	1,58443	,43618	92,75472
3,71633	1,62832	,45521	90,62466
3,77403	1,67439	,47553	88,42503
3,83167	1,72036	,49613	86,26648
3,89275	1,76902	,51830	84,02449
3,92326	1,79332	,52949	82,92145
3,95374	1,81759	,54076	81,82921
4,01865	1,86924	,56501	79,54263
4,05105	1,89502	,57725	78,42206
4,08340	1,92076	,58955	77,31415
4,15298	1,97611	,61629	74,97926
4,21380	2,02452	,63995	72,98843
4,23064	2,03793	,64655	72,44301
4,29592	2,08992	,67232	70,38958
4,32673	2,11448	,68457	69,44011
4,39692	2,17048	,71274	67,32773
4,46492	2,22481	,74031	65,33656
4,54008	2,28496	,77110	63,20652
4,56480	2,30476	,78129	62,52586
4,60132	2,33405	,79641	61,53874

Table B-II-Continued

LHC ID	K	P	REK	Z	MACH	VPK	TG	VG	THETA-K	TPK	IG/IG0	PG/PG0	DG/DG0	SDK/DG0	CF	ISP	IT
4.67970																	
4.75872																	
4.78403																	
4.82240																	
4.90463																	
4.98690																	
5.02521																	
5.06813																	
5.08958																	
5.09495																	
5.10021																	
5.10568																	
5.11135																	
5.11725																	
5.12338																	
5.12975																	
5.13638																	
5.14326																	
5.15043																	
5.15789																	
5.16563																	
4.99524																	
4.99639																	
4.99758																	
4.99882																	
4.96638																	

TOTAL MASS FLOW = 6.833000E+03 N2 POINTS = 90

LHC ID	K	P	REK	Z	MACH	VPK	TG	VG	THETA-K	TPK	IG/IG0	PG/PG0	DG/DG0	SDK/DG0	CF	ISP	IT
2	4	1	7.42535E+00	1.68836	1.8856	3545.5	4830.0	6225.6	0.000	177280	3.19900E-03	19521	25260	23001	0.0000	0.00	5
2	4	2	3.326045E+01	5.891127E+03	0.	0.	0.	0.	4.891883E+03	4.963567E+03	2.04901E-02	3.80575E-02	3.80575E-02	5.943395E-03	4.920000E-06	0.00	5
3	4	1	9.577902E+01	5.644717E+03	0.	0.	0.	0.	5.1048841E+03	4.972180E-02	4.972180E-02	9.235174E-02	9.235174E-02	1.632000E-05	1.632000E-05	0.00	5
4	1	7.96359E+02	5.449110E+03	0.	0.	0.	0.	0.	5.111033E+03	7.748285E-02	1.435143E-01	1.435143E-01	2.290000E-05	2.290000E-05	2.290000E-05	0.00	5
5	2	7.47764E+02	5.300421E+03	0.	0.	0.	0.	0.	5.156357E+03	6.160763E-02	1.144281E-01	1.144281E-01	3.620000E-05	3.620000E-05	3.620000E-05	0.00	5
6	3	8.450134E+02	5.175471E+03	0.	0.	0.	0.	0.	5.193135E+03	1.750418E-02	1.750418E-02	3.25173E-02	3.25173E-02	3.620000E-05	3.620000E-05	0.00	5
2	4	1	6.72285E+00	8.144651E+03	1.8856	3545.5	4830.0	6225.6	17.941	150726	3.384637E-03	19521	25260	23001	0.0000	0.00	4
2	4	2	7.922436E+00	7.964660E+03	1.8856	3545.5	4830.0	6225.6	17.941	150726	2.211960E-03	1.95900E-03	1.95900E-03	5.710418E-03	4.920000E-06	0.00	4
3	2	3.93149E+01	7.707752E+03	1.8856	3545.5	4830.0	4830.0	6225.6	17.941	150726	6.309088E-03	2.484439E-03	2.484439E-03	1.632000E-05	1.632000E-05	0.00	4
4	4	4.919493E+01	7.442032E+03	1.8856	3545.5	4830.0	4830.0	6225.6	17.941	150726	2.268877E-03	8.934551E-04	8.934551E-04	2.290000E-05	2.290000E-05	0.00	4
5	5	5.187359E+01	7.194270E+03	1.8856	3545.5	4830.0	4830.0	6225.6	17.941	150726	2.27253E-04	8.934551E-05	8.934551E-05	2.940000E-05	2.940000E-05	0.00	4
6	1	2.13285E+02	6.984916E+03	1.8856	3545.5	4830.0	4830.0	6225.6	17.941	150726	-7.12780E-08	-3.037195E-08	-3.037195E-08	3.620000E-05	3.620000E-05	0.00	4
2	4	1	1.4382	4.46676	2.9174	3511.6	8327.9	16.212	16.212	156188	0.2924	0.5204	0.2924	0.0000	0.00	0.00	4
1	1	6.60129E+00	8.197273E+03	1.8856	3545.5	4830.0	4830.0	6225.6	17.941	150726	3.405285E-03	1.302905E-03	1.302905E-03	4.920000E-06	4.920000E-06	0.00	4
2	7	7.62095E+00	8.016930E+03	1.8856	3545.5	4830.0	4830.0	6225.6	17.941	150726	2.163946E-02	8.279934E-03	8.279934E-03	9.840000E-06	9.840000E-06	0.00	4

Table B-II-Continued

3	2	3,399,326+01	7,759,639E+03	1,844,250E+01	4,170,000E+03	2,923,559E+03	1,118,919E+03	1,632,000E-05
4	2	8,232,518+01	7,492,019E+03	1,806,970E+01	17,000,000E+03	4,243,202E+04	1,523,903E+04	9,900,000E-05
5	2	8,454,165+01	7,245,495E+03	1,752,916E+01	17,000,000E+03	2,128,653E+05	-3,110,129E-05	2,940,000E-05
2	4	2,229,600	4,157,544	2,956,634	71,118,689,13	16,549,555,338	1,027,591,050,222	1,017,920,000,000
1	1	1,501,608E+00	5,258,535E+03	1,863,131E+01	5,535,523E+03	3,423,976E+03	1,264,415E+03	4,920,000E-06
2	7	5,284,415E+00	6,078,231E+03	1,875,825E+01	4,170,000E+03	1,830,173E+02	6,788,765E-03	9,840,000E-06
3	2	2,271,616E+01	7,821,245E+03	1,871,885E+01	4,170,000E+03	-1,371,253E+03	-5,803,914E+04	1,632,000E-05
4	4	4,647,138E+01	7,552,064E+03	1,832,333E+01	4,170,000E+03	-2,437,808E+03	-9,001,155E+04	2,290,000E-05
2	4	2,349,503	4,727,750	3,009,134	15,849,15	19,010,546,445	1,026,131,047,52	1,000,000,000,000
1	1	1,516,955E+00	8,338,005E+03	1,906,988E+01	3,147,801E+03	3,440,350E+03	1,209,574E+03	4,920,000E-06
2	7	2,203,439E+00	8,159,273E+03	1,916,259E+01	4,021,469E+03	6,718,959E+03	2,362,275E+03	9,840,000E-06
3	2	1,693,695E+01	7,904,917E+03	1,910,633E+01	4,170,000E+03	-1,322,650E+02	-4,650,219E+03	1,632,000E-05
2	4	2,531,138	4,955,530	3,081,933	9,857,719	19,696,533,317	1,023,711,044,37	1,000,000,000,000
1	1	1,410,642E+00	8,484,355E+03	1,972,498E+01	3,140,181E+03	2,729,013E+03	8,899,017E+04	4,920,000E-06
2	6	6,631,153E+00	8,273,662E+03	1,977,517E+01	3,758,863E+03	3,122,230E+03	1,018,568E+03	9,840,000E-06
2	4	2,722,14	5,192,96	3,151,532	9,867,915	20,399,523,13	1,021,461,041,02	1,000,000,000,000
1	1	1,267,244E+00	8,555,971E+03	2,040,223E+01	3,329,823E+03	-2,607,534E+03	-7,564,559E+04	4,920,000E-06
2	4	2,124,09	4,154,466	2,917,359	9,832,410	17,862,561,56	1,028,410,506,64	1,000,000,000,000
1	1	1,582,374E+00	8,194,045E+03	1,798,044E+01	3,157,686E+03	3,377,486E+03	1,257,657E+03	4,920,000E-06
2	7	5,303,395E+00	8,014,750E+03	1,815,705E+01	4,170,000E+03	2,189,957E+02	8,154,631E+03	9,840,000E-06
3	2	2,701,05E+01	7,758,301E+03	1,816,303E+01	4,170,000E+03	1,058,991E+02	3,943,311E+03	1,632,000E-05
4	4	4,665,526E+01	7,493,199E+03	1,783,017E+01	4,170,000E+03	2,197,552E+03	8,182,919E+04	2,290,000E-05
5	7	7,670,91E+01	7,249,026E+03	1,733,392E+01	4,170,000E+03	3,182,934E+04	1,185,213E+04	2,940,000E-05
6	1	1,122,117E+02	7,034,070E+03	1,679,033E+01	4,170,000E+03	-7,804,211E+06	-2,906,014E+06	3,620,000E-05
2	4	2,198,05	4,640,81	2,951,634	7,347,42	9,837,819	1,027,311,049,12	1,000,000,000,000
1	1	1,543,364E+00	8,248,691E+03	1,825,575E+01	3,153,767E+03	3,401,771E+03	1,226,701E+03	4,920,000E-06
2	7	3,460,366E+00	8,069,061E+03	1,840,518E+01	4,170,000E+03	2,082,720E+02	7,522,672E+03	9,840,000E-06
3	2	2,173,12E+01	7,812,280E+03	1,840,195E+01	4,170,000E+03	1,949,408E+03	1,787,699E+03	1,632,000E-05
4	4	4,568,178E+01	7,545,498E+03	1,806,303E+01	4,170,000E+03	1,948,189E+04	7,036,681E+03	2,290,000E-05
5	7	6,212,92E+01	7,298,720E+03	1,756,214E+01	4,170,000E+03	8,205,929E+03	-2,963,937E+03	2,940,000E-05
2	4	2,289,91	4,757,39	2,992,734	3,042,718	18,511,548,95	1,025,981,047,33	1,014,730,000,000
1	1	1,498,694E+00	8,312,072E+03	1,858,995E+01	3,149,303E+03	3,423,652E+03	1,191,574E+03	4,920,000E-06
2	7	1,239,90E+00	8,132,419E+03	1,810,365E+01	4,069,421E+03	1,594,641E+02	5,550,714E+03	9,840,000E-06
3	2	1,507,52E+01	7,876,094E+03	1,869,244E+01	4,170,000E+03	-2,185,710E+03	-7,607,187E+04	1,632,000E-05
4	4	4,442,731E+01	7,606,041E+03	1,846,649E+01	4,170,000E+03	-2,454,036E+03	-8,541,073E+04	2,290,000E-05
2	4	2,415,94	4,918,21	3,046,933	7,374,0	18,983,539,83	1,024,291,044,99	1,000,000,000,000
1	1	1,431,492E+00	8,393,614E+03	1,904,488E+01	3,143,575E+03	3,403,799E+03	1,126,100E+03	4,920,000E-06
2	6	7,970,40E+00	8,214,870E+03	1,913,361E+01	3,862,322E+03	8,066,802E+03	2,668,790E+03	9,840,000E-06
3	2	0,484,50E+01	7,961,344E+03	1,909,921E+01	4,170,000E+03	-1,328,107E-02	-4,393,859E+03	1,632,000E-05
2	4	2,603,54	5,156,15	3,121,132	9,829,718	19,682,527,64	1,022,010,417,0	1,000,000,000,000
1	1	1,328,049E+00	8,503,384E+03	1,971,333E+01	3,359,735E+03	2,038,652E+03	6,250,149E+04	4,920,000E-06
2	6	2,448,73E+00	8,329,915E+03	1,976,018E+01	3,645,128E+03	3,129,716E+03	9,595,159E+04	9,840,000E-06

Table B-II-Continued

3,82791	1,56672	4,0024	86,31179
3,88518	1,61130	4,1818	84,33139
3,94538	1,65814	4,3734	82,28638
4,00550	1,70493	4,5680	80,27693
4,06935	1,75450	4,7776	78,18648
4,10123	1,77927	4,8636	77,15697
4,13308	1,80402	4,9903	76,13700
4,20094	1,85672	5,2203	74,00318
4,23483	1,88354	5,3365	72,95673
4,26867	1,90932	5,4534	71,92190
4,34147	1,96588	5,7076	69,74123
4,40215	2,01597	5,9330	67,87886
4,47489	2,06961	6,1831	65,90474
4,54488	2,12409	6,4371	63,98655
4,56588	2,14044	6,5140	63,41934
4,64081	2,19885	6,7902	61,43719
4,67716	2,22723	6,9255	60,49117
4,75739	2,26991	7,2264	58,46222
4,83274	2,34890	7,5121	56,64182
4,91821	2,41594	7,8396	54,65038
4,97663	2,46187	8,0653	53,32741
5,06649	2,53267	8,4154	51,37036
5,15615	2,60354	8,7678	49,50042
5,21652	2,65139	9,0068	48,27385
5,31015	2,72584	9,3798	46,46843
5,35936	2,76459	9,5704	37,29842
5,39630	2,79980	9,7024	29,10168
5,41227	2,81507	9,7556	26,21764
5,43097	2,83362	9,8151	23,27125
5,45040	2,85374	9,8740	20,50708
5,47077	2,87559	9,9322	18,20323
5,49156	2,89932	9,9895	16,03902
5,51406	2,92510	1,00458	14,09498

TOTAL MASS FLOW = 6.8330000E+03										NO. POINTS = 76						
LRC ID	K	P	REK	Z	MACH	VG	THETA-K	THETA-G	IG/TGO	TPK	PG/PGO	DG/DGO	SDK/DG	CF	ISP	IT
					VPK						DPK/DG	DPK/DPU		RPK		
3	3	0,00000	1,82623	1,9141	4753,7	6355,9	0,000	0,76059	1,7576	1,23109	1,23466	0,0000	0,00	5		
1	7,000917E+00	6,20388E+03	0,				4,818479E+03	3,214112E-03	5,461356E-03	5,161356E-03	4,920000E-06					
2	3,146806E+01	6,013104E+03	0,				4,893900E+03	2,069462E-02	3,516389E+02	3,516389E+02	9,840000E-06					
3	9,043978E+01	5,781861E+03	0,				4,984915E+03	5,053016E-02	4,585987E+02	4,585987E+02	1,632000E-05					
4	1,698629E+02	5,560665E+03	0,				5,052528E+03	7,912382E-02	1,344456E+01	1,344456E+01	2,290000E-05					
5	2,599726E+02	5,407996E+03	0,				5,110136E+03	6,131319E-02	1,072726E+01	1,072726E+01	2,940000E-05					
6	3,633532E+02	5,279915E+03	0,				5,140885E+03	1,798803E-02	3,056492E-02	3,056492E-02	5,620000E-05					
3	4	2,18081	4,73256	2,9517	3471,6	8376,2	17,797	55546	82647	82647	0,0000	0,0000	0,00	4		
1	1,483690E+00	8,247337E+03	1,790684E+01	3,533286E+03			3,373573E+03	1,161933E-03	1,161933E-03	1,161933E-03	4,920000E-06					
2	7,080471E+00	8,068922E+03	1,807243E+01	4,170000E+03			2,147550E+02	7,524333E+03	7,524333E+03	7,524333E+03	9,840000E-06					
3	2,140562E+01	7,813086E+03	1,809799E+01	4,170000E+03			1,265592E+02	4,434233E+03	4,434233E+03	4,434233E+03	1,632000E-05					

CHARACTERISTICS 3-46 (LAST)
ARE OMITTED

Table B-II-Continued

TWO-PHASE PLUME PROG. HAS BEEN COMPLETED

CP TIME = 489,422 PP TIME = 246,239

SLINES

BEGINNING OF STREAMLINE GENERATION PROGRAM

CP TIME = 489,431 PP TIME = 247,752

STREAMLINE(1) = 0,00000 PERCENT OF THE TOTAL MASS FLOW
 ZINIT = 0,000000 (NONDIMENSIONAL = S/RC)
 PINIT = 1992,764306 (PSIA)
 TINIT = 6128,734834 (DFG, R)
 VINIT = 1918,291211 (FT/SEC)
 ZFINAL = 11,540129 (NONDIMENSIONAL = Z/RC)
 MGKSK = 73 (NO. OF PRESSURE TABLE POINTS)

POINT NO.	AXIAL DISTANCE (Z/RC)	RADIAL DISTANCE (R/RC)	STREAMLINE DISTANCE (S/RC)	PRESSURE (PSIA)
1	1,250	0,000	0,000	1992,764
2	1,162	0,000	,088	1968,198
3	1,073	0,000	,177	1939,718
4	,985	0,000	,265	1906,875
5	,896	0,000	,354	1869,199
6	,808	0,000	,442	1826,204
7	,719	0,000	,531	1777,410
8	,631	0,000	,619	1727,201
9	,542	0,000	,708	1693,414
10	,454	0,000	,796	1652,289
11	,365	0,000	,885	1604,440
12	,277	0,000	,973	1550,596
13	,188	0,000	1,062	1480,280
14	,100	0,000	1,150	1430,930
15	,011	0,000	1,239	1376,494
16	,077	0,000	1,327	1317,779
17	,166	0,000	1,416	1246,342
18	,254	0,000	1,504	1186,698

Table B-II-Continued

19	,343	0,000	1,593	1116,877
20	,431	0,000	1,600	1057,315
21	,800	0,000	2,000	806,477
22	,863	0,000	2,133	770,934
23	,967	0,000	2,217	732,580
24	1,055	0,000	2,305	693,313
25	1,145	0,000	2,395	652,519
26	1,241	0,000	2,491	611,134
27	1,341	0,000	2,591	568,816
28	1,448	0,000	2,698	526,072
29	1,563	0,000	2,813	482,766
30	1,688	0,000	2,938	439,223
31	1,826	0,000	3,076	395,468
32	1,980	0,000	3,230	351,779
33	2,211	0,000	3,461	295,815
34	2,313	0,000	3,563	269,062
35	2,395	0,000	3,645	254,118
36	2,526	0,000	3,776	226,334
37	2,596	0,000	3,846	214,670
38	2,657	0,000	3,917	202,486
39	2,766	0,000	4,016	187,451
40	2,924	0,000	4,174	165,741
41	3,008	0,000	4,258	154,696
42	3,095	0,000	4,345	145,360
43	3,219	0,000	4,469	131,440
44	3,423	0,000	4,673	112,893
45	3,532	0,000	4,782	103,419
46	3,643	0,000	4,893	96,422
47	3,958	0,000	5,208	77,591
48	4,126	0,000	5,376	69,366
49	4,301	0,000	5,551	62,617
50	4,679	0,000	5,929	49,984
51	4,892	0,000	6,142	43,846
52	5,113	0,000	6,363	39,296
53	5,592	0,000	6,842	30,684
54	6,124	0,000	7,374	23,949
55	6,541	0,000	7,791	21,099
56	6,801	0,000	8,051	20,967
57	6,969	0,000	8,219	20,251
58	7,110	0,000	8,360	19,551
59	7,255	0,000	8,505	19,935
60	7,404	0,000	8,654	19,982
61	7,561	0,000	8,811	20,057
62	7,723	0,000	8,973	20,123
63	7,896	0,000	9,146	20,196
64	8,075	0,000	9,325	20,171
65	8,268	0,000	9,518	19,915
66	8,466	0,000	9,716	19,849
67	8,676	0,000	9,926	19,856
68	8,893	0,000	10,143	19,904
69	9,131	0,000	10,381	19,929
70	9,396	0,000	10,646	18,291
71	9,680	0,000	10,900	17,336
72	9,974	0,000	11,204	16,215
73	10,290	0,000	11,540	15,392

Table B-II-Continued

STREAMLINE(2) = 20,00000 PERCENT OF THE TOTAL MASS FLOW
 ZINIT = 0,000000 (NONDIMENSIONAL = Z/RC)
 PINIT = 2007,823437 (PSIA)
 TINIT = 6136,185482 (DEG, R)
 VINIT = 1858,421073 (FT/SEC)
 ZFINAL = 10,434325 (NONDIMENSIONAL = Z/RC)
 MGKSK = 56 (NO. OF PRESSURE TABLE POINTS)

POINT NO.	AXIAL DISTANCE (Z/RC)	RADIAL DISTANCE (R/RC)	STREAMLINE DISTANCE (S/RC)	PRESSURE (PSIA)
1	.1250	.560	0,000	2007,823
2	.1162	.547	.069	1981,789
3	.1073	.535	.179	1951,099
4	.985	.524	.268	1915,353
5	.896	.513	.357	1874,112
6	.808	.502	.446	1826,909
7	.719	.492	.535	1773,265
8	.631	.476	.625	1749,073
9	.542	.471	.714	1704,692
10	.454	.466	.802	1653,410
11	.365	.461	.891	1595,816
12	.277	.456	.980	1532,585
13	.188	.451	1,068	1477,028
14	.100	.449	1,157	1416,022
15	.011	.448	1,245	1351,434
16	.077	.447	1,334	1283,990
17	.166	.447	1,422	1213,088
18	.254	.448	1,511	1144,993
19	.343	.450	1,599	1075,117
20	.431	.453	1,688	1008,222
21	.749	.449	2,005	781,204
22	.807	.471	2,067	751,428
23	.946	.519	2,215	677,937

Table B-II-Continued

24	1,082	,561	2,357	608,307
25	1,217	,600	2,407	542,034
26	1,349	,635	2,457	479,876
27	1,479	,665	2,768	424,826
28	1,607	,691	2,898	376,329
29	1,736	,716	3,029	333,252
30	1,872	,743	3,168	293,268
31	2,015	,772	3,314	257,000
32	2,168	,805	3,471	223,123
33	2,332	,843	3,639	192,423
34	2,510	,885	3,822	164,404
35	2,705	,933	4,023	141,668
36	2,882	,985	4,201	127,590
37	3,105	1,002	4,429	114,027
38	3,358	1,055	4,687	101,460
39	3,648	1,116	4,984	89,382
40	4,105	1,210	5,450	74,033
41	4,320	1,255	5,670	67,940
42	4,488	1,289	5,841	63,737
43	4,774	1,347	6,133	57,292
44	4,924	1,377	6,286	54,289
45	5,081	1,408	6,446	51,376
46	5,301	1,452	6,670	47,649
47	5,660	1,523	7,036	42,318
48	5,856	1,562	7,237	39,716
49	6,057	1,601	7,441	37,301
50	6,355	1,659	7,745	34,057
51	6,844	1,753	8,243	29,536
52	7,112	1,804	8,515	27,408
53	7,374	1,853	8,782	25,547
54	8,153	1,999	9,574	20,908
55	8,573	2,078	10,002	18,877
56	8,998	2,155	10,434	17,113

Table B-II-Continued

STREAMLINE(S) = 40,00000 PERCENT OF THE TOTAL MASS FLOW
 ZINIT = 0,000000 (NONDIMENSIONAL = S/RC)
 PINIT = 2028,364264 (PSIA)
 TINIT = 6146,272736 (DEG, R)
 VINIT = 1774,130855 (FT/SEC)
 ZFINAL = 10,421796 (NONDIMENSIONAL = Z/RC)
 MGKSK = 55 (NO. OF PRESSURE TABLE POINTS)

POINT NO.	AXIAL DISTANCE (Z/RC)	RADIAL DISTANCE (R/RC)	STREAMLINE DISTANCE (S/RC)	PRESSURE (PSIA)
1	=1,250	,799	0,000	2028,364
2	=1,162	,781	,090	1999,334
3	=1,073	,762	,181	1965,110
4	=,985	,745	,271	1925,349
5	=,896	,728	,361	1879,629
6	=,808	,712	,451	1827,471
7	=,719	,697	,541	1768,371
8	=,631	,676	,632	1707,895
9	=,542	,667	,721	1712,268
10	=,454	,659	,810	1650,323
11	=,365	,651	,898	1582,554
12	=,277	,644	,987	1509,524
13	=,188	,638	1,076	1464,486
14	=,100	,635	1,164	1392,638
15	=,011	,633	1,253	1318,565
16	,077	,632	1,341	1242,894
17	,166	,633	1,430	1170,601
18	,254	,634	1,518	1094,832
19	,343	,638	1,607	1023,362
20	,431	,643	1,696	949,990
21	,696	,643	1,960	752,060
22	,716	,650	1,981	741,362
23	,854	,696	2,127	665,075
24	,993	,741	2,273	586,250
25	1,131	,786	2,419	508,925
26	1,271	,831	2,566	435,225
27	1,413	,877	2,714	370,151
28	1,556	,923	2,865	314,575
29	1,702	,971	3,019	266,777
30	1,851	1,020	3,176	228,607
31	2,003	1,068	3,335	203,830
32	2,159	1,115	3,498	187,352
33	2,325	1,166	3,671	172,308
34	2,500	1,218	3,854	157,990
35	2,687	1,275	4,050	144,262

Table B-II-Continued

36	2,889	1,334	4,260	131,120
37	3,108	1,399	4,260	118,411
38	3,349	1,470	4,260	106,251
39	3,555	1,499	4,947	96,996
40	3,827	1,566	5,228	86,339
41	4,137	1,643	5,547	76,011
42	4,495	1,731	5,915	65,989
43	5,061	1,872	6,499	53,372
44	5,332	1,939	6,778	48,430
45	5,542	1,991	6,994	45,049
46	5,901	2,081	7,365	39,930
47	6,090	2,128	7,559	37,548
48	6,287	2,177	7,763	35,258
49	6,565	2,246	8,049	32,363
50	7,018	2,358	8,518	28,300
51	7,267	2,420	8,773	26,351
52	7,522	2,483	9,035	24,555
53	7,899	2,576	9,424	21,913
54	8,522	2,733	10,066	17,538
55	8,867	2,823	10,422	15,352

STREAMLINE(4) = 60,00000 PERCENT OF THE TOTAL MASS FLOW
 ZINIT = 0,000000 (NONDIMENSIONAL = S/RG)
 PINIT = 2053,317024 (PSIA)
 TINIT = 6158,412074 (DEG, R)
 VINIT = 1567,048615 (FT/SEC)
 ZFINAL = 9,236019 (NONDIMENSIONAL = Z/RG)
 MGKSK = 51 (NO. OF PRESSURE TABLE POINTS)

POINT NO.	AXIAL DISTANCE (Z/RG)	RADIAL DISTANCE (R/RG)	STREAMLINE DISTANCE (S/RG)	PRESSURE (PSIA)
1	1,250	,992	0,000	2053,317
2	1,162	,966	,092	2019,760
3	1,073	,941	,184	1980,745
4	,985	,917	,276	1935,960
5	,896	,895	,367	1894,962
6	,808	,874	,458	1827,235
7	,719	,854	,549	1762,205
8	,631	,831	,640	1782,140

Table B-II-Continued

9	1,542	1,812	1,730	1714,942
10	1,454	1,807	1,812	1642,099
11	1,365	1,797	1,812	1563,922
12	1,277	1,788	1,997	1480,801
13	1,188	1,781	1,086	1442,231
14	1,100	1,777	1,174	1360,393
15	1,011	1,775	1,263	1277,440
16	922	1,774	1,351	1193,909
17	833	1,775	1,440	1118,471
18	744	1,779	1,528	1035,535
19	655	1,784	1,617	961,009
20	566	1,791	1,706	881,700
21	477	1,795	1,815	717,171
22	388	1,809	1,960	693,268
23	299	1,852	2,104	608,907
24	210	1,897	2,250	521,435
25	121	1,945	2,398	436,550
26	32	1,996	2,549	363,736
27	1,388	1,051	2,705	300,922
28	1,537	1,108	2,865	259,784
29	1,690	1,167	3,029	238,081
30	1,846	1,225	3,195	219,675
31	2,007	1,283	3,366	202,352
32	2,171	1,341	3,540	186,125
33	2,341	1,399	3,720	170,940
34	2,518	1,457	3,906	156,551
35	2,706	1,520	4,104	142,859
36	2,906	1,585	4,314	129,878
37	3,120	1,656	4,540	117,497
38	3,351	1,732	4,783	105,732
39	3,604	1,814	5,049	94,526
40	3,881	1,905	5,341	83,896
41	4,181	1,992	5,673	76,402
42	4,424	2,030	5,899	67,350
43	4,781	2,130	6,270	58,696
44	5,195	2,247	6,699	50,387
45	5,853	2,433	7,384	40,085
46	6,169	2,524	7,712	36,114
47	6,414	2,594	7,967	33,325
48	6,836	2,716	8,407	28,081
49	7,059	2,782	8,639	25,094
50	7,294	2,854	8,885	22,149
51	7,629	2,961	9,236	18,321

Table B-II-Continued

STREAMLINE(S) = 80,00000 PERCENT OF THE TOTAL MASS FLOW
 Z' INIT = 0,000000 (NONDIMENSIONAL = Z/RC)
 P' INIT = 2081,153171 (PSIA)
 T INIT = 6171,809471 (DEG, R)
 V INIT = 1540,268632 (FT/SEC)
 Z FINAL = 8,644886 (NONDIMENSIONAL = Z/RC)
 MGKSK = 49 (NO. OF PRESSURE TABLE POINTS)

POINT NO.	AXIAL DISTANCE (Z/RC)	RADIAL DISTANCE (R/RC)	STREAMLINE DISTANCE (S/RC)	PRESSURE (PSIA)
1	1,250	1,166	0,000	2081,153
2	1,162	1,131	,095	2041,593
3	1,073	1,098	,190	1996,673
4	,985	1,066	,283	1946,054
5	,896	1,032	,376	1889,211
6	,808	1,011	,469	1825,507
7	,719	,988	,560	1754,245
8	,631	,963	,652	1790,229
9	,542	,944	,742	1711,576
10	,454	,932	,832	1627,907
11	,365	,919	,921	1539,285
12	,277	,909	1,010	1445,883
13	,188	,902	1,099	1409,973
14	,100	,897	1,188	1318,953
15	,011	,894	1,276	1227,595
16	,077	,894	1,365	1136,380
17	,166	,897	1,453	1056,140
18	,254	,902	1,542	966,216
19	,343	,910	1,631	887,173
20	,431	,920	1,720	801,994
21	,522	,930	1,811	675,103
22	,614	,944	1,925	641,228
23	,706	,955	1,966	614,682
24	,796	,964	2,000	593,222
25	,885	1,021	2,188	467,783
26	1,026	1,071	2,367	382,882
27	1,171	1,126	2,492	313,344
28	1,318	1,185	2,651	286,172
29	1,468	1,244	2,812	264,654
30	1,622	1,303	2,976	244,259
31	1,779	1,363	3,144	225,057
32	1,940	1,424	3,316	207,084
33	2,106	1,486	3,494	190,025
34	2,278	1,549	3,677	174,106
35	2,456	1,615	3,867	159,176
36	2,643	1,682	4,066	145,173
37	2,839	1,752	4,274	132,022
38	3,047	1,827	4,492	119,582

Table B-II-Continued

39	3,269	1,906	4,730	107,882
40	3,507	1,991	4,774	96,825
41	3,766	2,084	5,118	86,398
42	4,049	2,184	5,558	76,594
43	4,360	2,295	5,889	67,395
44	4,610	2,341	6,143	61,312
45	4,960	2,449	6,509	53,710
46	5,360	2,572	6,928	46,470
47	5,825	2,718	7,415	37,957
48	6,591	2,988	8,227	19,963
49	6,977	3,147	8,645	14,839

END OF STREAMLINE GENERATION PROGRAM
 MGKS INPUT TAPE HAS BEEN PREPARED

CP TIME = 492,122 PP TIME = 264,634

Table B-II--Continued

```

09/15/71 COPE 3,2,0=MDAC6500= VERSION N 06/28/71
09,57,55,B929806
09,57,56,SER,B24929
-09,57,56,H612,2,1500,800,600,12000,135000,
09,57,56,1DB24929 MARKHOFFMAN A03833888047612 40HA12 9615780010
09,57,56,REQUEST,CONTAM,MY, (14640)
09,57,56, (33 ASSIGNED, REEL 14640 )
09,57,56,REQUEST,TAPE9,MY, (RESERVE)
09,57,56, 100
09,57,56, (21 ASSIGNED, REEL 53929 )
09,57,56,COPYBF (CONTAM,REL)
09,58,14,COPYBF (CONTAM,TAPE4)
09,58,21,COPYBF (CONTAM,UCONT)
09,58,30,REWIND (REL)
09,58,30,REWIND (TAPE4)
09,58,30,REWIND (UCONT)
09,58,30,RETURN (CONTAM)
09,58,30,RFL,100,
09,58,30,DECIMAL=CP= 000 SEC,,PP= 039 SEC,,OCTAL=FL=012K,
09,58,30,RFL,60000,
09,59,09,DECIMAL=CP= 000 SEC,,PP= 000 SEC,,OCTAL=FL=000K,
09,59,09,UPDATE (P=UCONT)
10,01,31, UPDATING FINISHED
10,01,32,RUN (S,,1001,COMPILE)
10,01,47,REWIND (LGO)
10,01,47,RFL,100,
10,01,47,DECIMAL=CP= 017 SEC,,PP= 056 SEC,,OCTAL=FL=060K,
10,01,47,RFL,135000,
10,01,53,DECIMAL=CP= 000 SEC,,PP= 000 SEC,,OCTAL=FL=000K,
10,01,53,COPYLIB (LG1,LGO,REL)
10,01,53, COPYLIB
10,01,53,
10,01,53,*** COPYLIB
-10,02,31,EXECUTION FL=037000, ADD 10000 FOR CP LOADER FL,
10,02,31,DECIMAL=CP= 001 SEC,,PP= 022 SEC,,OCTAL=FL=135K,
10,03,50,DECIMAL=CP= 002 SEC,,PP= 024 SEC,,OCTAL=FL=037K,
10,03,50,END COPYLIB
10,03,51,REWIND (LG1)
10,03,51,LISTIT (LG1)
-10,05,01, CATALOG FINISHED
10,05,01,SETCURE,
10,05,01,LOAD (LG1)
10,05,51,ROLLOUT COMPLETED, (FL 135000)
10,14,19,ROLLIN COMPLETED,
10,14,54,NOGO,
-10,14,55,RFL,115000,
10,14,55,DECIMAL=CP= 013 SEC,,PP= 061 SEC,,OCTAL=FL=135K,
10,14,55,AFILE,
10,20,13,ROLLOUT COMPLETED, (FL 115000)

```

Table B-II--Concluded

10,25,07,ROLLIN COMPLETED,
10,30,02,STOP
10,30,03,REWIND(TAPE9)
10,30,03,COPYCF(TAPE9,OUTPUT)
10,30,06,RETURN(TAPE9)
10,30,09,CP 492,137 SEC,
10,30,09,PP 267,273 SEC,
10,30,09,SS 409,000 SEC,
R929R06, 011906 LINES PRINTED,

#####

Appendix C

KINCON

NONEQUILIBRIUM CHEMICAL KINETICS
AND CONDENSATION COMPUTER
PROGRAM

A Multiphase Reacting Gas
Streamtube Model

Program Number H860

TABLE OF CONTENTS

Section		Page
C. 1	INTRODUCTION	365
C. 2	ANALYSIS	367
	a. Conservation Equations	367
	b. Condensation Equations	372
C. 3	NUMERICAL METHOD	374
C. 4	PROGRAM OVERLAY STRUCTURE	377
C. 5	PROGRAM SUBROUTINES	378
	a. Main Overlay	378
	b. LINK 10 Subroutines	381
	c. LINK 20 Subroutines	381
	d. LINK 30 Subroutines	382
	e. LINK 41 Subroutines	384
	f. LINK 42 Subroutines	388
C. 6	PROGRAM USER'S MANUAL	415
	a. Operation Mode	416
	b. \$THERMO	416
	c. Thermodynamic Data	418
	d. Title Card	422
	e. Species Cards	422
	f. Reaction Cards	423
	g. \$PROPEL	424
C. 7	OUTPUT FOR A SAMPLE CASE	434
	a. Reaction-Rate Screening Case	434
	b. Oblique Shock Case	434
	c. Normal Shock-Stagnation Streamline Case	434
	d. Automated Kinetics and Condensation Case	434
C. 8	REFERENCES	458

TABLES

<u>Table</u>	<u>Page</u>
C-I Species Residing on Master Thermodynamic Tape	420
C-II Sample Listing For Thermodynamic Function Cards For N ₂	421
C-III Card Listing For Rate-Screening Case	435
C-IV Sample Reaction-Screening Output	437
C-V Final Summary Output After Screening - Results of Original and Screened Runs	438
C-VI Card Listing For Oblique Shock Calculation in Air	439
C-VII Pressure Table	440
C-VIII Shock Calculation	441
C-IX Card Listing For Normal Shock Stagnation Streamline Calculation in Air	442
C-X Input Velocity Distribution Table	443
C-XI Sample Output For Normal Shock Calculation	444
C-XII Kincon Sample Case - Data Listing	446
C-XIII Streamline Generation Program	447
C-XIV Initial Conditions Kinetic Streamtube Calculation Axial Position = 0, Input Normalizing Axial Scale Factor (FT) 8, 10000E-03	449
C-XV Kinetic Streamtube Conditions Axial Position	450
C-XVI Kinetic Streamtube Conditions Axial Position	451
C-XVII Area Ratio Table	452
C-XVIII Initial Conditions Kinetic Streamtube Calculation Axial Position = 2, 49885E+01 Input Normalizing Axial Scale Factor (FT) 8, 10000E-03	454

<u>Table</u>		<u>Page</u>
C-XIX	Kinetic Streamtube Conditions Axial Position	455
C-XX	Kinetic Streamtube Conditions Axial Position	456

LIST OF ABBREVIATIONS AND SYMBOLS

A, a	Cross-sectional area of the streamtube
a_j, b_j	Reaction-rate parameters
C_p	Specific heat at constant pressure
c_i	Mass fraction of i^{th} species
f_i	Free energy of i^{th} species
g	Mass fraction of condensed phase
\dot{H}	Energy addition rate, per unit normalized length, per unit initial streamtube mass flux
h	Enthalpy
h'	Enthalpy of condensed phase
J	Nucleation rate, critical-size nuclei formed per unit volume, per unit time
k	Boltzmann constant
K_j	Equilibrium constant
k_j, k_{kj}	Reaction-rate parameters
\dot{M}	Momentum flux, per unit normalized length, per unit initial streamtube mass flux
M_j	Third-body reaction term
\bar{M}_i	Chemical symbol for the i^{th} species
m	Mass addition rate, per unit normalized length per unit initial streamtube mass flux
m_{ji}	Reaction-rate ratio
m_i	Molecular weight of i^{th} species
N_a	Avogadro's number
n	Total number of species

n_j	Reaction-rate parameters
P, P_i	Pressure and partial pressure of i^{th} species, respectively
R	Gas constant of the mixture
\mathcal{R}	Universal gas constant
r^*	Normalization factor for x
r^{**}	Critical droplet radius
\dot{s}_i	i^{th} species mass addition rate, per unit normalized length, per unit initial streamtube mass flux
T	Temperature
V	Flow velocity
X_j	Species production-rate term
x	Axial distance
γ	Ratio of specific heats
σ	Surface tension
η	Condensation coefficient
ν_{ij}, ν'_{ij}	Stoichiometric coefficients
ρ	Density
ω_i	Production rate of i^{th} species

SUBSCRIPT

D	Droplet
L	Liquid
V	Vapor
VS	Saturated vapor
i	i^{th} species
j	j^{th} reaction

Appendix C

KINCON

NONEQUILIBRIUM CHEMICAL KINETICS AND CONDENSATION COMPUTER PROGRAM

A Multiphase Reacting Gas Streamtube Model

C. 1 INTRODUCTION

The computer program described in this appendix is a subprogram to the Plume Contamination Effects Prediction Computer Program, CONTAM, and performs chemical-kinetic and single-species condensation calculations along gas-phase streamlines as computed by the Multiphase Nozzle and Plume Transport Computer Program, MULTRAN. KINCON may also be used as an independent computer program on any third-generation computer with a core exceeding 135, 000 words and a Fortran IV processor.

The present computer program is based on the ICRPG One-Dimensional Kinetic Nozzle Analysis Computer Program, ODK (References C-1 and C-2), and on modifications to the ODK by Dynamic Science Corporation under contract to McDonnell Douglas Astronautics Company (Reference C-3). The purpose of the original program was to provide an automated engineering tool for the kinetic analysis of one-dimensional chemically reacting gas systems. To this end, a number of options were included in the program to aid the user. These included a mass, momentum, and energy streamtube addition option, generalized oblique shock calculation, normal shock-stagnation streamline calculation, area-defined streamtube option, and a reaction screening option. Modifications performed under the present study include the addition of a thermodynamic nonequilibrium condensation model and the automation of the program to perform successive kinetics and condensation calculations for a series of streamlines.

Species and reactions are input to the program in symbolic form. The user may input arbitrary species (up to 40) and arbitrary gas phase reactions (up to 150). Specified third-body reaction rate ratios may be employed. A comprehensive library of thermochemical data is available as part of the computer program. This data may be expanded by input of tables punched directly from the JANAF format. Automatic plotting of temperature, density, and species concentration is available. A unique feature of the program is its ability to integrate—with complete numerical stability—the differential equations governing the kinetic system.

Section C.2 contains a discussion of physical assumptions. The equations governing the inviscid, one-dimensional flow of a chemically reacting gas mixture are given in the form in which they are integrated in the computer program.

Section C.3 contains a discussion of the integration method used in the computer program.

Section C.4 contains a description of the program overlay structure.

Section C.5 contains a detailed engineering and programming description of the logic and the calculations performed in the computer program.

Section C.6 contains a program user's manual describing the use of the computer program with an explanation of the program input and output.

Section C.7 contains input and output for a sample case.

C. 2 ANALYSIS

The method of solution consists of integrating the conservation equations for the chemical system in such a form that the chemistry is generalized for binary exchange and dissociation-recombination reactions. Condensed phase products are considered by a single-species nonequilibrium condensation option.

a. Conservation Equations

The KINCON computer program integrates a set of simultaneous differential equations along a pressure-defined streamtube (i. e., $P(x)$ and $dP(x)/dx$ are known). These differential equations represent the conservation of species, mass, momentum, and energy for the system as expressed by Equations (C-5), (C-6), (C-7), and (C-8) below.

The conservation equations governing the inviscid flow of reacting gas mixtures have been given by Hirschfelder, Curtiss, and Bird (Reference C-4), Penner (Reference C-5), and others. The following basic assumptions are made in the derivation of these equations.

1. Mass (\dot{m} , \dot{s}_i), momentum (\dot{M}), and energy (\dot{H}) addition rates are defined for the system.
2. The gas is inviscid.
3. Each component of the gas is a perfect gas.
4. The internal degrees of freedom of each component of the gas are in equilibrium.

In one-dimensional flow, the conservation equations have the form¹

$$\text{species} \quad \frac{d}{dx} [(1 + \bar{m}) c_i] = \dot{s}_i + (1 + m) \frac{\omega_i r^*}{\rho V} \quad (\text{C-1})$$

$$\text{mass} \quad \frac{d}{dx} (1 + \bar{m}) = \dot{m} \quad (\text{C-2})$$

$$\text{momentum} \quad \frac{d}{dx} [(1 + \bar{m}) V] = \dot{M} - \frac{(1 + \bar{m})}{\rho V} \frac{dP}{dx} \quad (\text{C-3})$$

¹The independent variable, x , is taken as unitless with r^* as the conversion factor to units. The quantity $1 + \bar{m}$ represents the streamtube mass flux normalized by the initial streamtube mass flux; i. e., $1 + \bar{m} = (\rho Va)/(\rho Va)_0$

energy

$$\frac{d}{dx} \left[(1 + \bar{m}) h_T \right] = \dot{H},$$

(C-4)

$$h_T = \sum_{i=1}^n c_i h_i + \frac{V^2}{2}$$

If the expansion process is specified by the pressure distribution as a function of distance, Equations (C-1 through C-4) can be written as

$$\frac{dc_i}{dx} = \frac{\dot{s}_i - \dot{m}c_i}{1 + \bar{m}} + \frac{\dot{\omega}_i r^*}{\rho V} \quad (C-5)$$

$$\frac{dV}{dx} = \frac{\dot{M} - \dot{m}V}{1 + \bar{m}} - \frac{1}{\rho V} \frac{dP}{dx} \quad (C-6)$$

$$\frac{dT}{dx} = \frac{1}{C_p} \left[\frac{\dot{H} - \dot{m} h_T}{1 + \bar{m}} - \frac{V (\dot{M} - \dot{m}V)}{1 + \bar{m}} + \frac{1}{\rho} \frac{dP}{dx} - \sum_{i=1}^n h_i \frac{dc_i}{dx} \right] \quad (C-7)$$

$$\frac{d\rho}{dx} = \left[\frac{1}{P} \frac{dP}{dx} - \frac{1}{T} \frac{dT}{dx} - \frac{1}{R} \left(\sum_{i=1}^n R_i \frac{dc_i}{dx} \right) \right] \rho \quad (C-8)$$

where

$$C_p = \sum_{i=1}^n c_i C_{pi} \quad (C-9)$$

$$\gamma = \frac{C_p}{(C_p - R)} \quad (C-10)$$

$$h_i = \int_0^T C_{pi} dT + h_{i0} \quad (C-11)$$

For each component of the gas, the equation of state is

$$P_i = \rho_j R_i T \quad (C-12)$$

Summing over all the components of the mixture, the overall equation of state is obtained

$$P = \rho RT = \rho T \sum_{i=1}^n c_i R_i \quad (C-13)$$

The net species production rate ω_i for each species (component) is calculated from

$$\omega_i = \bar{m}_i \rho^2 \sum_{j=1}^n (\nu'_{ij} - \nu_{ij}) X_j \quad (C-14)$$

where

$$X_j = \left[K_j \prod_{i=1}^n c_i^{\nu_{ij}} - \rho^\lambda \prod_{i=1}^n c_i^{\nu'_{ij}} \right] k_j M_j \quad (C-15)$$

and λ depends on the order of the reaction and M_j is calculated only for dissociation-recombination reactions.

The equilibrium constant, K_j , is

$$K_j = e^{-\Delta F/RT} \quad (C-16)$$

$$\Delta F = \sum_{i=1}^n f_i \nu_{ij} - \sum_{i=1}^n f_i \nu'_{ij}$$

The computer program considers chemical reactions defined by the generalized chemical reaction equation

$$\sum_{i=1}^n \nu_{ij} \bar{M}_i \rightleftharpoons \sum_{i=1}^n \nu'_{ij} \bar{M}_i \quad (C-17)$$

where v_{ij} and v'_{ij} are the stoichiometric coefficients to be used in Equation (C-15) while \bar{M}_i represents the symbol for the i^{th} chemical species.

The reaction rates, k_j , for the j^{th} reaction appearing in Equation (C-15) are represented in the Arrhenius form

$$k_j = a_j T^{-n_j} e^{-b_j/\mathcal{R}T} \quad (\text{C-18})$$

where

- a_j is the pre-exponential coefficient
- n_j is temperature dependence of the pre-exponential factor
- b_j is the activation energy

Since each dissociation-recombination reaction has a distinct reaction rate associated with each third body, the net production rate for each dissociation-recombination reaction should be calculated from

$$X_j = \sum_{k=1}^n \left[K_j \prod_{i=1}^n c_i^{v_{ij}} - \rho \prod_{i=1}^n c_i^{v'_{ij}} \right] c_k k_{kj} \quad (\text{C-19})$$

rather than Equation (C-15). However, Benson and Fueno (Reference C-6) have shown theoretically that the temperature-dependence of recombination rates is approximately independent of the third body. Assuming that the temperature dependence of recombination rates is independent of the third body, the recombination rate associated with the k^{th} species (third body) can be represented as

$$k_{kj} = a_{kj} T^{-n_j} e^{-b_j/\mathcal{R}T} \quad (\text{C-20})$$

where only the constants a_{kj} are different for different species (third bodies). From Equation (C-19) it can be shown that

$$X_j = \left[K_j \prod_{i=1}^n c_i^{v_{ij}} - \rho \prod_{i=1}^n c_i^{v'_{ij}} \right] \left[\sum_{i=1}^n \frac{a_{ij}}{a_{kj}} c_i \right] a_{kj} T^{-n_j} e^{-b_j/\mathcal{R}T} \quad (\text{C-21})$$

Thus, the recombination rates associated with each third body can be considered as in Equation (C-15) by calculating the general third body term M_j as

$$M_j = \sum_{i=1}^n m_{ji} c_i \quad (C-22)$$

where m_{ji} is the ratio a_{ij}/a_{kj} .

In order to numerically integrate Equations (C-1), (C-5), (C-6), and (C-7), it is necessary to input the following type of information concerning the chemical system:

Boundary Conditions:

- x_0 initial axial position
- P_0 initial pressure
- T_0 initial temperature
- V_0 Initial velocity
- x_{max} final axial position
- $P(x)$ table of pressure versus axial position
- $dP(x)/dx$ table of pressure derivatives versus axial position

Species Information:²

- \bar{M}_i species name
- \bar{m}_i species molecular weight
- $C_{pi}(T)$ species specific heat
- $h_i(T)$ species enthalpy
- $f_i(T)$ species free energy

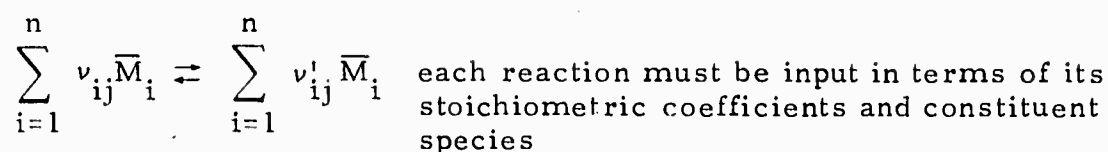
²The items C_{pi} , h_i , and f_i are not available directly in the appropriate units. The computer program calculates these items for each species from the JANAF data for:

$$- \frac{\begin{matrix} H^\circ - H^\circ_{298} & C_p \text{ vs } T \\ F^\circ - H^\circ_{298} & \text{vs } T \end{matrix}}{T} \text{ vs } T$$

and

$$H^\circ_{f,298}$$

Reaction Information:



a_j, n_j, b_j constants defining k_j , the reaction rates

m_{ji} third body reaction-rate ratios

Miscellaneous Information:

r^* normalization factor for x

Mass, Momentum, Energy, and Species Addition Functions:

$\dot{m}(x)$ mass addition rate, per unit normalized length, per unit initial streamtube mass flux

$\dot{M}(x)$ Momentum flux, per unit normalized length, per unit initial streamtube mass flux

$\dot{H}(x)$ energy addition rate, per unit normalized length, per unit initial streamtube mass flux

$\dot{s}_i(x)$ i^{th} species mass addition rate, per unit normalized length, per unit initial streamtube mass flux

A considerable amount of data (such as JANAF tables defining C_{pi} , h_i , and f_i , reaction rate parameters and cards defining chemical reactions) are available with the computer program. Details concerning input to the computer program are given in Subsection C.6.

For the area defined option including mass, energy, and momentum addition, the pressure profile is obtained by an iteration to obtain the pressure profile such that $\left| \frac{A(x) \text{ obtained} - A(x) \text{ input}}{A(x) \text{ input}} \right| < \epsilon$ where ϵ is an input convergence criteria.

b. Condensation Equations

Dropwise condensation of a single gaseous species is computed from classical liquid drop theory. In addition to the assumptions noted above, the condensation analysis assumes the following:

1. Condensed phase mass is uniformly distributed.
2. Droplets are spherical.
3. Droplets are small and follow gas streamlines.
4. Volume occupied by condensed phase is small compared to gas volume.

Two distinct processes are treated, nucleation and droplet growth. The nucleation process (spontaneous self-nucleation) occurs in the expanding supersaturated vapor and involves the clustering of vapor molecules to give rise to very small nuclei (radius of 10 to 100 Å). Only nuclei reaching the critical drop radius r^{**} can exist and grow. Critical drop radius is given by Frenkel (Reference C-7)

$$r^{**} = \frac{2\sigma}{\rho_L R_v T \ln\left(\frac{p_v}{p_{vs}}\right)} \quad (C-23)$$

The nucleation rate, J , represents the number of critical-size nuclei formed per unit volume per unit time and is calculated from the expression by Stever (Reference C-8)

$$J = \left(\frac{p_v}{kT}\right)^2 \frac{1}{\rho_L} \left(\frac{2\sigma m_i}{\pi N a}\right)^{1/2} \exp\left(-\frac{4\pi\sigma r^{**2}}{3 kT}\right) \quad (C-24)$$

Once a suitable number of nuclei are formed in the vapor, the process of droplet growth accounts for the actual condensation. Droplet growth occurs through the collision of vapor molecules and stable liquid droplets.

The net flux of vapor to the droplet surface is computed from kinetic theory considerations where droplets are typically smaller than the mean free path of the gas. The droplet growth equation of Hill (Reference C-9) is utilized

$$\frac{dr}{dx} = \frac{\eta}{\rho_L V} \frac{1}{(2\pi R_v)^{1/2}} (\beta - \beta_D) \quad (C-25)$$

where

$$\beta = \frac{p_v}{T^{1/2}}$$

$$\beta_D = \frac{p_D}{T_D^{1/2}}$$

Droplet temperature is assumed to be that of the saturated vapor.

The appropriate mass, momentum, and energy addition rates are computed internally from the following expressions

$$\begin{aligned} \dot{m} &= -\frac{dg}{dx} && \text{Mass} \\ \dot{M} &= \dot{m}V + g \frac{(1 - \bar{m})}{\rho V} \frac{dp}{dx} && \text{Momentum} \\ \dot{H} &= (1 - 2g) \dot{m}h' - (1 + \bar{m}) g \frac{dh'}{dx} && \text{Energy} \\ \dot{S}_i &= \dot{m}, \quad i = \text{condensing species} && \text{Species} \\ &= 0 \text{ for other species} \end{aligned}$$

The rate-of-change of condensed-phase mass fraction, dg/dx , is evaluated by summing the mass of all droplets formed upstream of a specific location, x , as follows

$$\frac{dg}{dx} = \frac{4\pi\rho_L}{\rho V} \left[\frac{1}{3} r^{**}(x) J(x) \frac{A(x)}{A_0} + \frac{dr}{dx} \int_{x_0}^x r(x, \xi)^2 J(\xi) \frac{A(\xi)}{A_0} d\xi \right] \quad (C-26)$$

where the integral is replaced by a summation for numerical evaluation.

C.3 NUMERICAL METHOD

It has been shown (e. g., Reference C-10) that explicit methods of numerical integration are unstable when applied to relaxation equations [such as Equations (C-1), (C-5), (C-6), and (C-7)], unless the integration step size is of the order of the characteristic relaxation distance. Since in the near equilibrium flow regime the characteristic relaxation distance is typically many orders of magnitude smaller than characteristic physical dimensions of the system of interest, the use of explicit methods to integrate relaxation equations often results in excessively long computation times. An implicit integration method which is inherently stable in all flow situations (whether near equilibrium or frozen) is therefore used by the computer program. With this method, step sizes which are of the order of the physical dimensions of the system of interest can be used, reducing the computation time per case by several orders of magnitude when compared with conventional explicit integration methods.

Consider N first-order simultaneous differential equations

$$\frac{dy_i}{dx} = f_i(X, y_1, \dots, y_N) \quad i = 1, 2, \dots, N \quad (C-27)$$

with known partial derivatives (i. e. the Jacobian for the system)³

$$a_i = \frac{\partial f_i}{\partial x} \quad (C-28)$$

$$\beta_{i,j} = \frac{\partial f_i}{\partial y_j} \quad (C-29)$$

The following implicit difference equations are used by the computer program to determine the $y_{i,n+1}$, (the subscript n denotes the n^{th} integration step)

$$y_{i,n+1} = y_{i,n} + k_{i,n+1} \quad h = x_{n+1} - x_n \quad (C-30)$$

where

$$k_{i,n+1} = \left[f_{i,n} + a_{i,n} h + \sum_{j=1}^N \beta_{i,j,n} k_{j,n+1} \right] \cdot h \quad (C-31)$$

for the initial step and for restart (first order).

$$k_{i,n+1} = \frac{1}{3} \left[k_{i,n} + 2 \left(f_{i,n} + a_{i,n} h + \sum_{j=1}^N \beta_{i,j,n} k_{j,n+1} \right) \cdot h \right] \quad (C-32)$$

³The computer program uses analytic expressions for calculation of the partial derivatives, a_i , β_{ij} .

for equal steps (second order with $h =$ previous h)

$$k_{i,n+1} = \frac{h_{n+1}^2}{(2h_{n+1} + h_n) \cdot h_n} \left[k_{i,n} + \left[f_{i,n} + a_{i,n} h_{n+1} + \sum_{j=1}^N \beta_{i,j,n} k_{j,n+1} \right] \cdot \frac{h_n}{h_{n+1}} (h_{n+1} + h_n) \right] \quad (C-33)$$

for unequal steps (2nd order with $h \neq$ previous h)

A derivation of these equations is given in Reference C-2.

If the flow is frozen, the explicit form of the above equations can be used ($\beta_{ij} = 0$); i. e., Equations (C-31), (C-32), and (C-33) are each reduced from an NXN system of linear simultaneous equations to N explicit equations ($N = 3 +$ number of species).

Control of the integration step size, h , is provided by calculating estimates for the truncation error and comparing these to an input criterion, δ .

The step size is halved if for any $i = 1, 2, \dots, N$

$$E_i > \delta$$

The step size is doubled if for all $i = 1, 2, \dots, N$

$$E_i < \frac{\delta}{10}$$

where

$$E_i = \left| \frac{k_{i,n+1} - 2k_{i,n} + k_{i,n-1}}{3k_{i,n+1} - k_{i,n}} \right| \quad (C-34)$$

The above expression for E_i is derived in Reference C-2.

C. 4 PROGRAM OVERLAY STRUCTURE

OVERLAY (FFILE, 6, 0)

			SCREEN DRIVER FIND STOICC SPLN AF073C GTF STF APPROX		
<u>LINK 10</u>	<u>LINK 20</u>	<u>LINK 30</u>	<u>LINK 41</u>	<u>LINK 42</u>	<u>LINK 50</u>
TTAPE COLOUT	ECNV INPUT NUMBER SPRXIN	STFSET	ADDFIT CONVRT PACKIP PRES SLP TCALC	DERIV EF FLU ADDXXX IAUX 1 IAUX ITER INT LESK MAIN OUTPUT OUTXXX PLTSUB PRNTCK UTIL SHOCK SCRX TREE CONAD VAPOR DROPS	DSCPLT MAXMIN SCAL

C. 5 PROGRAM SUBROUTINES

This section contains a description of the program subroutines. These descriptions are given in the order that the subroutines appear—link 10 through 50—on the overlay chart of Subsection C. 4. The order of execution of the program links is described below.

The main program sets up master limits for the chemistry, initializes certain logical control variables, and calls subroutine DRIVER. Subroutine DRIVER provides the overall logic control for the program.

After the program is loaded, LINK 10 is executed either to prepare a master tape containing JANAF Thermochemical Data from card input or to summarize the current master file used. LINK 20 is then executed to perform program input and species selection functions.

LINK 30 is then executed to prepare a blocked tape of packed and converted thermochemical data to be used by the kinetic calculation links. LINK 41 is then executed to prepare species and reaction information, pressure table and derivatives, and mass, energy, momentum, and species tables for the kinetic calculation. LINK 42 is executed to perform the kinetic expansion and condensation computation.

LINK 50 is executed to prepare plot output if requested.

a. Main Overlay

(1) Program SCREEN

This subroutine provides overlay communication, defines the labeled common blocks, sets maximum limits for the chemical tables, and initializes certain logical control variables. It calls subroutine DRIVER.

(2) Subroutine DRIVER

This subroutine performs the overall logic for the program.

(3) Subroutine FIND

Provides indices of the table entries which bracket the value of a current variable. The subroutine saves its place in the table.

(4) Subroutine STOICC

Provides up to ten reactants indices and ten product indices from the master stoichiometric coefficient table.

(5) Subroutine AFØ73C

This subroutine provides overlay linkage between the kinetic packing link, LINK 41 and the kinetic expansion computation link, LINK 42.

(6) Subroutine GTF

This subroutine computes the effective gas constant, gaseous heat capacity, γ , $\partial\gamma/\partial T$, $\partial\gamma/\partial C_i$ from the following formulae:

$$R = \sum_{i=1}^{NSP} C_i \cdot R_i$$

$$C_p = \sum_{i=1}^{NSP} C_i \cdot C_{p_i}$$

$$\gamma = \frac{C_p}{C_p - R}$$

$$\frac{\partial\gamma}{\partial T} = - \frac{\gamma \cdot (\gamma - 1)}{C_p} \cdot \sum_{i=1}^{NSP} C_i \cdot \frac{\partial C_{p_i}}{\partial T}$$

$$\frac{\partial\gamma}{\partial C_i} = \gamma \cdot (\gamma - 1) \cdot \left[\frac{R_i}{R} - \frac{C_{p_i}}{C_p} \right] \quad i = 1, \dots, NSP$$

(7) Subroutine SPLN

Performs cubic interpolation for a function and its first two derivatives. Given function values y_n and y_{n+1} and first derivative values y'_n and y'_{n+1} at x_n and x_{n+1} , this subroutine evaluates $y(x)$, $y'(x)$, and $y''(x)$ for $x_n \leq x < x_{n+1}$ using:

$$y = A(x - x_n)^3 + B(x - x_n)^2 + C(x - x_n) + D$$

$$y' = 3A(x - x_n)^2 + 2B(x - x_n) + C$$

$$y'' = 6A(x - x_n) + 2B$$

where:

$$A = \frac{1}{h^3} \cdot \left[(y'_{n+1} + y'_n) h - 2k \right]$$

$$B = -\frac{1}{h^2} \cdot \left[(y'_{n+1} + 2y'_n) h - 3k \right]$$

$$C = y'_n$$

$$D = y_n$$

$$h = x_{n+1} - x_n$$

$$k = y_{n+1} - y_n$$

(8) Subroutine STF

Using the SPLN interpolation subroutine, this subroutine computes the heat capacity and its temperature derivatives, enthalpy, and free energy, at the current temperature for all gaseous chemical species.

(9) Subroutine APPROX

This subroutine provides extension of the thermochemical data between the temperatures 9,000 and 20,000°R. A message is provided each time an approximation is calculated. The approximation formulae are given below with X = 9,000°R:

$$C_{P_T} = C_{P_X}$$

$$H_T = H_X + C_{P_X} * \Delta T$$

$$F_T = F_X - \left[\frac{H_T^\circ - H_{298}^\circ}{T} - \frac{H_T^\circ - H_{298}^\circ}{X} - C_{P_T} \log \left(\frac{T}{X} \right) \right]$$

b. LINK 10 Subroutines

(1) Subroutine TTAPE

This subroutine generates a master JANAF thermochemical tape which is subsequently utilized by Subroutine STFSET. The tape is written in the binary mode with the thermodynamic functions in caloric units. The thermodynamic functions for each species include:

<u>Function</u>	<u>Units</u>
C_p°	cal/mole-°K
$H^\circ - H^\circ_{298}$	k-cal/mole
$-\frac{(F^\circ - H^\circ_{298})}{T}$	cal/mole-°K

given at 100°K temperature increments over the range 100°K to 5,000°K, inclusive. Reference may be made to Subsection C.6, the Program Users Manual, for a complete description of thermodynamic input format and output options.

(2) Subroutine COLCUT

Provides columnar output of species names for those species residing on the master thermo file.

c. LINK 20 Subroutine

(1) Subroutine ECVN

This subroutine translates a BCD string of characters, into one floating point numeric value. E, I, and F formats are permitted with the result always a floating point number. It is called by subroutine SPRXIN to decode numeric fields in the species and reactions cards.

(2) Subroutine INPUT

This subroutine performs specific case input for the program. It performs the following functions:

1. Variable initialization to nominal values.
2. Read title card.
3. Call subroutine SPRXIN to input the species and reactions cards.

4. Read \$PROPEL namelist for case input data.
5. Check input mole or mass fractions for unity ($\pm 1.0E-4$).
6. Read initial conditions and pressure table from Tape 8 when operated in automatic mode.

(3) Subroutine NUMBER

This subroutine converts a one-character BCD number to a FORTRAN integer number. It is called by subroutine ECVN to decode free field numeric data.

(4) Subroutine SPRXIN

This subroutine processes the species and reactions cards. Species symbols, numeric mass or mole fractions, symbolic reactions, and rate parameters are processed. Reference may be made to Subsection C. 6, the Program Users Manual, for a complete description of input requirements.

d. LINK 30 Subroutines

(1) Subroutine STFSET

This subroutine uses the master JANAF tape written by subroutine TTAPE, to generate a species thermal-function tape (KSTF) in blocked form for the kinetic calculations. The tabulated functions on the master tape are:

<u>Function</u>	<u>Units</u>
$Cp'_i = Cp^\circ_i$	cal/mole-°K
$H'_i = [H^\circ - H^\circ_{298}]_i$	kcal/mole
$F'_i = - \left[\frac{F^\circ - H^\circ_{298}}{T} \right]_i$	cal/mole-°K

For the kinetic calculations the above functions must be converted to the ft/sec °R units system by the following:

<u>Function</u>	<u>Conversion</u>	<u>Internal Units</u>
Cp_i	$= [Cp_i' \cdot R_i] / 1.98726$	$ft^2/sec^2 \cdot ^\circ R$
H_i	$= \left(H_i' + \Delta H^\circ F_i \right) R_i \cdot 905.770$	ft^2/sec^2
F_i	$= F_i' / 1.98726$	unitless

These converted functions are then written in 900 °R temperature blocks. The free energy and heat capacity derivatives are computed using the formulae below with $\Delta T = 180.0$.

The function derivatives are computed according to the following formulae:

$$\frac{d\eta}{dT}(i, T_1) = \frac{4 \cdot \eta(i, T_2) - 3 \cdot \eta(i, T_1) - \eta(i, T_3)}{2 \cdot \Delta T}$$

$$\frac{d\eta}{dT}(i, T_j) = \frac{\eta(i, T_j + \Delta T) - \eta(i, T_j - \Delta T)}{2 \cdot \Delta T}$$

$$\frac{d\eta}{dT}(i, T_{50}) = \frac{3 \cdot \eta(i, T_{50}) - 4 \cdot \eta(i, T_{49}) + \eta(i, T_{48})}{2 \cdot \Delta T}$$

where η_i may be species heat capacity Cp' or free energy F' .

e. LINK 41 Subroutines

(1) Subroutine ADDFIT

For mass, energy, momentum and species addition functions, this subroutine calculates addition function tables and their derivatives from the input tables using one of the following options:

1. Simple differencing.
2. Spline fit.
3. Input derivative tables.
4. Parabolic fit.

The addition functions are normalized, modified by the appropriate multiplicative constants if required, and output in tabular form.

If single species condensation option is utilized, addition functions are not input but computed internally. No operations are performed by ADDFIT.

(2) Subroutine CONVRT

This subroutine converts input data from the externally input units to internally used computation units. In order to conserve computation time during the kinetic expansion, parameters such as molecular weights are included in these conversions. Primed numbers are input quantities.

(a) Dissociation-Recombination Reaction Rate Ratio

Input units: unitless

Internal units: (lbs-mass/lb-mole)⁻¹

Formula: $XMM_{j,i} = XMM'_{j,i} / MW_i$

(b) Pre-exponential Reaction Rate Ratio

Dissociation-recombination reactions

Input units: cm, °K, g-mole, sec

Internal units: ft³, °R, lb-mole, sec

$$A_j = \frac{A'_j \cdot (.0160183)^\eta \cdot 1.8^{XN_j}}{\prod_{i=1}^n MW_i^{\nu'_{ij}}}$$

Where η depends on the order of the reaction.

and

$$0.0160183 = \frac{3.531 \cdot 10^{-5} \text{ft}^3}{1 \text{cm}^3} \cdot \frac{1 \text{g-mass}}{2.2 \cdot 10^{-3} \text{lb-mass}}$$

(c) Exponential Term

Input units: kcal/mole

Internal units: °R

$$\text{Formula: } B_j = B'_j \cdot 905.770$$

where

$$905.770 = \frac{1000 \text{ cal}}{1 \text{ kcal}} \cdot \frac{1}{1.98726 \text{ cal/mole-}^\circ\text{K}} \cdot \frac{1.8^\circ\text{R}}{1.0^\circ\text{K}}$$

(d) Equilibrium Constant Multiplicative Factor

Input units: not input

Internal units: (lb-mass) - °R/ft³

Formula:

$$\text{DATEF(J)} = \frac{\prod_{i=1}^n \text{MW}_i^{v'_{ij}}}{\prod_{i=1}^n \text{MW}_i^{v_{ij}} \cdot 0.73034}$$

where

$$0.73034 = 49,721.011 \frac{\text{ft-poundals}}{(\text{lb-mole}) \cdot ^\circ\text{R}} \cdot \frac{1 \text{atmos}}{68,059.59 \text{ poundals/ft}^2}$$

(e) Heats of Reaction

Input units: Kcal/mole (via heats of formation)

Internal units: °R

$$\text{Formula: } \text{DELH(J)} = \text{DELH(J)}' \cdot 905.770$$

(f) Pressure

Input units: PSIA

Internal units: poundals/ft²

Formula: $P = P' \cdot 4633.056$

where

$$4633.056 = \frac{144 \text{ in}^2}{1 \text{ ft}^2} \cdot 32.174 \frac{\text{ft}}{\text{sec}^2}$$

(3) Subroutine PACK1P

On the basis of those species currently being considered, this subroutine packs species and reaction information from the master tables into those control sections utilized by the kinetic calculation links.

The following is a description of the subroutine functions:

1. The reaction rate parameters for the reactions to be considered are selected from tape unit KREAX.
2. The symbolic reactions and their input rate parameters are printed.
3. Reaction mass balance is checked for a tolerance of $\pm 1.0 \text{ E-}10$.
4. Heats of reaction are computed.

(4) Subroutine PRES

This subroutine provides a pressure table and its derivatives suitable for processing by the kinetic calculation links. For a normal shock stagnation streamline, velocity table and its derivatives are provided in a form suitable for processing by the kinetic calculation links.

(5) Subroutine SLP (X, Y, N, MFLAG, YP, W1, W2, W3, IFLAG)

The purpose of this subroutine is to supply derivatives for a tabulated function. The end point derivatives may be specified or are calculated internally by parabolic interpolation. Interior point derivatives may be found by a cubic spline fit procedure.

Calling Sequence:

- X is a table of independent variables, x_i
Y is a table of the dependent variables, y_i
N is the number of entries in each of the tables X, Y, and YP. $i = 1, \dots, N$

MFLAG this entry is a flag, m, such that

m > 0 implies x is equally spaced

m < 0 implies x is not equally spaced

|m| = 1 y' will be continuous

|m| = 2 y' and y'' will be continuous

YP is a table of the derivative, y'_i

W1 working storage of length N

W2 working storage of length N

W3 working storage of length N

IFLAG this entry is a flag, i, such that

i = 0 implies value for YP(1) and YP(N) will be calculated internally by parabolic differencing

i = 1 implies values for YP(1) and YP(N) will be input

Method:

The cubic spline fit procedure utilizes the interpolation formula given within the description of subroutine SPLN, i. e. :

$$y = A(x - x_0)^3 + B(x - x_0)^2 + C(x - x_0) + D$$

$$y' = 3A(x - x_0)^2 + 2B(x - x_0) + C$$

$$y'' = 6A(x - x_0) + 2B$$

The piecewise cubic fit to a tubular function by the above relations will yield a discontinuity in the second derivative y'', between adjacent fits of:

$$y''_{1_{01}} - y''_{1_{12}} = \frac{1}{h_{01}} \left(2y'_0 + 4y'_1 - 6 \frac{k_{01}}{h_{01}} \right) - \frac{1}{h_{12}} \left(6 \frac{k_{12}}{h_{12}} - 4y'_1 - 2y'_2 \right)$$

where

$$h_{01} = x_1 - x_0$$

$$h_{12} = x_2 - x_1$$

$$k_{01} = y_1 - y_0$$

$$k_{12} = y_2 - y_1$$

The method consists of setting the left-hand side of the above relation equal to zero so that the second derivative is continuous across juncture points. As applied to a tabular function, the above procedure results in a set of linear simultaneous equations (tri-diagonal) to be solved for the y'_1 , provided that values for y' at the end points are known.

(6) Subroutine TCALC

This is a dummy subroutine to permit the user to generate the addition function tables using his own supplied subroutine. It must be replaced with the appropriate TCALC routine and used in conjunction with the IADDOP = 2 option.

f. LINK 42 Subroutines

This link contains the one dimensional kinetic expansion subroutines.

The implicit integration method, used to integrate the fluid dynamic and chemical relaxation equations, requires the values of the partial derivatives of all total derivatives with respect to every variable. The program will generate a matrix of partial derivatives such that the entry in the n^{th} row and the m^{th} column is the partial derivative of $d[n]/dx$ with respect to m . This matrix is called BETA(I, J). The velocity, density, and temperature-fluid dynamic variables considered for every case reside in rows 1, 2, and 3 respectively. The chemical species occupy rows 4 through the number of species plus 3. The following notation will be used to denote partial derivatives:

$$\beta(A, B) = \frac{\partial \left[\frac{\partial A}{\partial x} \right]}{\partial B}$$

To facilitate the identification of program variables with the engineering notation, the following format will be used where applicable:

engineering notation-program variable-equation

The program will also generate a matrix which will be solved for the variable increments for each integration step. This matrix will expand or contract, depending on the number of chemical species to be considered.

The total derivatives f_i and partial derivatives β_{ij} have been separated into two components: (1) adiabatic component with no mass, momentum, or species addition, and (2) addition component due to mass, momentum, energy, or species addition. Subroutines DERIV and FLU calculate the adiabatic components and subroutine ADDXXX calculates the addition component. When no mass, momentum, energy, or species addition functions are input, the addition component calculations are bypassed.

For the single-species condensation option, subroutines CONAD, VAPOR and DRØPS compute the mass, momentum, and energy addition functions used by ADDXXX to calculate addition components.

(1) Subroutine DERIV

This subroutine computes the adiabatic components of total derivatives f_i and the partial derivatives $\beta(i, j)$ for the chemical relaxation equations.

Notation: i = Species subscript

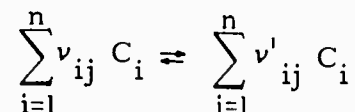
j = Reaction subscript

ℓ = Total number of chemical reactions

m = Number of dissociation-recombination reactions

n = Total number of gaseous species

The generalized chemical reaction which is handled by this subroutine is defined by:



with:

$$\psi_{ij} = \nu'_{ij} - \nu_{ij}$$

The reverse reaction rate constant is defined by the equation:

$$k_j \quad SK(J) = A_j \cdot T^{-XN_j} \cdot \exp(-B_j/T)$$

The net production rate for a reaction is given by:

$$X_j \quad X(J) = \left[K_j \cdot \prod_{i=1}^n C_i^{\nu_{ij}} - \rho^\lambda \cdot \prod_{i=1}^n C_i^{\nu'_{ij}} \right] \cdot k_j \cdot M_j$$

where:

$\lambda = 1$ for a dissociation-recombination reaction

$= 0$ for a binary exchange reaction

and

$$M_j = \sum_{i=1}^n XMM_{j,i} \cdot C_i \quad \text{for a dissociation-recombination reaction}$$

$$= 1 \quad \text{for a binary exchange reaction}$$

The net individual species production rate is given by the equation:

$$\frac{dC_i}{dx} \quad FN(I) = \bar{K}_i \cdot \sum_{j=1}^l \psi_{ij} \cdot X_j$$

where:

$$\bar{K}_i = (MW_i \cdot \rho \cdot r^*)/V$$

The partial derivatives of the net species production rate with respect to the chemical species, the gas velocity, the gas density, and the gas temperature are:

$$\beta(C_k, C_i) \quad BT(I, K) = \bar{K}_i \cdot \sum_{j=1}^l \frac{\partial X_j}{\partial C_i} \quad \begin{array}{l} i = 1, \dots, \text{NSP} \\ k = 1, \dots, \text{NSP} \end{array}$$

$$\beta(C_i, V) \quad PHI(I, 1) = -\frac{1}{V} \frac{dC_i}{dx} \quad i = 1, \dots, \text{NSP}$$

$$\beta(C_i, \rho) \quad PHI(I, 2) = \frac{1}{\rho} \cdot \frac{dC_i}{dx} + \bar{K}_i \cdot \sum_{j=1}^m \frac{\partial X_j}{\partial \rho} \quad i = 1, \dots, \text{NSP}$$

$$\beta(C_i, T) \quad PHI(I, 3) = \bar{K}_i \sum_{j=1}^l \frac{\partial X_j}{\partial T} \quad i = 1, \dots, \text{NSP}$$

The equilibrium constants and their temperature derivatives are computed only for dissociation-recombination reactions; those quantities for the binary exchange reactions are computed by products and ratios of the dissociation-recombination reaction equilibrium constants and derivatives.

(2) Subroutine EF

This subroutine computes the dissociation-recombination reaction equilibrium constants and their temperature derivatives from the following formulae:

$$K_j \quad EK(J) = \frac{DATEF(J)}{T} \cdot \exp \left[\frac{-\Delta H_j}{T} - \sum_{i=1}^n Ft_i \cdot v_{ij} + \sum_{i=1}^n Ft_i \cdot v'_{ij} \right]$$

$$\frac{dK_j}{dT} \quad DKT(J) = \left[\frac{-\sum_{i=1}^n \left(\frac{Ht_i}{R_i} \right) \cdot v_{ij} + \sum_{i=1}^n \left(\frac{Ht_i}{R_i} \right) \cdot v'_{ij}}{T} - 1 \right] \cdot \frac{K_j}{T}$$

where:

Ft_i = species free energy at the current temperature

Ht_i = species enthalpy at the current temperature

ΔH_j = heat of reaction for the J^{th} reaction

DATEF(j) = is discussed in Subsection C. 5, e(2)

(3) Subroutine FLU

This subroutine computes the adiabatic component of the total derivatives f_i and the partial derivatives α_i and $\beta(i, j)$ for the fluid dynamic equations. Pressure defined fluid dynamic equations are used. The summation terms, energy exchange term B, the diabatic heat addition term A, the Mach number, and all the partial derivatives of these terms are computed. The pressure and its derivatives are obtained from the pressure table.

For a stagnation streamline calculation, the pressure derivatives are obtained from the relationship:

$$\frac{dP}{dx} = -\rho \cdot V \frac{dV}{dx}$$

where V and dV/dx are defined by input tables.

Notes: $\Phi(i, \ell)$, $\ell = 1, 2, 3$ are defined under Subroutine DERIV
 $\Phi(i, 1)$, = $\beta(C_i, V)$; $\Phi(i, 2)$ = $\beta(C_i, \rho)$; $\Phi(i, 3)$ = $\beta(C_i, T)$

The following relationships may be helpful:

$$f_i = \frac{dC_i}{dx}; f_i = \frac{r^* \cdot \omega_i \cdot R \cdot T}{P \cdot V}; \frac{dC_i}{dx} = \frac{\omega_i r^*}{\rho \cdot V}$$

Computation of the Summation Terms and their derivatives:

First Summation

$$S1 \quad S1 = \frac{1}{R} \cdot \sum_{i=1}^n \frac{dC_i}{dx} \cdot R_i$$

$$\frac{\partial S1}{\partial V} \quad DS1V = \frac{1}{R} \cdot \sum_{i=1}^n \Phi(i, 1) \cdot R_i$$

$$\frac{\partial S1}{\partial \rho} \quad DS1R\emptyset = \frac{1}{R} \cdot \sum_{i=1}^n \Phi(i, 2) \cdot R_i$$

$$\frac{\partial S1}{\partial T} \quad DS1T = \frac{1}{R} \cdot \sum_{i=1}^n \Phi(i, 3) \cdot R_i$$

$$\frac{\partial S1}{\partial C_i} \quad DS1C(I) = \frac{1}{R} \cdot \left[\sum_{i=1}^n \beta(C_j, C_i) \cdot R_j - S1 \cdot R_i \right]$$

$i = 1, \dots, NSP$

Second Summation

$$S2 \quad S2 = \frac{1}{R \cdot T} \cdot \sum_{i=1}^n \frac{dC_i}{dx} \cdot h_i$$

$$\frac{\partial S2}{\partial V} \quad DS2V = \frac{1}{R \cdot T} \cdot \sum_{i=1}^n \Phi(i, 1) \cdot h_i$$

$$\frac{\partial S_2}{\partial p} \quad DS2R\emptyset \quad = \frac{1}{R \cdot T} \cdot \sum_{i=1}^n \Phi(i, 2) \cdot h_i$$

$$\frac{\partial S_2}{\partial T} \quad DS2T \quad = \frac{1}{R \cdot T} \cdot \sum_{i=1}^n \left[\Phi(i, 3) \cdot h_i + \frac{dC_i}{dx} \cdot C_{p_i} \right] - \frac{S_2}{T}$$

$$\frac{\partial S_2}{\partial C_i} \quad DS2C(I) \quad = \frac{1}{R} \cdot \left[\sum_{j=1}^n \frac{\beta(C_j, C_i) \cdot h_j}{T} - S_2 \cdot R_i \right]$$

$i = 1, \dots, NSP$

Computation of the Energy Exchange Term B and its Derivatives:

$$B \quad BB \quad = \frac{\gamma-1}{\gamma} \cdot S_2$$

$$\frac{\partial B}{\partial V} \quad DBBV \quad = \frac{\gamma-1}{\gamma} \cdot \frac{\partial S_2}{\partial V}$$

$$\frac{\partial B}{\partial p} \quad DBBRO \quad = \frac{\gamma-1}{\gamma} \cdot \frac{\partial S_2}{\partial p}$$

$$\frac{\partial B}{\partial T} \quad DBBT \quad = \frac{\gamma-1}{\gamma} \cdot \frac{\partial S_2}{\partial T} + \frac{S_2}{\gamma^2} \cdot \frac{\partial \gamma}{\partial T}$$

$$\frac{\partial B}{\partial C_i} \quad DBBC(I) \quad = \frac{\gamma-1}{\gamma} \cdot \frac{\partial S_2}{\partial C_i} + \frac{S_2}{\gamma^2} \cdot \frac{\partial \gamma}{\partial C_i} \quad i = 1, \dots, NSP$$

Computation of the Diabatic Heat Addition Term A and its Derivatives:

$$A \quad AA \quad = S_1 - B$$

$$\frac{\partial A}{\partial V} \quad DAAV \quad = \frac{\partial S_1}{\partial V} - \frac{\partial B}{\partial V}$$

$$\begin{aligned} \frac{\partial A}{\partial p} \quad \text{DAARO} &= \frac{\partial S1}{\partial p} - \frac{\partial B}{\partial p} \\ \frac{\partial A}{\partial T} \quad \text{DAAT} &= \frac{\partial S1}{\partial T} - \frac{\partial B}{\partial T} \\ \frac{\partial A}{\partial C_i} \quad \text{DAAC(1)} &= \frac{\partial S1}{\partial C_i} - \frac{\partial B}{\partial C_i} \quad i = 1, \dots, \text{NSP} \end{aligned}$$

Computation of the Mach Number and its Derivatives:

$$\begin{aligned} M^2 \quad \text{XM2} &= \frac{V^2}{\gamma \cdot R \cdot T} \\ \frac{\partial M^2}{\partial V} \quad \text{DM2V} &= \frac{2 \cdot M^2}{V} \\ \frac{\partial M^2}{\partial T} \quad \text{DM2T} &= -\frac{M^2}{T} - \frac{M^2}{\gamma} \cdot \frac{\partial \gamma}{\partial T} \\ \frac{\partial M^2}{\partial C_1} \quad \text{DM2C(1)} &= -M^2 \cdot \left[\frac{\partial \gamma}{C_1} \cdot \frac{1}{\gamma} + \frac{R_i}{R} \right] \quad i = 1, \dots, \text{NSP} \\ \frac{dV}{dx} \quad \text{FNX(1)} &= -\frac{1}{\rho \cdot V} \cdot \frac{dP}{dx} \\ \frac{\partial[\text{FNX(1)}]}{\partial x} \quad \text{AL(1)} &= -\frac{1}{\rho \cdot V} \cdot \frac{d^2 P}{dx^2} \\ \beta(V, V) \quad \text{BETA (1, 1)} &= -\frac{1}{V} \cdot \frac{dV}{dx} \\ \beta(V, \rho) \quad \text{BETA(1, 2)} &= -\frac{1}{\rho} \cdot \frac{dV}{dx} \end{aligned}$$

The Gas Density derivatives are Computed:

$$\frac{d\rho}{dx} \quad \text{FNX(2)} \quad = \quad \rho \cdot \left[\frac{dP}{dx} \cdot \frac{1}{\gamma \cdot P} - A \right]$$

$$\frac{\partial[\text{FNX(2)}]}{\partial x} \quad \text{AL(2)} \quad = \quad \frac{\rho}{\gamma \cdot P} \cdot \left[\frac{d^2P}{dx^2} - \left(\frac{dP}{dx} \right)^2 \cdot \frac{1}{P} \right]$$

$$\beta(\rho, V) \quad \text{BETA(2, 1)} \quad = \quad - \rho \cdot \frac{\partial A}{\partial V}$$

$$\beta(\rho, \rho) \quad \text{BETA(2, 2)} \quad = \quad - \frac{1}{\rho} \cdot \frac{d\rho}{dx} - \rho \cdot \frac{\partial A}{\partial \rho}$$

$$\beta(\rho, T) \quad \text{BETA(2, 3)} \quad = \quad - \rho \cdot \frac{\partial A}{\partial T} - \frac{\rho}{P \cdot \gamma^2} \cdot \frac{\partial \gamma}{\partial T} \cdot \frac{dP}{dx}$$

$$\beta(\rho, C_i) \quad \text{BETA(2, i+3)} \quad = \quad - \frac{\rho}{\gamma^2 P} \cdot \frac{\partial \gamma}{\partial C_i} \cdot \frac{dP}{dx} - \rho \cdot \frac{\partial A}{\partial C_i} \quad i = 1, \dots, \text{NSP}$$

The Gas Temperature derivatives are computed:

$$\frac{dT}{dx} \quad \text{FNX(3)} \quad = \quad T \cdot \left[\frac{\gamma-1}{\gamma} \cdot \frac{1}{P} \cdot \frac{dP}{dx} - B \right]$$

$$\frac{\partial[\text{FNX(3)}]}{\partial x} \quad \text{AL(3)} \quad = \quad \frac{\gamma-1}{\gamma} \cdot \frac{T}{P} \cdot \left[\frac{d^2P}{dx^2} - \left(\frac{dP}{dx} \right)^2 \cdot \frac{1}{P} \right]$$

$$\beta(T, V) \quad \text{BETA(3, 1)} \quad = \quad - T \cdot \frac{\partial B}{\partial V}$$

$$\beta(T, \rho) \quad \text{BETA(3, 2)} \quad = \quad - T \cdot \frac{\partial B}{\partial \rho}$$

$$\beta(T, T) \quad \text{BETA}(3, 3) = \frac{1}{T} \cdot \frac{dT}{dx} + T \cdot \frac{1}{\gamma^2 \cdot P} \cdot \frac{dP}{dx} \cdot \frac{\partial \gamma}{\partial T} - T \cdot \frac{\partial B}{\partial T}$$

$$\beta(T, C_i) \quad \text{BETA}(3, i+3) = T \cdot \left[\frac{1}{\gamma^2 \cdot P} \cdot \frac{dP}{dx} \cdot \frac{\partial \gamma}{\partial C_i} - \frac{\partial B}{\partial C_i} \right]$$

$i = 1, \dots, \text{NSP}$

For an adiabatic area defined calculation, the total derivatives f_i and the partial derivatives a_i and β_{ij} for the fluid dynamic equations are computed using the following area defined equations:

The area ratio and its derivatives are computed from:

$$a = Y^2$$

$$\frac{da}{dx} = 2 \cdot Y \cdot \frac{dY}{dx}$$

$$\frac{d^2 a}{dx^2} = 2 \cdot \left[Y \frac{d^2 Y}{dx^2} + \left(\frac{dY}{dx} \right)^2 \right]$$

where Y , dY/dx , $d^2 Y/dx^2$ are computed via interpolation in the table of derivatives of the input wall table generated in Subroutine SLP.

The Gas Velocity derivatives are computed:

$$\frac{dV}{dx} \quad \text{FNX}(1) = \frac{V}{M^2 - 1} \cdot \left[\frac{1}{a} \frac{da}{dx} - A \right]$$

$$\frac{\partial [\text{FNX}(1)]}{\partial x} \quad \text{AL}(1) = \frac{V}{M^2 - 1} \cdot \frac{1}{a} \cdot \left[\frac{d^2 a}{dx^2} - \frac{1}{a} \left(\frac{da}{dx} \right)^2 \right]$$

$$\beta(V, V) \quad \text{BETA}(1, 1) = \frac{1}{V} \cdot \frac{dV}{dx} - \frac{1}{M^2 - 1} \cdot \frac{dV}{dx} \cdot \frac{\partial M^2}{\partial V} - \frac{V}{M^2 - 1} \cdot \frac{\partial A}{\partial V}$$

$$\beta(V, \rho) \quad \text{BETA}(1, 2) \quad = \quad - \frac{V}{M^2 - 1} \cdot \frac{\partial A}{\partial \rho}$$

$$\beta(V, T) \quad \text{BETA}(1, 3) \quad = \quad - \frac{1}{M^2 - 1} \cdot \frac{dV}{dx} \cdot \frac{\partial M^2}{\partial T} - \frac{V}{M^2 - 1} \cdot \frac{\partial A}{\partial T}$$

$$\beta(V, C_i) \quad \text{BETA}(1, i+3) \quad = \quad - \frac{1}{M^2 - 1} \cdot \frac{dV}{dx} \cdot \frac{\partial M^2}{\partial C_i} - \frac{V}{M^2 - 1} \cdot \frac{\partial A}{\partial C_i}$$

$$i = 1, \dots, \text{NSP}$$

The Gas Density derivatives are computed:

$$\frac{d\rho}{dx} \quad \text{FNX}(2) \quad = \quad -\rho \cdot \left[\frac{M^2}{M^2 - 1} \cdot \left(\frac{1}{a} \cdot \frac{da}{dx} - A \right) + A \right]$$

$$\frac{\partial[\text{FNX}(2)]}{\partial x} \quad \text{AL}(2) \quad = \quad -\rho \cdot \frac{M^2}{M^2 - 1} \cdot \frac{1}{a} \cdot \left[\frac{d^2 a}{dx^2} - \frac{1}{a} \left(\frac{da}{dx} \right)^2 \right]$$

$$\beta(\rho, V) \quad \text{BETA}(2, 1) \quad = \quad \rho \cdot \left[\frac{1}{(M^2 - 1)^2} \cdot \left(\frac{1}{a} \frac{da}{dx} - A \right) \cdot \frac{\partial M^2}{\partial V} + \frac{1}{M^2 - 1} \cdot \frac{\partial A}{\partial V} \right]$$

$$\beta(\rho, \rho) \quad \text{BETA}(2, 2) \quad = \quad \frac{1}{\rho} \cdot \frac{d\rho}{dx} + \frac{\rho}{M^2 - 1} \cdot \frac{\partial A}{\partial \rho}$$

$$\beta(\rho, T) \quad \text{BETA}(2, 3) \quad = \quad \rho \cdot \left[\frac{1}{(M^2 - 1)^2} \cdot \left(\frac{1}{a} \frac{da}{dx} - A \right) \cdot \frac{\partial M^2}{\partial T} + \frac{1}{M^2 - 1} \cdot \frac{\partial A}{\partial T} \right]$$

$$\beta(\rho, C_i) \quad \text{BETA}(2, i+3) = \rho \cdot \left[\frac{1}{(M^2-1)^2} \cdot \left(\frac{1}{a} \frac{da}{dx} - A \right) \frac{\partial M^2}{\partial C_i} + \frac{1}{M^2-1} \cdot \frac{\partial A}{\partial C_i} \right] \quad i = 1, \dots, \text{NSP}$$

The Gas Temperature derivatives are computed:

$$\frac{dT}{dx} \quad \text{FNX}(3) = -T \cdot \left[(\gamma-1) \cdot \frac{M^2}{M^2-1} \cdot \left(\frac{1}{a} \frac{da}{dx} - A \right) + B \right]$$

$$\frac{\partial[\text{FNX}(3)]}{\partial x} \quad \text{AL}(3) = -T \cdot \frac{M^2}{M^2-1} \cdot \frac{\gamma-1}{a} \cdot \left[\frac{d^2 a}{dx^2} - \frac{1}{a} \cdot \left(\frac{da}{dx} \right)^2 \right]$$

$$\beta(T, V) \quad \text{BETA}(3, 1) = T \cdot \left[\frac{\gamma-1}{(M^2-1)^2} \left(\frac{1}{a} \frac{da}{dx} - A \right) \cdot \frac{\partial M^2}{\partial V} + \gamma-1 \cdot \frac{M^2}{M^2-1} \cdot \frac{\partial A}{\partial V} - \frac{\partial B}{\partial V} \right]$$

$$\beta(T, \rho) \quad \text{BETA}(3, 2) = T \cdot \left[\gamma-1 \cdot \frac{M^2}{M^2-1} \cdot \frac{\partial A}{\partial \rho} - \frac{\partial B}{\partial \rho} \right]$$

$$\beta(T, T) \quad \text{BETA}(3, 3) = \frac{1}{T} \cdot \frac{dT}{dx} + T \cdot \left[\frac{\gamma-1}{(M^2-1)^2} \left(\frac{1}{a} \frac{da}{dx} - A \right) \frac{\partial M^2}{\partial T} + \gamma-1 \cdot \frac{M^2}{M^2-1} \cdot \frac{\partial A}{\partial T} - \frac{\partial B}{\partial T} - \frac{M^2}{(M^2-1)} \cdot \left(\frac{1}{a} \frac{da}{dx} - A \right) \frac{\partial \gamma}{\partial T} \right]$$

$$\beta(T, C_i) \quad \text{BETA}(3, i+3) = T \cdot \left[\frac{\gamma - 1}{(M^2 - 1)^2} \cdot \left(\frac{1}{a} \frac{da}{dx} - A \right) \cdot \frac{\partial M^2}{\partial C_i} \right. \\ \left. + \gamma - 1 \cdot \frac{M^2}{M^2 - 1} \cdot \frac{\partial A}{\partial C_i} - \frac{\partial B}{\partial C_i} - \frac{M^2}{M^2 - 1} \cdot \left(\frac{1}{a} \frac{da}{dx} - A \right) \frac{\partial \gamma}{\partial C_i} \right] \quad i = 1, \dots, \text{NSP}$$

(4) Subroutine ADDXXX

This subroutine calculates the addition component of the total derivatives f_i and the partial derivatives a_i and β_{ij} and calculates the total and partial derivatives.

The addition components of the total derivatives are presented below:

$$\frac{dV}{dx} \Big|_{\text{add}} = \frac{\dot{M} - \dot{m}V}{1 + \bar{m}}$$

$$\frac{dC_i}{dx} \Big|_{\text{add}} = \frac{\dot{S}_i - \dot{m}C_i}{1 + \bar{m}_i}$$

$$\frac{dT}{dx} \Big|_{\text{add}} = \frac{1}{C_p} \left[\frac{E - \dot{m} H_T}{1 + \bar{m}} - \frac{V(\dot{M} - \dot{m}V)}{1 + \bar{m}} - \sum_{i=1}^{\text{nsp}} h_i \left(\frac{\dot{S}_i - \dot{m}C_i}{1 + \bar{m}} \right) \right]$$

$$\frac{d\rho}{dx} \Big|_{\text{add}} = \frac{-\rho}{T} \frac{dT}{dx} \Big|_{\text{add}} - \sum_{i=1}^{\text{nsp}} \frac{R_i}{R} \rho \frac{dC_i}{dx} \Big|_{\text{add}}$$

On option the adiabatic and addition components of the total derivatives are output from this subroutine.

(5) Subroutine IAUX1 (HL, H, QK, RK, JX)

This subroutine performs implicit integration according to the method discussed in Subsection C.3. The increments for the chemical species concentrations and the fluid dynamic variables at the forward point are calculated by solving the appropriate set of nonhomogeneous algebraic equations.

The calling sequence parameters are:

HL—last integration step size

H —current integration step size

QK—last increments for variables

RK—computed increments for variables

JX— 1 initial 3 steps

2 general step

3 special step

4 restart step

The total derivatives, $f_{i,n}$, and partial derivatives, $\beta_{i,j,n}$ at the back point are calculated in subroutines DERIV and FLU.

The special step calculation is used only in halving the step size if required.

After each integration step, subroutine IAUX obtains the derivatives at the then current axial position.

For implicit integration the equations used are:

Initial Step and Restart

$$k_{i,1} = \left[f_{i,0} + \alpha_{i,0} h + \sum_{j=1}^N \beta_{i,j,0} k_{j,1} \right] \cdot h$$

General Step

$$k_{i,n+1} = \frac{1}{3} \left[k_{i,n} + 2 \cdot \left(f_{i,n} + \alpha_{i,n} h + \sum_{j=1}^N \beta_{i,j,n} k_{j,n+1} \right) \cdot h \right]$$

Special Step

$$k_{i, n+1} = \frac{h_{n+1}^2}{(2h_{n+1} + h_n) \cdot h_n} \left[k_{i, n} + \left[f_{i, n} + \alpha_{i, n} h_{n+1} + \sum_{j=1}^N \beta_{i, j, n} k_{j, n+1} \right] \cdot \frac{h_n}{h_{n+1}} (h_{n+1} + h_n) \right]$$

(6) Subroutine IAUX (HL, H, QK, RK, JX)

This subroutine performs the iteration for the area defined, mass energy, momentum addition calculation. If the problem is pressure defined or an adiabatic-area-defined calculation, this subroutine merely calls Subroutine IAUX1 and then updates the derivatives at the forward point by calling Subroutine DERIV.

For the area defined, mass, energy, momentum addition calculation, the iteration proceeds as described below.

Prediction:

$$\frac{dP}{dx} = R \cdot T \cdot \frac{d\rho}{dx} + R \cdot \rho \cdot \frac{dT}{dx}$$

where

$$\frac{d\rho}{dx} = -\frac{1}{a} \frac{da}{dx} \cdot \rho \cdot \frac{M^2}{(M^2 - 1)}$$

$$\frac{dT}{dx} = -\frac{1}{a} \frac{da}{dx} \cdot T \cdot (\gamma - 1) \cdot \frac{M^2}{(M^2 - 1)}$$

if

$$0.99 < M^2 < 1.01,$$

then

$$\frac{dP}{dx} = 0.005 \cdot \frac{P}{H}$$

i

$$\frac{da}{dx} = 0.0,$$

then dP/dx from the previous step is used as the first estimate.

Iteration: Subroutine ITER is called successively to use the secant method to provide new estimates for dP/dx such that

$$f(A_{\text{calc}} - A_{\text{input}}) < \epsilon$$

Convergence: Convergence is obtained when

$$\left| \frac{A_{\text{calc}} - A_{\text{input}}}{A_{\text{input}}} \right| < \epsilon$$

and the pressure at the forward point is computed from

$$P_{i+1} = P_i + \left. \frac{dP}{dx} \right|_i \cdot H$$

(7) ITER (F1, X1, XNEW, NØØ)

The purpose of this subroutine is to find the root or zero of the algebraic equation

$$f(X) = 0$$

using the method of secant or false position. In particular this subroutine is designed to take advantage of the fact that the secant method will always find the root of the above equation if the root has been spanned.

Calling Sequence:

- F1 is the value of the dependent variable, f, corresponding to the value of X1. (Input)
- X1 is the value of the independent variable, X, which corresponds to F1. (Input)
- XNEW is the predicted or new value of the independent variable. (Output)
- NØØ is a flag such that
- NØØ = -1 the first time ITER is called. (Input)
- NØØ = +1 upon subsequent calls. (Output)

Restrictions:

The user is expected to check for convergence as there are no internal checks made in ITER. A literal must not be input to this subroutine.

Method:

Subroutine ITER utilizes the secant method predictor formula

$$X_{i+1} = X_i - f_i \cdot (X_i - X_{i-1}) / (f_i - f_{i-1})$$

where the subscript i refers to the current value of X and f except for the first iteration in which the value of X is perturbed only slightly. When the root has been spanned, the subroutine saves 2 back values of f and X in order that the root may always be straddled and thus found. The linkage to the subroutine is set up so that if bounds on the root are known, then the value of XNEW may be disregarded and bounded values may be used for the first two guesses. This type of linkage necessitates that the value of X1 must be set equal to XNEW or the bounded value of X. In order to accelerate convergence, if the error within the bounded domain of the dependent variable exceeds a ratio of 10, then the new value of X is set equal to one half of the range.

(8) Subroutine INT

Provides control for the implicit integration procedure, determines the proper set of nonhomogeneous equations to solve, and, after

each integration step, computes the next integration step size according to the following relations:

$$h_{n+2} = 2h_{n+1}, \quad \left| \frac{k_{i,n+1} - 2k_{i,n} + k_{i,n-1}}{3k_{i,n+1} - k_{i,n}} \right| \leq \frac{\delta}{10} \quad \text{MAX}$$

$$h_{n+2} = \frac{1}{2} h_{n+1}, \quad \left| \frac{k_{i,n+1} - 2k_{i,n} + k_{i,n-1}}{3k_{i,n+1} - k_{i,n}} \right| > \delta \quad \text{MAX}$$

$$h_{n+2} = h_{n+1}, \quad \frac{\delta}{10} \leq \left| \frac{k_{i,n+1} - 2k_{i,n} + k_{i,n-1}}{3k_{i,n+1} - k_{i,n}} \right| \leq \delta \quad \text{MAX}$$

On option, (JF=1) only the fluid dynamic variables are used in determining the next integration step size.

If the step size is halved for the fourth step, the integration is restarting using one-half the original step size.

The correspondence between equation number and physical property is:

<u>Equation Number</u>	<u>Property</u>
1	Velocity of gas
2	Density of gas
3	Temperature of gas
4 → NSP+3	Gaseous species mass fraction (1 → NSP) corresponds to (4 → NSP + 3)

(9) Subroutine LESK(Y)

This subroutine is a single precision linear equation solver which is used to perform the matrix inversions required by subroutine IAUX. Gaussian elimination is used with row interchange taking place to position maximum pivot elements after the rows are initially scaled.

(10) Subroutine MAIN

Provides overall logic control for the kinetic calculations, controls the shock calculation for both generalized oblique shock and the normal shock for the stagnation streamline, and prints the summary for the maximum and minimum reaction net production rates.

The normal shock calculation equations are presented below:

$$P_2 = \rho_1 V_1^2 + P_1 - (\rho_1 V_1) V_2$$

$$h_2 = \frac{V_1^2}{2} - \frac{V_2^2}{2} + h_1$$

$$T_2 = f(h_2)$$

$$\rho_2 = \frac{P_2}{R \cdot T_2}$$

(11) Subroutine OUTPUT

This subroutine provides conversion from internal computational units to output engineering units. The following output parameters are computed by this subroutine:

The pressure (in PSIA) is computed from:

$$P_{\text{(PSIA)}} = P/4633.056$$

The gaseous species mole fractions are computed from:

$$C_{i, m} = \frac{R_i}{R} \cdot C_i$$

The gas molecular weight is computed from:

$$MW = 49721.011/R$$

The percentage mass fraction change is computed from:

$$\Delta(\text{Mass Fraction}) = 100.0 \cdot \left(1.0 - \sum_{i=1}^n C_i \right)$$

The gas heat capacity is computed from:

$$C_{p_g} \text{ (BTU/LB-}^\circ\text{R)} = 3.9969 \cdot 10^{-5} \cdot C_{p_g}$$

The gas static enthalpy is computed from:

$$H_g \text{ (BTU/LB)} = 3.9969 \cdot 10^{-5} \sum_{i=1}^n C_i \cdot \left(h_i - 905.770 \cdot R_i \cdot \Delta H_{F_i}^\circ \right)$$

The percentage enthalpy change is computed from:

$$\Delta H_T = \frac{100 \cdot \left(H_c - \sum_{i=1}^{\text{NSP}} C_i \cdot h_i - v^2 / 2 \right)}{\text{HREF}}$$

where

$$\text{HREF} = \sum_{i=1}^{\text{NSP}} C_i \cdot \left(h_i - 905.770 \cdot R_i \cdot \Delta H_{F_i}^\circ \right)$$

evaluated at the initial conditions in Subroutine CONVRT.

The real gas constant and frozen gamma [Subsection C. 5f(2) (EF)] the enthalpy in internal units, the kinetic coupling terms A and B [Subsection C. 5f(3) (FLU)], the maximum relative error [Subsection C. 5t(8) (INT)], and the species concentrations in molecules per cc are also output.

(12) Subroutine OUTXXX

This subroutine is identical except in name to subroutine UTIL. It is used during the iteration for θ , the shock angle, during a generalized oblique shock calculation.

(13) Subroutine PLTSUB

This subroutine saves the current values of the variables requested for plotting and generates the proper labels and formatting for processing by subroutine DSCPLT. Plot information is saved on logical unit IPTAPE.

(14) Subroutine PRNTCK

For the option to print starting at step ND1, printing every ND3rd step up to step ND2, this subroutine checks whether or not the current step should be printed. If it is to be printed this subroutine calls OUTPUT.

(15) Subroutine UTIL (F1, X1, XNEW, NOO)

The purpose of this subroutine is to find the root or zero of the algebraic equation

$$f(X) = 0$$

using the method of secant or false position. In particular this subroutine is designed to take advantage of the fact that the secant method will always find the root of the above equation if the root has been spanned.

Calling Sequence:

- F1 is the value of the independent variable, f, corresponding to the value of X1. (Input)
- X1 is the value of the independent variable, X, which corresponds to F1. (Input)
- XNEW is the predicted or new value of the independent variable. (Output)
- NOO is a flag such that
- NOO = -1 the first time ITER is called. (Input)
- NOO = +1 upon subsequence calls. (Output)

Restrictions:

The user is expected to check for convergence as there are no internal checks made in UTIL. A literal must not be input to this subroutine.

Method:

Subroutine UTIL utilizes the secant method predictor formula

$$X_{i+1} = X_i - f_i \cdot (X_i - X_{i-1}) / (f_i - f_{i-1})$$

where the subscript i refers to the current value of X and f except for the first iteration in which the value of X is perturbed only slightly. When the root has been spanned the subroutine saves 2 back values of f and X in order that the root may always be straddled and thus found. The linkage to the subroutine is set up so that if bounds on the root are known, then the value of XNEW may be disregarded and bounded values may be used for the first two guesses. This type of linkage necessitates that the value of X1 must be set equal to XNEW or the bounded value of X. In order to accelerate convergence, if the error within the bounded domain of the dependent variable exceeds a ratio of 10, then the new value of X is set equal to one half of the range.

(16) Subroutine SHOCK

This subroutine calculates the downstream oblique shock conditions for an arbitrary pressure rise. The chemistry is assumed frozen across the shock. The method used is an iteration on the shock angle, θ , using the following:

$$1. \quad \theta^{(0)} = \arcsin \left[\sqrt{\frac{\frac{P_2}{P_1} (\gamma_1 + 1) + (\gamma_1 - 1)}{2 \gamma_1 M_1^2}} \right]$$

$$2. \quad u_1^{(i+1)} = V_1 \sin \theta^{(i)}$$

$$3. \quad v_2^{(i+1)} = V_1 \cos \theta^{(i)}$$

$$u_2^{(i+1)} = \frac{P_1 - P_2 + \rho_1 \left[u_1^{(i+1)} \right]^2}{\rho_1 u_1^{(i+1)}}$$

$$H_2^{(i+1)} = H_1 + \frac{1}{2} \left[u_1^{(i+1)} \right]^2 - \frac{1}{2} \left[u_2^{(i+1)} \right]^2$$

$$4. \quad T_2^{(i+1)} = f(H_2^{(i+1)}), \text{ obtained by iteration using subroutine UTIL.}$$

$$5. \quad \rho_{2a}^{(i+1)} = \frac{P_2}{R T_2^{(i+1)}}$$

$$\rho_{2b}^{(i+1)} = \frac{\rho_1 u_1^{(i+1)}}{u_2^{(i+1)}}$$

$$6. \quad \text{if } \left| \frac{\rho_{2a}^{(i+1)} - \rho_{2b}^{(i+1)}}{\rho_{2a}^{(i+1)}} \right| < \epsilon \text{ go to 9.}$$

7. Call OUTXXX to obtain new value for $\theta^{(i)}$ using secant method

8. Go to 2.

9. Compute and output downstream conditions:

$$Y_2 = \frac{C_P(T_2)}{C_P(T_2) - R}$$

$$V_2 = \sqrt{u_2^2 + v_2^2}$$

$$M_2 = \frac{V_2}{\sqrt{\gamma_2 R T_2}}$$

If the upstream Mach number is less than one, no shock calculation is possible and the calculation is terminated at this point.

If the specified conditions are inconsistent, i. e., if

$$\sqrt{\frac{\frac{P_2}{P_1} (\gamma_1 + 1) + (\gamma_1 - 1)}{2 \gamma_1 M_1^2}} > 1.0$$

a normal shock calculation is attempted using $\theta = \pi/2$ and no iteration. An error message is provided for both of the above error conditions.

(17) Subroutine SCRX

This subroutine screens the reaction set at each axial station for those reactions which are necessary to assure a relative accuracy for a specified chemical species. Summaries of an ordered set of those reactions which produce and those reactions which destroy the specified species, along with total production and destruction rates are provided.

The subroutine screens those reactions which produce or destroy the specified species and retains those which produce or destroy the species at a rate greater than the input criterion (a percentage of the total production or destruction per unit normalized length). A logical vector is generated with the entry TRUE if the reaction is required or FALSE if the reaction is not required.

(18) Subroutine TREE (L, LIND, N)

The purpose of this subroutine is to reorder an input vector L containing N components so that

$$L(1) \leq L(2) \leq \dots \leq L(N).$$

L may be either real or integer.

The vector LIND must be input as a vector of integers 1, 2, . . . N. The vector LIND will be output as a vector containing the integer numbers which were the original position numbers of the L components.

The method used by subroutine TREE is described by ALGORITHM 245, TREE SORT 3 by Robert W. Floyd, "Communications of the ACM." December, 1964.

(19) Subroutine CONAD

This subroutine calculates the mass, momentum, energy, and species addition functions to the gas phase streamtube resulting from the condensation of a single gaseous species.

Subroutine VAPOR is called at each integration step to determine location of current thermodynamic state relative to liquid-vapor or solid-vapor coexistence line on the pressure, temperature (P, T) surface.

Once condensing vapor becomes saturated, the critical droplet radius and nucleation rate are computed. The addition function components are not calculated until the nucleation rate surpasses a threshold value EJMIN (input under \$PROPEL). The addition functions are computed from the following:

$$\dot{m} = dg/dx$$

$$\dot{M} = \dot{m}V + g \frac{(1+m)}{\rho V} dp/dx$$

$$\dot{H} = (1 - 2g) \dot{m}h' - (1 + \bar{m}) \dot{g} \frac{dh'}{dT} \frac{dT}{dx}$$

$$\dot{S}_i = \dot{m}, \text{ for } i = \text{condensing species}$$

$$= 0, \text{ for remaining species}$$

The rate of change of the condensed mass fraction is obtained from

$$\frac{dg}{dx} = \frac{4\pi\rho_L}{\rho V} \left[\frac{1}{3} r^{**}(x) J(x) \frac{A(x)}{A_0} + \frac{dr}{dx} \int_{x_0}^x r(x, \xi)^2 J(\xi) \frac{A(\xi)}{A_0} d\xi \right]$$

The liquid droplet properties are obtained from Subroutine DROPS.

(20) Subroutine VAPOR (PV, PVS, DPVSDT, TS, IP, JJ, ISAT)

This routine computes for a specified species JJ the vapor pressure (PV), saturated vapor properties, and the location of the current state with respect to both the triple point and the liquid-vapor or solid-vapor coexistence line. Vapor pressure is computed from

$$P_v = C_i \frac{R_i}{R} P$$

For pressures and temperatures above the triple point, the saturated vapor pressure (PVS) corresponding to temperature T, derivative of PVS with respect to T, and saturated vapor temperature (TS) corresponding to pressure P are obtained from expressions of the form

$$PVS = C_1 + C_2/T + C_3/T^2$$

$$TS = 1. / [C_4 + C_5 \ln (PV) + C_6 \ln^2 (PV)]$$

$$DPVSDT = -PVS (C_2 - 2.0 C_3/T) / T^2$$

At or below the triple point, the following expressions are used

$$PVS = \exp (C_8 - C_7/T)$$

$$TS = C_7 / [C_8 - \ln (PV)]$$

$$DPVSDT = PVS C_7/T^2$$

where the constants C_1 through C_8 are determined from data and are input under \$PROPEL. Preliminary values of these constants for water vapor are stored internally and need not be entered.

The additional parameters in the calling statement are

IP = 0 Current state corresponds to triple point

= 1 Above triple point

= 2 Below triple point

ISAT = 0 Vapor is unsaturated

= 1 Vapor is saturated

(21) Subroutine DROPS

This subroutine computes liquid droplet properties and derivatives as a function of temperature. Above the triple point, latent heat and density are computed from

$$L = A_1 - A_2 T - A_3 T^2$$

$$\rho = A_4 - A_5 T_D + A_6 T_D^2$$

$$\sigma = A_{11} - A_{12} T_D$$

At or below the triple point, the following are used

$$L = A_7 - A_8 T$$

$$\rho = A_9 - A_{10} T_D$$

$$\sigma = A_{11} - A_{12} T_D$$

First and second derivatives with respect to temperature are obtained by differentiating the above expressions. The coefficients A_1 through A_{12} are input under \$PROPEL. Preliminary values of these constants for water vapor are stored internally.

g. LINK 50 Subroutines

(1) Subroutine LINK 50

This subroutine reads the quantities saved for plotting from logical unit IPTAPE into the proper buffer areas and calls subroutine DSCPLT for the actual plotting.

(2) Subroutine DSCPLT

This subroutine is a generalized plotting routine utilizing Calcomp software to produce plots. It requires subroutines SCAL and MAXMIN.

(3) Subroutine MAXMIN

This subroutine finds the maximum and minimum entries in an array.

(4) Subroutine SCAL(XMAX, XMIN, XI, DX, XO, XE)

Given the maximum and minimum of a variable and the number of units (inches, cm., etc.) available for plotting, this routine:

1. Determines the most efficient scale per plotting unit of the form $1.0 \cdot 10^a$, $2.0 \cdot 10^a$, $5.0 \cdot 10^a$ where a is an integer.
2. Adjusts the minimum scale value so that the plot begins at a multiple of the scale value.

Calling Sequence:

XMAX = the maximum value of the variable (input)

XMIN = the minimum value of the variable (input)

XI = the number of units (in., cm, etc.) available for plotting (input)

DX = the scale selected for the plot grid (output)

XO = the first plot grid value (output)

XE = the last plot grid value (output)

The algorithm used is given below:

$$W = \frac{XMAX - XMIN}{XI}$$

Then select $s = 1, 2, \text{ or } 5$ such that

$$W = DX \text{ is a minimum}$$

where

$$A = 1 + \log\left(\frac{W}{s}\right)$$

$$B = [A], [A] = \text{the greatest integer strictly less than } A, \\ \text{e.g. } [1.2] = 1, [0] = -1$$

or

$$B = [A] - 1 \text{ if } A = [A]' \text{ or } A < 0$$

$$C = s 10^B$$

$$D = \left\lfloor \frac{XMIN}{C} \right\rfloor C$$

or

$$D = \left(\left\lfloor \frac{XMIN}{C} \right\rfloor - 1 \right) C \text{ if } C \cdot D > XMIN$$

$$E = W/C$$

and

$$DX = C$$

$$XO = D$$

$$XE = E$$

also

$$\text{if } W=0 \text{ then } DX=XO=XE=0$$

C.6 PROGRAM USER'S MANUAL

This program was developed on the CDC 6500 computer using the FORTRAN IV language. Conversion to another computer system should be straight forward provided sufficient core storage (135,000 words) is available. Program overlay extends three levels deep including the executive level, when used as a subprogram to CONTAM.

The description of the operation mode and input to the computer program is divided into the following six Subsections:

- C. 6. 1 OPERATION MODE—Automatic or manual.
- C. 6. 2 \$THERMØ—Namelist input which controls the thermodynamic data input.
- C. 6. 3 THERMODYNAMIC DATA—Optional.

- C. 6. 4 TITLE CARD—Also serves for plot labels.
- C. 6. 5 SPECIES CARDS—Species to be considered and their initial concentrations.
- C. 6. 6 REACTION CARDS—Input of reactions and rate data.
- C. 6. 7 \$PRØPEL—Namelist input for a specific case.

Card listings for the complete input for several sample cases are given in Section C. 7.

a. Operation Mode

Two modes of operation (automatic or manual) are available and specified through input variable KMØDE in the executive program, CONTAM.

(1) Manual Mode (KMØDE = 1)

In the manual mode of operation the KINCON subprogram is independent of the other subprograms. The user is free to specify, via input data (cards), the streamtube initial conditions, boundary conditions, and program options. A complete set of data (inputs described in Subsections C. 6b through C. 6g) is required for each streamtube calculation. However, if a specific nozzle/plume streamtube, generated by either the nozzle or plume portion of MULTRAN is desired; subprogram SLINES may be utilized in conjunction with MULTRAN to specify initial conditions and pressure distribution while operating in the manual mode. The variable NSL, which specifies the number of streamtubes processed by subprogram SLINES, is input through either the executive program or SLINES and is tested to determine if input data from SLINES via TAPE 8 is to be used in the manual mode of operation.

If NSL = 0, TAPE 8 will not be read and all data must be input.

If NSL / 0, the initial values (Z, PI, T, V, and EXIT), as well as the streamtube pressure distribution (NTB, ZTB (I), and PTB (I)) are read from TAPE 8. If successive cases are run, TAPE 8 will be read successively until either the final case is completed or the number of streamtubes on TAPE 8 is exhausted. It should be noted that any or all data read from Tape 8 may be overridden by card input.

(2) Automatic Mode (KMØDE = 0)

The automatic mode of operation is designed to calculate both chemical-kinetic and single-species condensation effects (a two-pass calculation performed in that order) for a number of streamtubes calculated by MULTRAN and SLINE subprograms. This mode requires only one set of input data and is utilized in conjunction with subprogram SLINES (or a TAPE 8 previously generated by SLINES).

In the automatic mode, KINCON will accept input data describing initial gas-phase composition, chemical reaction and rate coefficients, and pertinent integration control parameters (described in Subsections C.6.b through C.6.g). Initial streamtube conditions and pressure distribution are read from TAPE 8, and kinetics calculation is then performed along the pressure-defined streamline. During the kinetics calculation pass the vapor pressure of the condensible species is compared with the saturated vapor surface to determine the vapor state. Once the saturated vapor state is reached, the streamtube conditions at the saturation point (location, temperature, pressure, velocity, and species composition) are written onto TAPE 1. The streamtube area ratio, referenced to the saturation point, is then computed and written on TAPE 1 during the subsequent integration.

TAPE 1 thus contains, at the completion of the kinetics pass, the initial conditions and area ratio distribution for the streamtube beginning at the saturation point.

If the saturation point is countered on the kinetics pass, a second pass is made to compute condensation. This pass, utilizing TAPE 1 generated during the kinetics pass, invokes frozen-chemistry and single-species condensation options to compute condensation effects along the area defined streamtube. Following the completion of the condensation calculation, initial conditions for the next streamtube are read from TAPE 8 and the calculation procedure is repeated until all streamtubes have been completed. If the saturation point is not reached on a given kinetics pass, the condensation calculation pass is not performed and the program proceeds to the next streamtube.

Inputs in the automatic mode consist of all inputs described in Subsections C.6.b through C.6.f and a limited number of inputs in \$PROPEL. Inputs required in \$PROPEL are the following:

RSTAR	Axial distance normalizing factor (nozzle throat radius)
PRINT VARIABLES	(ND1, ND2, ND3)
INTEGRATION VARIABLES	(IH, HMIN, HMAX, DEL, JF)

Inputs that are available but not required include MISCELLANEOUS VARIABLES (except IFLAST), INTERMEDIATE OUTPUT VARIABLES, and certain CONDENSATION OPTION VARIABLES.

b. \$THERMØ

Permits the generation of a master thermodynamic file or the use of a tape file previously generated master thermodynamic file.

<u>Variable</u>	<u>Value</u>	<u>Description</u>
NUCHEM	= 1	A master thermodynamic file will be generated for this case on tape unit 4. Species and thermodynamic data will be read from unit INTAPE (nominal=5, the input file) and a new thermodynamic file will be generated on unit 4. The new thermodynamic file will be end-filed and rewound after generation.
	= 0	A previously generated master thermodynamic file will be used for this case. The master thermodynamic file must be file TAPE 4. No other input variables are required for this option.
MAXSP	= Input	If a master thermodynamic file is to be generated this variable specifies the number of species for the master file.
LIST	= 1	A list of species named for those species master file will be output.
	= 0	This output will be deleted.
LISTX	= 1	Thermodynamic functions (CP, H, F) will be output for each species (one page per species, 52 lines per page). Species names, molecular weights, and heats of formation will also be printed.
	= -1	Only a table of species names, molecular weights, and heats of formation will be printed.
	= 0	The above output will be deleted.
INTAPE	= Input	Tape file from which thermodynamic data is to be read (nominal = 5).

\$END

c. Thermodynamic Data

For a NUCHEM = 1 option in \$THERMØ the program will read MAXSP Master Species cards containing: species symbolic identifier, molecular weight, and ΔH°_{F298} , and then read MAXSP sets of thermodynamic data (CP, H, F) checking names and card sequences. The Master Species cards must be sequenced sequentially in columns 41-50 (I10 format) and must correspond directly to the order in which the thermodynamic data is to be read. Thermodynamic functions consist of 10 cards per function, 5 values per card corresponding to temperature values of 100 → 5,000°K at 100°K

intervals. Table C-I lists the species for which thermodynamic data is currently available. For species which do not appear in Table C-I, this input may be obtained directly from the JANAF tables. Table C-II is a sample listing of the thermodynamic function input for the species N₂.

Master Species Cards

<u>Column</u>	<u>Information</u>
1 - 10	Not used.
11 - 16	Species Symbolic Identifier, 6 alphanumeric characters (left justified).
17 - 20	Not used.
21 - 30	Species molecular weight (F) format.
31 - 40	Species ΔH°_{F298} (F) format, K cal/mole.
41 - 50	Right justified sequence number used for sequence checking on input (I10 format).
51 - 80	Not used.

It should be noted that a species is identified by the name assigned by the user. In general this name is the chemical symbol, e.g., O, O₂, H, H₂. However, it may be useful to define a dummy species with all the properties of another species but which may be treated in a special manner, e.g., the percentage of the total amount of a species which is designated as an inert (possibly to simulate incomplete mixing or combustion). This may be done by defining species O and OX where OX is identical to O except in name, but does not appear in any reaction.

Master Thermodynamic Function Cards

<u>Column</u>	<u>Information</u>
1	Not used.
2 - 10	Function value at $(100 + 500 (n-1))$ °K, n = card number.
11	Not used.
12 - 20	Function value at $(200 + 500 (n-1))$ °K.
21	Not used.
22 - 30	Function value at $(300 + 500 (n-1))$ °K.
31	Not used.
32 - 40	Function value at $(400 + 500 (n-1))$ °K.
41	Not used.
42 - 50	Function value at $(500 + 500 (n-1))$ °K.
51 - 60	Not used.
61 - 66	Species symbolic identifier, left justified.
67 - 68	Not used.
69 - 70	Function Definition CP, H, or F, left justified.
73 - 76	The word CARD.
77 - 78	Card number 1-10 right justified.
79 - 80	Not used.

Species symbolic identifier, function definition, and card numbers are checked for consistency on input.

Table C-I. SPECIES RESIDING ON MASTER THERMODYNAMIC TAPE

1 H ₂ O	19 SF ₄	37 RCL ₃	55 C ₂ F ₂	73 COF ₂	90 ALF
2 H ₂	20 SF ₆	38 BF	56 O ₃	74 NO ₃	91 ALF ₂
3 OH	21 C	39 BF ₂	57 HO ₂	75 NH	92 ALF ₃
4 O ₂	22 CO ₂	40 BF ₃	58 NO ₂ ⁻	76 NH ₂	93 ALOCL
5 O	23 CO	41 BOCL	59 NA	77 NH ₃	94 ALOF
6 H	24 C ₂	42 BOF	60 NA ⁺	78 BH	95 ALCLF
7 ARGON	25 CH	43 BCLF	61 NAO	79 BH ₂	96 ALCL ₂ F
8 F ₂	26 CH ₂	44 BCL ₂ F	62 CF ₂	80 BH ₃	97 ALCL ₂ F ₂
9 HF	27 CH ₃	45 BCLF ₂	63 CF ₃	81 B ₂ H ₆	98 OH ⁻
10 F	28 CH ₄	46 B	64 CF ₄	82 B ₂ O ₂	99 CH ₂ O
11 N ₂	29 C ₂ H ₂	47 CL	65 C ₂ F ₄	83 B ₂ O ₃	100 NaOH
12 NO	30 CN	48 CL ₂	66 NO ₂	84 AL	101 NAH
13 NO ⁺	31 HCN	49 N	67 N ₂ O	85 AL ₂ O	102 H ₂ Z
14 O ₂ ⁻	32 BO	50 HCL	68 HCO	86 AL ₂ O	103 HZ
15 O ⁻	33 BO	51 CLF	69 HCO ⁺	87 ALCL	104 OHX
16 F ⁻	34 BO ₂	52 CNCL	70 C ₂ H	88 ALCL ₂	105 PHOTON
17 F ⁻	35 BCL	53 CNF	71 H ₃ O ⁺	89 ALCL ₃	106 OZ
18 S	36 BCL ₂	54 CF	72 H ₂ O ₂		

Table C-II. SAMPLE LISTING FOR THERMODYNAMIC
FUNCTION CARDS FOR N₂

6,9560,	5,9570,	6,9610,	6,9900,	7,0690,	N2	CP	CARD 1
7,1960,	7,3500,	7,5120,	7,6700,	7,8150,	N2	CP	CARD 2
7,9450,	8,0610,	8,1620,	8,2520,	8,3300,	N2	CP	CARD 3
8,3980,	8,4580,	8,5120,	8,5590,	8,6010,	N2	CP	CARD 4
8,6380,	8,6720,	8,7030,	8,7310,	8,7560,	N2	CP	CARD 5
8,7790,	8,8000,	8,8200,	8,8380,	8,8550,	N2	CP	CARD 6
8,8710,	8,8860,	8,9000,	8,9140,	8,9270,	N2	CP	CARD 7
8,9390,	8,9500,	8,9620,	8,9720,	8,9830,	N2	CP	CARD 8
8,9930,	9,0020,	9,0120,	9,0210,	9,0300,	N2	CP	CARD 9
9,0390,	9,0480,	9,0570,	9,0660,	9,0740,	N2	CP	CARD 10
1,3790,	,6830,	,0130,	,7100,	1,4130,	N2	H	CARD 1
2,1250,	2,8530,	3,5960,	4,3550,	5,1290,	N2	H	CARD 2
5,9170,	6,7180,	7,5290,	8,3500,	9,1790,	N2	H	CARD 3
10,0150,	10,8580,	11,7070,	12,5600,	13,4180,	N2	H	CARD 4
14,2800,	15,1460,	16,0150,	16,8860,	17,7610,	N2	H	CARD 5
18,6380,	19,5170,	20,3980,	21,2800,	22,1650,	N2	H	CARD 6
23,0510,	23,9390,	24,8290,	25,7190,	26,6110,	N2	H	CARD 7
27,5050,	28,3990,	29,2950,	30,1910,	31,0890,	N2	H	CARD 8
31,9880,	32,8880,	33,7880,	34,6900,	35,5930,	N2	H	CARD 9
36,4960,	37,4000,	38,3060,	39,2120,	40,1190,	N2	H	CARD 10
51,9570,	46,4070,	45,7700,	46,0430,	46,5610,	N2	F	CARD 1
47,1430,	47,7310,	48,3030,	48,8530,	49,3780,	N2	F	CARD 2
49,8790,	50,3570,	50,8130,	51,2480,	51,6650,	N2	F	CARD 3
52,0650,	52,4480,	52,8160,	53,1710,	53,5130,	N2	F	CARD 4
53,8420,	54,1600,	54,4600,	54,7660,	55,0550,	N2	F	CARD 5
55,3350,	55,6060,	55,8700,	56,1270,	56,3760,	N2	F	CARD 6
56,6190,	56,8560,	57,0870,	57,3120,	57,5320,	N2	F	CARD 7
57,7470,	57,9570,	58,1620,	58,3620,	58,5590,	N2	F	CARD 8
58,7510,	58,9400,	59,1240,	59,3050,	59,4820,	N2	F	CARD 9
59,6570,	59,8270,	59,9950,	60,1600,	60,3220,	N2	F	CARD 10

d. Title Card

The title card contains free field information which will be written as a header label for the program output. The first 40 characters will be written as a label on each plot if plotting is requested.

e. Species Cards

This input is prefixed by a single card with SPECIES in columns 1 to 7 and with the words MASS FRACTIONS or MOLE FRACTIONS in columns 9-22. If the identifier for mass or mole fractions is omitted, mass fractions are assumed. Up to 40 species cards may be input. Only those species specified by input species cards will be considered. The order of the input species cards is independent of the order in which the species appear on the master thermodynamic data file. However, the order of the input species cards does define the species order for the specific calculation, and other input referencing individual species must refer to the order of the input species cards. Species Cards are described below:

<u>Column</u>	<u>Function</u>
1 - 10	Not used.
11 - 16	Symbol (left justified).
17 - 20	Not used.
21 - 60	Value of initial species concentration (if zero must be input as 0.0) free field F or E format.
61 - 80	User identification if desired.

Symbols for Species Identification

A chemical species is identified symbolically by six alphanumeric characters as follows:

The species symbol must agree with that given on its master species card (columns 11-16) used in generating the master thermodynamic file. If the species is ionized, the degree of ionization is indicated by a + (or -) sign followed by an integer describing the degree of ionization (if no integer is given the species will be assumed singly ionized). The species symbol may not contain the characters * or =. The special species symbol PHOTON is reserved for specifying radiative reactions.

Examples:

<u>Symbol</u>	<u>Interpretation</u>
CL	Cl
NA+	NA ⁺
K+2	K ⁺⁺
CL2-2	Cl ₂ ⁻
H2O2	H ₂ O ₂

f. Reaction Cards

This input is prefixed by a single card with REACTIØNS in columns 1 to 9. Up to 15 dissociation reactions and a total 150 reactions may be input following this card. Only one card per reaction is permitted. Cards specifying dissociation-recombination reactions must precede cards specifying exchange reactions. The content and format of the reaction cards are defined as follows:

(1) Each card is divided into five fields, separated by commas. Each field contains:

Field 1	the reaction.
Field 2	A = followed by the value of A.
Field 3	N = followed by the value of N.
Field 4	B = followed by the value of B, the activation energy (Kcal/mole).
Field 5	available for comments.

Rules for specifying the reaction are given in C.6.e(2) below. The values A, N, and B define the reverse reaction rate, k, as

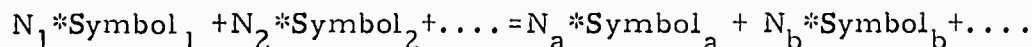
$$k = A \cdot T^{-N} \cdot e^{-(B/RT)}$$

All three reaction rate parameters must be input. The numeric value of each parameter may be specified in either I, F, or E format. If E format is used, the E must appear before the exponent.

There may be no blanks between the characters A and equal sign, the N and equal sign, and the B and equal sign.

Input rate parameters are in units of cc, °K, mole, sec.

(2) The general form of a reaction is:



where the left-hand side represents reactants and the right-hand side represents products.

Each symbol must be as defined on an input species card (see the description of SPECIES CARDS).

The multipliers, N, must be integers and represent stoichiometric coefficients. If no stoichiometric coefficient is given, the value 1 is assumed.

It is required that

$$N_1 + N_2 + \dots \leq 10$$

and

$$N_a + N_b + \dots \leq 10$$

Examples:

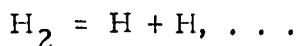
<u>Reaction</u>	<u>Interpretation</u>
NA++CL- = NACL	Na ⁺ + Cl ⁻ = NaCl
B+2+M-2 = BM	B ⁺⁺ + M ⁻⁻ = BM
BE+2+2*ØH- = BEØHØH	Be ⁺⁺ + 2ØH ⁻ = Be (ØH) ₂

(3) The dissociation-recombination reactions specifying third-body terms must precede other types of reactions, and must be followed by the directive:

Column 1

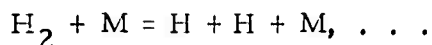
END TBR REAX

All reactions prior to the above directive will have a third-body term added to each side of the reaction. For example:



END TBR REAX

is the same as



where M is a generalized third body. Specific third-body effects may be included by inputting specific third-body reaction rate ratios XMM (J, I).

(4) Radiative reactions may be considered using the special species PHØTØN. The PHØTØN may only appear on the left-hand side of the equal sign for a reaction.

(5) The reaction set is terminated by a card containing LAST CARD in columns 1 to 9.

g. \$PRØPEL

<u>Case Variables</u>	<u>Units</u>	
*Z	Initial normalized axial position	None
*PI	Initial pressure	PSIA
*T	Initial temperature	°R
*V	Initial velocity	ft/sec
RSTAR	Axial distance normalizing factor (normally throat radius for nozzle calculations)	Inches

*EXIT Normalized axial distance for run termination None
 NØCHEM = 1 if a frozen chemistry case is desired None

Plot Variables (plotting not available in automatic mode of operation)

IFP = 1 Plotting requested
 ITP = 1 Plot temperature
 IRØP = 1 Plot density
 ICHEMP (1) = Species numbers for desired species concentration plots, up to 30 species
 IXP = 1 Plot functions vs normalized distance
 MLP = 1 Plot species MØLE fractions
 MSP = 1 Plot species MASS fractions

Print Variables

ND1 Print every ND3rd step beginning with the ND1st step
 ND2 until the ND2nd step. (The initial conditions and the
 ND3 EXIT point are always printed.)

Integration Variables

HI Initial normalized step size
 HMIN Minimum normalized step size
 HMAX Maximum normalized step size
 DEL Relative error criterion
 JF = 0 all variables considered for step size control
 = 1 only fluid dynamic variables considered for step size control.

The variable which controls the step size; i. e., has the maximum relative error; is printed in the normal output under Integration Parameters, labeled Governing Equation. The number: variable correspondence is as follows: 1=T; 2=RO; 3=V, 4=Species 1; 5=Species 2; . . . NSP + 3 = Species NSP.

Table Input Variables

*NTB Number of input table entries for pressure table (101).
 JPFLAG Determines the type of differentiation used to obtain derivatives for all input tables. Reference should be made to Mass, Momentum, Energy and Species Addition Functions for other input tables controlled by JPFLAG.

*Values are read from TAPE 8 and need not be input when operated in automatic mode (KMØDE = 0) or in a manual mode (KMØDE = 1) and using streamtube data from TAPE 8 (NSL ≠ 0). If input, they will override TAPE 8 values for first streamtube only.

= 1 derivatives of input table obtained by simple difference formulae with second derivatives defined as 0. Normally used in automatic mode.

= 2 derivatives of input tables obtained by SPLINE fit ($NTB \leq 20$).

= 3 derivatives input along with tables.

= 4 derivatives of input tables obtained by parabolic differentiation ($NTB \leq 20$).

*PSCALE = Multiplicative constant for the input pressure table.

*ZTB (1) = Normalized axial positions for input tabular values for pressure table (always input).

*PTB (1) = Pressure table (PSIA) (always input).

*DPTB (1) = Pressure table derivative (for JPFLAG = 3 option).

Miscellaneous Variables

XMM (J,I) Reaction rate ratio effect on reaction J of species I.

TU (1) Temperature above which approximate extension of JANAF tables will occur for each species (nominal = 9,000°R).

IFLAST For overlay reasons must be set = 1 on the last case of a run.

TSTOP Time at which a run will arbitrarily be terminated (CP time). Ignore in automatic mode.

Intermediate Output

IDQDN = 1 Print total derivatives.

IDXJDN = 1 Print individual reaction net production rates.

IEQOUT = 1 Print equilibrium constant and its temperature dependence in internal units.

IRATE = 1 Print reaction forward and reverse rates in internal units.

*Values are read from TAPE 8 and need not be input when operated in automatic mode ($KM\emptyset DE = 0$) or in a manual mode ($KM\emptyset DE = 1$) and using streamtube data from TAPE 8 ($NSL / 0$). If input, they will override TAPE 8 values for first streamtube only.

IMASDX = 1 For an IADDF = 1 option print chemical and addition function components of total derivatives.

IØPXF = 1 Print influence coefficient vectors.

IØPVAR (1) = Set consecutive entries equal to K for variables for which influence coefficient vectors are to be output, where

<u>K</u>	<u>Variable</u>
1	V
2	RØ
3	T
4	Species number 1
.	.
.	.
.	.
NSP+3	Species number NSP

For example: IØPVAR(1) = 4, 3, will output influence coefficient vectors for species number 1 and for temperature.

Mass, Momentum, Energy, and Species Addition Functions

Variable

IADDF = 1 Addition functions will be input.

IXTB = Number of entries in addition function tables ≤ 40 .

IADDØP = 0 Addition functions input via tables.

= 1 Addition functions defined via multiplicative factors. See EFACT (I), XMFACT (I), SPFACT (I, J) below. Note that IXTB factors must be input.

= 2 A subroutine for addition calculation will be supplied by the user.

XADSCL = Multiplicative scale factor for all addition functions. Note that input of XADSCL as $1.0/(\rho \cdot V \cdot A)$ will provide automatic normalization (per unit initial streamtube mass flux) for input addition functions.

ADDX (I) = Table of normalized axial stations for all input addition functions.

- ADDMAS (I) = Mass addition rate, per unit normalized length, per unit initial streamtube mass flux (unitless).
- ADDE (I) = Energy addition rate, per unit normalized length, per unit initial streamtube mass flux (BTU/lb).
- ADDEX (I) = Auxiliary energy addition rate, per unit normalized length, per unit initial streamtube mass flux (BTU/lb) which will be added to the energy addition rate ADDE (I). Note that ADDEX (I) is independent of EFACT (I) for IADDOP = 1 option and will be added to ADDE (I) before modification by XADSCL.
- ADDMOM (I) = Momentum flux, per unit normalized length, per unit initial streamtube mass flux (ft/sec).
- NPINT (I) = Species number (for current case) to relate species addition functions to specific species. See example under ADDSP (I, J).
- NSPADD = Number of entries in NPINT (I) table.
- ADDSP (I, J) = Species mass addition rate per unit normalized length, per unit initial streamtube mass flux (unitless).
- I=1, . . . IXTB corresponding to number of entries
- J=1, . . . NSPADD
- e. g. , NSPADD = 2
 NPINT = 3, 5
 ADDSP (I, 1) corresponds to Species 3
 ADDSP (I, 2) corresponds to Species 5
- EFACT (I) = For IADDOP = 1, ADDE (I) computed as ADDMAS(O) *EFACT(I).
- XMFACT (I) = For IADDOP = 1, ADDMOM (I) computed as ADDMAS (I) *XMFACT (I).
- SPFACT (I, J) = For IADDOP = 1, ADDSP (I, J) computed as ADDMAS (I) *SPFACT (I, J).
- IHTOTF - 1 Restart flag indicating that a case is being restarted and directing the initial enthalpy to be HTOTX.
- HTOTX - Initial enthalpy if a case has been restarted (ft²/sec²).

- DMASDX (I) = For JPFLAG = 3 option, derivative of the mass addition rate $d(\text{ADDMAS})/d\bar{x}$.
- DEDXT (I) = For JPFLAG = 3 option, derivative of the total energy addition rate $d(\text{ADDE}+\text{ADDEX})/d\bar{x}$.
- DMØMDX (I) = For JPFLAG = 3 option, derivative of the momentum addition rate $d(\text{ADDMØM})/d\bar{x}$.
- DSPDX (I, J) = For JPFLAG = 3 option, derivative of the species addition rate $d(\text{ADDSP})/d\bar{x}$.

Generalized Oblique Shock Calculation

A generalized oblique shock calculation is specified by input of a pressure table containing a pressure discontinuity, and a pointer designating the shock location.

		UNITS
NSHØCK	= Pointer designating the last entry in the pressure table prior to the shock. For example:	None
	$\frac{P_2}{P_1} = \frac{\text{PTB}(\text{NSHØCK}+1)}{\text{PTB}(\text{NSHØCK})}$	
	Entries NSHØCK and NSHØCK+1 in the pressure table must have the same axial position.	
SHKBUG	= 1.0 provides intermediate output. 0.0 provides no intermediate output.	None
SMAXIT	= Maximum number of iterations during a generalized oblique shock calculation.	None
SKEPS(1)	= Relative convergence criterion for temperature iteration during a generalized oblique shock calculation.	None
SKEPS(2)	= Relative convergence criterion for overall iteration during a generalized oblique shock calculation.	None

Normal Shock Stagnation Streamline Calculation

The normal shock stagnation streamline calculation option performs a normal shock calculation from specified upstream and downstream velocities and continues the calculation as a velocity defined streamtube.

		<u>UNITS</u>
NSTAGV	= 1 specifies a normal shock stagnation streamline calculation.	None
VEL1	= Upstream velocity for the normal shock calculation.	ft/sec
VTB(1)	= Array defining the velocity as a function of normalized axial distance. VTB(1) is defined as the downstream velocity for the normal shock calculation.	ft/sec
NVTB	= Number of entries in the velocity profile NVTB \leq 101.	None

Reaction Screening Input Variables

If a reaction screening calculation is requested, the program performs a two-pass calculation. The first pass utilizes the complete reaction set and determines those reactions which must be retained to satisfy the input criteria for each species screened. The second pass redoes the first calculation with an edited reaction set and provides a summary page comparing both calculations.

		<u>UNITS</u>
ISCRF	= 1, specifies a reaction screening case for ISCSP (I) species.	None
ISCSP(1)	= Species number for those species to be screened \leq 40.	None
EPSCR(1)	= Relative retention criterion for each species to be screened. Defined as the maximum change in mass fraction relative to production or destruction of the species per unit normalized length for all reactions involving the corresponding species \leq 40.	None
ISCBUG	= 1, provides intermediate output during the reaction screening procedure.	None

Area Defined Option Input

Area Defined Calculation With Mass, Energy or Momentum Addition:

ITAREA	=	Input maximum number of iterations for area ratio calculation. A nonzero value for ITAREA triggers the area ratio iteration logic. After maximum iterations, the program outputs an error message, accepts the most recent values, and continues.
ABAR(1)	=	Area ratio table (A/A_0).
XARTAB(1)	=	Normalized axial coordinates for the input area ratio table.
DABARX(1)	=	Derivative with respect to normalized axial distance of the input area ratio table (if input derivative option used).
NPATAB	=	Number of entries in area ratio table ≤ 40 .
ICALDA	=	0 derivative of area ratio table controlled by JPFLAG.
	=	1, 2, 3, 4 replaces JPFLAG control for area ratio table ONLY.
AREPS	=	Relative convergence criterion for area ratio iteration.

Single Species Condensation Option

Condensation calculations require the use of both the mass, momentum, and energy addition option and the area-defined streamtube option. The pertinent parameters for these options are included below:

*IADDF	=	1	Addition function option will be utilized.
*IADDØP	=	3	Single species condensation routines will provide addition functions.
*ITAREA	=		Maximum number of iterations for area ratio calculation.
*XARTAB(1)	=		Normalized axial coordinate for input area ratio table.
*ABAR(1)	=		Area ratio table (A/A_0).

*Values for these variables are calculated internally when operated in automatic mode ($KMØDE = 0$) and need not be input.

- *NPATAB = Number of entries in area ratio table ≤ 40 .
- *DABARX (1) = Derivative with respect to normalized axial distance of input area ratio table (if input derivative option used).
- AREPS = Relative convergence criterion for area ratio iteration.
- *NØCHEM = 1 Frozen chemistry option is utilized.
- ICØND = Number signifying the location of condensing species with respect to the species input order.

The following inputs describe the vapor/liquid properties. A preliminary set of constants for water is stored internally and will be used if the following inputs are ignored. If improved values for water are available or if a different condensing species is being considered, some or all of the following may be input:

- TLIM = Limiting temperature for saturated vapor test. State of condensible vapor will not be tested above TLIM (units = $^{\circ}\text{R}$).
- EJMIN = Threshold value for nucleation rate below which condensation effects will not be computed (units = $1/\text{ft}^3\text{-sec}$).
- ETA = Condensation (or sticking) coefficient for water vapor/liquid.
- PCØNST (I) = Array of constants utilized in describing vapor state (see subroutine VAPØR).
- PCØNST (1) = C_1 (atm)
- PCØNST (2) = C_2 (atm - $^{\circ}\text{R}$)
- PCØNST (3) = C_3 (atm - $(^{\circ}\text{R})^2$)
- PCØNST (4) = C_4 ($1/^{\circ}\text{R}$)
- PCØNST (5) = C_5 ($1/^{\circ}\text{R}$)
- PCØNST (6) = C_6 ($1/^{\circ}\text{R}$)
- PCØNST (7) = C_7 ($^{\circ}\text{R}$)
- PCØNST (8) = C_8 (-)

*Values for these variables are calculated internally when operated in automatic mode (KMØDE = 0) and need not be input.

- PCØNST (9) = Triple point pressure
(poundal/ft²)
- PCØNST (10) = Triple point temperature
(°R)
- DCØNST (I) = Array of constants utilized in describing
liquid droplet properties (see Subroutine
DRØPS)
- DCØNST (1) = A₁ (BTU/lb)
- DCØNST (2) = A₂ (BTU/lb)-°R)
- DCØNST (3) = A₃ (BTU/lb)-°R²)
- DCØNST (4) = A₄ (lb/ft³)
- DCØNST (5) = A₅ (lb/ft³) - °R)
- DCØNST (6) = A₆ (lb/ft³ - °R²)
- DCØNST (7) = A₇ (BTU/lb)
- DCØNST (8) = A₈ (BTU/lb - °R)
- DCØNST (9) = A₉ (lb/ft³)
- DCØNST (10) = A₁₀ (lb/ft³ - °R)
- DCØNST (11) = A₁₁ (Poundal/ft)
- DCØNST (12) = A₁₂ (Poundal/ft - °R)
- DCØNST (13) = Condensed phase heat
capacity (BTU/lb - °R)

C. 7 SAMPLE CASES

A sample case illustrating the abilities of the KINCON program as a subprogram to CONTAM has been presented in the program description of CONTAM, Section 7. 0. In this mode, the KINCON program analyzes the nonequilibrium chemical kinetics and condensation of plume species for prediction of contamination effects on bodies submerged in bipropellant plumes. Several additional KINCON program options are available when run in the manual mode as an independent program. Sample cases are included in this appendix to illustrate these options.

a. Reaction-Rate Screening Case

Computer input card listing and selected output for the rate screening of pure-air chemistry system are presented in Tables C-III through C-V. The original system consists of a set of 14 species and 37 reactions as presented in the card-image listing in Table C-III. The complete reaction set is utilized on the first calculation pass. Those reactions which must be retained to satisfy the input criteria for each species screened are determined. A second pass recomputes the case using the edited reaction set and provides a summary page comparing both results.

Output for a rate-screening case differs from a standard kinetics run only by the addition of intermediate reaction-rate printout for each screened species at each output station and a summary page comparing the results of the original and edited reaction sets. Table C-IV contains the reaction rate output for screened species E-(electron) at axial position 20. 0. A similar page is output for each remaining screened species. The summary page is included in Table C-V.

b. Oblique Shock Case

Card image listing for an oblique shock calculation in air is included in Table C-VI. A discontinuity in the input pressure table identifies the shock location as shown in pressure table output, Table C-VII. Results of the shock calculation are presented in Table C-VIII. The output for the integration to and from the shock is the same as the standard kinetics output and has been omitted.

c. Normal Shock-Stagnation Streamline Case

Card-image listing for a normal shock stagnation streamline calculation in air is included in Table C-IX. The streamline downstream of the normal shock is defined through an input velocity distribution table. Velocity table is output as shown in Table C-X. The normal shock calculation output is included in Table C-XI. The remaining output for this case is of the same format as the standard kinetics run and has been omitted.

d. Automated Kinetics and Condensation Case

The following sample case was completed to illustrate the operation of the KINCON subprogram in the automatic mode including both kinetics and water vapor condensation passes in a single case. The test case corresponds to a streamline bounding 90% of the total mass flow for a typical MMH/NTO

Table C-III. CARD LISTING FOR RATE-SCREENING CASE

THERMO		PROGRAM SCREEN	
PURE AIR SCREENING SPECIES			
N2	1,769000E		
O2	6,227936E		
NO	4,939180E-3		
	1,418422E-5		
O	1,889173E-7		
NO+	3,921985E-7		
O2-	2,560473E-11		
O-	1,964042E-7		
E-	7,978542E-12		
NO2	2,622374E-7		
N2O	7,536638E-9		
NO2-	1,100075E-10		
O3	4,975525E-6		
NO3	9,995519E-11		
REACTIONS			
O2 = O + O	A = 1.1E+15, B = 1.2, C = 0.0		
N2 = N + N	A = 1.5E+17, B = 0.02, C = 0.0		
NO = N + O	A = 4.0E+15, B = 0.0, C = 0.0		
NO2 = NO + O	A = 1.0E+15, B = 0.0, C = -1.79		
NO = NO+ + E-	A = 8.67E+26, B = 2.5, C = 0.0		
O3 = O + O2	A = 1.82E+19, B = 2.0, C = 0.0	I = ALL	12,49
O2- = O2 + E-	A = 3.9E+16, B = 0.0, C = 0.0		14,24
O- = O + E-	A = 3.0E+16, B = 0.0, C = 0.0		15,23
NO2- = NO2 + E-	A = 1.45E+19, B = 0.0, C = 0.0	I = NO2 (NO2 XRM)	16,77
NO2- = NO + O-	A = 3.2E+15, B = 0.0, C = 0.0		17,151
END TBR REAX			
NO + O = NO2	A = 1.3E+14, B = -1.5, C = 5.94		1 4
N2 + O = NO + N	A = 1.3E+14, B = 0.0, C = 0.0		12 5
N2 + O2 = NO + NO	A = 5.0E+10, B = 0.0, C = 79.5		20 6
NO + NO = N2O + O	A = 1.2E+14, B = 0.0, C = 27.7		21 51
NO + NO = N + NO2	A = 3.0E+12, B = 0.0, C = 0.0		22 52
NO + O2 = O + NO2	A = 1.8E+13, B = 0.0, C = 1.15		23 56
O2 + O2 = O + O3	A = 2.15E+13, B = 0.0, C = 5.44		24 54
NO + O2 = N + O3	A = 3.0E+11, B = 0.0, C = 0.0		25 55
NO2 + O2 = NO + O3	A = 4.0E+11, B = 0.0, C = 2.07		26 57
NO3 + O2 = NO2 + O3	A = 4.2E+10, B = 0.0, C = 0.0		27 139
N2 + O2 = N2O + O	A = 3.0E+17, B = 0.0, C = 24.0		28 50
N2O + O = N + NO2	A = 4.2E+10, B = 0.0, C = 0.0		29 53
N2 + NO = N2O + N	A = 1.2E+8, B = 0.0, C = 0.0		30 141
O2 + E- = O- + O	A = 4.4E+13, B = 0.0, C = 0.0		31 78
O3 + E- = O- + O2	A = 4.0E+8, B = -0.83, C = 9.34		32 79
O3 + E- = O2- + O	A = 1.0E+14, B = 0.0, C = 0.0		33 80
N2O + E- = O- + N2	A = 6.0E+8, B = 0.0, C = 0.0		34 81
NO2 + E- = O- + NO	A = 1.0E+14, B = 0.0, C = 0.0		35 159
NO + E- = O- + N	A = 9.4E+14, B = 0.0, C = 0.0		36 160

NOT REPRODUCIBLE

Table C-III-Concluded

$NO2 + E = NO + O$, $A = 9.6E+13$, $N = 0.0$, $B = 0.0$	37	162
$O2 + O = O2 + O$, $A = 4.3E+13$, $N = 0.0$, $B = 0.0$	38	162
$O2 + NO2 = O2 + NO2$, $A = 4.8E+14$, $N = 0.0$, $B = 0.0$	39	131
$NO2 + O = NO2 + O$, $A = 7.2E+14$, $N = 0.0$, $B = 0.0$	40	154
$N + O = NO + O$, $A = 1.44E+21$, $N = 1.5$, $B = 0.0$	41	7
$NO + O2 = NO + O2$, $A = 3.0E+19$, $N = 1.0$, $B = 0.0$	42	12P
$NO + O = NO + O$, $A = 3.5E+19$, $N = 1.0$, $B = 0.0$	43	129
$NO + NO2 = NO + NO2$, $A = 3.6E+19$, $N = 1.0$, $B = 0.0$	44	142
LAST CARD		
PSPROPEL		
$NT=5$, $PT(1)=5*1.0$, $ZTR(1)=0.0, 10.0, 20.0, 30.0, 1.0E4$, $Z=0.0$, $PI=1.0$,		
$PI = 1.0$, $PSCALE=0.0208$, $NO3=1$, $EVITE=0.42$, $I=47L0.0$, $V=3800.0$, $RSTAR=12.0$,		
$H1=0.1$, $HMI7=0.1$, $HMAX=9.0$, $DBL=0.005$, $JF=1$,		
$ISCRF=1$, $ISCRF(1)=9.0, 7.6, 12.17, 14$, $CPSCF(1)=4*1.0E-2, 3*1.0E-2$,		
$NC3=2$, $IFPEL$,		
$ICQXX=1$,		
\$END		

NOT REPRODUCIBLE

Table C-IV. SAMPLE REACTION-SCREENING OUTPUT

REACTIONS INVOLVING SPECIES E		AT AXIAL POSITION	2.00000E-01
PRODUCTION		DESTRUCTION	
D(C(I))/DX	REACTION	D(C(I))/DX	REACTION
8.69563475E-21	25	7.53288250E-20	5
3.18730759E-20	9	4.95092844E-14	34
2.19782268E-18	28	6.41667151E-14	24
1.91513964E-17	29		
5.43746279E-17	27		
1.55960595E-15	26		
1.00316791E-14	8		
2.20229032E-14	30		
2.32151600E-14	7		
NET PRODUCTION		5.69051127E-14	
NET DESTRUCTION		1.13676075E-13	

Table C-V. FINAL SUMMARY OUTPUT AFTER SCREENING - RESULTS OF ORIGINAL AND SCREENED RUNS

VARIABLE	ORIG FINAL COND	SCREENED FINAL COND
VEL	3,80000000E+03	3,80000000E+03
DENS	1,17993504E-05	1,17993504E-05
TEMP	4,70000501E+03	4,70000501E+03
N2	7,60000253E-01	7,60000253E-01
O2	2,25934373E-01	2,25934373E-01
NO	4,04039502E-03	4,04039501E-03
N	5,62376673E-07	5,62376794E-07
O	1,00229198E-02	1,00229198E-02
NO+	3,90949443E-07	3,90950464E-07
O2-	2,80312862E-10	2,80494462E-10
O-	2,03467463E-09	2,03513961E-09
E-	7,05313769E-12	7,05313731E-12
NO2	1,08509134E-06	1,08509778E-06
N2O	1,08161532E-08	1,08141731E-08
NO2-	1,02571348E-10	1,02570492E-10
O3	5,70692828E-09	5,70186569E-09
NO3	9,98670043E-11	9,99081900E-11

THE FOLLOWING REACTIONS WERE OMITTED ON THE SCREENED CALCULATION

REACTION	5
REACTION	9
REACTION	10
REACTION	18
REACTION	19
REACTION	20
REACTION	25
REACTION	27
REACTION	28
REACTION	29
REACTION	35

NOT REPRODUCIBLE

Table C-VI. CARD LISTING FOR OBLIQUE SHOCK CALCULATION IN AIR

```

THERMO
NLCHEN=0, L1S1=1,
SEND
BLUNT BODY INVISCID FIELD STREAMTUBE NO. 2U
SPECIES MASS FRACTIONS
N2 .781184
O2 .209476
NO .0
N .0
C .0
NO+ .0
F= .0
ARGON .00934

REACTIONS
N2 = 2*N, A=1.0E18, N=1.0, B=0.0, REACTION 1
O2 = 2*O, A=1.9E16, N=0.5, B=0.0, REACTION 2
NO = N + O, A=6.0E16, N=0.5, B=0.0, REACTION 3

END TBR REAX
NC + O = C2 + N, A=1.8E 8, N=1.5, B=6.001, REACTION 6
N2 + O = NO + N, A=1.5E13, N=0.0, B=0.0, REACTION 7
N2 + O2 = 2*NO, A=1.0E13, N=0.0, B=79.488, REACTION 8
N + O = NO + E, A=2.8E20, N=1.2, B=0.0, REACTION 9

LAST CARD
SROPEL
Z=0.0, PI=9.2004, T=431.41, V=22500., RSTAR=5, EXIT=056928, PSCALE=00694444,
H1=1.E=4, HMIN=1.E=4, HMAX=1.0, DEL=0.1, ND3=10, JPELAGE=1,
NSMCK=3,
TCOND(1)=4000.,
NTB=10,
ZTB(1)=1., P=5,
ZTB(3)=0.0, O=0.0, I=491961.6, 548852.11, 607338.21, 724302.31, 837449.52, 060573,
PTB(1)=9.2004, 9.2004,
PTB(3)=9.2004, 180.96, 147.18, 107.68, 100.42, 117.28, 144.31, 158.45,
EXIT= 49, 7663,
$END

```

NOT REPRODUCIBLE

Table C-VII. PRESSURE TABLE

***** SHOCK OCCURS AT TABLE ENTRY 3 *****			
I	X	P	DP/DX
1	-1.00000000E+00	9.20040000E+00	0.
2	-5.00000000E-01	9.20040000E+00	0.
3	0.	9.20040000E+00	0.
4	0.	1.80960000E+02	=2.26413425E+01
5	1.49196100E+00	1.47180000E+02	=1.11897475E+01
6	6.54885200E+00	1.07680000E+02	=4.62266508E+00
7	1.16073380E+01	1.00420000E+02	6.32600681E-01
8	2.17243020E+01	1.17280000E+02	2.16953827E+00
9	3.18374490E+01	1.44310000E+02	1.35712132E+00
10	5.20605730E+01	1.58450000E+02	6.99199590E-01

Table C-VIII. SHOCK CALCULATION

 BEGIN SHOCK CALCULATION, AXIAL POSITION = 0.0000

CALCULATED SHOCK CONDITIONS

SHOCK ANGLE (DEG) 1.07112538E+01
 DEFLECT ANG (DEG) 8.47695096E+00
 P2/P1 1.96687101E+01

PROPERTY	UPSTREAM	DOWNSTREAM
PRESSURE (PSIA)	6.38916258E+02	1.25666586E+00
TEMPERATURE (DEG-R)	4.31411921E+02	1.75017828E+03
DENSITY (LBM/FT3)	3.98120375E+04	1.93016028E-03
MACH NUMBER	2.20478049E+01	1.10106903E+01
FROZEN GAMMA	1.40065148E+00	1.33856013E+00

Table C-IX. CARD LISTING FOR NORMAL SHOCK STAGNATION
STREAMLINE CALCULATION IN AIR

```

3THERNO
NLCHEM=9, LIST=1,
SENC
STAGNATION STREAMLINE PASS NO, 1
SPECIES MASS FRACTIONS
N2 .781184
O2 .209476
NO .0
H .0
O .0
CO+ .0
F .0
ARGON .00934

REACTIONS
N2 = 2*O, A=1.0E18, N=1.0, B=0.0, REACTION 1
O2 = 2*O, A=1.0E16, N=0.5, B=0.0, REACTION 2
NO = N + O, A=5.0E16, N=0.5, B=0.0, REACTION 3
END THR REAX

NO + O = O2 + N, A=1.8E 8, N=1.5, B=6.001, REACTION 6
N2 + O = NO + N, A=1.5E13, N=0.0, B=0.0, REACTION 7
N2 + O2 = 2*NO, A=1.0E13, N=0.0, B=79.488, REACTION 8
N + O = NO + E, A=2.3E20, N=1.2, B=0.0, REACTION 9
LAST CARD
$PROPEL
Z=0., PI=0.063892, T=433.6, V=1701.6, RSTAR=0.75, EXITE=0.0514,
PTR(1)=0.063892,
HI=1.E=4, HMIN=1.E=4, HMAX=1.0, DEL=0.1, NDS=10. JPFLAG=1,
NSTAGV=1, VELI=22400.,
NVT=21,
ZTR(1)=0., U0257., O0514., O0771., O1028., O1285., O1542., O1799., O2056., O2313,
ZTR(11)=.02570., O2827., O3084., O3341., O3596., O3855., O4112., O4369., O4626., O4883,
ZTR(21)=.05140,
VTR(1)= 1701.6, 1615.3, 1529.1, 1442.9, 1356.7, 1270.7, 1184.8, 1098.9, 1013.1,
VTR(10)=927.5, 841.9, 756.5, 671.3, 586.2, 501.3, 416.7, 332.1, 248.1, 164.4, 84.1, 95., 1,
ND3=5,
SENC

```

Table C-X. INPUT VELOCITY DISTRIBUTION TABLE

V E L O C I T Y T A B L E			
1	0,	1,70160000E+03	-3,35797665E+04
2	2,57000000E-03	1,61530000E+03	-3,35603113E+04
3	5,14000000E-03	1,52910000E+03	-3,35603113E+04
4	7,71000000E-03	1,44280000E+03	-3,35408560E+04
5	1,02600000E-02	1,35670000E+03	-3,34924903E+04
6	1,26500000E-02	1,27070000E+03	-3,34435798E+04
7	1,54200000E-02	1,18480000E+03	-3,34241245E+04
8	1,79900000E-02	1,09890000E+03	-3,34046693E+04
9	2,05600000E-02	1,01310000E+03	-3,33463035E+04
10	2,31300000E-02	9,27500000E+02	-3,33073930E+04
11	2,57000000E-02	8,41900000E+02	-3,32464825E+04
12	2,82700000E-02	7,56500000E+02	-3,31906615E+04
13	3,08400000E-02	6,71300000E+02	-3,31422957E+04
14	3,34100000E-02	5,86200000E+02	-3,30739300E+04
15	3,59800000E-02	5,01300000E+02	-3,29766537E+04
16	3,85500000E-02	4,16700000E+02	-3,29182879E+04
17	4,11200000E-02	3,32100000E+02	-3,28415564E+04
18	4,36900000E-02	2,48100000E+02	-3,26264591E+04
19	4,62600000E-02	1,64400000E+02	-3,18681323E+04
20	4,88300000E-02	8,41950000E+01	-3,19844358E+04
21	5,14000000E-02	0,	-3,27607004E+04

NOT REPRODUCIBLE

Table C-XI. SAMPLE OUTPUT FOR NORMAL SHOCK CALCULATION

NORMAL SHOCK STAGNATION STREAMLINE CALCULATION REQUESTED

CALCULATED SHOCK CONDITIONS

PROPERTY	UPSTREAM	DOWNSTREAM
PRESSURE (PSIA)	6,38920000E+02	3,97035865E+01
TEMPERATURE (DEG-R)	4,33600000E+02	3,21130576E+04
DENSITY (LBF/FT3)	3,96107490E-04	3,32356308E-03

NOT REPRODUCIBLE

engine. The initial streamtube temperature was purposely reduced from the original combustion chamber value to ensure condensation within the region of interest.

A card-image listing of the case is shown in Table C-XII. The streamline conditions (initial pressure, temperature, and velocity) including the pressure distribution were obtained from the output of the MULTRAN subprogram and are presented in Table C-XIII. Printout of the input data and the pressure distribution table were omitted since that information is available in Tables C-XII and C-XIII. The initial streamline conditions for the kinetics pass are presented in Table C-XIV.

The water vapor saturation point is reached at station 24.988 as shown in the station output, Table C-XV. Conditions at the saturation point are saved as initial conditions for subsequent condensation calculation pass. An area ratio table is constructed as the integration continues downstream as can be seen by the area ratio printout. Table C-XVI shows the termination of the kinetics pass when the static temperature dropped below 180 °R. The condensation calculation pass begins at the saturation point and follows the area ratio table computed during the kinetics pass. Table C-XVII presents this area ratio table plus the first derivative as output at the beginning of the condensation pass. Initial conditions for the condensation pass are included in Table C-XVIII; intermediate printout of pertinent water vapor properties and nucleation rate are also shown. Variables include

- PV = vapor pressure (atm)
- PVS = saturated vapor pressure (atm)
- PRATIO = PV/PVS
- RS = critical droplet radius (cm)
- EJ = nucleation rate (1/cm³ sec)
- TS = saturated vapor temperature (°R)

As the flow continues to expand to higher degrees of supersaturation, the nucleation rate increases triggering droplet growth (condensation). Tables C-XIX and C-XX present the output at typical locations in the condensing region. These tables illustrate the additional printout in the condensing region (where nucleation rate is greater than threshold value). The FORTRAN symbols correspond to the symbols used in the analysis in the following manner for primary variables of interest;

- RPRIME = r'
- XMBAR = \bar{m}
- HINT = $\int_0^x \dot{H} dx$
- G = g

Table C-XII. KINCON SAMPLE CASE-DATA LISTING

```

STHERMO 5
AUTOMATED KINCON TEST CASE
SPECIES MASS FRACTIONS
CO2      ,0652
H2O      ,2738
-----
CO       ,2017
H2       ,020
N2       ,42509761
-----
NO       ,002
OH       ,00967
O2       ,000764
-----
C        1,69E-11
H        ,00115
N        1,39E-6
O        ,000817

REACTIONS
O2 = 2*O,      A=3,3E17,      N=1,0,      B=0,0,      REACTION 1
N2 = 2*N,      A=9,6E17,      N=1,0,      B=0,0,      REACTION 2
NO = N + O,    A=7,2E15,      N=0,5,      B=0,0,      REACTION 3
H2 = 2*H,      A=5,0E18,      N=1,0,      B=0,0,      REACTION 4
H2O = H + OH,  A=1,17E17,     N=0,0,      B=0,0,      REACTION 5
OH = H + O,    A=2,3E16,      N=0,0,      B=0,0,      REACTION 6
CO2 = CO + O,  A=5,1E15,      N=0,0,      B=3,5A,     REACTION 7
CO = C + O,    A=6,0E8,       N=0,0,      B=5A,,      REACTION 8
END TBR REAX
NO + O = O2 + N, A=3,0E11,      N=-0,5,     B=7,13,     REACTION 9
NO + N = N2 + O, A=9,0E13,      N=0,0,      B=75,5,     REACTION 10
N2 + O2 = 2*NO, A=1,0E13,      N=0,0,      B=79,48A,   REACTION 11
CO + O2 = CO2 + O, A=1,9E13,      N=0,0,      B=54,15,    REACTION 12
CC + N = C + NO, A=1,3E10,      N=-0,1,     B=0,5,      REACTION 13
CC + O = C + O2, A=2,4E13,      N=0,0,      B=1,99,     REACTION 14
CC + H = C + OH, A=1,2E14,      N=0,0,      B=25,83,    REACTION 15
CO2 + H = CO + OH, A=5,6E11,      N=0,0,      B=1,08,     REACTION 16
OH + O = H + O2, A=2,24E14,     N=0,0,      B=16,A,     REACTION 17
OH + H2 = H2O + H, A=8,41E13,     N=0,0,      B=20,1,     REACTION 18
2*OH = H2O + O,  A=5,75E13,     N=0,0,      B=18,A,     REACTION 19
H2 + O = OH + H, A=7,33E12,     N=0,0,      B=0,0,      REACTION 20
H2 + O2 = 2*OH,  A=4,98E23,     N=2,5,      B=85,7,     REACTION 21
NO + CO = CO2 + N, A=1,0E13,      N=0,0,      B=9,93,     REACTION 22
NO + H = OH + N,  A=3,4E13,      N=0,0,      B=1,38,     REACTION 23
CC + CO = CO2 + C, A=1,0E13,      N=0,0,      B=9,93,     REACTION 24

LAST CARD
SROPEL
RSTAR=0,0972,JPFLAG=1,DEL=.01,  MD3=10,HI=.0001,  HMIN=.0001,  HMAX=1.0,
TCOND(1)=12*0.,T=2500.,
AREPS=.001,ETA=0.1,TCOND(1)=12*0.,IDCOND=2,
SEND

```

NOT REPRODUCIBLE

Table C-XIII. STREAMLINE GENERATION PROGRAM

CP TIME = 33,799 PP TIME = 192,713

STREAMLINE(1) = 90,0000 PERCENT OF THE TOTAL MASS FLOW
 ZINIT = 0,00000 (NONDIMENSIONAL * S/RC)
 PINIT = 67,524369 (PSIA)
 TINIT = 5453,270529 (DEG, R)
 VINIT = 2587,734814 (FT/SEC)
 ZFINAL = 44,569804 (NONDIMENSIONAL * Z/RC)
 NGKSK = 78 (NO. OF PRESSURE TABLE POINTS)

POINT NO.	AXIAL DISTANCE (Z/RC)	RADIAL DISTANCE (R/RC)	STREAMLINE DISTANCE (S/RC)	PRESSURE (PSIA)
1	6,237351E-01	1,010896E+00	0,	6,752437E+01
2	5,613616E-01	9,992094E+01	6,345886E+02	6,550104E+01
3	4,989881E-01	9,884265E+01	1,267576E+01	6,466242E+01
4	4,366146E-01	9,792893E+01	1,897968E+01	6,246165E+01
5	3,742411E-01	9,713276E+01	2,526764E+01	6,019785E+01
6	3,118675E-01	9,645190E+01	3,154204E+01	5,839127E+01
7	2,494940E-01	9,589293E+01	3,780439E+01	5,614706E+01
8	1,871205E-01	9,545219E+01	4,405729E+01	5,386846E+01
9	1,247470E-01	9,512955E+01	5,030298E+01	5,155861E+01
10	6,237351E-02	9,492547E+01	5,654367E+01	4,951774E+01
11	3,552714E-15	9,484006E+01	6,278160E+01	4,715078E+01
12	6,237351E-02	9,487171E+01	6,901903E+01	4,478359E+01
13	1,247470E-01	9,502609E+01	7,525830E+01	4,274839E+01
14	1,871205E-01	9,529274E+01	8,150134E+01	4,038052E+01
15	2,494940E-01	9,567607E+01	8,775046E+01	3,804044E+01
16	3,118675E-01	9,617624E+01	9,400784E+01	3,573715E+01
17	3,742411E-01	9,680336E+01	1,002766E+00	3,374438E+01
18	4,366146E-01	9,753766E+01	1,065571E+00	3,152130E+01
19	4,989881E-01	9,838889E+01	1,128522E+00	2,935697E+01
20	5,613616E-01	9,935746E+01	1,191643E+00	2,726202E+01
21	6,548790E-01	1,003425E+00	1,285678E+00	2,445532E+01
22	6,681853E-01	1,006635E+00	1,299366E+00	2,406621E+01
23	8,230535E-01	1,047388E+00	1,459507E+00	1,980347E+01
24	8,840405E-01	1,063762E+00	1,522653E+00	1,899437E+01
25	9,959586E-01	1,095271E+00	1,638922E+00	1,758742E+01
26	1,109730E+00	1,126632E+00	1,756937E+00	1,667694E+01
27	1,226214E+00	1,158689E+00	1,877752E+00	1,572658E+01
28	1,345742E+00	1,191324E+00	2,001655E+00	1,479170E+01
29	1,468845E+00	1,224672E+00	2,129195E+00	1,386588E+01
30	1,596016E+00	1,258866E+00	2,260882E+00	1,295506E+01
31	1,727683E+00	1,294023E+00	2,397162E+00	1,206744E+01
32	1,864462E+00	1,330303E+00	2,538672E+00	1,120840E+01
33	2,007078E+00	1,367891E+00	2,686158E+00	1,037966E+01

Table C-XIII-Concluded

34	2,156435E+00	1,407000E+00	2,840550E+00	9,581216E+00
35	2,313262E+00	1,447797E+00	3,002596E+00	8,816376E+00
36	2,478760E+00	1,490560E+00	3,173530E+00	8,084436E+00
37	2,655024E+00	1,535883E+00	3,35528E+00	7,368069E+00
38	2,845226E+00	1,584638E+00	3,551879E+00	6,652436E+00
39	3,048344E+00	1,636619E+00	3,761543E+00	5,971779E+00
40	3,269320E+00	1,693105E+00	3,989624E+00	5,314822E+00
41	3,508983E+00	1,754318E+00	4,236981E+00	4,702522E+00
42	3,773142E+00	1,821724E+00	4,509604E+00	4,121188E+00
43	4,065000E+00	1,896143E+00	4,810801E+00	3,581002E+00
44	4,392306E+00	1,979536E+00	5,148564E+00	3,075581E+00
45	4,761856E+00	2,073639E+00	5,529907E+00	2,610257E+00
46	5,185288E+00	2,181412E+00	5,966838E+00	2,183015E+00
47	5,675233E+00	2,306087E+00	6,472398E+00	1,797046E+00
48	6,251182E+00	2,452654E+00	7,066704E+00	1,451938E+00
49	6,625002E+00	2,547389E+00	7,452340E+00	1,272373E+00
50	7,074635E+00	2,660688E+00	7,916029E+00	1,086394E+00
51	7,815313E+00	2,849148E+00	8,680306E+00	8,667201E-01
52	8,571396E+00	3,041428E+00	9,460456E+00	7,013092E-01
53	9,265366E+00	3,218157E+00	1,017658E+01	5,882468E-01
54	9,975806E+00	3,399777E+00	1,090986E+01	4,941469E-01
55	1,068503E+01	3,581162E+00	1,164192E+01	4,249876E-01
56	1,067373E+01	3,574772E+00	1,165490E+01	4,264300E-01
57	1,076811E+01	3,604541E+00	1,175387E+01	5,163831E-01
58	1,113066E+01	3,702849E+00	1,212951E+01	4,638904E-01
59	1,125574E+01	3,738687E+00	1,225963E+01	4,641027E-01
60	1,142516E+01	3,787626E+00	1,243597E+01	4,589467E-01
61	1,156782E+01	3,829747E+00	1,258472E+01	4,641766E-01
62	1,180306E+01	3,899483E+00	1,283008E+01	4,481104E-01
63	1,207228E+01	3,977769E+00	1,311045E+01	4,802594E-01
64	1,242947E+01	4,074703E+00	1,348056E+01	5,042020E-01
65	1,285652E+01	4,183837E+00	1,392133E+01	4,871803E-01
66	1,314293E+01	4,257693E+00	1,421712E+01	4,860031E-01
67	1,357414E+01	4,370228E+00	1,466277E+01	4,534370E-01
68	1,411218E+01	4,512423E+00	1,521928E+01	4,268618E-01
69	1,478154E+01	4,686822E+00	1,591098E+01	3,989918E-01
70	1,663745E+01	5,120941E+00	1,781699E+01	2,243533E-01
71	1,816543E+01	5,496204E+00	1,939037E+01	1,536901E-01
72	1,906691E+01	5,647968E+00	2,030454E+01	1,482508E-01
73	2,135328E+01	6,248347E+00	2,266842E+01	1,130785E-01
74	2,379229E+01	6,939570E+00	2,520350E+01	4,096669E-02
75	2,684459E+01	8,144826E+00	2,848513E+01	1,523652E-02
76	2,942882E+01	9,186441E+00	3,127138E+01	9,973209E-03
77	3,145359E+01	9,973589E+00	3,344378E+01	7,958811E-03
78	4,158523E+01	1,454961E+01	4,456980E+01	2,352045E-03

Table C-XIV. INITIAL CONDITIONS KINETIC STREAMTUBE CALCULATION AXIAL POSITION = 0.
 INPUT NORMALIZING AXIAL SCALE FACTOR (FT) 8.10000E-03

FLOW PROPERTIES		KINETIC COUPLING TERMS	
MACH NUMBER	0.0000000000000000	COUPLING TERM A	0.0000000000000000
PRESSURE (PSIA)	0.0000000000000000	COUPLING TERM B	-0.0000000000000000
VELOCITY (FT/SEC)	0.0000000000000000	INTEGRATION PARAMETERS	
TEMPERATURE (DEG-R)	0.0000000000000000	CURRENT STEP SIZE	1.0000000000000000
DENSITY (LB/FT3)	0.0000000000000000	PERCENT ENTHALPY CHANGE	0.
ENTHALPY (BTU/LB)	0.0000000000000000	1.0 = SUMMATION C(I)	-1.0000000000000000
GAS MOLECULAR WEIGHT	0.0000000000000000	MAXIMUM RELATIVE ERROR	0.
HEAT CAPACITY (BTU/LB-DEG-R)	0.0000000000000000	GOVERNING EQUATION	0
PROPER GAMMA	0.0000000000000000		
GAS CONDUCTIVITY (BTU/SEC-FT-DEG-R)	0.0000000000000000		
SUM C(I)*H(I) (PTE/SEC)	-0.1000000000000000		

CHEMICAL COMPOSITION									
NO.	SPECIES	MASS FRACTION	MOLE FRACTION	MOLEC/CC	NO. SPECIES	MASS FRACTION	MOLE FRACTION	MOLEC/CC	
1	O2	0.920000E+02	0.915223E+02	7.0793E+17	2	H2O	2.730000E+01	2.990922E+01	7.2621E+18
3	CO	3.017000E+01	1.417122E+01	3.4400E+18	4	H2	2.000000E+02	1.052403E+01	4.7400E+18
5	N2	4.050976E+01	2.906157E+01	7.2506E+18	6	NO	2.000000E+03	1.311665E+03	3.1848E+16
7	OH	9.670000E+03	1.118931E+08	2.7168E+17	8	O2	7.640000E+04	4.698654E+04	1.1409E+16
9	C	1.400000E+11	2.740000E+11	6.7235E+08	10	H	1.150000E+03	2.245264E+02	5.4516E+17
11	N	1.300000E+06	1.950049E+06	4.7416E+13	18	O	6.170000E+04	7.569186E+04	1.8427E+16

NOT REPRODUCIBLE

Table C-XV. KINETIC STREAMTUBE CONDITIONS AXIAL POSITION 2.41693E+01

FLOW PROPERTIES		KINETIC COUPLING TERMS					
MACH NUMBER	5.74884214E+00	COUPLING TERM A	7.66871295E+06				
PRESSURE (PSIA)	6.78062174E+02	COUPLING TERM B	-7.81553792E+06				
VELOCITY (FT/SEC)	7.44408137E+03	INTEGRATION PARAMETERS					
TEMPERATURE (DEGR)	4.8786590E+02	CURRENT STEP SIZE	1.02400000E+01				
DENSITY (LB/FT3)	2.33488281E+04	PERCENT ENTHALPY CHANGE	-2.19847381E+00				
ENTHALPY=H0 (BTU/LB)	-1.78964723E+01	1.0 = SUMMATION C(I)	1.43600687E+11				
GAS MOLECULAR WEIGHT	1.98938856E+01	MAXIMUM RELATIVE ERROR	1.07717726E+03				
HEAT CAPACITY (BTU/LB=DEGR)	3.66045862E+01	GOVERNING EQUATION					
FROZEN GAMMA	1.37535284E+00		3				
GAS CONDUCTIVITY (BTU/SEC-R)	3.49941178E+03						
SUM C(I)*H(I) (FT2/SEC2)	-5.47937080E+07						
CHEMICAL COMPOSITION							
NO.	SPECIES	MASS FRACTION	MOLEC/CC	NO.	SPECIES	MASS FRACTION	MOLEC/CC
1	CO2	7.116331E+02	3.216600E+02	4	H2O	2.627214E+01	3.121762E+01
3	CO	1.979046E+01	1.405496E+01	4	H2	1.999614E+02	1.973140E+01
5	N2	4.250984E+01	3.018460E+01	6	NO	2.001244E+03	1.326677E+03
7	OH	1.748476E+06	2.045071E+06	8	O2	3.837964E+04	2.385905E+04
9	C	4.029950E+12	6.674541E+12	10	H	7.265474E+04	1.437803E+02
11	N	1.876187E+08	2.664416E+08	12	O	7.349727E+07	9.138047E+07
SATURATION POINT H2O AT Z = 2.4988500E+01							
	P =	4.9890143E+02	T =	4.5431785E+02	V =	7.4871320E+03	
	Z =	2.4988500E+01	AREA RATIO =	1.0000000E+00			
	Z =	2.5193300E+01	AREA RATIO =	1.0577367E+00			
	Z =	2.5398108E+01	AREA RATIO =	1.1238478E+00			
	Z =	2.5602900E+01	AREA RATIO =	1.1971106E+00			
STEP SIZE HALVED AT Z = 2.5602900E+01							

Table C-XVI. KINETIC STREAMTUBE CONDITIONS AXIAL POSITION 3.52285E+01

FLOW PROPERTIES		KINETIC COUPLING TERMS	
MACH NUMBER	9.09020824E+00	COUPLING TERM A	5.56793392E+07
PRESSURE (PSIA)	6.97243082E+03	COUPLING TERM B	-5.63243932E+07
VELOCITY (FT/SEC)	7.86861495E+03	INTEGRATION PARAMETERS	
TEMPERATURE (DEGR)	2.1453395E+02	CURRENT STEP SIZE	4.09600000E+01
DENSITY (LB/FT3)	2.77268073E+05	PERCENT ENTHALPY CHANGE	-5.04339509E+00
ENTHALPY/HO (BTU/LB)	-1.1631592E+02	1.0 = SUMMATION C(I)	-1.41113787E+11
GAS MOLECULAR WEIGHT	1.98930921E+01	MAXIMUM RELATIVE ERROR	2.00803912E+04
HEAT CAPACITY (BTU/LB=DEGR)	3.51453953E+01	GOVERNING EQUATION	
FROZEN GAMMA	1.39712569E+00		2
GAS CONDUCTIVITY (BTU/SEC2/DEGR)	2.49941089E+03		
SUM C(I)*H(I) (FT2/SEC2)	-5.72561720E+07		

CHEMICAL COMPOSITION									
NO.	SPECIES	MASS FRACTION	MOLE FRACTION	MOLEC/CC	NO. SPECIES	MASS FRACTION	MOLE FRACTION	MOLEC/CC	
1	CO2	7.116335E+02	3.216602E+02	9.3960E+14	2	H2O	2.827214E+01	3.121763E+01	9.1190E+15
3	CO	1.979046E+01	1.405406E+01	4.1056E+15	4	H2	1.999619E+02	1.973145E+0	5.7638E+15
5	N2	4.250984E+01	3.018461E+01	8.8172E+15	6	NO	2.001243E+03	1.326677E+03	3.8754E+13
7	OH	1.636699E+06	1.914335E+06	5.5920E+10	8	O2	3.837967E+04	2.385906E+04	6.9695E+12
9	C	4.029764E+12	6.474254E+12	1.9496E+05	10	H	7.285006E+04	1.437727E+02	4.1997E+14
11	N	1.869501E+08	2.654922E+08	7.7553E+08	12	O	8.333111E+07	1.03671E+06	3.0265E+10

TEMPERATURE		176.204 IS OUTSIDE THERMAL TABLES	
Z#	3.6047700E+01	AREA RATIO#	6.9523233E+00
Z#	3.6866900E+01	AREA RATIO#	7.3103800E+00
Z#	3.7686100E+01	AREA RATIO#	7.7198414E+00
Z#	3.8505300E+01	AREA RATIO#	8.1616624E+00
Z#	3.9324500E+01	AREA RATIO#	8.6731070E+00
Z#	4.0143700E+01	AREA RATIO#	9.2586952E+00
Z#	4.0962900E+01	AREA RATIO#	9.9366756E+00
Z#	4.1782100E+01	AREA RATIO#	1.0732400E+01

Table C-XVII. AREA RATIO TABLE

I	X	A	DA/DX CALCED
1	2,49885000E+01	1,00000000E+00	0,
2	2,51933000E+01	1,05773674E+00	3,02360939E=01
3	2,53981000E+01	1,12384704E+00	3,40268291E=01
4	2,56029000E+01	1,19711063E+00	3,75357475E=01
5	2,58077000E+01	1,27759346E+00	4,12841205E=01
6	2,60125000E+01	1,36421039E+00	4,52888593E=01
7	2,62173000E+01	1,46309663E+00	4,93586234E=01
8	2,64221000E+01	1,56838331E+00	5,34413881E=01
9	2,66269000E+01	1,68199256E+00	5,74269561E=01
10	2,68317000E+01	1,80360412E+00	6,11919442E=01
11	2,70365000E+01	1,93263476E+00	6,46070464E=01
12	2,72413000E+01	2,06823459E+00	6,75455096E=01
13	2,74461000E+01	2,20930117E+00	6,98907936E=01
14	2,76509000E+01	2,35450728E+00	7,15425464E=01
15	2,78557000E+01	2,50233944E+00	7,24198945E=01
16	2,80605000E+01	2,65113916E+00	7,24603912E=01
17	2,82653000E+01	2,79913720E+00	7,16138891E=01
18	2,84701000E+01	2,94446965E+00	7,12583409E=01
19	2,87261000E+01	3,12754171E+00	7,43507550E=01
20	2,89321000E+01	3,32514552E+00	7,96910279E=01
21	2,92893000E+01	3,57636158E+00	8,32199903E=01
22	2,95965000E+01	3,83644914E+00	8,48097857E=01

Table C-XVII-Conclusion

23	2,99037000E+01	4,09743291E+00	8,37479712E+01
24	3,02109000E+01	4,35099667E+00	8,00741677E+01
25	3,05181000E+01	4,58940859E+00	7,27663481E+01
26	3,09277000E+01	4,87258586E+00	6,17132385E+01
27	3,14397000E+01	5,15815780E+00	5,32042607E+01
28	3,19517000E+01	5,41739749E+00	4,85100428E+01
29	3,25661000E+01	5,70457492E+00	4,17098491E+01
30	3,33853000E+01	6,01534988E+00	3,44497609E+01
31	3,44093000E+01	6,33955291E+00	3,51928117E+01
32	3,60477000E+01	6,95232330E+00	3,95030554E+01
33	3,68669000E+01	7,31038000E+00	4,62962601E+01
34	3,76861000E+01	7,71084136E+00	5,19581533E+01
35	3,85053000E+01	8,16166239E+00	5,87320313E+01
36	3,93245000E+01	8,67310696E+00	6,69575694E+01
37	4,01437000E+01	9,25069520E+00	7,71221106E+01
38	4,09629000E+01	9,93667562E+00	8,99477990E+01
39	4,17821000E+01	1,07323999E+01	9,71343169E+01

Table C-XVIII. INITIAL CONDITIONS KINETIC STREAMTUBE CALCULATION AXIAL POSITION = 2.49885E+01 INPUT NORMALIZING AXIAL SCALE FACTOR (FT) 8.10000E-03

FLOW PROPERTIES		KINETIC COUPLING TERMS	
MACH NUMBER	5.98764801E+00	COUPLING TERM A	0.
PRESSURE (PSIA)	4.98901428E+02	COUPLING TERM B	0.
VELOCITY (FT/SEC)	7.48713199E+03	INTEGRATION PARAMETERS	
TEMPERATURE (DEG-R)	4.94317844E+02	CURRENT STEP SIZE	1.00000000E+03
DENSITY (LB/FT3)	2.03556393E+04	PERCENT ENTHALPY CHANGE	-2.2979991E+00
ENTHALPY-HO (BTU/LB)	-3.01629119E+01	1.0 = SUMMATION C(I)	-1.43529633E+11
GAS MOLECULAR WEIGHT	1.98930875E+01	MAXIMUM RELATIVE ERROR	0.
HEAT CAPACITY (BTU/LB-DEGR)	3.64976731E+01	GOVERNING EQUATION	0
FROZEN GAMMA	1.37686669E+00		
GAS CONDUCTIVITY (BTU/SEC-R)	2.49941144E+03		
SUM C(I)*M(I) (BT2/SEC2)	-5.51006316E+07		

CHEMICAL COMPOSITION									
NO.	SPECIES	MASS FRACTION	MOLE FRACTION	MOLEC/CC	NO. SPECIES	MASS FRACTION	MOLE FRACTION	MOLEC/CC	
1	CO2	7.116331E+02	3.216601E+02	3.1753E+19	2	H2O	2.827214E+01	3.121782E+01	3.0817E+16
3	CO	1.979646E+01	1.405406E+01	1.38725E+16	4	H2	1.999613E+02	1.973141E+01	1.9478E+16
5	N2	4.250984E+01	3.018461E+01	2.9797E+16	6	NO	2.001243E+03	1.326677E+03	1.3097E+14
7	OH	1.728320E+06	2.021497E+06	1.9956E+11	8	O2	3.837964E+04	2.385905E+04	2.3553E+13
9	C	4.029866E+12	6.474421E+12	6.8888E+05	10	H	7.289369E+04	1.437781E+02	1.4193E+15
11	N	1.874259E+08	2.661679E+08	2.6275E+09	12	O	7.512937E+07	9.34095E+07	9.2212E+10

MBAR = 0.		MBAR*1 = 0.		AREA RATIO = 1.00000E+00	
Z #	2.4989500E+01	PV#	1.0602199E+03	PVS #	9.2499474E+04
ITARCT#	0	RS#	9.9825604E+07	EXPJ#	0.
				PRATIO#	1.1461902E+00
				EJ#	0.
				TS#	456.866
Z #	2.4990500E+01	PV#	1.0602177E+03	PVS #	9.2498817E+04
ITARCT#	0	RS#	9.9821973E+07	EXPJ#	0.
				PRATIO#	1.1461960E+00
				EJ#	0.
				TS#	456.866
Z #	2.4991500E+01	PV#	1.0602133E+03	PVS #	9.2496871E+04
ITARCT#	0	RS#	9.9809744E+07	EXPJ#	0.
				PRATIO#	1.1462153E+00
				EJ#	0.
				TS#	456.866
Z #	2.4992500E+01	PV#	1.0602066E+03	PVS #	9.2493633E+04
ITARCT#	0	RS#	9.9788890E+07	EXPJ#	0.
				PRATIO#	1.1452482E+00
				EJ#	0.
				TS#	456.866
Z #	2.4993500E+01	PV#	1.0601889E+03	PVS #	9.2484828E+04
ITARCT#	0	RS#	9.9731984E+07	EXPJ#	0.
				PRATIO#	1.1463382E+00
				EJ#	0.
				TS#	456.866
Z #	2.4994500E+01	PV#	1.0601823E+03	PVS #	9.2471538E+04
ITARCT#	0	RS#	9.9646081E+07	EXPJ#	0.
				PRATIO#	1.1464742E+00
				EJ#	0.
				TS#	456.866

Table C-XIX. KINETIC STREAMTUBE CONDITIONS AXIAL POSITION 2.70052E+01

FLOW PROPERTIES		KINETIC COUPLING TERMS							
MACH NUMBER	6.07098473E+00	COUPLING TERM A	0.						
PRESSURE (PSIA)	1.62814224E+02	COUPLING TERM B	0.						
VELOCITY (FT/SEC)	7.59405872E+03	INTEGRATION PARAMETERS							
TEMPERATURE (DEG C)	3.55392215E+02	CURRENT STEP SIZE	2.00000000E+03						
DENSITY (LB/FT ³)	1.05047495E+04	PERCENT ENTHALPY CHANGE	-1.91610421E+00						
ENTHALPY (BTU/LB)	-6.67331061E+01	1.0 * SUMMATION C(I)	-1.22426513E+11						
GAS MOLECULAR WEIGHT	1.98931189E+01	MAXIMUM RELATIVE ERROR	7.04105856E+01						
HEAT CAPACITY (BTU/LB-DEGR)	3.60747119E+01	GOVERNING EQUATION							
PROZEN GAMMA	1.38297669E+00	3							
GAS CONDUCTIVITY (BTU/SEC-FT)	2.40940375E+03								
SUM C(I)*H(I) (FT ² /SEC ²)	-5.60142370E+07								
CHEMICAL COMPOSITION									
NO.	SPECIES	MASS FRACTION	MOLE FRACTION	MOLEC/CC	NO.	SPECIES	MASS FRACTION	MOLE FRACTION	MOLEC/CC
1	CO2	7.116439E+02	3.216654E-02	1.3315E+15	2	H2O	2.827104E+01	3.121667E-01	1.2922E+16
3	CO	1.979076E+01	1.405519E-01	5.8181E+15	4	H2	1.909645E+02	1.973174E-01	8.1679E+15
5	N2	4.251048E+01	3.018511E-01	1.2495E+16	6	NO	2.001274E+03	1.326499E-03	5.4918E+13
7	OH	1.729346E+06	2.021531E-06	8.3681E+10	8	O2	3.878022E+04	2.395945E-04	9.8765E+12
9	C	4.029928E+12	6.674532E-12	2.7629E+05	10	H	7.295479E+04	1.437405E-02	5.19517E+14
11	N	1.874287E+08	2.661723E-08	1.1018E+09	12	O	7.513071E+07	9.341151E-07	3.8667E+10
<p>NSA4 = 1.52987E+05 MPAR=1 = 9.99985E+01 AREA RATIO = 1.90994E+00</p> <p>Z = 2.7007250E+01 PVS = 3.4558156E+04 PVS = 8.6252116E+07 PRATIO = 4.005644E+02 TS = 434.737</p> <p>YED=2 = 1.0210476E+13 DELZ = 2.000000E+03 RPRIME = 1.4689714E+12 YERM1 = 9.19241558E+21</p> <p>EB = 1.0720532E+04 XBAR = 1.5298692E+05 WNY = 1.063246E+01 G = 1.5298692E+05</p> <p>BB = 1.7671834E+20 DMRX = 5.4480244E+05 DGR = 1.186473E+04 B-DH = 1.0237643E+12</p> <p>DMPOY = 1.3965942E+04 RSTAK = 9.831743E+10 J RATE = 4.6754794E+22 M-PRIME = -1.7496817E+08</p> <p>XMDY = 1.11884737E+04 TFAC = 9.997633E+01 E = 8.3038854E+01</p> <p>Z = 2.7007250E+01 PVS = 3.4558156E+04 PVS = 8.6252116E+07 PRATIO = 4.005644E+02 TS = 434.737</p> <p>YFACT=0 RSE=3.8891461E+04 EXPJ=1.7922668E+05 EJM=1.5811361E+18</p> <p>Z = 2.7009250E+01 PVS = 3.45717867E+04 PVS = 8.5417438E+07 PRATIO = 4.0410797E+02 TS = 436.717</p> <p>YFACT=0 RSE=2.9948836E+08 EXPJ=1.2276672E+05 EJM=1.7137061E+18</p> <p>Z = 2.7011250E+01 PVS = 3.4477629E+04 PVS = 8.4577772E+07 PRATIO = 4.0764409E+02 TS = 436.697</p> <p>YFACT=0 RSE=2.9955378E+08 EXPJ=1.7540244E+05 EJM=1.7478482E+18</p> <p>STEP SIZE HALVED AT Z = 2.7311250E+01</p> <p>Z = 2.7109250E+01 PVS = 3.4477650E+04 PVS = 8.5417458E+07 PRATIO = 4.0353704E+02 TS = 436.497</p> <p>YFACT=0 RSE=2.9975443E+08 EXPJ=1.2211981E+05 EJM=1.7007262E+18</p> <p>Z = 2.7010250E+01 PVS = 3.4557531E+04 PVS = 8.4995551E+07 PRATIO = 4.0540384E+02 TS = 436.687</p> <p>YFACT=0 RSE=2.9958790E+08 EXPJ=1.2342973E+05 EJM=1.7175175E+18</p> <p>Z = 2.7011250E+01 PVS = 3.4437426E+04 PVS = 8.4574112E+07 PRATIO = 4.0718637E+02 TS = 436.677</p> <p>YFACT=0 RSE=2.9942002E+08 EXPJ=1.2475764E+05 EJM=1.7345295E+18</p>									

Table C-XX. KINETIC STREAMTUBE CONDITIONS AXIAL POSITION 2.90277E+01

FLOW PROPERTIES		KINETIC COUPLING TERMS	
MACH NUMBER	7.39920083E+00	COUPLING TERM A	0.
PRESSURE (PSIA)	6.59610248E+03	COUPLING TERM B	0.
VELOCITY (FT/SEC)	7.65226399E+03	INTEGRATION PARAMETERS	
TEMPERATURE (DEGR)	3.00035213E+02	CURRENT STEP SIZE	5.00000000E+04
DENSITY (LB/FT3)	9.91076152E+05	PERCENT ENTHALPY CHANGE	-2.71582302E+00
ENTHALPY/HO (BTU/LB)	-8.27515332E+01	1.0 * SUMMATION C(I)	-4.23483471E-12
GAS MOLECULAR WEIGHT	1.98975622E+01	MAXIMUM RELATIVE ERROR	1.33814552E+03
HEAT CAPACITY (BTU/LB-DEGR)	3.57963888E+01	GOVERNING EQUATION	
FROZEN GAPMA	1.34698720E+00	3	
GAS CONDUCTIVITY (BTU/SEC-DEGR)	2.49884035E+03		
SUM C(I)=H(I) (FT2/SEC2)	-5.62218244E+07		

CHEMICAL COMPOSITION

NO.	SPECIES	MASS FRACTION	MOLE FRACTION	MOLEC/CC	NO.	SPECIES	MASS FRACTION	MOLE FRACTION	MOLEC/CC
1	CO2	7.131691E+02	3.224268E+02	6.1886E+14	2	H2O	2.811733E+01	3.105386E+01	5.9604E+15
3	CO	1.983386E+01	1.408846E+01	2.7041E+15	4	H2	2.003931E+02	1.977844E+01	3.7962E+15
5	N2	4.260199E+01	3.029696E+01	5.8073E+15	6	NO	2.009563E+03	1.329839E+03	2.5525E+13
7	OH	1.732051E+06	2.026316E+06	3.8892E+10	8	O2	3.846248E+04	2.391592E+04	4.5903E+12
9	C	4.038563E+12	6.690331E+12	1.2841E+05	10	H	7.381089E+04	1.441709E+02	2.7662E+14
11	N	1.878304E+08	2.668024E+08	5.1209E+08	12	O	7.529173E+07	9.363262E+07	1.7972E+10

MBAR	=2.15566E+03	MBAR*1	= 9.97844E+01	AREA RATIO	= 3.36225E+00
Z	= 2.9027750E+01	DELZ	= 5.0000000E+04	RPRIME	= 4.3365606E+12
TERM2	= 2.638930E+15	XMBAR	= -2.15566365E+03	WINT	= 1.5012744E+01
S	= -1.008496E+06	DARDX	= 4.038563E+12	DODX	= 1.3381455E+03
BB	= 1.3242819E+21	RSTAR	= 7.1500577E+10	J RATE	= 7.8795803E+23
DMPDT	= -1.3974599E+04	TFAC	= 9.9663642E+01	E	= 9.4144203E+00
XMDOT	= -1.3573893E+03	X1OH	= -1.0460248E+01	TERM1	= 3.4893905E+24
				G	= 2.1556656E+03
				DODX	= 1.3381455E+03
				HPRIME	= -1.7472215E+08

DHPDX = dh'/dx
DGDx = dg/dx
DRDX = dr/dx
RSTAR = r^{**}
JRATE = J
HPRIME = h'
DHPDT = dh'/dT
XMDOT = \dot{m}
XMOM = \dot{M}
E = \dot{H}

All values of variables printed out under the above symbols are in the internal computing units of poundal, pound mass, BTU, foot, and second.

C. 8 REFERENCES

- C-1. J. R. Kliegel, and H. M. Frey. One-Dimensional Reacting Gas Nonequilibrium Performance Program. 02874-6003-R000, March, 1967, TRW Systems, Redondo Beach, Calif.
- C-2. J. R. Kliegel, H. M. Frey, G. R. Nickerson, and T. J. Tyson. ICRPG One-Dimensional Kinetic Nozzle Analysis Computer Program. Published by Dynamic Science, under contract NAS7-443, July 1968.
- C-3. H. M. Frey and G. R. Nickerson. SCREEN, A Computer Program for the Screening of Chemically Reacting Gas Mixtures. Published by Dynamic Science under Contract to McDonnell Douglas Astronautics Company, TR-141-1-CS, February, 1970.
- C-4. J. O. Hirschfelder, C. F. Curtiss, and R. B. Bird. Molecular Theory of Gases and Liquids. Wiley, (New York), 1954.
- C-5. S. S. Penner. Chemistry Problems in Jet Propulsion. Pergamon, (New York), 1957.
- C-6. S. W. Benson and T. Fueno. "Mechanism of Atom Recombination by Consecutive Vibrational Deactivations." Journal of Chemical Physics, Vol. 36, 1962, pp 1597-1607.
- C-7. J. Frankel. Kinetic Theory of Liquids. Oxford University Press. (London), 1946.
- C-8. H. G. Stever. Condensation in High-Speed Flows. High-Speed Aerodynamics and Jet Propulsion. Vol. III, Princeton University Press, (Princeton, N. J.), 1958.
- C-9. P. G. Hill. "Condensation of Water Vapor During Supersonic Expansion in Nozzles." Journal of Fluid Mechanics, Vol 25, 1966.
- C-10. T. J. Tyson and J. R. Kliegel. "An Implicit Integration Procedure for Chemical Kinetics." AIAA 6th Aerospace Sciences Meeting, Paper No. 68-180, January 1968.

Appendix D

SURFACE

DEPOSITION AND SURFACE EFFECTS
COMPUTER PROGRAM

A Plume Impingement, Deposition, Abrasion, and
Surface Contamination Effects Model

Program Number P1942

TABLE OF CONTENTS

<u>Section</u>		
D. 1	INTRODUCTION	465
	a. The SURFACE Program	465
	b. Scope	465
D. 2	ANALYSIS	466
	a. Summary	466
	b. Configuration	468
	c. Initial Condition	469
	d. Test Effects	470
	e. Identification of Exposure Type	471
	f. Impingement	471
	g. Transformation of Coordinates	472
	h. Plume Impingement Effects	472
	i. New Condition of Surface	474
D. 3	PROGRAM OVERLAY STRUCTURE	474
D. 4	SUBROUTINES	474
	a. Subroutine HCØNDF	475
	b. Subroutine HCØNDØ	475
	c. Subroutine REDRHØ	475
	d. Subroutine REDRØD	475
	e. Subroutine REDVIS	475
	f. Subroutine WEBBER	475
	g. Subroutine GETSUR	476
	h. Subroutine WARD	476
	i. Subroutine MINSUR	476
	j. Subroutine INTER	476
	k. Subroutine MAXSUR	476
	l. Subroutine INTRA	477
	m. Subroutine EXTRAP	477
	n. Subroutine ENTER	477
	o. Subroutine HØTPAR	477
	p. Subroutine FINDR	477
	q. Subroutine CØTRN	478
	r. Subroutine TRNCØR	478

Preceding page blank

D. 5	PROGRAM USER'S MANUAL	478
	a. General	478
	b. Data Input	478
D. 6	OUTPUT DESCRIPTION	491

TABLES

<u>Table</u>		<u>Page</u>
D-I	Input Data for SURFACE	492
D-II	Satellite Configuration	497
D-III	Projections	500
D-IV	Properties of Structural Materials	501
D-V	Operating Conditions	502
D-VI	SURFACE Properties Input	504
D-VII	Spacecraft Exterior Materials—SEEK Values Input for Initial Conditions	508
D-VIII	Current Condition of Satellite Exterior	510
D-IX	Effective Heat Transfer Constants—Initial Conditions	512
D-X	Spacecraft Exterior Materials After Plume or Space Exposure	512
D-XI	Current Condition of Satellite Exterior for Assigned Post-Plume Conditions	513
D-XII	Effective Heat Transfer Constants—After Assigned Exposure to Plume	515
D-XIII	Impingement of Plume on Satellite	516
D-XIV	Coordinate Transformation	517
D-XV	Physical Properties of Impinged Segment Surfaces	518
D-XVI	Wear Constants of Materials on Surface	519
D-XVII	Arbitrary Plume Characteristics for Testing Program	520

Appendix D

SURFACE

DEPOSITION AND SURFACE EFFECTS
COMPUTER PROGRAM

A Plume Impingement, Deposition, Abrasion, and
Surface Contamination Effects Model

D. 1 INTRODUCTION

a. The SURFACE Program

The computer program described in this appendix is a subprogram to the Plume Contamination Effects Prediction Computer Program, CONTAM, and computes the effect of direct plume impingement on sensitive satellite surfaces in terms of changes in the thermal and optical properties of the surfaces. Required input to the SURFACE subprogram includes:

(1) The gasdynamic, thermodynamic, and chemical constitution description of a plume as computed by the MULTRAN subprogram (Appendix B) and KINCON (Appendix C).

(2) A configurational and material description of the sensitive surfaces of the spacecraft.

b. Scope

The scope of this portion of the study was initially limited to definition of the basic components of a computer model of direct plume impingement contamination effects caused by a limited number of species on selected sensitive surfaces. The objective of this initial approach was to demonstrate that the determination of surface effects was amenable to modeling by a computer program.

The program development proceeded faster than anticipated, and the program is much more nearly complete than expected. The program currently is a system model consisting of a general configurational description of a satellite with multiple thrusters, an extensive list of structural

materials which may be included as part of the surface, and many of the expected plume contaminant species. The model of the plume-surface interactions is, however, still restricted to a limited set of steady-state conditions. A brief description of the model and computer program will be presented along with a sample output of the program.

Because the simplified program model is now operational, numerical values for "surface effects" can be calculated. Hence, there is a temptation to try to use the program to get valid answers to questions about plume-surface interactions. It cannot be too strongly emphasized that the current program may not give valid answers except in the simplest cases; therefore, engineering judgment must be exercised.

D. 2 ANALYSIS

a. Summary

(1) Configuration

The basic configuration of a model satellite: location of thrusters, materials of construction at various locations (segments), and properties of the structural materials are input to SURFACE first. Properties of typical deposit materials are then entered. A segment-by-segment mechanical description of the satellite is constructed and printed out.

(2) Initial Condition

The optical and thermal properties of the surface materials are matched to the segment structure of the satellite, and a segment-by-segment listing of the current optical/thermal condition is printed. At the same time, the average α , ϵ , and α/ϵ ratios for the whole satellite are calculated and then listed.

(3) Test Effects

The next portion, use of which is optional, consists of input of arbitrary or precalculated data about the current conditions of selected segments after plume exposure, and then determination and listing of the current segment-by-segment optical/thermal condition, plus averaged α , ϵ , and the α/ϵ ratio. This portion can be used either to checkout the calculations of surface condition or to calculate the effects of surface plume interactions observed in tests or calculated by means other than this program.

(4) Segments Impinged

Based on a knowledge of the basic plume structure, as determined by the MULTRAN subprogram (or, in the manual mode, from test or other computed data), the SURFACE subprogram then determines and lists

the location of all portions of the spacecraft upon which the plume impinges. This permits the elimination of those spacecraft surfaces which will not be affected by the thruster impingement, thereby preventing unnecessary computations.

Transformation of coordinates from satellite-based to thruster-based are calculated at this point, in order to accept data from MULTRAN and KINCON. The data to be transformed may be entered by card or may have been calculated earlier.

(5) Plume Impingement Calculations

The program then assembles and lists a file of properties of the current surfaces of the plume-impinged segments identified earlier.

Characteristic properties of the plume are then input based on the results of KINCON and MULTRAN. The thruster pulse is sliced into selected increments, and the program calculates the gross effect of impingement on the surface material of each satellite segment during the time slice, thus determining whether abrasion or deposition (treated as mutually exclusive) occurs. After deciding the type of effect, the detailed effects on each segment are determined. The process is then repeated for subsequent slices, with the surface condition after each slice used as input for the next. When the calculation is completed for the total pulse, the final conditions for the affected segments are listed.

(6) Final Condition

The program then returns to calculation of the current optical/thermal surface condition, α , ϵ , and the α/ϵ ratio.

(7) Recycling

Reentry to calculate the effects of a new pulse can then be accomplished.

(8) Future Work

Among the parameters of major importance to the calculation of surface effects which are not yet embodied in the program are:

- Effects of exposure to space vacuum between pulses.
- Effects of transient conditions during pulse (start-up and tail-off).
- Sticking of droplets to surface.
- Heat transfer to surface during deposition.

Future work on SURFACE will emphasize modification of the program to include these effects.

b. Configuration

(1) Satellite Structure

SURFACE accepts card data input to describe the external surface of the satellite. The surface is divided into a number of segments (variable at will), and each segment location is given in a cylindrical coordinate system. Additional inputs include the locations of all projections from the surface, the height of such projections, and the angle they present to the main axis of the satellite. The initial surface temperature at each location is noted. The program prints a set of tables showing all configuration data.

In the satellite-based cylindrical coordinate system, the origin is placed at the vertex of the satellite nose, with the satellite axis lying on the X-axis. The coordinates of any point in this system are given in terms of (X, R, θ) , with θ measured in radians from the horizontal Y-axis.

For purposes of locating the various conditions and effects on the surface of the satellite, the exterior is divided into segments, each with a specified area. Each segment is given an identification number, and its location is recorded in the cylindrical coordinates of its midpoint. The shapes of the segments are appropriate to the surfaces they lie on—squares on the cylindrical surface, annular segments and circles for the ends. The assignments are completely flexible and can be changed by simply changing the data cards. In general, there is no need to describe the satellite exterior completely. If the general areas which can interact with the plume are already known, then the input can be limited to these areas.

(2) Projection Configuration

Card data are accepted to describe the configuration and structure of projections above the satellite surface, including sensors, solar cells, and thrusters. Tables are printed showing the data for each projection. If a projection is in contact with two or more segments only the contacted segment with the lowest I. D. number reports information about the location of the projection.

(3) Structural Materials

Card data are accepted to describe the structural-mechanical properties of typical materials used for exterior structures of satellites. Materials include aluminum, gold plating, solar-cell-cover glasses, infrared ports, windows, ultraviolet ports, and white and black thermal-control coatings. Typical or handbook data are currently input. Definitive data

for specific alloys or compositions can be added easily when information on their behavior is required. The input data are listed.

(4) Optical and Thermal Coefficients for Structural Materials

Card data are accepted to define properties such as a solar absorptivity, thermal emissivity, transmittivity at selected wavelengths, etc., as functions of surface finish for the structural materials. Typical or handbook data are currently supplied. Specific data inputs for selected compositions of materials can be added as required. The input data are listed.

(5) Physicochemical Properties of Propellants and Deposits

Card data are accepted to define the physical and chemical properties of plume species and deposits at selected reference temperatures. Properties of propellants at other temperatures are then calculated. However, there are not sufficient data for most of the condensed reaction products for accurate extrapolation of these properties, and most of the data for these materials are treated as constant with temperature.

The methods used to calculate the properties are described in Appendix A, Subsection A. 2c(2).

(6) Optical and Thermal Coefficients for Deposits

Card data are accepted to define thermal and optical coefficients— α , ϵ , τ , and ρ —as functions of temperature. Input data are listed.

c. Initial Condition

(1) Initial Assignment of Materials

Card data are accepted to assign specific structural materials to each satellite segment. As many as three layers of materials may be assigned to any segment. The data are entered into two arrays; one is the surface description array, and the other is a transfer matrix used to search for properties corresponding to the materials and their conditions.

A table is printed showing the materials assigned to each segment of the satellite and projections.

(2) Optical/Thermal Surface Parameters

This segment takes the transfer matrix and searches the stored optical and thermal coefficients for the appropriate data. Interpolations/extrapolations are conducted if the specific data needed have not been entered during input.

The optical and thermal properties of structural materials are tabulated as functions of surface finish; the properties of the deposits are given as functions of surface temperature.

The interpolation-extrapolation routines include the following features:

- No extrapolation of optical/thermal properties is done below the value given for the lowest temperature or surface finish in the tables; the minimum value is used.
- Extrapolation above the highest temperature/surface finish is a simple linear ratio from the values for the two greatest temperatures/surface finishes.
- Interpolation is by ratio from the nearest adjacent values, using essentially the method given by Wiberg¹.
- The new description of the surface is printed out.

(3) Effective Values of Heat Transfer Coefficients

This segment calculates the values for solar absorptivity and thermal emissivity and their ratio, averaged over the whole satellite exterior (excluding projections). The calculated values are printed out.

d. Test Effects

A flag is set during initialization to activate or bypass this module.

(1) Surface State

Card data are input describing the physical state of selected structural segments. Such data include presence of deposits, thickness of deposit and/or thickness of original surface, surface finish, and surface temperature. The data are listed.

(2) Optical/Thermal Surface Parameters and Heat Transfer Coefficients

The program then returns to the calculation of surface parameters and coefficients described above in D. 2c (2) and (3), and lists the values obtained.

¹ K. B. Wiberg, "Subroutine LOCATN," Computer Programming for Chemists, W. A. Benjamin, Inc., New York (1965).

e. Identification of Exposure Type

A flag is used to signify whether plume exposure or space exposure has occurred, or whether all exposures are over and the surface state should be recalculated. This flag can be preset during initialization, or set automatically when the end of a plume exposure computation is reached. If the exposure is to a plume, a branch is made to a routine which identifies the segments which are directly exposed. Space exposure involves the whole spacecraft, and no selection of segments is necessary.

If the flag indicates that the exposure is to a space environment, the computation is terminated because routines to determine the effects of space exposure have not yet been included in SURFACE.

f. Impingement

The intercept of the plume with the satellite is calculated. The variables used are satellite configuration, thruster location, and plume geometry. The impinged segments are placed in the array named AFFSEG (affected segments).

The areas impinged by the plume are functions of the geometry of the plume and the configuration of the satellite. In the subsequent sub-routines, the border of the impinged area is found by simultaneous solution of the equations of plume and surface, and then the surface description array SURDES is searched to find all segments whose coordinates are on or inside the border. These segment identification numbers are put into the array called AFFSEG.

A paraboloid shape for the plume is assumed. The latus rectum of the plume paraboloid, which defines the shape of the plume, is equal to four times P. P is a function of thruster size, configuration, etc., and of the time in the cycle (pulse transient).

The computation is done in two separate segments. The first is the intersection of the plume with the satellite surface. Currently this segment is restricted to satellites of cylindrical cross-section. The second segment determines the intersection with projections. The computation assumes a plane surface on the projection, but it can lie at any solid angle to the axis of the plume. The configuration of the system used for these calculations is the data originally entered in the program (Section D. 2. (b)). There is no provision for recalculating the intersection of movable projections after they have changed position.

g. Transformation of Coordinates

The MULTRAN and KINCØN subprograms treat the plume in thruster-based cylindrical coordinates. In order to identify the locations of impinged satellite surfaces in the plume, a transformation to satellite-based coordinates is performed on the plume flow field. These calculations require inclusion of a radial angle in the plume coordinates because the cylindrical symmetries of the isolated plume are lost in the presence of the satellite structure. The origin for measuring this angle is defined by the plane in which the central axis of the thruster and the central axis of the satellite both lie.

h. Plume Impingement Effects

(1) Surface Properties

The physical and mechanical properties of the surfaces of the affected segments are found and entered in the array SEARCH. These properties determine the type of interaction with the plume.

(2) Surface Effects

The results of the impingement of the plume on the segment surfaces are calculated for brief time increments, using plume characteristics read in at this point. The only mode used in program checkout has assumed uniform plume characteristics over all affected segments, but this is not a program-imposed limit. Impingement on one location by the plumes from two separate thrusters fired simultaneously is not treated; however, sequential firing of two or more thrusters may be treated.

As a first step, the abrasion wear is calculated. If the wear depth is less than 0.1 microinch, deposition from the plume is assumed to be the major process, and the program branches to the calculation of deposit formation. The results of either process are stored temporarily. The effects are then calculated for the next time interval, using the results from the previous interval as the base. When the exposure is completed, the final results are entered into the array EFFECT.

(3) Abrasion

All abrasion is assumed to be the result of impacting particles (droplets). There are no provisions for abrasive wear resulting from gas impact or for thermal ablation. If abrasion occurs, the impacting drops are assumed to depart along with the abraded surface material. There are no provisions for deposition of preexisting drops. The wear relation used is the fatigue wear term of Neilson and Gilchrist². The rate of material

²J. H. Neilson and A. Gilchrist, Wear, Vol. 11, pp. 111-122 (1968).

removed per weight of impinging condensed phase is calculated by means of tabulated values for the fatigue wear parameter for several materials, plus constants for the equation used to calculate the value at specific velocities.

The wear rate constant (lb_m material removed per lb_m material impinged) for a particular material is a function of the impingement velocity up to a lower critical velocity; it then becomes constant. The critical velocity is a property of the material undergoing abrasion. Some data available suggest that there are upper critical velocities at which the form of the wear equation changes, but the data are insufficient for definitive application, therefore the program does not model the changes.

In the calculation of abrasion effects, the droplets are grouped into two size categories: the uncombusted material (large) and the condensed combustion products (small). An average diameter is used for each size category.

Two effects are calculated—the wear depth and the surface finish. If the abrasion is sufficient to completely remove the surface layer, subsequent calculations are conducted with the characteristics of the newly exposed layer.

(4) Deposition

The model used for the deposition process is a relatively simple one which is an analogy between heat and mass transfer, based on Trebal's model³. The model uses heat transfer coefficients, without data on mass transfer or deposition rates. However, the model does not include thermal effects of the deposition process or of chemical reactions between deposited species.

The determination of deposition requires the diffusivities of the condensing species in the gas stream. These are calculated from the boiling point, molecular radius, and density. The assumption is made that each condensable species diffuses independently through a medium consisting solely of nitrogen gas. Next, using the specific heat, viscosity, and molecular weight of the plume, the Prandtl number and Schmidt number are calculated; and then the mass transfer coefficient is determined. The deposition per time slice is then calculated.

The program then calculates the identity of the species on the surface, considering the species present, those depositing, and the likely chemical reactions between them.

The calculations are repeated for the entire engine pulse. The results of the deposition (species and depth) are then entered in EFFECT. The surface finish (roughness) of the deposits is not calculated at the present time; a value of 25 microns is arbitrarily applied to each deposit.

³R. E. Trebal, Illustration 3.4, Mass Transfer Operations, 2nd Ed. (1968).

i New Condition of Surface

The program returns to the section which calculates the current optical/thermal properties as described previously.

D.3 PROGRAM OVERLAY STRUCTURE

ØVERLAY (HFILE, 7, 0)

SURFACE (H411)

GETSUR

MINSUR

MAXSUR

INTER

INTRA

EXTRAP

ENTER

HØTPAR

FINDR

CØRTRN

WEBBER

WARD

REDRHØ

REDRØD

HCØNDF

HCØNDØ

REDVIS

TRNCØR

D.4 SUBROUTINES

There are 18 subroutines used in SURFACE. They are described briefly, in order of appearance in the program, in the following sections.

a. Subroutine HCØNDF

Approximates the enthalpy of the condensed phase fuel as a function of temperature, similar to HCØNDF in TCC, but with the addition of a term for the heat capacity of the solid phase.

If

$$T < M. p.$$

then

$$H_F = C_{P_{solid}} \times T$$

If

$$T \geq M. p.$$

then

$$H_F = C_{P_{solid}} \times M. p. + \Delta H_{fusion} + C_{P_{liquid}} \times (T - M. p.)$$

b. Subroutine HCØNDØ

Approximates the enthalpy of the oxidizer by a method analogous to the method for fuel in HCØNDF above.

c. Subroutine REDRHØ

Approximates the reduced density of a liquid as a function of reduced temperature along the saturation line. Identical to REDRHØ in TCC.

d. Subroutine REDRØD

Approximates the reduced density difference (reduced density of liquid minus reduced density of vapor) as a function of reduced temperature. Identical with REDRØD in TCC.

e. Subroutine REDVIS

Approximates the reduced viscosity of a liquid as a function of reduced temperature. Identical to REDVIS in TCC.

f. Subroutine WEBBER

This subroutine is used to calculate the reduced properties of fuel and oxidizer at selected temperatures; vapor pressure, density, O/F density ratio, viscosity, and surface temperature. The calculations are outlined in Section A.2c (2).

g. Subroutine GETSUR

This subroutine is used to find the optical and thermal properties corresponding to the surface roughness or temperature. The files are first searched to find if the needed value is entered. If it is not, other subroutines are used for extrapolation/interpolation.

GETSUR is also called by subroutine ENTER.

h. Subroutine WARD

This subroutine, called only from subroutine GETSUR, is used to transfer all lower layers upward one layer in the segment description if the data indicate a zero or negative thickness for the top layer.

i. Subroutine MINSUR

This subroutine, called from subroutine GETSUR directly, or by subroutines INTER and INTRA in turn called from GETSUR, is used when there is no value of a selected surface thermal/optical property corresponding to the surface finish of interest. It searches through the tabulation until the entry corresponding to the least increase in finish is found.

j. Subroutine INTER

This subroutine, called from subroutine GETSUR only, is used to interpolate values for surface optical/thermal properties when no values corresponding to the surface finish of interest are available in the tabulation. It searches to find the closest lower and higher values, and the corresponding roughnesses. A factor is calculated from the roughnesses

$$Q = \frac{R_{\phi} - R_L}{R_U - R_L}$$

The surface property required is then calculated.

$$S_{\phi} = (S_U - S_L) * Q + S_L$$

where S indicates the surface property, R the roughness, ϕ the property of interest, L the lower value, and U the upper value.

k. Subroutine MAXSUR

This subroutine, called from GETSUR, INTER, and INTRA is the mirror image of MINSUR. It is used to find the value of a surface property corresponding to the least decrease in surface finish.

l. Subroutine INTRA

This subroutine, called from GETSUR only, is used to interpolate values for surface optical/thermal properties when interpolation is necessary on the surface finish entry as well as the desired property entry. The interpolation routines are the same as in INTER.

m. Subroutine EXTRAP

This subroutine, called from GETSUR, is in part a dummy subroutine. The routine is to be used to interpolate surface physical and chemical properties for plume deposits at various temperatures; however, for most of the possible deposits, there are insufficient data entered to determine trends accurately enough for interpolation. Only for N_2O_4 and MMH can properties be extrapolated, and then only the physical properties. Subroutine WEBBER is called for these cases; in all others, a statement is printed saying that the extrapolations cannot be performed.

n. Subroutine ENTER

This subroutine, called from the program SURFACE, is used to enter changed surface conditions and properties of segments into the files in which the original input data are stored. The old file is searched for the segment of interest; then the data for the segment are compared with the changed data. If the layer structure has changed (new or changed composition layer from deposition, or layer removed by abrasion), the required shifts are made in the locations of the filed data, and then the individual items of changed data are entered into the correct locations.

o. Subroutine HØTPAR

This subroutine is called by the program SURFACE. It calculates the overall effective values for α , ϵ , and the α/ϵ ratio corresponding to a particular set of surface conditions. Local values of α , ϵ , and the area of each segment are read from the files. The products of α time area and of ϵ times area for each segment are separately summed, then divided by the total area. Projections such as solar cells are not included in the calculation.

p. Subroutine FINDR

This subroutine is called by the program SURFACE. FINDR determines the ID number and coordinates of all satellite body segments which are wet by the plume. The subroutine is currently limited to satellites with a cylindrical shape and plumes which are paraboloids of revolution.

When specific values for thruster location and the latus rectum of the plume are entered, the segments which are wetted are determined.

q. Subroutine CØRTRN

This subroutine is called from the program SURFACE. It is used to transform coordinates from the satellite based X, R, θ cylindrical system to the cylindrical system based on any thruster of known position. The transformation is by standard analytical geometry equations.

r. Subroutine TRNCOR

This subroutine, called from SURFACE, is the inverse of the previous one. It transforms coordinates from a thruster-based system to the satellite-based system.

D. 5 PROGRAM USER'S MANUAL

a. General

The SURFACE program is the fourth link of the CONTAM computer program. It may be run as a subprogram to CONTAM under control of subroutine EXEC, or as an independent program. It was developed on a CDC 6500 computer using FORTRAN IV language. The SURFACE program requires 175,000g words of core storage. Conversion to another computer system should be straightforward, providing that sufficient core is available.

b. Data Input

The following input properties are required for SURFACE:

Propellant Properties and Thruster Characteristics (INPUT 1)

External Materials

Satellite Configuration

Projection(s) Configuration(s)

Structural Materials

Propellant Temperature (Test Case)

Optical/Thermal Properties

Segment Structure

Program Option Selection

Modified Surface Conditions (Test Case)

Program Option Selections

Pulse Characteristics

Program Option Selection

Coordinate Transformation

Thruster to Satellite
Satellite to Thruster

Molecular Weight

Wear Constants

Plume Characteristics

Velocity Limits

Heat Transfer Coefficients

Plume Physical Properties

Plume Configuration Change

DATA statements are not used for numerical data inputs.

The inputs are described in the following sections. Table D-1 at the end of this subsection is a listing of the card image for some of the inputs.

(1) Initialization Data

These are separate cards in the FORTRAN program. They follow the heading INITIALIZE.

<u>ITEM NAME</u>	<u>USE</u>	<u>INITIAL VALUE</u>
DELTMA	Variable time slice	0.0
DELP	Change in P, controlling plume shape	0.0
IGØ	Counter for number of exposure cycles	0.0
NF1	Counter for number of segments wet by plumes	0.0
NTR	Thruster identification number	0.0
ZTEST	Error flag; if greater than zero, program aborts	0.0

<u>ITEM NAME</u>	<u>USE</u>	<u>INITIAL VALUE</u>
RUNFLAG	Flag indicating availability of exposure data; 0 = no data	1.0
IA	Flag to indicate whether data to be processed related to initial conditions (IA = 0) or exposure results (IA > 0)	0.0
EXTYPE	Flag indicating type of exposure; -1 = no exposure; 0 = plume; +1 = space.	-1.0
P	Controls plume shape; P = 1/4 latus rectum of plume paraboloid	0.0
ITRNCL	Flag for coordinate transformation calculations -1 = satellite to thruster 0 = none +1 = both types +2 = thruster to satellite	
KSTP	Controls use of DELP to change P	
RLOOPN	Counter for number of pulse slices processed	0.0

(2) Propellant Properties and Thrustor Characteristics

This data input is identical to that described for the TCC program in Appendix A, Section A.6, and it follows the same INPUT 1 procedure. When all the links in the overall program CONTAM have been installed, this input will be deleted, and the data will be read from the TCC input.

(3) External Materials - Array NAME

<u>ITEM NAME</u>	<u>INPUT FORMAT</u>	<u>MEANING OR USE</u>	<u>UNITS</u>
NAME (n)	6H	Names of structural	-
n = 1 - 25	Two cards	materials and deposits	

Note: There are many unassigned NAME's for inclusion of new materials.

(4) Satellite Configuration - Array SURDES

<u>ITEM NAME</u>	<u>INPUT FORMAT</u>	<u>MEANING OR USE</u>	<u>UNITS</u>
M1S	5X, 15	Number of rows in SURDES = number of segments	-
M2S(=11)	5X, 15	Number of columns in SURDES = number of segment descriptors	-

The above two items are input on one card.

TOTAR	10X, F10.0	Area of satellite	Ft ²
SURDES(M1S, 1)	F8.0	Segment ID No.	-
, 2)	F8.0	X - coordinate	Ft
, 3)	F8.0	R - coordinate	Ft
, 4)	F8.0	Theta coordinate	Radian
, 5)	F8.0	Area	Ft ²
, 6)	F8.0	X distance to nearest plume vertex	Ft
, 7)	F8.0	Surface temperature	Deg R
, 8)	F8.0	Height of projection (if any) from segment	Ft
, 9)	F8.0	Lambda direction cosine of projection surface referred to satellite axis	-
, 10)	F8.0	Mu direction cosine	-
, 11)	F8.0	Nu direction cosine	-

SURDES (n, 1-10) are on one card, SURDES (n, 11) is on a second card. There are hence M1S pairs of cards.

(5) Projection Configuration - Includes More Array SURDES

<u>ITEM NAME</u>	<u>INPUT FORMAT</u>	<u>MEANING OR USE</u>	<u>UNITS</u>
PRJN (n)	10X, A6	Name of projection	-

n is ID of satellite segment that projection is attached to

<u>ITEM NAME</u>	<u>INPUT FORMAT</u>	<u>MEANING OR USE</u>	<u>UNIT</u>
TRX (m)	5X, F10.0	If PRJN = THRUSTOR,	Ft
m is the counter NTR		TRX is the X-coordinate. For any other PRJN, TRX is the area of the segment and its name is changed to AREA	Ft ²
TRR (m)	5X, F5.0	If PRJN = THRUSTOR	Ft
		TRR is the R-coordinate. For any other PRJN, TRX is changed to M11S, the number of segments.	-
TRTHET (m)	5X, F5.0	If PRJN = THRUSTOR,	Radians
		TRTHET is the - coordinate. For other PRJN, TRTHET is changed to M22S, the number of data points for the segments.	-

The above 4 items are on one card. There are as many cards as there are projections. The sequence of cards is interrupted by the descriptive cards, next detailed, whenever the projection is not a thrustor.

SURDES (n, 1) (n = M1S + 1 to M11S)	F7.0	ID No. of segment on projection	-
SURDES (n, 2)	F9.0	X-coordinate of segment	Ft
, 3)	F8.0	R-coordinate of segment	Ft
, 4)	F9.0	θ-coordinate	Radians
, 5)	F6.0	Area	Ft ²
, 6)	F9.0	X-distance to nearest plume vertex	Ft
, 7)	F8.0	Surface temperature	Deg R

The above 7 items are on one card. There are M11S cards. M3S is set equal to M1S, and M1S increased by M11S.

(6) Structural Materials - Array MATERIAL and File 1, MAT

<u>ITEM NAME</u>	<u>INPUT FORMAT</u>	<u>MEANING OR USE</u>	<u>UNITS</u>
MT1S	10X, 15	Number of rows in MATERIAL	-
MT2S	10X, 15	Number of columns in MATERIAL	-

The above two items are on one card.

MATERIAL (n, 1)	F3.0	Material code number	-
, 2)	F7.0	Melting point	Deg R
, 3)	E10.7	Vickers hardness	kg/mm ²
, 4)	E10.7	Bulk modulus	Lb/in. ²
, 5)	F6.0	Surface tension	Dyne/cm
, 6)	F8.3	Heat capacity	BTU/lb-deg R
, 7)	F8.3	Thermal conductivity	BTU-in./ft ² -sec-deg R
, 8)	E10.7	Yield Strength	Lb/in. ²
, 9)	F5.2	Density	Lb/ft ³

The above nine items are entered on one card for each segment. There are MT1S cards.

(7) Propellant Temperature - Test Case

<u>ITEM NAME</u>	<u>INPUT FORMAT</u>	<u>MEANING OR USE</u>	<u>UNITS</u>
TTANKF	10X, F10.0	Fuel temperature	Deg K
TTANKO	10X, F10.0	Oxidizer temperature	Deg K

The above two items are entered on one card.

(8) Deposits - Array CHEMIC and File 3, CHEM

<u>ITEM NAME</u>	<u>INPUT FORMAT</u>	<u>MEANING OR USE</u>	<u>UNITS</u>
JC1S	10X, 15	Number of rows in CHEMIC	-
JC2S	10X, 15	Number of columns in CHEMIC	-

The above two items are on one card.

CHEMIC (n, 1)	F8.4	Material code number	-
n = 1, - JC1S			
, 2)	F8.4	Freezing point	Deg R
, 3)	F8.4	Density (solid)	Lb/Ft ³
, 4)	F8.4	Critical temperature	Deg R
, 5)	F8.4	Boiling point	Deg R
, 6)	F8.4	Heat of fusion	BTU/lb
, 7)	F8.4	Thermal conductivity (solid)	BTU-in. / ft ² -sec-deg R
, 8)	F8.4	Thermal conductivity (liquid)	BTU-in. / ft ² -sec-deg R
, 9)	F8.4	Heat capacity (solid)	BTU/lb-deg R
, 10)	F8.4	Heat capacity (liquid)	BTU/lb-deg R

The above 10 items are on one card for each material.

<u>ITEM NAME</u>	<u>INPUT FORMAT</u>	<u>MEANING OR USE</u>	<u>UNITS</u>
CHEMIC (n, 11)	F8.4	Refractive index (liquid)	-
, 12)	F8.4	Molecular radius	Angstrom

The above 2 items are on one card for each material. There are JC1S pairs of cards.

(9) Optical Thermal Properties - Array PRØPTY and File 2, PROP

This input recycles once for each material entry in the array NAME. It reads the control cards (number of rows and columns), then the data cards for NAME (1). Then it recycles and reads the control card and data cards for NAME (2), etc. If NAME (n) is unassigned, it proceeds directly to NAME (n + 1). Note that the code number for each material (the first column in PRØPTY) is supplied by the FØRTRAN program.

<u>ITEM NAME</u>	<u>INPUT FORMAT</u>	<u>MEANING OR USE</u>	<u>UNITS</u>
N1S	5X, 15	Number of rows in PRØPTY	-
N2S	5X, 15	Number of columns in PRØPTY	-

The above two items are on one card.

PRØPTY (n, 1)	Assigned by program	Material code number	-
n = 1 - N1S			
, 2)	F10.4	Surface finish for structural materials or temperature for deposits	Mu-in. Deg R
, 3)	F10.4	Solar absorptivity	-
, 4)	F10.4	Thermal emissivity	-
, 5)	F10.4	Diffuse solar reflectivity	-
, 6)	F10.4	Specular solar reflectivity	-
, 7)	F10.4	Thermal reflectivity	-
, 8)	F10.4	Thermal conductivity	BTU-in. / ft ² -sec- deg R
, 9)	F10.4	Infrared transmittance (15 micron)	-

The above 8 items are on one card per surface finish or temperature.

<u>ITEM NAME</u>	<u>INPUT FORMAT</u>	<u>MEANING OR USE</u>	<u>UNITS</u>
PRØPTY (n, 10)	F10.4	Visible transmittance (0.5 micron)	-
, 11)	F10.4	Ultraviolet transmit- tance (0.1 micron)	-

The above 2 items are on one card per surface finish or temperature. There are N1S pairs of cards.

(10) Segment Structure - Array SURDES

In this deck, the array is filled column-by-column instead of row-by-row.

<u>ITEM NAME</u>	<u>INPUT FORMAT</u>	<u>MEANING OR USE</u>	<u>UNITS</u>
SURDES (n, 12) n = 1, M1S	20F4.0 (7 cards)	Code number of material in top layer, all seg- ments in sequence	-
, 13)	8E10.7 (17 cards)	Thickness of top layer	In.
, 14)	16F5.0 (9 cards)	Surface finish of top layer	Mu-in.
, 25) n = 1-9 and 41-M3S	20F4.0 (5 cards)	Code number of material for 2nd layer	-
, 26)	8E10.7 (12 cards)	Thickness of 2nd layer	In.
, 27)	16F5.0 (6 cards)	Surface finish of 2nd layer	Mu-in.

(11) Program Option Selection

<u>ITEM NAME</u>	<u>INPUT FORMAT</u>	<u>USE</u>
RUNFLAG	10X, I3	If zero, go to exposure routines If positive, go to surface condition routines

(12) Modified Surface Conditions - Test Case - Array EFFECT

<u>ITEM NAME</u>	<u>INPUT FORMAT</u>	<u>MEANING OR USE</u>	<u>UNITS</u>
IIS	5X, 15 (one card)	Number of segments with changed conditions - number of rows for EFFECT	-
EFFECT (n, 1) n = 1-IIS	G10.6	X-coordinate of segment	Ft
, 2)	G10.6	Y-coordinate	Ft
, 3)	G10.6	θ -coordinate	Rad
, 4)	G10.6	ID number	-
, 5)	G10.6	Surface temperature	Deg R
, 6)	G10.6	Top layer material code	-
, 7)	G10.6	Thickness	In.
, 8)	G10.6	Surface finish	Mu-in.
The above eight entries are on one card.			
, 9)	G10.6	2nd layer material code	-
, 10)	G10.6	Thickness	In.
, 11)	G10.6	Surface finish	Mu-in.

The above three entries are on one card. There are IIS pairs of cards.

(13) Program Option Selection

<u>ITEM NAME</u>	<u>INPUT FORMAT</u>	<u>USE</u>
RUNFLAG	10X, 13 (one card)	See (11)
EXTYPE	(10X, F10.0 (one card)	If: -1, no exposure 0, plume exposure +1, space exposure

(14) Pulse Characteristics - Impingement Locations

<u>ITEM NAME</u>	<u>INPUT FORMAT</u>	<u>MEANING OR USE</u>	<u>UNITS</u>
TRSLOC	10X, F5.0	θ -coordinate of active thruster	Rad
TOTIME	5X, F5.0	Pulse duration	Sec

The above two items are on a single data card.

P	10X, F10.0	P is 1/4 the latus rectum of the plume	-
---	------------	--	---

The above item is alone on a card.

<u>ITEM NAME</u>	<u>INPUT FORMAT</u>	<u>MEANING OR USE</u>	<u>UNITS</u>
NTR	10X, 15	Thruster number	-
P	10X, F10.0	1/4th latus rectum	-

The above two items are on a single data card. One card is inserted for each impingement case of interest. The loop is terminated when NTR is given a value of 999.

(15) Program Option Selection

<u>ITEM NAME</u>	<u>INPUT FORMAT</u>	<u>USE</u>
ITRNCL	10X, 15	Selects which of the coordinate transformations should be calculated. (See Initialization.)

(16) Coordinate Transformation (Test Case)

(a) Thruster-Based to Satellite-Based

<u>ITEM NAME</u>	<u>INPUT FORMAT</u>	<u>MEANING OR USE</u>	<u>UNITS</u>
NTR	10X, 15	Thruster number	-
N	10X, 15	Case number for thruster NTR	-

The above two items are input on a single card.

<u>ITEM NAME</u>	<u>INPUT FORMAT</u>	<u>MEANING OR USE</u>	<u>UNITS</u>
ZZ(NTR, N)	10X, F10.0	Axial coordinate in thruster system	Ft
RR(NTR, N)	10X, F10.0	Radial coordinate	Ft
THE(NTR, N)	10X, F10.0	Angular coordinate	Rad

The above three items are input on a single card. The subroutine CORTRN repeats the above inputs until it finds a value of -1 for NTR.

(b) Satellite-Based to Thruster-Based

The program does not require special input for this transformation. It automatically uses the coordinates of the segments identified as being impinged by the plume.

(17) Molecular Weight - Array MØLWT

<u>ITEM NAME</u>	<u>INPUT FORMAT</u>	<u>MEANING OR USE</u>	<u>UNITS</u>
MØLWT(n) n is the code number of deposited materials, 19-25	7(5X, F5.0) one card	Molecular weight of species in gas state	Lb-mole/lb

(18) Wear Constants - Array SCRPTTE

<u>ITEM NAME</u>	<u>INPUT FORMAT</u>	<u>MEANING OR USE</u>	<u>UNITS</u>
SCRPTTE (n, 1) n is code number of material	5X, F5.0	Material code number	-
, 2)	10X, G10.0	Wear constant	Lb mass/ lb impinging
, 3)	5X, G10.0	Lower critical velocity	Ft/sec
, 4)	5X, F10.0	Exponent	-

The above four items are input on a single data card. Input is one card for each material in numerical order of the material code.

(19) Plume Characteristics (Test Case)

<u>ITEM NAME</u>	<u>INPUT FORMAT</u>	<u>MEANING OR USE</u>	<u>UNITS</u>
NTR	5X, I5	Thruster number	-
SDRPDM(NTR)	5X, G10.0	Small drop diameter	In.
LDRPDM(NTR)	5X, G10.0	Large drop diameter	In.
SDVEL(NTR)	5X, G10.0	Small drop velocity	Ft/sec
LDVEL(NTR)	5X, G10.0	Large drop velocity	Ft/sec

The above 5 items are input on a single data card

SDAIMP(NTR)	5X, G10.0	Small drop impingement angle	Rad
LDAIMP(NTR)	5X, G10.0	Large drop impingement angle	Rad
SDMAPS(NTR)	5X, G10.0	Small drop flow concentration	Lb/ft ² -sec
LDMAPS(NTR)	5X, G10.0	Large drop flow concentration	Lb/ft ² -sec

The above 4 items are input on a single data card.

PMCMP(1) 1 = deposite code number = 19 - 25	7(5X, F5.0) one card	Concentration of condensables in gas phase of plume	Lb/ft ³
---	-------------------------	---	--------------------

(20) Velocity Limits - for Material Wear

<u>ITEM NAME</u>	<u>INPUT FORMAT</u>	<u>MEANING OR USE</u>	<u>UNITS</u>
VUP1	5X, F10.0	High velocity lower critical limit	Ft/sec
VUP2	5X, F10.0	High velocity upper critical limit	Ft/sec

The above 2 items are input on a single data card.

(21) Heat Transfer Coefficients (Test Case)

<u>ITEM NAME</u>	<u>INPUT FORMAT</u>	<u>MEANING OR USE</u>	<u>UNITS</u>
HTRNH1	10X, F10.0	Heat transfer coefficient from plume to surface at velocity G1	BTU-in. / ft ² -sec- deg R
HTRNH2	10X, F10.0	Heat transfer coefficient at G2	BTU-in. / ft ² -sec- deg R
G1	10X, F10.0	Superficial velocity	Lb/ft ² - sec
G2	10X, F10.0	Superficial velocity	Lb/ft ² - sec

The above 4 items are input using a single data card.

(22) Plume Physical Properties (Test Case)

<u>ITEM NAME</u>	<u>INPUT FORMAT</u>	<u>MEANING OR USE</u>	<u>UNITS</u>
PMTP	5X, F10.0	Temperature of plume	Deg R
PMPRS	5X, F10.0	Pressure	Lb/in. ²
PMRHØ	5X, F10.0	Vapor density	Lb/ft ³

The above 3 items are input using a single data card.

(23) Plume Configuration Change

<u>ITEM NAME</u>	<u>INPUT FORMAT</u>	<u>MEANING OR USE</u>	<u>UNITS</u>
DELP	5X, F10.0	Causes change in plume shape	-

Table D-1 is a listing of the card image for some of the inputs.

D.6 OUTPUT DESCRIPTION

The output of the SURFACE program consists of a set of tables which contain lists of data of interest. Copies of the tables (or portions thereof) are presented to illustrate the following discussion.

The first output (Table D-II) lists the configuration of the basic satellite and shows the location of all segments and projections. The second

Table D-I. Continued

115,	10,825	1,195	5,7596	1,0	6,725	520,	-1,	-1,	-1,
116,	10,825	0,0	0,0	2,0	6,725	520,	+2,5	999,	999,
PROJECTN= THRSTR AREA 0,0 M11S= 0,0 M22S= 0,0									
PROJECTN= THRSTR AREA 0,0 M11S= 0,0 M22S=1,571									
PROJECTN= THRSTR AREA 0,0 M11S= 0,0 M22S=3,142									
PROJECTN= THRSTR AREA 0,0 M11S= 0,0 M22S=4,712									
PROJECTN= SOLGEL AREA 20,0 M11S= 20,0 M22S= 7,									
7301,	6,4362	3,562	2,19911	1,0	7,2662	550,0			
7302,	6,4052	4,161	1,499	1,0	7,0052	560,0			
7303,	6,4032	4,056	2,19911	1,0	7,0032	560,0			
7304,	6,5962	3,951	2,899	1,0	7,0962	560,0			
7305,	6,4201	5,122	1,591	1,0	7,0201	560,0			
7306,	6,4151	5,030	2,19911	1,0	7,0151	560,0			
7307,	6,4121	4,954	2,827	1,0	7,0121	560,0			
7308,	6,2320	6,100	1,503	1,0	7,0320	560,0			
7309,	6,2270	6,020	2,19911	1,0	7,0270	560,0			
7310,	6,2220	5,940	2,835	1,0	7,0220	560,0			
7311,	6,7230	6,203	-2,835	1,0	7,1230	510,0			
7312,	6,7130	6,1131	-2,19911	1,0	7,1130	510,0			
7313,	6,7130	5,033	-1,503	1,0	7,1130	510,0			
7314,	6,9111	5,235	-2,897	1,0	7,3111	510,0			
7315,	6,9061	5,1371	-2,19911	1,0	7,3061	510,0			
7316,	6,9011	5,0392	-1,501	1,0	7,3011	510,0			
7317,	7,0992	4,270	-2,599	1,0	7,4992	510,0			
7318,	7,0942	4,1551	-2,19911	1,0	7,4942	510,0			
7319,	7,0892	4,038	-1,499	1,0	7,4892	510,0			
7320,	7,3722	2,6011	-2,19911	1,0	7,7722	520,0			
PROJECTN= THRSTR TRX 11,05 TOR 1,E-STRHT 0,0									
M11S = 9 M22S = 9									
1	1279,	2,7E	1	9,0E	6 200,	0,215	0,457	47,E	3169,
2	1700,	5,5E	2	9,9E	6 200,	0,17	,00182	5,0E	4 162,
3	1320,	4,9E	2	9,9E	6 200,	0,18	,00242	5,E	3 132,
4	425,	4,9E	2	9,9E	6 200,	0,20	,0098	5,E	3 397,
5	1390,	4,9E	2	9,9E	6 200,	0,19	,0026	5,E	3 135,
6	-1,	-1,	-1,	-1,	-1,	-1,	-1,	-1,	-1,
7	2440,	5,6E	1	1,1E	7 1120,	0,081	0,405	3,E	3128,
8	6700,	2,E	2	-1,	-1,	0,38	,00234	-1,	118,
9	5270,	2,E	2	-1,	-1,	,25	,0067	-1,	356,
TTANKO= 273,2 PROPELLANT TEMPERATURES									
TTANKO= 560,0									
TTANKO= 7									
TTANKO= 12									
19,	471,37	110,6	776,4	529,2	68,51	-1,	,002509	0,295	0,3783
1,420	3,710								
20,	413,2	110,3	-1,	569,	92,9	-1,	,00336	0,656	-1,
1,340	4,085								
21,	442,	-1,	1052,	648,	97,3	-1,	-1,	0,358	0,7
-1,	4,547								
22,	-1,	-1,	-1,	-1,	-1,	-1,	-1,	-1,	-1,
-1,	5,05								
23,	-1,	-1,	-1,	-1,	-1,	-1,	-1,	-1,	-1,
-1,	5,298								
24,	-1,	-1,	-1,	-1,	-1,	-1,	-1,	-1,	-1,
-1,	5,444								
25,	491,0	57,2	1165,	671,	143,2	,004167	,00113	0,149	1,
1,36303	3,140								
M11S= 29 M22S= 19									
0,0	0,2	0,011	0,04	-1,0	-1,0	-1,0	0,457	0	

OPTICAL/THERMAL CHARACTERISTICS
(ONE SHEET OMITTED)

Table D-I-Continued

NOT REPRODUCIBLE

OPT	.75	0.0																	
	N1S=	1	N2S=	10															
T	10.	-1.	-1.	-1.	-1.	-1.	-1.	.00242	.5										
I	.98	0.																	
	N1S=	1	N2S=	10															
A	2.5	-1.	-1.	-1.	-1.	-1.	-1.	.098	.85										
L	.75	0.																	
	N1S=	1	N2S=	10															
/	1.	-1.	-1.	-1.	-1.	-1.	-1.	.0026	0.0										
T	.98	.65																	
	N1S=	2	N2S=	10															
H	0.1	0.10	0.02	0.90	0.007	-1.	-1.	.606	.0										
E	0.0	0.0																	
R	1.0	0.25	0.04	0.55	0.007	-1.	-1.		0.00										
M	0.0	0.0																	
	N1S=	2	N2S=	10															
A	10.0	0.96	0.85	0.25	-1.	-1.	-1.	.0233	0.00										
L	0.0	0.0																	
	60.0	0.89	0.77	0.02	-1.	-1.	-1.		0.00										
P	0.0	0.0																	
	N1S=	2	N2S=	10															
O	10.0	0.12	0.93	0.05	-1.	-1.	-1.	.0067	0.00										
P	0.0	0.0																	
	60.0	0.21	0.95	0.02	-1.	-1.	-1.		0.00										
E	0.0	0.0																	
	N1S=	1	N2S=	7															
A	560.0	-1.	-1.	-1.	0.0755	-1.	-1.	.00239											
T	N1S=	1	N2S=	7															
L	560.0	-1.	-1.	-1.	-1.	-1.	-1.	.00336											
E	N1S=	1	N2S=	1															
S	560.0																		
	N1S=	1	N2S=	1															
	560.0																		
	N1S=	1	N2S=	3															
	560.0	.45	.75																
	N1S=	1	N2S=	7															
	560.0	-1.	-1.	-1.	-1.	-1.	-1.	.00113											
	7.	7.	7.	7.	7.	7.	7.	7.	7.	7.	7.	7.	7.	7.	7.	7.	7.	7.	7.
	1.	1.	1.	1.	1.	1.	1.	1.	1.	1.	1.	1.	1.	1.	1.	1.	1.	1.	1.
	9.	1.	9.	1.	1.	9.	1.	9.	1.	1.	9.	1.	9.	1.	9.	1.	9.	1.	1.
	9.	8.	9.	8.	9.	8.	9.	8.	9.	8.	9.	8.	9.	8.	9.	8.	9.	8.	8.
	9.	9.	9.	9.	9.	9.	9.	9.	9.	9.	9.	9.	9.	9.	9.	9.	9.	9.	9.
	3.	3.	3.	3.	3.	3.	3.	3.	3.	3.	3.	3.	3.	3.	3.	3.	3.	3.	3.
	3.E=	4	3.E=	4	3.E=	4	3.E=	4	3.E=	4	3.E=	4	3.E=	4	3.E=	4	3.E=	4	1.5E=
	3.E=	4	1.E=	1	1.E=	1	1.E=	1	1.E=	1	1.E=	1	1.E=	1	1.E=	1	1.E=	1	1.E=
	1.E=	1	1.E=	1	1.E=	1	1.E=	1	1.E=	1	1.E=	1	1.E=	1	1.E=	1	1.E=	1	1.E=
	1.E=	1	1.E=	1	1.E=	1	1.E=	1	1.E=	1	1.E=	1	1.E=	1	1.E=	1	1.E=	1	1.E=
	1.E=	1	1.E=	1	1.E=	1	1.E=	1	1.E=	1	1.E=	1	1.E=	1	1.E=	1	1.E=	1	1.E=
	5.E=	3	1.E=	1	5.E=	3	1.E=	1	1.E=	1	5.E=	3	1.E=	1	1.E=	1	5.E=	3	5.E=
	1.E=	1	1.E=	1	5.E=	3	1.E=	1	5.E=	3	1.E=	1	1.E=	1	1.E=	1	5.E=	3	5.E=
	1.E=	1	5.E=	3	1.E=	1	1.E=	1	5.E=	3	1.E=	1	5.E=	3	1.E=	1	5.E=	3	1.E=
	1.E=	1	5.E=	3	1.E=	1	5.E=	3	1.E=	1	5.E=	3	1.E=	1	5.E=	3	1.E=	1	5.E=
	5.E=	3	7.E=	3	7.E=	3	5.E=	3	7.E=	3	5.E=	3	7.E=	3	5.E=	3	7.E=	3	7.E=
	5.E=	3	7.E=	3	5.E=	3	7.E=	3	7.E=	3	5.E=	3	7.E=	3	5.E=	3	7.E=	3	5.E=
	7.E=	3	7.E=	3	7.E=	3	7.E=	3	7.E=	3	7.E=	3	7.E=	3	7.E=	3	7.E=	3	7.E=
	7.E=	3	7.E=	3	7.E=	3	7.E=	3	7.E=	3	7.E=	3	7.E=	3	7.E=	3	7.E=	3	7.E=
	5.E=	3	5.E=	3	5.E=	3	5.E=	3	5.E=	3	5.E=	3	5.E=	3	5.E=	3	5.E=	3	5.E=

Table D-II. SATELLITE CONFIGURATION

ID NO.	S E G M E N T				X DIST SEGMENT TO PLUME VERTEX (FT)	SURFACE TEMPERATURE (DEG R)	HEIGHT OF PROJECTION (FT)	DIRECTION COSINES OF NORMAL TO PROJECTION TANGENT PLANE		
	X COORD. (FT)	R COORD. (FT)	THETA (RAD)	AREA (SQFT)				LAMBDA	MU	NU
1	0,000	0,000	0,00000	1	3,600	520,0	-1,0	-1,0	-1,0	
2	,305	,590	1,44720	1	3,295	520,0	-1,0	-1,0	-1,0	
3	,305	,590	3,14159	1	3,295	520,0	-1,0	-1,0	-1,0	
4	,305	,590	5,23600	1	3,295	520,0	-1,0	-1,0	-1,0	
5	,620	1,200	,42830	1	2,980	520,0	-1,0	-1,0	-1,0	
6	,620	1,200	1,57080	1	2,980	520,0	-1,0	-1,0	-1,0	
7	,620	1,200	3,14159	1	2,980	520,0	-1,0	-1,0	-1,0	
8	,620	1,200	4,79818	1	2,980	520,0	-1,0	-1,0	-1,0	
9	,620	1,200	5,45460	1	2,980	520,0	-1,0	-1,0	-1,0	
10	1,325	1,600	,31416	1	2,275	520,0	-1,0	-1,0	-1,0	
11	1,325	1,600	,94248	1	2,275	520,0	-1,0	-1,0	-1,0	
12	1,325	1,600	1,57080	1	2,275	520,0	-1,0	-1,0	-1,0	
13	1,325	1,600	2,19911	1	2,275	520,0	-1,0	-1,0	-1,0	
14	1,325	1,600	2,82743	1	2,275	520,0	-1,0	-1,0	-1,0	
15	1,325	1,600	3,45575	1	2,275	520,0	-1,0	-1,0	-1,0	
16	1,325	1,600	4,08407	1	2,275	520,0	-1,0	-1,0	-1,0	
17	1,325	1,600	4,71240	1	2,275	520,0	-1,0	-1,0	-1,0	
18	1,325	1,600	5,34070	1	2,275	520,0	-1,0	-1,0	-1,0	
19	1,325	1,600	5,96902	1	2,275	520,0	-1,0	-1,0	-1,0	
20	2,325	1,600	,31416	1	1,725	520,0	-1,0	-1,0	-1,0	
21	2,325	1,600	,94248	1	1,725	520,0	-1,0	-1,0	-1,0	
22	2,325	1,600	1,57080	1	1,725	520,0	-1,0	-1,0	-1,0	
23	2,325	1,600	2,19911	1	1,725	520,0	-1,0	-1,0	-1,0	
24	2,325	1,600	2,82743	1	1,725	520,0	-1,0	-1,0	-1,0	
25	2,325	1,600	3,45575	1	1,725	520,0	-1,0	-1,0	-1,0	
26	2,325	1,600	4,08407	1	1,725	520,0	-1,0	-1,0	-1,0	
27	2,325	1,600	4,71240	1	1,725	520,0	-1,0	-1,0	-1,0	
28	2,325	1,600	5,34070	1	1,725	520,0	-1,0	-1,0	-1,0	
29	2,325	1,600	5,96902	1	1,725	520,0	-1,0	-1,0	-1,0	
30	3,325	1,600	,31416	1	,725	520,0	1,5	NOT APPLICABLE	NOT APPLICABLE	
31	3,325	1,600	,94248	1	,725	520,0	-1,0	-1,0	-1,0	
32	3,325	1,600	1,57080	1	,725	520,0	1,5	NOT APPLICABLE	NOT APPLICABLE	
33	3,325	1,600	2,19911	1	,725	520,0	-1,0	-1,0	-1,0	
34	3,325	1,600	2,82743	1	,725	520,0	-1,0	-1,0	-1,0	
35	3,325	1,600	3,45575	1	,725	520,0	1,5	NOT APPLICABLE	NOT APPLICABLE	
36	3,325	1,600	4,08407	1	,725	520,0	-1,0	-1,0	-1,0	
37	3,325	1,600	4,71240	1	,725	520,0	1,5	NOT APPLICABLE	NOT APPLICABLE	
38	3,325	1,600	5,34070	1	,725	520,0	-1,0	-1,0	-1,0	
39	3,325	1,600	5,96902	1	,725	520,0	-1,0	-1,0	-1,0	
40	4,325	1,600	,31416	1	,725	520,0	-1,0	-1,0	-1,0	
41	4,325	1,600	,94248	1	,725	520,0	-1,0	-1,0	-1,0	
42	4,325	1,600	1,57080	1	,725	520,0	-1,0	-1,0	-1,0	
43	4,325	1,600	2,19911	1	,725	520,0	-1,0	-1,0	-1,0	
44	4,325	1,600	2,82743	1	,725	520,0	-1,0	-1,0	-1,0	
45	4,325	1,600	3,45575	1	,725	520,0	-1,0	-1,0	-1,0	
46	4,325	1,600	4,08407	1	,725	520,0	-1,0	-1,0	-1,0	
47	4,325	1,600	4,71240	1	,725	520,0	-1,0	-1,0	-1,0	
48	4,325	1,600	5,34070	1	,725	520,0	-1,0	-1,0	-1,0	
49	4,325	1,600	5,96902	1	,725	520,0	-1,0	-1,0	-1,0	
50	5,325	1,600	,31416	1	1,725	520,0	-1,0	-1,0	-1,0	
51	5,325	1,600	,94248	1	1,725	520,0	-1,0	-1,0	-1,0	
52	5,325	1,600	1,57080	1	1,725	520,0	-1,0	-1,0	-1,0	
53	5,325	1,600	2,19911	1	1,725	520,0	-1,0	-1,0	-1,0	
54	5,325	1,600	2,82743	1	1,725	520,0	-1,0	-1,0	-1,0	

NOT REPRODUCIBLE

Table D-II-Conclusion

55	5,325	1,600	3,45575	1	1,725	520,0	-1,0	-1,0	-1,0	-1,0	
56	5,325	1,600	4,08407	1	1,725	520,0	-1,0	-1,0	-1,0	-1,0	
57	5,325	1,600	4,71240	1	1,725	520,0	-1,0	-1,0	-1,0	-1,0	
58	5,325	1,600	5,34070	1	1,725	520,0	-1,0	-1,0	-1,0	-1,0	
59	5,325	1,600	5,96902	1	1,725	520,0	-1,0	-1,0	-1,0	-1,0	
60	6,325	1,600	3,1414	1	2,725	520,0	-1,0	-1,0	-1,0	-1,0	
61	6,325	1,600	,9424A	1	2,725	520,0	-1,0	-1,0	-1,0	-1,0	
62	6,325	1,600	1,57080	1	2,725	520,0	-1,0	-1,0	-1,0	-1,0	
63	6,325	1,600	2,19911	1	2,725	520,0	-1,0	-1,0	-1,0	-1,0	
64	6,325	1,600	2,82743	1	2,725	520,0	-1,0	-1,0	-1,0	-1,0	
65	6,325	1,600	3,45575	1	2,725	520,0	-1,0	-1,0	-1,0	-1,0	
66	6,325	1,600	4,08407	1	2,725	520,0	-1,0	-1,0	-1,0	-1,0	
67	6,325	1,600	4,71240	1	2,725	520,0	-1,0	-1,0	-1,0	-1,0	
68	6,325	1,600	5,34070	1	2,725	520,0	-1,0	-1,0	-1,0	-1,0	
69	6,325	1,600	5,96902	1	2,725	520,0	-1,0	-1,0	-1,0	-1,0	
70	7,325	1,600	,31416	1	3,725	520,0	-1,0	-1,0	-1,0	-1,0	
71	7,325	1,600	,9424A	1	3,725	520,0	-1,0	-1,0	-1,0	-1,0	
72	7,325	1,600	1,57080	1	3,725	520,0	-1,0	-1,0	-1,0	-1,0	
73	7,325	1,600	2,19911	1	3,725	520,0	-1,0	4,0	,9820	,1000	,0500
74	7,325	1,600	2,82743	1	3,725	520,0	-1,0	-1,0	-1,0	-1,0	
75	7,325	1,600	3,45575	1	3,725	520,0	-1,0	-1,0	-1,0	-1,0	
76	7,325	1,600	4,08407	1	3,725	520,0	-1,0	-1,0	-1,0	-1,0	
77	7,325	1,600	4,71240	1	3,725	520,0	-1,0	-1,0	-1,0	-1,0	
78	7,325	1,600	5,34070	1	3,725	520,0	-1,0	-1,0	-1,0	-1,0	
79	7,325	1,600	5,96902	1	3,725	520,0	-1,0	-1,0	-1,0	-1,0	
80	8,325	1,600	,31416	1	4,725	520,0	-1,0	-1,0	-1,0	-1,0	
81	8,325	1,600	,9424A	1	4,725	520,0	-1,0	-1,0	-1,0	-1,0	
82	8,325	1,600	1,57080	1	4,725	520,0	-1,0	-1,0	-1,0	-1,0	
83	8,325	1,600	2,19911	1	4,725	520,0	-1,0	-1,0	-1,0	-1,0	
84	8,325	1,600	2,82743	1	4,725	520,0	-1,0	-1,0	-1,0	-1,0	
85	8,325	1,600	3,45575	1	4,725	520,0	-1,0	-1,0	-1,0	-1,0	
86	8,325	1,600	4,08407	1	4,725	520,0	-1,0	-1,0	-1,0	-1,0	
87	8,325	1,600	4,71240	1	4,725	520,0	-1,0	-1,0	-1,0	-1,0	
88	8,325	1,600	5,34070	1	4,725	520,0	-1,0	-1,0	-1,0	-1,0	
89	8,325	1,600	5,96902	1	4,725	520,0	-1,0	-1,0	-1,0	-1,0	
90	9,325	1,600	,31416	1	5,725	520,0	-1,0	-1,0	-1,0	-1,0	
91	9,325	1,600	,9424A	1	5,725	520,0	-1,0	-1,0	-1,0	-1,0	
92	9,325	1,600	1,57080	1	5,725	520,0	-1,0	-1,0	-1,0	-1,0	
93	9,325	1,600	2,19911	1	5,725	520,0	-1,0	-1,0	-1,0	-1,0	
94	9,325	1,600	2,82743	1	5,725	520,0	-1,0	-1,0	-1,0	-1,0	
95	9,325	1,600	3,45575	1	5,725	520,0	-1,0	-1,0	-1,0	-1,0	
96	9,325	1,600	4,08407	1	5,725	520,0	-1,0	-1,0	-1,0	-1,0	
97	9,325	1,600	4,71240	1	5,725	520,0	-1,0	-1,0	-1,0	-1,0	
98	9,325	1,600	5,34070	1	5,725	520,0	-1,0	-1,0	-1,0	-1,0	
99	9,325	1,600	5,96902	1	5,725	520,0	-1,0	-1,0	-1,0	-1,0	
100	10,325	1,600	,31416	1	6,725	520,0	-1,0	-1,0	-1,0	-1,0	
101	10,325	1,600	,9424A	1	6,725	520,0	-1,0	-1,0	-1,0	-1,0	
102	10,325	1,600	1,57080	1	6,725	520,0	-1,0	-1,0	-1,0	-1,0	
103	10,325	1,600	2,19911	1	6,725	520,0	-1,0	-1,0	-1,0	-1,0	
104	10,325	1,600	2,82743	1	6,725	520,0	-1,0	-1,0	-1,0	-1,0	
105	10,325	1,600	3,45575	1	6,725	520,0	-1,0	-1,0	-1,0	-1,0	
106	10,325	1,600	4,08407	1	6,725	520,0	-1,0	-1,0	-1,0	-1,0	
107	10,325	1,600	4,71240	1	6,725	520,0	-1,0	-1,0	-1,0	-1,0	
108	10,325	1,600	5,34070	1	6,725	520,0	-1,0	-1,0	-1,0	-1,0	
109	10,325	1,600	5,96902	1	6,725	520,0	-1,0	-1,0	-1,0	-1,0	
110	10,825	1,195	,52360	1	6,725	520,0	-1,0	-1,0	-1,0	-1,0	
111	10,825	1,195	1,57080	1	6,725	520,0	-1,0	-1,0	-1,0	-1,0	
112	10,825	1,195	2,61800	1	6,725	520,0	-1,0	-1,0	-1,0	-1,0	
113	10,825	1,195	3,66520	1	6,725	520,0	-1,0	-1,0	-1,0	-1,0	
114	10,825	1,195	4,71240	1	6,725	520,0	-1,0	-1,0	-1,0	-1,0	
115	10,825	1,195	5,75960	1	6,725	520,0	-1,0	-1,0	-1,0	-1,0	
116	10,825	0,000	0,00000	2	6,725	520,0	2,5	NOT APPLICABLE			

NOTE: VALUES OF -1,0 INDICATE NO DATA ENTERED,
EXTERNAL TOTAL AREA 117,00 SQUARE FEET

NOT REPRODUCIBLE

(Table D-III) provides data on the projections present, identifying them as to type and location. Items which themselves are considered to consist of segments have their structures detailed.

The next few outputs (Tables D-IV to D-VI) consist of listings of properties of materials; structural materials, propellants, deposits (not illustrated), and thermal/optical properties (only first page of listing included).

Table D-VII, a partial listing, shows the structure of the segments of the spacecraft, with the materials called out for each segment.

The first output showing results of program computations is Table D-VIII. In this table, the structure and thermal/optical properties for each segment in its initial condition are detailed. Table D-IX presents the effective absorptivity, emissivity, and their ratio for the complete satellite.

The set of changed segment surface conditions which were input as data are listed in Table D-X, and the effect that these changes have on the segment properties is printed in Table D-XI. Note the changes in segments 51, 52 and 53 (see Table D-VIII, and D-XI), and the way the changes correspond to the input shown in Table D-X. The effect on the spacecraft's thermal condition may be noted by comparing Tables D-IX and D-XII.

The calculated impingement of the plume on the satellite for various plume geometries and nozzle selections is given in Table D-XIII, while D-XIV shows the results of coordinate transformation calculations. The inputs to the thruster-to-satellite table are arbitrary selections, but those for the satellite-to-thruster transformation are the segments impinged by the plume (Table D-XIII).

The mechanical properties of impinged segments are presented in Table D-XV, and Table D-XVI lists the wear constants of all materials of interest.

The important characteristics of the plume which relate to damage to the satellite surfaces are given in Table D-XVII.

The output after calculating the effects of the plume on the surface has the same format as that from the arbitrary changes (Table D-XI); therefore, no copy is presented.

Table D-III. PROJECTIONS

THRUSTORS LOCATED AT SEGMENT NOS,	X (FT)	R (FT)	THETA (RAD)
30	3,600	2,600	3,14160
32	3,600	2,600	1,571000
35	3,600	2,600	3,142000
37	3,600	2,600	4,712000

SOLCEL AT SEGMENT NO, 73

S E G M E N T					X DIST	SURFACE
ID	X	R	THETA	AREA	SEGMENT	TEMPER.
NO.	COORD. (FT)	COORD. (FT)	(RAD)*	(SQFT)	TO PLUME VERTEX (FT)	ATURE (DEG R)
7301	6,886	2,582	2,19911	1	3,286	570,0
7302	6,600	4,161	1,49900	1	3,000	500,0
7303	6,603	4,056	2,19911	1	3,003	500,0
7304	6,598	3,951	2,89900	1	2,998	500,0
7305	6,420	5,122	1,50100	1	2,820	500,0
7306	6,415	5,038	2,19911	1	2,815	500,0
7307	6,410	4,954	2,89700	1	2,810	500,0
7308	6,232	6,100	1,50300	1	2,632	500,0
7309	6,227	6,020	2,19911	1	2,627	500,0
7310	6,222	5,940	2,89500	1	2,622	500,0
7311	6,723	6,200	-2,89500	1	3,123	510,0
7312	6,718	6,119	-2,19911	1	3,118	510,0
7313	6,713	6,038	-1,50300	1	3,113	510,0
7314	6,911	5,255	-2,89700	1	3,311	510,0
7315	6,906	5,137	-2,19911	1	3,306	510,0
7316	6,901	5,039	-1,50100	1	3,301	510,0
7317	7,099	4,275	-2,89900	1	3,499	510,0
7318	7,094	4,155	-2,19911	1	3,494	510,0
7319	7,089	4,035	-1,49900	1	3,489	510,0
7320	7,572	2,681	-2,19911	1	3,772	520,0

* NEGATIVE VALUE FOR ANGLE SIGNALS THAT SEGMENT IS ON SIDE OF PROJECTION FACING AWAY FROM THE PLUME.

NOTE: VALUES OF -1,0,,,0 INDICATE NO DATA ENTERED

AREA OF SOLCEL IS 20.0 SQUARE FEET.

THRUSTORS LOCATED AT SEGMENT NOS,	X (FT)	R (FT)	THETA (RAD)
116	11,050	,000	0,000000

TOTAL SATELLITE AREA, INCLUDING PROJECTIONS, IS 137,00 SQUARE FEET.

Table D-IV. PROPERTIES OF STRUCTURAL MATERIALS

MATERIAL	CODE NO.	MELTING POINT (DEG R)	VICKERS HARDNESS (KG/50UM)	BULK MODULUS (PSI)	SURFACE ENERGY (DYNE/CM)	HEAT CAPACITY (BTU/LB-DEG)	THERMAL CONDUCTIVITY (BTU-IN/ SQFT-DEG-SEC)	YIELD STRENGTH (PSI)	DENSITY (LB/CUFT)
ALUMIN	1	1279.00	27.00E+00	98.00E+05	900.000	.215	.457	47,000E+03	169.00
CINCO	2	1700.00	55.00E+01	59.00E+05	200.000	.170	.302	50,000E+03	162.00
SOLCEL	3	1320.00	49.00E+01	99.00E+05	200.000	.180	.002	80,000E+02	139.00
INPORT	4	425.00	45.00E+01	99.00E+05	200.000	.200	.098	80,000E+02	390.00
UVPART	5	1390.00	49.00E+01	99.00E+05	200.000	.180	.003	80,000E+02	135.00
UMASND	6	21.00	10.00E+01	10.00E+01	1.000	-.100	-1.000	10,000E+01	1.00
GOLD	7	2440.00	58.00E+01	11,000E+04	1120.000	.131	.806	30,000E+02	1238.00
BLACK	8	6700.00	20.00E+01	10,000E+01	1.000	.360	.023	10,000E+01	118.00
WHITE	9	3270.00	20.00E+01	10,000E+01	1.000	.250	.007	10,000E+01	354.00

NOTE: VALUES OF -1.0000 INDICATE NO DATA ENTERED

NOT REPRODUCIBLE

Table D-V. OPERATING CONDITIONS

EXTERNAL PRESSURE (PSIA)	WALL TEMPERATURE (DEG R)
0,000000	529,200000

FUEL PROPERTIES

BOILING POINT (DEG R)	FREEZING POINT (DEG R)	CRITICAL TEMP, (DEG R)	CRITICAL PRESS, (PSIA)
648,000000	399,600000	1069,200000	1195,000000
VAPOR CP, (BTU/LB-DEG)	LIQUID CP, (BTU/LB-DEG)	SOLID CP, (BTU/LB-DEG)	MOL. WEIGHT
,995000	,690000	,522292	46,074000
LATENT HEAT VAP, (BTU/LB)	LATENT HEAT FUS, (BTU/LB)	LIG. THERM. COND, (BTU-IN/SQFT-DEG-SEC)	ACCOM. COEFF.
378,000000	121,500000	,000484	,100000
REFERENCE TEMP, (DEG R)	SPECIFIC GRAVITY	VISCOSITY (POISE)	SURFACE TENSION (DYNE/CM)
540,000000	,870000	,010400	34,000000

OXIDIZER PROPERTIES

BOILING POINT (DEG R)	FREEZING POINT (DEG R)	CRITICAL TEMP, (DEG R)	CRITICAL PRESS, (PSIA)
529,200000	471,600000	777,600000	1441,300000
VAPOR CP, (BTU/LB-DEG)	LIQUID CP, (BTU/LB-DEG)	SOLID CP, (BTU/LB-DEG)	MOL. WEIGHT
,295000	,378300	,295000	46,005000
LATENT HEAT VAP, (BTU/LB)	LATENT HEAT FUS, (BTU/LB)	LIG. THERM. COND, (BTU-IN/SQFT-DEG-SEC)	ACCOM. COEFF.
178,200000	68,760000	,000024	,100000
REFERENCE TEMP, (DEG R)	SPECIFIC GRAVITY	VISCOSITY (POISE)	SURFACE TENSION (DYNE/CM)
540,000000	1,434000	,003940	28,000000

Table D-V-Concluded

GENERAL INSTRUCTIONS

STOP TIME TIME INTERVAL
 (SEC) (SEC)
 .064000 .000100

KNUDSEN-LANGMUIR COEFFICIENTS

CNSTHF	CNSTHD	CNSTVF	CNSTVO
2.8571428571E-06	3.0000000000E-07	2.9697757560E-05	2.9675511683E-05

CALINGEART-DAVIS COEFFICIENTS

$\ln(P) = A + (B/(T-43.0))$ FOR P IN MM, T IN DEG K

FUEL		OXIDIZER	
A	B	A	B
24.185411	-3283.087298	26.755098	-3244.533651

VAPOR ENTHALPY AT THE BOILING POINT

FUEL	OXIDIZER
(BTU/LB)	(BTU/LB)
234.843895	251.758080

PARACHOR

FUEL	OXIDIZER
127.88111	73.79814

Table D-VI-Continued

WHITE

SURFACE FINISH (REFLECTIVITY) (DIFFUSE) (SPECULAR) THERMAL CONDUCTIVITY (BTU-IN/FT-DEG-SEC) TRANSMITTANCE (0.1 MICRON(VIS) 0.5 MICRON(IR) 15 MICRON(VIS) 0.1 MICRON(UV))

10,0000 .1200 .9300 .0500 -1.0000 -1.0000 0.0000 0.0000 0.0000 0.0000 0.0000 0.0000

60,0000 .2100 .9500 .0200 -1.0000 -1.0000 -1.0000 0.0000 0.0000 0.0000 0.0000 0.0000

NOTE: VALUES OF -1.0000 INDICATE NO DATA ENTERED

2304

TEMPERATURE (DEG F) ABSORPTIVITY (SOLAR) (THERMAL) (DIFFUSE) (SPECULAR) REFLECTIVITY (DIFFUSE) (SPECULAR) THERMAL CONDUCTIVITY (BTU-IN/FT-DEG-SEC) TRANSMITTANCE (0.1 MICRON(VIS) 0.5 MICRON(IR) 15 MICRON(VIS) 0.1 MICRON(UV))

560,0000 -1.0000 -1.0000 -1.0000 .0755 -1.0000 -1.0000 .0024 -1.0000 -1.0000 -1.0000 -1.0000

NOTE: VALUES OF -1.0000 INDICATE NO DATA ENTERED

4903

TEMPERATURE (DEG F) ABSORPTIVITY (SOLAR) (THERMAL) (DIFFUSE) (SPECULAR) REFLECTIVITY (DIFFUSE) (SPECULAR) THERMAL CONDUCTIVITY (BTU-IN/FT-DEG-SEC) TRANSMITTANCE (0.1 MICRON(VIS) 0.5 MICRON(IR) 15 MICRON(VIS) 0.1 MICRON(UV))

560,0000 -1.0000 -1.0000 -1.0000 -1.0000 -1.0000 -1.0000 .0034 -1.0000 -1.0000 -1.0000 -1.0000

NOTE: VALUES OF -1.0000 INDICATE NO DATA ENTERED

4903

TEMPERATURE (DEG F) ABSORPTIVITY (SOLAR) (THERMAL) (DIFFUSE) (SPECULAR) REFLECTIVITY (DIFFUSE) (SPECULAR) THERMAL CONDUCTIVITY (BTU-IN/FT-DEG-SEC) TRANSMITTANCE (0.1 MICRON(VIS) 0.5 MICRON(IR) 15 MICRON(VIS) 0.1 MICRON(UV))

560,0000 -1.0000 -1.0000 -1.0000 -1.0000 -1.0000 -1.0000 -1.0000 -1.0000 -1.0000 -1.0000 -1.0000

NOTE: VALUES OF -1.0000 INDICATE NO DATA ENTERED

4903

Table D-VI—Concluded

MMH20

TEMPERATURE (DEG R) ABSORB TIVITY (SOLAR) (THERMAL) (DIFFUSE) (SPECULAR) REFLECTIVITY THERMAL CONDUCTIVITY (BTU-IN/FT-DEG-SEC) TRANSMITTANCE (MICRON) 0.15 MICRON (UV) 0.15 MICRON (UV) 0.15 MICRON (UV)

560.0000 -1.0000 -1.0000 -1.0000 -1.0000 -1.0000 -1.0000 -1.0000 -1.0000 -1.0000

MMH03

TEMPERATURE (DEG R) ABSORB TIVITY (SOLAR) (THERMAL) (DIFFUSE) (SPECULAR) REFLECTIVITY THERMAL CONDUCTIVITY (BTU-IN/FT-DEG-SEC) TRANSMITTANCE (MICRON) 0.15 MICRON (IR) 0.15 MICRON (VIS) 0.15 MICRON (UV)

560.0000 -1.0000 -1.0000 -1.0000 -1.0000 -1.0000 -1.0000 -1.0000 -1.0000 -1.0000

NOTE: VALUES OF -1.0000 INDICATE NO DATA ENTERED

MMH20

TEMPERATURE (DEG R) ABSORB TIVITY (SOLAR) (THERMAL) (DIFFUSE) (SPECULAR) REFLECTIVITY THERMAL CONDUCTIVITY (BTU-IN/FT-DEG-SEC) TRANSMITTANCE (MICRON) 0.15 MICRON (UV) 0.15 MICRON (UV) 0.15 MICRON (UV)

560.0000 .4500 .7500 -1.0000 -1.0000 -1.0000 -1.0000 -1.0000 -1.0000 -1.0000

NOTE: VALUES OF -1.0000 INDICATE NO DATA ENTERED

WATER

TEMPERATURE (DEG R) ABSORB TIVITY (SOLAR) (THERMAL) (DIFFUSE) (SPECULAR) REFLECTIVITY THERMAL CONDUCTIVITY (BTU-IN/FT-DEG-SEC) TRANSMITTANCE (MICRON) 0.15 MICRON (IR) 0.15 MICRON (VIS) 0.15 MICRON (UV)

560.0000 -1.0000 -1.0000 -1.0000 -1.0000 4.5000 .0011 -1.0000 -1.0000 -1.0000

NOTE: VALUES OF -1.0000 INDICATE NO DATA ENTERED

Table D-VIII. CURRENT CONDITION OF SATELLITE EXTERIOR-INITIAL CONDITIONS

IC	X	R	THETA	AREA	PLUVE X	TEMP	PRUN HGT	LAMBDA	MU	NU	TRN(1,1)
1	0.000	0.000	0.7000	1	-0.000	522.0	-1.0	-1.0000	-1.0000	-1.0000	0.0000
	MATL	DEPTH	FINISH	ABSRTY	EMISIV	REF(1,F)	REF(1,S)	REF(1,M)	TRM COND	TRN(1,5)	TRN(1,1)
	7	0.000	1.0000	.2000	.0400	.0070	-1.0000	.0000	.0000	0.0000	0.0000
	1	ALUMI	2.0000	.0200	.0500	.0000	-1.0000	.0000	.4570	0.0000	0.0000
	-1	SOLE	-1.0000	-1.0000	-1.0000	-1.0000	-1.0000	-1.0000	-1.0000	-1.0000	-1.0000
2	0.590	0.590	1.7472	1	-0.195	522.0	-1.0	-1.0000	-1.0000	-1.0000	0.0000
	MATL	DEPTH	FINISH	ABSRTY	EMISIV	REF(1,F)	REF(1,S)	REF(1,M)	TRM COND	TRN(1,5)	TRN(1,1)
	7	0.000	1.0000	.2000	.0400	.0070	-1.0000	.0000	.0000	0.0000	0.0000
	1	ALUMI	2.0000	.0200	.0500	.0000	-1.0000	.0000	.4570	0.0000	0.0000
	-1	SOLE	-1.0000	-1.0000	-1.0000	-1.0000	-1.0000	-1.0000	-1.0000	-1.0000	-1.0000
3	0.595	0.590	3.1450	1	-0.195	522.0	-1.0	-1.0000	-1.0000	-1.0000	0.0000
	MATL	DEPTH	FINISH	ABSRTY	EMISIV	REF(1,F)	REF(1,S)	REF(1,M)	TRM COND	TRN(1,5)	TRN(1,1)
	7	0.000	1.0000	.2000	.0400	.0070	-1.0000	.0000	.0000	0.0000	0.0000
	1	ALUMI	2.0000	.0200	.0500	.0000	-1.0000	.0000	.4570	0.0000	0.0000
	-1	SOLE	-1.0000	-1.0000	-1.0000	-1.0000	-1.0000	-1.0000	-1.0000	-1.0000	-1.0000
4	0.595	0.590	5.9360	1	-0.195	522.0	-1.0	-1.0000	-1.0000	-1.0000	0.0000
	MATL	DEPTH	FINISH	ABSRTY	EMISIV	REF(1,F)	REF(1,S)	REF(1,M)	TRM COND	TRN(1,5)	TRN(1,1)
	7	0.000	1.0000	.2000	.0400	.0070	-1.0000	.0000	.0000	0.0000	0.0000
	1	ALUMI	2.0000	.0200	.0500	.0000	-1.0000	.0000	.4570	0.0000	0.0000
	-1	SOLE	-1.0000	-1.0000	-1.0000	-1.0000	-1.0000	-1.0000	-1.0000	-1.0000	-1.0000
5	0.620	1.200	1.2330	1	-0.190	522.0	-1.0	-1.0000	-1.0000	-1.0000	0.0000
	MATL	DEPTH	FINISH	ABSRTY	EMISIV	REF(1,F)	REF(1,S)	REF(1,M)	TRM COND	TRN(1,5)	TRN(1,1)
	7	0.000	1.0000	.2000	.0400	.0070	-1.0000	.0000	.0000	0.0000	0.0000
	1	ALUMI	2.0000	.0200	.0500	.0000	-1.0000	.0000	.4570	0.0000	0.0000
	-1	SOLE	-1.0000	-1.0000	-1.0000	-1.0000	-1.0000	-1.0000	-1.0000	-1.0000	-1.0000

Table D-VIII-Concluded

ID	X	R	T-BETA	AREA	PLUME X	TEMP	PRJN HGT	LAMBDA	MU	TRN(1,1)
50	5.325	1.600	1.7420	1	1.725	525.0	51.0	1.0000	1.0000	0.0000
	MATL NAME	DEPTH	FINISH	ABSRTY	EMISY	REF(CIF)	REF(SPC)	REF(TM)	T-RM CONE	TRN(1,5)
	1 ALUMIN	.1000	16.0000	.2280	.0800	.5291	.7500	.4473	.4570	0.0000
	-1 NONE	-1.0000	-1.0000	-1.0000	-1.0000	-1.0000	-1.0000	-1.0000	-1.0000	-1.0000
	-1 NONE	-1.0000	-1.0000	-1.0000	-1.0000	-1.0000	-1.0000	-1.0000	-1.0000	-1.0000
51	5.325	1.600	1.7420	1	1.725	525.0	51.0	1.0000	1.0000	0.0000
	MATL NAME	DEPTH	FINISH	ABSRTY	EMISY	REF(CIF)	REF(SPC)	REF(TM)	T-RM CONE	TRN(1,5)
	1 ALUMIN	.1000	16.0000	.2280	.0800	.5291	.7500	.4473	.4570	0.0000
	-1 NONE	-1.0000	-1.0000	-1.0000	-1.0000	-1.0000	-1.0000	-1.0000	-1.0000	-1.0000
	-1 NONE	-1.0000	-1.0000	-1.0000	-1.0000	-1.0000	-1.0000	-1.0000	-1.0000	-1.0000
52	5.325	1.600	1.7420	1	1.725	525.0	51.0	1.0000	1.0000	0.0000
	MATL NAME	DEPTH	FINISH	ABSRTY	EMISY	REF(CIF)	REF(SPC)	REF(TM)	T-RM CONE	TRN(1,5)
	1 ALUMIN	.1000	16.0000	.2280	.0800	.5291	.7500	.4473	.4570	0.0000
	-1 NONE	-1.0000	-1.0000	-1.0000	-1.0000	-1.0000	-1.0000	-1.0000	-1.0000	-1.0000
	-1 NONE	-1.0000	-1.0000	-1.0000	-1.0000	-1.0000	-1.0000	-1.0000	-1.0000	-1.0000
53	5.325	1.600	1.7420	1	1.725	525.0	51.0	1.0000	1.0000	0.0000
	MATL NAME	DEPTH	FINISH	ABSRTY	EMISY	REF(CIF)	REF(SPC)	REF(TM)	T-RM CONE	TRN(1,5)
	1 ALUMIN	.1000	16.0000	.2280	.0800	.5291	.7500	.4473	.4570	0.0000
	-1 NONE	-1.0000	-1.0000	-1.0000	-1.0000	-1.0000	-1.0000	-1.0000	-1.0000	-1.0000
	-1 NONE	-1.0000	-1.0000	-1.0000	-1.0000	-1.0000	-1.0000	-1.0000	-1.0000	-1.0000
54	5.325	1.600	1.7420	1	1.725	525.0	51.0	1.0000	1.0000	0.0000
	MATL NAME	DEPTH	FINISH	ABSRTY	EMISY	REF(CIF)	REF(SPC)	REF(TM)	T-RM CONE	TRN(1,5)
	1 ALUMIN	.1000	16.0000	.2280	.0800	.5291	.7500	.4473	.4570	0.0000
	-1 NONE	-1.0000	-1.0000	-1.0000	-1.0000	-1.0000	-1.0000	-1.0000	-1.0000	-1.0000
	-1 NONE	-1.0000	-1.0000	-1.0000	-1.0000	-1.0000	-1.0000	-1.0000	-1.0000	-1.0000
55	5.325	1.600	1.7420	1	1.725	525.0	51.0	1.0000	1.0000	0.0000
	MATL NAME	DEPTH	FINISH	ABSRTY	EMISY	REF(CIF)	REF(SPC)	REF(TM)	T-RM CONE	TRN(1,5)
	1 ALUMIN	.1000	16.0000	.2280	.0800	.5291	.7500	.4473	.4570	0.0000
	-1 NONE	-1.0000	-1.0000	-1.0000	-1.0000	-1.0000	-1.0000	-1.0000	-1.0000	-1.0000
	-1 NONE	-1.0000	-1.0000	-1.0000	-1.0000	-1.0000	-1.0000	-1.0000	-1.0000	-1.0000

NOT REPRODUCIBLE

Table D-IX. EFFECTIVE HEAT TRANSFER CONSTANTS

SUM OF SEGMENT AREAS ■ 117.00

EFFECTIVE SOLAR ABSORPTIVITY ■ .323

EFFECTIVE THERMAL EMISSIVITY ■ .409

AVERAGE VALUE ALPHA/EPSILON RATIO FOR WHOLE SPACECRAFT ■ .7890

Table D-X. SPACECRAFT EXTERIOR MATERIALS AFTER PLUME OR SPACE EXPOSURE

SEGMENT NO.	TEMPERATURE (DEG R)	T O P L A Y E R		2 ND L A Y E R	
		MATERIAL FINISH	DEPTH (IN)	MATERIAL FINISH	DEPTH (IN)
42	600.0	ALUMIN	.0950	UNASND	.1000
51	610.0	WHITE	.0020	ALUMIN	.1000
52	650.0	ALUMIN	.0950	UNASND	.1000
53	610.0	ERODED	0.0000	ALUMIN	.1000
61	780.0	ALUMIN	.0980	UNASND	.1000
62	900.0	ALUMIN	.0780	UNASND	.1000
63	780.0	ALUMIN	.0980	UNASND	.1000
72	630.0	HOLE	.0500	UNASND	.1000
82	610.0	ALUMIN	.1000	UNASND	.1000
92	580.0	BLACK	.0057	ALUMIN	.1000

NOTE: VALUES OF 0.0000 INDICATE NO DATA ENTERED

Table D-XI-Concluded

ID	X	R	THETA	AREA	PLUME X	TEMP	PRJN HGT	LAMBDA	MU	NU	
50	5.325	1.600	.31416	1	1.725	520.0	1.0	1.0000	1.0000	1.0000	
MATRL NAME	DEPTH	FINISH	ABSRTY	EMISTY	REF(DIF)	REF(SPC)	REF(TH)	TMRM COND	TRN(15)	TRN(5)	TRN(1)
1 ALUMIN	.1000	16.0000	.2260	.0800	.5291	.7600	.4473	.4570	0.0000	0.0000	0.0000
-1 NONE	-1.0000	-1.0000	-1.0000	-1.0000	-1.0000	-1.0000	-1.0000	-1.0000	-1.0000	-1.0000	-1.0000
-1 NONE	-1.0000	-1.0000	-1.0000	-1.0000	-1.0000	-1.0000	-1.0000	-1.0000	-1.0000	-1.0000	-1.0000
ID	X	R	THETA	AREA	PLUME X	TEMP	PRJN HGT	LAMBDA	MU	NU	
51	5.325	1.600	.74248	1	1.725	610.0	1.0	1.0000	1.0000	1.0000	
MATRL NAME	DEPTH	FINISH	ABSRTY	EMISTY	REF(DIF)	REF(SPC)	REF(TH)	TMRM COND	TRN(15)	TRN(5)	TRN(1)
9 WHITE	.0020	80.0000	.2100	.9500	.0200	10.0000	10.0000	.0067	0.0000	0.0000	0.0000
1 ALUMIN	.1000	39.0000	.3760	.5620	.5000	.0971	.2000	.4570	0.0000	0.0000	0.0000
-1 NONE	-1.0000	-1.0000	-1.0000	-1.0000	-1.0000	-1.0000	-1.0000	-1.0000	-1.0000	-1.0000	-1.0000
ID	X	R	THETA	AREA	PLUME X	TEMP	PRJN HGT	LAMBDA	MU	NU	
52	5.325	1.600	1.97060	1	1.725	650.0	1.0	1.0000	1.0000	1.0000	
MATRL NAME	DEPTH	FINISH	ABSRTY	EMISTY	REF(DIF)	REF(SPC)	REF(TH)	TMRM COND	TRN(15)	TRN(5)	TRN(1)
1 ALUMIN	.0950	250.0000	.6000	.3400	.5000	.9000	.2000	.4570	0.0000	0.0000	0.0000
-1 NONE	-1.0000	-1.0000	-1.0000	-1.0000	-1.0000	-1.0000	-1.0000	-1.0000	-1.0000	-1.0000	-1.0000
-1 NONE	-1.0000	-1.0000	-1.0000	-1.0000	-1.0000	-1.0000	-1.0000	-1.0000	-1.0000	-1.0000	-1.0000
ID	X	R	THETA	AREA	PLUME X	TEMP	PRJN HGT	LAMBDA	MU	NU	
53	5.325	1.600	2.11911	1	1.725	610.0	1.0	1.0000	1.0000	1.0000	
MATRL NAME	DEPTH	FINISH	ABSRTY	EMISTY	REF(DIF)	REF(SPC)	REF(TH)	TMRM COND	TRN(15)	TRN(5)	TRN(1)
1 ALUMIN	.1000	39.0000	.3760	.5620	.5000	.0971	.2000	.4570	0.0000	0.0000	0.0000
-1 NONE	-1.0000	-1.0000	-1.0000	-1.0000	-1.0000	-1.0000	-1.0000	-1.0000	-1.0000	-1.0000	-1.0000
-1 NONE	-1.0000	-1.0000	-1.0000	-1.0000	-1.0000	-1.0000	-1.0000	-1.0000	-1.0000	-1.0000	-1.0000
ID	X	R	THETA	AREA	PLUME X	TEMP	PRJN HGT	LAMBDA	MU	NU	
54	5.325	1.600	2.02743	1	1.725	520.0	1.0	1.0000	1.0000	1.0000	
MATRL NAME	DEPTH	FINISH	ABSRTY	EMISTY	REF(DIF)	REF(SPC)	REF(TH)	TMRM COND	TRN(15)	TRN(5)	TRN(1)
1 ALUMIN	.1000	16.0000	.2260	.0800	.5291	.7600	.4473	.4570	0.0000	0.0000	0.0000
-1 NONE	-1.0000	-1.0000	-1.0000	-1.0000	-1.0000	-1.0000	-1.0000	-1.0000	-1.0000	-1.0000	-1.0000
-1 NONE	-1.0000	-1.0000	-1.0000	-1.0000	-1.0000	-1.0000	-1.0000	-1.0000	-1.0000	-1.0000	-1.0000

Table D-XII. EFFECTIVE HEAT TRANSFER CONSTANTS—
AFTER EXPOSURE TO PLUME

SUM OF SEGMENT AREAS = 117.00

EFFECTIVE SOLAR ABSORPTIVITY = .336

EFFECTIVE THERMAL EMISSIVITY = .445

AVERAGE VALUE, ALPHA/EPSILON RATIO FOR WHOLE SPACECRAFT = .7548

Table D-XIII. IMPINGEMENT OF PLUME ON SATELLITE

FROM THRUSTOR NO. 1 WHEN P = .90 ID NOS.
42
52
62
72
82
92
102
PROJECTION SEGMENTS IMPINGED BY THRUSTOR NO. 2 WHEN P = 2.000
7301
7302
7303
7304
7305
7306
7308
7309
PROJECTION SEGMENTS IMPINGED BY THRUSTOR NO. 1 WHEN P = .200
0

Table D-XIV. COORDINATE TRANSFORMATION

THRUSTOR SYSTEM		TO	SATELLITE SYSTEM			
AXIAL COORDINATE		RADIAL COORDINATE	ANGULAR COORDINATE			
ZZ	X	RR	R	THE	THETA	
(FT)	(FT)	(FT)	(FT)	(RAD)	(RAD)	
1,7300	5,3300	1,0000	1,6000	3,1416	0,0000	
4,0700	7,6700	1,5000	4,0886	2,9870	0,0972	

THRUSTOR-BASED COORDINATES
OF PLUME IMPINGED SEGMENTS

SEG	AXIAL	RADIAL	ANGULAR
ID	DIST	DIST	COORD
	Z (FT)	R (FT)	THE (RAD)
42	0,72500	1,00000	-1,57079
52	1,72500	1,00000	-1,57079
62	2,72500	1,00000	-1,57079
72	3,72500	1,00000	-1,57079
82	4,72500	1,00000	-1,57079
92	5,72500	1,00000	-1,57079
102	6,72500	1,00000	-1,57079
7301	3,28620	1,60140	0,32485
7302	3,00820	1,57876	1,38058
7303	3,00820	2,47949	0,27839
7304	2,99820	4,17552	0,40647
7305	2,82010	2,53483	1,42940
7306	2,81510	3,30863	0,46236
7308	2,63200	3,51040	1,45280
7309	2,62700	4,20414	0,57046

* ANGLE FROM LINE JOINING
AXES OF SATELLITE AND THRUSTOR

Table D-XV. PHYSICAL PROPERTIES OF IMPINGED SEGMENT SURFACES

MATERIAL	CODE NO.	MELTING POINT (DEG R)	VICKERS HARDNESS (KG/SQMM)	BULK MODULUS (PSI)	SURFACE ENERGY (DYNE/CM)	HEAT CAPACITY (BTU/LB-DEG)	CONDUCTIVITY (BTU-IN/ SQFT-DEG-SEC)	YIELD STRENGTH (PSI)	DENSITY (LB/CUFT)	SEG ID
ALUMIN	1	1279.00	27.000E+00	98.000E+05	900.000	.215	.457	47.000E+03	169.00	42
ALUMIN	1	1279.00	27.000E+00	98.000E+05	900.000	.215	.457	47.000E+03	169.00	52
ALUMIN	1	1279.00	27.000E+00	98.000E+05	900.000	.215	.457	47.000E+03	169.00	62
ALUMIN	1	1279.00	27.000E+00	98.000E+05	900.000	.215	.457	47.000E+03	169.00	72
ALUMIN	1	1279.00	27.000E+00	98.000E+05	900.000	.215	.457	47.000E+03	169.00	82
BLACK	8	6709.00	20.000E+01	-10.000E+01	-1.000	.360	.023	-10.000E+01	118.00	92
WHITE	9	5270.00	20.000E+01	-10.000E+01	-1.000	.250	.007	-10.000E+01	356.00	102
ALUMIN	1	1279.00	27.000E+00	98.000E+05	900.000	.215	.457	47.000E+03	169.00	7301
SOLCEL	3	1320.00	49.000E+01	99.000E+05	200.000	.180	.002	80.000E+02	139.00	7302
SOLCEL	3	1320.00	49.000E+01	99.000E+05	200.000	.180	.002	80.000E+02	139.00	7303
SOLCEL	3	1320.00	49.000E+01	99.000E+05	200.000	.180	.002	80.000E+02	139.00	7304
SOLCEL	3	1320.00	49.000E+01	99.000E+05	200.000	.180	.002	80.000E+02	139.00	7305
SOLCEL	3	1320.00	49.000E+01	99.000E+05	200.000	.180	.002	80.000E+02	139.00	7306
SOLCEL	3	1320.00	49.000E+01	99.000E+05	200.000	.180	.002	80.000E+02	139.00	7307
SOLCEL	3	1320.00	49.000E+01	99.000E+05	200.000	.180	.002	80.000E+02	139.00	7308
SOLCEL	3	1320.00	49.000E+01	99.000E+05	200.000	.180	.002	80.000E+02	139.00	7309

NOTE: VALUES OF 01.0...0 INDICATE NO DATA ENTERED

Table D-XVI. WEAR CONSTANTS OF MATERIALS ON SURFACE

NAME	ID	WEAR CONSTANT (FT-LB/LB)	VELOCITY LOWER LIMIT (FT/SEC)	EXPONENT (SLOPE)	MOLECULAR WEIGHT (VAPOR)
ALUMIN	1	3.000E+06	460	-3.3125	-1.0
WINDOW	2	5.000E+04	170	-3.5625	-1.0
SOLCEL	3	5.000E+04	170	-3.5625	-1.0
IRPORT	4	5.000E+04	170	-3.5625	-1.0
UVPORT	5	5.000E+04	170	-3.5625	-1.0
UNASND	6	-1.000E+00	-1	-1.0000	-1.0
GOLD	7	3.000E+06	460	-3.3125	-1.0
BLACK	8	1.200E+04	200	-2.5000	-1.0
WHITE	9	1.200E+04	200	-2.5000	-1.0
TFE	18	1.500E+05	1000	-2.5000	-1.0
N2O4	19	1.000E+04	220	-3.0000	46.0
HN03	20	1.000E+04	220	-3.0000	63.0
MMH	21	1.000E+04	220	-3.0000	46.0
MMHN2O	22	1.000E+04	220	-3.0000	64.0
MMHN03	23	1.000E+04	220	-3.0000	109.0
MHNH2O	24	1.000E+04	220	-3.0000	154.0
WATER	25	1.000E+04	220	-3.0000	18.0

NOTE: VALUES OF -1.0...0 INDICATE NO DATA ENTERED

HIGH VELOCITY LOWER LIMITS FOR ALL MATERIALS

HIGH VELOCITY (FT/SEC)	HYPER VELOCITY (FT/SEC)
3000	900000

Table D-XVII. ARBITRARY PLUME CHARACTERISTICS FOR TESTING PROGRAM

THRUSTER NUMBER	DROP DIAMETER		DROP VELOCITY		IMPINGEMENT ANGLE		CONCENTRATION		TEMPERATURE	PRESSURE	DENSITY
	SMALL (IN.)	LARGE (IN.)	SMALL (FT/SEC)	LARGE (FT/SEC)	SMALL (RAD)	LARGE (RAD)	SMALL (LB/SEC)	LARGE (LB/SEC)	(DEG R)	(PSIA)	(LB/CUFT)
2	.0200	.2000	2000	1500	.15708	.09123	.0030	.0010	2000	27.0	.0030

SUPERFICIAL HEAT TRANSFER											
VELOCITY COEFFICIENT											
(LB/SOFT-SEC) (BTU-IN/SOFT-SEC-DEG R)											

25.0 .620											
50.0 1.040											
